THE SYNTHESIS AND STUDY OF TF ANTIGEN FUNCTIONALIZED DENDRIMERS AND DENDRIMER END GROUP CHARACTERIZATION AND INDIUM(III) PROMOTED GLYCOSYLATION

by

Amanda Lynn Mattson

A dissertation submitted in partial fulfillment
of the requirements for the degree

of

Doctor of Philosophy

in

Chemistry

MONTANA STATE UNIVERSITY
Bozeman, Montana

April 2017

©COPYRIGHT

by

Amanda Lynn Mattson

2017

All Rights Reserved

DEDICATION

This dissertation is dedicated to my parents, who have been my lifelong source of unconditional support and encouragement. I love you.

ACKNOWLEDGEMENTS

I would like to thank my advisor, Dr. Mary Cloninger, for her years of constant support and guidance. She has fostered a lab environment that has come to feel like my second family. I would like to thank the members of the Cloninger group: Dr. Anna Michel, Dr. Candace Goodman, Jessica Ennist, Harrison VanKoten, Dr. Jon Cousin, Sam Bernhard, Mackenzie Fricke, and Jessi Langlais, who have been wonderfully supportive throughout all of my life events, chemistry related or otherwise. I would like to thank Dr. Kristian Schlick for teaching me everything I know in lab and Garrett Moraski for his valuable advice and immeasurable patience. Thank you to Kyle Tweedy for his work on the TF antigen project and Kevin Poffenberger, Scott Jungwirth, and Dr. Robert Usselman for their work on EPR. I would like to thank the members of my committee: Dr. Tom Livinghouse, Dr. Ed Dratz, Dr. Valérie Copié, and Dr. Sharon Neufeldt for sacrificing their time and energy to assist in my pursuit of a PhD. I would like to thank my family for all of their encouragement, especially my brother, Mark Mattson, for being my on-call librarian. Finally, I would like to thank my best friend and husband, Scott, who has made countless sacrifices in his life to ensure my success and happiness.

TABLE OF CONTENTS

1. INTRODUCTION TO TF ANTIGEN, GALECTIN-3, MULTIVALENCY, AND DENDRIMERS 1

Background 1
Introduction to Galectin-3 3
TF Antigen and Galectin-3 4
Multivalency 7
Multivalent Displays of TF Antigen 9
Polyamidoamine Dendrimers 15
Lactose Functionalized Dendrimers and Galectin-3 17
Summary of the Research Described Herein 18
Hypothesis 19
Conclusion 20

2. SYNTHESIS OF TF ANTIGEN FUNCTIONALIZED DENDRIMERS 22

Background 22
Previous Synthetic Routes 23
Synthesis of TF Antigen 25
PAMAM Dendrimer Functionalization 31
Conclusion 35
Experimental Procedures 35
General Methods 35

3. THE STUDY OF TF ANTIGEN FUNCTIONALIZED DENDRIMERS IN HOMOTYPIC CELLULAR AGGREGATION ASSAYS 62

Background 62
TF Antigen Functionalized Dendrimers 66
Results 67
Discussion 69
Conclusion 72
Experimental Procedures 73
Dendrimers 73
Cell culture methods 73
Homotypic cellular aggregation assay 74
Data analysis 74
Statistical analysis 76

TABLE OF CONTENTS — CONTINUED

4. CHARACTERIZATION OF DENDRIMERS BEARING CLUSTERS OF END GROUPS 77

Background 77
Results and Discussion 80
Conclusion 87
Experimental Procedures 88
General Methods 88

5. USING INDIUM(III) AS A PROMOTER FOR GLYCOSYLATION 102

Contribution of Authors and Coauthors 11702
Manuscript information page 11703
Discussion 11706
Experimental 117
General Methods 117
General procedure for optimization of reaction conditions 118
General procedure for mannopyranoside and galactopyranoside derivatives 118
General procedure for evaluation of the reversibility of the reaction 119
General procedure for acetonide protected derivatives using $In(OTf)_3$ 119
General procedure for preparation of disaccharides 120

6. SUMMARY AND CONCLUSIONS 130

REFERENCES CITED 133

APPENDICES 152

APPENDIX A: Relevant Spectral Data from Chapter 2 153
APPENDIX B: Supplemental Data from Chapter 3 209
APPENDIX C: Relevant Spectral Data from Chapter 4 220
APPENDIX D: Relevant Spectral Data from Chapter 5 287
APPENDIX E: Copyright Infromation for Reprinted Materials 302
Figure 2 303
Figures 5 and 6 303
Figures 7, 16, 17, 18 304
Figure 9 310
Figure 10 31
Figure 11 318

LIST OF TABLES

Table Page

1. Percent loading of **18**, **19**, **20**, and **21** with TF antigen 33

2. Acetylation of dendrimer end groups 33

3. Amounts used for dendrimers **29-34**.....91

4. Amounts used for dendrimers **35-40**.....94

5. Amounts used for dendrimers **41-46**.....96

6. Amounts used for dendrimers **47-52**.....98

7. Summary of cellular aggregation assay data 210

LIST OF SCHEMES

Scheme Page

1. Synthesis of benzylidene derivatives trichloroacetimidates **4** and **8**, and attempted glycosylation 26

2. Part 1 of the synthesis of TF antigen via an azide protection 29

3. Part 2 of the synthesis of TF antigen; the formation of the disaccharide 29

4. Glycosylation attempt using N-phenyl-2,2,2-trifluoroacetimidate 30

5. Part 3 of the synthesis of TF antigen- azide reduction and methyl ester deprotection 31

6. The functionalization of PAMAM dendrimers with TF antigen 34

7. The formation of sodium 3,5-bis-(3-(3-(*N*-oxy-2,2,6,6-tetramethylpiperidine-4-yl)-thioureido)propoxy) benzoate **27** 81

8. Preparation of generation 4 dendrimers with radical end groups clustered in groups of two 84

LIST OF FIGURES

Figure Page

1. The structure of TF antigen....1

2. MUC1 protein structure....2

3. Demonstration of a segment of the MUC1 glycosylation on healthy cells vs cancer cells....2

4. Representation of Galectin 3....3

5. TF antigen in the binding pocket of galectin-3's carbohydrate recognition domain....5

6. Hydrogen bonding interactions of TF antigen in the binding pocket of galectin-3....5

7. Galectin-3 re-patterning the surface of cancer cells....6

8. Demonstration of the different types of multivalency....8

9. BSA and TT proteins functionalized with MUC1 mimicking protein chains which were glycosylated with variants of TF antigen....10

10. KLH protein functionalized with carbohydrate clusters....11

11. TF antigen functionalized gold nanoparticles....13

12. Generation 2 polyamidoamine dendrimer....16

13. Retrosynthesis of TF antigen.....22

14. Example of neighboring group participation....23

15. Proposed intermediate of nickel catalyzed glycosylation....25

16. The effect of lactose functionalized dendrimers on A549 cells....64

17. The effect of lactose functionalized dendrimers on A549 cells....65

LIST OF FIGURES — CONTINUED

Figure Page

18. Schematic representation of the effects of galectin-3 and dendrimers on cancer cellular aggregation 66

19. Generations 2, 3, 4, and 6 TF antigen functionalized dendrimers 67

20. Graphs showing µM TF antigen functionalized dendrimer vs. percent free cells 69

21. Example image of 6 images stitched together in Microsoft Image Composite Editor 75

22. Example image of inverted color in Gimp 2.8....75

23. Example image of increased contrast in Gimp 2.8 76

24. Peaks A and B in the EPR spectrum are used to determine line broadening effects....80

25. Theoretical line broadening graphs....80

26. EPR spectra of compound **27** at increasing concentrations....82

27. Comparison of line broadening between Compound **27** and 4-amino-TEMPO 83

28. EPR spectra of dendrimers **47-52** 85

29. A/B height ratios of dendrimers **47-52** plotted in comparison with the theoretical extremes 86

30. Dendrimer **47** EPR....99

31. Dendrimer **48** EPR....99

32. Dendrimer **49** EPR....100

33. Dendrimer **50** EPR....100

34. Dendrimer **51** EPR....101

LIST OF FIGURES — CONTINUED

Figure Page

35. Dendrimer **52** EPR 101

36. Full ^{1}H NMR spectrum of compound **1** 154

37. Full ^{1}H NMR spectrum of compound **2** 155

38. Full ^{1}H NMR spectrum of compound **3** 156

39. Full ^{1}H NMR spectrum of compound **4** 157

40. Full ^{1}H NMR spectrum of compound **5** 158

41. Full ^{13}C NMR spectrum of compound **5** 159

42. Full ^{19}F NMR spectrum of compound **5** 160

43. Full ^{1}H NMR spectrum of compound **6** 161

44. Full ^{13}C NMR spectrum of compound **6** 162

45. Full ^{19}F NMR spectrum of compound **6** 163

46. Full ^{1}H NMR spectrum of compound **7** 164

47. Full ^{13}C NMR spectrum of compound **7** 165

48. Full ^{19}F NMR spectrum of compound **7** 166

49. Full ^{1}H NMR spectrum of compound **8** 167

50. Full ^{13}C NMR spectrum of compound **8** 168

51. Full ^{19}F NMR spectrum of compound **8** 169

52. Full ^{1}H NMR spectrum of compound **9** 170

53. Full ^{1}H NMR spectrum of compound **10** 171

LIST OF FIGURES — CONTINUED

Figure Page

54. Full ^{1}H NMR spectrum of compound **11** 172

55. Full ^{1}H NMR spectrum of compound **12** 173

56. Full ^{13}C NMR spectrum of compound **12** 174

57. Full ^{1}H NMR spectrum of compound **13** 175

58. Full ^{13}C NMR spectrum of compound **13** 176

59. Full ^{1}H NMR spectrum of compound **14** 177

60. Full ^{13}C NMR spectrum of compound **14** 178

61. Full ^{1}H NMR spectrum of compound **15** 179

62. Full ^{13}C NMR spectrum of compound **15** 180

63. Full ^{1}H NMR spectrum of compound **16** 181

64. Full ^{13}C NMR spectrum of compound **16** 182

65. Full ^{1}H NMR spectrum of compound **17** 183

66. Full ^{13}C NMR spectrum of compound **17** 184

67. Full ^{1}H NMR spectrum of compound **18** 185

68. Full ^{13}C NMR spectrum of compound **18** 186

69. Smoothed MALDI TOF spectrum for compound **18** 187

70. Full ^{1}H NMR spectrum of compound **19** 188

71. Full ^{13}C NMR spectrum of compound **19** 189

72. Smoothed MALDI TOF spectrum for compound **19** 190

73. Full ^{1}H NMR spectrum of compound **20** 191

LIST OF FIGURES — CONTINUED

Figure Page

74. Full ^{13}C NMR spectrum of compound **20** 192

75. Smoothed MALDI TOF spectrum for compound **20** 193

76. Full ^{1}H NMR spectrum of compound **21** 194

77. Full ^{13}C NMR spectrum of compound **21** 195

78. Smoothed MALDI TOF spectrum for compound **21** 196

79. Full ^{1}H NMR spectrum of compound **22** 197

80. Full ^{13}C NMR spectrum of compound **22** 198

81. Smoothed MALDI TOF spectrum for compound **22** 199

82. Full ^{1}H NMR spectrum of compound **23** 200

83. Full ^{13}C NMR spectrum of compound **23** 201

84. Smoothed MALDI TOF spectrum for compound **23** 202

85. Full ^{1}H NMR spectrum of compound **24** 203

86. Full ^{13}C NMR spectrum of compound **24** 204

87. Smoothed MALDI TOF spectrum for compound **24** 205

88. Full ^{1}H NMR spectrum of compound **25** 206

89. Full ^{13}C NMR spectrum of compound **25** 207

90. Smoothed MALDI TOF spectrum for compound **25** 208

91. Untreated A549 cells 211

92. 57 μM G2-TF antigen functionalized dendrimer 211

LIST OF FIGURES — CONTINUED

Figure Page

93. 114 µM G2-TF antigen functionalized dendrimer.....212

94. 171 µM G2-TF antigen functionalized dendrimer.....212

95. 228 µM G2-TF antigen functionalized dendrimer.....213

96. 33 µM G3-TF antigen functionalized dendrimer.....213

97. 66 µM G3-TF antigen functionalized dendrimer.....214

98. 99 µM G3-TF antigen functionalized dendrimer.....214

99. 132 µM G3-TF antigen functionalized dendrimer.....215

100. 12 µM G4-TF antigen functionalized dendrimer.....215

101. 24 µM G4-TF antigen functionalized dendrimer.....216

102. 36 µM G4-TF antigen functionalized dendrimer.....216

103. 48 µM G4-TF antigen functionalized dendrimer.....217

104. 4 µM G6-TF antigen functionalized dendrimer.....217

105. 8 µM G6-TF antigen functionalized dendrimer.....218

106. 12 µM G6-TF antigen functionalized dendrimer.....218

107. 16 µM G6-TF antigen functionalized dendrimer.....219

108. Full ^{1}H NMR spectrum of compound **26**.....221

109. Full ^{13}C NMR spectrum of compound **26**.....222

110. Full ^{1}H NMR spectrum of Methyl 3,5-bis-(3-(tert-butyloxycarbonylamido)propoxy)benzoate.....223

111. Full ^{13}C NMR spectrum of Methyl 3,5-bis-(3-(tert-butyloxycarbonylamido)propoxy)benzoate.....224

LIST OF FIGURES — CONTINUED

Figure Page

112. Full ^{1}H NMR spectrum of compound **28** 225

113. Full ^{13}C NMR spectrum of compound **28** 226

114. Full ^{1}H NMR spectrum of compound **29** 227

115. Full ^{13}C NMR spectrum of compound **29** 228

116. Smoothed MALDI TOF spectrum for compound **29** 229

117. Full ^{1}H NMR spectrum of compound **30** 230

118. Full ^{13}C NMR spectrum of compound **30** 231

119. Smoothed MALDI TOF spectrum for compound **30** 232

120. Full ^{1}H NMR spectrum of compound **31** 233

121. Full ^{13}C NMR spectrum of compound **31** 234

122. Smoothed MALDI TOF spectrum for compound **31** 235

123. Full ^{1}H NMR spectrum of compound **32** 236

124. Full ^{13}C NMR spectrum of compound **32** 237

125. Smoothed MALDI TOF spectrum for compound **32** 238

126. Full ^{1}H NMR spectrum of compound **33** 239

127. Full ^{13}C NMR spectrum of compound **33** 240

128. Smoothed MALDI TOF spectrum for compound **33** 241

129. Full ^{1}H NMR spectrum of compound **34** 242

130. Full ^{13}C NMR spectrum of compound **34** 243

LIST OF FIGURES — CONTINUED

Figure Page

131. Smoothed MALDI TOF spectrum for compound **34** 244

132. Full ^{1}H NMR spectrum of compound **35**.....245

133. Full ^{13}C NMR spectrum of compound **35**.....246

134. Smoothed MALDI TOF spectrum for compound **35** 247

135. Full ^{1}H NMR spectrum of compound **36**.....248

136. Full ^{13}C NMR spectrum of compound **36**.....249

137. Smoothed MALDI TOF spectrum for compound **36** 250

138. Full ^{1}H NMR spectrum of compound **37**.....251

139. Full ^{13}C NMR spectrum of compound **37**.....252

140. Smoothed MALDI TOF spectrum for compound **37** 253

141. Full ^{1}H NMR spectrum of compound **38**.....254

142. Full ^{13}C NMR spectrum of compound **38**.....255

143. Smoothed MALDI TOF spectrum for compound **38** 256

144. Full ^{1}H NMR spectrum of compound **39**.....257

145. Full ^{13}C NMR spectrum of compound **39**.....258

146. Smoothed MALDI TOF spectrum for compound **39** 259

147. Full ^{1}H NMR spectrum of compound **40**.....260

148. Full ^{13}C NMR spectrum of compound **40**.....261

149. Smoothed MALDI TOF spectrum for compound **40** 262

150. Full ^{1}H NMR spectrum of compound **41**.....263

LIST OF FIGURES — CONTINUED

Figure Page

151. Full ^{13}C NMR spectrum of compound **41** 264

152. Smoothed MALDI TOF spectrum for compound **41** 265

153. Full ^{1}H NMR spectrum of compound **42** 266

154. Full ^{13}C NMR spectrum of compound **42** 267

155. Smoothed MALDI TOF spectrum for compound **42** 268

156. Full ^{1}H NMR spectrum of compound **43** 269

157. Full ^{13}C NMR spectrum of compound **43** 270

158. Smoothed MALDI TOF spectrum for compound **43** 271

159. Full ^{1}H NMR spectrum of compound **44** 272

160. Full ^{13}C NMR spectrum of compound **44** 273

161. Smoothed MALDI TOF spectrum for compound **44** 274

162. Full ^{1}H NMR spectrum of compound **45** 275

163. Full ^{13}C NMR spectrum of compound **45** 276

164. Smoothed MALDI TOF spectrum for compound **45** 277

165. Full ^{1}H NMR spectrum of compound **46** 278

166. Full ^{13}C NMR spectrum of compound **46** 279

167. Smoothed MALDI TOF spectrum for compound **46** 280

168. Smoothed MALDI TOF spectrum for compound **47** 281

169. Smoothed MALDI TOF spectrum for compound **48** 282

LIST OF FIGURES — CONTINUED

Figure Page

170. Smoothed MALDI TOF spectrum for compound **49** 283

171. Smoothed MALDI TOF spectrum for compound **50** 284

172. Smoothed MALDI TOF spectrum for compound **51** 285

173. Smoothed MALDI TOF spectrum for compound **52** 286

LIST OF ABBREVIATIONS

Boc: tert-butoxy carbamate
BORSM: based on recovered starting material
CRD: carbohydrate recognition domain
DBU: 1,8-diazabicyclo[5.4.0]undec-7-ene
DIEA: N,N-diisopropylethylamine
DMA: dimethylacetamide
DMAP: 4-dimethylaminopyridine
DMF: dimethylformamide
DMSO: dimethyl sulfoxide
EDC: N-(3-dimethylaminopropyl)-N'-ethylcarbodiimide
EPR: electron paramagnetic resonance
EDTA: ethylenediaminetetraacetic acid
Gal: galactose
GalNAc: N-acetylgalactosamine
HOAt: 1-hydroxy-7-azabenzotriazole
MALDI: matrix-assisted laser desorption ionization
MUC1: Mucin 1
NHS: N-hydroxysuccinamide
NMR: nuclear magnetic resonance
PAMAM: polyamidoamine
PBS: phosphate buffered saline
PEG: polyethylene glycol
*p*TsOH: *p*-toluenesulfonic acid
PyAOP: (7-azabenzotriazol-1-yloxy)tripyrrolidinophosphonium hexafluorophosphate
Ser: serine
T3P: propane phosphonic acid anhydride
TEA: triethylamine
TEMPO: 2,2,6,6-tetramethyl-piperidine-1-oxyl
TF: Thomsen-Friedenreich
TFA: trifluoroacetic acid
THF: tetrahydrofuran
Thr: threonine

ABSTRACT

Polyamidoamine (PAMAM) dendrimers were functionalized with the Thomsen-Friedenreich (TF) antigen to study the multivalent effects on the galectin-3 mediated homotypic aggregation of A549 cells. TF antigen functionalized dendrimers of generations 2, 3, 4, and 6 were found to induce cellular aggregation. This is in contrast with previously observed results using lactose functionalized dendrimers, in which lactose functionalized generation 2 dendrimers were able to inhibit cellular aggregation. Additionally, TF antigen functionalized generation 6 dendrimers did not induce cellular aggregation as effectively as lactose functionalized generation 6 dendrimers. These preliminary results suggest that when compared to lactose functionalized dendrimers, the stronger galectin-3 binding affinity for TF antigen dendrimers may allow for more galectin-3 recruitment, creating aggregates with less freedom to rearrange into an optimized conformation. This suggests the reversibility of the binding event is important for effective protein interactions.

The synthesis of TF antigen was achieved using indium triflate catalyzed glycosylation reactions. The development of indium(III) as a glycosylation promoter involved the analysis of indium bromide, indium chloride, and indium triflate for use in glycosylation reactions with a variety of alcohol acceptors. $In(OTf)_3$ mediated glycosylations of acetonide protected mannosides afforded exclusively alpha products in high yields. Acetylated mannosides gave moderate yields of exclusively alpha products using $InBr_3$ and $InCl_3$. Benzylated galactosides gave moderate yields of alpha, beta product mixtures using $In(OTf)_3$, with beta products formation being favored. Indium(III) was also used to synthesize alpha-1-2-dimannoside and alpha-galactose-1-2-mannoside in high yield.

Additionally, spin labelled PAMAM dendrimers were preliminarily studied via electron paramagnetic resonance (EPR) to analyze the spatial arrangement of end groups. Dendrimers were functionalized with 2,2,6,6-tetramethylpiperidine-1-oxyl (TEMPO) covalently tethered as a dimer. At low percent loading, a strong effect arising from the dimeric spin-labeled end groups was observed. EPR spectra of dendrimers bearing a higher loading of the dimeric spin-labeled end groups indicated that the end group arrangement approached a random distribution at approximately 40 to 50 percent loading. This suggests that covalently clustered pairs of end groups are significantly different from randomly distributed end groups on PAMAM dendrimers at low loading and become equivalent to randomly functionalized dendrimers around 50% functionalization.

CHAPTER ONE

INTRODUCTION TO TF ANTIGEN, GALECTIN-3, MULTIVALENCY, AND DENDRIMERS

Background

An antigen is a compound that is specifically recognized by antibodies, usually invoking an immune response. The Thomsen-Friedenreich (TF) antigen is a known tumor-associated glycoantigen with the structure of β-Gal-1-3-α-GalNAc-Thr/Ser, as shown in figure 1.[1] The threonine or serine is embedded in a mucin protein called MUC1, a large, transmembrane protein that is heavily glycosylated on healthy epithelial cells.[2] MUC1 extends far from the cell surface relative to other proteins (figure 2) and the extensive glycosylation protects the cell surface from outside forces.[3]

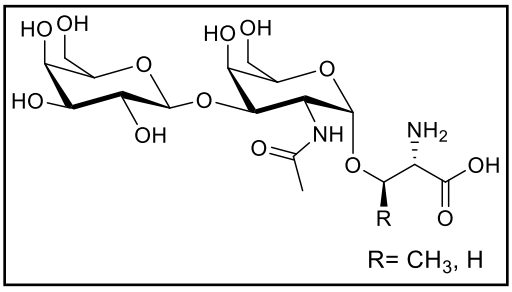


Figure 1. The structure of TF antigen.

In healthy cells, TF antigen's structure is masked under a layer of carbohydrates.[4-6] Through the loss of this carbohydrate layer (figure 3), the structure of TF antigen has been shown to be unmasked in approximately 90% of human carcinomas, becoming a cancer cell specific surface marker.[5] Once unmasked, TF antigen is the natural ligand for

galectin-3,[7] a protein that has been implicated in many processes of cancer progression including cellular adhesion,[8-12] tumor progression,[13-15] metastasis,[16-18] angiogenesis,[19] and anti-apoptosis.[14, 20]

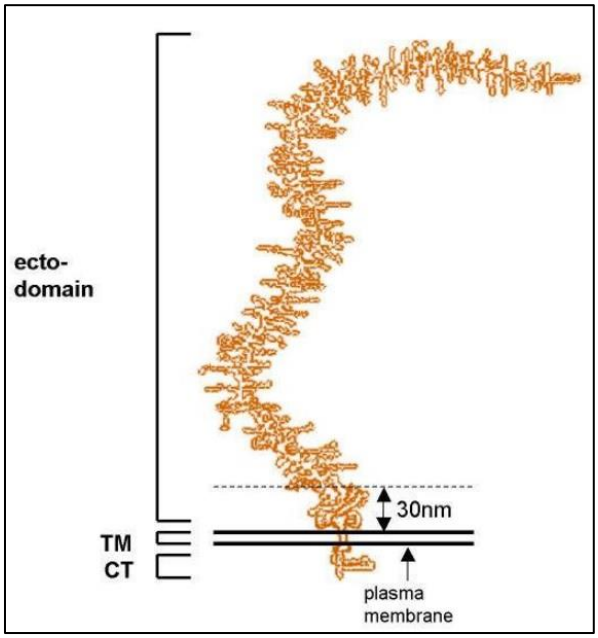


Figure 2. MUC1 protein structure. Figure shows size differences between the cytoplasmic domain (CT), the transmembrane domain (TM), and the extracellular domain. 30 nm shows the distance most proteins extend from the cellular membrane. Reprinted from Brayman *et al*[2] under CC-BY 4.0 license.

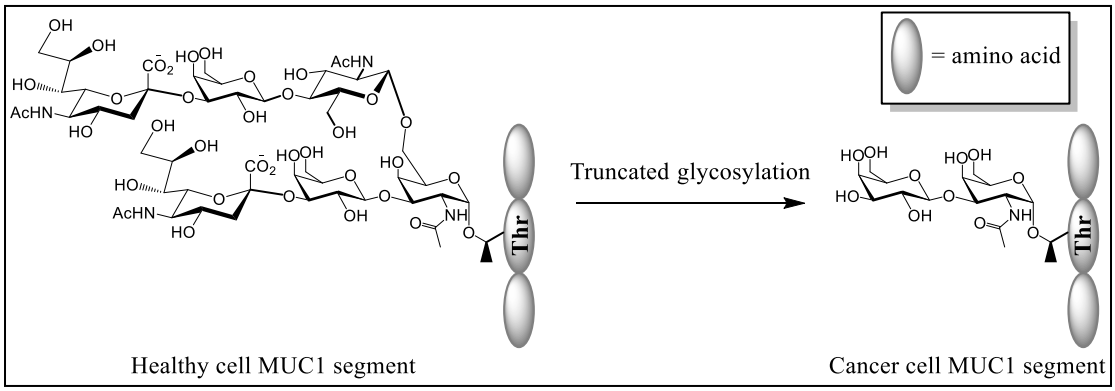


Figure 3. Demonstration of a segment of the MUC1 glycosylation on healthy cells vs cancer cells. Figure based on the model in Hang *et al.*[6]

Introduction to Galectin-3

A galectin is a protein that binds beta galactosides. There are 15 known galectins found in mammals, all containing a conserved amino acid sequence in the carbohydrate recognition domain (CRD).[21] These varying galectins have different functions depending on their location throughout the body. Galectin-3 is the most widely studied galectin, due to its many reported roles in cancer cell processes, as stated previously. Galectin-3 is the only galectin that is a chimeric protein, meaning it has two distinct regions: the conserved CRD and an N-terminal collagen like tail (figure 4A).[22] The CRD contains a curved beta sheet binding pocket that selectively binds beta galactosides, such as TF antigen, lactose, and N-acetyllactosamine.[7, 23] The protein tail is unstructured and composed of tandem repeating units rich in proline, glycine, tyrosine, and alanine.[24] The tail gives galectin-3 the ability to oligomerize through intermolecular interactions between protein tails (figure 4B).[25, 26] This oligomerization is key to the function of galectin-3 in cellular adhesion. Studies have shown that loss of protein function is observed when the N-terminal domain is removed.[27-30]

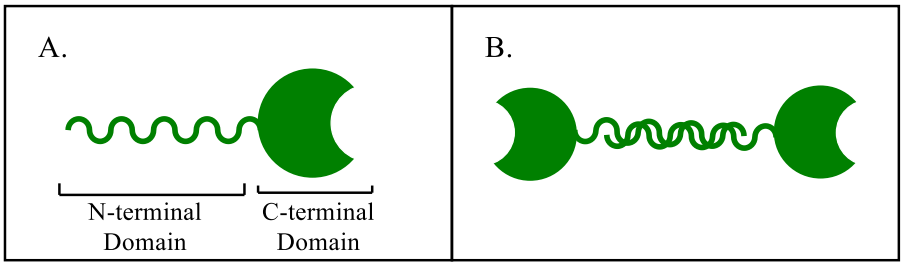


Figure 4. (A) Representation of Galectin 3 with the c-terminal carbohydrate recognition domain and the n-terminal unstructured tail, (B) representation of galectin-3 tail oligomerization.

Galectin-3 exists in low levels in healthy cells and has been shown to regulate inflammatory and immune responses,[21, 31, 32] maintain cell homeostasis,[33-35] regulate cell growth and proliferation,[36, 37] inhibit apoptosis,[36, 38] and play an important role in embryonic implantation.[39-41] These functions are obtained mainly through the regulation of cellular adhesion. Galectin-3 has been found to be overexpressed in a wide variety of cancers such as ovarian cancer,[42] colorectal carcinoma,[43] gastric cancer,[44, 45] pancreatic cancer,[46] breast cancer,[12, 47, 48] esophageal cancer, [49] melanoma,[50] thyroid cancer,[51, 52] lung cancer,[53] and liver cancer,[54, 55] with higher rates of expression generally correlating to worse patient outcomes.[18] Due to its role in so many types of cancers, the study of galectin-3 and its natural ligand, TF antigen, is of great importance.

TF Antigen and Galectin-3

Galectin-3 binds a variety of beta galactosides such as galactose, N-acetylgalactose, lactose, and N-acetyllactosamine, listed in order of increasing affinity, however its natural ligand with the strongest binding affinity is TF antigen.[7] Bian *et al*. examined the crystal structure of the CRD with several ligands, TF antigen being the most pertinent to this research. The CRD is composed of a 5 stranded anti-parallel beta sheet and a 6 stranded anti-parallel beta sheet creating a beta sandwich structure. The TF antigen is in a chair conformation and interacts with six key amino acids in the binding pocket as well as two conserved water molecules, shown in figure 6. A key aspect of the binding event is a hydrogen bonding network formed between Arg186, water molecule 1, Glu165, water molecule 2, and C4 and the oxygen in the ring of the N-acetylgalactosaminoside portion of the TF antigen, shown in figure 5 and figure 6.

This hydrogen bonding network is unique to TF antigen recognition and is not seen in galectin-3 binding with any of the other mentioned ligands.

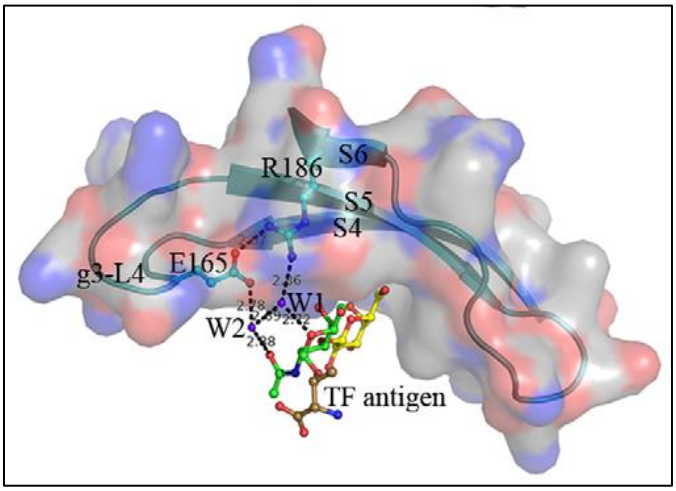


Figure 5. TF antigen in the binding pocket of galectin-3's carbohydrate recognition domain. The hydrogen bonding network is demonstrated with dotted lines and the two water molecules are labeled W1 and W2. Reprinted from Bian *et al*[7] under CC-BY 4.0 license.

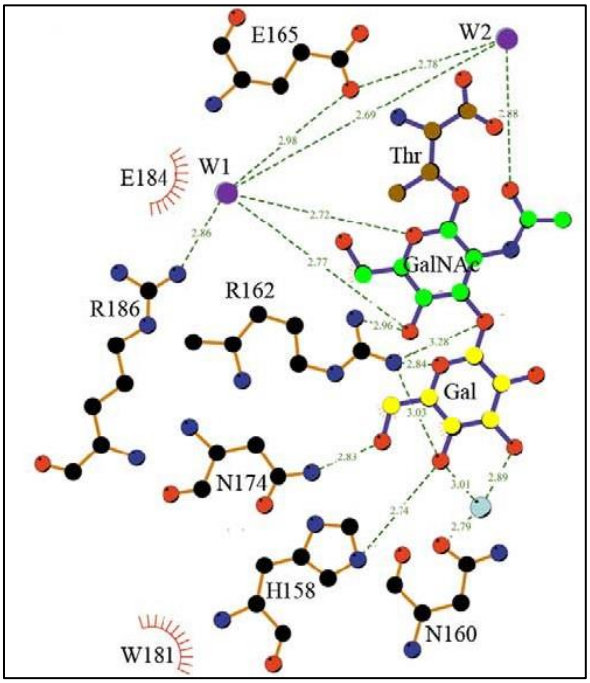


Figure 6. Hydrogen bonding interactions of TF antigen in the binding pocket of galectin-3. Reprinted from Bian *et al*[7] under CC-BY 4.0 license.

The main functions of galectin-3 in cancer are achieved through its ability to induce cellular adhesion. This cellular adhesion is achieved through its interaction with TF antigen on the cell surface. The galectin-3 CRDs interact with TF antigen on MUC1, and the N-terminal tails interact with the tails of other galectin-3 proteins creating cross linking. This clusters the MUC1 together and re-patterns the surface of the cell (figure 7).[10] When the MUC1 proteins are clustered together on the cell, shorter adhesion molecules such as E-selectin and integrins are exposed allowing the cell to adhere to other cells. This cellular adhesion will be the focus of the research in chapter 3.

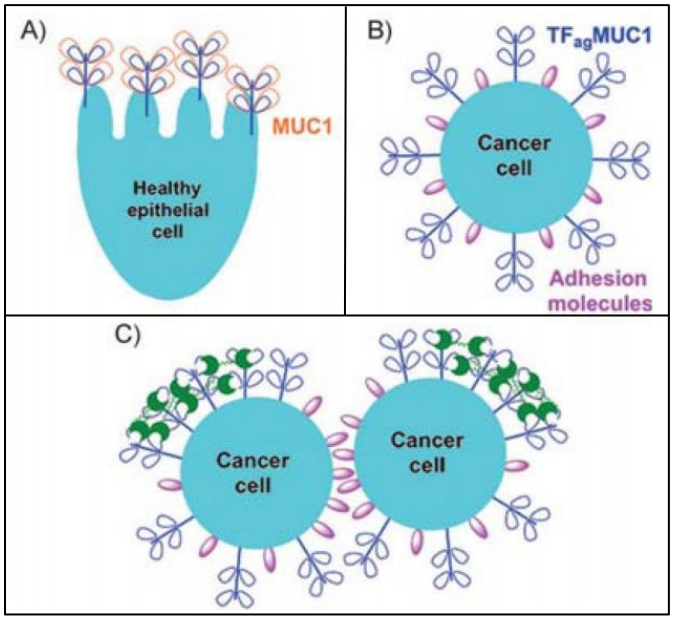


Figure 7. Galectin-3 re-patterning the surface of cancer cells. (A) a healthy epithelial cell expressing normally glycosylated MUC1 on the apical surface, (B) overly expressed and aberrantly glycosylated MUC1 spread across the entire surface on cancer cells, (C) galectin-3 (shown in green) polarizing MUC1 on the cell surface, exposing adhesion molecules (shown in purple) and inducing cellular aggregation. Reprinted with permission from Michel *et al*.[56] adapted from Yu *et al*.[10]

Multivalency

Typically, interactions between a protein and its ligand are too weak and transient to be biologically relevant. To overcome this, multivalency is frequently observed. Mutivalency is multiple ligands on one entity interacting with multiple receptors on another entity, thereby enhancing the binding affinity and increasing the length of time for the binding event.[57]

There are several different types of multivalency in nature. One example of multivalency is when the binding entity contains multiple ligands that can interact with a receptor. When one ligand is released from the receptor, another adjacent ligand can bind, increasing the local concentration of ligands around the receptor and increasing the amount of time the binding entity as a whole spends interacting with the receptor. This is known as the statistical effect (figure 8B).

A second example of multivalency is known as the chelate effect. In this example, two or more adjacent receptors interact with multiple ligands. If these ligands are all independent of each other, binding is weak. However, if these ligands are covalently linked, the binding is stronger (figure 8C). The attached ligands are entropically favorable over multiple independent ligands because the independent ligands have a greater degree of freedom.

A third example of multivalency is known as receptor clustering wherein a multivalent display of ligands interacts with multiple receptors, bringing those receptors clustered together (figure 8D). A variation of this is seen in galectin-3 re-patterning the

surface of a cancer cell. The galectin-3 oligomers interact with the TF antigen on MUC1 and cluster the MUC1 on the cell surface.

Another important aspect of multivalency is the ability of multivalent receptors to interact either with multiple ligands on a molecule or with ligands across separate molecules (figure 8E). When the multivalent receptor is able to span separate molecules linking them together, a matrix formation may occur.

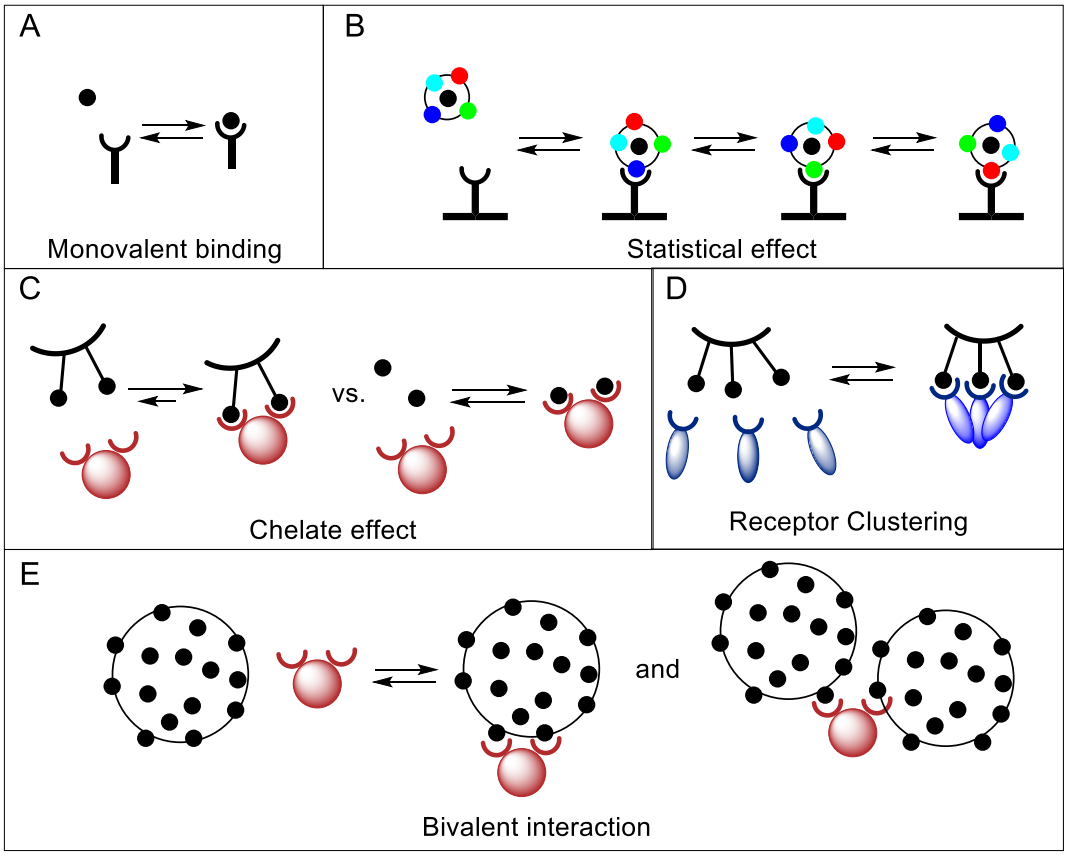


Figure 8. Schematic Representation of different types of multivalency.

Multivalent Displays of TF Antigen

Because TF antigen is a cellular surface marker that is masked on healthy cells, but is unmasked in 90% of carcinomas, it is an attractive target for anticancer research. Targeting this molecule should afford therapeutics that specifically target cancer cells while bypassing healthy cells. Additionally, because TF antigen has been demonstrated to play a key role in metastasis, the ability to block this compound could protect patients against tumor metastasis. TF antigen has also become an attractive target for cancer vaccines. Theoretically, if a vaccine were able to stimulate the immune system to recognize TF antigen, the immune system could attack cancer cells displaying TF antigen and inhibit tumor formation. There have been numerous examples exploring TF antigen as a potential vaccine.

A popular vaccine technique attaches TF antigen to a protein that is known to cause an immune response, therefore teaching the immune system to recognize and attack TF antigen. These are called carrier proteins. Zhang *et al*. attached TF antigen to keyhole limpet hemocyanin (KLH), a molluscan protein, and patients with breast cancer, ovarian cancer, and colon cancer were immunized with these compounds. A single molecule of TF antigen on the protein failed to elicit an immune response; however, a significantly stronger immune response was observed when this glycoprotein was combined with DETOX adjuvant (an additive that invokes an immune response) or when clusters of TF antigen were attached to the protein.[58-60] However, the serum from these patients with higher levels of antibodies only moderately recognized breast and colon cancer cells, and the studies showed no data supporting a correlation between the vaccine and improved

patient outcomes. This indicates the compounds were able to stimulate an immune response, but not a response specific to TF antigen.

Hoffmann-Röder *et al*. multivalently functionalized bovine serum albumin (BSA) and tetanus toxoid (TT) proteins with MUC1 mimicking protein chains, each of which were functionalized with a single TF antigen (figure 9).[61] BSA contained seven glycopeptide units and TT contained around 20 glycopeptide units. Vaccination with these glycoproteins resulted in a significant immune response in mice. Additionally, both C6 hydroxyl groups of the disaccharide were replaced with fluorine to protect the sugar from enzyme degradation. The fluorinated glycoproteins also elicited a significant immune response in mice.

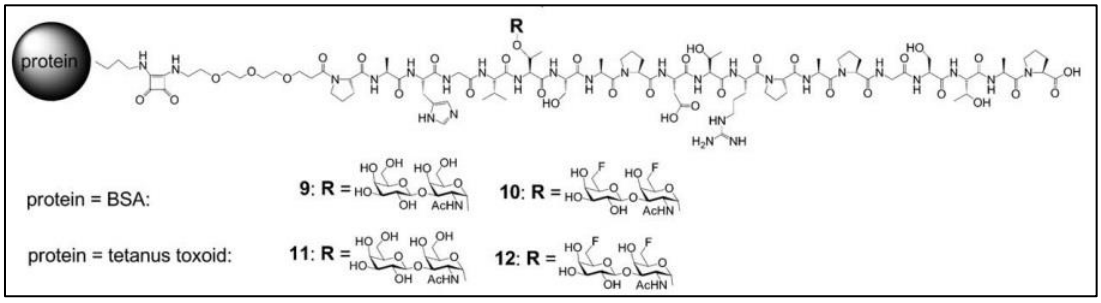


Figure 9. BSA and TT proteins functionalized with MUC1 mimicking protein chains which were glycosylated with variants of TF antigen. Reprinted with permission from Hoffmann-Röder *et al*.[61]

Ragupathi *et al*. functionalized KLH protein with heterogeneous carbohydrate clusters containing a TF antigen along with four or five other tumor related carbohydrates: Tn, STn, , Globo-H, and either Lewis^y or GM2, the structures of which are shown in figure 10.[62, 63] Each KLH protein was functionalized with 228 or 505 of the carbohydrate clusters. Mice injected with these glycoproteins had a significantly higher

immune response than those injected with only the carbohydrate cluster or the carbohydrate cluster on a Pam_3Cys conjugate. The glycoprotein induced a significant increase in antibodies specific for all the tumor related carbohydrates except Lewis^y.

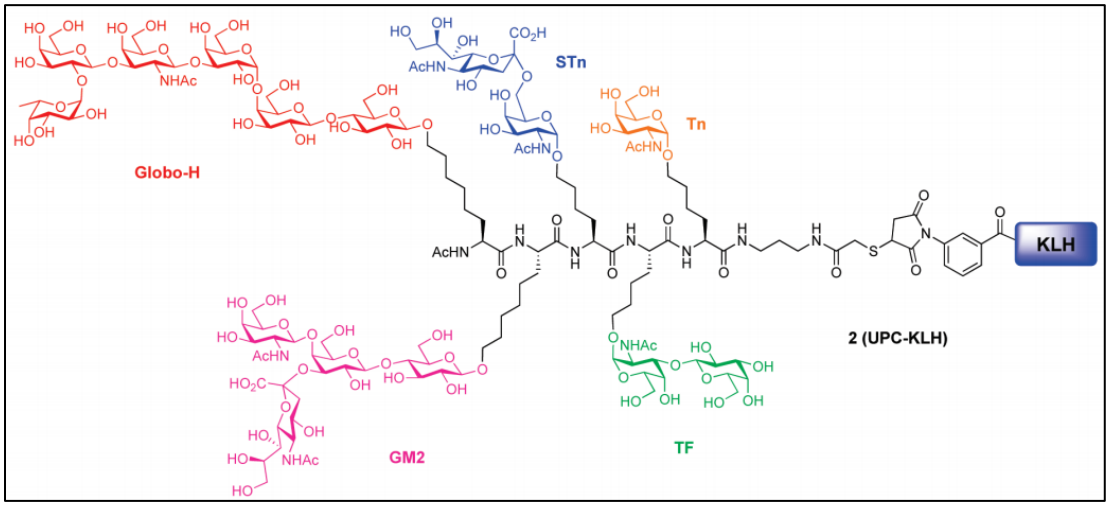


Figure 10. KLH protein functionalized with carbohydrate clusters. Reprinted with permission from Zhu *et al*.[63]

Wilkinson *et al*. created glycosylated lipopeptides using the Pam_3Cys conjugate, a compound shown to stimulate an immune response. A MUC1 peptide sequence glycosylated with TF antigen in five locations was attached to the Pam_3Cys.[64] This was also combined with a tetanus toxin t-cell epitope fragment. These TF antigen compounds were compared to similar compounds that were either Tn antigen functionalized or unglycosylated. While all compounds induced an immune response in mice, compounds with the tetanus toxin fragment gave an enhanced immune response over compounds without it and TF antigen afforded an enhanced immune response over Tn antigen. Interestingly, the unglycosylated compounds elicited a higher immune response than

those functionalized with Tn antigen, demonstrating the MUC1 peptide sequence alone is capable of inducing an immune response.

Sun *et al*. functionalized a carrier protein, CRM197, with between 4 and 11 TF antigen units or N-modified TF antigen units with increasing levels of fluorination on the N-acetyl group. These glycoproteins were used to stimulate an immune response in mice.[65] The fluorinated compounds induced a larger immune response than the unmodified TF antigen protein, and all antibodies produced recognized native TF antigen displaying cells. However, the antibodies produced by the native TF antigen protein reacted more strongly to the native TF antigen cells than the antibodies produced in higher numbers by the modified species.

Cremer *et al*. synthesized a peptide cluster containing a central core with three branches extending from the core. One branch had a MUC1 amino acid sequence with a Tn antigen carbohydrate, one branch had a MUC1 amino acid sequence with a TF antigen carbohydrate, and the third branch had a PADRE amino acid sequence which is a universal T-helper epitope.[66] This glycopeptide complex induced a strong immune response in mice, generating antibodies that specifically recognize tumor cells bearing TF antigen.

Biswas *et al*. synthesized gold nanoparticles functionalized with TF antigen conjugated by a combined alkane/PEG linker, as shown in figure 11.[67, 68] These TF antigen functionalized gold nanoparticles were between 1.5 and 3.5 nm with 20 sugars per nanoparticle for TF antigen attached by serine and 70 sugars per nanoparticle for TF antigen attached by threonine. These nanoparticles proved to be significantly more

cytotoxic to galectin-3 positive cancer cells than to galectin-3 negative cancer cells, with the threonine linked particles being 3-4 times more cytotoxic than the serine linked particles. It was also shown that the threonine linked nanoparticles activated an apoptosis pathway through interaction with galectin-3.

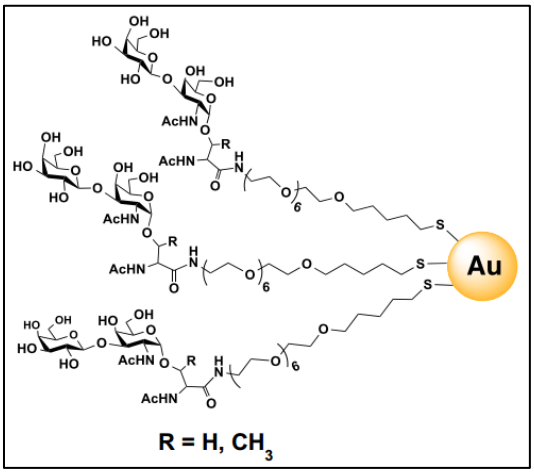


Figure 11. TF antigen functionalized gold nanoparticles. Reprinted with permission from Biswas *et al*.[67]

Briñas *et al*., from the same research group, then heterogeneously functionalized gold nanoparticles with 3 entities: a MUC4 peptide chain with TF antigen units attached, Cd3 which is a 28 residue peptide that is a B-cell activating adjuvant, and a spacer linker that helps to control the polydispersity of the gold nanoparticles formed.[69, 70] The TF antigen was placed at different locations of the MUC4 chain and in one case two TF antigen molecules were appended on MUC4. While all of the particles elicited an immune response in mice, particles displaying one TF antigen per MUC4 unit created a stronger immune response than the particle displaying two TF antigen on MUC4. The sera from the mice was shown to recognize the MUC4 sequence with the specific location of TF antigen with which it was vaccinated, as well as the MUC4 sequence

alone. This demonstrates the importance of the peptide sequence in immune response recognition as well as the ability to generate immune response specificity.

To avoid negative aspects of proteins carriers, such as protein aggregation and an unwanted immune response specific to the linker used rather than the carbohydrate, Trabbic *et al*. created a purely carbohydrate cluster composed of a polysaccharide backbone with branches displaying the disaccharide portion of TF antigen.[71] These polysaccharides are zwitterionic through carboxylic acids and amines, which was proven to be essential in producing biological activity. Mice immunized with this compound were compared to mice immunized with the polysaccharide backbone without TF antigen attached. Both sets of mice showed an increased immune response over those given PBS, however, only mice immunized with the TF antigen displaying compounds elicited antibodies selective and specific to TF antigen. These selective antibodies were then tested against human breast cancer cells (MCF-7) and human colon cancer cells (HCT-116). Increased binding was shown for the breast cancer cells, but not for the colon cancer cells, presumably due to the fact that the breast cancer cells express a higher number of TF antigen markers than the colon cancer cells.

The collective of these results sets an exciting foundation for the possibility of using multivalent displays of TF antigen in the future. These early results suggest that it is likely possible to use synthetic TF antigen systems to invoke a specific immune response that would be capable of recognizing TF antigen displaying cancer cells. However, the failure of these vaccines in human trials demonstrated that eliciting an immune response is not equivalent to affording protection from disease. Several of these

studies demonstrated the need to distinguish a general immune response from an immune response that is specific to native TF antigen displayed on the cell. Incorporating a MUC1 mimicking peptide sequence has been proven to induce this targeted immune response. At this time, a lack of successful vaccines in human trials suggests more work is needed in this area to understand the specific processes of immune recognition.

Baek *et al*. created polyamidoamine (PAMAM) dendrimers that were functionalized with the disaccharide portion of TF antigen.[72] Generations 0, 1, 2, and 3 dendrimers were used and loaded with 4, 8, 16, and 32 TF antigens units respectively. These dendrimers were used in enzyme linked immunosorbent assays (ELISAs) to demonstrate binding between TF antigen and mouse monoclonal IgG antibody. Binding strength positively correlated to increased valency, with potencies of 460, 960, 1700, and 3800 times stronger than the monovalent TF antigen for generations 0, 1, 2, and 3 respectively.[73] TF antigen functionalized dendrimers incorporating an N,N'-bis(acrylamide)acetic acid core with 2, 4, or 6 sugars showed significantly less potent binding than all the PAMAM core dendrimers, with potencies 13.3, 120.5, and 47.8 times stronger than monomeric TF antigen.[74] Although the different frameworks afforded compounds with very different potencies, these experiments demonstrate the multivalent effect on protein-carbohydrate binding that can be induced by TF antigen functionalized dendrimers.

Polyamidoamine Dendrimers

This dissertation will focus on using polyamidoamine (PAMAM) dendrimers as a multivalent framework to display TF antigen with the native amino acid linker. PAMAM

dendrimers are polymers made of repeating subunits that extend symmetrically and radially from the core. The size of the dendrimer is increased by alternating reactions of two Michael additions of acrylic acid methyl ester to a terminal primary amine followed by amidation of the methyl esters with ethylene diamine.[75] This allows control over the growth of the dendrimer size, unlike standard polymerization reactions. Each time these reactions are employed, the number of terminal primary amines doubles, and the resulting dendrimer is referred to as a new generation. This results in a framework that is highly uniform and easily controlled in size and polydispersity. Generation 0 dendrimers, abbreviated as G0, have four terminal primary amines, generation 1 dendrimers (G1) have eight, generation 2 dendrimers (G2) have sixteen, and so on, as demonstrated in figure 12.

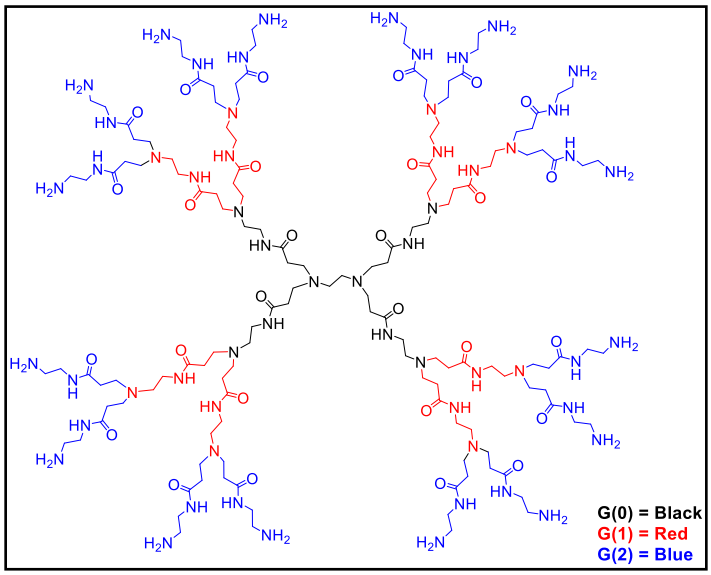


Figure 12. Generation 2 polyamidoamine dendrimer with generation 0 shown in black, generation 1 shown in red, and generation 2 shown in blue.

This polyamidoamine framework is favorable because it mimics the amide backbone of proteins and is highly flexible and dynamic. The dendrimers are able to mimic globular proteins while having higher stability to light, temperature, and pH due to the lack of a tertiary folded structure.[76] PAMAM dendrimers have also been shown to be non-immunogenic and non-toxic when the terminal amines are functionalized and neutral.[77, 78] The terminal amines can be functionalized with a wide variety of molecules to be displayed in a multivalent fashion. Dendrimers that are functionalized with carbohydrates are referred to as glycodendrimers and have been used to probe protein-carbohydrate interactions[79-84] as well as interactions between carbohydrates and cellular surfaces.[56, 85, 86]

Lactose Functionalized Dendrimers and Galectin-3

In previous work from this lab, lactose functionalized dendrimers were used to probe the galectin-3 induced cellular aggregation of three cell lines, A549 cells being pertinent to this dissertation.[56] Lactose was chosen because it is a ligand that will bind galectin-3. Although lactose has a weaker affinity for galectin-3 than that of TF antigen (220 μM K_D vs 47 μM K_D),[7, 87] the synthesis of lactose functionalized dendrimers is far less labor intensive and far less expensive than that of TF antigen functionalized dendrimers. Generations 4 and 6 lactose functionalized dendrimers induced additional cellular aggregation above what is seen for untreated cells. Adding excess galectin-3 induces additional cellular aggregation. Generation 2 lactose dendrimers were capable of inhibiting this additional aggregation, returning cells to aggregation levels seen in untreated cells. Generation 3 lactose functionalized dendrimers were capable of slightly

inhibiting aggregation but were not able to return the cells to aggregation levels of untreated cells.

The results of lactose functionalized dendrimers indicate the size of the dendrimer is important when it comes to multivalent displays interacting with galectin-3 at the cellular surface. Larger generations of dendrimers are capable of binding multiple galectin-3 lectins and creating large crosslinked networks, which were observed using dynamic light scattering and fluorescence microscopy experiments in this lab.[84] The lactose functionalized dendrimer nucleation of protein assembly increased the cancer cellular aggregation. Smaller generations of dendrimers were not capable of binding multiple galectin-3 lectins in the same way, and were therefore unable to form large crosslinked networks. It seems that smaller generation dendrimers are able to divert galectin-3 from binding cell surface MUC1, which disrupts the galectin-3 induced cellular aggregation. Although lactose has a weaker binding constant than the TF antigen displayed on the cellular surface, the multivalent display of lactose enables lactose functionalized dendrimers to bind competitively.

Summary of the Research Described Herein

This dissertation reports the synthesis of TF antigen functionalized PAMAM dendrimers for the elucidation of the role of galectin-3 in cancer progression. Key steps in the synthesis include two separate glycosylation reactions using catalytic indium triflate. The most difficult step involves a glycosylation reaction yielding an alpha linkage to threonine, when neighboring group participation of NAc on C-2 would afford beta. To circumvent this interaction, C-2 was protected with a nonparticipating azide and

the alpha linkage was achieved through the use of a more polar solvent and strong acid catalyst. This synthesis is discussed further in chapter 2.

A549 lung cancer cells, which express endogenous galectin-3,[56] are used in homotypic cancer cellular aggregation assays, discussed in chapter 3. By multivalently displaying TF antigen, the glycodendrimers are able to probe the interaction between naturally expressed TF antigen on MUC1 and galectin-3. Endogenous galectin-3 induces small amounts of cellular aggregation. The glycodendrimer's effect on cellular aggregation signals the extent to which the multivalent display of MUC1's native ligand is competing with the natural galectin-3/TF antigen interaction. These results are compared to those from the lactose dendrimers to examine any differences observed from use of a stronger ligand.

This dissertation will discuss the synthetic route taken to create TF antigen dendrimers and the subsequent study of these compounds with A549 lung cancer cells. It will also discuss progress toward the characterization of the relative locations of end groups on dendrimers (chapter 4). Finally, the development of Indium (III) as a glycosylation promoter that was further employed in the synthesis of TF antigen is discussed (chapter 5).

Hypothesis

Because lactose functionalized second and third generation dendrimers inhibited galectin-3 induced cellular aggregation while fourth and sixth generation dendrimers induced cellular aggregation, the hypothesis that guided this work is that TF antigen functionalized dendrimers will also serve as effective tools for the study and mediation of

cancer cellular aggregation processes. Because TF antigen is the natural ligand and has a stronger monovalent binding constant for galectin-3 than does lactose, similar cellular aggregation trends were expected to emerge at lower dendrimer concentrations than those required for lactose functionalized dendrimers. More definitive results using TF antigen functionalized third and fourth generation dendrimers were also anticipated, as lactose functionalized third and fourth generation dendrimers had low activity in cellular aggregation assays presumably due to the low monovalent binding constant for lactose and galectin-3.

Conclusion

In conclusion, the Thomsen-Friedenreich (TF) antigen is a base for the carbohydrate layer on the membrane bound protein MUC1. In approximately 90% of carcinomas, truncated glycosylation exposes TF antigen, making it a surface marker specific to cancer cells. TF antigen is the natural ligand for the protein galectin-3, and the interaction between the two is important for cellular adhesion, tumor progression, metastasis, angiogenesis, and anti-apoptosis in cancer. The ability to specifically target TF antigen should lead to the ability to specifically target cancer cells and block the cancer functions in which it is involved. Several attempts to use TF antigen in vaccines to stimulate the immune system against cancerous cells have shown promising preliminary results, but significant results in human trials have not yet been obtained. Additional frameworks which multivalently display TF antigen have been slow to emerge because of the challenge of obtaining sufficient quantities of TF antigen and are limited to one gold

nanoparticle example. In one interesting prior example, the TF antigen disaccharide was appended to the dendrimer without the key serine/threonine linking amino acid.

Previously, this lab has shown that lactose functionalized PAMAM dendrimers are able to alter the galectin-3 induced aggregation of cancer cells. Small generations inhibit aggregation, while large generations increase aggregation. This dissertation reports the synthesis of TF antigen functionalized PAMAM dendrimers and the study of their effects on the cellular aggregation of A549 cancer cells. The multivalent interaction between TF antigen and galectin-3 is almost certainly critical for mediation of the cellular recognition events important in cancer processes and the synthesis of TF antigen functionalized dendrimers that is reported herein broadens the available toolkit for research in this area. The TF antigen functionalized dendrimers are important tools for more fully discerning the function of galectin-3 in cancer progression.

CHAPTER TWO

THE SYNTHESIS OF TF ANTIGEN FUNCTIONALIZED DENDRIMERS

Background

The structure of TF antigen is β-Gal-1-3-α-GalNAc-Thr/Ser,[88] with the obvious synthetic route utilizing two glycosylation reactions to link the galactoside, N-acetylgalactosaminoside, and amino acid, as shown in figure 13. The C2 positions of the galactoside and N-acetylgalactosaminoside are capable of controlling the stereochemistry of the anomeric bond formed during the glycosylation. Conveniently, the C2 position of the galactose is oriented to give the desired beta linkage, when acetylated, via neighboring group participation (figure 14). However, the neighboring group participation of the N-acetyl on the C2 of the N-acetylgalactosaminoside is oriented to give the undesired beta linkage to the amino acid. Because of this, steps must be taken to avoid this interaction and to favor the formation of the desired alpha linkage.

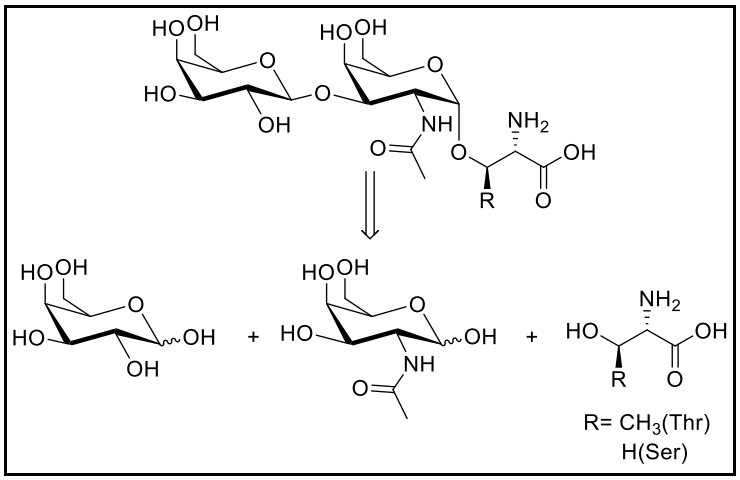


Figure 13. Retrosynthesis of TF antigen.

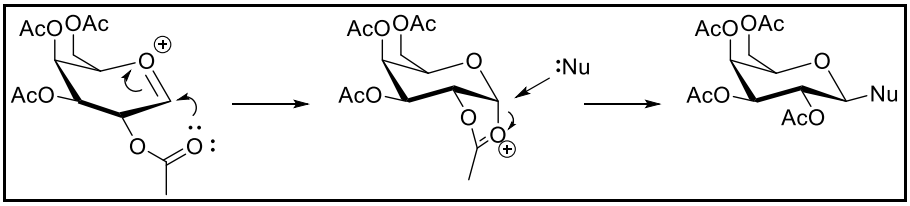


Figure 14. Example of neighboring group participation.

Previous Synthetic Routes

The synthesis of the disaccharide portion of TF antigen was first reported in 1981 through a glycosyl halide.[89] This synthesis employed a previously reported method[90] in which an azide was used at the C2 position to avoid unfavorable neighboring group participation, while a beta halide at the anomeric position was used to invert the stereochemistry during glycosylation to yield the alpha anomeric bond. The use of an azide at the C2 position to favor the alpha product has been used consistently throughout a number of synthetic routes with glycosyl halides,[91-93] selenoglycosides,[94] glycosyl nitrates,[95, 96] thioglycosides,[97, 98] and trichloroacetimidates.[68, 99] While a few of these methods rely on the inversion of anomeric stereochemistry to yield the alpha linkage, most rely on combinations of a strong promoter, more polar solvent (usually THF), and low temperatures to favor the formation of the alpha bond, with varying results as to yields and alpha selectivity. With the exception of the trichloroacetimidate, these glycoside donors are highly reactive and difficult to use. The trichloroacetimidate provides a convenient and stable intermediate that is easy to store and use.[100] There has been one example in which N-acetylgalactosamine was used directly through a C4:C6 benzylidene acetal, which was theorized to hold O4 and O6 in orientations that stabilize the anomeric effect, favoring the alpha bond formation.[101]

There have also been attempts to use enzymes to create the desired stereochemistry of TF antigen. In one notable attempt, α-N-acetylgalactosaminidase from beef liver was used to create the alpha linkage between galactosamine and threonine or serine.[102] However this work concluded that due low yields and an impure mixture of products, the purely synthetic route was superior for the formation of the alpha linkage. There have also been examples of using an enzyme to create the beta 1, 3-linkage between galactose and N-acetylgalactosamine.[102, 103] However, these gave moderate yields (around 20-30% reported in reference 102), and the preparation of the enzymes was labor intensive. Due to the relative ease of this glycosylation synthetically, it can be concluded that the synthetic route is more straightforward.

The most similar synthesis to the target of this research was reported in 2001 when the disaccharide portion of TF antigen was put on PAMAM dendrimer.[72] This work replaced the amino acid portion of TF antigen with a thioether linker, used to attach the disaccharide to generations 0, 1, 2, and 3 PAMAM dendrimers. The synthesis of the disaccharide was achieved through activation of galactosyl bromide for the beta glycosylation. The alpha glycosylation was achieved on N-acetylglucosamine through reflux with $BF_3 \bullet OEt_2$ and allyl alcohol, followed by C4 epimerization to afford alpha N-acetylgalactosyl allyl alcohol. The thiol was added to the alkene through radical initiated photoactivation to give the thioether linker that was used to attach the disaccharide to the dendrimer.

Instead of methods avoiding the troublesome orientation of the N-acetyl group at C2, there has been a method reported in which the stereochemistry of the amine on C2 is

used as a directing group in order to direct the amino acid to approach axially.[104] This is attempted by functionalizing the C2 amine with various benzylidene derivatives and using a nickel catalyst, which interacts with the lone pair on the amine and directs the amino acid to approach axially to form the alpha bond, as shown in figure 15.

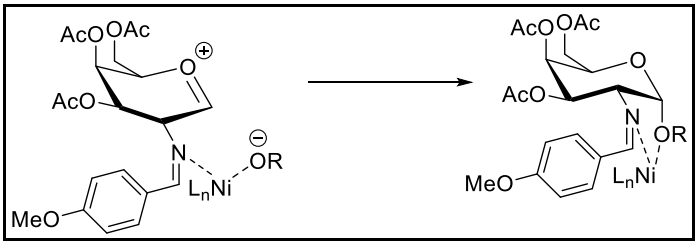
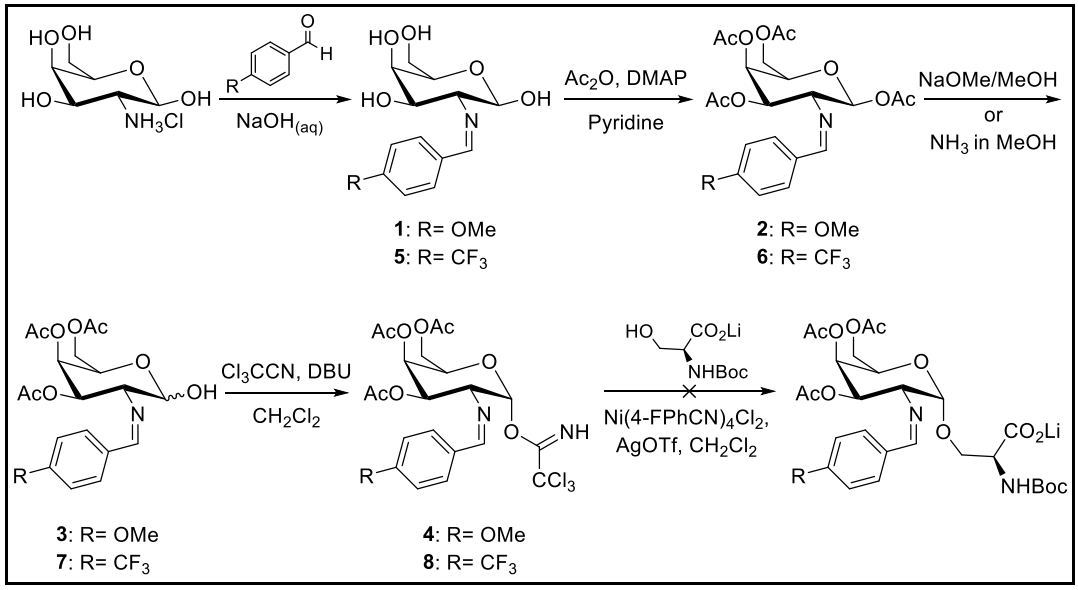


Figure 15. Proposed intermediate of nickel catalyzed glycosylation adapted from Mensah *et al*.[104]

Synthesis of TF Antigen

Due to the potential simplicity of the method described above,[104] this use of a nickel catalyst was the first synthetic route attempted, as summarized in scheme 1. The first attempt functionalized the amine with anisaldehyde in aqueous NaOH to yield **1**, followed by global acetylation with Ac_2O in pyridine and catalytic DMAP to yield **2**. The anomeric position was selectively deprotected with dilute NaOMe in MeOH to afford **3**, followed by the formation of alpha trichloroacetimidate **4** using trichloroacetonitrile and DBU. Due to the lability of the imine, these steps were highly sensitive and the products were difficult to purify. Deviations from the published procedure were required in order to obtain enough material to proceed. Upon attempting the nickel catalyzed glycosylation, insufficient product was produced to be isolated or carried forward.



Scheme 1. Synthesis of benzylidene derivatives trichloroacetimidates **4** and **8**, and attempted glycosylation.

This route was attempted once more by replacing anisaldehyde with 4-(trifluoromethyl)benzaldehyde due to promising results reported.[104] The formation of **5** and **6** were achieved by slight variations on the procedures reported above for **1** and **2**, and **7** and **8** were accomplished through slight variations on the published procedures.[104] However, when this glycosylation was attempted, again, no isolable product was produced. It is possible that this glycosylation method is highly sensitive to protecting group variations, and the deviation of serine protecting groups from those in the published procedure led to significantly lower yields. There have been additional reports of difficulty using similar chemistry.[105, 106] Due to the difficult use of these compounds and the low glycosylation yields, this synthetic route was abandoned for a more classical approach.

Due to the large amount of literature describing the successful use of an azide at C2, this approach was used here. $In(OTf)_3$ was used as a catalyst in both glycosylation

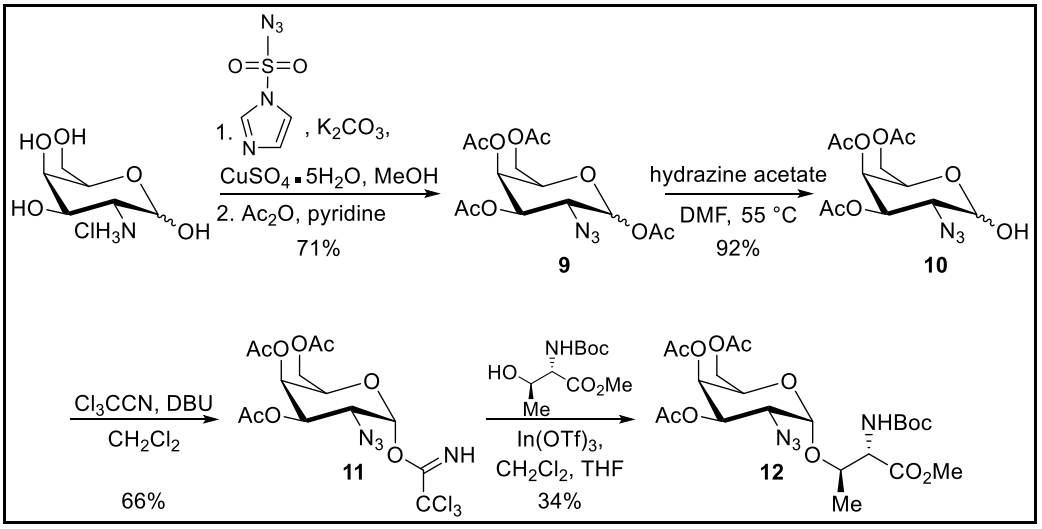
reactions for the synthesis shown in schemes 2 and 3. Indium(III) was screened in a variety of glycosylation reactions that are discussed in depth in chapter 5. Three indium(III) species were evaluated for these studies: $InCl_3$, $InBr_3$, and $In(OTf)_3$. The indium complex generally converts from the trigonal planar geometry of the trivalent species to an octahedral geometry for the hexavalent species, with some variations depending on the complexity of the ligand.[107] The ligand coordination of the indium halide species has been experimentally determined as 50% ionic,[108] with $InBr_3$ having slightly more ionic character and a lower energetic barrier for dissociation than $InCl_3$.[109, 110]

One possible mechanism for the indium promoted glycosylation involves the coordination of the glycosylation byproduct, trichloroacetamide, to the indium. There is reason to believe the trichloroacetamide can displace the halide or triflate ligands. First, the average bond lengths for indium-chloride and indium-triflate bonds are 2.53 Å[107] and 2.58 Å,[111] respectively, indicating that these are relatively weak bonds. The average length for an indium-amide bond is 2.07 Å,[107] demonstrating indium's significantly stronger affinity for amide ligands over halides or triflates. The possible involvement of an amide-coordinated indium species in the glycosylation mechanism is also supported by the known reactivity of indium(III) halides in water. Indium halide ligands are readily displaced to form $In(OH_2)_6^{3+}$ with indium-oxygen bond lengths of 2.11 Å.[107, 112] The similar bond lengths of the indium hydrate complex and indium-amide complex suggests the amide ligand could in this reaction displace the halide or triflate ligands in a similar fashion as has been observed with water.

For the glycosylation reactions in the synthesis of TF antigen, $In(OTf)_3$ was experimentally determined to be most effective. $In(OTf)_3$ was first used by the Trost group in 1997 as a ruthenium cocatalyst for the formation of diketones.[113] $In(OTf)_3$ was first reported as a lone catalyst by the Frost group in 1999 as a promoter for a hetero Diels-Alder reaction[114] and has been employed in a wide variety of reactions.[115] Further discussion on indium(III) in glycosylation reactions can be found in chapter 5.

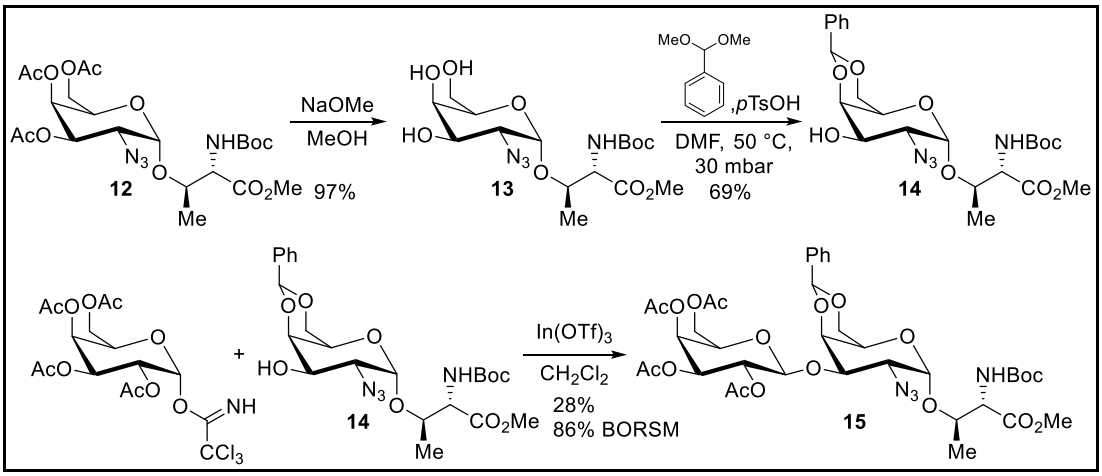
Compound **9** was made from a published procedure[116] where galactosamine was protected with an azide at C2 using imidazole-1-sulfonyl azide in the presence of K_2CO_3 and $CuSO_4 \bullet 5H_2O$, in methanol, followed by global acetylation using Ac_2O and pyridine. The anomeric position was selectively deprotected using hydrazine acetate to afford **10,** and alpha trichloroacetimidate **11** was achieved through the use of trichloroacetonitrile and DBU in CH_2Cl_2.[117]

To favor the formation of the alpha bond to threonine in the glycosylation step, a 3:1 ratio of CH_2Cl_2: THF was used, as has been previously reported.[68] However, unlike previous reports, the current synthesis used $In(OTf)_3$ as a catalyst, which gave **12** in 34% yield, a yield comparable to most other methods discussed above. No beta product was observed in this reaction. $In(OTf)_3$ is a catalyst that has not been reported for this glycosylation previously and its development is further discussed in chapter 5.



Scheme 2. Part 1 of the synthesis of TF antigen via an azide protection.

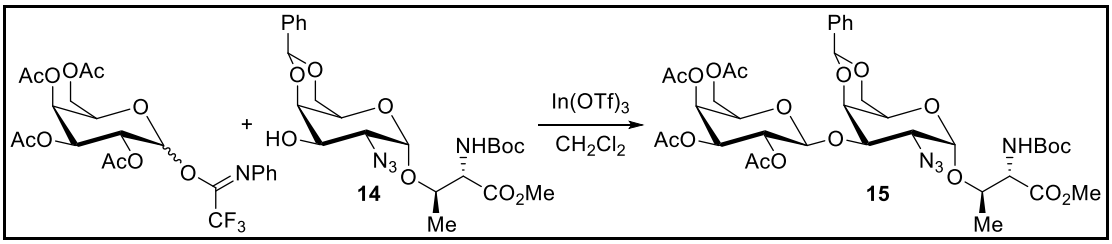
Compound **12** was deacetylated under Zemplén conditions in dry methanol (to protect the methyl ester from hydrolysis) to give **13.** The 4:6 benzylidene acetal **14** was made using benzaldehyde dimethyl acetal with trace *p*TsOH in DMF at 50 °C and under reduced pressure. This selective protection of C4 and C6 left C3 open for glycosylation.



Scheme 3. Part 2 of the synthesis of TF antigen; the formation of the disaccharide.

$In(OTf)_3$ was used again as the glycosylation catalyst to give entirely beta linked disaccharide **15** in a 28% yield with significant recovery of **14** giving an 86% BORSM

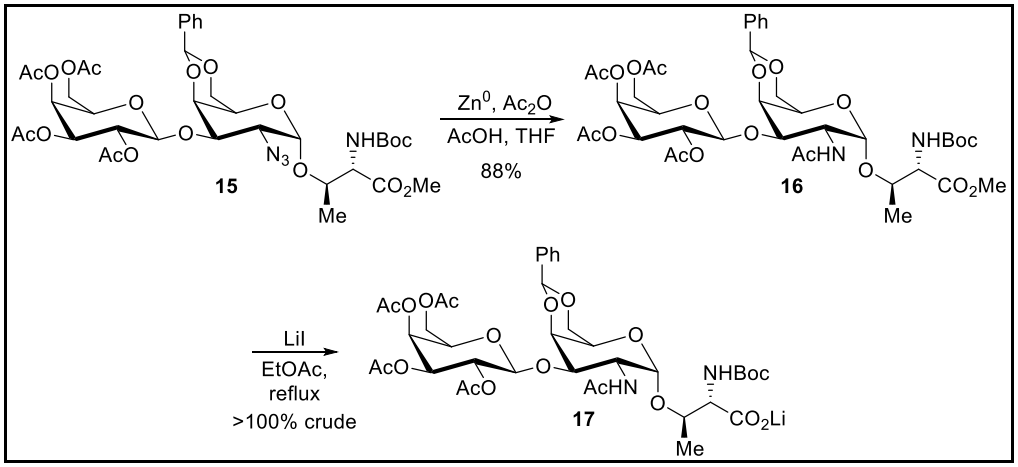
yield. Increasing the equivalents of the galactose trichloroacetimidate did not give higher yields of **15** but did decrease the amount of **14** recovered. This low yield is explained by the well documented side product of trichloroacetimidate rearrangement in which the nitrogen of the trichloroacetimidate leaving groups acts as a nucleophile attacking the anomeric position to form a trichloroacetamide.[118] This side product often forms when the glycosyl acceptor is bulky, as is **14**. To attempt to avoid this rearrangement, an N-phenyl-2,2,2-trifluoroacetimidate was tested as a glycosyl donor, as shown in scheme 4. Initial tests showed such lower yields than those of the traditional trichloroacetimidate that this route was abandoned. It is possible that further optimization of solvents, temperatures, and catalysts could lead to success with this glycosyl donor.



Scheme 4. Glycosylation attempt using N-phenyl-2,2,2-trifluoroacetimidate.

The azide of **15** was reduced to the amine and subsequently acetylated in one step using zinc dust in the presence of Ac_2O and AcOH in THF from a reported procedure[68], to give **16.** Lithium iodide was used in refluxing EtOAc to give carboxylate **17** with slight modifications from a literature procedure.[119] While this procedure gives no side reactions on the sugar itself, the lithium iodide also attacks the EtOAc and produces lithium acetate. The presence of lithium acetate was convenient as acetylation of any unfunctionalized terminal amines on the dendrimer often helps with dendrimer solubility

in water,[120, 121] as well as decreasing any cytotoxicity of the dendrimer.[122-124] This step produced a combination of **17**, lithium acetate, and excess lithium iodide that was used as a crude mixture to functionalize the PAMAM dendrimers.



Scheme 5. Part 3 of the synthesis of TF antigen- azide reduction and methyl ester deprotection.

PAMAM Dendrimer Functionalization

Generations 2, 3, 4, and 6 PAMAM dendrimers were functionalized with protected TF antigen **17** using an EDC coupling with 1-hydroxy-7-azabenzotriazole (HOAt) and collidine in DMSO. Several coupling conditions were screened to increase dendrimer loading, including EDC/NHS, T3P/pyridine (also collidine), and PyAOP/ HOAt/ DIEA. The combination of EDC and HOAt gave the most favorable loadings of 38%, 38%, 45%, and 27% for **18**, **19**, **20**, and **21** respectively, with the rest of the end groups being acetylated.

The percent loadings of the dendrimers were calculated by taking the average of the loadings calculated via ^{1}H NMR and via MALDI. Percent loadings via ^{1}H NMR were

calculated by integrating the overlapping signals of dendrimer amides at 8.23 – 7.68 ppm and comparing it to the integration of the benzylidene acetal proton on TF antigen at 5.51 ppm. The overlapping signals of the dendrimer amides consist of 28, 60, 124, and 508 protons for G2, G3, G4, and G6 respectively. By setting the multiplet equal to this known number, the integration of the TF antigen proton gives the number of TF antigen units attached to the dendrimer. The ratio of TF antigen to acetate groups on dendrimer (represented by R in the equations below) was calculated by integrating the methyl peak of the NAc at C2 on TF antigen and the methyl peak of the NAc on the dendrimer. Because both peaks are CH_3 peaks, the ratio gives the direct ratio for the end groups on dendrimer.

This sugar to acetate ratio (R) was used in calculating percent loading via MALDI. A representative molecular weight (rep. MW) was calculated by taking the molecular weight of adding one TF antigen on dendrimer (MW_{TF}) and adding the molecular weight of adding an acetate on dendrimer (MW_{Ac}) multiplied by the ratio calculated via ^{1}H NMR (R), as shown in equation 1. The molecular weight of unfunctionalized dendrimer was subtracted from the molecular weight of functionalized dendrimer giving the weight of the sum of end groups added to the dendrimer. This was divided by the calculated representative molecular weight of the end groups to give the number of TF antigen functionalizing the dendrimer, as shown in equation 2. This number was then multiplied by the acetate to TF antigen ratio to give the number of acetate groups on the dendrimer, as shown in equation 3.

Equations used to calculate loading via MALDI.

$$(\text{Rep. MW}) = (MW_{TF}) + R\times(MW_{Ac}) = 822.82 + R\times 42.05 \qquad \text{(eq. 1)}$$

$$(\#\text{ of TF antigen}) = \frac{(MW_{\text{loaded dendrimer}}) - (MW_{\text{PAMAM dendrimer}})}{(\text{Rep. MW})} \qquad \text{(eq. 2)}$$

$$(\#\text{ of Ac}) = R\times(\#\text{ of TF antigen}) \qquad \text{(eq. 3)}$$

Final loading numbers were calculated by taking the average of the number of end groups calculated via ^{1}H NMR and the number of end groups calculated via MALDI, as shown in tables 1 and 2. Final percent loading was calculated by taking the number of end groups functionalized with TF antigen and dividing by the theoretical number of end groups that can be functionalized for each dendrimer (16, 32, 64, and 256 for G2, G3, G4, and G6 respectively).

Compound	Generation	# of TF antigen via ^{1}H NMR	# of TF antigen via MALDI	Average # of TF antigen	% loading
18	2	5	7	6	38 %
19	3	12	11	12	38 %
20	4	28	30	29	45 %
21	6	59	76	68	27 %

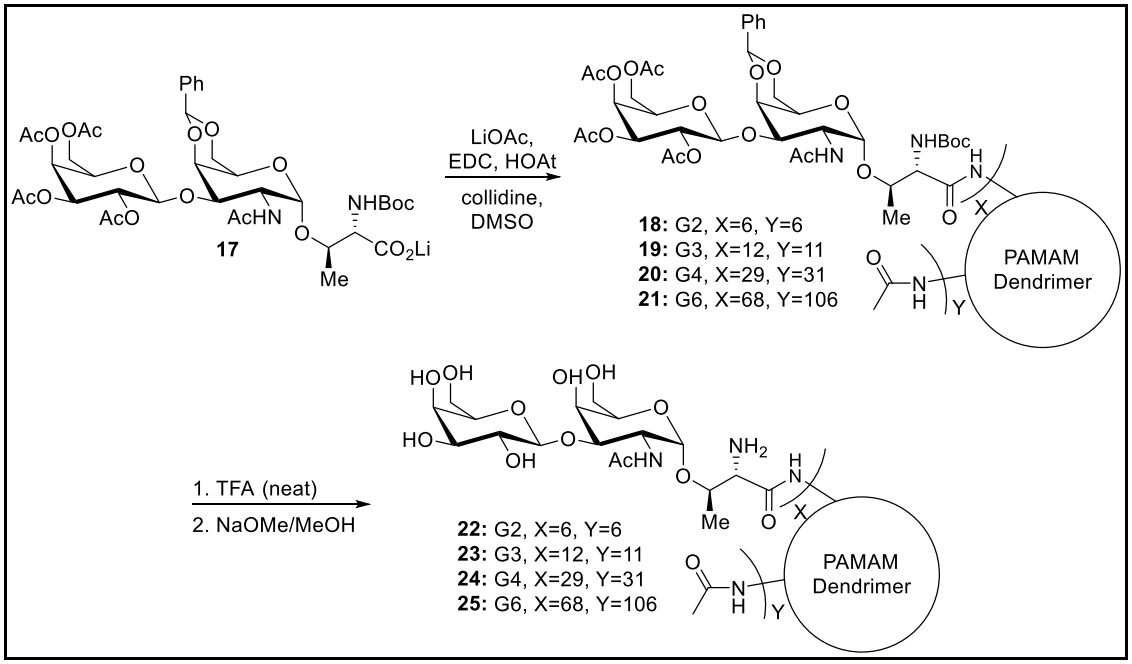
Table 1. Percent loading of **18**, **19**, **20**, and **21** with TF antigen

Compound	Generation	# of Ac via ^{1}H NMR	# of Ac via MALDI	Average # of Ac
18	2	5	7	6
19	3	11	10	11
20	4	30	32	31
21	6	119	92	106

Table 2. Acetylation of dendrimer end groups

Dendrimer loadings between 30 and 50 percent have proven favorable in some cases as these loading have roughly the same protein binding with those of higher loading,[81] and sometimes even exhibit tighter binding.[80] This is due to a balance between the number of sugars available for the binding pocket, increasing the statistical chance of binding, and too many sugars crowding the binding pocket and contributing unfavorable interactions.

The dendrimers were exposed to 2-(2-isothiocyanatoethoxy)-ethanol to check for any unfunctionalized terminal amines. Both NMR and MALDI confirmed no isothiocyanato tether had been added, suggesting all accessible terminal amines had been functionalized. The TF antigen was deprotected with neat TFA followed by Zemplén conditions to yield final products **22**, **23**, **24**, **25** as TF antigen functionalized dendrimers.



Scheme 6. The functionalization of PAMAM dendrimers with TF antigen.

Conclusion

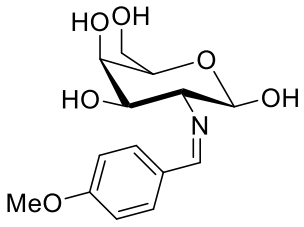
In conclusion, TF antigen was successfully synthesized using an azide at the C2 position of galactosamine. The formation of the alpha linkage was accomplished using 3:1 CH_2Cl_2: THF and $In(OTf)_3$ as a catalyst that has not been reported before for this glycosylation. $In(OTf)_3$ was successfully used again to form the beta linkage of the disaccharide. This protected TF antigen was attached to generations 2, 3, 4, and 6 PAMAM dendrimers and subsequently deprotected to produce TF antigen functionalized dendrimers for use in cellular aggregation studies discussed in chapter 3.

Experimental Procedures

General Methods

General reagents were purchased from Sigma-Aldrich and Fisher Scientific chemical companies. PAMAM dendrimers were purchased from Dendritech, inc. Dendrimer ^{13}C and ^{1}H NMR spectra included in this manuscript were recorded at Montana State University on a Bruker AVANCE III 500 MHz NMR spectrometer, equipped with a liquid nitrogen-cooled Prodigy^{TM} cryoprobe and SampleJet^{TM} automatic sample loading system. Carbohydrate ^{13}C and ^{1}H NMR spectra were recorded on a Bruker DRX 500 MHz spectrometer. Partial protons are reported in NMR data representing peak ratios due to the large number of protons in each dendrimer and the variability in the number of the functionalized end groups within a single sample. ^{1}H NMR chemical shifts are reported in ppm with the residual solvent peak as the internal standard (d_6-DMSO: δ 2.50 ppm; $CDCl_3$: δ 7.26 ppm) with the format as follows:

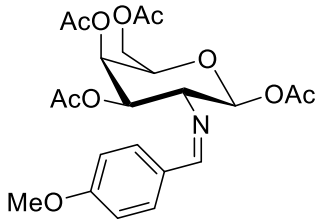
chemical shift, multiplicity (s = singlet, bs = broad singlet, d = doublet, dd = doublet of doublets, t = triplet, q = quartet, m = multiplet), coupling constants, integration, and assignment. ^{13}C NMR chemical shifts are reported in ppm with the residual solvent peak as the internal standard (DMSO: δ 39.52 ppm; $CDCl_3$: δ 77.16 ppm). Mass spectrometry data was obtained on a Bruker Autoflex III MALDI-TOF in positive linear mode with an acceleration voltage of 19 kilovolts. MALDI samples were prepared in a matrix: analyte ratio of 1000:1 or 500:1 with 3-indoleacrylic acid as the matrix and DMF as the solvent. A 1 µL aliquot of solution was used on the MALDI plate. Bovine serum albumin (MW 66,431 g/mol), trypsinogen (MW 23,981 g/mol), and myoglobin (MW 16,952 g/mol) were used as external standards. The molecular weight was calculated with a peak centroid based on a peak width of approximately 2,000 for G2 dendrimers, 5,000 for G3 and G4 dendrimers, and 10,000 for G6 dendrimers. Relevant spectra can be found in Appendix A.



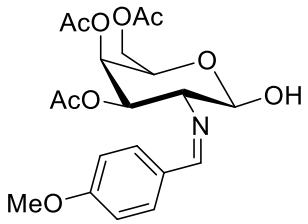
2-deoxy-2-p-methoxybenzylideneamino-β-D-galactopyranose (1).

D-galactosamine hydrochloride (2.44 g, 11.3 mmol) was dissolved in a 1.3 M aqueous NaOH solution (10.5 mL) and the flask was blanketed with argon. Anisaldehyde (2.54 mL, 20.9 mmol) was added and allowed to vigorously stir at 21 °C to form a turbid solution. Once a white precipitate had formed, the reaction was allowed to cool at 0 °C

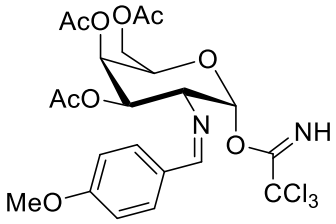
for 1 h. The solid was collected by vacuum filtration, rinsed with H_2O (2 × 20 mL) and 1:1 MeOH: Et_2O (2 × 20 mL), and concentrated *in vacuo* for 12 h to give 2.85 g (85%) of product as a light yellow solid. ^{1}H NMR (500 MHz, d_6-DMSO) δ 8.09 (s, 1H), 7.63 (d, *J* = 8.5 Hz, 2H), 6.94 (d, *J* = 8.5 Hz, 2H), 6.42 (d, *J* = 6.9 Hz, 1H), 4.62 – 4.56 (m, 2H), 4.51 (d, *J* = 6.9 Hz, 1H), 4.40 (d, *J* = 4.2 Hz, 1H), 3.76 (s, 3H), 3.62 (bs, 1H), 3.58 – 3.45 (m, 3H), 3.42 (t, *J* = 5.8 Hz, 1H), 3.05 (t, *J* = 8.6 Hz, 1H) ppm. Consistent with literature values.[125]



2-deoxy-2-p-methoxybenzylideneamino-1,3,4,6-tetra-*O*-acetyl-β-D-galactopyranose (2). Compound **1** (2.54 g, 8.54 mmol) was suspended in Ac_2O (10 mL, 106.0 mmol) and cooled to 0 °C. Pyridine (16 mL, 198.6 mmol) and DMAP (32.6 mg, 0.27 mmol) were added and the solid slowly dissolved. This was allowed to warm to 21 °C and stir for 3 h. The reaction was cooled to 0 °C, poured onto ice (120 mL), and collected by vacuum filtration. The solid was rinsed with H_2O (50 mL) and Et_2O (50 mL) and concentrated *in vacuo* to give 2.10 g (53 % yield) of product as white solid. ^{1}H NMR (500 MHz, $CDCl_3$) δ 8.18 (s, 1H), 7.64 (d, *J* = 8.5 Hz, 2H), 6.89 (d, *J* = 8.5 Hz, 2H), 5.90 (d, *J* = 8.2 Hz, 1H), 5.43 (d, *J* = 2.5 Hz, 1H), 5.22 (dd, *J* = 10.3, 3.0 Hz, 1H), 4.23 – 4.11 (m, 3H), 3.82 (s, 3H), 3.60 (t, *J* = 9.2 Hz, 1H), 2.15 (s, 3H), 2.03 (s, 3H), 2.00 (s, 3H), 1.86 (s, 3H) ppm. Consistent with literature values.[125]

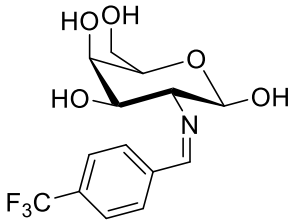


2-deoxy-2-p-methoxybenzylideneamino-3,4,6-tri-*O*-acetyl-β-D-galactopyranose (3). Compound **2** (117.0 mg, 0.25 mmol) was suspended in MeOH (10.2 mL) and vortexed until dissolved. A 0.66 M NaOMe in MeOH solution (73 µL, 0.048 mmol) was added dropwise while stirring. This was allowed to stir at 21 °C for 15 min, diluted with H_2O (10 mL) and extracted with CH_2Cl_2 (2 × 10 mL). The organic layer was dried over $MgSO_4$, filtered, and concentrated *in vacuo* to give 98.3 mg (92% yield) of crude product as a light yellow solid, which was used without further purification. ^{1}H NMR (500 MHz, $CDCl_3$) δ 8.20 (s, 1H), 7.63 (d, *J* = 8.6 Hz, 2H), 6.83 (d, *J* = 8.5 Hz, 2H), 5.36 (d, *J* = 2.2 Hz, 1H), 5.16 (dd, *J* = 10.4, 2.9 Hz, 1H), 5.06 (d, *J* = 7.7 Hz, 1H), 4.19 – 4.07 (m, 3H), 3.78 (s, 3H), 3.43 (dd, *J* = 10.0, 8.1 Hz, 1H), 2.13 (s, 3H), 2.03 (s, 3H), 1.83 (s, 3H) ppm. Consistent with literature values.[104]



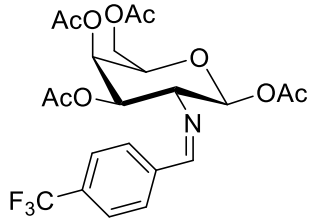
2-deoxy-2-p-methoxybenzylideneamino-3,4,6-tri-*O*-acetyl-α-D-galactopyranosyl trichloroacetimidate (4). Compound **3** (295.1 mg, 0.70 mmol) and trichloroacetonitrile (290 µL, 2.89 mmol) were dissolved in CH_2Cl_2 (2.3 mL) and cooled

to 0 °C. DBU (6.0 µL, 0.04 mmol) was added and allowed to stir at 0 °C for 3 h. The reaction was concentrated *in vacuo* and purified by flash column chromatography (6:4 Hexanes: EtOAc) to give 165.4 mg (42% yield) of product as a yellow solid. R_f = 0.16. ^{1}H NMR (500 MHz, $CDCl_3$) δ 8.59 (s, 1H), 8.25 (s, 1H), 7.60 (d, *J* = 8.6 Hz, 2H), 6.86 (d, *J* = 8.6 Hz, 2H), 5.99 (d, *J* = 8.1 Hz, 1H), 5.47 (d, *J* = 2.6 Hz, 1H), 5.33 (dd, *J* = 10.4, 3.1 Hz, 1H), 4.28 – 4.15 (m, 3H), 3.81 (s, 3H), 3.74 (dd, *J* = 10.0, 8.5 Hz, 1H), 2.17 (s, 3H), 2.04 (s, 3H), 1.89 (s, 3H) ppm. Consistent with literature values.[104]



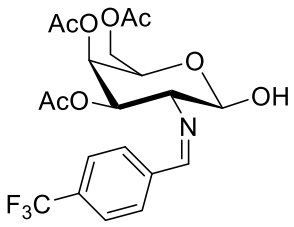
2-deoxy-2-(4-trifluoromethyl-benzylideneamino)-β-D-galactopyranose (5). D-galactosamine hydrochloride (1.07 g, 4.96 mmol) was dissolved in a 1.4 M aqueous NaOH solution (4.4 mL) and the flask was blanketed with argon. 4-(trifluoromethyl)benzaldehyde (1.25 mL, 9.19 mmol) was added and the mixture was vortexed on high for 3 min, turning the solution a cloudy white. This was cooled to 0 °C and allowed to stir for 1 h. The reaction was diluted with H_2O (30 mL), washed with $CHCl_3$ (2 × 15 mL), and extracted with EtOAc (5 × 30 mL). The combined organic layer was washed with H_2O (20 mL), dried over $MgSO_4$, and concentrated *in vacuo* to give 0.89 g (53 % yield) of crude product as a light yellow solid, which was used without further purification. ^{1}H NMR (500 MHz, d_6-DMSO) δ 8.28 (s, 1H), 7.93 (d, *J* = 8.1 Hz, 2H), 7.77 (d, *J* = 8.1 Hz, 2H), 6.51 (d, *J* = 6.8 Hz, 1H), 4.66 (t, *J* = 7.2 Hz, 1H), 4.61 (m,

2H), 4.51 (d, *J* = 4.2 Hz, 1H), 3.65 (bs, 1H), 3.61 – 3.42 (m, 4H), 3.21 – 3.13 (m, 1H) ppm; ^{13}C NMR (125 MHz, d_6-DMSO) δ 161.3, 140.3, 129.0, 126.0, 125.9, 96.4, 75.7, 75.1, 71.8, 67.5, 61.1 ppm; ^{19}F NMR (282 MHz, d_6-DMSO) δ -61.11 ppm.

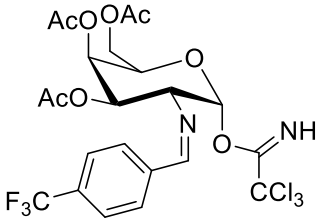


2-deoxy-2-(4-trifluoromethyl-benzylideneamino)-1,3,4,6-tetra-*O*-acetyl-β-D-galactopyranose (6). Compound **5** (129.9 mg, 0.39 mmol) was suspended in Ac_2O (450 µL, 0.48 mmol) and cooled to 0 °C. Pyridine (805 µL, 9.97 mmol) and DMAP (1.7 mg, 0.01 mmol) were added, and the mixture was allowed to stir until the solid was dissolved. The reaction was allowed to warm to 21 °C and stir for 4 h. Ice (6 mL) was added and the reaction was extracted with EtOAc (2 × 6 mL). To the organic layer, a 10% aqueous Na_2CO_3 solution (5 mL) was added and allowed to stir vigorously for 1 h. The aqueous layer was removed and the organic layer was washed with H_2O (5 mL), dried over $MgSO_4$, filtered, and concentrated *in vacuo*. The solid was purified by flash column chromatography (7:3 Hexanes: EtOAc + 4% TEA) to give 91.7 mg (47% yield) of product as a yellow solid. R_f = 0.33. ^{1}H NMR (500 MHz, $CDCl_3$) δ 8.32 (s, 1H), 7.82 (d, *J* = 8.0 Hz, 2H), 7.65 (d, *J* = 8.0 Hz, 2H), 5.94 (d, *J* = 8.2 Hz, 1H), 5.45 (d, *J* = 2.9 Hz, 1H), 5.25 (dd, *J* = 10.4, 3.2 Hz, 1H), 4.24 – 4.12 (m, 3H), 3.67 (dd, *J* = 10.1, 8.5 Hz, 1H), 2.16 (s, 3H), 2.04 (s, 3H), 2.01 (s, 3H), 1.87 (s, 3H) ppm; ^{13}C NMR (126 MHz, $CDCl_3$) δ

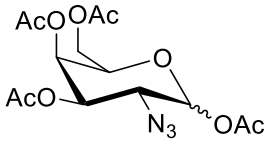
170.4, 170.1, 169.6, 168.6, 163.8, 138.3, 128.7, 125.7, 125.7, 93.2, 71.9, 71.3, 68.9, 65.8, 61.2, 20.7, 20.7 (2C), 20.5 ppm; ^{19}F NMR (282 MHz, $CDCl_3$) δ -62.90 ppm.



2-deoxy-2-(4-trifluoromethyl-benzylideneamino)-3,4,6-tri-*O*-acetyl-β-D-galactopyranose (7). Compound **6** (131.9 mg, 0.26 mmol) was dissolved in dry THF (1.3 mL) and cooled to 0 °C. A 7 N NH_3 in MeOH solution (565 µL) was added dropwise, and the reaction was allowed to warm to 21 °C and stir for 2 h. The reaction was concentrated *in vacuo* to give 120.9 mg (100% yield) of crude product mixed with starting material as a yellow solid, which was used without further purification. ^{1}H NMR (500 MHz, d_6-DMSO) δ 8.55 (s, 1H), 7.90 (d, *J* = 8.0 Hz, 2H), 7.70 (d, *J* = 8.0 Hz, 2H), 6.44 (d, *J* = 3.5 Hz, 1H), 5.60 – 5.54 (m, 2H), 4.61 (t, *J* = 6.4 Hz, 1H), 4.27 – 4.07 (m, 3H), 2.16 (s, 3H), 1.99 (s, 3H), 1.85 (s, 3H) ppm; ^{13}C NMR (126 MHz, d_6-DMSO) δ 170.7, 170.7, 170.0, 164.3, 139.1, 128.5, 125.3, 125.2, 95.6, 71.8, 71.7, 70.6, 66.3, 61.6, 19.2 (2C), 19.0 ppm; ^{19}F NMR (282 MHz, d_6-DMSO) δ -64.34 ppm.

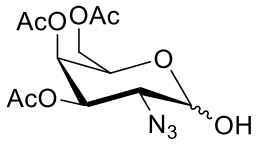


2-deoxy-2-(4-trifluoromethyl-benzylideneamino)-3,4,6-tri-*O*-acetyl-α-D-galactopyranosyl trichloroacetimidate (8). Compound **7** (120.9 mg, 0.26 mmol) was dissolved in CH_2Cl_2 (1.4 mL) and cooled to 0 °C. Trichloroacetonitrile (79.7 µL, 0.79 mmol) and DBU (20.2 µL, 0.14 mmol) were added and allowed to stir for 4 h at 0 °C. The reaction was concentrated *in vacuo* and purified by flash column chromatography (7:3 Hexanes: EtOAc + 4% TEA) to give 91.7 mg (47% yield) of product as a yellow solid. R_f = 0.33. ^{1}H NMR (500 MHz, $CDCl_3$) δ 8.55 (s, 1H), 8.40 (s, 1H), 7.79 (d, *J* = 8.0 Hz, 2H), 7.63 (d, *J* = 8.0 Hz, 2H), 6.44 (d, *J* = 3.4 Hz, 1H), 5.61 – 5.57 (m, 2H), 4.57 (t, *J* = 6.5 Hz, 1H), 4.28 – 4.01 (m, 3H), 2.17 (s, 3H), 2.02 (s, 3H), 1.88 (s, 3H) ppm; ^{13}C NMR (126 MHz, $CDCl_3$) δ 170.4, 170.1, 169.8, 163.6, 160.9, 138.6, 128.7, 125.6, 125.6, 96.1, 69.4, 68.6, 66.5, 66.3, 61.6, 20.7 (2C), 20.6 ppm; ^{19}F NMR (282 MHz, $CDCl_3$) δ -62.88 ppm.



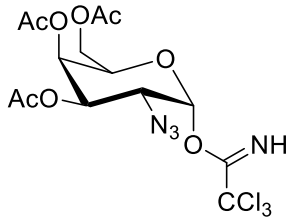
1,3,4,6-Tetra-*O*-acetyl-2-azido-2-deoxy-α,β-D-galactopyranose (9). D-galactosamine hydrochloride (5.51 g, 25.6 mmol) and K_2CO_3 (9.56 g, 69.2 mmol) were suspended in MeOH (130 mL). $CuSO_4 \cdot 5H_20$ (73.0 mg, 0.29 mmol) and imidazole-

1-sulfonyl azide hydrochloride (6.45 g, 30.8 mmol) were added to the suspension, allowed to stir at 21 °C for 3 h, and concentrated *in vacuo*. The solid was dissolved in pyridine (102 mL) and cooled to 0 °C. Ac_2O (76 mL, 804 mmol) was added and the solution was allowed to stir at 21 °C for 28.5 h. The reaction was diluted with EtOAc (500 mL) and washed with 10% aqueous HCl solution (2 × 200 mL), saturated $NaHCO_3$ solution (3 × 200 mL), and 10% aqueous Na_2CO_3 solution (2 × 200 mL). The organic layer was dried over $MgSO_4$ and concentrated *in vacuo*. The solid was purified by flash column chromatography (7:3 Hexanes: EtOAc + 2% TEA) to give 6.82 g (71% yield) of product as a yellow solid. α:β = 27:73. R_f = 0.25. ^{1}H NMR (500 MHz, $CDCl_3$) δ 6.27 (d, *J* = 3.2 Hz, 0.27H), 5.51 (d, *J* = 8.5 Hz, 0.73H), 5.43 (s, 0.27H), 5.33 (d, *J* = 2.6 Hz, 0.73H), 5.26 (dd, *J* = 11.0, 2.5 Hz, 0.27H), 4.86 (dd, *J* = 10.8, 3.1 Hz, 0.73H), 4.26-4.21 (m, 0.33H), 4.13 – 4.01 (m, 2H), 3.99-3.95 (m, 0.67H), 3.89 (dd, *J* = 11.0, 3.3 Hz, 0.27H), 3.83 – 3.75 (m, 0.73H), 2.15 (s, 2.27H), 2.12 (m, 3.73H), 2.02 (m, 3H), 1.99 (s, 3H) ppm. Consistent with literature values.[117]



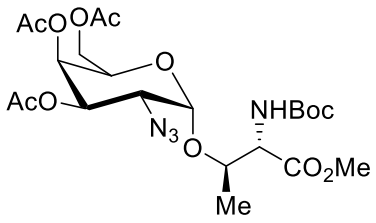
3,4,6-Tri-*O*-acetyl-2-azido-2-deoxy-α,β-D-galactopyranose (10). Hydrazine acetate (37.3 mg, 0.40 mmol) and compound **9** (114.5 mg, 0.31 mmol) were dissolved in DMF (0.32 mL) and allowed to stir at 55 °C for 30 min. The reaction was diluted with H_2O (0.8 mL) and extracted with EtOAc (0.8 mL and 0.4 mL). The combined organic layers were washed with saturated $NaHCO_3$ solution (3 × 0.4 mL) and brine

(3 × 0.4 mL), dried over $MgSO_4$, and concentrated *in vacuo* to give 93.8 mg (92% yield) of product as a yellow solid. ^{1}H NMR (500 MHz, $CDCl_3$) δ 5.41 (bs, 0.46H), 5.37 (m, 0.70H), 5.34 (d, *J* = 3.0 Hz, 0.26H), 5.29 (d, *J* = 2.5 Hz, 0.43H), 4.77 (dd, *J* = 10.9, 3.2 Hz, 0.43H), 4.66 (d, *J* = 8.0 Hz, 0.42H), 4.42 (t, *J* = 6.6 Hz, 0.7H), 4.12 – 4.01 (m, 2.30H), 3.88 (t, *J* = 6.4 Hz, 0.45H), 3.68 (dd, *J* = 11.0, 3.2 Hz, 0.50H), 3.62 (dd, *J* = 10.7, 8.1 Hz, 0.42H), 2.11 (d, *J* = 4.8 Hz, 3H), 2.03 – 1.99 (m, 6H) ppm. Consistent with literature values.[117]



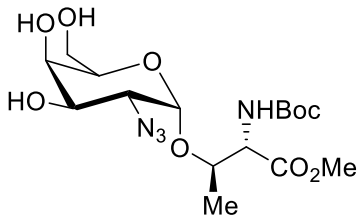
3,4,6-Tri-*O*-acetyl-2-azido-2-deoxy-α-D-galactopyranosyl trichloroacetimidate (11). DBU (0.765 mL, 5.1 mmol) and compound **10** (1.79 g, 5.4 mmol) were dissolved in dry CH_2Cl_2 (30 mL) and allowed to stir for 10 min at 0 °C. Trichloroacetonitrile (5.44 mL, 54.3 mmol) was added and allowed to stir at 0 °C for 2 h. The reaction was concentrated *in vacuo* and dissolved in 7:3 Hexanes: EtOAc + 1% TEA (30 mL) with a minimum amount of CH_2Cl_2 added to dissolve the solid. This was filtered over a silica plug with excess 7:3 hexanes: EtOAc + 1% TEA, concentrated *in vacuo,* and purified by flash column chromatography (7:3 Hexanes: EtOAc + 1% TEA) to give 1.69 g (66% yield) of product as a yellow solid. R_f = 0.29. ^{1}H NMR (500 MHz, $CDCl_3$) δ 8.77 (s, 1H), 6.48 (d, *J* = 3.4 Hz, 1H), 5.52 (d, *J* = 2.5 Hz, 1H), 5.35 (dd, *J* = 11.2, 2.5 Hz, 1H),

4.39 (t, *J* = 6.5 Hz, 1H), 4.12 (dd, *J* = 11.2, 6.5 Hz, 1H), 4.06 – 3.98 (m, 2H), 2.15 (s, 3H), 2.05 (s, 3H), 1.98 (s, 3H) ppm. Consistent with literature values.[117]

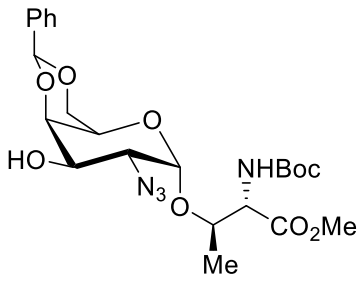


***O*-(3,4,6-tri-*O*-acetyl-2-azido-2-deoxy-α-D-galactopyranosyl)-*N*-(*tert*-butoxycarbonyl)-L-threonine methyl ester (12).** *N*-(*tert*-Butoxycarbonyl)-L-threonine methyl ester (0.99 g, 4.2 mmol) and compound **11** (1.69 g, 3.6 mmol) were dried at 50×10^{-3} mbar for 1 h. The solid was dissolved in dry 3:1 CH_2Cl_2:THF (70 mL) and allowed to stir with 3 g of 4 Å activated sieves for 30 min. $In(OTf)_3$ (0.12 g, 0.21 mmol) was added and allowed to stir for 2 h at 21 °C. Solid $NaHCO_3$ (5 g) was added and allowed to stir for 20 min. This was filtered over a neutral alumina plug with excess CH_2Cl_2, concentrated *in vacuo*, and purified by flash column chromatography (6:4 Hexanes: EtOAc) to give 0.66 g (34% yield) of product as a light yellow solid. R_f = 0.47. ^{1}H NMR (500 MHz, $CDCl_3$) δ 5.35 (d, *J* = 2.7 Hz, 1H, H-4), 5.22 (d, *J* = 9.5 Hz, 1H, N**H**Boc), 5.16 (dd, *J* = 11.1, 2.7 Hz, 1H, H-3), 4.93 (d, *J* = 3.5 Hz, 1H, H-1), 4.36-4.27 (m, 2H, CH_3C**H**, C**H**NHBoc), 4.17 (t, *J* = 6.4 Hz, 1H, H-5), 4.00 (d, *J* = 6.4 Hz, 2H, 2H-6), 3.70 (s, 3H, CO_2Me), 3.59 (dd, *J* = 11.1, 3.5 Hz, 1H, H-2), 2.06 (s, 3H, OAc), 1.97 (s, 3H, OAc), 1.96 (s, 3H, OAc), 1.40 (s, 9H, Boc), 1.24 (d, *J* = 6.3 Hz, 3H, C**H**$_3$CH) ppm; ^{13}C NMR (125 MHz, $CDCl_3$) δ 170.9, 170.3, 170.0, 169.9, 156.0, 99.5,

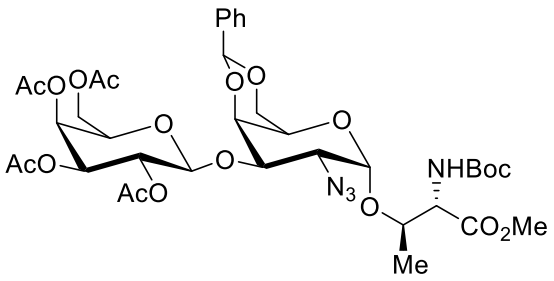
80.1, 77.5, 68.3, 67.4, 66.9, 61.7, 58.1, 57.7, 52.5, 28.2, 20.6, 20.5 (2C), 18.2 ppm; HRMS (micro-TOF) *m/z* 547.2221 (calculated *m/z* M+H = 547.2246 for $C_{22}H_{34}N_4O_{12}$).



***O*-(2-azido-2-deoxy-α-D-galactopyranosyl)-*N*-(*tert*-butoxycarbonyl)-L-threonine methyl ester (13).** Compound **12** (100.1 mg, 0.18 mmol) was dissolved in dry MeOH (7.2 mL) and a 1 M NaOMe in dry MeOH solution (120 µL) was added dropwise over 5 min. This was allowed to stir for 25 min at 21 °C. Amberlite® IR120, H resin (50 mg) was added and allowed to stir until the pH reached 7 (litmus). This was filtered and concentrated *in vacuo*. The solid was dissolved in EtOAc (4 mL), washed with H_2O (0.5 mL), dried over $MgSO_4$, filtered, and concentrated *in vacuo* to give 74.8 mg (97% yield) of product as a white solid. ^{1}H NMR (500 MHz, $CDCl_3$) δ 5.50 (d, *J* = 9.4 Hz, 1H, N**H**Boc), 4.98 (d, *J* = 3.4 Hz, 1H, H-1), 4.40 – 4.31 (m, 2H, CH_3C**H**, C**H**NHBoc), 4.12 (bs, 1H, H-4), 3.99 (dd, *J* = 10.6, 2.6 Hz, 1H, H-3), 3.91 – 3.73 (m, 6H, H-5 2H-6, 3O**H**), 3.80 (s, 3H, CO_2Me), 3.56 (dd, *J* = 10.6, 3.4 Hz, 1H, H-2), 1.47 (s, 9H, Boc), 1.28 (d, *J* = 6.2 Hz, 3H, C**H**$_3$CH) ppm; ^{13}C NMR (125 MHz, $CDCl_3$) δ 171.4, 156.2, 99.5, 80.3, 76.7, 70.2, 69.9, 68.1, 62.4, 60.6, 58.2, 52.7, 28.3, 18.4 ppm; HRMS (micro-TOF) *m/z* 443.1808 (calculated *m/z* M+Na = 443.1748 for $C_{16}H_{28}N_4O_9$).

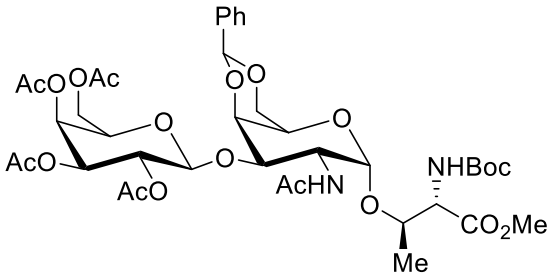


***O*-(2-azido-4:6-*O*-benzylidene-2-deoxy-α-D-galactopyranosyl)-*N*-(*tert*-butoxycarbonyl)-L-threonine methyl ester (14).** Benzaldehyde dimethyl acetal (125 µL, 0.83 mmol) and compound **13** (74.8 mg, 0.18 mmol) were dissolved in dry DMF (435 µL) and a trace amount of *p*TsOH was added. This was allowed to stir at 50 °C under reduced pressure (30 mbar) for 2 h. The reaction was diluted with EtOAc (3 mL) and washed with H_2O (0.5 mL). The organic layer was dried over $MgSO_4$, filtered, concentrated *in vacuo*, and purified by flash column chromatography (6:4 hexanes: EtOAc) to give 62.6 mg (69% yield) of product as a white solid. R_f = 0.36. ^{1}H NMR (500 MHz, $CDCl_3$) δ 7.45 (dd, *J* = 6.5, 2.9 Hz, 2H, Ph), 7.38 – 7.33 (m, 3H, Ph), 5.54 (s, 1H, Ph-C**H**), 5.37 (d, *J* = 9.4 Hz, 1H, N**H**Boc), 4.97 (d, *J* = 3.3 Hz, 1H, H-1), 4.35 (dd, *J* = 6.3, 2.0 Hz, 1H, CH_3C**H**), 4.30 (dd, *J* = 9.4, 2.0 Hz, 1H, C**H**NHBoc), 4.25 – 4.18 (m, 2H, H-4, H-6a), 4.09 – 4.01 (m, 2H, H-3, H-6b), 3.76 (s, 3H, CO_2Me), 3.74 (bs, 1H, H-5), 3.57 (dd, *J* = 10.5, 3.3 Hz, 1H, H-2), 2.57 (d, *J* = 10.6 Hz, 1H, C-3O**H**), 1.46 (s, 9H, Boc), 1.26 (d, *J* = 6.3 Hz, 3H, C**H**$_3$CH) ppm; ^{13}C NMR (125 MHz, $CDCl_3$) δ 171.0, 156.2, 137.2, 129.4, 128.3, 126.2, 101.2, 99.7, 80.1, 76.9, 75.3, 69.1, 67.4, 63.2, 61.1, 58.2, 52.6, 28.3, 18.5 ppm; HRMS (micro-TOF) *m/z* 507.2091 (calculated *m/z* M-H = 507.2086 for $C_{23}H_{32}N_4O_9$).



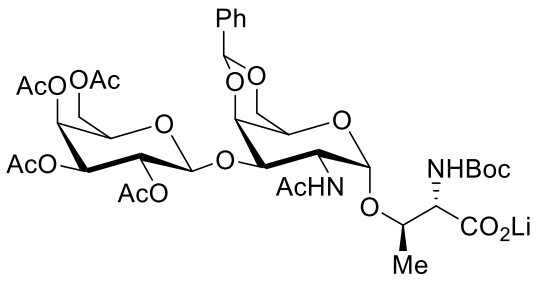
***O*-(2,3,4,6-Tetra-*O*-acetyl-β-D-galactopyranosyl-(1→3)-2-azido-4:6-*O*-benzylidene-2-deoxy-α-D-galactopyranosyl)-*N*-(*tert*-butoxycarbonyl)-L-threonine methyl ester (15).** 2,3,4,6-Tetra-*O*-acetyl-α-D-galactopyranosyl trichloroacetimidate (147.0 mg, 0.30 mmol) and compound **14** (137.9 mg, 0.27 mmol) were dried at 50×10^{-3} mbar for 1 h. The solid was dissolved in dry CH_2Cl_2 (2.9 mL). $In(OTf)_3$ (4.9 mg, 0.0087 mmol) was added and allowed to stir for 25 min at 21 °C. Solid $NaHCO_3$ (1 g) was added and allowed to stir for 20 min. This was filtered over a neutral alumina plug with excess CH_2Cl_2, concentrated *in vacuo*, and purified by flash column chromatography (1:1 Hexanes: EtOAc) to give 63.9 mg (28% yield, 86% BORSM yield) of product as a white solid. R_f = 0.30. ^{1}H NMR (500 MHz, $CDCl_3$) δ 7.52 – 7.48 (m, 2H, Ph), 7.38 - 7.32 (m, 3H, Ph), 5.52 (s, 1H, Ph-C**H**), 5.39 (d, *J* = 3.0 Hz, 1H, H-4'), 5.36 (d, *J* = 9.5 Hz, 1H, N**H**Boc), 5.27 (dd, *J* = 10.4, 7.9 Hz, 1H, H-2'), 5.04 – 4.98 (m, 2H, H-3', H-1), 4.77 (d, *J* = 7.9 Hz, 1H, H-1'), 4.39 (dd, *J* = 6.3, 2.1 Hz, 1H, CH_3C**H**), 4.35 (d, *J* = 2.9 Hz, 1H, H-4), 4.35 - 4.30 (m, 1H, C**H**NHBoc), 4.26 – 4.17 (m, 2H, H-6a, H-6a'), 4.11 (dd, *J* = 11.2, 6.7 Hz, 1H, H-6b'), 4.03 (d, *J* = 12.4 Hz, 1H, H-6b), 3.99 – 3.92 (m, 2H, H-5', H-3), 3.80 (dd, *J* = 10.8, 3.4 Hz, 1H, H-2), 3.76 (s, 3H, CO_2Me), 3.68 (bs, 1H, H-5), 2.15 (s, 3H, OAc), 2.04 (s, 3H, OAc), 2.04 (s, 3H, OAc), 1.97 (s, 3H, OAc), 1.46 (s, 9H, Boc), 1.29 (d, *J* = 6.3 Hz, 3H, C**H**$_3$CH) ppm; ^{13}C NMR (125 MHz, $CDCl_3$) δ

171.0, 170.3, 170.1, 169.4, 156.1, 137.5, 128.9, 128.1, 126.1, 102.4, 100.7, 99.6, 80.2, 76.5, 75.8, 75.7, 71.1, 70.9, 69.1, 68.7, 67.0, 63.5, 61.4, 59.2, 58.1, 58.1, 52.5, 28.3, 20.7, 20.7 (2C), 20.5, 18.7 ppm; HRMS (micro-TOF) *m/z* 861.2992 (calculated *m/z* M+Na = 861.3012 for $C_{37}H_{50}N_4O_{18}$).



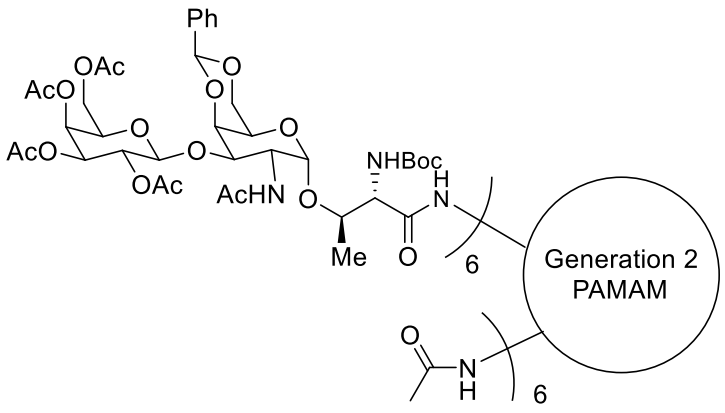
***O*-(2,3,4,6-Tetra-*O*-acetyl-β-D-galactopyranosyl-(1→3)-2-acetamido-4:6-*O*-benzylidene-2-deoxy-α-D-galactopyranosyl)-*N*-(*tert*-butoxycarbonyl)-L-threonine methyl ester (16).** Compound **15** (26.4 mg, 31.5 μmol) was dissolved in THF (525 μL), AcOH (260 μL), and Ac_2O (86.9 μL). Zn dust (0.265 g, 4.05 mmol) was added and allowed to vigorously stir for 4 h at 21 °C. The suspension was filtered over a celite plug with THF (10 mL). This was diluted with EtOAc (5 mL) and washed with saturated $NaHCO_3$ solution (3 × 5 mL) and 10% aqueous Na_2CO_3 solution (2 × 200 mL). The organic layer was dried over $MgSO_4$, filtered, concentrated *in vacuo*, and purified by flash column chromatography (EtOAc) to give 23.6 mg (88% yield) of product as a white solid. R_f = 0.48. ^{1}H NMR (500 MHz, $CDCl_3$) δ 7.52 – 7.49 (m, 2H, Ph), 7.38 – 7.28 (m, 3H, Ph), 5.66 (d, *J* = 8.8 Hz, 1H, N**H**Ac), 5.52 (s, 1H, Ph-C**H**), 5.38 (d, *J* = 3.0 Hz, 1H, H-4'), 5.22 (d, *J* = 7.9 Hz, 1H, N**H**Boc), 5.18 (dd, *J* = 10.3, 7.8 Hz, 1H, H-2'), 4.97 (dd, *J* = 10.3, 3.0 Hz, 1H, H-3'), 4.93 (d, *J* = 2.8 Hz, 1H, H-1), 4.74 (d, *J* = 7.8 Hz, 1H, H-1'),

4.61 (m, 1H, H-2), 4.32 (d, *J* = 9.4 Hz, 1H, C**H**NHBoc), 4.26 (d, *J* = 2.9 Hz, 1H, H-4), 4.24 – 4.16 (m, 3H, CH_3C**H**, H-6a, H-6a'), 4.16 – 4.10 (m, 1H, H-6b'), 4.03 (d, *J* = 12.3 Hz, 1H, H-6b), 3.92 (m, 1H, H-5'), 3.84 (d, *J* = 10.9 Hz, 1H, H-3), 3.72 (s, 3H, CO_2Me), 3.65 (bs, 1H, H-5), 2.14 (s, 3H, OAc), 2.03 (s, 6H, OAc), 2.00 (s, 3H, NH**Ac**), 1.95 (s, 3H, OAc), 1.45 (s, 9H, Boc), 1.28 (d, *J* = 6.0 Hz, 3H, C**H**$_3$CH); ^{13}C NMR (125 MHz, $CDCl_3$) δ 171.8, 170.4, 170.3, 170.2, 169.7, 169.5, 155.7, 137.6, 128.8, 128.1, 126.2, 101.0, 100.7, 100.4, 76.8, 75.5, 74.0, 71.0, 70.9, 69.1, 68.8, 67.0, 63.6, 61.4, 58.0, 52.5, 48.1, 28.3, 25.0, 23.4, 20.7 (3C), 20.6, 18.5 ppm; ; HRMS (micro-TOF) *m/z* 853.3239 (calculated *m/z* M-H = 853.3237 for $C_{39}H_{54}N_2O_{19}$).



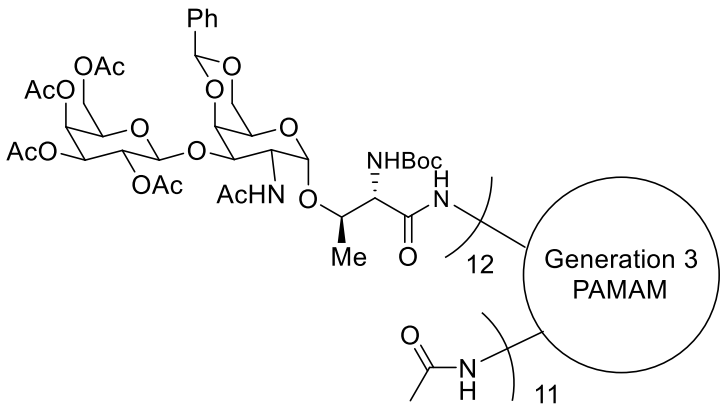
***O*-(2,3,4,6-Tetra-*O*-acetyl-β-D-galactopyranosyl-(1→3)-2-acetamido-4:6-*O*-benzylidene-2-deoxy-α-D-galactopyranosyl)-*N*-(*tert*-butoxycarbonyl)-L-threonine lithium carboxylate (17).** Compound **16** (63.5 mg, 0.074 mmol) and lithium iodide (61.4 mg, 0.46 mmol) were dissolved in dry EtOAc (740 µL), blanketed under an argon atmosphere, and allowed to stir under reflux for 20 h. The reaction was concentrated *in vacuo*, dissolved in H_2O (1 mL) and washed with $CHCl_3$ (1 mL). The organic layer was extracted with H_2O (1 mL) and the combined aqueous layers were washed with $CHCl_3$ (3 × 1 mL). The H_2O was removed *in vacuo* to give product mixed with lithium acetate

and presumably excess LiI (130.1 mg, > 100% crude yield) as a yellow solid, which was used without further purification. ^{1}H NMR (600 MHz, d_6-DMSO) δ 8.25 (d, *J* = 9.2 Hz, 1H, N**H**Ac), 7.45 – 7.30 (m, 5H, Ph), 6.02 (d, *J* = 7.4 Hz, 1H, N**H**Boc), 5.49 (s, 1H, Ph-C**H**), 5.22 (d, *J* = 3.0 Hz, 1H, H-4'), 5.03 (dd, *J* = 10.0, 3.0 Hz, 1H, H-3'), 4.90 – 4.78 (m, 3H, H-1, H-1', H-2'), 4.35 (s, 1H, H-4), 4.20 (m, 2H, H-2, H-5'), 4.08 – 3.96 (m, 5H, H-3, H-6a', H-6a, H-6b, CH_3C**H**), 3.74 (d, *J* = 12.3 Hz, 1H, C**H**NHBoc), 3.70 (s, 1H, H-6b'), 3.55 (s, 1H, H-5), 2.07 (s, 3H, OAc), 1.99 (s, 3H, OAc), 1.96 (s, 3H, OAc), 1.87 (s, 3H, OAc), 1.85 (s, 3H, NH**Ac**), 1.36 (s, 9H, Boc), 1.04 (d, *J* = 6.1 Hz, 3H, C**H**$_3$CH) ppm; ^{13}C NMR (150 MHz, d_6-DMSO) δ 172.3, 170.7, 170.4, 170.3, 170.0, 169.4, 155.5, 138.9, 129.2, 128.5, 126.6, 101.4, 100.3, 98.9, 78.3, 77.0, 75.8, 75.2, 70.9, 70.3, 69.3, 68.7, 67.8, 63.3, 62.0, 58.7, 47.7, 28.8, 23.3, 21.2, 21.1, 21.0, 20.9, 18.1 ppm; HRMS (micro-TOF) *m/z* 839.3034 (calculated *m/z* M = 839.3081 for $C_{38}H_{51}N_2O_{19}$).



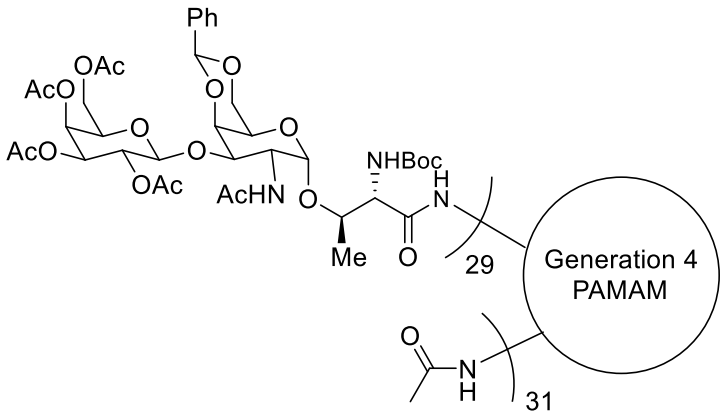
***O*-(2,3,4,6-Tetra-*O*-acetyl-β-D-galactopyranosyl-(1→3)-2-acetamido-4:6-*O*-benzylidene-2-deoxy-α-D-galactopyranosyl)-*N*-(*tert*-butoxycarbonyl)-L-threonine functionalized Generation 2 PAMAM dendrimer (18).** Generation 2 polyamidoamine

dendrimer (4.5 mg, 1.38 µmol) was combined with crude compound **17** (22.7 mg, 26.8 µmol) and lyophilized to give a yellow solid. EDC (50.9 mg, 265.5 µmol) and collidine (105 µL, 788.5 µmol) were dissolved in DMSO (840 µL) and added to the solid and allowed to stir until the solid dissolved. 1 M HOAt in DMA (265 µL) was added dropwise while stirring resulting in a bright yellow liquid. This was allowed to stir for 16 h at 21 °C. The dendrimer was purified by dialysis with 3500 Da MWCO tubing in 250 mL DMSO for 72 h, changing the DMSO every 6 h. The liquid was lyophilized to give 17.3 mg (> 100% yield) of product as a yellow solid with residual DMSO. ^{1}H NMR (600 MHz, d_6-DMSO) δ 8.16 – 7.68 (m, 1.00H), 7.47 – 7.34 (m, 1.12H), 7.27 (d, *J* = 7.1 Hz, 0.16H), 6.76 (d, *J* = 8.9 Hz, 0.14H), 5.51 (s, 0.19H), 5.29 (d, *J* = 3.3 Hz, 0.18H), 5.07 (dd, *J* = 10.4, 3.2 Hz, 0.18H), 4.92 (dd, *J* = 10.1, 8.2 Hz, 0.19H), 4.82 (d, *J* = 8.0 Hz, 0.17H), 4.76 (bs, 0.20H), 4.32 (bs, 0.24H), 4.25 – 4.11 (m, 0.73H), 4.10 – 3.98 (m, 0.85H), 3.84 (d, *J* = 11.3 Hz, 0.20H), 3.70 (bs, 0.19H), 3.08 (bs, 2.19H), 2.66 (bs, 0.92H), 2.43 (bs, 0.62H), 2.20 (bs, 1.10H), 2.11 (s, 0.56H), 2.03 (s, 0.59H), 1.99 (s, 0.63H), 1.90 (s, 0.59H), 1.87 (s, 0.55H), 1.79 (s, 0.56H), 1.44 (s, 1.70H), 1.11 (d, *J* = 5.2 Hz, 0.57H) ppm; ^{13}C NMR (150 MHz, d_6-DMSO) δ 172.2, 172.2, 172.1, 172.1, 171.7, 171.7, 170.5, 170.4, 170.4, 170.0, 169.9, 169.5, 169.3, 156.2, 138.9, 129.3, 128.5, 126.7, 101.8, 100.4, 99.9, 79.1, 75.9, 75.6, 70.9, 70.3, 69.1, 68.8, 67.8, 63.2, 61.9, 58.8, 52.6, 50.0, 47.7, 38.9, 38.8, 38.6, 37.4, 33.7, 28.7, 23.4, 23.1, 21.1, 20.9, 20.9, 20.8, 19.1 ppm; MALDI-TOF (pos) m/z = 8895.



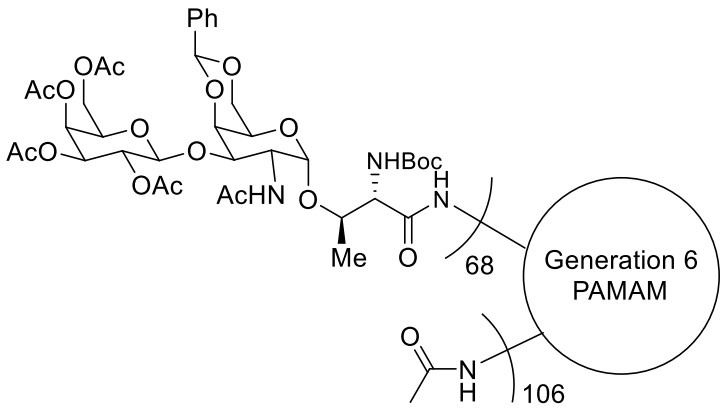
***O*-(2,3,4,6-Tetra-*O*-acetyl-β-D-galactopyranosyl-(1→3)-2-acetamido-4:6-*O*-benzylidene-2-deoxy-α-D-galactopyranosyl)-*N*-(*tert*-butoxycarbonyl)-L-threonine functionalized Generation 3 PAMAM dendrimer (19).** Generation 3 polyamidoamine dendrimer (5.7 mg, 0.83 µmol) was combined with crude compound **17** (26.8 mg, 31.7 µmol) and lyophilized to give a yellow solid. EDC (48.6 mg, 253.5 µmol) and collidine (105 µL, 788.5 µmol) were dissolved in DMSO (700 µL) and added to the solid and allowed to stir until the solid dissolved. 1 M HOAt in DMA (255 µL) was added dropwise while stirring resulting in a bright yellow liquid. This was allowed to stir for 16 h at 21 °C. The dendrimer was purified by dialysis with 3500 Da MWCO tubing in 250 mL DMSO for 72 h, changing the DMSO every 6 h. The liquid was lyophilized to give 21.0 mg (> 100% yield) of product as a yellow solid with residual DMSO. ^{1}H NMR (600 MHz, d_6-DMSO) δ 8.16 – 7.73 (m, 1.00H), 7.48 – 7.34 (m, 1.01H), 7.28 (d, *J* = 10.0 Hz, 0.09H), 6.78 (d, *J* = 9.1 Hz, 0.12H), 5.51 (s, 0.17H), 5.29 (d, *J* = 2.2 Hz, 0.20H), 5.07 (dd, *J* = 11.1, 1.7 Hz, 0.22H), 4.94 – 4.90 (m, 0.22H), 4.82 (d, *J* = 7.9 Hz, 0.18H), 4.76 (bs, 0.20H), 4.32 (bs, 0.27H), 4.25 – 4.11 (m, 0.81H), 4.11 – 3.98 (m, 0.86H), 3.84 (d, *J* = 10.8 Hz, 0.24H), 3.70 (bs, 0.27H), 3.07 (bs, 2.49H), 2.66 (bs, 1.21H), 2.43 (bs, 0.62H),

2.19 (bs, 1.06H), 2.11 (s, 0.59H), 2.04 (s, 0.55H), 1.99 (s, 0.62H), 1.90 (s, 0.59H), 1.87 (s, 0.54H), 1.79 (s, 0.55H), 1.44 (s, 1.54H), 1.11 (d, J = 4.9 Hz, 0.56H) ppm; ^{13}C NMR (150 MHz, d_6-DMSO) δ 172.1, 171.7, 170.5, 170.5, 170.4, 170.0, 169.9, 169.5, 169.3, 156.2, 138.9, 129.3, 128.5, 126.7, 101.8, 100.4, 99.9, 79.1, 75.9, 75.6, 70.9, 70.3, 69.1, 68.8, 67.8, 63.2, 61.9, 58.7, 52.6, 50.0, 47.7, 39.2, 38.9, 38.8, 38.6, 37.4, 33.7, 28.7, 28.5, 23.4, 23.1, 21.1, 20.9 (2C), 20.8, 19.2 ppm; MALDI-TOF (pos) m/z = 16220.



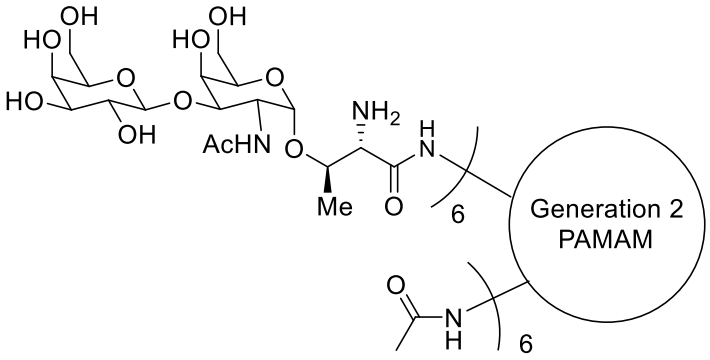
***O*-(2,3,4,6-Tetra-*O*-acetyl-β-D-galactopyranosyl-(1→3)-2-acetamido-4:6-*O*-benzylidene-2-deoxy-α-D-galactopyranosyl)-*N*-(*tert*-butoxycarbonyl)-L-threonine functionalized Generation 4 PAMAM dendrimer (20).** Generation 4 polyamidoamine dendrimer (6.1 mg, 0.45 μmol) was combined with crude compound **17** (29.4 mg, 34.7 μmol) and lyophilized to give a yellow solid. EDC (52.7 mg, 274.9 μmol) and collidine (110 μL, 826.0 μmol) were dissolved in DMSO (750 μL) and added to the solid and allowed to stir until the solid dissolved. 1 M HOAt in DMA (275 μL) was added dropwise while stirring resulting in a bright yellow liquid. This was allowed to stir for 16 h at 21 °C. The dendrimer was purified by dialysis with 3500 Da MWCO tubing in

250 mL DMSO for 72 h, changing the DMSO every 6 h. The liquid was lyophilized to give 22.2 mg (> 100% yield) of product as a yellow solid with residual DMSO. ^{1}H NMR (600 MHz, d_6-DMSO) δ 8.17 – 7.70 (m, 1.00H), 7.51 – 7.34 (m, 1.71H), 7.27 (d, *J* = 4.6 Hz, 0.09H), 6.76 (d, *J* = 8.6 Hz, 0.12H), 5.51 (s, 0.23H), 5.29 (d, *J* = 2.7 Hz, 0.24H), 5.07 (dd, *J* = 10.5, 2.6 Hz, 0.24H), 4.96 – 4.88 (m, 0.27H), 4.82 (d, *J* = 8.0 Hz, 0.23H), 4.76 (bs, 0.22H), 4.32 (bs, 0.30H), 4.26 – 4.11 (m, 1.00H), 4.11 – 3.98 (m, 1.01H), 3.84 (d, *J* = 11.1 Hz, 0.20H), 3.70 (bs, 0.21H), 3.08 (bs, 3.16H), 2.66 (bs, 1.57H), 2.43 (bs, 0.93H), 2.19 (bs, 1.72H), 2.10 (s, 0.78H), 2.03 (s, 0.82H), 1.99 (s, 0.83H), 1.90 (s, 0.79H), 1.87 (s, 0.79H), 1.79 (s, 0.73H), 1.44 (s, 2.34H), 1.11 (d, *J* = 4.2 Hz, 0.85H) ppm; ^{13}C NMR (150 MHz, d_6-DMSO) δ 172.1, 170.5, 170.4, 170.4, 170.0, 169.5, 169.3, 156.2, 138.9, 129.3, 128.5, 126.7, 101.8, 100.4, 99.9, 79.1, 75.9, 75.6, 70.9, 70.3, 69.1, 68.8, 67.8, 63.2, 61.9, 58.8, 57.5, 52.6, 50.0, 47.7, 38.8, 38.3, 37.4, 33.6, 28.7, 23.4, 23.1, 21.1, 20.9, 20.9, 20.8, 19.2 ppm; MALDI-TOF (pos) m/z = 39225.



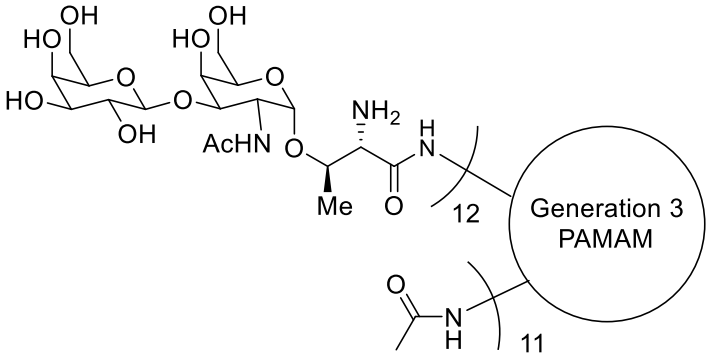
***O*-(2,3,4,6-Tetra-*O*-acetyl-β-D-galactopyranosyl-(1→3)-2-acetamido-4:6-*O*-benzylidene-2-deoxy-α-D-galactopyranosyl)-*N*-(*tert*-butoxycarbonyl)-L-threonine functionalized Generation 6 PAMAM dendrimer (21).** Generation 6 polyamidoamine dendrimer (5.4 mg, 0.11 μmol) was combined with crude compound **17** (27.8 mg, 32.8 μmol) and lyophilized to give a yellow solid. EDC (49.9 mg, 260.3 μmol) and collidine (105 μL, 788.5 μmol) were dissolved in DMSO (750 μL) and added to the solid and allowed to stir until the solid dissolved. 1 M HOAt in DMA (260 μL) was added dropwise while stirring resulting in a bright yellow liquid. This was allowed to stir for 16 h at 21 °C. The dendrimer was purified by dialysis with 3500 Da MWCO tubing in 250 mL DMSO for 72 h, changing the DMSO every 6 h. The liquid was lyophilized to give 24.1 mg (> 100% yield) of product as a yellow solid with residual DMSO. ^{1}H NMR (600 MHz, d_6-DMSO) δ 8.23 – 7.77 (m, 1.00H), 7.48 – 7.23 (m, 1.09H), 6.76 (d, *J* = 7.5 Hz, 0.09H), 5.52 (s, 0.16H), 5.28 (s, 0.15H), 5.06 (d, *J* = 10.6 Hz, 0.15H), 4.97 – 4.88 (m, 0.17H), 4.83 (d, *J* = 6.5 Hz, 0.14H), 4.75 (bs, 0.15H), 4.32 (bs, 0.16H), 4.26 – 4.11 (m, 0.58H), 4.10 – 3.97 (m, 0.70H), 3.85 (d, *J* = 9.8 Hz, 0.23H), 3.70 (bs, 0.23H), 3.08 (bs, 2.12H), 2.71 (bs, 1.23H), 2.28 (bs, 1.42H), 2.10 (s, 0.49H), 2.03 (s, 0.52H), 1.99 (s,

0.53H), 1.90 (s, 0.50H), 1.87 (s, 0.48H), 1.80 (s, 0.72H), 1.43 (s, 1.61H), 1.11 (bs, 0.52H) ppm; ^{13}C NMR (150 MHz, d_6-DMSO) δ 170.5, 170.4, 170.4, 170.0, 169.6, 169.3, 156.3, 138.9, 129.3, 128.5, 126.7, 101.7, 100.4, 99.9, 79.1, 75.6, 70.9, 70.3, 68.8, 67.8, 63.2, 61.9, 58.8, 52.5, 49.9, 47.7, 40.9, 38.9, 28.7, 23.4, 23.1, 21.1, 20.9, 20.9, 20.8, 19.2 ppm; MALDI-TOF (pos) m/z = 103355.



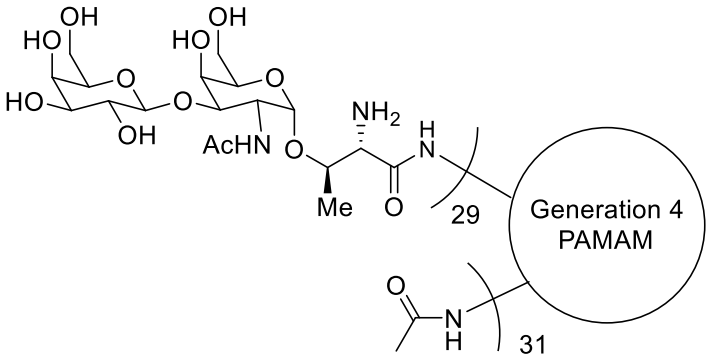
β-D-galactopyranosyl-(1→3)-2-acetamido-2-deoxy-α-D-galactopyranosyl-L-threonine functionalized Generation 2 PAMAM dendrimer (22). Compound **18** (7.7 mg, 0.87 μmol) was dissolved in neat TFA (700 μL) and was allowed to stir for 30 min at 21 °C. A 2.5 M NaOMe in dry MeOH solution (3.0 mL) was added slowly while stirring and was then added dropwise until the pH reached 9 (litmus). This was allowed to stir at 21 °C for 1 h and the dendrimer was purified by dialysis with 3500 Da MWCO tubing in 200 mL H_2O for 6 h, changing the H_2O once at 3 h, followed by 200 mL DMSO for 24 h, changing the DMSO every 8 h. The liquid was lyophilized to give 3.7 mg (65% yield) of product as a light yellow solid. ^{1}H NMR (600 MHz, d_6-DMSO) δ 8.14 – 7.69 (m, 1H), 7.49 (d, *J* = 5.0 Hz, 0.13H), 4.70 (bs, 0.14H), 4.64 (d, *J* = 2.5 Hz, 0.18H), 4.51 (bs, 0.33H), 4.30 (d, *J* = 11.8 Hz, 0.32H), 4.22 (d, *J* = 7.1 Hz,

0.17H), 4.14 – 4.05 (m, 0.26H), 3.90 (bs, 0.12H), 3.85 (bs, 0.17H), 3.62 (t, *J* = 5.4 Hz, 0.21H), 3.60 – 3.53 (m, 0.40H), 3.51 – 3.34 (m, 1.12H), 3.17 – 3.19 (m, 0.33H), 3.00 (bs, 1.92H), 2.58 (bs, 1.05H), 2.36 (bs, 0.63H), 2.12 (bs, 1.14H), 1.76 (s, 0.44H), 1.73 (s, 0.54H), 1.11 (d, *J* = 5.6 Hz, 0.53H) ppm; ^{13}C NMR (151 MHz, d_6-DMSO) δ 172.1, 171.8, 170.5, 169.9, 158.2, 158.0, 156.3, 120.9, 118.9, 116.9, 114.9, 105.0, 100.0, 99.2, 77.5, 76.2, 75.7, 73.7, 71.9, 71.1, 68.6, 68.1, 61.1, 61.0, 52.6, 50.0, 48.9, 39.0, 38.9, 38.9, 38.7, 37.3, 33.7, 23.3, 23.1, 19.1 ppm; MALDI-TOF (pos) m/z = 6540.



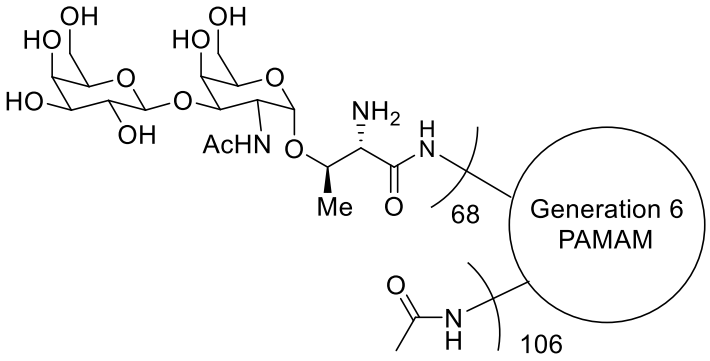
β-D-galactopyranosyl-(1→3)-2-acetamido-2-deoxy-α-D-galactopyranosyl-L-threonine functionalized Generation 3 PAMAM dendrimer (23). Compound **19** (8.2 mg, 0.51 μmol) was dissolved in neat TFA (800 μL) and was allowed to stir for 30 min at 21 °C. A 2.5 M NaOMe in dry MeOH solution (3.5 mL) was added slowly while stirring and was then added dropwise until the pH reached 9 (litmus). This was allowed to stir at 21 °C for 1 h and the dendrimer was purified by dialysis with 3500 Da MWCO tubing in 200 mL H_2O for 6 h, changing the H_2O once at 3 h, followed by 200 mL DMSO for 24 h, changing the DMSO every 8 h. The liquid was lyophilized to give 5.2 mg (86% yield) of product as a light yellow solid. ^{1}H NMR (600 MHz,

d_6-DMSO) δ 8.17 – 7.78 (m, 1H), 7.58 (d, *J* = 5.4 Hz, 0.15H), 4.78 (bs, 0.16H), 4.71 (d, *J* = 2.2 Hz, 0.14H), 4.59 (bs, 0.28H), 4.37 (d, *J* = 15.7 Hz, 0.29H), 4.29 (d, *J* = 7.3 Hz, 0.16H), 4.23 – 4.11 (m, 0.25H), 3.97 (bs, 0.14H), 3.92 (s, 0.16H), 3.74 – 3.68 (m, 0.15H), 3.67 – 3.61 (m, 0.27H), 3.57 – 3.42 (m, 0.70H), 3.24 – 3.16 (m, 0.37H), 3.08 (bs, 1.28H), 2.66 (bs, 0.82H), 2.43 (bs, 0.52H), 2.20 (bs, 0.89H), 1.84 (s, 0.25H), 1.80 (s, 0.34H), 1.17 (d, *J* = 5.9 Hz, 0.33H) ppm; ^{13}C NMR (151 MHz, d_6-DMSO) δ 172.1, 171.8, 170.6, 170.0, 158.4, 158.2, 158.0, 157.8, 120.9, 118.9, 116.9, 114.9, 105.0, 99.1, 77.5, 76.2, 75.7, 73.7, 71.9, 71.1, 68.6, 68.1, 61.1, 61.0, 59.8, 52.6, 50.0, 49.1, 49.0, 38.9, 38.8, 37.4, 33.7, 23.3, 23.1, 19.1 ppm; MALDI-TOF (pos) m/z = 8550.



β-D-galactopyranosyl-(1→3)-2-acetamido-2-deoxy-α-D-galactopyranosyl-L-threonine functionalized Generation 4 PAMAM dendrimer (24). Compound **20** (4.9 mg, 0.12 μmol) was dissolved in neat TFA (500 μL) and was allowed to stir for 30 min at 21 °C. A 2.5 M NaOMe in dry MeOH solution (2.0 mL) was added slowly while stirring and was then added dropwise until the pH reached 9 (litmus). This was allowed to stir at 21 °C for 1 h and the dendrimer was purified by dialysis with 3500 Da MWCO tubing in 200 mL H_2O for 6 h, changing the H_2O once at 3 h, followed by

200 mL DMSO for 24 h, changing the DMSO every 8 h. The liquid was lyophilized to give 2.7 mg (69% yield) of product as a yellow solid. ^{1}H NMR (500 MHz, d_6-DMSO) δ 8.18 – 7.74 (m, 1H), 7.56 (d, *J* = 5.7 Hz, 0.11H), 4.84 – 4.69 (m, 0.33H), 4.58 (bs, 0.36H), 4.37 (bs, 0.30H), 4.29 (d, *J* = 7.1 Hz, 0.20H), 4.22 – 4.12 (m, 0.32H), 4.01 – 3.90 (m, 0.35H), 3.76 – 3.60 (m, 0.62H), 3.60 – 3.43 (m, 1.06H), 3.08 (bs, 2.03H), 2.66 (bs, 1.22H), 2.43 (bs, 0.62H), 2.20 (bs, 1.32H), 1.84 (s, 0.31H), 1.80 (s, 0.50H), 1.18 (d, *J* = 5.7 Hz, 0.42H) ppm; ^{13}C NMR (126 MHz, d_6-DMSO) δ 172.1, 171.8, 170.6, 170.0, 158.5, 158.2, 158.0, 119.1, 116.7, 105.0, 99.1, 77.5, 75.8, 73.7, 71.9, 71.2, 68.6, 68.1, 61.1, 61.0, 59.8, 52.6, 50.0, 49.0, 38.9, 38.8, 37.4, 33.7, 23.3, 23.1, 19.0 ppm; MALDI-TOF (pos) m/z = 31510.



β-D-galactopyranosyl-(1→3)-2-acetamido-2-deoxy-α-D-galactopyranosyl-L-threonine functionalized Generation 6 PAMAM dendrimer (25). Compound **21** (5.0 mg, 0.048 μmol) was dissolved in neat TFA (500 μL) and was allowed to stir for 30 min at 21 °C. A 2.5 M NaOMe in dry MeOH solution (2.0 mL) was added slowly while stirring and was then added dropwise until the pH reached 9 (litmus). This was allowed to stir at 21 °C for 1 h and the dendrimer was purified by dialysis with 3500 Da

MWCO tubing in 200 mL H_2O for 6 h, changing the H_2O once at 3 h, followed by 200 mL DMSO for 24 h, changing the DMSO every 8 h. The liquid was lyophilized to give 2.3 mg (61% yield) of product as a yellow solid. ^{1}H NMR (500 MHz, d_6-DMSO) δ 8.17 – 7.73 (m, 1H), 7.57 (d, *J* = 4.8 Hz, 0.07H), 4.82 – 4.68 (m, 0.17H), 4.58 (bs, 0.19H), 4.43 – 4.25 (m, 0.28H), 4.23 – 4.11 (m, 1H), 4.00 – 3.89 (m, 0.15H), 3.70 (bs, 0.15H), 3.68 – 3.60 (m, 0.28H), 3.59 – 3.42 (m, 0.82H), 3.08 (bs, 1.98H), 2.66 (bs, 1.06H), 2.43 (bs, 0.42H), 2.20 (bs, 1.08H), 1.84 (s, 0.31H), 1.80 (s, 0.59H), 1.17 (d, *J* = 5.0 Hz, 0.37H) ppm; ^{13}C NMR (126 MHz, d_6-DMSO) δ 172.1, 171.8, 170.0, 170.0, 158.2, 158.0, 157.7, 119.1, 116.7, 104.9, 77.5, 75.8, 73.7, 71.9, 71.7, 71.2, 68.6, 68.2, 61.1, 61.0, 52.7, 50.0, 49.0, 38.9, 38.8, 37.4, 33.7, 23.3, 23.1, 19.2 ppm; MALDI-TOF (pos) m/z = 77880.

CHAPTER THREE

THE STUDY OF TF ANTIGEN FUNCTIONALIZED DENDRIMERS IN HOMOTYPIC CELLULAR AGGREGATION ASSAYS

Background

Cellular assays are a means to study cellular processes in a straightforward environment outside the body. Removing the complex *in vivo* environment allows for the isolated study of specific pathways. The preliminary *in vitro* study allows for a greater understanding of the pathway *in vivo* and sets the groundwork for further *in vivo* research. Homotypic aggregation assays allow for the study of the cellular adhesion of one cell type with itself. Aggregation assays have been used to study the effect of galectins in homotypic[56, 86, 126, 127] and heterotypic[10, 20, 126] cellular aggregation. For this dissertation, homotypic aggregation was analyzed with the human cell line, A549. This cell line is a non-small cell lung carcinoma.[128] These cells have been shown to overexpress galectin-3, which contributes to cellular aggregation.[56, 129]

Previous work from this lab demonstrated that generation 4 and 6 lactose functionalized dendrimers increased cellular aggregation.[56] The extent of cellular aggregation was determined by measuring the percent of un-aggregated (free) cells in solution, the process of which will be discussed in further detail in the experimental section of this chapter. In this previous work, between 70 and 80 percent of the untreated A549 cells in the control experiments were free cells.

In the presence of generation 6 lactose functionalized dendrimer, A549 cells demonstrated an increase in the number of aggregated cells as the concentration of the dendrimer was increased. A statistically significant difference from free cells was observed at 6 μM of dendrimer with about 60% free cells and 12 μM of dendrimer with about 30% free cells (figure 16B), demonstrating significant aggregation caused by relatively small amounts of dendrimer. Generation 4 dendrimers increased aggregation slightly at 8 μM to about 60% free cells, but additional dendrimer did not produce an increase in aggregation (figure 16A). This suggests generation 6 lactose dendrimers are able to bind multiple galectin-3 and form large crosslinking networks that increase cellular aggregation, as illustrated in figure 18D. Generation 4 dendrimers are smaller than generation 6 dendrimers (45 Å vs 67 Å) and while generation 4 dendrimers can still crosslink and increase aggregation, they are not able to do so to the extent of generation 6. Generation 2 and 3 lactose functionalized dendrimers were shown to have no significant effect on the aggregation of native A549 cells (figures 17A and 17B), demonstrating that they are not large enough to bind multiple galectin-3 lectins and create large crosslinked galectin-3/glycodendrimer networks.

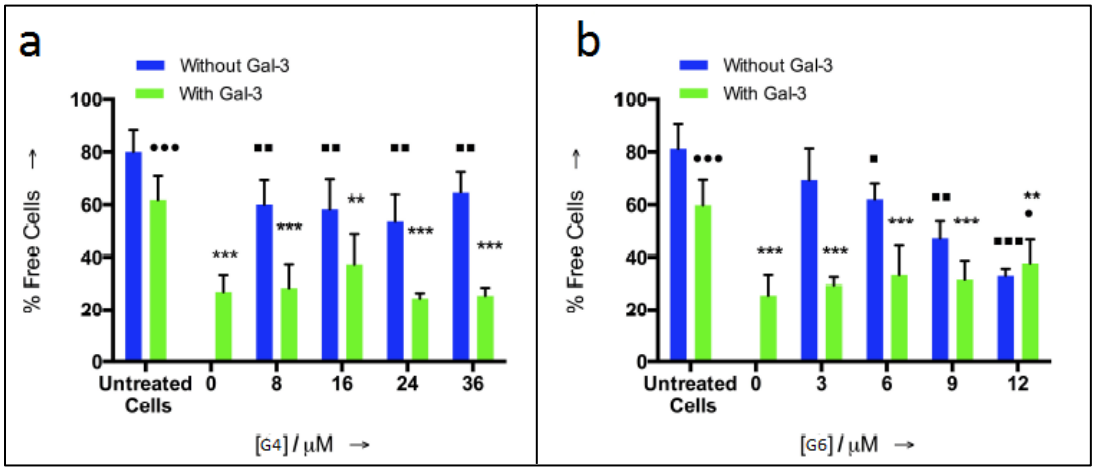


Figure 16. The effect of lactose functionalized dendrimers on A549 cells with and without added galectin-3. (A) Generation 4 dendrimer, (B) Generation 6 dendrimer. Statistical significance is shown: with respect to untreated cells (squares), with respect to the galecin-3 standard (circles), and with respect to untreated cells in the galectin standard experiment (stars). *P < 0.05, **P < 0.01, ***P < 0.001. Figure reprinted with permission from Michel *et al*.[56]

When extra galectin-3 was added to the cells, an increase in aggregation was observed, reducing the free cells to about 25% of the sample. Generation 2 lactose functionalized dendrimers were demonstrated to inhibit galectin-3 induced aggregation at 60 μM to about 55% free cells and maintained this level at increasing concentrations (figure 17A). Generation 3 dendrimers were demonstrated to inhibit galectin-3 induced aggregation slightly at 36 μM to about 45% free cells, but aggregation was never inhibited to the extent observed with generation 2 (figure 17B). Generation 4 and 6 lactose functionalized dendrimers were shown to have no significant effect on cells with increased aggregation from excess galectin-3 (figure 16A and 16B). This demonstrated the smaller dendrimers' ability to divert galectin-3 from the native multivalent cell surface interactions and inhibit the galectin-3 induced aggregation, as illustrated in figure 18C. The multivalency of lactose on small dendrimers created a strong enough binding

event to compete with the natural TF antigen ligand for galectin-3 binding. The larger dendrimers are not able to disrupt aggregation because they form the crosslinked networks previously discussed.

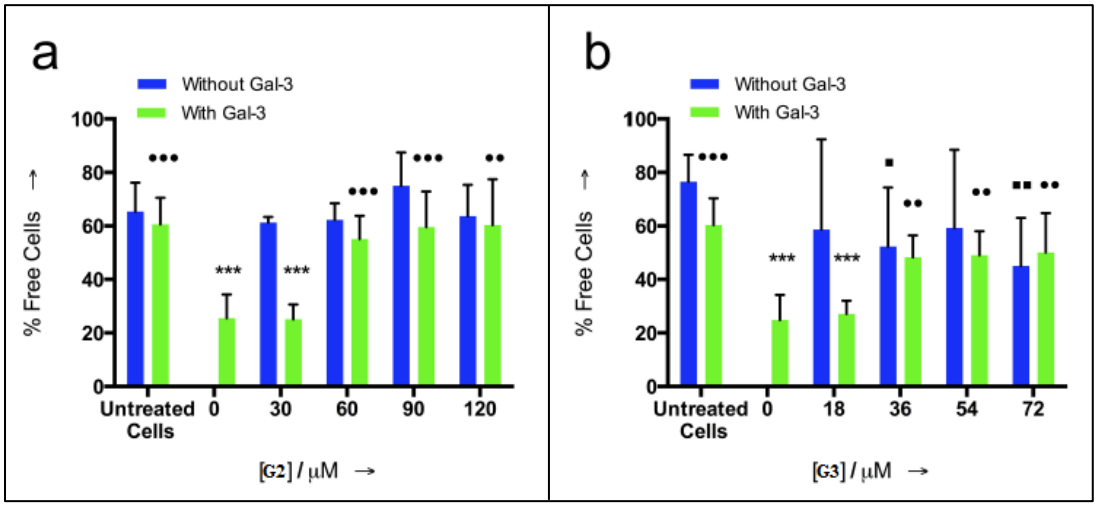


Figure 17. The effect of lactose functionalized dendrimers on A549 cells with and without added galectin-3. (A) Generation 2 dendrimer, (B) Generation 3 dendrimer. Statistical significance is shown: with respect to untreated cells (squares), with respect to the galecin-3 standard (circles), and with respect to untreated cells in the galectin standard experiment (stars). *P < 0.5, **P < 0.01, ***P < 0.001. Figure reprinted with permission from Michel *et al.*[56]

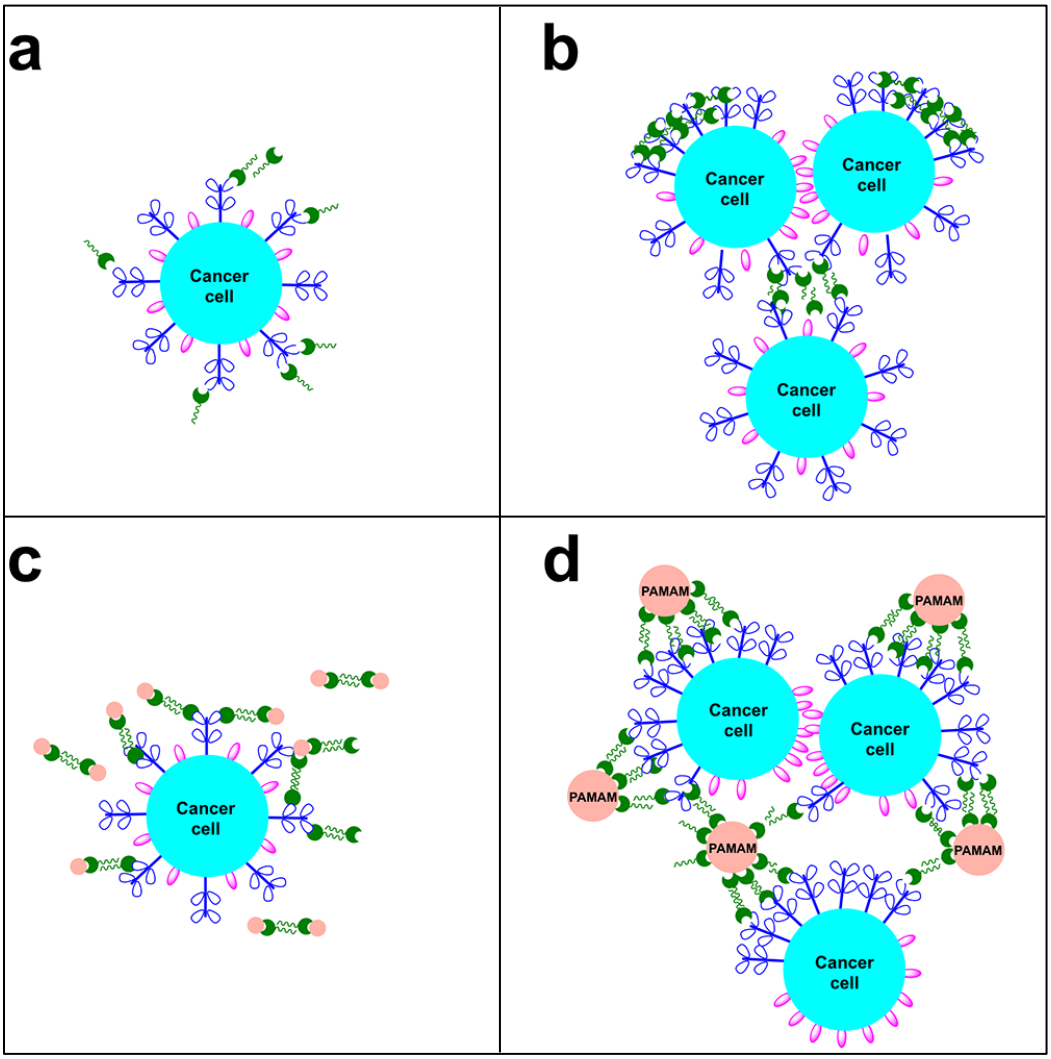


Figure 18. Schematic representation of the effects of galectin-3 and dendrimers on cancer cell aggregation. Galectin-3 is represented in green. MUC1 is represented in blue. Dendrimers are represented by pink circles. Adhesion molecules are shown in pink on the cell surface. (A) Cancer cell with MUC1 covering the surface, (B) Galectin-3 polarizing the surface of the cell and causing aggregation, (C) Small dendrimers diverting galectin-3 from polarizing the cell surface, (D) Large dendrimers forming crosslinking networks and increasing aggregation. Figure reprinted with permission from Michel *et al*.[56]

TF Antigen Functionalized Dendrimers

In order to determine the effect of ligand affinity, TF antigen functionalized dendrimers were evaluated in cellular aggregation assays with A549 cells analogous to

the assay performed with lactose functionalized dendrimers. TF antigen functionalized dendrimers were synthesized for generation 2, 3, 4, and 6 displaying 6, 12, 29, and 68 sugars, respectively (figure 19). The synthesis and characterization of these dendrimers is discussed in depth in chapter 2. Lactose functionalized dendrimers displayed 11, 22, 40, and 99 sugars for generations 2, 3, 4, and 6, respectively.[130] As the effect of multivalency is the focus of the study, all TF antigen dendrimer concentrations were made with respect to the molar concentration of sugars in solution. This sugar concentration remained constant across generations and matched those of the lactose functionalized dendrimers used previously. When the number of sugars in solution is equal, any differences observed can be attributed to the differences in monomeric affinities or to how those sugars are arranged multivalently.

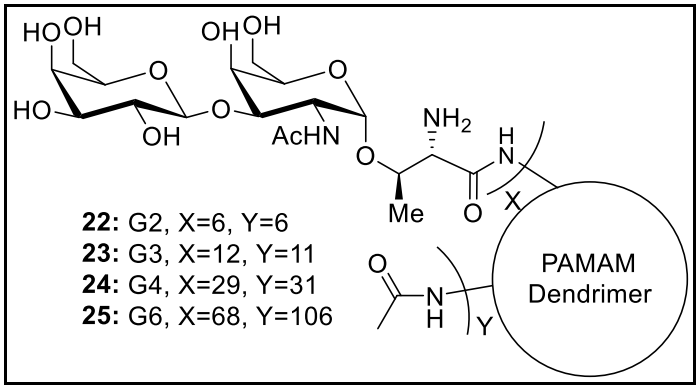


Figure 19. Generations 2, 3, 4, and 6 TF antigen functionalized dendrimers.

Results

A549 cells were incubated for 1 hour with increasing amounts of dendrimer and the percent of free cells was calculated. For this study, untreated A549 cells consistently exhibited between 80 to 90 percent free cells. Surprisingly, all four generations induced

cellular aggregation as the molarity of dendrimer increased (figure 20). Generation 2 dendrimer demonstrated a statistically significant increase in aggregation at 171 µM with about 60% free cells. Generation 3 dendrimer demonstrated an increase in aggregation at 99 µM with about 55% free cells. Generation 4 dendrimer demonstrated an increase in aggregation at 12 µM with 75% free cells. This was a less extreme change than generations 2 and 3, however a statistical significance was observed due to the smaller standard deviation, and aggregation continued to increase as dendrimer concentration increased, as with other generations. Generation 6 dendrimer demonstrated an increase in aggregation at 8 µM with 75 % free cells, and an increase of aggregation was observed as dendrimer concentration was increased. The molarity reported in figure 20 is with respect to the dendrimer. On the graphs, each increase in dendrimer concentration is an increase in an equal number of sugars across generations. All data summarized in figure 20 is displayed in Table 7 of appendix B.

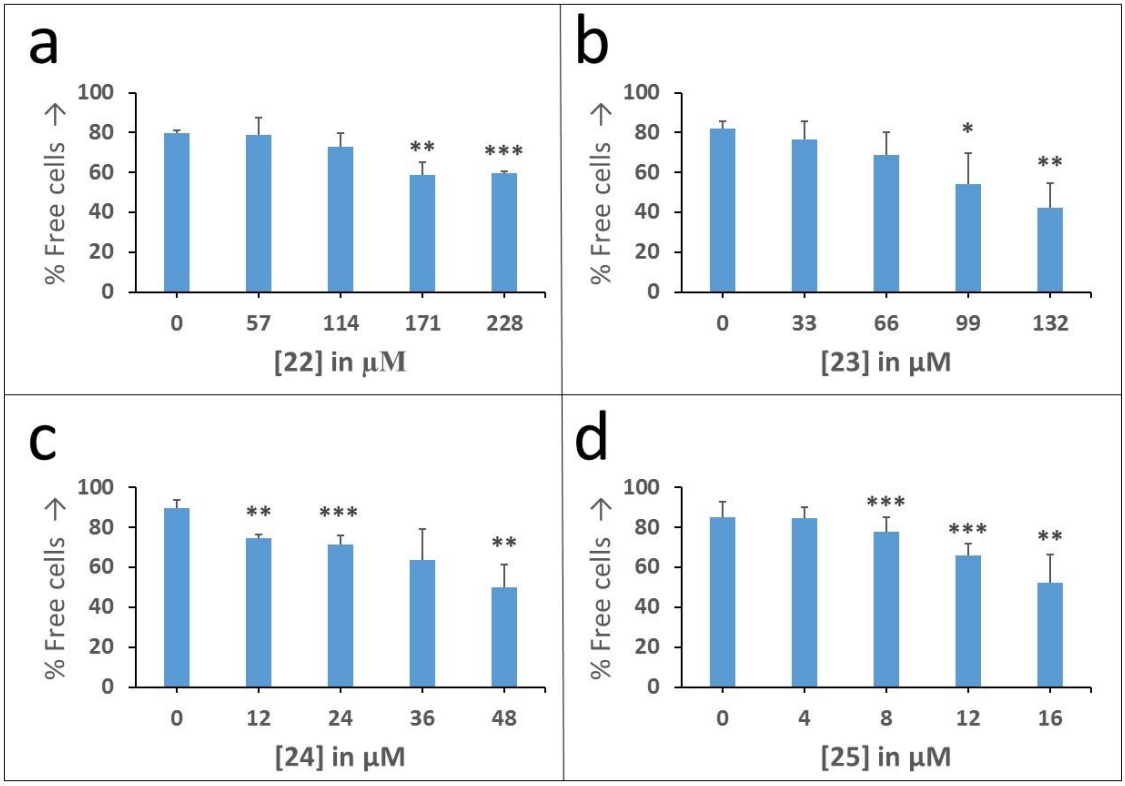


Figure 20. Graphs showing µM TF antigen functionalized dendrimer vs. percent free cells. (A) Generation 2, (B) Generation 3, (C) Generation 4, (D) Generation 6. *P < 0.1, **P < 0.05, ***P < 0.01.

Discussion

Contrary to observations with lactose functionalized dendrimers, all generations of TF antigen functionalized dendrimers induced aggregation. There was not a significant difference in aggregation observed between generations, with highest dendrimer molarities giving 60%, 42%, 50%, and 52% free cells for generations 2, 3, 4, and 6, respectively. Presumably, continued increases in the concentrations of the dendrimers would further increase cellular aggregation, however larger quantities of dendrimer must be produced to conduct these experiments. The increased aggregation for TF antigen

functionalized dendrimers relative to lactose functionalized dendrimers is presumably due to galectin-3's higher binding affinity for TF antigen. It seems the stronger binding affinity allows TF antigen functionalized dendrimers to bind to multiple galectin-3 lectins even with smaller generations. Small lactose functionalized dendrimers, on the other hand, were not able to nucleate the formation of large enough aggregates of galectin-3 to cause cellular aggregation. This indicates that the TF antigen/galectin-3 binding is less reversible, and crosslinked networks of galectin-3/TF antigen functionalized dendrimers are formed that increase cellular aggregation regardless of the dendrimer generation.

Interestingly, generation 6 TF antigen functionalized dendrimers induced less aggregation than generation 6 lactose functionalized dendrimers. This is perhaps due to the more reversible nature of the monovalent lactose/galectin-3 interaction. If lactose binding to galectin-3 is more reversible, then the aggregate is capable of rearrangement to obtain the most stable conformation, allowing more crosslinking and more aggregation of cancer cells for generation 6. If TF antigen/galectin-3 binding is less reversible, then the binding is less capable of rearrangement to obtain the most stable conformation for galectin-3/TF antigen functionalized dendrimers.

Previous examples of this type of dendrimer behavior have been demonstrated in this lab. Dimannose functionalized dendrimers were studied with a strong binding protein, cyanovirin-N, and a weaker binding protein, Concanavalin A (Con A).[131] The dendrimers bound the maximum number of Con A proteins capable of fitting on the dendrimer surface, but significantly less cyanovirin-N proteins were bound than were able to fit on the surface. In this case, the reversibility of the Con A/mannose interaction

allowed the protein to move around the surface to achieve the most stable conformation. The bound Con A proteins were able to adjust so that complete surface coverage of the glycodendrimer was obtained. However, the stronger binding strength of the cyanovirin-N protein to dimmanosides did not allow for the same degree of reversibility in the dendrimer/protein binding interaction. The proteins were held in the first conformation established because k_{off} was significantly reduced, not allowing for rearrangement of the cyanovirin-N/glycodendrimer into an ideal packing pattern.

Another example that demonstrates the importance of the monovalent affinity on multivalent binding interactions was reported by Candace Goodman with biotin functionalized dendrimers binding with streptavidin.[132] In this study, the size and shape of aggregates formed by the dendrimer and protein in solution were assessed. The streptavidin/biotin functionalized dendrimer aggregation was compared to aggregates formed by concanavalin A and mannose functionalized dendrimers as well as aggregates formed by galectin-3 and lactose functionalized dendrimers. The streptavidin/biotin dendrimers produced irregularly shaped and highly polydisperse aggregates in comparison to the galectin-3/lactose dendrimers, which were spherical in shape and had a lower polydispersity. This suggests the irreversibility of the streptavidin/biotin binding creates highly heterogeneous, complex crosslinked networks, while the reversibility of the galectin-3/lactose binding allows for more uniform networks to be formed. However, Con A with mannose functionalized dendrimers also produced irregularly shaped, highly polydisperse aggregates despite Con A having a binding constant for mannose similar to that of galectin-3 for lactose. Both Con A and streptavidin are tetramers with four binding

sites per protein, and galectin-3 contains only one binding site per protein, suggesting the nature of the protein's multivalency may also be highly significant in the formations of the crosslinking networks.

For the purposes of this study, the systems being compared both contain galectin-3, so the protein multivalency variable is removed. It is also notable that monovalent binding between TF antigen and galectin-3 is reversible. It is the current hypothesis that the multivalent display of TF antigen creates a much stronger binding event that is less reversible than when lactose is used multivalently. In order to test the hypothesis that TF antigen functionalized dendrimers are able to form large crosslinking networks regardless of size, dynamic light scattering experiments with galectin-3 must be conducted to examine the size and polydispersity of the lectin/glycodendrimer aggregates that are formed. A comparison of these results with those of lactose dendrimers and galectin-3 will give further insight into the disparity seen between the two dendrimers in cellular aggregation.

Conclusion

In conclusion, TF antigen functionalized dendrimers were evaluated for their effect on homotypic aggregation of A549 cells, and results from these assays were compared to results previously reported for lactose functionalized dendrimers. Larger generations of lactose functionalized dendrimers induced cellular aggregation, while smaller generations of lactose functionalized dendrimers inhibited galectin-3 induced cellular aggregation. In contrast, all generations of TF antigen functionalized dendrimers induced cellular aggregation. The most likely explanation for the differences observed for

the two systems is that TF antigen binds to galectin-3 more strongly than lactose, giving multivalent TF antigen the ability to form large crosslinking networks regardless of dendrimer size. Additional in depth studies are needed to determine the validity of this hypothesis.

Experimental Procedures

Dendrimers

TF antigen functionalized dendrimers were synthesized as described in chapter 2. Dendrimers were dissolved in ultrapure water, filtered over a 0.22 μm filter, and the water was removed by lyophilization. The dendrimers were then dissolved in ultrapure water at varying concentrations so the number of sugars per milliliter was equivalent to that used for lactose functionalized dendrimers. Generation 2 was dissolved at 2.37 mg/mL, generation 3 at 2.71 mg/mL, generation 4 at 2.31 mg/mL, and generation 6 at 2.40 mg/mL.

Cell Culture Methods

Human cell line A549 was purchased from ATCC and cultured as recommended in F-12K media supplemented with 10% fetal bovine serum (FBS) and 100 units/mL penicillin-streptomycin. The cells were incubated at 37 °C with 5% CO_2 in air atmosphere. For these experiments, cells were used that had been passaged less than 6 times. Cells were dissociated from growth dishes using Trypsin/ EDTA (0.25%/ 0.02%).

Homotypic Cellular Aggregation Assay

Cells were counted using a hemocytometer and suspended in serum free media (SFM, F-12K) at 16 million cells per mL. Decreasing amounts (53, 43, 33, 23, and 13 µL) of SFM were added to separate 1.6 mL Eppendorf tubes. The cell suspension (15 µL, 240,000 cells) was added to each tube, and increasing amounts (0, 10, 20, 30, and 40 µL) of dendrimer solution were added to the respective tubes so the final volume of each tube was 68 µL. The contents of the tube were gently mixed, and this was allowed to gently rotate for 1 h at 37 °C, after which 3 aliquots of 10 µL each each were viewed on a Nikon Eclipse TS-100 phase contrast microscope under 4x magnification. Two images were taken of each aliquot for analysis. Each assay was repeated in triplicate.

Data Analysis

Each tube yielded 6 images that were stitched together using Microsoft Image Composite Editor 2.0 with the planar motion setting and structured 2×3 (figure 21). This composite image was edited using Gimp 2.8 to invert the color so cells would appear black (figure 22) and the contrast was increased (threshold 90) (figure 23) so cells could be easily detected by the image analysis software, Pixcavator 5.1. The image was also resized to 1833×918 to allow Pixcavator 5.1 to read the image. Pixcavator 5.1 was set to recognize single cells at 30 pixels. The aggregate size data obtained from Pixcavator 5.1 was analyzed in Microsoft Excel with cell aggregates being labelled as anything larger than 120 pixels. The sum of all dark areas less than 120 pixels was divided by the sum of all total dark areas to give the percent of free cells. Select images for cellular assays can be found in appendix B.

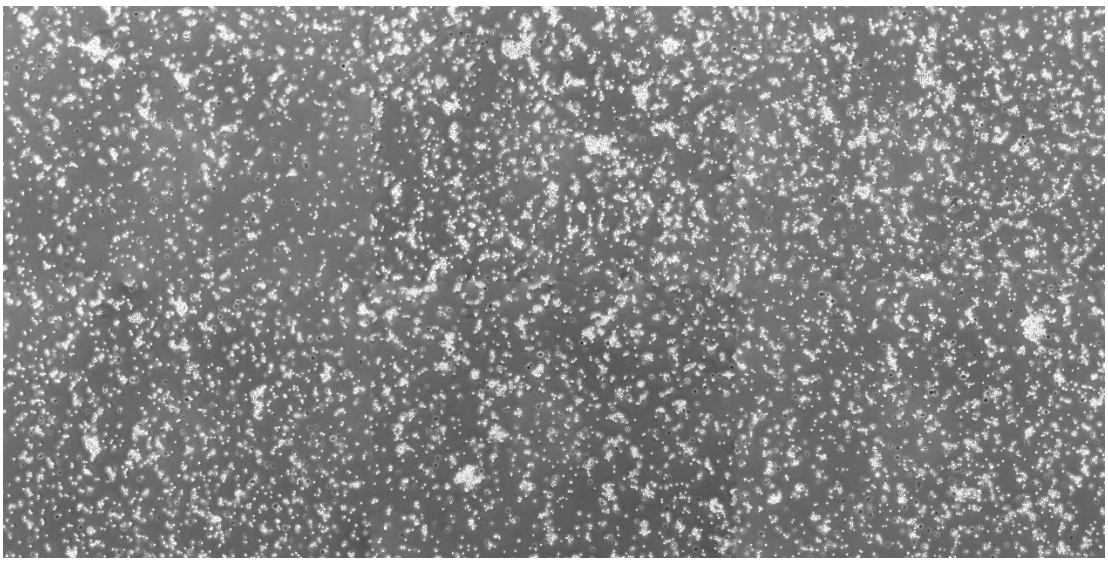


Figure 21. Example image of 6 images stitched together in Microsoft Image Composite Editor. Cells are shown as white.

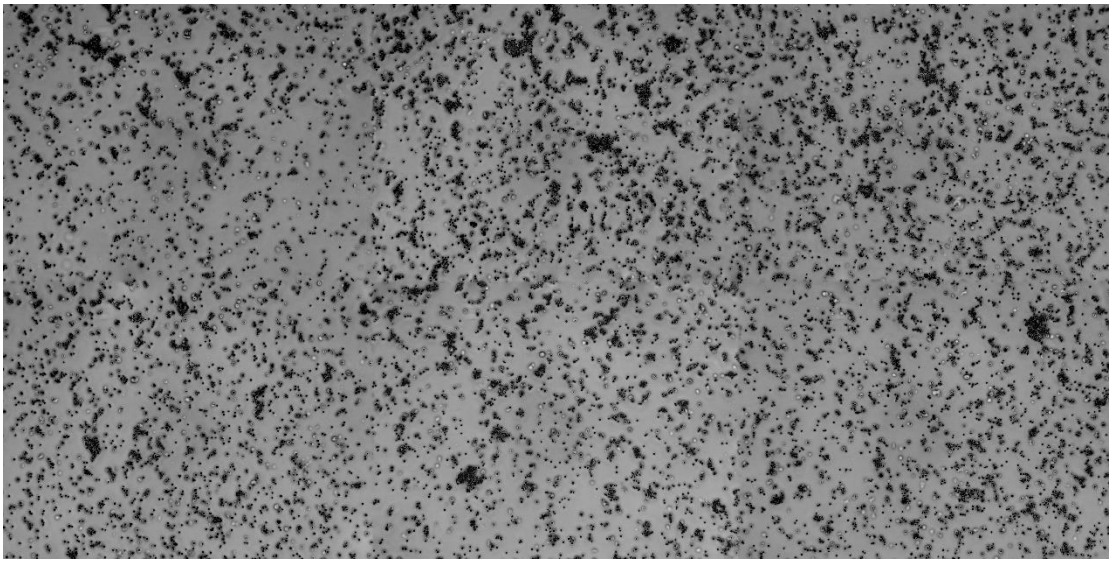


Figure 22. Example image of inverted color in Gimp 2.8. Cells are shown as black.

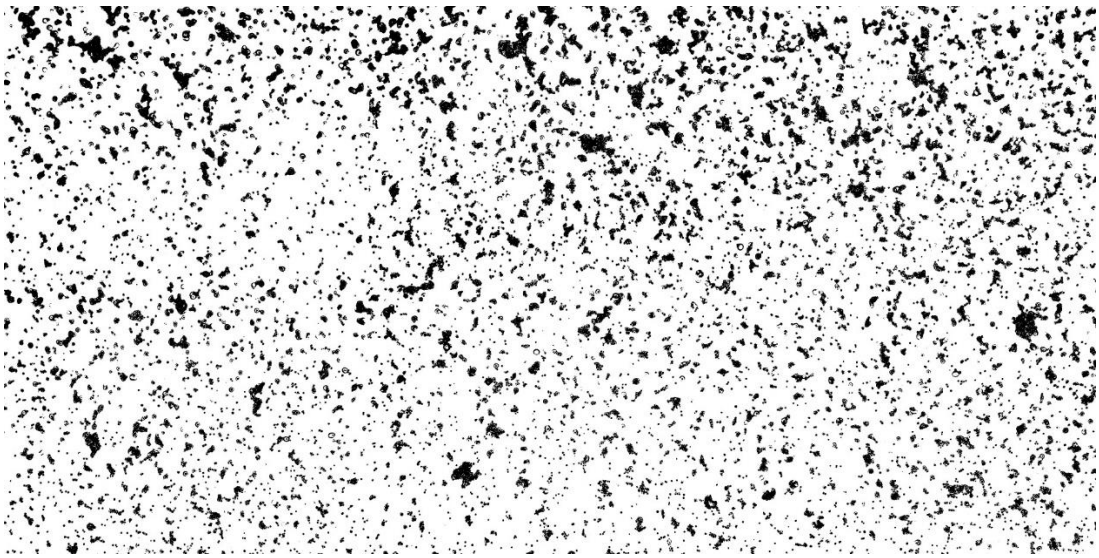


Figure 23. Example image of increased contrast in Gimp 2.8. Cells are shown as black.

Statistical Analysis

Statistical significance was determined using the unpaired two-tailed student's t-test. *P < 0.1, **P < 0.05, ***P < 0.01. Data are mean ± SD, n = 3. Statistical significance reported is with respect to untreated cells.

CHAPTER FOUR

CHARACTERIZATION OF DENDRIMERS BEARING CLUSTERS OF END GROUPS

Background

Dendrimers are highly branched macromolecules that are being used for a variety of biomedical applications such as drug delivery, tissue engineering, and imaging agents.[133, 134] Dendrimers are also used in a variety of analytical applications including light harvesting, fluorescent sensing, guest encapsulation, gas sensing, and catalysis.[135] Many dendrimers bear more than one type of functional group attached to the terminal end groups. Several techniques to synthesize these heterofunctionalized dendrimers have been reported,[136-140] the simplest of which adds the different end groups either simultaneously or sequentially in solution in the desired molar ratios.[82, 141] Heterofunctionalized therapeutic dendrimers are useful in that they are able to accommodate the active compound end groups, such as targeting agents or a prodrug, along with end groups to decrease the dendrimer's cytotoxicity,[78] or to work as imaging agents.[142-145] Heterofunctionalized dendrimers have also been used to improve MRI contrast agents by decreasing the molecular tumbling time for the MRI imaging agents currently being employed.[146] The ability to arrange the end groups of heterofunctionalized dendrimers into specific patterns can be very important, as in the case of partially functionalized tri-mannoside clustered dendrimers. These glycodendrimers have binding affinity for Concanavalin A equal to fully functionalized

un-patterned mannose dendrimers with a significant amount of end groups remaining available for functionalization with a variety of other compounds.[147]

Spin labeled dendrimers have been used in electron paramagnetic resonance (EPR) studies to study solvent and temperature effects on the nature of the dendrimer,[148] dendrimer interactions with peptides,[149] polynucleotides,[150] and select amino acids,[151] as well as intermolecular interactions between dendrimers.[152] EPR of spin-labeled compounds was also used to probe the structure of brush polymers,[153] as well as the interactions between double stranded DNA and spermine-based dendrons.[154] Previously, this lab has used spin labeled polyamidoamine dendrimers to show that end group functionalization occurs in a random manner.[141, 155, 156] Adjacent binding sites reactive toward different ligands have been observed in nature and the binding strength is increased when both ligands are present.[157-161] This type of binding is referred to as heterobivalent binding. A bi-functionalized dendrimer bearing a random distribution of end groups may not be sufficient to position the distinct ligands for binding to both sites. In this case, clustered end groups may be necessary to hold the different ligands near each other on the surface of the dendrimer.

Because it has been shown that specifically patterning the end groups can have a significant effect on the dendrimer's functionality, as seen with the tris-mannoside clustered dendrimers[147] and in the case of heterobivalent binding,[161] the focus of this work is to compare the end group distribution of dendrimers containing spins covalently linked in clusters to the end group distribution of dendrimers bearing a random distribution of spins. In a study using a temporary linker, the range of motion for the end

groups was determined to be so dynamic that a covalent linkage is necessary to keep end groups near each other in space.[156]

To determine the patterning of end groups, the line broadening of the EPR spectrum is analyzed for varying percent loadings of dendrimers with spin labels. It has been shown that the line broadening can be calculated by taking the peak height ratio for peaks A and B in the EPR spectrum, as shown in figure 24.[141] A larger A/B height ratio correlates to more line broadening. Increased line broadening correlates to a closer proximity of dendrimer end groups. Figure 25 shows that when the line broadening (A/B height ratio) is plotted against the percent loading of the spin label, 2,2,6,6-Tetramethyl-piperidine-1-oxyl (TEMPO), three graphs emerge depending on whether the end groups are arranged randomly, clustered, or as far apart as possible. The clustered and maximally separated graphs are previously reported theoretical calculations, while the random distribution graph is previously reported experimental data.[141] It should be noted that the node that appears in the clustered line broadening curve is artifactual. Thus far, this analysis has given line broadening curves that fit the random distribution model for all functionalized PAMAM dendrimers that have been studied including a range of sterically hindered end groups,[141] mannose functionalized engroups,[155] and end groups temporarily clustered with boron.[156] In this report, dendrimers bearing covalently linked clusters of end groups that afford a non-random end group distribution are described.

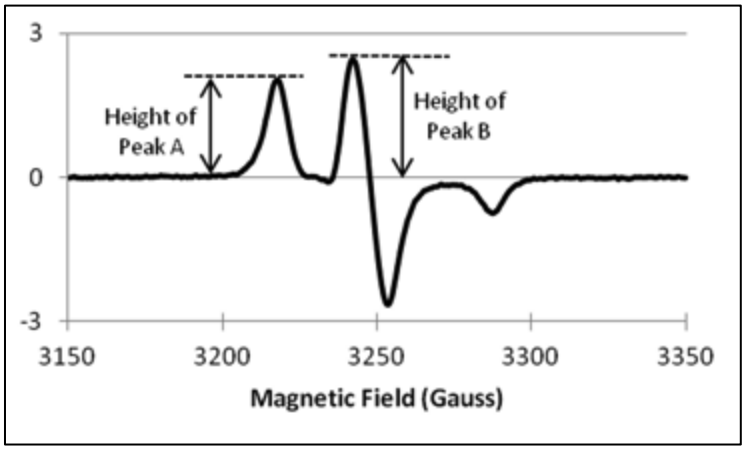


Figure 24. Peaks A and B in the EPR spectrum are used to determine line broadening effects.

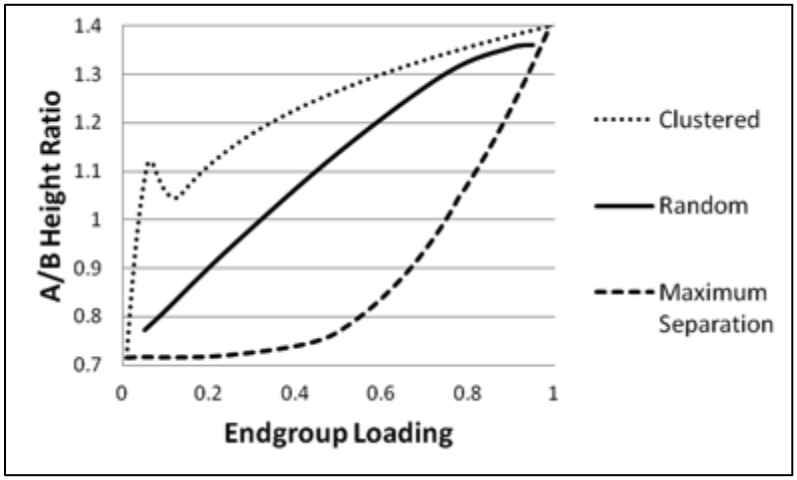
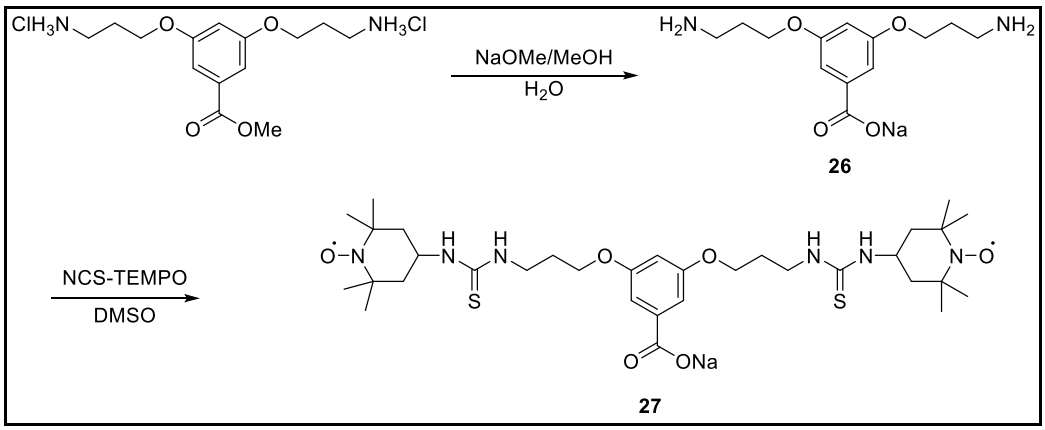


Figure 25. Theoretical line broadening graphs for clustered end groups (small dashed) and maximally separated end groups (large dashed) with the line broadening graph for experimentally determined random end groups (solid). Figure adapted from Walter *et al*.[141]

Results and Discussion

To characterize the changes in the line broadening in the EPR spectrum that occur upon covalent linkage of spins, sodium 3,5-bis-(3-(3-(*N*-oxy-2,2,6,6-tetramethylpiperidine-4-yl)-thioureido)propoxy) benzoate (**27**) was synthesized as shown in scheme 7.



Scheme 7. The formation of sodium 3,5-bis-(3-(3-(*N*-oxy-2,2,6,6-tetramethylpiperidine-4-yl)-thioureido)propoxy) benzoate **27**.

The ammonium salts of methyl 3,5-bis-(3-aminopropoxy)benzoate dihydrochloride were reduced using sodium methoxide in a mixture of methanol and water, required for solvation, which converted the methyl ester into carboxylate **26**. Carboxylate **26** was combined with two equivalents of 4-isothiocyanato-2,2,6,6-tetramethylpiperidine-1-oxyl (NCS-TEMPO) to give compound **27**. No purification was performed for these steps as the only impurities were unreactive salts. EPR data was collected for compound **27** at increasing concentrations, and the line broadening was calculated for each concentration using the A/B peak height ratio.[141] The EPR spectra for **27** at various concentrations are shown in figure 26, where peak A has been normalized to 1 for ease of visual comparison. The height decrease for peak B indicates an increase in line broadening.

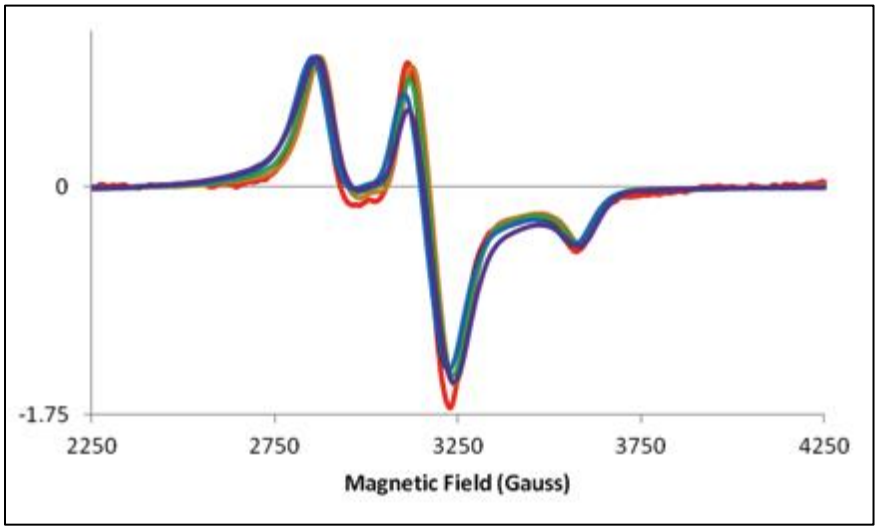


Figure 26. EPR spectra of compound **27** at increasing concentrations: red: 5 mM, orange: 25 mM, green: 50 mM, blue: 75 mM, purple 100 mM.

The A/B ratios for the spectra of **27** were plotted against the concentrations of radicals in solution and were compared to that of the 4-amino-TEMPO monomer in equal concentrations (figure 27). A higher A/B peak height ratio corresponds to more spectral line broadening. This graph indicates that there is more line broadening for 4-amino-TEMPO than for compound **27** when the concentration is greater than 75 mM on a per spin basis. Due to the fact that compound **27** has two radicals per molecule, there are half as many molecules in solution as there are for 4-amino-TEMPO at the equivalent concentration. Thus, there is a greater distance between molecules and therefore less intermolecular line broadening for **27** than for 4-amino-TEMPO. At concentrations below 75 mM, dimer **27** shows greater line broadening than that of 4-amino-TEMPO monomer and appears to be reaching a minimum A/B value. Presumably, this minimum A/B value correlates to the intramolecular line broadening associated with the dimer (**27)**. When the dendrimer is functionalized with **27**, the local concentration of the spins will be altered,

eliminating the possibility of intermolecular line broadening. EPR data is collected at a dendrimer concentration low enough to ensure no intermolecular line broadening can occur, thus any line broadening observed is intramolecular on the dendrimer surface.

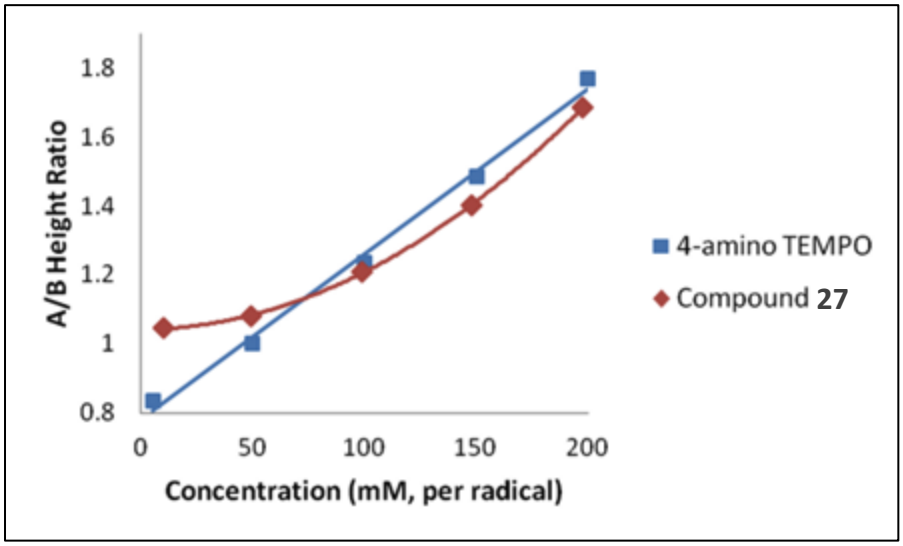
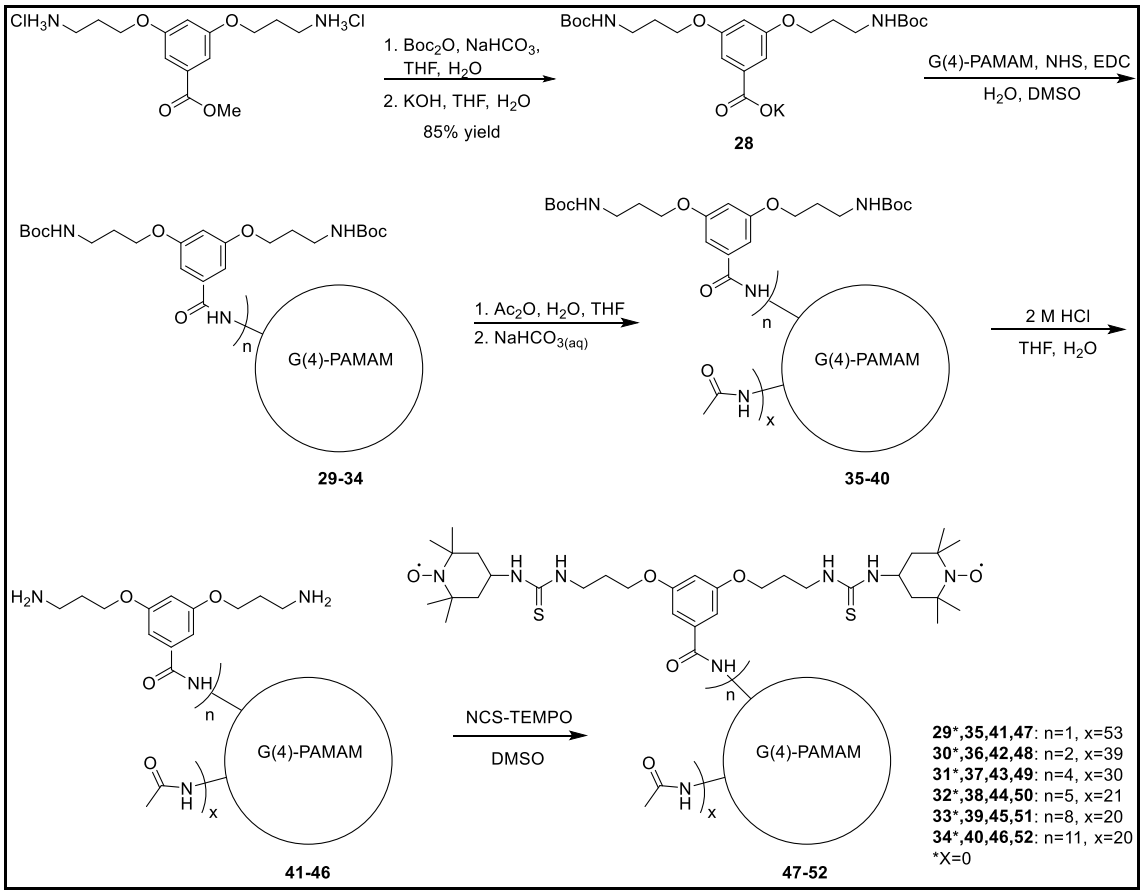


Figure 27. Comparison of line broadening between Compound **27** and 4-amino-TEMPO at increasing concentrations.

Functionalization of G(4) PAMAM dendrimer using compound **27** was attempted with both EDC/NHS coupling and ethyl chloroformate/TEA coupling. Unfortunately, both sets of reaction conditions produced significant radical quenching. Hence, the functionalization of generation 4 PAMAM dendrimer to create di-spin end groups was performed as shown in scheme 8. The amines of methyl 3,5-bis-(3-aminopropoxy)benzoate dihydrochloride were Boc protected followed by the use of potassium hydroxide to convert the methyl ester to a carboxylate producing carboxylate **28** in an 85% yield. Carboxylate **28** was used for functionalization of G(4) PAMAM dendrimer in varying percent loadings using NHS and EDC coupling to afford dendrimers **29-34**. A maximum loading of 11 functionalized end groups was reached,

apparently due to the steric bulk of **28** leaving no space for additional functionalization. At this point, any accessible unfunctionalized reactive amino termini were acetylated using acetic anhydride, producing dendrimers **35-40**. Two molar hydrochloric acid was used to remove the Boc protecting groups from **35-40**, yielding dendrimers **41-46**. The free amines were functionalized with NCS-TEMPO, producing dendrimers **47-52**.



Scheme 8. Preparation of generation 4 dendrimers with radical end groups clustered in groups of two.

EPR spectra for dendrimers **47-52** were collected and peak A was normalized to 1, as shown in figure 28. The line broadening effects of the resulting spectra were examined. Because the functionalized end group is so large, the maximum loading that

could be achieved is 40%. Therefore, the line broadening effects in the spectra are small. Percent loading was calculated by multiplying the number of functionalized end groups, n, by two because there are two spins per end group, and assuming 100% loading was n= 55 based on the molecular weight of the unfunctionalized G(4)-PAMAM as determined by MALDI-TOF MS.[162] This allowed the percent loadings to be accurately compared to those of the generation 4 PAMAM dendrimers functionalized with TEMPO in a random distribution that have been previously studied.[141]

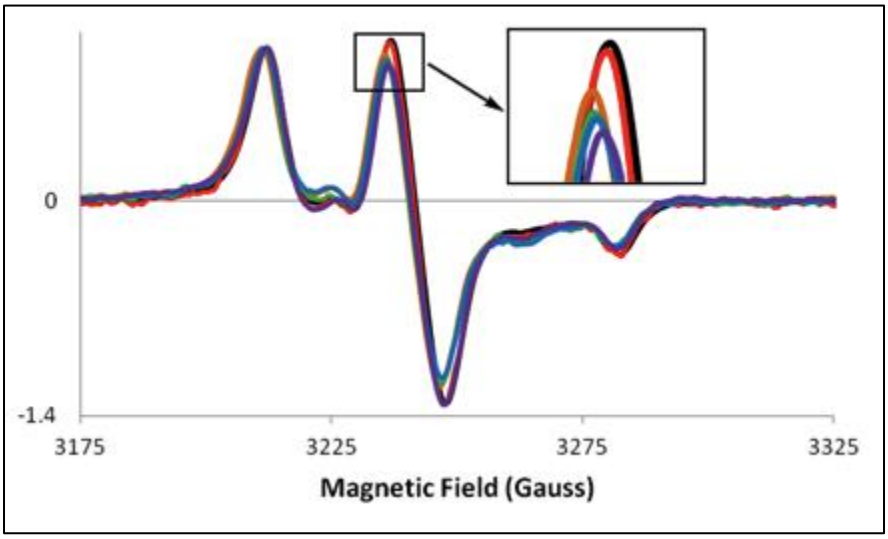


Figure 28. EPR spectra of dendrimers **47-52**. Black: n=1 (4%), Red: n= 2 (7%), Orange: n= 4 (15%), Green: n= 5 (18%), Blue: n= 8 (29%), Purple: n= 11 (40%), where n is the number of end groups functionalized, and percent is the percent loading.

The A/B height ratios of the EPR spectra are as follows: 4%: 0.95, 7%: 0.97, 15%: 1.04, 18%: 1.08, 29%: 1.10, and 40%: 1.13. By plotting the A/B height ratios against the percent loading and in comparison to the other graphs, a more accurate representation of the line broadening is displayed. Figure 29 shows that the line broadening of dendrimers **47-52** aligns reasonably well with the theoretical model for the

clustered distribution at lower loadings and falls between the curves for the random distribution and the clustered distribution at higher loadings. The results in figure 29 are as expected because **47-52** have a random distribution of end groups with two spin labels per end group. The theoretical model is for the more extreme example in which all spin labels are clustered together. When comparing the line broadening results from figure 27 and figure 29, a trend is observed in which the curves for tethered TEMPO and the curves for untethered TEMPO differ most at lower concentrations and begin to converge as concentrations increase. Absolute comparisons between the A/B ratios of two graphs cannot be made, due to the fact that a system in which spins are on a dendrimer cannot be compared to a system in which spins are free in solution, as has been previously reported.[162]

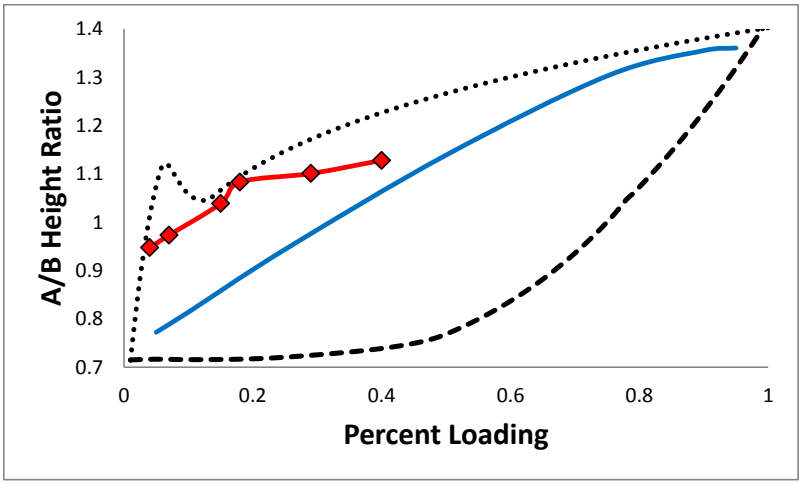


Figure 29. A/B height ratios of dendrimers **47-52** (red line) plotted in comparison with the theoretical extremes, fully clustered end groups (small dashed) and maximally separated end groups (large dashed) and the experimentally determined values for a random distribution of TEMPO (blue line), values taken from Walter *et al*.[141]

In an attempt to show reproducibility of these finding, the synthesis of dendrimers **47-52** was attempted numerous times. In each attempt, significant radical quenching was

observed. Because the step previous to NCS-TEMPO addition required 2 M HCl, addition of NaOMe was crucial to remove any acid remaining on the dendrimer. However, higher additions of NaOMe resulted in increased radical quenching, suggesting the radical is sensitive to basic conditions on the time scale of days. Therefore, dendrimers where allowed to stir in 1 M NaOMe for 24 hours and dialyzed before exposure to NCS-TEMPO. Subsequent attempts using this method gave inconclusive results due to the discovery that several batches of NCS-TEMPO were partially quenched before use. Further work is needed to re-synthesize dendrimer **47-52** with active radicals to reproduce the results reported here.

Conclusion

In conclusion, a new dendrimer has been synthesized in which dimers of spin labeled end groups are incorporated onto the dendrimer. The line broadening curve for dendrimers **47-52** with di-spin end groups aligns well with the theoretical model for the clustered distribution at lower loadings and falls between the curves for the random distribution and the clustered distribution at higher loadings. The experimentally obtained values for **47-52** suggest that covalent linkage of heterobivalent ligands is most important for percent loadings below 50% on the dendrimer. Further work is needed to demonstrate the reproducibility of these preliminary results. Because di-spin labeled dendrimers provide insight into the properties of covalently linked end groups, this study has important implications for the development of heterobifunctionalized dendrimers that are becoming increasingly important for a wide variety of applications.

Experimental Procedures

General Methods

All chemicals unless otherwise specified were purchased from Sigma-Aldrich or Fisher Scientific. Generation 4 polyamidoamine dendrimer was purchased from Dendritech, Inc. Methyl 3,5-bis-(3-aminopropoxy)benzoate dihydrochloride was purchased from Syrwit Technology Co., ltd. NCS-TEMPO was purchased from Tokyo Chemical Industry Co., ltd. ^{13}C and ^{1}H NMR were recorded on a Bruker DRX 500 MHz spectrometer. Partial protons are reported in NMR data representing peak ratios due to the large number of protons in each dendrimer and the variability in the number of the functionalized end groups within a single sample. Mass spectrometry data was obtained on a Bruker Autoflex III MALDI-TOF in positive linear mode with an acceleration voltage of 19 kilovolts. MALDI samples were prepared in a 10000:1 matrix: analyte ratio with 3-indoleacrylic acid as the matrix and DMF as the solvent. The molecular weight was calculated with a peak centroid based on a peak width of approximately 5,000. EPR spectra were obtained on a Varian E-109 X-band spectrometer with a lab built computer interface. Dendrimers were dissolved in a 3:1 mixture of DMSO/glycerol at approximately 1×10^{-4} M. Serial dilutions were performed to ensure concentrations were below the threshold for intermolecular line broadening. Samples were scanned at a power of 0.0002 mW. The field was scanned over a range of 200 G with 100 kHz modulation at an amplitude of 1 G. The scan rate was 100 G/min. with a time constant of 250 ms. Relevant spectra can be found in Appendix C.

Sodium (3-aminopropoxy)benzoate (26). Methyl 3,5-bis-(3-aminopropoxy)benzoate dihydrochloride (44.4 mg, 0.13 mmol) was dissolved in 4:1 MeOH: H_2O (1.5 mL) and added to a 5 mL round bottom flask charged with 1 mL MeOH/NaOMe (3.5 equiv. NaOMe). This was allowed to stir at 21 °C for 17 h and concentrated *in vacuo*, affording 35.0 mg (>100% yield) of crude product as a white powder with unreactive salts. ^{1}H NMR (500 MHz, D_2O) δ 6.87 (s, 2H), 6.33 (s, 1H), 3.79 (t, J= 6.7 Hz, 4H), 2.54 (appt. t, J= 7.2 Hz, 4H), 1.65 (dt, J= 6.7, 13.8 Hz, 4H) ppm; ^{13}C NMR (125 MHz, D_2O) δ 174.2, 159.2, 139.0, 107.9, 104.4, 66.7, 37.7, 31.5 ppm; HRMS (micro-TOF) *m/z*= 269.1497 g/mol (calculated M+H = 269.1501 g/mol for $C_{13}H_{20}N_2O_4$).

Sodium 3,5-bis-(3-(3-(*N*-oxy-2,2,6,6-tetramethylpiperidine-4-yl)-thioureido)propoxy) benzoate (27). Crude compound **26** (35.0 mg) was suspended in DMSO (2 mL) and NCS-TEMPO (64.1 mg, 0.30 mmol) was slowly added to the reaction flask wrapped in aluminum foil. This was allowed to stir at 21 °C for 24 h. The reaction was concentrated *in vacuo* giving an orange powder in a crude yield of greater than 100% due to salts. HRMS (micro-TOF) *m/z* = 717.3431 g/mol (calculated M+H = 717.3444 g/mol for $C_{33}H_{53}N_6NaO_6S_2^{2\bullet}$).

Methyl 3,5-bis-(3-(tert-butyloxycarbonylamido)propoxy)benzoate. A solution of methyl 3,5-bis-(3-aminopropoxy)benzoate dihydrochloride (0.43 g, 1.21 mmol) and $NaHCO_3$ (0.41 g, 4.88 mmol) in H_2O (10 mL) was combined with a solution of di-tert-butyl dicarbonate (0.53 g, 2.43 mmol) in THF (6 mL) and was allowed to stir at 21 ºC for 20 h. The THF was removed *in vacuo* and the resulting mixture was diluted with H_2O

(20 mL) and extracted with Et_2O (3 × 40 mL). The combined Et_2O layers were washed with brine (2 × 40 mL) and dried over $MgSO_4$. The reaction was concentrated *in vacuo* affording 0.57 g (96% yield) of product as a white solid. ^{1}H NMR (500 MHz, $CDCl_3$) δ 7.15 (d, J=2.4 Hz, 2H), 6.61 (t, J= 2.4 Hz, 1H), 4.70 (s, 2H, N-H), 4.01 (t, J= 6.1 Hz, 4H), 3.88 (s, 3H, Me-H), 3.30 (appt. q, J= 6.1 Hz, 4H), 1.96 (p, J= 6.1 Hz, 4H), 1.42 (s, 18H, Boc-H) ppm; ^{13}C NMR (125 MHz, $CDCl_3$) δ 166.7, 159.8, 156.0, 131.9, 107.8, 106.5, 79.2, 66.0, 52.2, 37.8, 29.4, 28.4 ppm; HRMS (micro-TOF) m/z = 483.2925 (calculated m/z M+H = 483.2706 for $C_{24}H_{38}N_2O_8$). Consistent with literature values.[163]

Potassium 3,5-bis-(3-(tert-butyloxycarbonylamido)propoxy)benzoate (28). Methyl 3,5-bis-(3-(tert-butyloxycarbonylamido)propoxy)benzoate (0.21 g, 0.44 mmol) was dissolved in THF (8.5 mL) and a solution of potassium hydroxide (25.1 mg, 0.45 mmol) dissolved in H_2O (1 mL) was added. The mixture was allowed to stir at 21 °C for 19 h. The THF was removed *in vacuo*, leaving a white solid. This solid was dissolved in H_2O (35 mL) and washed with Et_2O (2 × 20 mL). The aqueous layer was concentrated *in vacuo* yielding 0.18 g (89% yield) of product as a white solid. ^{1}H NMR (500 MHz, D_2O) δ 6.92 (s, 2H), 6.46 (s, 1H), 3.90 (t, J= 6.3 Hz, 4H), 3.06 (appt. t, J= 6.05 Hz, 4H), 1.79-1.70 (m, 4H), 1.19 (s, 18H, Boc-H) ppm; ^{13}C NMR (125 MHz, D_2O) δ 174.2, 159.1, 158.0, 139.2, 108.1, 104.7, 80.7, 66.3, 37.2, 28.5, 27.7 ppm; HRMS (micro-TOF) *m/z* = 491.2529 (calculated M+H = 491.2369 for $C_{23}H_{35}N_2NaO_8$). Consistent with literature values.[163]

3,5-Bis[3-(tert-butyloxycarbonylamido)propyloxy]benzoamide functionalized generation 4 polyamidoamine dendrimers (29-34). The following solutions were made: 0.41 M EDC in 2:1 DMSO: H_2O, 0.63 M NHS in DMSO, and 0.44 M potassium 3,5-Bis[3-(tert-butyloxycarbonylamido)propyloxy]benzoate (**28**) in 2:3 DMSO: H_2O. Exact amounts used for each reaction are summarized in Table 3. The appropriate aliquots of each solution for each dendrimer were mixed in 6 different 1 dram vials and allowed to stir for 15 min at 21 °C. Generation 4 PAMAM dendrimer was transferred into 6 different 1 dram vials and dissolved in enough DMSO so that the final volume would equal 2.7 mL. The corresponding solutions of EDC, NHS, and compound **28** were added to the dendrimer solutions while stirring to achieve the varying percent loadings. This was allowed to stir at 21 °C for 16 h. The solutions were dialyzed separately in H_2O (3 × 500 mL) for 2 h each and concentrated *in vacuo*.

Prod.	G(4) PAMAM mg (mol)	EDC mg (mol)	NHS mg (mol)	**3** mg (mol)	N[1] (loading)[2]	% Yield[3]
29	35.3 mg (2.59×10^{-6} mol)	5.5 mg (3.57×10^{-5} mol)	2.9 mg (2.50×10^{-5} mol)	1.8 mg (3.57×10^{-6} mol)	1 (4%)	96%
30	32.9 mg (2.42×10^{-6} mol)	10.3 mg (6.65×10^{-5} mol)	5.4 mg (4.65×10^{-5} mol)	3.4 mg (6.65×10^{-6} mol)	2 (7%)	quant.
31	30.6 mg (2.25×10^{-6} mol)	14.4 mg (9.27×10^{-5} mol)	7.5 mg (6.49×10^{-5} mol)	4.7 mg (9.27×10^{-6} mol)	4 (15%)	95%
32	30.2 mg (2.22×10^{-6} mol)	18.9 mg (1.22×10^{-4} mol)	9.8 mg (8.54×10^{-5} mol)	6.2 mg (1.22×10^{-5} mol)	5 (18%)	quant.
33	29.9 mg (2.20×10^{-6} mol)	28.1 mg (1.81×10^{-4} mol)	14.6 mg (1.27×10^{-4} mol)	9.2 mg (1.81×10^{-5} mol)	8 (29%)	quant.
34	29.5 mg (2.17×10^{-6} mol)	36.9 mg (2.38×10^{-4} mol)	19.2 mg (1.67×10^{-4} mol)	12.1 mg (2.38×10^{-5} mol)	11 (40%)	quant.

1. N = the number of end groups functionalized.
2. % loading = N divided by 55 (total number of end groups) and multiplied by 2 (for the number of spins per end group).
3. Quant. means quantitative yield

Table 3. Amounts used for dendrimers **29-34**.

Dendrimer **29**. ^{1}H NMR (500 MHz, 3:2 d_8-THF: D_2O) δ 4.01 (s, 0.05H), 3.48-3.15 (m, 2.45H), 3.12 (bs, 0.2H), 2.79 (bs, 2.49H), 2.59 (bs, 1.00H), 2.48-2.30 (m, 1.98H), 1.92-

1.86 (m, 0.04H), 1.37 (s, 0.13H, Boc-H) ppm; ^{13}C NMR (125 MHz, 3:2 d_8-THF: D_2O) δ 174.88, 174.68, 174.31, 164.46, 51.69, 49.44, 44.03, 40.61, 40.29, 39.97, 38.83, 36.98, 36.71, 36.51, 33.07, 27.90, 25.09, 13.73 ppm; MALDI-TOF (pos) *m/z* = 14100.

Dendrimer **30**. ^{1}H NMR (500 MHz, 3:2 d_8-THF: D_2O) δ 4.00-3.91 (m, 0.07H), , 3.41-3.10 (m, 2.64H), 3.07 (bs, 0.15H), 2.90-2.66 (m, 2.32H), 2.54 (bs, 1.00H), 2.45-2.26 (m, 2.00H), 1.90-1.79 (m, 0.07H), 1.31 (s, 0.25H, Boc-H) ppm; ^{13}C NMR (125 MHz, 3:2 d_8-THF: D_2O) δ 174.78, 174.51, 174.13, 173.82, 159.85, 51.55, 49.31, 44.03, 43.85 40.48, 40.15, 39.76, 39.14, 38.70, 36.88, 36.57, 36.37, 32.92, 27.76, 24.97, 13.59 ppm; MALDI-TOF (pos) *m/z* = 14400.

Dendrimer **31**. ^{1}H NMR (500 MHz, 3:2 d_8-THF: D_2O) δ 4.04-3.95 (m, 0.10H) 3.49-3.12 (m, 2.78H), 2.91 (bs, 0.59H), 2.77 (bs, 1.64H), 2.66-2.30 (m, 1.00H), 2.49-2.29 (m, 2.00H), 1.94-1.84 (m, 0.11H), 1.35 (s, 0.40H, Boc-H) ppm; ^{13}C NMR (125 MHz, 3:2 d_8-THF: D_2O) δ 176.68, 172.98, 172.59, 172.23, 158.10, 157.97, 157.38, 49.71, 47.51, 41.92, 37.81, 37.31, 36.85, 35.04, 34.72, 31.10, 27.44, 25.90, 23.13 ppm; MALDI-TOF (pos) *m/z* = 15400.

Dendrimer **32**. ^{1}H NMR (500 MHz, 3:2 d_8-THF: D_2O) δ 4.02-3.91 (m, 0.14H) 3.46-3.07 (m, 2.88H), 2.92 (bs, 0.39H), 2.74 (bs, 1.69H), 2.64-2.47 (m, 1.00H), 2.34 (bs, 1.83H), 1.91-1.79 (m, 0.15H) 1.32 (s, 0.53H, Boc-H) ppm; ^{13}C NMR (125 MHz, 3:2 d_8-THF: D_2O) δ 178.50, 174.91, 174.45, 174.09, 159.97, 159.83, 156.69, 136.10, 105.81, 105.73, 66.04, 51.60, 49.40, 39.59, 39.17, 38.72, 36.92, 36.58, 32.97, 29.30, 27.77, 25.00 ppm; MALDI-TOF (pos) *m/z* = 15900.

Dendrimer **33**. ^{1}H NMR (500 MHz, 3:2 d_8-THF: D_2O) δ 6.99 (s, 0.11H), 6.56 (s, 0.05H), 4.00 (bs, 0.16H), 3.49-3.09 (m, 3.15H), 3.00 (bs, 0.18H), 2.77 (bs, 1.65H), 2.67-2.51 (m, 1.00H), 2.37 (bs, 2.13H), 1.96-1.80 (m, 0.21H) 1.35 (s, 0.93H, Boc-H) ppm; ^{13}C NMR (125 MHz, 3:2 d_8-THF: D_2O) δ 172.58, 172.18, 171.87, 158.10, 157.94, 154.79, 134.24, 103.94, 76.67, 64.17, 49.73, 47.53, 37.69, 37.32, 36.85, 35.28, 35.07, 34.71, 31.12, 27.43, 25.90, 23.12 ppm; MALDI-TOF (pos) *m/z* = 17000.

Dendrimer **34**. ^{1}H NMR (500 MHz, 3:2 d_8-THF: D_2O) δ 6.95 (s, 0.12H), 6.52 (s, 0.05H), 3.96 (bs, 0.32H), 3.47-3.06 (m, 3.60H), 2.74 (bs, 1.78H), 2.55 (bs, 1.00H), 2.33 (bs, 2.07H), 1.85 (bs, 0.32H) 1.31 (s, 1.27H, Boc-H) ppm; ^{13}C NMR (125 MHz, 3:2 d_8-THF: D_2O) δ 174.40, 174.27, 174.02, 173.68, 159.97, 159.79, 156.63, 136.12, 105.80, 78.45, 66.02, 51.63, 49.42, 39.56, 39.19, 38.72, 37.15, 36.95, 36.57, 35.93, 35.48, 33.01, 29.32, 27.78 ppm; MALDI-TOF (pos) *m/z* = 18500.

3,5-Bis[3-(tert-butyloxycarbonylamido)propyloxy]benzoamide and acetyl bifunctionalized generation 4 polyamidoamine dendrimers (35-40). Exact amounts used for each reaction are summarized in Table 4. Dendrimers (**29-34**) were dissolved in the corresponding amount of 3:2 THF: H_2O to create a 1 mM solution. Ac_2O (275 equiv.) was added to the solutions which were allowed to stir for 3.5 h at 21 °C. A 1 M aqueous solution of $NaHCO_3$ (825 equiv.) was added slowly over a 20 min period. The solutions were allowed to stir uncapped for 1.5 h and dialyzed separately in alternating H_2O (500 mL) and MeOH (500 mL) twice for 2 h each. The reactions were concentrated *in vacuo*.

Product	**29-34** mg (mol)	Ac_2O mg (mol)	$NaHCO_3$ mg (mol)	N[1]	% yield
35	(**29**) 25.5 mg (1.81×10^{-6} mol)	50.8 mg (4.98×10^{-4} mol)	126.5 mg (1.51×10^{-3} mol)	53	90%
36	(**30**) 26.9 mg (1.87×10^{-6} mol)	52.6 mg (5.15×10^{-4} mol)	126.6 mg (1.51×10^{-3} mol)	39	76%
37	(**31**) 16.7 mg (1.08×10^{-6} mol)	30.3 mg (2.97×10^{-4} mol)	73.3 mg (8.73×10^{-4} mol)	30	80%
38	(**32**) 26.7 mg (1.68×10^{-6} mol)	47.2 mg (4.62×10^{-4} mol)	116.5 mg (1.39×10^{-3} mol)	21	68%
39	(**33**) 28.9 mg (1.70×10^{-6} mol)	47.7 mg (4.67×10^{-4} mol)	117.9 mg (1.40×10^{-3} mol)	20	80%
40	(**34**) 19.0 mg (1.03×10^{-6} mol)	28.8 mg (2.82×10^{-4} mol)	72.8 mg (8.67×10^{-4} mol)	20	94%

1. N = number of acetylated end groups

Table 4. Amounts used for dendrimers **35-40**.

Dendrimer **35**. ^{1}H NMR (500 MHz, CD_3OD) δ 3.46-3.15 (m, overlap with solvent peak precludes integration), 2.77 (bs, 1.91H), 2.57 (bs, 1.00H), 2.35 (bs, 1.70H), 1.93 (s, 0.87H), 1.41 (s, 0.07H, Boc-H) ppm; ^{13}C NMR (125 MHz, CD_3OD) δ 173.68, 173.26, 172.02, 52.08, 49.77, 49.69, 48.44, 43.76, 38.78, 38.63, 37.27, 33.37, 21.48 ppm; MALDI-TOF (pos) *m/z* = 16800.

Dendrimer **36**. ^{1}H NMR (500 MHz, CD_3OD) δ 6.95 (s, 0.01H), 3.44-3.14 (m, overlap with solvent peak precludes integration), 2.77 (bs, 1.82H), 2.56 (bs, 1.00H), 2.35 (bs, 1.84H), 1.93 (s, 0.68H), 1.41 (s, 0.13H, Boc-H) ppm; ^{13}C NMR (125 MHz, CD_3OD) δ 173.71, 173.29, 172.07, 52.07, 49.76, 43.73, 38.78, 38.64, 37.24, 33.32, 27.48, 21.50 ppm; MALDI-TOF (pos) *m/z* = 16800.

Dendrimer **37**. ^{1}H NMR (500 MHz, CD_3OD) δ 6.95 (s, 0.03H), 6.63 (s, 0.02H), 3.99 (s, 0.11H), 3.55-3.13 (m, overlap with solvent peak precludes integration), 2.77 (bs, 1.75H), 2.57 (bs, 1.00H), 2.35 (bs, 1.89H), 1.93 (s, 0.55H), 1.40 (s, 0.35H, Boc-H) ppm; ^{13}C

NMR (125 MHz, CD_3OD) δ 173.71, 173.30, 172.08, 159.52, 52.07, 49.77, 38.78, 37.30, 33.41, 27.48, 21.52 ppm; MALDI-TOF (pos) *m/z* = 17200.

Dendrimer **38**. ^1H NMR (500 MHz, CD_3OD) δ 6.95 (s, 0.02H), 4.01 (s, 0.12H), 3.49-3.14 (m, overlap with solvent peak precludes integration), 2.77 (bs, 1.77H), 2.56 (bs, 1.00H), 2.35 (bs, 1.92H), 1.93 (bs, 0.39H), 1.40 (s, 0.45H, Boc-H) ppm; ^{13}C NMR (125 MHz, CD_3OD) δ 173.69, 173.28, 160.24, 159.52, 157.10, 136.17, 105.74, 78.56, 65.56, 52.09, 49.77, 38.80, 37.31, 36.52, 33.44, 29.36, 27.50 ppm; MALDI-TOF (pos) *m/z* = 16600.

Dendrimer **39**. ^1H NMR (500 MHz, CD_3OD) δ 6.95 (s, 0.07H), 6.62 (s, 0.02H), 4.01 (s, 0.28H), 3.50-3.14 (m, overlap with solvent peak precludes integration), 2.77 (bs, 1.86H), 2.56 (bs, 1.00H), 2.35 (bs, 2.05H), 1.97-1.86 (m, 0.40H), 1.40 (s, 0.91H, Boc-H) ppm; ^{13}C NMR (125 MHz, CD_3OD) δ 173.69, 173.28, 160.24, 159.52, 157.10, 136.17, 105.74, 78.56, 65.56, 52.09, 49.77, 38.80, 37.31, 36.52, 33.44, 29.36, 27.50 ppm; MALDI-TOF (pos) *m/z* = 17800.

Dendrimer **40**. ^1H NMR (500 MHz, CD_3OD) δ 6.95 (s, 0.13H), 6.62 (s, 0.07H), 3.99 (s, 0.32H), 3.49-3.09 (m, overlap with solvent peak precludes integration), 2.76 (bs, 1.69H), 2.55 (bs, 1.00H), 2.34 (bs, 2.25H), 1.98-1.83 (m, 0.44H), 1.40 (s, 1.28H, Boc-H) ppm; ^{13}C NMR (125 MHz, CD_3OD) δ 173.69, 160.24, 105.75, 99.99, 78.56, 65.53, 52.09, 49.79, 37.05, 33.36, 29.34, 27.50 ppm; MALDI-TOF (pos) *m/z* = 19300.

3,5-Bis (3-amino-propoxy) benzoamide and acetyl bifunctionalized generation 4 polyamidoamine dendrimers (41-46). Exact amounts used are summarized in Table 5. Dendrimers (**35-40**) were suspended in THF (0.4 mL) and a

5 M HCl aqueous solution (0.2 mL) was added while stirring, causing the dendrimers to dissolve. The solutions were allowed to stir at 21 °C for 16.5 h. The solutions were quenched with a saturated $NaHCO_3$ solution (1.1 mL) and allowed to stir for 30 min. The solutions were dialyzed separately in H_2O (3 × 500 mL) followed by DMSO (1 × 250 mL) for 1.5 h each. The reactions were concentrated *in vacuo.*

Product	**35-40** mg (mol)	% Yield
41	(**35**) 27.5 mg (1.64×10^{-6} mol)	49%
42	(**36**) 24.0 mg (1.43×10^{-6} mol)	50%
43	(**37**) 14.8 mg (8.60×10^{-7} mol)	60%
44	(**38**) 18.9 mg (1.14×10^{-6} mol)	55%
45	(**39**) 24.3 mg (1.37×10^{-6} mol)	68%
46	(**40**) 18.6 mg (9.64×10^{-7} mol)	39%

Table 5. Amounts used for dendrimers **41-46.**

Dendrimer **41**. ^{1}H NMR (500 MHz, d_6-DMSO) δ 8.21-7.70 (m, 1.31H), 3.33 (s, 0.90H), 3.24-2.93 (m, 3.58H), 2.79-2.45 (m, overlap with solvent peak precludes integration), 2.38 (bs, 1.00H), 2.15 (bs, 2.11H), 1.75 (s, 0.92H) ppm; ^{13}C NMR (125 MHz, d_6-DMSO) δ 172.08, 171.77, 169.91, 52.57, 50.03, 44.99, 40.90, 38.88, 38.80, 37.37, 33.74, 23.04 ppm; MALDI-TOF (pos) *m/z* = 14900.

Dendrimer **42**. ^{1}H NMR (500 MHz, d_6-DMSO) δ 8.30-7.75 (m, 1.16H), 3.31 (s, 2.52H), 3.22-2.92 (m, 3.25H), 2.74-2.46 (m, overlap with solvent peak precludes integration), 2.39 (bs, 1.00H), 2.15 (bs, 2.09H), 1.75 (s, 0.72H) ppm; ^{13}C NMR (125 MHz, d_6-DMSO) δ 172.09, 169.92, 52.57, 50.06, 40.90, 38.89, 37.37, 33.75, 23.04 ppm; MALDI-TOF (pos) *m/z* = 16100.

Dendrimer **43**. ^{1}H NMR (500 MHz, d_6-DMSO) δ 8.33-7.71 (m, 1.25H), 3.31 (s, 1.91H), 3.21-2.93 (m, 3.94H), 2.77-2.45 (m, overlap with solvent peak precludes integration), 2.39 (bs, 1.00H), 2.16 (bs, 2.54H), 1.75 (s, 0.61H) ppm; ^{13}C NMR (125 MHz, d_6-DMSO) δ 172.08, 169.92, 52.55, 50.02, 40.90, 38.89, 37.39, 33.74, 23.04 ppm; MALDI-TOF (pos) *m/z* = 16000.

Dendrimer **44**. ^{1}H NMR (500 MHz, d_6-DMSO) δ 8.30-7.73 (m, 1.06H), 6.94 (s, 0.03H), 6.56 (s, 0.02H), 3.99 (s, 0.13H), 3.32 (s, 0.95H), 3.22-2.92 (m, 3.06H), 2.74-2.45 (m, overlap with solvent peak precludes integration), 2.38 (bs, 1.00H), 2.15 (bs, 2.13H), 1.75 (s, 0.47H) ppm; ^{13}C NMR (125 MHz, d_6-DMSO) δ 172.10, 169.91, 52.54, 50.05, 40.91, 38.89, 37.41, 33.73, 23.04 ppm; MALDI-TOF (pos) *m/z* = 16500.

Dendrimer **45**. ^{1}H NMR (500 MHz, d_6-DMSO) δ 8.33-7.73 (m, 1.18H), 6.94 (s, 0.08H), 6.55 (s, 0.07H), 3.99 (s, 0.31H), 3.31 (s, 2.02H), 3.22-2.91 (m, 3.64H), 2.77-2.44 (m, overlap with solvent peak precludes integration), 2.38 (bs, 1.00H), 2.16 (bs, 2.36H), 1.75 (s, 0.41H) ppm; ^{13}C NMR (125 MHz, d_6-DMSO) δ 171.83, 160.12, 106.10, 66.23, 52.57, 50.06, 40.91, 38.89, 37.39, 33.73, 30.87, 23.04 ppm; MALDI-TOF (pos) *m/z* = 17300.

Dendrimer **46**. ^{1}H NMR (500 MHz, d_6-DMSO) δ 8.33-7.71 (m, 1.26H), 6.95 (s, 0.10H), 6.56 (s, 0.06H), 4.01 (s, 0.56H), 3.42 (s, 3.71H), 3.28-2.90 (m, 5.00H), 2.80-2.45 (m, overlap with solvent peak precludes integration), 2.38 (bs, 1.00H), 2.16 (bs, 2.42H), 1.76 (s, 0.33H) ppm; ^{13}C NMR (125 MHz, d_6-DMSO) δ 171.88, 164.20, 160.07, 126.21, 106.12, 75.35, 66.15, 62.91, 52.56, 50.88, 50.02, 44.59, 40.90, 38.88, 37.38, 35.54, 33.77 ppm; MALDI-TOF (pos) *m/z* = 17600.

3,5-Bis[3-(3-(N-oxy-2,2,6,6-tetramethyl-piperidine-4-yl)-thioureido)-propoxy]benzoamide and acetyl bifunctionalized generation 4 polyamidoamine dendrimers (47-52). Exact amounts used are summarized in table 6. Dendrimers (**41-46**) were dissolved in a 34 mM solution of NaOMe in MeOH (0.3 mL) and allowed to stir for 1 h. An additional 0.1 mL of the NaOMe solution was added to each and allowed to stir for 1.75 h. The reactions were concentrated *in vacuo*. A solution of NCS-TEMPO in DMSO (0.12 M) was made and the appropriate aliquot was added to each reaction to give 70 equivalents of NCS-TEMPO per dendrimer. The reactions were vortexed until all dendrimer went into solution, wrapped in aluminum foil, and allowed to stir at 21 °C for 23 h. After which, an additional 70 equivalents of NCS-TEMPO was added to each. The reactions were concentrated *in vacuo*, re-dissolved in a minimum amount of DMSO, and allowed to continue to stir wrapped in aluminum foil for 3 d. The reactions were dialyzed separately in DMSO (3 × 80 mL) and concentrated *in vacuo*. Another 70 equivalents of NCS-TEMPO was added to each reaction and allowed to stir for 2 d, followed by an additional 70 equivalents of NCS-TEMPO and removal of DMSO *in vacuo*. The reactions were re-dissolved in a minimum amount of DMSO and were allowed to stir for 3 d. The reactions were dialyzed in DMSO (3 × 80 mL) and concentrated *in vacuo*.

Product	**41-46** mg (mol)	% Yield[1]
47	(**41**) 2.7 mg (1.81×10^{-7} mol)	67%
48	(**42**) 3.1 mg (1.93×10^{-7} mol)	19%
49	(**43**) 3.2 mg (2.00×10^{-7} mol)	quant.
50	(**44**) 2.8 mg (1.70×10^{-7} mol)	69%
51	(**45**) 3.1 mg (1.79×10^{-7} mol)	22%
52	(**46**) 2.8 mg (1.59×10^{-7} mol)	quant.

[1.] Quant. means quantitative yield.

Table 6. Amounts used for dendrimers **47-52**.

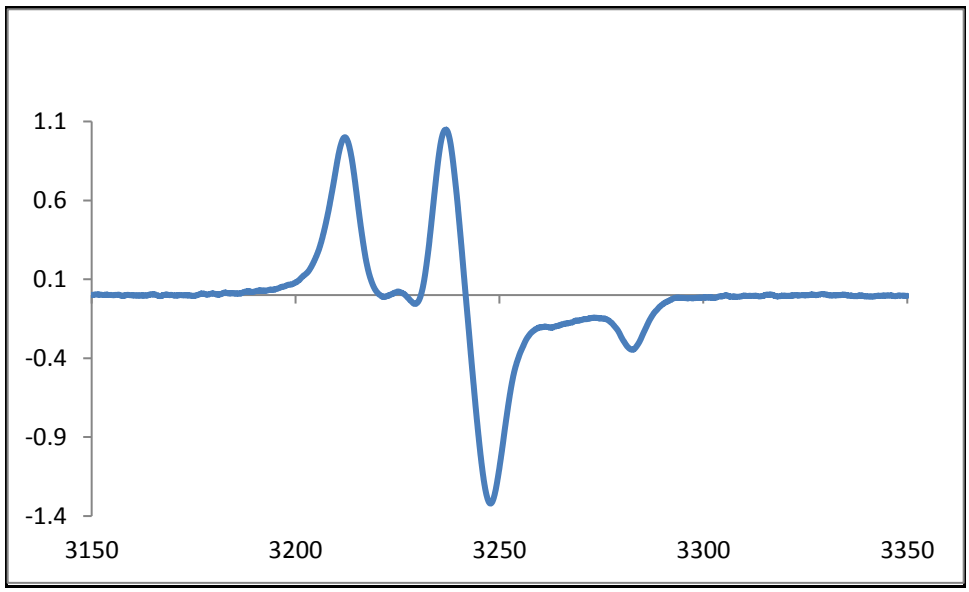


Figure 30. Dendrimer **47** EPR: A/B peak height ratio: 0.95
MALDI-TOF (pos) *m/z* = 16600.

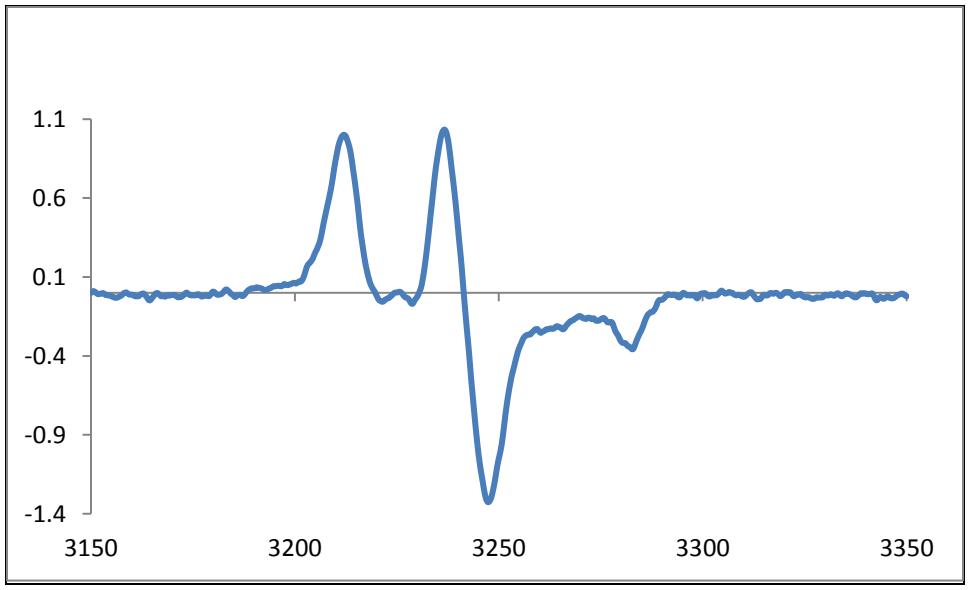


Figure 31. Dendrimer **48**. EPR: A/B peak height ratio: 0.97
MALDI-TOF (pos) *m/z* = 16900

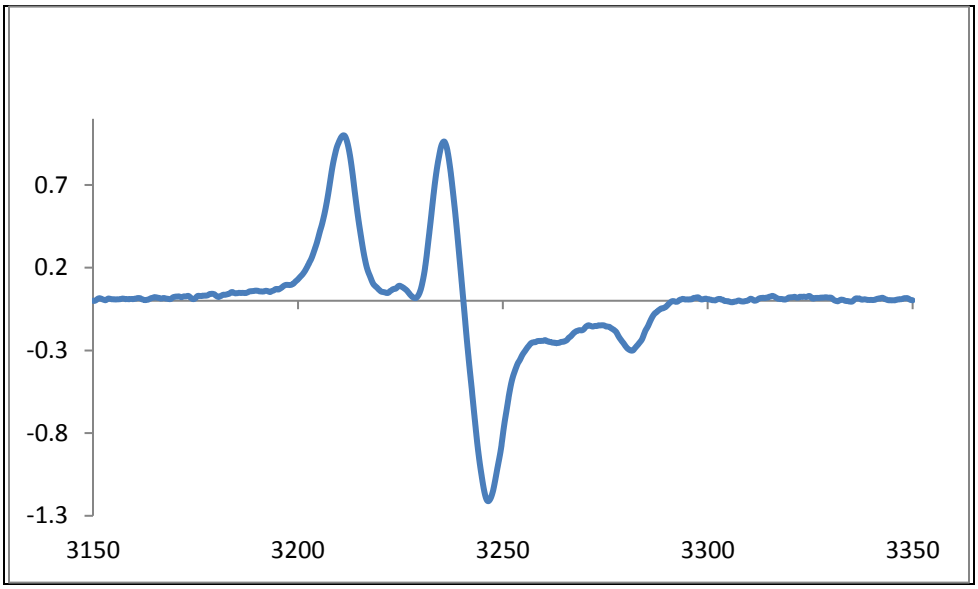


Figure 32. Dendrimer **49**. EPR: A/B peak height ratio: 1.04
MALDI-TOF (pos) *m/z* = 21300.

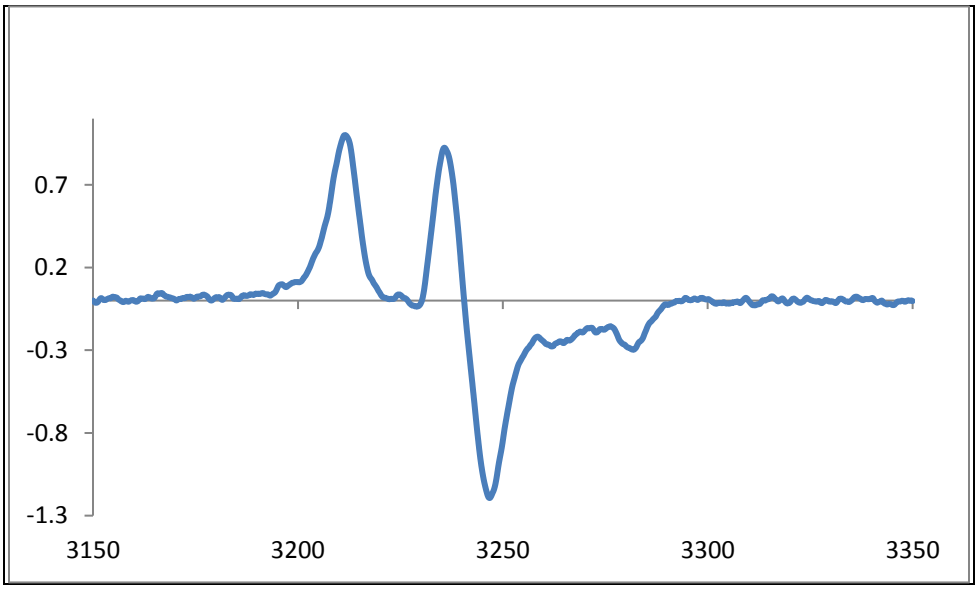


Figure 33. Dendrimer **50**. EPR: A/B peak height ratio: 1.08
MALDI-TOF (pos) *m/z* = 20800.

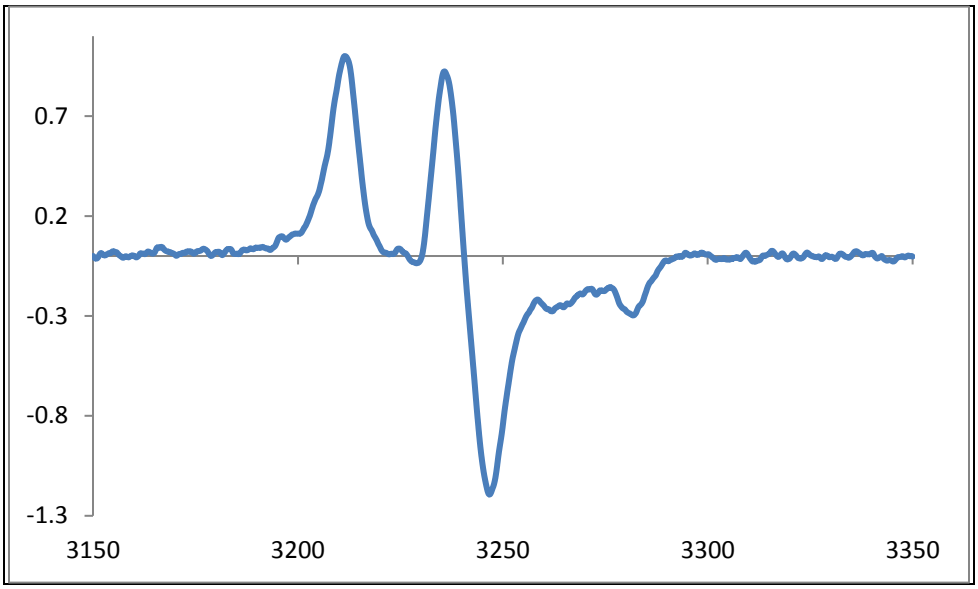


Figure 34. Dendrimer **51**. EPR: A/B peak height ratio: 1.10
MALDI-TOF (pos) *m/z* = 20800.

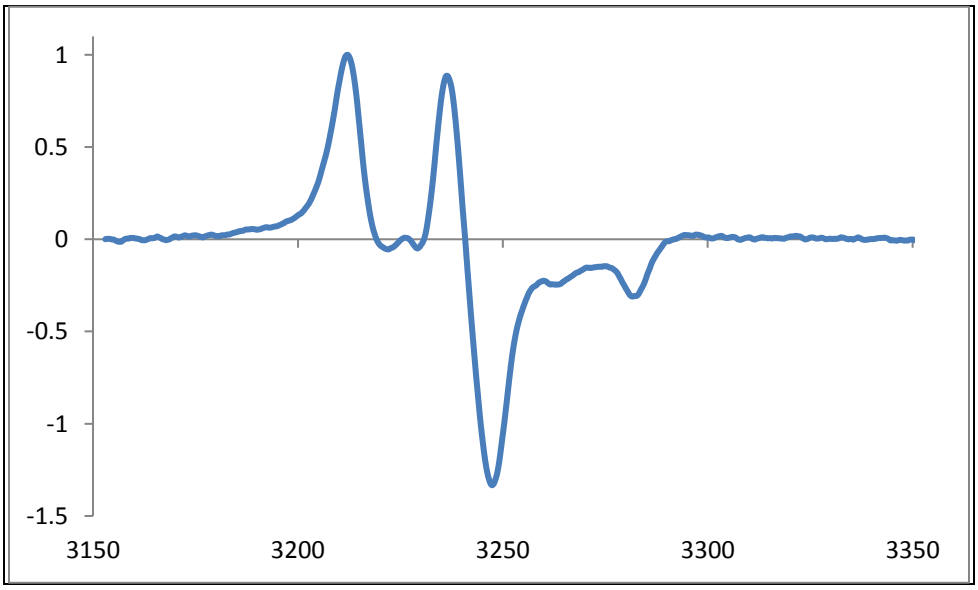


Figure 35. Dendrimer **52**. EPR: A/B peak height ratio: 1.13
MALDI-TOF (pos) *m/z* = 22500.

CHAPTER FIVE

USING INDIUM(III) AS A PROMOTER FOR GLYCOSYLATION

Contributions of Authors

Manuscript in Chapter 5

Author: Amanda L. Mattson

Contributions: Performed experiments and obtained results for all acetonide protected mannose experiments and for acetate protected mannose with 2-(2-azidoethoxy)ethyl alcohol and benzyl alcohol. Co-wrote initial draft of the manuscript.

Co-Author: Anna K. Michel

Contributions: Performed experiments and obtained results for all benzyl protected galactose experiments and for acetate protected mannose with n-butyl alcohol and t-amyl alcohol. Co-wrote initial draft of the manuscript.

Co-Author: Mary J. Cloninger

Contributions: Primary Investigator. Conceived of the project and provided funding. Provided guidance throughout the project. Provided feedback and edited drafts of the manuscript.

Manuscript Information Page

Amanda L. Mattson, Anna K. Michel, Mary J. Cloninger
Carbohydrate Research
Status of Manuscript: (Put an x in one of the options below)
____ Prepared for submission to a peer-reviewed journal
____ Officially submitted to a peer-review journal
____ Accepted by a peer-reviewed journal
_x__ Published in a peer-reviewed journal

Published by Elsevier
Carbohydrate Research 2012, 347 (1), 142–146.

Note

Using In(III) as a Promoter for Glycosylation[a]

Amanda L. Mattson, Anna K. Michel, Dr. Mary J. Cloninger*

Department of Chemistry and Biochemistry, 103 Chemistry and Biochemistry Building, Montana State University, Bozeman, MT 59717

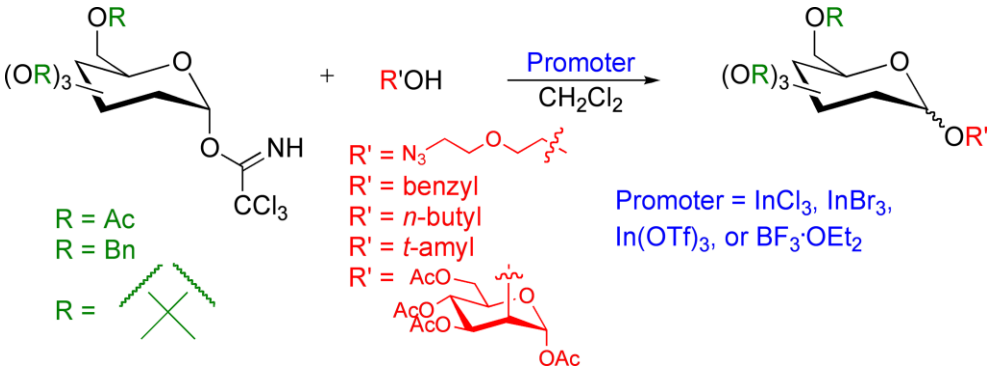
* Corresponding author. Tel: +1 406 994 3051; Fax: +1 406 994 5407; e-mail: mcloninger@chemistry.montana.edu

[a]Dedicated to Prof. Dr. András Lipták on the occassion of his 75th birthday.

Abstract. $InCl_3$, $InBr_3$, and $In(OTf)_3$ were tested as promoters in the preparation of glycosides from trichloroacetimidate precursors. A range of protecting groups and of alcohol acceptors were used to determine the versatility of these promoters. Disaccharide formation was demonstrated. In most cases, the In(III) compounds were shown to promote glycosylation better than the widely used promoter BF_3•OEt_2.

Keywords: Glycosylation, Trichloroacetimidate, Indium(III) promotion, $InBr_3$, $InCl_3$, $In(OTf)_3$

Graphical abstract.

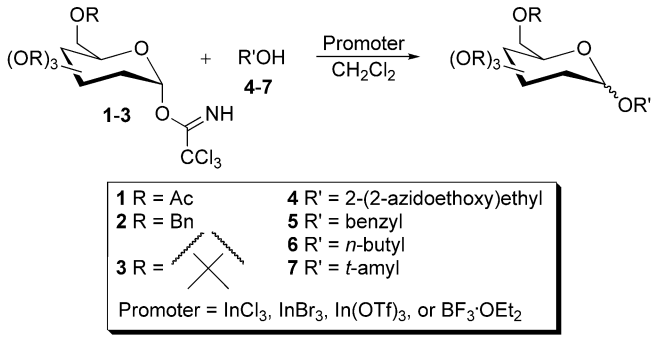


Glycosylation is one of the most widely used processes in carbohydrate chemistry. It is one of the most common post translational modifications[164] and thus is an important reaction in the synthesis and study of biologically relevant molecules. Synthetic methods of glycosylation require activation of the carbohydrate donor.[165-168] These reactions have been researched and reviewed extensively,[169, 170] and promotion of a trichloroacetimidate donor with a Lewis acid is common.[100, 168] Due to the broad scope of glycosylation reactions, there is a constant need for new promoters to fine tune the reaction for specific donors and acceptors. Several of these promoters are heavy metal based, which can be impractical due to the waste generated.[165, 171-173] BF_3•OEt_2 and TMSOTf are common alternatives as they avoid heavy metal waste,[100, 168] however these promoters are hygroscopic, and BF_3•OEt_2 requires distillation prior to use, which creates difficulty in utility.

This paper describes the use of indium(III) as an alternative to current promoters. In(III) is desirable when compared to other Lewis acids due to its stability in air and water[174, 175] and relatively low toxicity.[176] Since it is a weaker Lewis acid than the other heavy metal promoters, In(III) should be compatible with a wider range of substrates.[177] In carbohydrate synthesis, In(III) has been reported to catalyze peracetylation,[178] acetolysis, formation and hydrolysis of acetals, and formation of thioglycosides.[179, 180] In addition, $InCl_3$ has been reported as a glycosylation promoter using glycohalide donors,[181, 182] as well as peracetylated trichloroacetimidates.[183] While these sources focused on $InCl_3$, this paper broadens the scope to include other In(III) glycosylation promoters in the presence of a variety of protecting groups and alcohol acceptors.

To investigate glycosylation reactions with In(III), $InBr_3$, $InCl_3$, and $In(OTf)_3$ were used as promoters for the glycosylation of three trichloroacetimidate donors with four alcohol acceptors. The strategy for reaction development is shown in Scheme 1. Acetyl, benzyl, and acetonide protecting groups were chosen to provide a stability range that tested the limitations of the In(III) promoters. Primary, tertiary, and benzylic alcohols were chosen as glycosyl acceptors to demonstrate the steric range through which the varying In(III) compounds should be effective. The promoter BF_3•OEt_2 was used for comparison with In(III) reagents. Overall, this paper describes a simple reaction procedure for In(III) promoted glycosylation reactions.

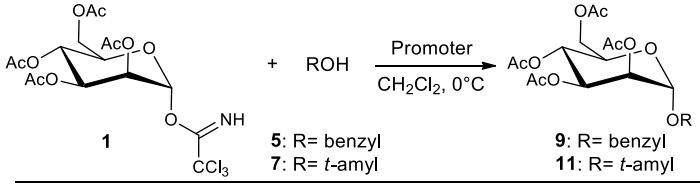
Scheme 1. In(III)-promoted glycosylation.



To identify optimal reaction conditions for each promoter, reactions were performed at a variety of different temperatures and with varying amounts of promoter. Reactions were monitored by ^1H NMR for the presence of the trichloroacetimidate starting material to determine how long the reactions should be performed. For acetyl protected mannosyl donor **1**, reactions at 0 ºC were found to be optimal. As shown in Table 1, using alcohols **5** and **7** as the acceptor, 0.5 equivalents of $InCl_3$ was necessary

with this Lewis acid. Only 10 mol % of $InBr_3$ was required (with decomposition becoming increasingly significant as larger amounts of $InBr_3$ were added). A trace amount of $In(OTf)_3$ was sufficient for glycosylation to occur in good yield. Thus, reactions using trichloroacetimidates **1**-**3** with alcohols **4**-**7** are reported using 0.1 equivalents of $InBr_3$, 0.25-0.5 equivalents of $InCl_3$, and 0.05 equivalents or a trace amount of $In(OTf)_3$. Additional optimization reactions are summarized in Table S1 of the Supplementary Data.

Table 1. Optimization of reaction conditions using **1** and **5** or **7**.

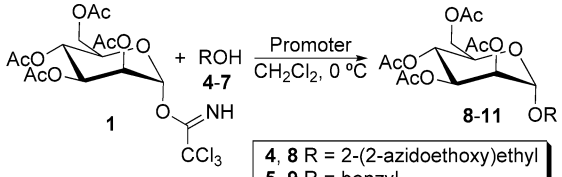


Alcohol	Promoter	Time (min)[a]	Yield (%)[b]
7	$InBr_3$ (0.9 equiv.)	20	63
7	$InBr_3$ (0.2 equiv.)	20	59
7	$InBr_3$ (0.1 equiv.)	30	75
7	$InBr_3$ (0.06 equiv.)	10	68
5	$InCl_3$ (0.5 equiv.)	20	72
5	$InCl_3$ (0.25 equiv.)	50	59
7	$In(OTf)_3$ (1.0 equiv.)	10	37
7	$In(OTf)_3$ (0.2 equiv.)	10	37
7	$In(OTf)_3$ (0.1 equiv.)	10	52
7	$In(OTf)_3$ (0.06 equiv.)	15	54
7	$In(OTf)_3$ (trace)	20	54
7	none	60	0

[a]Time to reaction completion.
[b]Yields determined by ^1H NMR spiked with a mesitylene standard.

A series of experiments were performed to compare In(III) promoters against the standard method of BF_3•OEt_2 in glycosylation promotion, and these studies are summarized in Tables 2-4. Reactions using the peracetylated mannosyl trichloroacetimidate **1** are reported in Table 2. In general, $InBr_3$ and $InCl_3$ were shown to perform better than BF_3•OEt_2, with preference toward $InBr_3$ or $InCl_3$ being acceptor dependant. With alcohols **4**-**6**, $In(OTf)_3$ afforded lower yields of glycosylation products, but this trend is not observed with trichloroacetimidates **2** and **3** (*vide infra*). NMR yields with alcohol **4** were so low that no isolated yield was attempted. Only the alpha product was observed, presumably due to the neighboring group participation of the acetyl group at C2 on the mannoside and due to the anomeric effect.

Table 2. Glycosylation results using peracetylated trichloroacetimidate **1**.



Product	Promoter (equiv.)	Time[a] (min.)	Yield (%)
8	$InBr_3$ (0.1)	30	42
8	$InCl_3$ (0.5)	20	45
8	$In(OTf)_3$ (0.05)	15	6[b]
8	BF_3•OEt_2 (0.2)	30	59
9	$InBr_3$ (0.1)	30	53
9	$InCl_3$ (0.5)	20	72
9	$In(OTf)_3$ (0.05)	15	31
9	BF_3•OEt_2 (0.2)	30	59
10	$InBr_3$ (0.1)	30	81
10	$InCl_3$ (0.5)	20	42
10	$In(OTf)_3$ (0.05)	15	33
10	BF_3•OEt_2 (0.2)	30	40
11	$InBr_3$ (0.1)	30	60
11	$InCl_3$ (0.5)	20	52
11	$In(OTf)_3$ (0.05)	15	57
11	BF_3•OEt_2 (0.2)	30	43

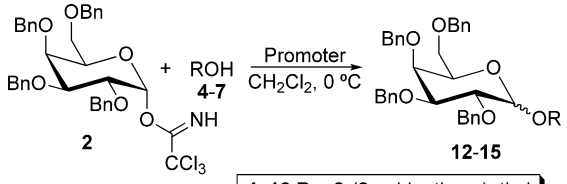
[a]Time to reaction completion.
[b]Yields determined by ^{1}H NMR spiked with a mesitylene standard.

The yields for reactions using the perbenzylated galactosyl trichloroacetimidate **2** are summarized in Table 3. Used in these catalytic amounts, In(III) was shown to be an effective promoter in all cases tested, with $In(OTf)_3$ giving yields of product formation consistently better than the BF_3•OEt_2 control. Yields for reactions with

$InBr_3$ were generally higher than those for reactions using $InCl_3$, with the exception of the more hindered alcohol **7**, which gave lower yields overall.

The experiments that are summarized in Table 3 using the perbenzylated galactosyl trichloroacetimidate **2** indicate that In(III) promoters can be catalytically used to effectively promote glycosylation reactions. However, since In(III) has been reported as a promoter of Friedel Crafts chemistry,[184, 185] formation of side products is likely to detrimentally affect reaction yields. Although the side products were not characterized, the increased complexity of the aromatic region in the ^{13}C and ^{1}H NMR spectra of crude product mixtures from **2** indicates their formation.

Table 3. Glycosylation results using perbenzylated trichloroacetimidate **2**.



4, **12** R = 2-(2-azidoethoxy)ethyl
5, **13** R = benzyl
6, **14** R = *n*-butyl
7, **15** R = *t*-amyl

Product	Promoter (equiv.)	Time[a] (min.)	Yield[b] (%)	α:β ratio[b]
12	$InBr_3$ (0.1)	30	57	1:10
12	$InCl_3$ (0.5)	20	48	1:30
12	$In(OTf)_3$ (0.05)	20	72	0:1
12	BF_3•OEt_2 (0.2)	30	65	0:1
13	$InBr_3$ (0.1)	30	61	0:1
13	$InCl_3$ (0.5)	20	53	0:1
13	$In(OTf)_3$ (0.05)	20	68	0:1
13	BF_3•OEt_2 (0.2)	30	60	0:1
14	$InBr_3$ (0.1)	30	57	0:1
14	$InCl_3$ (0.5)	20	53	0:1
14	$In(OTf)_3$ (0.05)	20	63	0:1
14	BF_3•OEt_2 (0.2)	30	61	0:1
15	$InBr_3$ (0.1)	30	30	1:3
15	$InCl_3$ (0.5)	20	33	2:7
15	$In(OTf)_3$ (0.05)	20	52	1:1
15	BF_3•OEt_2 (0.2)	30	24	2:7

[a]Time to reaction completion.
[b]Ratios determined by ^{1}H NMR after column purification.

For reactions using benzylated donor **2**, the β isomer is the major product in every case tested, and the most easily isolated, but α:β ratios vary depending on the acceptor used. Using $In(OTf)_3$ afforded the best results, but the conditions were optimized based on overall yield rather than anomeric ratios. It should be noted that time and strength of

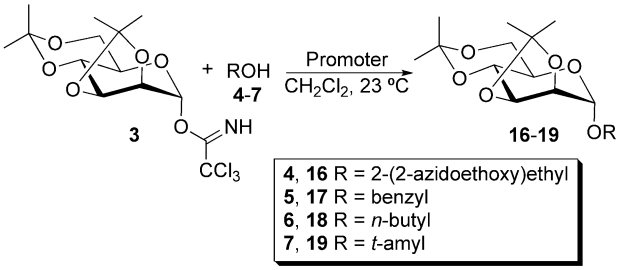
the acid promoter (as well as reaction temperature) may have a significant effect on the anomeric ratio of products. While the α product gains some anomeric stability, electrostatic interactions in the oxocarbenium ion half-chair intermediates should have a strong effect on product formation.[186] For **2**, since some unfavorable interactions are likely in both half-chairs, mixtures of α and β products form. For **3**, only one oxocarbenium ion can form, and only the α product is observed (see results below and figure S1 in the Supplementary Data for half-chair diagrams).

Products **14** and **15** were independently resubjected to the reaction conditions using one equivalent of $InBr_3$, $InCl_3$, or BF_3•OEt_2, and interconversion of the α and β isomers was not observed. The α:β ratio did change over time for **14** (see Table S3 in the Supplementary Data), but the ^{1}H NMR spectrum clearly indicated decomposition of **14**, and the α:β ratio doesn't reliably shift toward the ratio that was obtained in the reaction (in two trials, the α:β ratio shifts away from rather than toward the reaction ratio). These experiments indicate that the reaction occurs under kinetic control.

Glycosylation reactions using acetonide-protected mannoside **3** are summarized in Table 4. Optimization of these reactions requires a balance between the strength and quantity of the promoter that is present and the length of time that is required for the reaction to achieve completion. Reactions comparing temperatures and times were performed using alcohol **5**, and details are provided in Table S1 in the Supplementary Data. Above 20 mol% for $InBr_3$ and above trace amounts for $In(OTf)_3$, significant product degradation was observed. The length of reaction time required when using $InCl_3$ lead to significant product degradation. Removal of acetonide protecting groups using

$InCl_3$[187] and removal of various acetals and ketals using $In(OTf)_3$[188] have been reported. Deprotection is apparently a competitive reaction as the length of reaction and the quantity of promoter are increased, as seen by loss of protecting group peaks in the NMR spectra. Trace amounts of $In(OTf)_3$ proved to be the most effective catalyst for glycosylation of **3** and required no column chromatography for purification. No beta product was observed for reactions using acetonide-protected mannoside **3**, presumably due to the anomeric effect in conjunction with steric hindrance at the C2 position (see figure S1 in the Supplementary Information for diagrams).

Table 4. Glycosylation results using acetonide-protected trichloroacetimidate **3**.



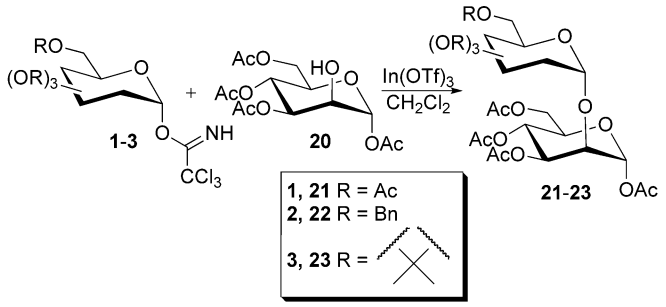
Product	Promoter (equiv.)	Time[a] (min.)	Yield (%)
16	$InBr_3$ (0.1)	25	29
16	$InCl_3$ (0.25)	45	35
16	$In(OTf)_3$ (trace)	25	92
16	$BF_3•OEt_2$ (0.2)	30	12
17	$InBr_3$ (0.1)	25	37
17	$InCl_3$ (0.25)	45	23
17	$In(OTf)_3$ (trace)	25	90
17	$BF_3•OEt_2$ (0.2)	30	20
18	$InBr_3$ (0.1)	25	12
18	$InCl_3$ (0.25)	45	0
18	$In(OTf)_3$ (trace)	25	78
18	$BF_3•OEt_2$ (0.2)	30	4
19	$InBr_3$ (0.1)	25	3
19	$InCl_3$ (0.25)	45	9
19	$In(OTf)_3$ (trace)	25	83
19	$BF_3•OEt_2$ (0.2)	30	6

[a]Time to reaction completion.

Overall, glycosylation of peracetylated mannosyl trichloroacetimidate **1** with simple alcohols afforded the highest yields using $InBr_3$ or $InCl_3$. $In(OTf)_3$ was the best promoter for reactions with perbenzylated galactosyl trichloroacetimidate **2** and acetonide protected mannosyl trichloroacetimidate **3**. Using these results, disaccharide-forming reactions were explored using **1**-**3** and acceptor **20**. Initial tests with $InBr_3$ afforded

significant amounts of unreacted **1** even when 20 mol % was used (rather than the 10 mol % that was used with **4**-**7**) and the reaction time was extended six-fold. $In(OTf)_3$ proved to be the preferred promoter for all three donors in disaccharide formation with **20**, and the results are shown in Table 5. Acetyl and acetonide protected mannosyl trichloroacetimidates gave high yields of disaccharides (78% and 94%, respectively) with only α-linked products observed and no column chromatography required in the case of acetonide protected mannosyl **3**. Benzylated galactosyl trichloroacetimidate **2** afforded a lower yield of α-linked product (27% yield) due to β product also being formed.

Table 5. $In(OTf)_3$ promoted disaccharide formations.



Product	Promoter (equiv.)	Temp (°C)	Time[a] (min.)	Yield (%)
21	$In(OTf)_3$ (0.05)	0	20	78
22	$In(OTf)_3$ (0.05)	0	30	27[b]
23	$In(OTf)_3$ (trace)	23	25	94

[a]Time to reaction completion.
[b]Yield is for α-linked product only.

In conclusion, $InBr_3$, $InCl_3$ and $In(OTf)_3$ were effective promoters of glycosylation reactions when used with the variety of protecting groups tested. With respect to acetylated mannosyl trichloroacetimidate **1**, $InBr_3$ or $InCl_3$ afforded the highest yields. All three of the In(III) promoters that were tested worked well with benzylated

galactosyl trichloroacetimidate **2**, with $In(OTf)_3$ giving slightly higher yields. When using acetonide protected mannosyl trichloroacetimidate **3**, trace amounts of $In(OTf)_3$ gave the highest yields and required no column chromatography for purification, while $InBr_3$ and $InCl_3$ gave lower yields equivalent to BF_3•OEt_2. A glycoside acceptor was also successfully added to the trichloroacetimidates using $In(OTf)_3$ as the promoter. Overall, In(III) afforded good to excellent yields of products without the requirement of distillation or an inert reaction atmosphere. The ability to vary ligands on In(III) also provides a broad range of promotion strength, enabling optimization of the conditions for desired reactions.

Experimental

General Methods

To obtain pure products, crude products were purified by column chromatography on 60 Å silica gel for acetyl protected mannosyls and benzyl protected galactosyls with hexane: ethyl acetate mobile phase in the indicated ratio. Acetonide protected manosyls were purified by column chromatography on 32-63μm neutral alumina with hexane: ethyl acetate mobile phase. An ice bath was used for reactions run at 0 °C. ^{13}C and ^{1}H NMR were recorded for purified compounds on a Bruker DRX 500 MHz Spectrometer using TMS as an internal standard. Mass spectra were obtained using a high-resolution Bruker micro-TOF system with electrospray ionization. Yields are either isolated yields or were calculated from crude ^{1}H NMR spectra using an internal mesitylene standard as specified. Ratios of alpha to beta diastereomers were determined using integrations of resonances in the ^{1}H NMR spectra or (for equivalent carbons) in the ^{13}C NMR spectra.[189]

Trichloroacetimidate starting materials[190] and acceptor **20**[191] were synthesized using previously described methods. Trace additions of $In(OTf)_3$ were performed by the addition of a visible amount less than 0.1mg.

General Procedure for Optimization of Reaction Conditions

Duplicate reactions were performed in parallel. A dry 4 mL scintillation vial was charged with the trichloroacetimidate starting material with a slight excess of alcohol and dissolved in enough dry CH_2Cl_2 to obtain a 50 mM solution of the trichloroacetimidate. The mixture was cooled if specified, and the promoter was added. BF_3•OEt_2 reactions were run under an argon atmosphere. Aliquots were taken from vial 1 and evaluated by ^{1}H NMR for reaction completion. When no starting material was observed, vial 2 was quenched with approximately 0.2 g dry $NaHCO_3$ for 20 min, diluted with 2 mL CH_2Cl_2 and filtered. The solvent was removed under reduced pressure. Yields of vial 2 were obtained from ^{1}H NMR spectra using an internal mesitylene standard. Reaction conditions for vial 2 reactions are provided in Table S1.

General Procedure for the Preparation of Mannopyranoside and Galactopyranoside Derivatives

A dry 4 mL scintillation vial was charged with the trichloroacetimidate starting material with a slight excess of alcohol and dissolved in enough dry CH2Cl2 to obtain a 50 mM solution of the trichloroacetimidate. The mixture was cooled if specified, and the promoter was added. BF3OEt2 reactions were run under an argon atmosphere. The reaction stirred for the specified time, quenched with approximately 0.2 g dry NaHCO3 for 20 min, diluted with 2mL CH2Cl2, and filtered. The solvent was removed under

reduced pressure. Chromatographic purification was performed (galactopyranoside products 8:2 hexane/EtOAc; acetyl protected mannopyranoside products either 7:3 hexane/EtOAc or 1:1 hexane/EtOAc; acetonide protected mannopyranoside products 7:3 hexane/ EtOAc + 0.5% DCM) to obtain pure samples. Exact reaction conditions are provided in Table S2 of the Supplementary data.

General Procedure for Evaluation of the Reversibility of the Reaction

A dry 2 mL scintillation vial was charged with the glycoside and a slight excess of alcohol and dissolved in enough dry CH_2Cl_2 to obtain a 50 mM solution of the trichloroacetimidate. The mixture was cooled to 0 °C, and the promoter was added. Reactions run with BF_3•OEt_2 were additionally purged with Ar. The reaction then stirred for 2h, then was diluted with 2 mL CH_2Cl_2 and quenched with 4 mL saturated $NaHCO_3$, washed with 4 mL brine, then dried over $MgSO_4$ and filtered. The solvent was removed under reduced pressure. The α:β ratios of crude products were obtained from ^{1}H NMR spectra. These reactions are summarized in Table S3 of the Supplementary Data.

General Procedure for the Preparation of Acetonide Protected Mannopyranoside Derivatives Using $In(OTf)_3$

A dry 4 mL scintillation vial was charged with the trichloroacetimidate **3** with a slight excess of alcohol and dissolved in enough dry CH_2Cl_2 to obtain a 50 mM solution of the trichloroacetimidate. Less than 0.1mg $In(OTf)_3$ was added and reaction stirred for 25 min. It was then quenched with approximately 0.2 g dry $NaHCO_3$ for 20 min. The solution was then filtered over a medium sized plug of alumina using CH_2Cl_2 as an

eluent. The solvent was removed under reduced pressure affording product with no further purification necessary.

General Procedure for Preparation of Disaccharides

A dry 4 mL scintillation vial was charged with the trichloroacetimidate starting material with a slight excess of 20 and dissolved in enough dry CH_2Cl_2 to obtain a 50 mM solution of the trichloroacetimidate. The mixture was cooled if specified, and the promoter was added. The reaction then stirred for the specified time, was quenched with 2 mL of saturated $NaHCO_3$ for 20 min, diluted with 2mL CH_2Cl_2, and filtered. The solvent was removed under reduced pressure. Chromatographic purification was performed (galactopyranoside product 6:4 hexane/EtOAc; acetyl protected mannopyranoside product 4:6 hexane/EtOAc). Acetonide protected mannopyranoside 23 was prepared via procedure 1.5 above. Exact reaction conditions are provided in Table S4 of the Supplementary data.

Acknowledgments

This work was supported by NIH R01 GM62444.

Supplementary Data

Using In(III) as a Promoter for Glycosylation

Anna K. Michel, Amanda L. Mattson, Dr. Mary J. Cloninger*

Department of Chemistry and Biochemistry, 103 Chemistry and Biochemistry Building, Montana State University, Bozeman, MT 59717

* Corresponding author. Tel: +1 406 994 3051; Fax: +1 406 994 5407; e-mail: mcloninger@chemistry.montana.edu

Table S1. Optimization of reactions for time, temperature, and promoter mole percent.

Product	Trichloro-acetimidate mg (#[a])	Alcohol mg (equiv, #)	Promoter	Promoter mg (equiv)	Temp. (°C)	Time (min.)[b]	Yield[c] (%)
11	50.5 (**1**)	9.6 (1.1, **7**)	$InBr_3$	34.1 (0.9)	0	20	63
11	48.2 (**1**)	9.6 (1.1, **7**)	$InBr_3$	8.6 (0.2)	0	20	59
11	50.7 (**1**)	9.6 (1.1, **7**)	$InBr_3$	3.8 (0.1)	0	30	75
11	100.0 (**1**)	18.9 (1.0, **7**)	$InBr_3$	4.1 (0.06)	0	10	68
11	53.8 (**1**)	14.2 (1.2, **5**)	$InCl_3$	12.3 (0.5)	0	20	55
11	53.8 (**1**)	14.2 (1.2, **5**)	$InCl_3$	5.9 (0.25)	0	50	58
11	52.7 (**1**)	12.3 (1.3, **7**)	$In(OTf)_3$	59.2 (1.0)	0	10	37
11	47.5 (**1**)	10.7 (1.3, **7**)	$In(OTf)_3$	11.3 (0.2)	0	10	37
11	47.5 (**1**)	10.4 (1.2, **7**)	$In(OTf)_3$	5.2 (0.1)	0	10	52
11	97.1 (**1**)	23.7 (1.2, **7**)	$In(OTf)_3$	6.7 (0.06)	0	15	54
11	104.7 (**1**)	24.3 (1.3, **7**)	$In(OTf)_3$	trace	0	20	54
11	50.7 (**1**)	10.9 (1.2, **7**)	$BF_3{\bullet}OEt_2$	2.9 (0.2)	0	30	53
11	100.1 (**1**)	28.9 (1.6, **7**)	$BF_3{\bullet}OEt_2$	121.4 (1.1)	0	120	61
14	51.9 (**2**)	7.1 (1.3, **6**)	$InBr_3$	25.2 (0.9)	0	30	decomp
14	50.5 (**2**)	6.2 (1.1, **6**)	$InBr_3$	1.0 (0.04)	0	45	65
14	50.9 (**2**)	5.9 (1.1, **6**)	$InBr_3$	2.5 (0.1)	0	30	67
14	48.7 (**2**)	7.3 (1.4, **6**)	$InCl_3$	16.0 (1.0)	0	45	50
14	50.3 (**2**)	7.7 (1.4, **6**)	$In(OTf)_3$	41.5 (1.0)	0	20	70
14	53.0 (**2**)	7.6 (1.3, **6**)	$In(OTf)_3$	4.1 (0.09)	0	20	78
14	52.0 (**2**)	5.6 (1.0, **6**)	$In(OTf)_3$	1.7 (0.04)	0	15	71
17	52.5 (**3**)	16.8 (1.2, **5**)	$InBr_3$	4.8 (0.1)	0	25	37
17	50.5 (**3**)	16.2 (1.2, **5**)	$InBr_3$	4.7 (0.1)	23	25	38
17	51.2 (**3**)	16.4 (1.2, **5**)	$BF_3{\bullet}OEt_2$	3.2 (0.2)	0	30	30
17	50.0 (**3**)	16.2 (1.2, **5**)	$BF_3{\bullet}OEt_2$	3.1 (0.2)	23	30	41
17	51.7 (**3**)	16.6 (1.2, **5**)	$InBr_3$	45.1 (1.0)	23	10	trace
17	51.6 (**3**)	16.5 (1.2, **5**)	$InBr_3$	9.4 (0.2)	23	20	30
17	51.8 (**3**)	16.6 (1.2, **5**)	$InBr_3$	4.7 (0.1)	23	25	42
17	105.5 (**3**)	33.8 (1.2, **5**)	$InBr_3$	4.7 (0.05)	23	30	40
17	44.6 (**3**)	14.3 (1.2, **5**)	$InCl_3$	12.1 (0.5)	23	20	13
17	42.4 (**3**)	13.6 (1.2, **5**)	$InCl_3$	6.4 (0.28)	23	45	21
17	53.8 (**3**)	17.2 (1.2, **5**)	$In(OTf)_3$	3.7 (0.05)	23	20	33
17	51.6 (**3**)	16.5 (1.2, **5**)	$In(OTf)_3$	trace	23	25	73
17	50.6 (**3**)	16.2 (1.2, **5**)	$BF_3{\bullet}OEt_2$	3.5 (0.2)	23	30	41
17	51.5 (**3**)	16.5 (1.2, **5**)	$BF_3{\bullet}OEt_2$	1.8 (0.1)	23	-	-

[a]# means the compound number, shown in Scheme 1 of the primary manuscript.
[b] dash indicates reaction never completed
[c]Yields determined by ^1H NMR spiked with a mesitylene standard.

Table S2. Conditions for glycosylation of trichloroacetimidates **1**–**3**.

Product	Trichloro-acetimidate mg (#[a])	Alcohol mg (equiv, #)	Promoter	Promoter mg (equiv)	Temp (°C)	Time (min.)	Yield (%)	α:β Ratio[b]
8	52.8 (**1**)	16.9 (1.2, **4**)	$InBr_3$	4.5 (0.1)	0	30	42	1:0
8	52.2 (**1**)	16.7(1.2, **4**)	$InCl_3$	11.1 (0.5)	0	20	45	1:0
8	32.8 (**1**)	10.5 (1.2, **4**)	$In(OTf)_3$	2.1 (0.06)	0	15	6[c]	1:0
8	49.7 (**1**)	15.9 (1.2, **4**)	$BF_3•OEt_2$	2.9 (0.2)	0	30	59	1:0
9	54.0 (**1**)	14.2 (1.2, **5**)	$InBr_3$	4.2 (0.1)	0	30	53	1:0
9	53.8 (**1**)	14.2 (1.2, **5**)	$InCl_3$	12.3 (0.5)	0	20	72	1:0
9	53.6 (**1**)	14.1 (1.2, **5**)	$In(OTf)_3$	3.5 (0.06)	0	15	31	1:0
9	49.8 (**1**)	13.1 (1.2, **5**)	$BF_3•OEt_2$	2.9 (0.2)	0	30	59	1:0
10	49.6 (**1**)	9.0 (1.2, **6**)	$InBr_3$	3.8 (0.1)	0	30	81	1:0
10	51.0 (**1**)	9.2 (1.2, **6**)	$InCl_3$	11.4(0.5)	0	20	42	1:0
10	53.0 (**1**)	9.6 (1.2, **6**)	$In(OTf)_3$	2.8 (0.05)	0	15	33	1:0
10	49.2 (**1**)	8.9 (1.2, **6**)	$BF_3•OEt_2$	2.8 (0.2)	0	30	40	1:0
11	49.5 (**1**)	10.6 (1.2, **7**)	$InBr_3$	4.0 (0.1)	0	30	60	1:0
11	53.3 (**1**)	11.5 (1.2, **7**)	$InCl_3$	12.6 (0.5)	0	20	52	1:0
11	53.9 (**1**)	11.6 (1.2, **7**)	$In(OTf)_3$	3.4 (0.06)	0	15	57	1:0
11	52.4 (**1**)	11.3 (1.2, **7**)	$BF_3•OEt_2$	3.0 (0.2)	0	30	43	1:0
12	33.6 (**2**)	7.7 (1.2, **4**)	$InBr_3$	2.0 (0.1)	0	30	57	1:10
12	35.9 (**2**)	8.2 (1.2, **4**)	$InCl_3$	6.0 (0.5)	0	45	48	1:30
12	36.0 (**2**)	8.3(1.2, **4**)	$In(OTf)_3$	1.7 (0.06)	0	20	72	0:1
12	32.3 (**2**)	7.4 (1.2, **4**)	$BF_3•OEt_2$	1.3 (0.2)	0	30	65	0:1
13	34.9(**2**)	6.6 (1.2, **5**)	$InBr_3$	2.4 (0.1)	0	30	61	0:1
13	30.6 (**2**)	5.8 (1.2, **5**)	$InCl_3$	4.8 (0.5)	0	45	53	0:1
13	31.1 (**2**)	5.9 (1.2, **5**)	$In(OTf)_3$	1.2 (0.05)	0	20	68	0:1
13	33.5 (**2**)	6.3 (1.2, **5**)	$BF_3•OEt_2$	1.3 (0.2)	0	30	60	0:1
14	31.2 (**2**)	4.1 (1.2, **6**)	$InBr_3$	1.7 (0.1)	0	30	57	0:1
14	32.2 (**2**)	4.2 (1.2, **6**)	$InCl_3$	5.2 (0.5)	0	45	53	0:1
14	32.9 (**2**)	4.3 (1.2, **6**)	$In(OTf)_3$	1.5 (.06)	0	20	63	0:1
14	32.0 (**2**)	4.2 (1.2, **6**)	$BF_3•OEt_2$	1.3 (0.2)	0	120	61	0:1
15	33.5 (**2**)	5.2 (1.2, **7**)	$InBr_3$	2.5 (0.1)	0	30	30	1:3
15	34.9 (**2**)	5.4(1.2, **7**)	$InCl_3$	5.4 (0.5)	0	45	33	2:7
15	32.4 (**2**)	5.0 (1.2, **7**)	$In(OTf)_3$	1.2 (0.05)	0	20	52	1:1
15	35.7 (**2**)	6.8 (1.2, **7**)	$BF_3•OEt_2$	1.5 (0.2)	0	120	25	2:7

[a]# means the compound number, shown in Scheme 1 of the primary manuscript.
[b]Ratios determined by ^1H NMR
[c]Yields determined by ^1H NMR spiked with a mesitylene standard.

Table S2 continued. Conditions for glycosylation of trichloroacetimidates **1**–**3**.

Product	Trichloro-acetimidate mg (#[a])	Alcohol mg (equiv, #)	Promoter	Promoter mg (equiv)	Temp. (°C)	Time (min.)	Yield (%)	α:β Ratio[b]
16	45.6(**3**)	19.2 (1.3, **4**)	$InBr_3$	3.7 (0.1)	23	25	29	1:0
16	44.7 (**3**)	18.8 (1.3, **4**)	$InCl_3$	6.7 (0.28)	23	45	35	1:0
16	43.2 (**3**)	18.2 (1.3, **4**)	$In(OTf)_3$	trace	23	30	92	1:0
16	43.8 (**3**)	18.5 (1.3, **4**)	BF_3•OEt_2	3.1 (0.2)	23	30	12	1:0
17	45.4 (**3**)	14.6 (1.2, **5**)	$InBr_3$	4.9 (0.1)	23	25	37	1:0
17	42.5 (**3**)	13.6 (1.2, **5**)	$InCl_3$	5.6 (0.24)	23	45	23	1:0
17	40.8 (**3**)	13.1 (1.2, **5**)	$In(OTf)_3$	trace	23	25	90	1:0
17	44.7 (**3**)	14.3 (1.2, **5**)	BF_3•OEt_2	3.1 (0.2)	23	30	20	1:0
18	43.4 (**3**)	9.5 (1.2, **6**)	$InBr_3$	4.8 (0.1)	23	25	12	1:0
18	43.0 (**3**)	9.5 (1.2, **6**)	$InCl_3$	6.1 (0.26)	23	45	0	1:0
18	43.2 (**3**)	9.5 (1.2, **6**)	$In(OTf)_3$	trace	23	25	78	1:0
18	43.1 (**3**)	9.5 (1.2, **6**)	BF_3•OEt_2	3.0 (0.2)	23	30	4	1:0
19	43.5 (**3**)	11.4 (1.2, **7**)	$InBr_3$	3.8 (0.1)	23	25	3	1:0
19	46.3 (**3**)	12.1 (1.2, **7**)	$InCl_3$	6.1 (0.24)	23	60	9	1:0
19	44.8 (**3**)	11.7 (1.2, **7**)	$In(OTf)_3$	trace	23	25	83	1:0
19	44.9 (**3**)	11.7 (1.2, **7**)	BF_3•OEt_2	3.1 (0.2)	23	30	6	1:0

[a]# means the compound number, shown in Scheme 1 of the primary manuscript.
[b]Ratios determined by ^{1}H NMR or ^{13}C NMR when specified.
[c]Yields determined by ^{1}H NMR spiked with a mesitylene standard.

Table S3. Reactions testing the reversibility of In(III)-promoted glycosylation.

Product	Glycoside mg (α:β)	Alcohol mg (equiv, #[a])	Promoter	Promoter mg (equiv)	Temp. (°C)	α:β Ratio[b]
14	51.8 (0:1)	10.4 (1.8, **6**)	BF_3•OEt_2	15.5 (1.4)	0	0:1
14	50.3 (0:1)	9.6 (1.8, **6**)	$InCl_3$	18.4 (1.1)	0	0:1
14	51.9 (0:1)	9.7 (1.7, **6**)	$InBr_3$	31.1 (1.2)	0	0:1
15	12.4 (1:7)	2.5 (1.4, **7**)	BF_3•OEt_2	3.3 (1.1)	0	1:9
15	12.1 (1:7)	2.5 (1.4, **7**)	$InCl_3$	5.3 (1.2)	0	1:5
15	10.7 (1:7)	2.4 (1.6, **7**)	$InBr_3$	7.7 (1.2)	0	1:2

[a]# means the compound number, shown in Scheme 1 of the primary manuscript.
[b]Yields determined by ^{1}H NMR spiked with a mesitylene standard.

Table S4. Conditions for formation of disaccharides **21-23**.

Product	Trichloro-acetimidate mg (#[a])	Acceptor sugar (20) mg (equiv)	$In(OTf)_3$ mg (equiv)	Temp. (°C)	Time (min.)	Yield[b] (%)	α:β Ratio[b]
21	55.5 (**1**)	47.9 (1.2)	3.2 (0.05)	0	20	78	1:0
22	38.0 (**2**)	23.5 (1.2)	1.5 (0.05)	0	30	27	1:0
23	45.9 (**3**)	43.6 (1.1)	trace	23	25	94	1:0

[a]# means the compound number, shown in Scheme 1 of the primary manuscript.
[b]Ratios determined by ^{1}H NMR.

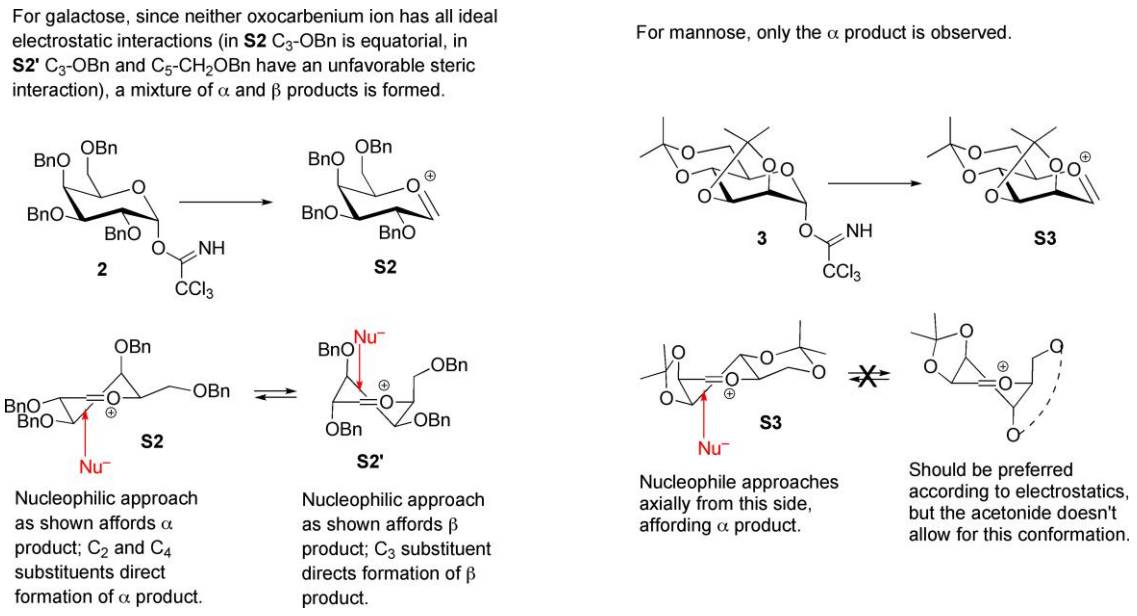


Figure S1. Half-chair diagrams to rationalize product formations.[186]

5-Azido-3-oxapentyl 2,3,4,6-tetra-*O*-acetyl-α-D-mannopyranoside (8). ^{1}H NMR (500 MHz, $CDCl_3$) δ 5.33 (dd, 1H, *J* = 10.0, 2.9 Hz, H-3), 5.29 - 5.21 (m, 2H, H-2, H-4), 4.84 (ap. s, 1H, H-1), 4.25 (dd, 1H, *J* = 12.4, 4.9 Hz, H-6a), 4.09 - 4.00 (m, 2H, H-6b, H-5), 3.79 (dd, 1H, *J* = 13.0, 5.8 Hz, C**H**$_2$$CH_2OCH_2$), 3.67 - 3.59 (m, 5H, C**H**$_2$C**H**$_2$OC**H**$_2$), 3.41 - 3.31 (m, 2H, C**H**$_2$$N_3$), 2.11 (s, 3H, COC**H**$_3$), 2.06 (s, 3H, COC**H**$_3$), 2.00 (s, 3H, COC**H**$_3$), 1.95 (s, 3H, COC**H**$_3$) ppm; ^{13}C NMR (125 MHz, $CDCl_3$) 170.7, 170.0, 169.9, 169.7, 97.7, 70.2, 70.0, 69.5, 69.0, 68.4, 67.3, 66.1, 62.4, 50.7, 20.9, 20.7 (3C) ppm; HRMS (micro-TOF) *m/z* 484.1505 (calculated *m/z* M+Na = 484.1543 for $C_{18}H_{27}N_3O_{11}Na$).

Benzyl 2,3,4,6-tetra-*O*-acetyl-α-D-mannopyranoside (9). ^{1}H NMR (500 MHz, $CDCl_3$) δ 7.36 - 7.26 (m, 5H, CH_2Ph-**H**), 5.33 (dd, 1H, *J* = 10.0, 3.1 Hz, H-3), 5.28 - 5.22 (m, 2H,

H-2, H-4), 4.85 (ap. s, 1H, H-1), 4.67 (d, 1H, *J* = 11.9 Hz, C**H₂**Ph-H), 4.53 (d, 1H, *J* = 11.9 Hz, C**H₂**Ph-H), 4.24 (dd, 1H, *J* = 12.1, 4.8 Hz, H-6a), 4.03 - 3.93 (m, 2H, H-6b, H-5), 2.10 (s, 3H, COC**H₃**), 2.07 (s, 3H, COC**H₃**), 1.99 (s, 3H, COC**H₃**), 1.95 (s, 3H, COC**H₃**) ppm; ^{13}C NMR (125 MHz, $CDCl_3$) 170.7, 170.0, 169.9, 169.8, 136.2, 129.7, 128.6, 128.2, 128.2, 96.7, 69.8, 69.5, 69.1, 68.6, 66.1, 62.4, 20.9, 20.7 (3C) ppm; HRMS (micro-TOF) *m/z* 461.1413 (calculated *m/z* M+Na = 461.1424 for $C_{21}H_{26}O_{10}Na$). Consistent NMR with literature values.[192]

Butyl 2,3,4,6-tetra-*O*-acetyl-α-D-mannopyranoside (10). ^{1}H NMR (500 MHz, $CDCl_3$) δ 5.32 (dd, 1H, *J* = 3.1, 10.0 Hz, H-3), 5.25 (t, 1H, *J* = 10.0 Hz, H-4), 5.21 (ap. s, 1H, H-2), 4.78 (s, 1H, H-1), 4.25 (dd, 1H, *J* = 5.3, 12.2 Hz, H-6a), 4.08 (appt. d, 1H, *J* = 12.2, H-6b), 3.92-3.99 (m, 1H, H-5), 3.61-3.70 (m, 1H OC**H₂**CH_2), 3.39-3.47 (m, 1H, OC**H₂**CH_2), 2.13 (s, 3H, COC**H₃**), 2.08 (s, 3H, COC**H₃**), 2.02 (s, 3H, COC**H₃**), 1.97 (s, 3H, COC**H₃**), 1.50-1.59 (m, 2H, OCH_2C**H₂**CH_2), 1.31-1.42 (m, 2H, CH_2C**H₂**CH_3), 0.91 (t, 3H, J = 7.4 Hz, CH_2C**H₃**); ^{13}C NMR (125 MHz, $CDCl_3$) 170.7, 170.1, 169.9, 169.8, 97.6, 69.7, 69.1, 68.4, 68.2, 66.3, 62.5, 31.3, 20.9, 20.7, 19.3, 13.8 ppm; HRMS (micro-TOF) *m/z* 427.1565 (calculated *m/z* M+Na = 427.1580 for $C_{18}H_{28}O_{10}Na$).

2-Methylbutyl 2,3,4,6-tetra-*O*-acetyl-α-D-mannopyranoside (11). ^{1}H NMR (500 MHz, $CDCl_3$) δ 5.37 (dd, 1H, *J* = 3.0, 10.0 Hz, H-3), 5.23 (t, 1H, *J* = 10.0 Hz, H-4), 5.07 (s, 1H, H-1), 5.02 (ap. s, 1H, H-2), 4.24 (dd, 1H, *J* = 5.4, 12.0 Hz, H-6a), 4.11-4.17 (m, 1H, H-5), 4.03 (d, 1H, *J* = 12.0 Hz, H-6b), 2.13 (s, 3H, COC**H₃**), 2.06 (s, 3H, COC**H₃**), 2.02 (s, 3H, COC**H₃**), 1.97 (s, 3H, COC**H₃**), 1.44-1.61 (m, 2H, CC**H₂**CH_3), 1.18 (d, 6H, *J* = 3.9 Hz, OC(C**H₃**)**₂**), 0.87 (t, 3H, *J* = 7.4 Hz, CH_2C**H₃**); ^{13}C NMR (125 MHz, $CDCl_3$) 170.7, 170.3, 170.0, 169.8, 92.0, 78.9, 71.3, 69.1, 68.1, 66.5, 62.7, 34.0, 25.8, 25.3, 21.0, 20.7, 8.4 ppm; HRMS (micro-TOF) *m/z* 441.1719 (calculated *m/z* M+Na = 441.1737 for $C_{19}H_{30}O_{10}Na$).

5-Azido-3-oxapentyl 2,3,4,6-tetra-*O*-benzyl-D-galactopyranoside (12). The values listed are for the β-product. ^{1}H NMR (500 MHz, $CDCl_3$) δ 7.22-7.39 (m, 20H, CH_2Ph**H**), 4.91-4.95 (m, 2H, C**H₂**Ph), 4.76 (d, 1H, *J* = 11.3 Hz, C**H₂**Ph), 4.72 (q, 2H, *J* = 11.8 Hz, C**H₂**Ph), 4.61 (d, 1H, *J* = 11.3 Hz, C**H₂**Ph), 4.37-4.41 (m, 3H, C**H₂**Ph and H-1), 4.02 (appt. m, 1H, H-5), 3.88 (d, 1H, *J* = 2.7 Hz, H-4), 3.81 (dd, 1H, *J* = 7.7, 9.7 Hz, H-2), 3.71-3.77 (m, 1H, H-6a), 3.66-3.71 (m, 1H, H-6b), 3.61 (ddd, 2H, *J* = 2.8, 4.4, 6.0 Hz, OC**H₂**CH_2OCH_2), 3.50-3.58 (m, 5H, H-3 and CH_2C**H₂**OC**H₂**CH_2) 3.27 (dd, 2H, *J* = 4.4, 9.2 Hz, CH_2C**H₂**N_3); ^{13}C NMR (125 MHz, $CDCl_3$) 138.9, 138.6, 138.5, 137.9, 127.5-128.4 (20C), 104.1, 82.1, 79.4, 75.0, 74.5, 73.5, 73.5, 73.4, 73.0, 70.4, 69.9, 69.0, 68.8, 50.7 ppm; HRMS (micro-TOF) *m/z* 676.2964 (calculated *m/z* M+Na = 676.2999 g/mol for $C_{38}H_{43}N_3O_7Na$).

Benzyl 2,3,4,6-tetra-*O*-benzyl-D-galactopyranoside (13). ^{1}H NMR (500 MHz, $CDCl_3$) Spectrum is not readily assignable but is provided below. ^{13}C NMR (125 MHz, $CDCl_3$) 102.88 (C1- β), 96.06 (C1-α); 13C peaks are consistent with literature.[189] HRMS (micro-TOF) *m/z* 653.2840 (calculated *m/z* M+Na = 653.2879 for $C_{41}H_{42}O_6Na$).

Butyl 2,3,4,6-tetra-*O*-benzyl-D-galactopyranoside (14). The values listed are for the β-product. ^{1}H NMR (500 MHz, $CDCl_3$) δ 7.24-7.43 (m, 20H, $CH_2Ph\mathbf{H}$), 4.95 (m, 2H, $C\mathbf{H_2}Ph$), 4.76 (m, 2H, $C\mathbf{H_2}Ph$), 4.73 (d, 1H, *J* = 11.8 Hz, $C\mathbf{H_2}Ph$), 4.64 (d, 1H, *J* = 11.8 Hz, $C\mathbf{H_2}Ph$), 4.44 (m, 2H, $C\mathbf{H_2}Ph$), 4.37 (d, 1H, *J* = 7.7, H-1), 3.93-4.01 (m, 1H, H-5), 3.90 (d, 1H, *J* = 2.7 Hz, H-4), 3.83 (dd, 1H, J *J* = 7.7, 9.7 Hz, H-2), 3.60 (dd, 2H, *J* = 1.6, 6.3 Hz, H-6a and H-6b), 3.50-3.55 (m, 3H, H-3 and $OC\mathbf{H_2}CH_2$), 1.57-1.71 (m, 2H, $CH_2C\mathbf{H_2}CH_2$), 1.35-1.5 (m, 2H $CH_2C\mathbf{H_2}CH_3$), 0.93 (t, 3H, *J* = 7.4 Hz, $CH_2C\mathbf{H_3}$); ^{13}C NMR (125 MHz, $CDCl_3$) 138.8, 138.7, 138.6, 138.0, (4C, quat. Cs) 127.6-128.4 (20C, aromatic Cs), 104.0 (C_1), 82.3, 79.6, 75.2, 74.5, 73.6 (2C), 73.4, 73.1, 69.6, 68.9, 31.8, 19.4, 13.9 ppm; HRMS (micro-TOF) *m/z* 619.2865 (calculated *m/z* M+Na = 619.3036 for $C_{38}H_{44}O_6Na$).

2-Methylbutyl 2,3,4,6-tetra-*O*-benzyl-D-galactopyranoside (15). The values listed are for the α-product. ^{1}H NMR (500 MHz, $CDCl_3$) δ 7.20-7.38 (m, 20H, $CH_2Ph\mathbf{H}$), 5.15 (d, 1H, *J* = 3.6 Hz, H-1), 4.94 (d, 1H, *J* = 11.4 Hz, $C\mathbf{H_2}Ph$), 4.79 (d, 1H, *J* = 11.7 Hz, $C\mathbf{H_2}Ph$), 4.73 (t, 2H, *J* = 12.0 Hz, $C\mathbf{H_2}Ph$), 4.67 (d, 1H, *J* = 11.7 Hz, $C\mathbf{H_2}Ph$), 4.54 (d, 1H, *J* = 11.4 Hz, $C\mathbf{H_2}Ph$), 4.42 (m, 2H, $C\mathbf{H_2}Ph$), 4.12 (m, 1H, H-5), 3.97-4.01 (m, 2H, H-4 and H-2), 3.94 (dd, 1H, *J* = 2.6, 10.2 Hz, H-3), 3.55 (m, 1H, H-6a) 3.46 (dd, 1H, *J* = 5.7, 9.1 Hz, H-6b), 1.45-1.61 (m, 2H, $CC\mathbf{H_2}CH_3$), 1.17 (s, 6H, $OC(C\mathbf{H_3})_2$), 0.88 (t, 3H, *J* = 7.5 Hz, $CH_2C\mathbf{H_3}$); ^{13}C NMR (125 MHz, $CDCl_3$) 140.0, 138.9, 138.8, 138.1, 127.3-128.3 (20C), 91.9, 79.2, 77.2, 76.7, 75.2, 74.7, 73.4, 73.2, 72.8, 69.0, 68.8, 34.6, 25.8, 25.5, 8.6 ppm; HRMS (micro-TOF) *m/z* 633.3163 (calculated *m/z* M+Na = 633.3192 for $C_{39}H_{46}O_6Na$).

5-Azido-3-oxapentyl 2,3:4,6-di-*O*-isopropylidene-α-D-mannopyranoside (16). ^{1}H NMR (500 MHz, $CDCl_3$) δ 4.99 (s, 1H, H-1), 4.75 (dd, 1H, *J* = 5.8, 3.6 Hz, H-3), 4.60 (d, 1H, *J* = 5.8 Hz, H-2) 4.40 - 4.34 (m, 1H, H-5), 4.10 - 4.05 (m, 1H, H-6e), 4.01 (dd, 1H, *J* = 8.6, 4.2 Hz , H-6a), 3.93 (dd, 1H, *J* = 7.6, 3.6 Hz, H-4), 3.73 - 3.76 (m, 1H, $C\mathbf{H_2}CH_2OCH_2$), 3.54 - 3.67 (m, 5H, $C\mathbf{H_2}C\mathbf{H_2}OC\mathbf{H_2}$), 3.36 (t, 2H, *J* = 4.5 Hz, $C\mathbf{H_2}N_3$), 1.43 (s, 3H, $C(C\mathbf{H_3})$), 1.42 (s, 3H, $C(C\mathbf{H_3})$), 1.35 (s, 3H, $C(C\mathbf{H_3})$), 1.29 (s, 3H, $C(C\mathbf{H_3})$) ppm; ^{13}C NMR (125 MHz, $CDCl_3$) 112.6, 109.2, 106.4, 85.0, 80.3, 79.4, 73.1, 70.2, 70.0, 66.8, 66.4, 50.6, 26.9, 25.8, 25.1, 24.5 ppm; HRMS (micro-TOF) *m/z* 374.1922 (calculated *m/z* M+H = 374.1927 for $C_{16}H_{28}N_3O_7$).

Benzyl 2,3:4,6-di-*O*-isopropylidene-α-D-mannopyranoside (17). ^{1}H NMR (500 MHz, $CDCl_3$) δ 7.36 - 7.26 (m, 5H), 5.06 (s, 1H), 4.78 (dd, 1H, J = 5.9, 3.6 Hz), 4.63 (ap. dd, 2H, *J* = 8.9, 6.7 Hz), 4.47 (d, 1H, *J* = 11.9 Hz), 4.39 (ddd, 1H, *J* = 7.7, 6.3, 4.3 Hz), 4.09 (dd, 1H, *J* = 8.7, 6.3 Hz), 3.99 - 3.93 (m, 2H), 1.44 (s, 3H), 1.44 (s, 3H), 1.37 (s, 3H), 1.30 (s, 3H) ppm; ^{13}C NMR (125 MHz, $CDCl_3$) 137.3, 128.5, 128.0, 127.9, 112.6, 109.2, 105.6, 85.1, 80.4, 79.6, 73.1, 69.1, 66.9, 26.9, 25.9, 25.2, 24.5 ppm; HRMS (micro-TOF) *m/z* 351.1801 (calculated *m/z* M+H = 351.1808 for $C_{19}H_{27}O_6$) Consistent with literature values.[193]

Butyl 2,3:4,6-di-O-isopropylidene-α-D-mannopyranoside (18). ^{1}H NMR (500 MHz, $CDCl_3$) δ 4.94 (s, 1H, H-1), 4.75 (dd, 1H, *J* = 5.8, 3.6 Hz, H-3), 4.55 (d, 1H, *J* = 5.8 Hz, H-2), 4.40 - 4.34 (m, 1H, H-5), 4.11 - 4.06 (m, 1H, H-6e), 4.01 (dd, 1H, *J* = 8.6, 4.2 Hz, H-6a), 3.89 (dd, 1H, *J* = 7.3, 3.6 Hz, H-4), 3.59 (dt, 1H, *J* = 9.6, 6.7 Hz, OC**H₂**CH_2), 3.35 (dt, 1H, *J* = 9.6, 6.7 Hz, OC**H₂**CH_2), 1.55 – 1.46 (m, 2H, OCH_2C**H₂**), 1.44 (s, 3H, C(C**H₃**)), 1.43 (s, 3H, C(C**H₃**)), 1.35 (s, 3H, C(C**H₃**)), 1.34 - 1.30 (m, 2H, CH_2C**H₂**CH_3), 1.29 (s, 3H, C(C**H₃**)), 0.88 (t, 3H, *J* = 7.4 Hz, CH_2C**H₃**) ppm; ^{13}C NMR (125 MHz, $CDCl_3$) 112.5, 109.2, 106.3, 85.1, 80.2, 79.5, 73.2, 67.2, 67.0, 31.4, 26.9, 25.9, 25.2, 24.5, 19.2, 13.8 ppm; HRMS (micro-TOF) *m/z* 317.1950 (calculated *m/z* M+H = 317.1964 for $C_{16}H_{29}O_6$)

2-Methylbutyl 2,3:4,6-di-O-isopropylidene-α-D-mannopyranoside (19). ^{1}H NMR (500 MHz, $CDCl_3$) δ 5.21 (ap. s, 1H, H-1), 4.80 - 4.74 (m, 1H, H-3), 4.51 (d, *J* = 5.7 Hz, 1H, H-2), 4.38 - 4.32 (m, 1H, H-5), 4.10 - 4.04 (m, 1H, H-6e), 4.01 - 3.94 (m, 2H, H-6a, H-4), 1.53 - 1.46 (m, 2H, C**H₂**CH_3), 1.45 (s, 3H, C(C**H₃**)), 1.42 (s, 3H, C(C**H₃**)), 1.35 (s, 3H, C(C**H₃**)), 1.29 (s, 3H, C(C**H₃**)), 1.16 (s, 6H, t-amyl C(C**H₃**)), 0.83 (t, *J* = 7.4 Hz, 3H, CH_2C**H₃**) ppm; ^{13}C NMR (125 MHz, $CDCl_3$) 112.3, 109.2, 101.5, 86.3, 79.9, 79.7, 73.2, 67.0, 34.1, 26.9, 26.4, 25.9, 25.6, 25.3, 24.4, 8.4 ppm; HRMS (micro-TOF) *m/z* 353.1928 (calculated *m/z* M+Na = 353.1940 for $C_{17}H_{30}NaO_6$)

2,3,4,6-Tetra-*O*-acetyl-α-D-mannopyranosyl-(1→2)-1,3,4,6-tetra-*O*-acetyl-α-D-mannopyranose (21). ^{1}H NMR (500 MHz, $CDCl_3$) δ d 5.76 (s, 1H), 5.45-5.48 (m, 1H), 5.28–5.36 (m, 3H), 5.09 (dd, *J* =2.4, 9.7 Hz, 1H), 4.98 (s, 1H), 4.39-4.41 (m, 1H), 4.31 (dd, *J* = 4.1, 12.2 Hz, 1H), 4.23 (dd, *J* = 4.29, 12.5 Hz, 1H), 4.14-4.16 (m, 2H), 4.01-4.03 (m, 1H), 3.76-3.78 (m, 1H) 1.99-2.13 (m, 24H) ppm; ^{13}C NMR (125 MHz, $CDCl_3$) 170.9, 170.6, 170.2, 169.8, 169.7, 169.5, 169.3, 168.3, 98.3, 90.9, 74.7, 73.1, 72.1, 69.9, 68.8, 68.3, 66.1, 65.6, 62.1, 61.7, 20.9, 20.8, 20.6, 20.5 ppm; HRMS (micro-TOF) *m/z* 701.1873 (calculated *m/z* M+Na = 701.1900 for $C_{48}H_{52}O_{15}Na$).

2,3,4,6-Tetra-*O*-(benzyl)-α-D-galactopyranosyl-(1→2)-1,3,4,6-tetra-*O*-acetyl-α-D-mannopyranose (22). ^{1}H NMR (500 MHz, $CDCl_3$) δ 7.19-7.42 (m, Ph**H,** 20H), 5.78 (s, 1H), 5.51 (t, *J* =9.6 Hz, 1H), 5.24 (d, *J* = 2.7 Hz, 1H), 5.13 (d, *J* = 9.6 Hz, 1H), 4.91 (dd, *J* = 11.7, 22.12 Hz, 2H), 4.82 (d, *J* = 11.6 Hz, 1H), 4.70-4.74 (m, 2H), 4.53 (d, *J* = 11.4 Hz, 1H), 4.35-4.39 (m, 3H), 4.28 (dd, *J* = 5.1, 12.2 Hz, 1H), 4.23 (s, 1H), 4.15 (d, *J* = 11.6 Hz, 1H), 4.06-4.09 (m, 2H), 4.01 (s, 1H), 3.78-3.80 (m, 1H), 3.53 (t, *J* = 8.2 Hz, 1H), 3.42-3.45 (m, 1H), 2.09 (s, 3H), 1.99 (s, 3H), 1.98 (s, 3H), 1.93 (s, 3H) ppm; ^{13}C NMR (125 MHz, $CDCl_3$) 170.8, 169.8, 169.3, 168.8, 138.8, 138.8, 138.6, 137.8, 128.4,127.3-128.4 (Ar-C, 20C), 97.5, 91.3, 78.6, 76.2, 73.5, 73.4, 73.3, 73.1, 72.8, 71.4, 69.8, 68.7, 66.1, 62.2, 20.7, 20.6 (3C) ppm; HRMS (micro-TOF) *m/z* 893.3347 (calculated *m/z* M+Na = 893.3360 for $C_{48}H_{52}O_{15}Na$). ^{1}H NMR is consistent with literature values.[194]

2,3:4,6-Di-O-isopropylidene-α-D-mannopyranosyl-(1→2)-1,3,4,6-tetra-*O*-acetyl-α-D-mannopyranose (23). ^{1}H NMR (500 MHz, $CDCl_3$) δ 5.71 (s, 1H), 5.26 (t, *J* = 9.9 Hz, 1H), 5.13 (s, 1H), 5.09 (dd, *J* = 9.9, 2.5 Hz, 1H), 4.83 – 4.74 (m, 2H), 4.35 (m, 1H), 4.24 (m, 2H), 4.18 (s, 1H), 4.04 (m, 3H), 3.98 – 3.92 (m, 1H), 3.76 – 3.69 (m, 1H), 2.18 (s, 3H), 2.05 (s, 3H), 2.04 (s, 3H), 1.99 (s, 3H), 1.42 (s, 3H), 1.36 (s, 3H), 1.30 (s, 3H), 1.30 (s, 3H) ppm; ^{13}C NMR (125 MHz, $CDCl_3$) 170.7, 169.8, 169.6, 169.0, 112.6, 109.1, 106.8, 91.3, 84.9, 80.7, 79.4, 73.2, 73.2, 72.9, 70.9, 66.3, 65.9, 62.1, 26.8, 25.8, 24.8, 24.3, 20.9, 20.8, 20.7, 20.6 ppm; HRMS (micro-TOF) *m/z* 613.2063 (calculated *m/z* M+Na =613.2108 for $C_{26}H_{38}NaO_{15}$)

Relevant spectra can be found in Appendix D.

CHAPTER SIX

SUMMARY AND CONCLUSIONS

The Thomsen-Friedenreich (TF) antigen has the structure of β-Gal-1-3-α-GalNAc-Thr/Ser and is a known tumor associated antigen. Its structure is masked under a carbohydrate layer on the surface of healthy cells and is unmasked in 90% of carcinomas through truncated glycosylation. Once unmasked, TF antigen is a surface marker specific for cancer cells and is the natural ligand for the protein galectin-3. Galectin-3 is over expressed in many types of cancer and has been implicated in many cancer processes such as cellular adhesion, angiogenesis, metastasis, and anti-apoptosis. Because of this, TF antigen and its relationship to galectin-3 is of interest.

TF antigen was synthesized through two separate glycosylation reactions using indium triflate as a catalyst. The stereochemistry for the beta 1,3 disaccharide linkage was achieved through neighboring group participation of acetylated C2' on the galactoside. The alpha linkage to threonine was achieved by azide protection of C2 on the galactosaminoside and the use of a more polar solvent. TF antigen was then attached to generations 2, 3, 4, and 6 polyamidoamine dendrimers to be displayed in a multivalent fashion.

TF antigen functionalized dendrimers were used to study galectin-3 interactions in homotypic cellular aggregation assays with A549 cells. All four generations of dendrimers induced cellular aggregation, suggesting TF antigen functionalized dendrimers are able to nucleate large enough protein aggregates with galectin-3 to form

crosslinking networks. This is in contrast to previous results observed with lactose functionalized dendrimers in which only generations 4 and 6 were able to induce cellular aggregation. Generations 2 and 3 lactose functionalized dendrimers were able to inhibit cellular aggregation. This indicates generations 2 and 3 TF antigen functionalized dendrimers are capable of binding more galectin-3 proteins than previously observed with lactose functionalized dendrimers, allowing larger dendrimer-protein aggregates to form. This ability to recruit more proteins per dendrimer is presumably due to TF antigen's stronger binding affinity for galectin-3 as its natural ligand. Further experiments are needed in order to test this hypothesis.

Additionally, further work was performed to characterize the distribution of dendrimer end groups. Spin labeled dendrimers can be used to study end group distribution through line broadening in the EPR spectrum. By quantifying the amount of line broadening observed in the spectrum, the relative location of dendrimer end groups can be determined. Generation 4 polyamidoamine dendrimers were functionalized with di-spin bearing end groups. When two spins were covalently linked, low loaded dendrimers closely matched the theoretically calculated pattern for clustered end groups. As dendrimer functionalization with the di-spin end groups increased, the surface pattern became closer to a random distribution. Significant radical quenching created problems in reproducing these results and further work is needed with active radicals.

Finally, indium(III) was proven to be a useful promoter in glycosylation reactions. Weaker Lewis acids, $InCl_3$ and $InBr_3$, performed better with acetylated mannose, while the stronger Lewis acid, $In(OTf)_3$, performed better with benzyl and acetonide protected

sugars. In the case of acetonide protected mannose, significant protecting group removal was observed with all indium(III) promoters above 0.05 equivalents. $In(OTf)_3$ was successful because it was strong enough to catalyze the glycosylation reaction in trace amounts, effectively avoiding acetonide deprotection. In glycosylation reactions forming disaccharides, $In(OTf)_3$ was the only promoter to give satisfactory yields, as a strong Lewis acid is often required in reactions with a bulky glycosyl acceptor. $In(OTf)_3$ was then used in the glycosylation reactions for the synthesis of TF antigen.

The research described herein provides further insight into the mechanism of TF antigen and galectin-3 in cancer processes, as well as further insight into the general use of dendrimers as multivalent scaffolds. The development of indium(III) as a glycosylation promoter and the newly described synthetic route to TF antigen provide a straightforward method to obtain TF antigen and will allow for further studies in the future. Further work is needed to fully understand the galectin-3 protein aggregation induced by the multivalent display of TF antigen. Future experiments using dynamic light scattering to observe the size, shape, and polydispersity of galectin-3/TF antigen functionalized dendrimer aggregates will give a better understanding of the processes taking place in cancer cellular aggregation.

REFERENCES CITED

1. Dippold, W.; Steinborn, A.; Meyer zum Büschenfelde, K. H., The role of the Thomsen-Friedenreich antigen as a tumor-associated molecule. *Environmental Health Perspectives* **1990,** *88*, 255-257.

2. Brayman, M.; Thathiah, A.; Carson, D. D., MUC1: A multifunctional cell surface component of reproductive tissue epithelia. *Reproductive biology and endocrinology : RB&E* **2004,** *2*, 4-4.

3. Von Mensdorff-Pouilly, S.; Moreno, M.; Verheijen, R. H. M., Natural and Induced Humoral Responses to MUC1. *Cancers* **2011,** *3* (3).

4. Sotozono, M. A.; Okada, Y.; Tsuji, T., THE THOMSEN-FRIEDENREICH ANTIGEN-RELATED CARBOHYDRATE ANTIGENS IN HUMAN GASTRIC INTESTINAL METAPLASIA AND CANCER. *Journal of Histochemistry & Cytochemistry* **1994,** *42* (12), 1575-1584.

5. Samuel, J.; Noujaim, A. A.; Maclean, G. D.; Suresh, M. R.; Longenecker, B. M., ANALYSIS OF HUMAN TUMOR ASSOCIATED THOMSEN-FRIEDENREICH ANTIGEN. *Cancer Research* **1990,** *50* (15), 4801-4808.

6. Hang, H. C.; Bertozzi, C. R., The chemistry and biology of mucin-type O-linked glycosylation. *Bioorganic & Medicinal Chemistry* **2005,** *13* (17), 5021-5034.

7. Bian, C.-F.; Zhang, Y.; Sun, H.; Li, D.-F.; Wang, D.-C., Structural Basis for Distinct Binding Properties of the Human Galectins to Thomsen-Friedenreich Antigen. *PLoS ONE* **2011,** *6* (9), e25007.

8. Springer, G. F.; Cheingsongpopov, R.; Schirrmacher, V.; Desai, P. R.; Tegtmeyer, H., PROPOSED MOLECULAR-BASIS OF MURINE TUMOR-CELL HEPATOCYTE INTERACTION. *Journal of Biological Chemistry* **1983,** *258* (9), 5702-5706.

9. Glinskii, O. V.; Li, F.; Wilson, L. S.; Barnes, S.; Rittenhouse-Olson, K.; Barchi, J. J.; Pienta, K. J.; Glinsky, V. V., Endothelial integrin α3β1 stabilizes carbohydrate-mediated tumor/endothelial cell adhesion and induces macromolecular signaling complex formation at the endothelial cell membrane. *Oncotarget* **2014,** *5* (5), 1382-1389.

10. Yu, L. G.; Andrews, N.; Zhao, Q.; McKean, D.; Williams, J. F.; Connor, L. J.; Gerasimenko, O. V.; Hilkens, J.; Hirabayashi, J.; Kasai, K.; Rhodes, J. M., Galectin-3 interaction with Thomsen-Friedenreich disaccharide on cancer-associated MUC1 causes increased cancer cell endothelial adhesion. *Journal of Biological Chemistry* **2007,** *282* (1), 773-781.

11. Qicheng, Z.; Barclay, M.; Hilkens, J.; Xiuli, G.; Barrow, H.; Rhodes, J. M.; Lu-Gang, Y., Interaction between circulating galectin-3 and cancer-associated MUC1 enhances tumour cellhomotypic aggregation and prevents anoikis. *Molecular Cancer* **2010,** *9*, 154-165.

12. Khaldoyanidi, S. K.; Glinsky, V. V.; Sikora, L.; Glinskii, A. B.; Mossine, V. V.; Quinn, T. P.; Glinsky, G. V.; Sriramarao, P., MDA-MB-435 Human Breast Carcinoma Cell Homo- and Heterotypic Adhesion under Flow Conditions Is Mediated in Part by Thomsen-Friedenreich Antigen-Galectin-3 Interactions. *Journal of Biological Chemistry* **2003,** *278* (6), 4127-4134.

13. Wolf, M. F.; Ludwig, A.; Fritz, P.; Schumacher, K., INCREASED EXPRESSION OF THOMSEN-FRIEDENREICH ANTIGENS DURING TUMOR PROGRESSION IN BREAST-CANCER PATIENTS. *Tumor Biology* **1988,** *9* (4), 190.

14. Liu, F.-T.; Rabinovich, G. A., Galectins as modulators of tumour progression. *Nat Rev Cancer* **2005,** *5* (1), 29-41.

15. Mori, Y.; Akita, K.; Yashiro, M.; Sawada, T.; Hirakawa, K.; Murata, T.; Nakada, H., Binding of Galectin-3, a β-Galactoside-binding Lectin, to MUC1 Protein Enhances Phosphorylation of Extracellular Signal-regulated Kinase 1/2 (ERK1/2) and Akt, Promoting Tumor Cell Malignancy. *The Journal of Biological Chemistry* **2015,** *290* (43), 26125-26140.

16. Sindrewicz, P.; Lian, L. Y.; Yu, L. G., Interaction of the Oncofetal Thomsen-Friedenreich Antigen with Galectins in Cancer Progression and Metastasis. *Frontiers in Oncology* **2016,** *6*.

17. Glinskii, O. V.; Sud, S.; Mossine, V. V.; Mawhinney, T. P.; Anthony, D. C.; Glinsky, G. V.; Pienta, K. J.; Glinsky, V. V., Inhibition of Prostate Cancer Bone Metastasis by Synthetic TF Antigen Mimic/Galectin-3 Inhibitor Lactulose-l-Leucine. *Neoplasia* **2012,** *14* (1), 65-73.

18. Zhao, Q. C.; Guo, X. L.; Nash, G. B.; Stone, P. C.; Hilkens, J.; Rhodes, J. M.; Yu, L. G., Circulating Galectin-3 Promotes Metastasis by Modifying MUC1 Localization on Cancer Cell Surface. *Cancer Research* **2009,** *69* (17), 6799-6806.

19. Nangia-Makker, P.; Honjo, Y.; Sarvis, R.; Akahani, S.; Hogan, V.; Pienta, K. J.; Raz, A., Galectin-3 Induces Endothelial Cell Morphogenesis and Angiogenesis. *The American Journal of Pathology* **2000,** *156* (3), 899-909.

20. Guha, P.; Kaptan, E.; Bandyopadhyaya, G.; Kaczanowska, S.; Davila, E.; Thompson, K.; Martin, S. S.; Kalvakolanu, D. V.; Vasta, G. R.; Ahmed, H., Cod glycopeptide with picomolar affinity to galectin-3 suppresses T-cell apoptosis and prostate cancer metastasis. *Proceedings of the National Academy of Sciences of the United States of America* **2013,** *110* (13), 5052-5057.

21. Norling, L. V.; Perretti, M.; Cooper, D., Endogenous galectins and the control of the host inflammatory response. *Journal of Endocrinology* **2009,** *201* (2), 169-184.

22. Balan, V.; Nangia-Makker, P.; Raz, A., Galectins as Cancer Biomarkers. *Cancers* **2010,** *2* (2), 592-610.

23. Zhuang, T.; Lee, H.-S.; Imperiali, B.; Prestegard, J. H., Structure determination of a Galectin-3–carbohydrate complex using paramagnetism-based NMR constraints. *Protein Science : A Publication of the Protein Society* **2008,** *17* (7), 1220-1231.

24. Pricci, F.; Leto, G.; Amadio, L.; Iacobini, C.; Romeo, G.; Cordone, S.; Gradini, R.; Barsotti, P.; Liu, F.-T.; Di Mario, U.; Pugliese, G., Role of galectin-3 as a receptor for advanced glycosylation end products. *Kidney International* **2000,** *58, Supplement 77*, S31-S39.

25. Nieminen, J.; Kuno, A.; Hirabayashi, J.; Sato, S., Visualization of Galectin-3 Oligomerization on the Surface of Neutrophils and Endothelial Cells Using Fluorescence Resonance Energy Transfer. *Journal of Biological Chemistry* **2007,** *282* (2), 1374-1383.

26. Hsu, D. K.; Zuberi, R. I.; Liu, F. T., Biochemical and biophysical characterization of human recombinant IgE-binding protein, an S-type animal lectin. *Journal of Biological Chemistry* **1992,** *267* (20), 14167-14174.

27. Sano, H.; Hsu, D. K.; Yu, L.; Apgar, J. R.; Kuwabara, I.; Yamanaka, T.; Hirashima, M.; Liu, F.-T., Human Galectin-3 Is a Novel Chemoattractant for Monocytes and Macrophages. *The Journal of Immunology* **2000,** *165* (4), 2156.

28. Nieminen, J.; St-Pierre, C.; Sato, S., Galectin-3 interacts with naive and primed neutrophils, inducing innate immune response. *Journal of Leukocyte Biology* **2005,** *78* (5), 1127-1135.

29. Kuwabara, I.; Liu, F. T., Galectin-3 promotes adhesion of human neutrophils to laminin. *The Journal of Immunology* **1996,** *156* (10), 3939.

30. Ochieng, J.; Green, B.; Evans, S.; James, O.; Warfield, P., Modulation of the biological functions of galectin-3 by matrix metalloproteinases. *Biochimica et Biophysica Acta (BBA) - General Subjects* **1998,** *1379* (1), 97-106.

31. Park, A.-M.; Hagiwara, S.; Hsu, D. K.; Liu, F.-T.; Yoshie, O., Galectin-3 Plays an Important Role in Innate Immunity to Gastric Infection by Helicobacter pylori. *Infection and Immunity* **2016,** *84* (4), 1184-1193.

32. Hsu, D. K.; Hammes, S. R.; Kuwabara, I.; Greene, W. C.; Liu, F. T., Human T lymphotropic virus-I infection of human T lymphocytes induces expression of the beta-galactoside-binding lectin, galectin-3. *The American Journal of Pathology* **1996,** *148* (5), 1661-1670.

33. Menini, S.; Iacobini, C.; Fantauzzi, C. B.; Pesce, C. M.; Pugliese, G., Role of Galectin-3 in Obesity and Impaired Glucose Homeostasis. *Oxidative Medicine and Cellular Longevity* **2016**.

34. Vasil'eva, O. A.; Yakushina, V. D.; Ryazantseva, N. V.; Novitsky, V. V.; Tashireva, L. A.; Starikova, E. G.; Zima, A. P.; Prokhorenko, T. S.; Krasnova, T. Y.; Nebesnaya, I. S., Regulation of gene expression of CD4+ T lymphocyte differentiation transcription factors by galectin-3 in vitro. *Molecular Biology* **2013,** *47* (6), 879-884.

35. Oliveira, F. L.; Brand, C.; Paula, A. A.; Arcanjo, K. D.; Hsu, D. K.; Fu-Tong, L.; Takiya, C. M.; Borojevic, R.; Chammas, R.; El-Cheikh, M. C., Lack of Galectin-3 Disturbs Mesenteric Lymph Node Homeostasis and B Cell Niches in the Course of Schistosoma mansoni Infection. *PLoS ONE* **2011,** *6* (5), 1-11.

36. Yang, R. Y.; Hsu, D. K.; Liu, F. T., Expression of galectin-3 modulates T-cell growth and apoptosis. *Proceedings of the National Academy of Sciences of the United States of America* **1996,** *93* (13), 6737-6742.

37. Szu-Chia, C.; Po-Lin, K., The Role of Galectin-3 in the Kidneys. *International Journal of Molecular Sciences* **2016,** *17* (4), 1-10.

38. Rabinovich, G. A.; Baum, L. G.; Tinari, N.; Paganelli, R.; Natoli, C.; Liu, F.-T.; Iacobelli, S., Galectins and their ligands: amplifiers, silencers or tuners of the inflammatory response? *Trends in Immunology* **2002,** *23* (6), 313-320.

39. Colnot, C.; Fowlis, D.; Ripoche, M. A.; Bouchaert, I.; Poirier, F., Embryonic implantation in Galectin 1 Galectin 3 double mutant mice. *Developmental Dynamics* **1998,** *211* (4), 306-313.

40. Yang, H.; Lei, C. X.; Zhang, W., Human chorionic gonadotropin (hCG) regulation of galectin-3 expression in endometrial epithelial cells and endometrial stromal cells. *Acta Histochemica* **2013,** *115* (1), 3-7.

41. Yang, H.; Lei, C.; Zhang, W., Expression of galectin-3 in mouse endometrium and its effect during embryo implantation. *Reproductive BioMedicine Online* **2012,** *24* (1), 116-122.

42. Cai, G.; Ma, X.; Chen, B.; Huang, Y.; Liu, S.; Yang, H.; Zou, W., Galectin-3 induces ovarian cancer cell survival and chemoresistance via TLR4 signaling activation. *Tumor Biology* **2016,** *37* (9), 11883-11891.

43. Gopalan, V.; Saremi, N.; Sullivan, E.; Kabir, S.; Lu, C.-T.; Salajegheh, A.; Leung, M.; Smith, R. A.; Lam, A. K.-y., The expression profiles of the galectin gene family in colorectal adenocarcinomas. *Human Pathology* **2016,** *53*, 105-113.

44. Tseng, P.-C.; Chen, C.-L.; Shan, Y.-S.; Lin, C.-F., An increase in galectin-3 causes cellular unresponsiveness to IFN-γ-induced signal transduction and growth inhibition in gastric cancer cells. *Oncotarget* **2016,** *7* (12), 15150-15160.

45. Miyazaki, J.; Hokari, R.; Kato, S.; Tsuzuki, Y.; Kawaguchi, A.; Nagao, S.; Itoh, K.; Miura, S., Increased expression of galectin-3 in primary gastric cancer and the metastatic lymph nodes. *Oncology Reports* **2002,** *9* (6), 1307-1312.

46. Song, S. M.; Ji, B. A.; Ramachandran, V.; Wang, H. M.; Hafley, M.; Logsdon, C.; Bresalier, R. S., Overexpressed Galectin-3 in Pancreatic Cancer Induces Cell Proliferation and Invasion by Binding Ras and Activating Ras Signaling. *Plos One* **2012,** *7* (8).

47. Shetty, P.; Bargale, A.; Patil, B. R.; Mohan, R.; Dinesh, U. S.; Vishwanatha, J. K.; Gai, P. B.; Patil, V. S.; Amsavardani, T. S., Cell surface interaction of annexin A2 and galectin-3 modulates epidermal growth factor receptor signaling in Her-2 negative breast cancer cells. *Molecular and Cellular Biochemistry* **2016,** *411* (1), 221-233.

48. Mayoral, M. A.; Mayoral, C.; Meneses, A.; Villalvazo, L.; Guzmán, A.; Espinosa, B.; Ochoa, J. L.; Zenteno, E.; Guevara, J., Identification of Galectin-3 and Mucin-Type O-Glycans in Breast Cancer and Its Metastasis to Brain. *Cancer Investigation* **2008,** *26* (6), 615-623.

49. Liang, N.; Song, X. M.; Xie, H.; Xu, D. G.; Liu, F. J.; Yu, X. S.; Tian, Y.; Liu, Z.; Qiao, L. L.; Zhang, J. D., Effect of galectin-3 on the behavior of Eca-109 human esophageal cancer cells. *Molecular Medicine Reports* **2015,** *11* (2), 896-902.

50. Braeuer, R. R.; Shoshan, E.; Kamiya, T.; Bar-Eli, M., The sweet and bitter sides of galectins in melanoma progression. *Pigment Cell & Melanoma Research* **2012,** *25* (5), 592-601.

51. Inohara, H.; Honjo, Y.; Yoshii, T.; Akahani, S.; Yoshida, J.; Hattori, K.; Okamoto, S.; Sawada, T.; Raz, A.; Kubo, T., Expression of galectin-3 in fine-needle aspirates as a diagnostic marker differentiating benign from malignant thyroid neoplasms. *Cancer* **1999,** *85* (11), 2475-2484.

52. Xu, X. C.; el-Naggar, A. K.; Lotan, R., Differential expression of galectin-1 and galectin-3 in thyroid tumors. Potential diagnostic implications. *The American Journal of Pathology* **1995,** *147* (3), 815-822.

53. Chung, L.-Y.; Tang, S.-J.; Wu, Y.-C.; Sun, G.-H.; Liu, H.-Y.; Sun, K.-H., Galectin-3 augments tumor initiating property and tumorigenicity of lung cancer through interaction with β-catenin. *Oncotarget* **2015,** *6* (7), 4936-4952.

54. Shan-Shan, J.; De-Sheng, W.; Qi-Jing, W.; Ke, P.; Yao-Jun, Z.; Yong-Qiang, L.; Jian-Jun, L.; Jing-Jing, Z.; Jia, H.; Lin, L.; Qiu-Zhong, P.; Jian-Chuan, X., Galectin-3 is

Associated with a Poor Prognosis in Primary Hepatocellular Carcinoma. *Journal of Translational Medicine* **2014,** *12* (1), 1-25.

55. Hsu, D. K.; Dowling, C. A.; Jeng, K. C. G.; Chen, J. T.; Yang, R. Y.; Liu, F. T., Galectin-3 expression is induced in cirrhotic liver and hepatocellular carcinoma. *International Journal of Cancer* **1999,** *81* (4), 519-526.

56. Michel, A. K.; Nangia-Makker, P.; Raz, A.; Cloninger, M. J., Lactose-Functionalized Dendrimers Arbitrate the Interaction of Galectin-3/MUC1 Mediated Cancer Cellular Aggregation. *Chembiochem* **2014,** *15* (14), 2106-2112.

57. Mammen, M.; Choi, S. K.; Whitesides, G. M., Polyvalent interactions in biological systems: Implications for design and use of multivalent ligands and inhibitors. *Angewandte Chemie-International Edition* **1998,** *37* (20), 2755-2794.

58. Zhang, S.; Walberg, L. A.; Ogata, S.; Itzkowitz, S. H.; Koganty, R. R.; Reddish, M.; Gandhi, S. S.; Longenecker, B. M.; Lloyd, K. O.; Livingston, P. O., Immune Sera and Monoclonal Antibodies Define Two Configurations for the Sialyl Tn Tumor Antigen. *Cancer Research* **1995,** *55* (15), 3364.

59. Livingston, P. O., Augmenting the immunogenicity of carbohydrate tumor antigens. *Seminars in Cancer Biology* **1995,** *6* (6), 357-366.

60. Slovin, S. F.; Ragupathi, G.; Musselli, C.; Fernandez, C.; Diani, M.; Verbel, D.; Danishefsky, S.; Livingston, P.; Scher, H. I., Thomsen-Friedenreich (TF) antigen as a target for prostate cancer vaccine: clinical trial results with TF cluster (c)-KLH plus QS21 conjugate vaccine in patients with biochemically relapsed prostate cancer. *Cancer Immunology, Immunotherapy* **2005,** *54* (7), 694-702.

61. Hoffmann-Roder, A.; Kaiser, A.; Wagner, S.; Gaidzik, N.; Kowalczyk, D.; Westerlind, U.; Gerlitzki, B.; Schmitt, E.; Kunz, H., Synthetic Antitumor Vaccines from Tetanus Toxoid Conjugates of MUC1 Glycopeptides with the Thomsen-Friedenreich Antigen and a Fluorine-Substituted Analogue. *Angewandte Chemie-International Edition* **2010,** *49* (45), 8498-8503.

62. Ragupathi, G.; Koide, F.; Livingston, P. O.; Cho, Y. S.; Endo, A.; Wan, Q.; Spassova, M. K.; Keding, S. J.; Allen, J.; Ouerfelli, O.; Wilson, R. M.; Danishefsky, S. J., Preparation and Evaluation of Unimolecular Pentavalent and Hexavalent Antigenic Constructs Targeting Prostate and Breast Cancer: A Synthetic Route to Anticancer Vaccine Candidates. *Journal of the American Chemical Society* **2006,** *128* (8), 2715-2725.

63. Zhu, J.; Wan, Q.; Lee, D.; Yang, G.; Spassova, M. K.; Ouerfelli, O.; Ragupathi, G.; Damani, P.; Livingston, P. O.; Danishefsky, S. J., From Synthesis to Biologics: Preclinical Data on a Chemistry Derived Anticancer Vaccine. *Journal of the American Chemical Society* **2009,** *131* (26), 9298-9303.

64. Wilkinson, B. L.; Malins, L. R.; Chun, C. K. Y.; Payne, R. J., Synthesis of MUC1-lipopeptide chimeras. *Chemical Communications* **2010,** *46* (34), 6249-6251.

65. Sun, S.; Zheng, X. J.; Huo, C. X.; Song, C. C.; Li, Q.; Ye, X. S., Synthesis and Evaluation of Glycoconjugates Comprising N-Acyl-Modified Thomsen-Friedenreich Antigens as Anticancer Vaccines. *Chemmedchem* **2016,** *11* (10), 1090-1096.

66. Cremer, G.-A.; Bureaud, N.; Piller, V.; Kunz, H.; Piller, F.; Delmas, A. F., Synthesis and Biological Evaluation of a Multiantigenic Tn/TF-Containing Glycopeptide Mimic of the Tumor-Related MUC1 Glycoprotein. *ChemMedChem* **2006,** *1* (9), 965-968.

67. Biswas, S.; Medina, S. H.; Barchi Jr, J. J., Synthesis and cell-selective antitumor properties of amino acid conjugated tumor-associated carbohydrate antigen-coated gold nanoparticles. *Carbohydrate Research* **2015,** *405*, 93-101.

68. Svarovsky, S. A.; Szekely, Z.; Barchi, J. J., Synthesis of gold nanoparticles bearing the Thomsen–Friedenreich disaccharide: a new multivalent presentation of an important tumor antigen. *Tetrahedron: Asymmetry* **2005,** *16* (2), 587-598.

69. Brinãs, R. P.; Sundgren, A.; Sahoo, P.; Morey, S.; Rittenhouse-Olson, K.; Wilding, G. E.; Deng, W.; Barchi, J. J., Design and Synthesis of Multifunctional Gold Nanoparticles Bearing Tumor-Associated Glycopeptide Antigens as Potential Cancer Vaccines. *Bioconjugate Chemistry* **2012,** *23* (8), 1513-1523.

70. Sundgren, A.; Barchi Jr, J. J., Varied presentation of the Thomsen–Friedenreich disaccharide tumor-associated carbohydrate antigen on gold nanoparticles. *Carbohydrate Research* **2008,** *343* (10–11), 1594-1604.

71. Trabbic, K. R.; Bourgault, J.-P.; Shi, M.; Clark, M.; Andreana, P. R., Immunological evaluation of the entirely carbohydrate-based Thomsen-Friedenreich - PS B conjugate. *Organic & Biomolecular Chemistry* **2016,** *14* (13), 3350-3355.

72. Baek, M.-G.; Rittenhouse-Olson, K.; Roy, R., Synthesis and antibody binding properties of glycodendrimers bearing the tumor related T-antigen. *Chemical Communications* **2001,** (3), 257-258.

73. Baek, M.-G.; Roy, R., Synthesis and protein binding properties of T-antigen containing GlycoPAMAM dendrimers. *Bioorganic & Medicinal Chemistry* **2002,** *10* (1), 11-17.

74. Roy, R.; Baek, M.-G., Glycodendrimers: novel glycotope isosteres unmasking sugar coding. Case study with T-antigen markers from breast cancer MUC1 glycoprotein. *Reviews in Molecular Biotechnology* **2002,** *90* (3–4), 291-309.

75. Dendrimers: Design, Synthesis and Chemical Properties. In *Dendrimers in Medicine and Biotechnology: New Molecular Tools*, Boas, U.; Christensen, J. B.; Heegaard, P. M. H., Eds. The Royal Society of Chemistry: 2006; 1-27.

76. Esfand, R.; Tomalia, D. A., Poly(amidoamine) (PAMAM) dendrimers: from biomimicry to drug delivery and biomedical applications. *Drug Discovery Today* **2001,** *6* (8), 427-436.

77. Roberts, J. C.; Bhalgat, M. K.; Zera, R. T., Preliminary biological evaluation of polyamidoamine (PAMAM) StarburstTM dendrimers. *Journal of Biomedical Materials Research* **1996,** *30* (1), 53-65.

78. Jevprasesphant, R.; Penny, J.; Jalal, R.; Attwood, D.; McKeown, N. B.; D'Emanuele, A., The influence of surface modification on the cytotoxicity of PAMAM dendrimers. *International Journal of Pharmaceutics* **2003,** *252* (1–2), 263-266.

79. Cloninger, M. J., Biological applications of dendrimers. *Current Opinion in Chemical Biology* **2002,** *6* (6), 742-748.

80. Woller, E. K.; Walter, E. D.; Morgan, J. R.; Singel, D. J.; Cloninger, M. J., Altering the Strength of Lectin Binding Interactions and Controlling the Amount of Lectin Clustering Using Mannose/Hydroxyl-Functionalized Dendrimers. *Journal of the American Chemical Society* **2003,** *125* (29), 8820-8826.

81. Wolfenden, M.; Cousin, J.; Nangia-Makker, P.; Raz, A.; Cloninger, M., Glycodendrimers and Modified ELISAs: Tools to Elucidate Multivalent Interactions of Galectins 1 and 3. *Molecules* **2015,** *20* (4).

82. Wolfenden, M. L.; Cloninger, M. J., Carbohydrate-Functionalized Dendrimers To Investigate the Predictable Tunability of Multivalent Interactions. *Bioconjugate Chemistry* **2006,** *17* (4), 958-966.

83. Roy, R.; Murphy, V. P.; Gabius, H.-J., Multivalent Carbohydrate-Lectin Interactions: How Synthetic Chemistry Enables Insights into Nanometric Recognition. *Molecules* **2016,** *21* (5).

84. Goodman, C. K.; Wolfenden, M. L.; Nangia-Makker, P.; Michel, A. K.; Raz, A.; Cloninger, M. J., Multivalent scaffolds induce galectin-3 aggregation into nanoparticles. *Beilstein Journal of Organic Chemistry* **2014,** *10*, 1570-1577.

85. Andreozzi, E.; Antonelli, A.; Cangiotti, M.; Canonico, B.; Sfara, C.; Pianetti, A.; Bruscolini, F.; Sahre, K.; Appelhans, D.; Papa, S.; Ottaviani, M. F., Interactions of Nitroxide-Conjugated and Non-Conjugated Glycodendrimers with Normal and Cancer Cells and Biocompatibility Studies. *Bioconjugate Chemistry* **2017,** *28* (2), 524-538.

86. Cousin, J. M.; Cloninger, M. J., Glycodendrimers: tools to explore multivalent galectin-1 interactions. *Beilstein Journal of Organic Chemistry* **2015,** *11*, 739-747.

87. Tejler, J.; Leffler, H.; Nilsson, U. J., Synthesis of O-galactosyl aldoximes as potent LacNAc-mimetic galectin-3 inhibitors. *Bioorganic & Medicinal Chemistry Letters* **2005,** *15* (9), 2343-2345.

88. Uhlenbruck, G.; Pardoe, G. I.; Bird, G. W. G., ON SPECIFICITY OF LECTINS WITH A BROAD AGGLUTINATION SPECTRUM .2. STUDIES ON NATURE OF T-ANTIGEN AND SPECIFIC RECEPTORS FOR LECTIN OF ARACHIS HYPOGOEA (GROUND-NUT). *Zeitschrift Fur Immunitats-Forschung Allergie Und Klinische Immunologie* **1969,** *138* (5), 423.

89. Ratcliffe, R. M.; Baker, D. A.; Lemieux, R. U., Synthesis of the T [β-d-Gal-(1→3)-α-d-GalNAc]-antigenic determinant in a form useful for the preparation of an effective artificial antigen and the corresponding immunoadsorbent. *Carbohydrate Research* **1981,** *93* (1), 35-41.

90. Paulsen, H.; Kolář, Č.; Stenzel, W., Synthesis of α-Glycosidically Linked Disaccharides of D-Galactosamine. *Angewandte Chemie International Edition in English* **1976,** *15* (7), 440-441.

91. Madsen, R.; Udodong, U. E.; Roberts, C.; Mootoo, D. R.; Konradsson, P.; Fraser-Reid, B., Studies Related to Synthesis of Glycophosphatidylinositol Membrane-Bound Protein Anchors. 6. Convergent Assembly of Subunits. *Journal of the American Chemical Society* **1995,** *117* (5), 1554-1565.

92. Rodriguez, M. C.; Yegorova, S.; Pitteloud, J.-P.; Chavaroche, A. E.; André, S.; Ardá, A.; Minond, D.; Jiménez-Barbero, J.; Gabius, H.-J.; Cudic, M., Thermodynamic Switch in Binding of Adhesion/Growth Regulatory Human Galectin-3 to Tumor-Associated TF Antigen (CD176) and MUC1 Glycopeptides. *Biochemistry* **2015,** *54* (29), 4462-4474.

93. Kuduk, S. D.; Schwarz, J. B.; Chen, X.-T.; Glunz, P. W.; Sames, D.; Ragupathi, G.; Livingston, P. O.; Danishefsky, S. J., Synthetic and Immunological Studies on Clustered Modes of Mucin-Related Tn and TF O-Linked Antigens: The Preparation of a Glycopeptide-Based Vaccine for Clinical Trials against Prostate Cancer. *Journal of the American Chemical Society* **1998,** *120* (48), 12474-12485.

94. Jiaang, W.-T.; Chang, M.-Y.; Tseng, P.-H.; Chen, S.-T., A concise synthesis of the O-glycosylated amino acid building block; using phenyl selenoglycoside as a glycosyl donor. *Tetrahedron Letters* **2000,** *41* (17), 3127-3130.

95. Lemieux, R. U.; Ratcliffe, R. M., The azidonitration of tri-O-acetyl-D-galactal. *Canadian Journal of Chemistry* **1979,** *57* (10), 1244-1251.

96. Svarovsky, S. A.; Barchi Jr, J. J., Highly efficient preparation of tumor antigen-containing glycopeptide building blocks from novel pentenyl glycosides. *Carbohydrate Research* **2003,** *338* (19), 1925-1935.

97. Bourgault, J. P.; Trabbic, K. R.; Shi, M.; Andreana, P. R., Synthesis of the tumor associative [small alpha]-aminooxy disaccharide of the TF antigen and its conjugation to a polysaccharide immune stimulant. *Organic & Biomolecular Chemistry* **2014,** *12* (11), 1699-1702.

98. Cato, D.; Buskas, T.; Boons, G.-J., Highly Efficient Stereospecific Preparation of Tn and TF Building Blocks Using Thioglycosyl Donors and the Ph 2 SO/Tf 2 O Promotor System*. *Journal of Carbohydrate Chemistry* **2005,** *24* (4-6), 503-516.

99. Keding, S. J.; Atsushi, E.; Biswas, K.; Zatorski, A.; Coltart, D. M.; Danishefsky, S. J., Hydroxynorleucine as a glycosyl acceptor is an efficient means for introducing amino acid functionality into complex carbohydrates. *Tetrahedron Letters* **2003,** *44* (16), 3413-3416.

100. Schmidt, R. R., New Methods for the Synthesis of Glycosides and Oligosaccharides - Are There Alternatives to the Koenigs-Knorr Method. *Angewandte Chemie-International Edition in English* **1986,** *25* (3), 212-235.

101. Yule, J. E.; Wong, T. C.; Gandhi, S. S.; Qiu, D.; Riopel, M. A.; Rao Koganty, R., Steric control of N-acetylgalactosamine in glycosidic bond formation. *Tetrahedron Letters* **1995,** *36* (38), 6839-6842.

102. Gambert, U.; Thiem, J., Chemoenzymatic synthesis of the Thomsen-Friedenreich antigen determinant. *Carbohydrate Research* **1997,** *299* (1–2), 85-89.

103. Wang, S.; Czuchry, D.; Liu, B.; Vinnikova, A. N.; Gao, Y.; Vlahakis, J. Z.; Szarek, W. A.; Wang, L.; Feng, L.; Brockhausen, I., Characterization of Two UDP-Gal:GalNAc-Diphosphate-Lipid beta 1,3-Galactosyltransferases WbwC from Escherichia coli Serotypes O104 and O5. *Journal of Bacteriology* **2014,** *196* (17), 3122-3133.

104. Mensah, E. A.; Yu, F.; Nguyen, H. M., Nickel-Catalyzed Stereoselective Glycosylation with C(2)-N-Substituted Benzylidene d-Glucosamine and Galactosamine Trichloroacetimidates for the Formation of 1,2-cis-2-Amino Glycosides. Applications to the Synthesis of Heparin Disaccharides, GPI Anchor Pseudodisaccharides, and α-GalNAc. *Journal of the American Chemical Society* **2010,** *132* (40), 14288-14302.

105. Tsai, Y.-H.; Gotze, S.; Vilotijevic, I.; Grube, M.; Silva, D. V.; Seeberger, P. H., A general and convergent synthesis of diverse glycosylphosphatidylinositol glycolipids. *Chemical Science* **2013,** *4* (1), 468-481.

106. Xiong, J.; Lu, Z.; Ding, N.; Ren, S.; Li, Y., Synthesis of the Pentasaccharide Moiety of Thornasterside A. *European Journal of Organic Chemistry* **2013,** *2013* (27), 6158-6166.

107. Petrosyants, S. P.; Ilyukhin, A. B., Indium(III) coordination compounds. *Russian Journal of Inorganic Chemistry* **2011,** *56* (13), 2047-2069.

108. Freeland, B. H.; Habeeb, J. J.; Tuck, D. G., COORDINATION-COMPOUNDS OF INDIUM .33. X-RAY PHOTOELECTRON-SPECTROSCOPY OF NEUTRAL AND ANIONIC INDIUM HALIDE SPECIES. *Canadian Journal of Chemistry-Revue Canadienne De Chimie* **1977,** *55* (9), 1527-1532.

109. Busev, A. I., *The Analytical Chemistry of Indium*. Pergamon Press: Oxford, London, New York, Paris, 1962; 287.

110. Hepler, L. G.; Hugus, Z. Z., Hydrolysis and Halide Complexing of Indium(III). *Journal of the American Chemical Society* **1952,** *74* (23), 6115-6116.

111. Macdonald, C. L. B.; Corrente, A. M.; Andrews, C. G.; Taylor, A.; Ellis, B. D., Indium(i) trifluoromethanesulfonate and other soluble salts for univalent indium chemistry. *Chemical Communications* **2004,** (2), 250-251.

112. Moeller, T., Contributions to the Chemistry of Indium. II. The Hydrolysis of Indium Trichloride Solutions. *Journal of the American Chemical Society* **1941,** *63* (5), 1206-1207.

113. Trost, B. M.; Portnoy, M.; Kurihara, H., A Ru-Catalyzed Three-Component Addition To Form 1,5-Diketones. *Journal of the American Chemical Society* **1997,** *119* (4), 836-837.

114. Ali, T.; Chauhan, K. K.; Frost, C. G., Indium triflate-an efficient catalyst for hetero Diels-Alder reactions. *Tetrahedron Letters* **1999,** *40* (30), 5621-5624.

115. Ghosh, R.; Maiti, S., Advances in indium triflate catalyzed organic syntheses. *Journal of Molecular Catalysis A: Chemical* **2007,** *264* (1–2), 1-8.

116. Lee, D. J.; Harris, P. W. R.; Brimble, M. A., Synthesis of MUC1 Neoglycopeptides using efficient microwave-enhanced chaotrope-assisted click chemistry. *Organic & Biomolecular Chemistry* **2011,** *9* (5), 1621-1626.

117. Kalidasan, K.; Su, Y.; Wu, X.; Yao, S. Q.; Uttamchandani, M., Fluorescence-activated cell sorting and directed evolution of [small alpha]-N-acetylgalactosaminidases using a quenched activity-based probe (qABP). *Chemical Communications* **2013,** *49* (65), 7237-7239.

118. Larsen, K.; Olsen, C. E.; Motawia, M. S., Acid-catalysed rearrangement of glycosyl trichloroacetimidates: a novel route to glycosylamines. *Carbohydrate Research* **2008,** *343* (2), 383-387.

119. Mayato, C.; Dorta, R. L.; Vázquez, J. T., Methyl esters: an alternative protecting group for the synthesis of O-glycosyl amino acid building blocks. *Tetrahedron Letters* **2008,** *49* (8), 1396-1398.

120. Zhuo, R. X.; Du, B.; Lu, Z. R., In vitro release of 5-fluorouracil with cyclic core dendritic polymer. *Journal of Controlled Release* **1999,** *57* (3), 249-257.

121. Majoros, I. J.; Keszler, B.; Woehler, S.; Bull, T.; Baker, J. R., Acetylation of Poly(amidoamine) Dendrimers. *Macromolecules* **2003,** *36* (15), 5526-5529.

122. Yang, K.; Weng, L.; Cheng, Y.; Zhang, H.; Zhang, J.; Wu, Q.; Xu, T., Host−Guest Chemistry of Dendrimer−Drug Complexes. 6. Fully Acetylated Dendrimers as Biocompatible Drug Vehicles Using Dexamethasone 21- Phosphate as a Model Drug. *The Journal of Physical Chemistry B* **2011,** *115* (10), 2185-2195.

123. Cheng, Y.; Zhao, L.; Li, Y.; Xu, T., Design of biocompatible dendrimers for cancer diagnosis and therapy: current status and future perspectives. *Chemical Society Reviews* **2011,** *40* (5), 2673-2703.

124. Jain, K.; Kesharwani, P.; Gupta, U.; Jain, N. K., Dendrimer toxicity: Let's meet the challenge. *International Journal of Pharmaceutics* **2010,** *394* (1–2), 122-142.

125. Silva, D. J.; Wang, H.; Allanson, N. M.; Jain, R. K.; Sofia, M. J., Stereospecific Solution- and Solid-Phase Glycosylations. Synthesis of β-Linked Saccharides and Construction of Disaccharide Libraries Using Phenylsulfenyl 2-Deoxy-2-Trifluoroacetamido Glycopyranosides as Glycosyl Donors1. *The Journal of Organic Chemistry* **1999,** *64* (16), 5926-5929.

126. Zou, J.; Glinsky, V. V.; Landon, L. A.; Matthews, L.; Deutscher, S. L., Peptides specific to the galectin-3 carbohydrate recognition domain inhibit metastasis-associated cancer cell adhesion. *Carcinogenesis* **2005,** *26* (2), 309-318.

127. Iurisci, I. D. A.; Cumashi, A.; Sherman, A. A.; Tsvetkov, Y. E.; Tinari, N.; Piccolo, E.; D'Egidio, M.; Adamo, V.; Natoli, C.; Rabinovich, G. A.; Iacobelli, S.; Nifantiev, N. E.; The Consorzio Interuniversitario Nazionale Per La Bio-Oncologia, I., Synthetic Inhibitors of Galectin-1 and -3 Selectively Modulate Homotypic Cell Aggregation and Tumor Cell Apoptosis. *Anticancer Research* **2009,** *29* (1), 403-410.

128. Giard, D. J.; Aaronson, S. A.; Todaro, G. J.; Arnstein, P.; Kersey, J. H.; Dosik, H.; Parks, W. P., IN-VITRO CULTIVATION OF HUMAN TUMORS - ESTABLISHMENT OF CELL LINES DERIVED FROM A SERIES OF SOLID TUMORS. *Journal of the National Cancer Institute* **1973,** *51* (5), 1417-1423.

129. Lieber, M.; Smith, B.; Szakal, A.; Nelsonrees, W.; Todaro, G., CONTINUOUS TUMOR-CELL LINE FROM A HUMAN LUNG CARCINOMA WITH PROPERTIES OF TYPE-II ALVEOLAR EPITHELIAL CELLS. *International Journal of Cancer* **1976,** *17* (1), 62-70.

130. Michel, A. K. Glycodendrimer Mediation of Galectin-3 Cancer Processes and Indium(III) as a Glycosylation Promoter. Montana State University, Bozeman, MT, 2014.

131. Mangold, S. L.; Morgan, J. R.; Strohmeyer, G. C.; Gronenborn, A. M.; Cloninger, M. J., Cyanovirin-N binding to Man[small alpha]1-2Man functionalized dendrimers. *Organic & Biomolecular Chemistry* **2005,** *3* (12), 2354-2358.

132. Goodman, C. K. Effect of monomeric binding affinity on scaffold mediated protein aggregation. Montana State University, Bozeman, MT, 2015.

133. Newkome, G. R.; Moorefield, C. N.; Vögtle, F., *Dendrimers and dendrons : concepts, syntheses, applications*. Wiley-VCH: Weinheim ; New York, 2001; p xii, 623 p.

134. Mintzer, M. A.; Grinstaff, M. W., Biomedical applications of dendrimers: a tutorial. *Chemical Society Reviews* **2011,** *40* (1), 173-190.

135. Astruc, D.; Boisselier, E.; Ornelas, C. t., Dendrimers Designed for Functions: From Physical, Photophysical, and Supramolecular Properties to Applications in Sensing, Catalysis, Molecular Electronics, Photonics, and Nanomedicine. *Chemical Reviews* **2010,** *110* (4), 1857-1959.

136. Grayson, S. M.; Fréchet, J. M. J., A New Approach to Heterofunctionalized Dendrimers: A Versatile Triallyl Chloride Core. *Organic Letters* **2002,** *4* (19), 3171-3174.

137. Goodwin, A. P.; Lam, S. S.; Fréchet, J. M. J., Rapid, Efficient Synthesis of Heterobifunctional Biodegradable Dendrimers. *Journal of the American Chemical Society* **2007,** *129* (22), 6994-6995.

138. Antoni, P.; Hed, Y.; Nordberg, A.; Nyström, D.; von Holst, H.; Hult, A.; Malkoch, M., Bifunctional Dendrimers: From Robust Synthesis and Accelerated One-Pot Postfunctionalization Strategy to Potential Applications. *Angewandte Chemie International Edition* **2009,** *48* (12), 2126-2130.

139. Navath, R. S.; Menjoge, A. R.; Wang, B.; Romero, R.; Kannan, S.; Kannan, R. M., Amino Acid-Functionalized Dendrimers with Heterobifunctional Chemoselective Peripheral Groups for Drug Delivery Applications. *Biomacromolecules* **2010,** *11* (6), 1544-1563.

140. Huang, H.; Li, J.; Liao, L.; Li, J.; Wu, L.; Dong, C.; Lai, P.; Liu, D., Poly(l-glutamic acid)-based star-block copolymers as pH-responsive nanocarriers for cationic drugs. *European Polymer Journal* **2012,** *48* (4), 696-704.

141. Walter, E. D.; Sebby, K. B.; Usselman, R. J.; Singel, D. J.; Cloninger, M. J., Characterization of Heterogeneously Functionalized Dendrimers by Mass Spectrometry and EPR Spectroscopy. *The Journal of Physical Chemistry B* **2005,** *109* (46), 21532-21538.

142. Hourani, R.; Jain, M.; Maysinger, D.; Kakkar, A., Multi-tasking with Single Platform Dendrimers for Targeting Sub-Cellular Microenvironments. *Chemistry – A European Journal* **2010,** *16* (21), 6164-6168.

143. Swanson, S. D.; Kukowska-Latallo, J. F.; Patri, A. K.; Chen, C.; Ge, S.; Cao, Z.; Kotlyar, A.; East, A. T.; Baker, J. R., Targeted gadolinium-loaded dendrimer nanoparticles for tumor-specific magnetic resonance contrast enhancement. *International Journal of Nanomedicine* **2008,** *3* (2), 201-210.

144. Amir, R. J.; Albertazzi, L.; Willis, J.; Khan, A.; Kang, T.; Hawker, C. J., Multifunctional Trackable Dendritic Scaffolds and Delivery Agents. *Angewandte Chemie International Edition* **2011,** *50* (15), 3425-3429.

145. Sharma, A.; Khatchadourian, A.; Khanna, K.; Sharma, R.; Kakkar, A.; Maysinger, D., Multivalent niacin nanoconjugates for delivery to cytoplasmic lipid droplets. *Biomaterials* **2011,** *32* (5), 1419-1429.

146. Klemm, P. J.; Floyd, W. C.; Smiles, D. E.; Fréchet, J. M. J.; Raymond, K. N., Improving T1 and T2 magnetic resonance imaging contrast agents through the conjugation of an esteramide dendrimer to high-water-coordination Gd(III) hydroxypyridinone complexes. *Contrast Media & Molecular Imaging* **2012,** *7* (1), 95-99.

147. Schlick, K. H.; Morgan, J. R.; Weiel, J. J.; Kelsey, M. S.; Cloninger, M. J., Clusters of ligands on dendrimer surfaces. *Bioorganic & Medicinal Chemistry Letters* **2011,** *21* (17), 5078-5083.

148. Bosman, A. W.; Janssen, R. A. J.; Meijer, E. W., Five Generations of Nitroxyl-Functionalized Dendrimers. *Macromolecules* **1997,** *30* (12), 3606-3611.

149. Klajnert, B.; Cangiotti, M.; Calici, S.; Majoral, J. P.; Caminade, A. M.; Cladera, J.; Bryszewska, M.; Ottaviani, M. F., EPR Study of the Interactions between Dendrimers and Peptides Involved in Alzheimer's and Prion Diseases. *Macromolecular Bioscience* **2007,** *7* (8), 1065-1074.

150. Ottaviani, M. F.; Sacchi, B.; Turro, N. J.; Chen, W.; Jockusch, S.; Tomalia, D. A., An EPR Study of the Interactions between Starburst Dendrimers and Polynucleotides. *Macromolecules* **1999,** *32* (7), 2275-2282.

151. Ottaviani, M. F.; Jockusch, S.; Turro, N. J.; Tomalia, D. A.; Barbon, A., Interactions of Dendrimers with Selected Amino Acids and Proteins Studied by Continuous Wave EPR and Fourier Transform EPR. *Langmuir* **2004,** *20* (23), 10238-10245.

152. Jockusch, S.; Turro, N. J.; Ottaviani, M. F.; Tomalia, D. A., An EPR and Fluorescence Depolarization Study of Intermolecular Interactions of Dendrimers at Medium and Highly Concentrated Aqueous Solutions. *Journal of Colloid and Interface Science* **2002,** *256* (1), 223-227.

153. Xia, Y.; Li, Y.; Burts, A. O.; Ottaviani, M. F.; Tirrell, D. A.; Johnson, J. A.; Turro, N. J.; Grubbs, R. H., EPR Study of Spin Labeled Brush Polymers in Organic Solvents. *Journal of the American Chemical Society* **2011,** *133* (49), 19953-19959.

154. Kurzbach, D.; Velte, C.; Arnold, P.; Kizilsavas, G.; Hinderberger, D., DNA condensation with spermine dendrimers: interactions in solution, charge inversion, and morphology control. *Soft Matter* **2011,** *7* (14), 6695-6704.

155. Samuelson, L. E.; Sebby, K. B.; Walter, E. D.; Singel, D. J.; Cloninger, M. J., EPR and affinity studies of mannose-TEMPO functionalized PAMAM dendrimers. *Organic & Biomolecular Chemistry* **2004,** *2* (21), 3075-3079.

156. Han, H. J.; Sebby, K. B.; Singel, D. J.; Cloninger, M. J., EPR Characterization of Heterogeneously Functionalized Dendrimers. *Macromolecules* **2007,** *40* (9), 3030-3033.

157. Koeller, K. M.; Smith, M. E. B.; Wong, C.-H., Tyrosine Sulfation on a PSGL-1 Glycopeptide Influences the Reactivity of Glycosyltransferases Responsible for Synthesis of the Attached O-Glycan. *Journal of the American Chemical Society* **2000,** *122* (4), 742-743.

158. Handlogten, Michael W.; Kiziltepe, T.; Moustakas, Demetri T.; Bilgiçer, B., Design of a Heterobivalent Ligand to Inhibit IgE Clustering on Mast Cells. *Chemistry & Biology* **2011,** *18* (9), 1179-1188.

159. Josan, J. S.; Handl, H. L.; Sankaranarayanan, R.; Xu, L.; Lynch, R. M.; Vagner, J.; Mash, E. A.; Hruby, V. J.; Gillies, R. J., Cell-Specific Targeting by Heterobivalent Ligands. *Bioconjugate Chemistry* **2011,** *22* (7), 1270-1278.

160. Yan, Y.; Chen, X., Peptide heterodimers for molecular imaging. *Amino Acids* **2011,** *41* (5), 1081-1092.

161. Choi, S.-k., *Synthetic Multivalent Molecules*. John Wiley & Sons, Inc.: Hoboken, New Jersey, USA, 2004; p 409.

162. Sebby, K. B.; Walter, E. D.; Usselman, R. J.; Cloninger, M. J.; Singel, D. J., End-Group Distributions of Multiple Generations of Spin-Labeled PAMAM Dendrimers. *The Journal of Physical Chemistry B* **2011,** *115* (16), 4613-4620.

163. Klopsch, R.; Koch, S.; Schlüter, A. D., Amino-Functionalized, Second-Generation Dendritic Building Blocks. *European Journal of Organic Chemistry* **1998,** *1998* (7), 1275-1283.

164. Zhao, Y. Y.; Takahashi, M.; Gu, J. G.; Miyoshi, E.; Matsumoto, A.; Kitazume, S.; Taniguchi, N., Functional roles of N-glycans in cell signaling and cell adhesion in cancer. *Cancer Science* **2008,** *99* (7), 1304-1310.

165. Mukaiyama, T.; Murai, Y.; Shoda, S., An Efficient Method for Glucosylation of Hydroxy Compounds Using Glucopyranosyl Fluoride. *Chemistry Letters* **1981,** (3), 431-432.

166. Dahmen, J.; Frejd, T.; Gronberg, G.; Lave, T.; Magnusson, G.; Noori, G., 2-Bromoethyl Glycosides - Synthesis and Characterization. *Carbohydrate Research* **1983,** *116* (2), 303-307.

167. Pougny, J. R.; Sinay, P., Reaction of Glucopyranosyl with Acetonitrile - Applications to Synthesis. *Tetrahedron Letters* **1976,** (45), 4073-4076.

168. Schmidt, R. R.; Michel, J., Facile Synthesis of Alpha-O-Glycosyl and Beta-O-Glycosyl Imidates - Preparation of Glycosides and Disaccharides. *Angewandte Chemie-International Edition in English* **1980,** *19* (9), 731-732.

169. Lindhorst, T. K., *Essentials of carbohydrate chemistry and biochemistry*. 2nd, rev. and updated ed.; Wiley-VCH: Weinheim, 2003; p xiii, 219.

170. Hanessian, S., *Preparative carbohydrate chemistry*. Marcel Dekker: New York, 1997; p xiii, 648.

171. Douglas, S. P.; Whitfield, D. M.; Krepinsky, J. J., Silver Trifluoromethanesulfonate(Triflate) Activation of Trichloroacetimidates in Glycosylation Reactions. *Journal of Carbohydrate Chemistry* **1993,** *12* (1), 131-136.

172. Adinolfi, M.; Barone, G.; Guariniello, L.; Iadonisi, A., Efficient activation of armed glycosyl trichloroacetimidates with Sm(OTf)(3) in the stereoselective glycosidation of saccharidic acceptors. *Tetrahedron Letters* **2000,** *41* (46), 9005-9008.

173. Adinolfi, M.; Barone, G.; Iadonisi, A.; Mangoni, L.; Schiattarella, M., Activation of disarmed 2-O-alkoxycarbonylated glycosyl trichloroacetimidates with lanthanide triflates: an efficient approach for the synthesis of 1,2-trans glycosides. *Tetrahedron Letters* **2001,** *42* (34), 5967-5969.

174. Loh, T. P.; Chua, G. L., Discovery of indium complexes as water-tolerant Lewis acids. *Chemical Communications* **2006,** (26), 2739-2749.

175. Frost, C. G.; Hartley, J. P., New applications of indium catalysts in organic synthesis. *Mini-Reviews in Organic Chemistry* **2004,** *1* (1), 1-7.

176. Asakura, K.; Satoh, H.; Chiba, M.; Okamoto, M.; Serizawa, K.; Nakano, M.; Omae, K., Genotoxicity Studies of Heavy Metals: Lead, Bismuth, Indium, Silver and Antimony. *Journal of Occupational Health* **2009,** *51* (6), 498-512.

177. Bandini, M.; Cozzi, P. G.; Giacomini, M.; Melchiorre, P.; Selva, S.; Umani-Ronchi, A., Sequential one-pot InBr3-catalyzed 1,4-then 1,2-nucleophilic addition to enones. *Journal of Organic Chemistry* **2002,** *67* (11), 3700-3704.

178. Bizier, N. P.; Atkins, S. R.; Helland, L. C.; Colvin, S. F.; Twitchell, J. R.; Cloninger, M. J., Indium triflate catalyzed peracetylation of carbohydrates. *Carbohydrate Research* **2008,** *343* (10-11), 1814-1818.

179. Das, S. K.; Roy, J.; Reddy, K. A.; Abbineni, C., A mild and convenient indium(III) chloride-catalyzed synthesis of thioglycosides. *Carbohydrate Research* **2003,** *338* (21), 2237-2240.

180. Giri, S. K.; Verma, M.; Kartha, K. P. R., Indium(III) Triflate: A Highly Efficient Catalyst for Reactions of Sugars. *Journal of Carbohydrate Chemistry* **2008,** *27* (8-9), 464-478.

181. Mukherjee, D.; Ray, P. K.; Chowdhury, U. S., Synthesis of glycosides via indium(III) chloride mediated activation of glycosyl halide in neutral condition. *Tetrahedron* **2001,** *57* (36), 7701-7704.

182. Ghosh, R. C., Arijit. , InCl3 - an efficient Lewis acid catalyst for stereoselective *O*-glycosidation reactions. *Indian Journal of Chemistry* **2002,** *41B*, 583-585.

183. Ghosh, R. C., Arijit; Maiti, Dilip K., InCl3.H2O: An efficient Lewis acid catalyst for stereoselective *O*-glycosidation reactions of per -*O*-acetylglycopyranosyl trichloroacetimidates. *Indian Journal of Chemistry* **2003,** *42B*, 602-604.

184. Kaneko, M.; Hayashi, R.; Cook, G. R., Intermolecular friedel-crafts reaction catalyzed by InCl3. *Tetrahedron Letters* **2007,** *48* (40), 7085-7087.

185. Thirupathi, P.; Kim, S. S., InBr3: A Versatile Catalyst for the Different Types of Friedel-Crafts Reactions. *Journal of Organic Chemistry* **2009,** *74* (20), 7755-7761.

186. Yang, M. T.; Woerpel, K. A., The Effect of Electrostatic Interactions on Conformational Equilibria of Multiply Substituted Tetrahydropyran Oxocarbenium Ions. *Journal of Organic Chemistry* **2009,** *74* (2), 545-553.

187. Pfrengle, F.; Dekaris, V.; Schefzig, L.; Zimmer, R.; Reissig, H. U., Indium Trichloride Mediated Cleavage of Acetonides in the Presence of Acid-Labile Functional Groups - Enhancing the Synthetic Utility of 1,3-Dioxolanyl-Substituted 1,2-Oxazines. *Synlett* **2008,** (19), 2965-2968.

188. Gregg, B. T.; Golden, K. C.; Quinn, J. F., Indium(III) Trifluoromethanesulfonate as an Efficient Catalyst for the Deprotection of Acetals and Ketals. *The Journal of Organic Chemistry* **2007,** *72* (15), 5890-5893.

189. Decoster, E.; Lacombe, J. M.; Strebler, J. L.; Ferrari, B.; Pavia, A. A., Another Approach to the Synthesis of Benzyl Derivatives of Reducing Monosaccharides - Study of Pyranose-Furanose Equilibria by C-13 Nmr. *Journal of Carbohydrate Chemistry* **1983,** *2* (3), 329-341.

190. Ren, T.; Liu, D. X., Synthesis of targetable cationic amphiphiles. *Tetrahedron Letters* **1999,** *40* (43), 7621-7625.

191. Gros, E. G. D., J.O.; Mastronardi, I. O., Methylation of carbohydrates bearing base-labile substituents, with diazomethane-boron trifluoride etherate. *Carbohydrate Research* **1967,** *4*, 432-434.

192. Polakova, M.; Roslund, M. U.; Ekholm, F. S.; Saloranta, T.; Leino, R., Synthesis of beta-(1 -> 2)-Linked Oligomannosides. *European Journal of Organic Chemistry* **2009,** (6), 870-888.

193. Yang, J. M.; Cooper-Vanosdell, C.; Mensah, E. A.; Nguyen, H. M., Cationic palladium(ii)-catalyzed stereoselective glycosylation with glycosyl trichloroacetimidates. *Journal of Organic Chemistry* **2008,** *73* (3), 794-800.

194. Mangold, S. L.; Morgan, J. R.; Strohmeyer, G. C.; Gronenborn, A. M.; Cloninger, M. J., Cyanovirin-N binding to Man alpha 1-2Man functionalized dendrimers. *Organic & Biomolecular Chemistry* **2005,** *3* (12), 2354-2358.

APPENDICES

APPENDIX A

RELEVANT SPECTRAL DATA FROM CHAPTER TWO

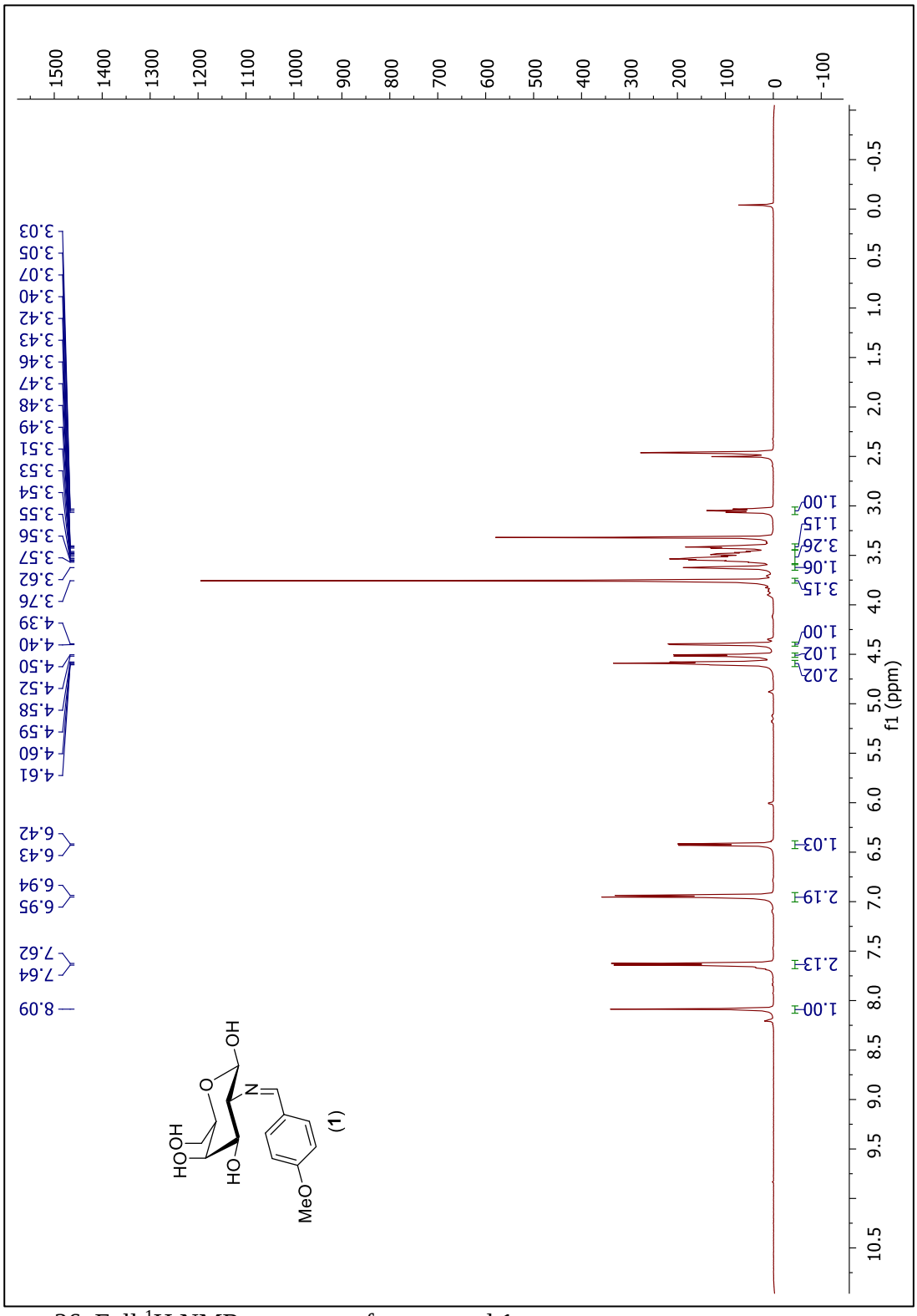


Figure 36. Full ^{1}H NMR spectrum of compound **1**.

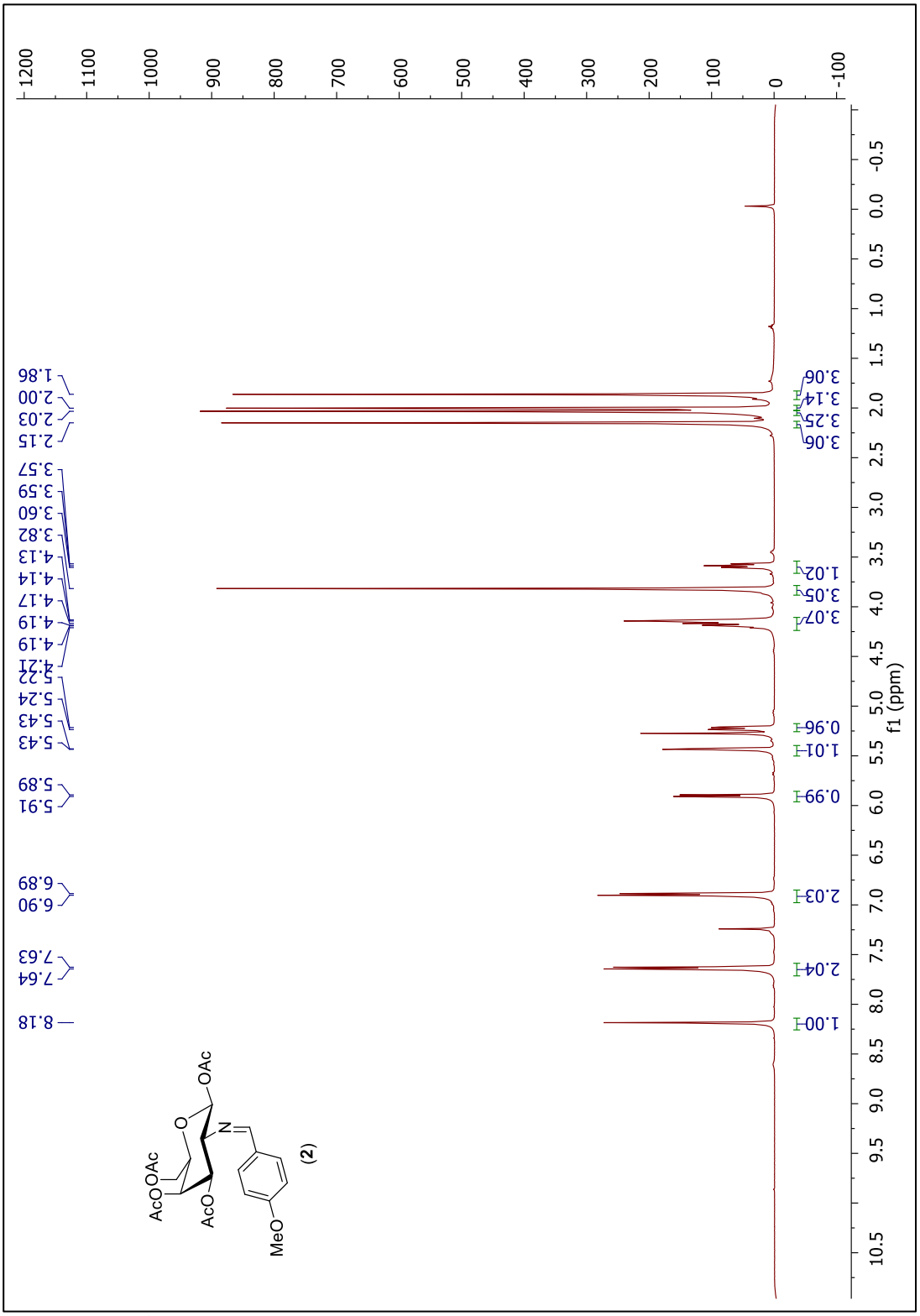


Figure 37. Full ^{1}H NMR spectrum of compound **2**.

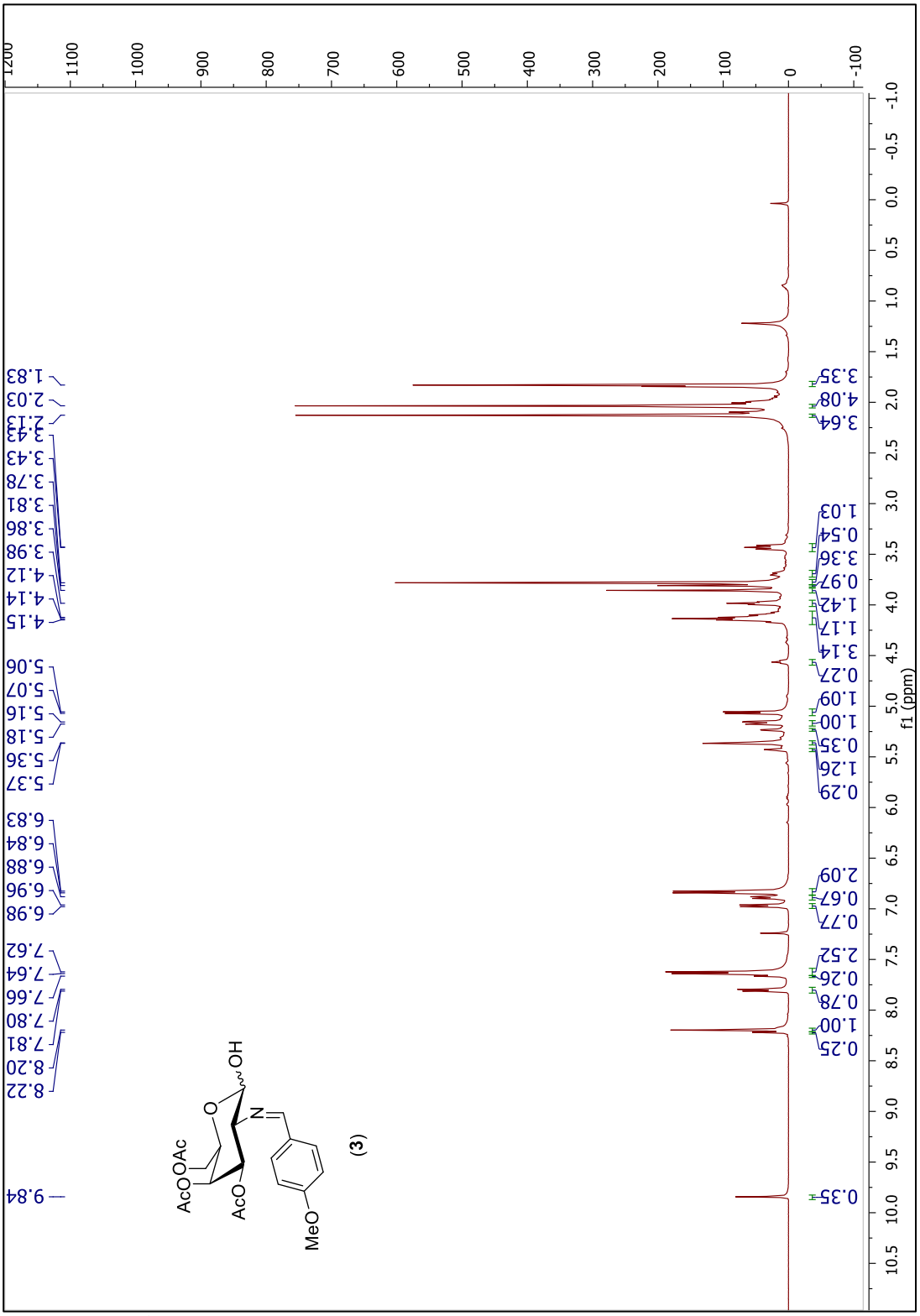


Figure 38. Full ^{1}H NMR spectrum of compound **3**.

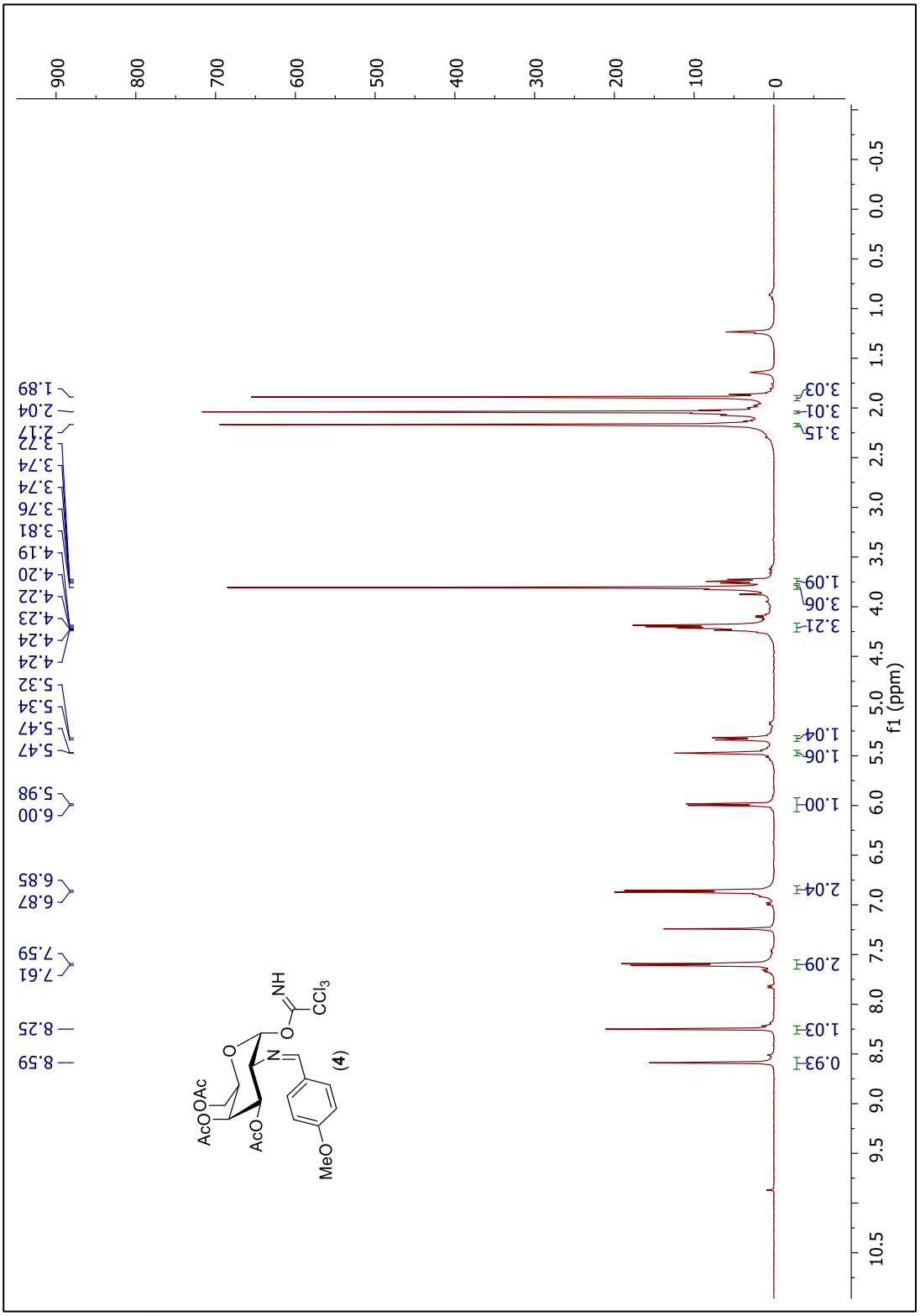


Figure 39. Full ^{1}H NMR spectrum of compound **4**.

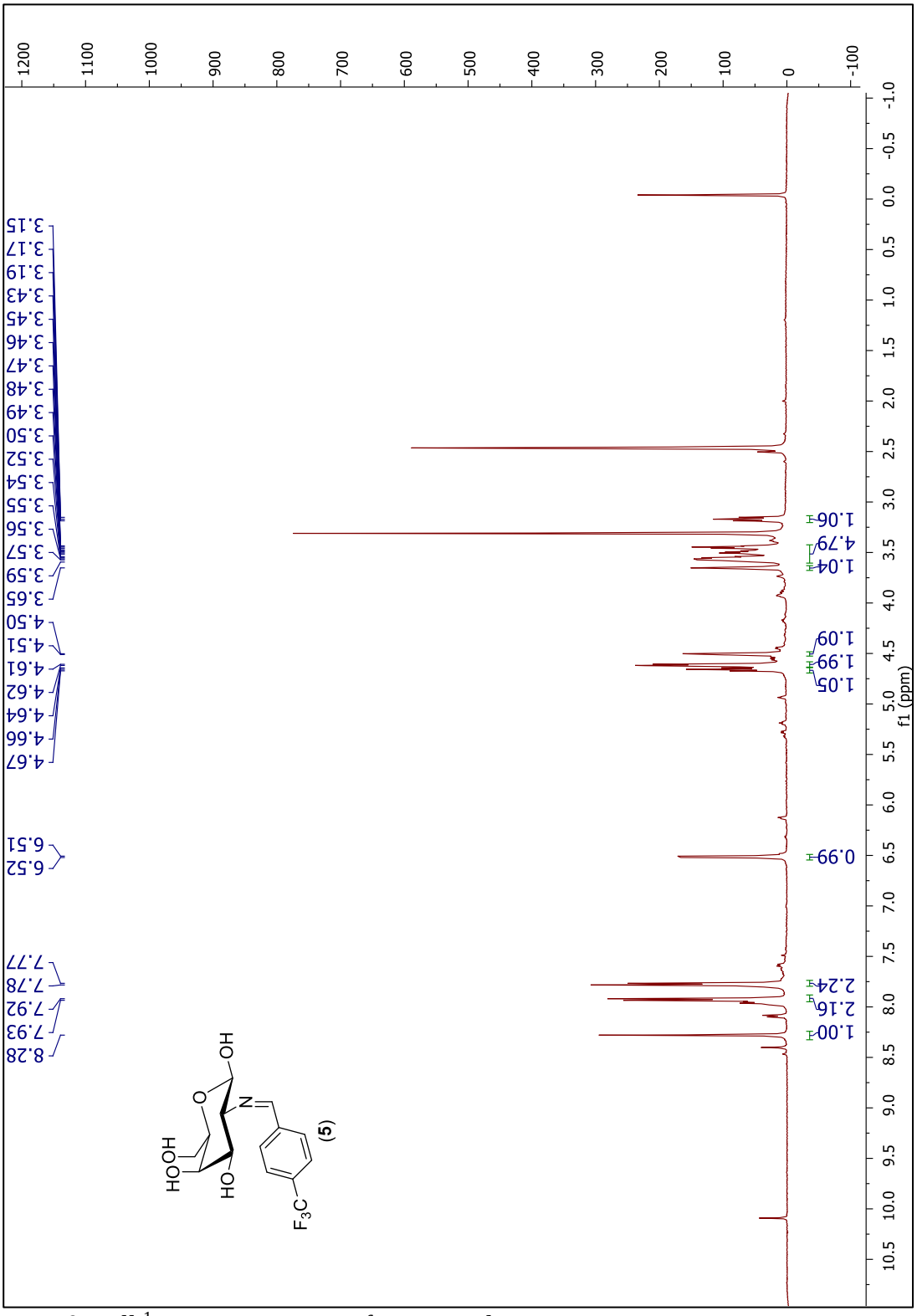


Figure 40. Full ^{1}H NMR spectrum of compound **5**.

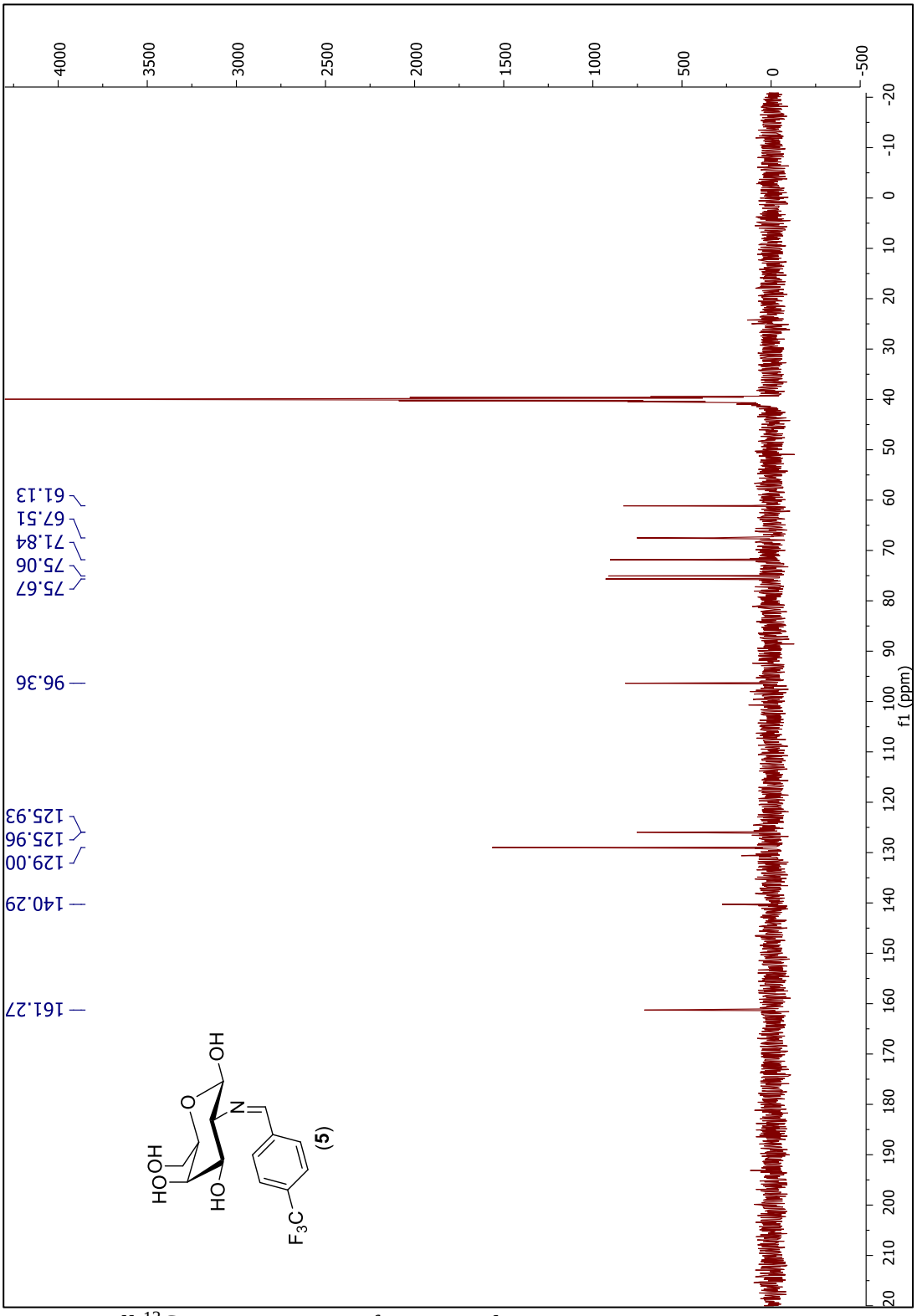


Figure 41. Full ^{13}C NMR spectrum of compound **5**.

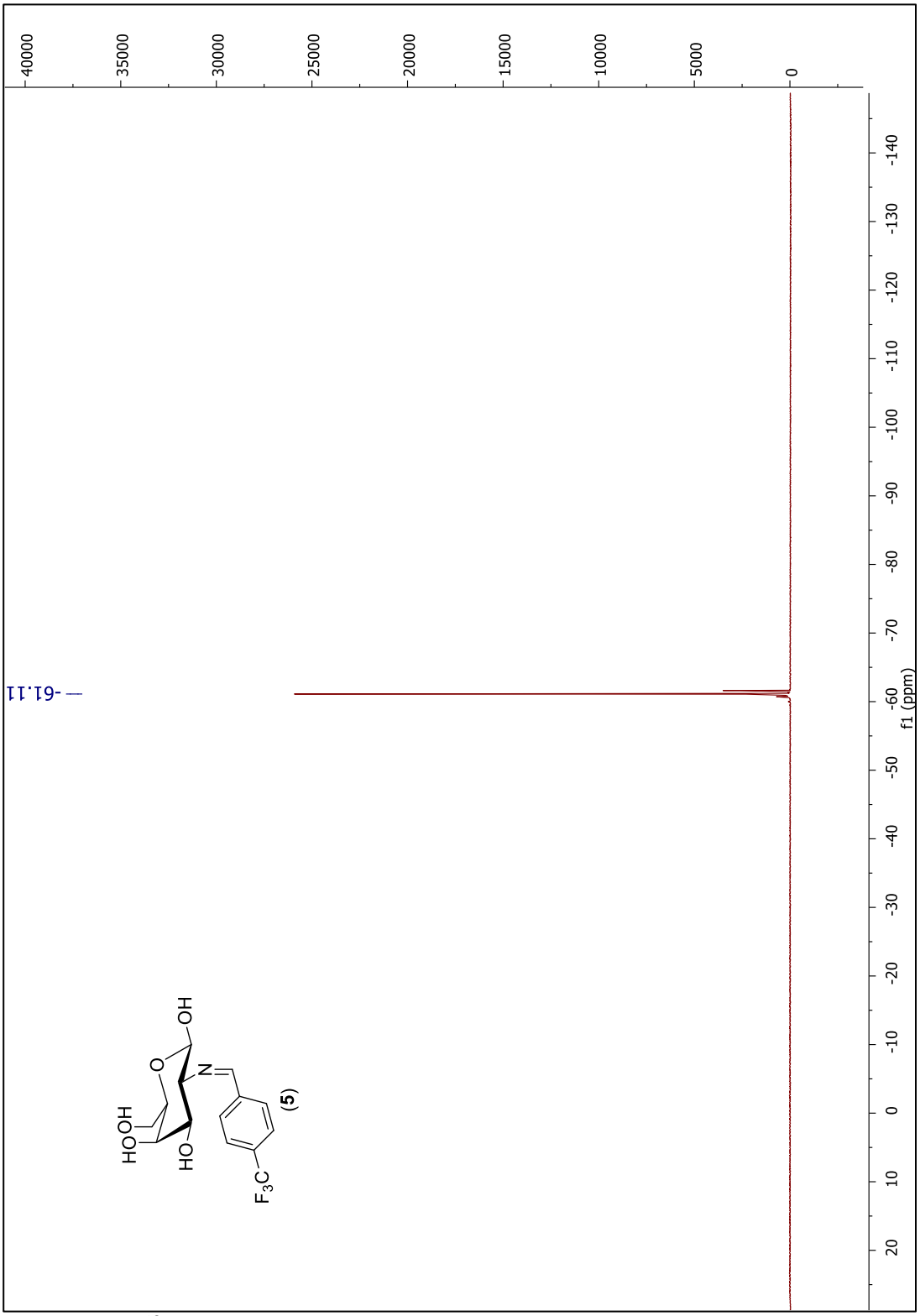


Figure 42. Full ^{19}F NMR spectrum of compound **5**.

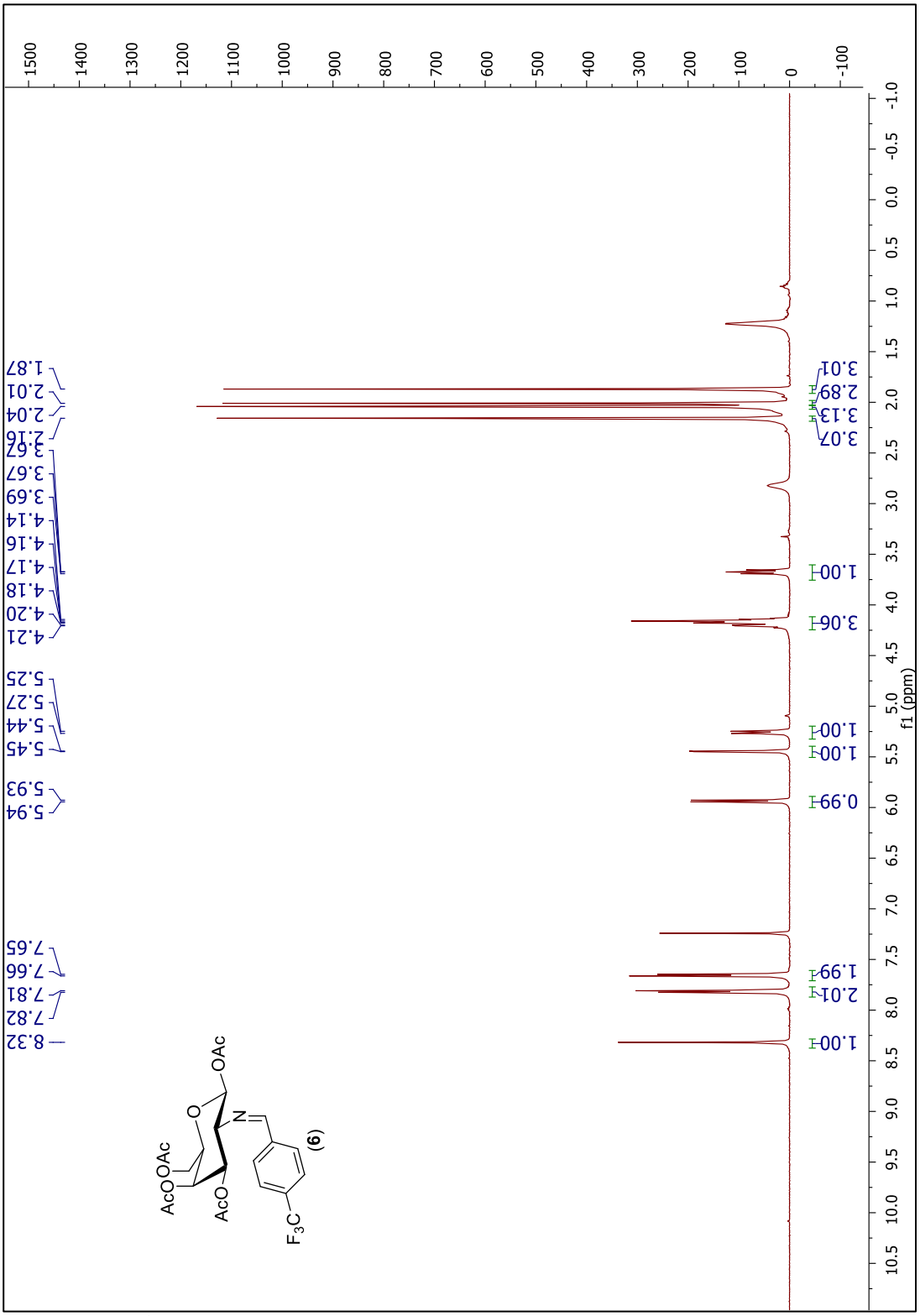


Figure 43. Full ^{1}H NMR spectrum of compound **6**.

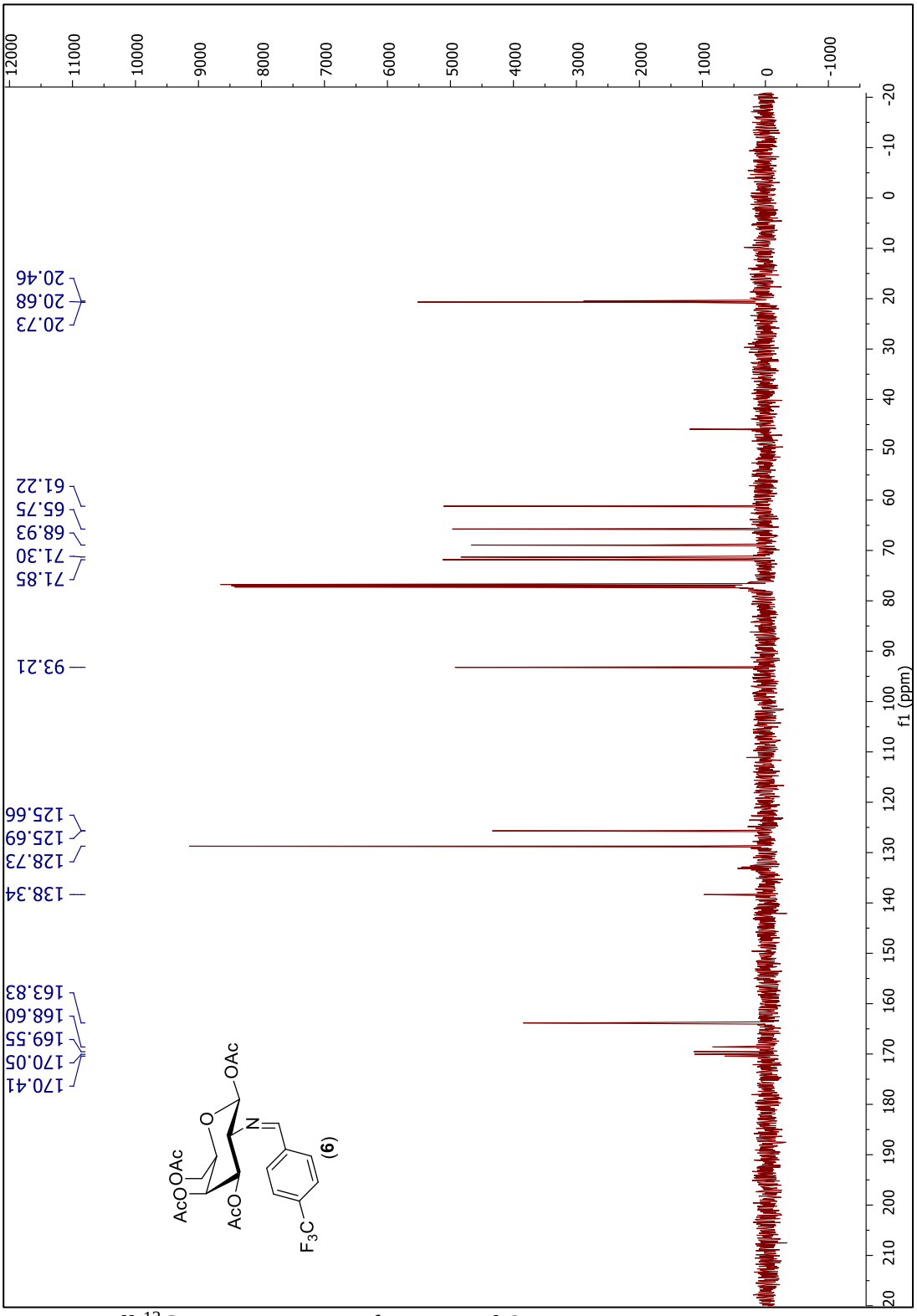


Figure 44. Full ^{13}C NMR spectrum of compound **6**.

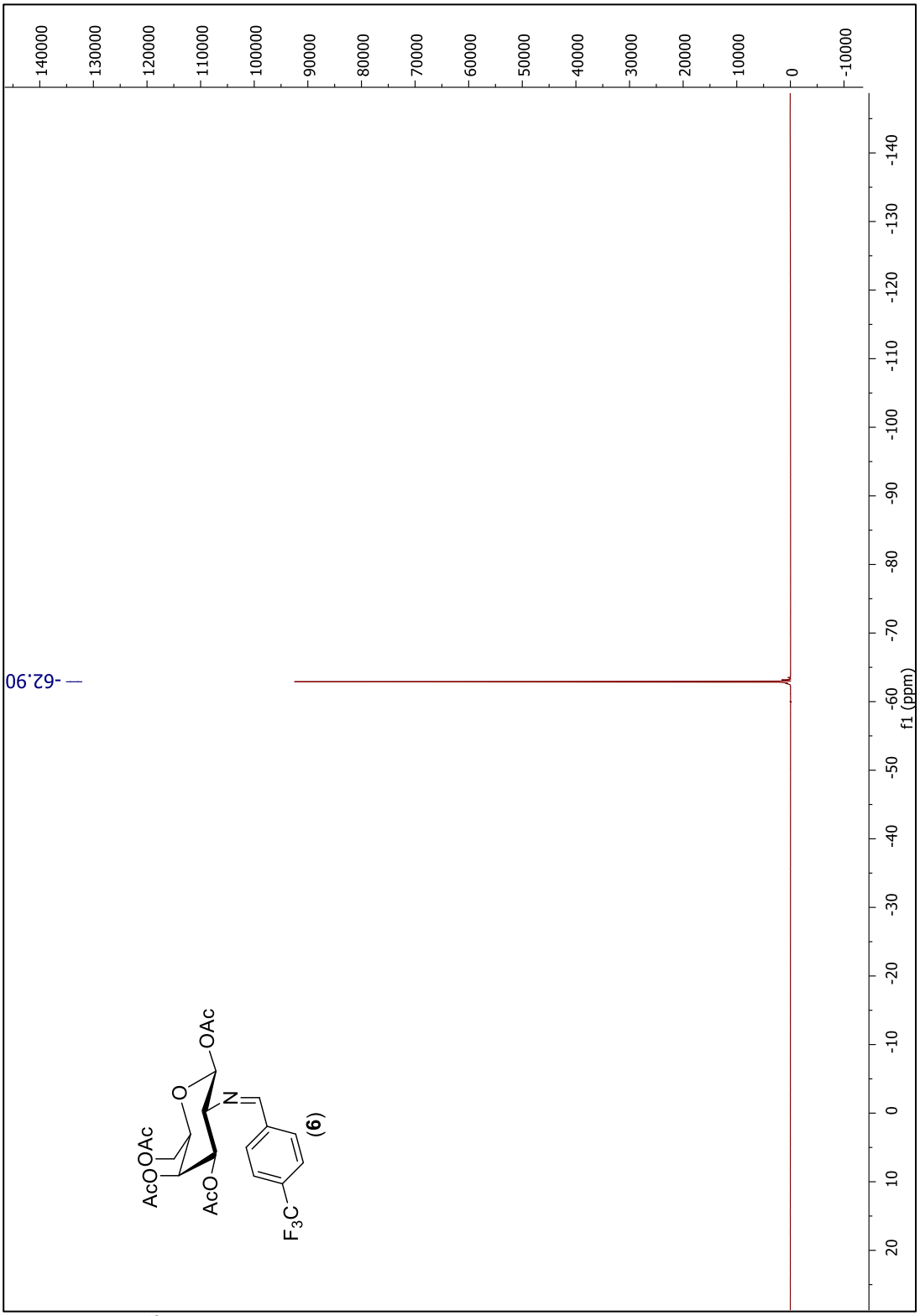


Figure 45. Full ^{19}F NMR spectrum of compound **6**.

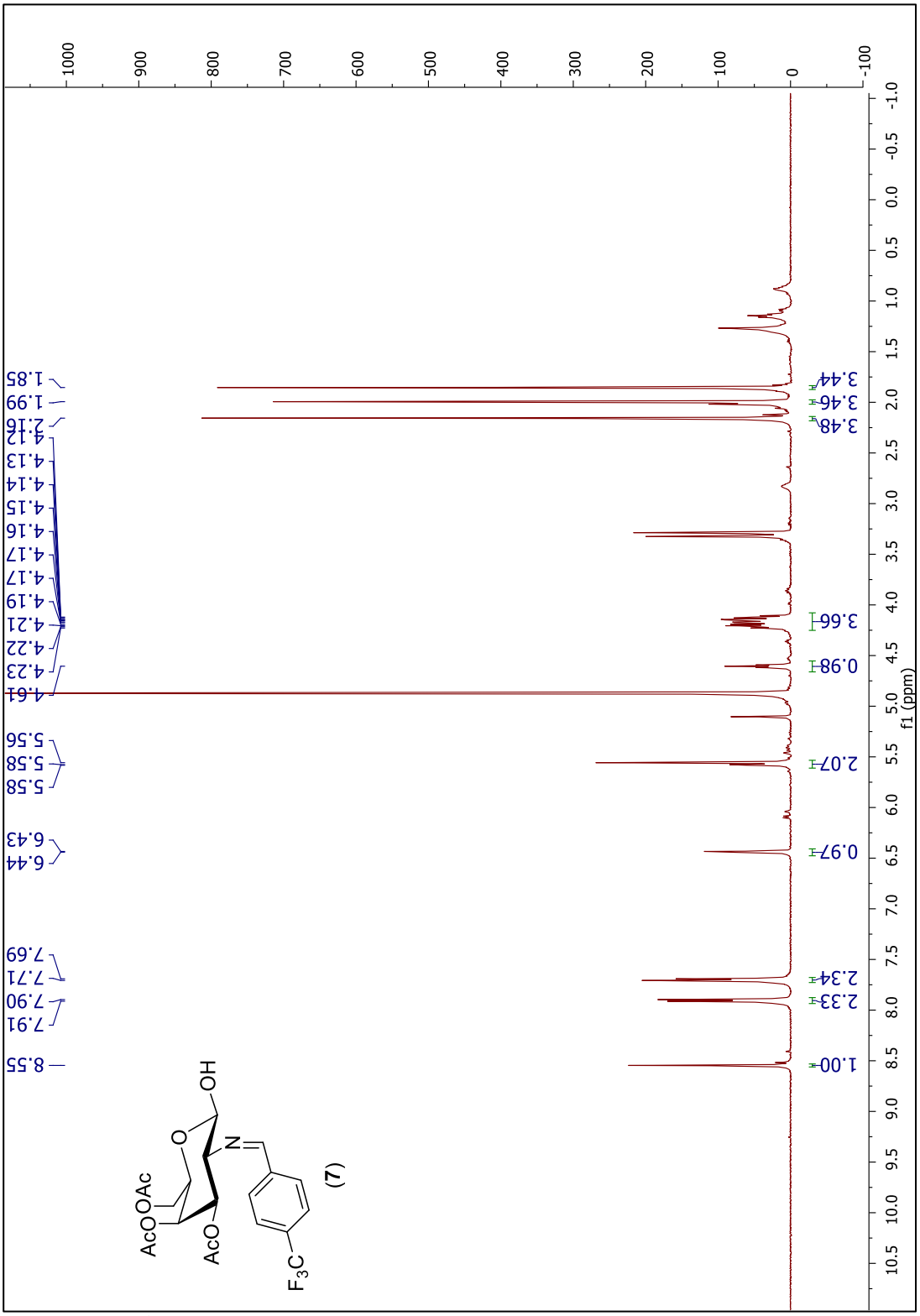


Figure 46. Full ^{1}H NMR spectrum of compound **7**.

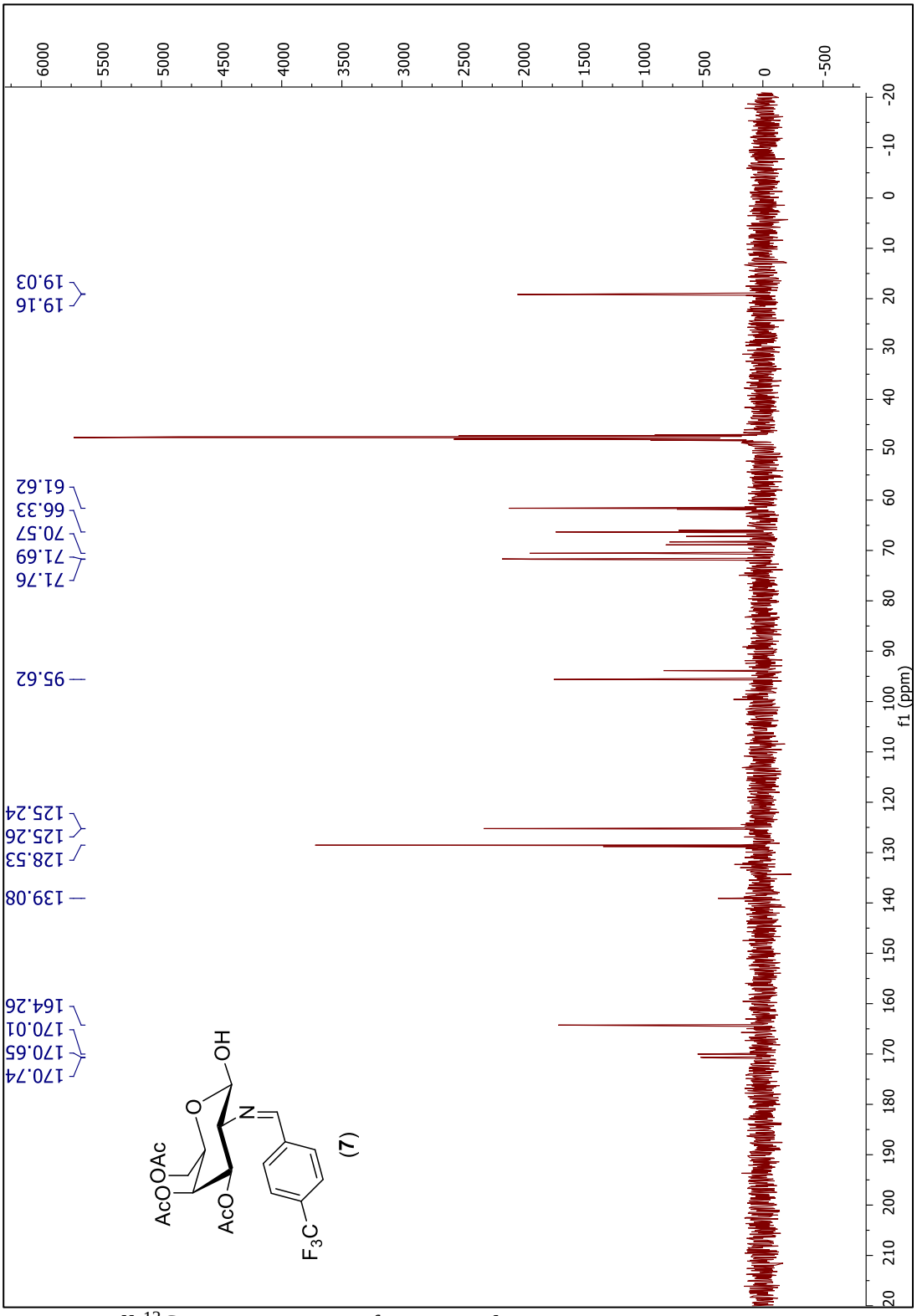


Figure 47. Full ^{13}C NMR spectrum of compound **7**.

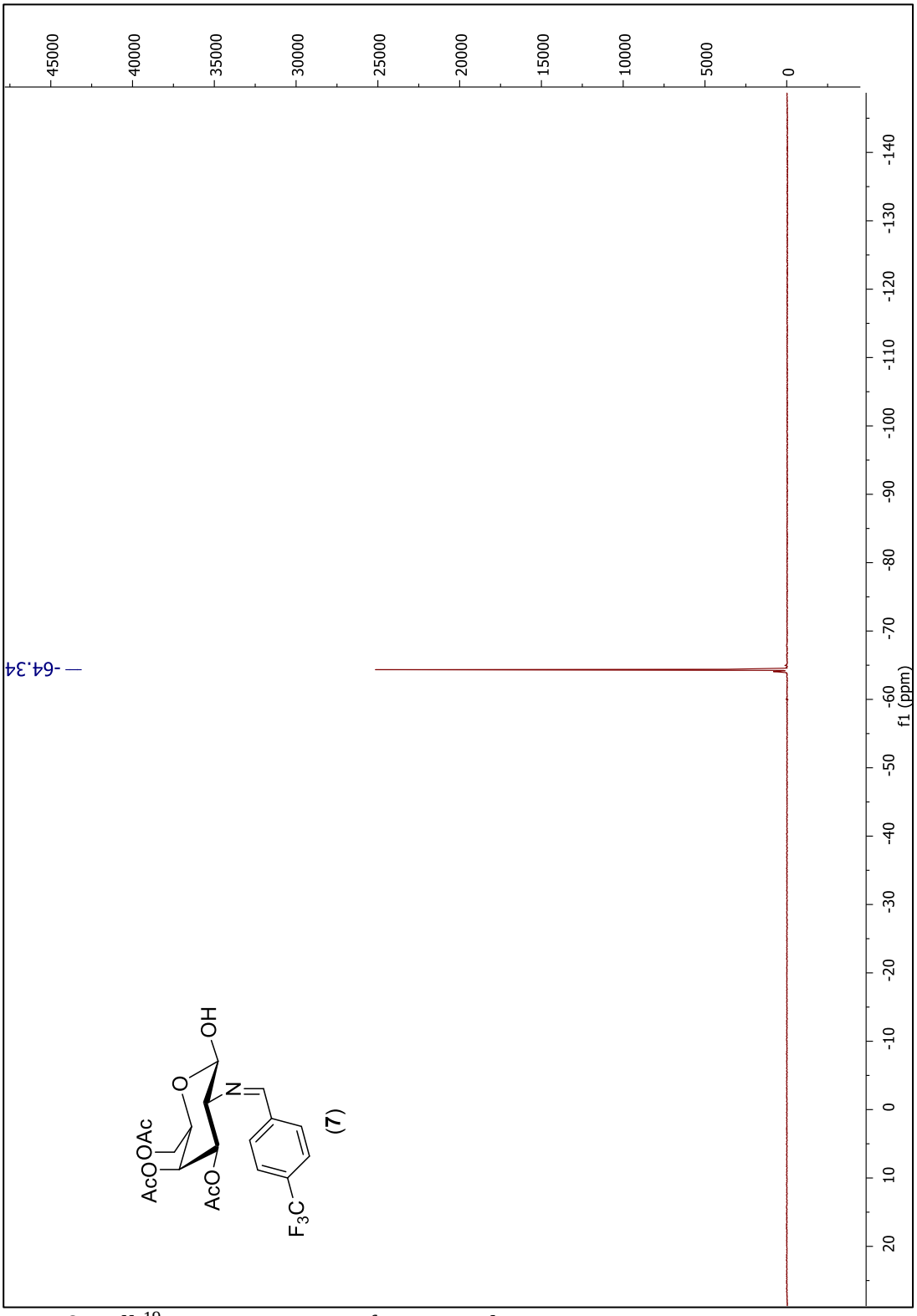


Figure 48. Full ^{19}F NMR spectrum of compound **7**.

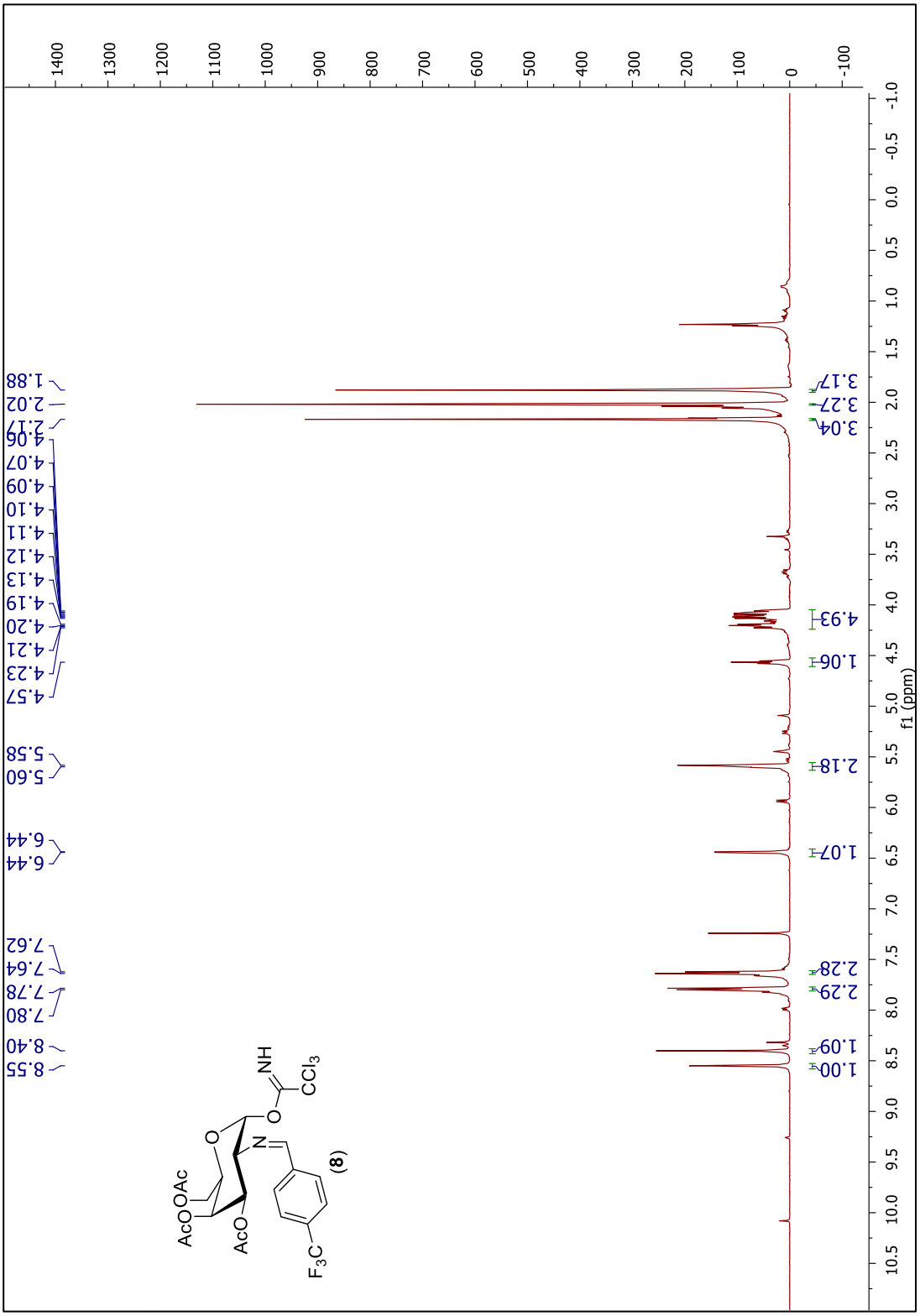


Figure 49. Full ^{1}H NMR spectrum of compound **8**.

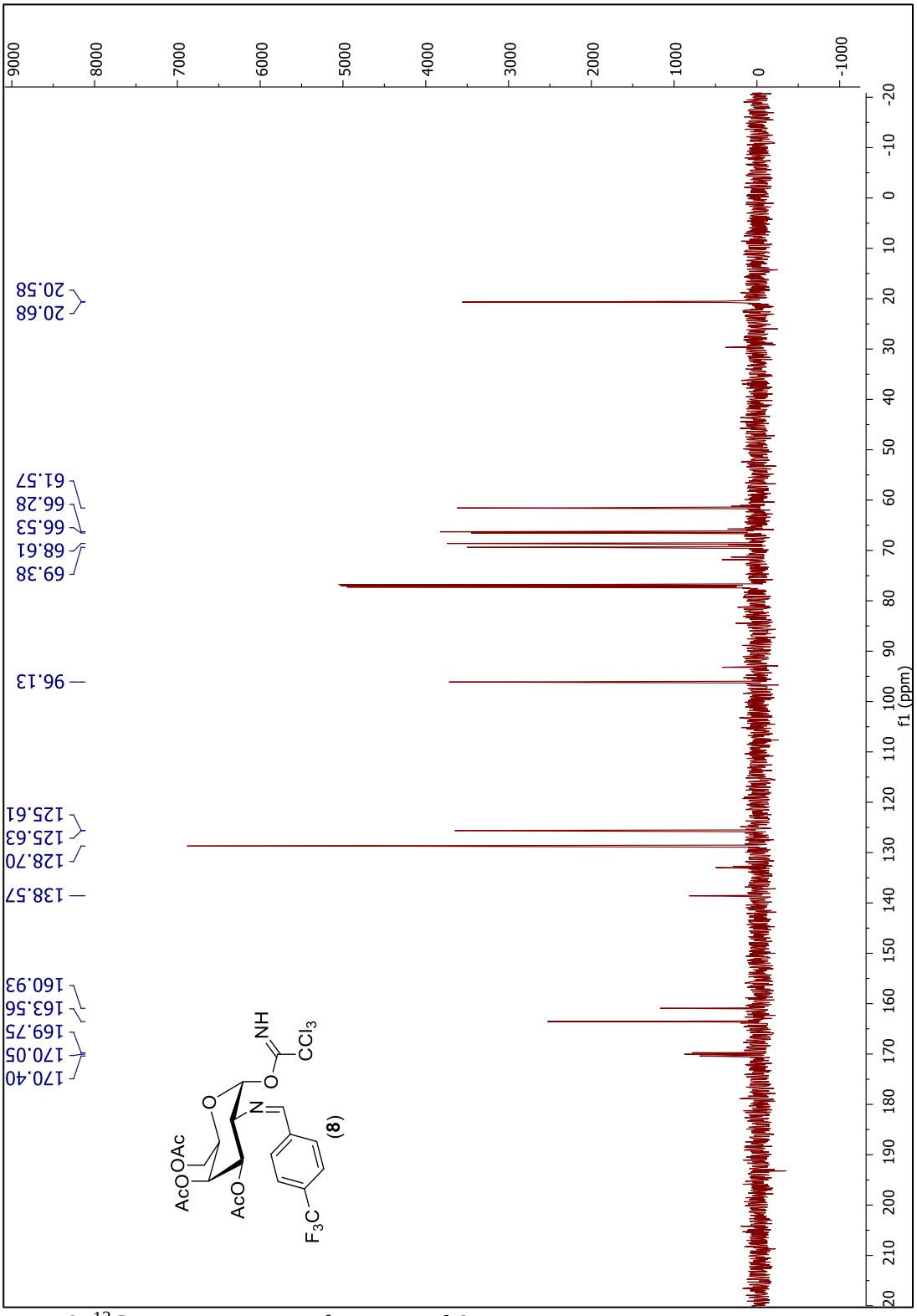


Figure 50. ^{13}C NMR spectrum of compound **8**.

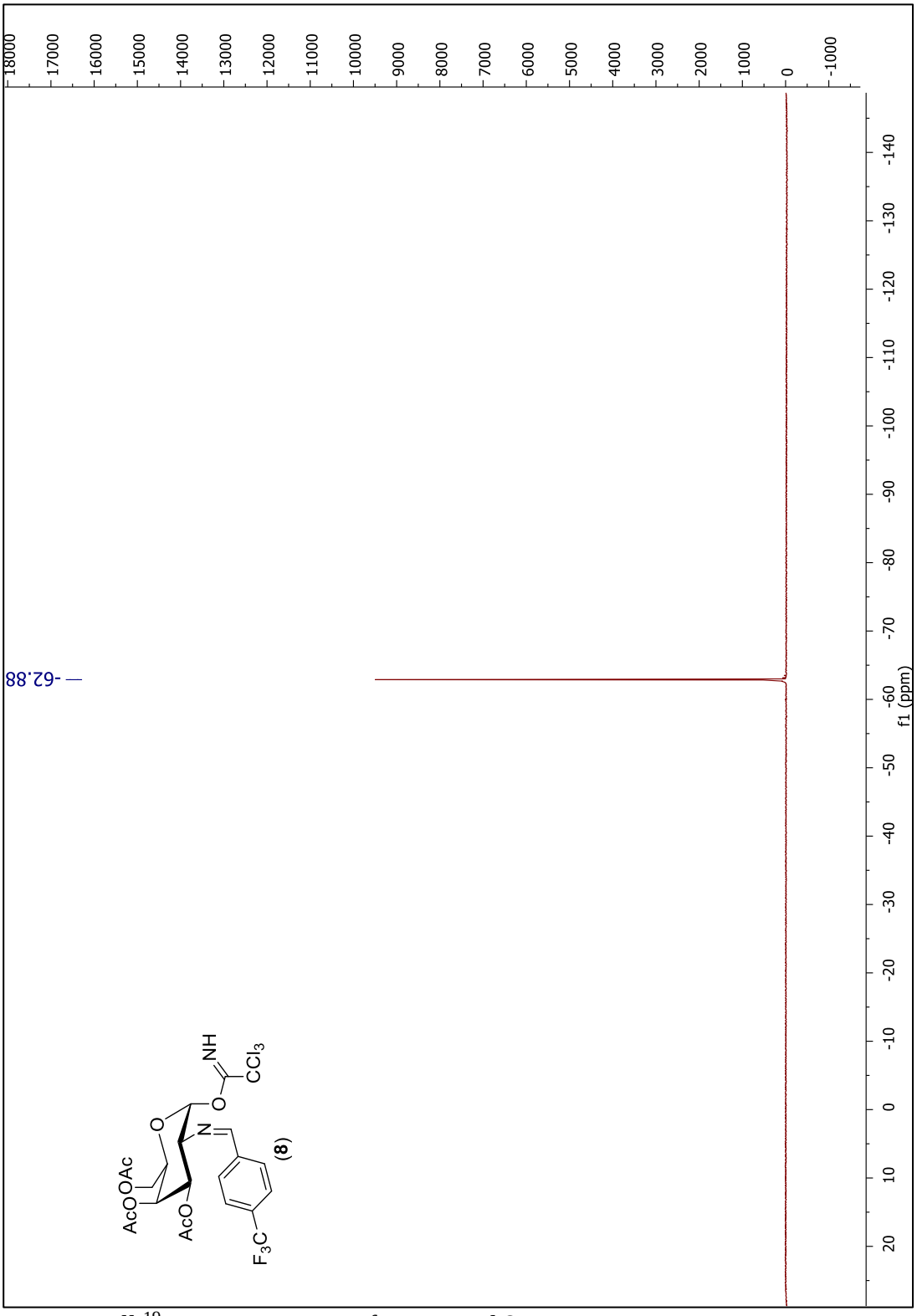


Figure 51. Full ^{19}F NMR spectrum of compound **8**.

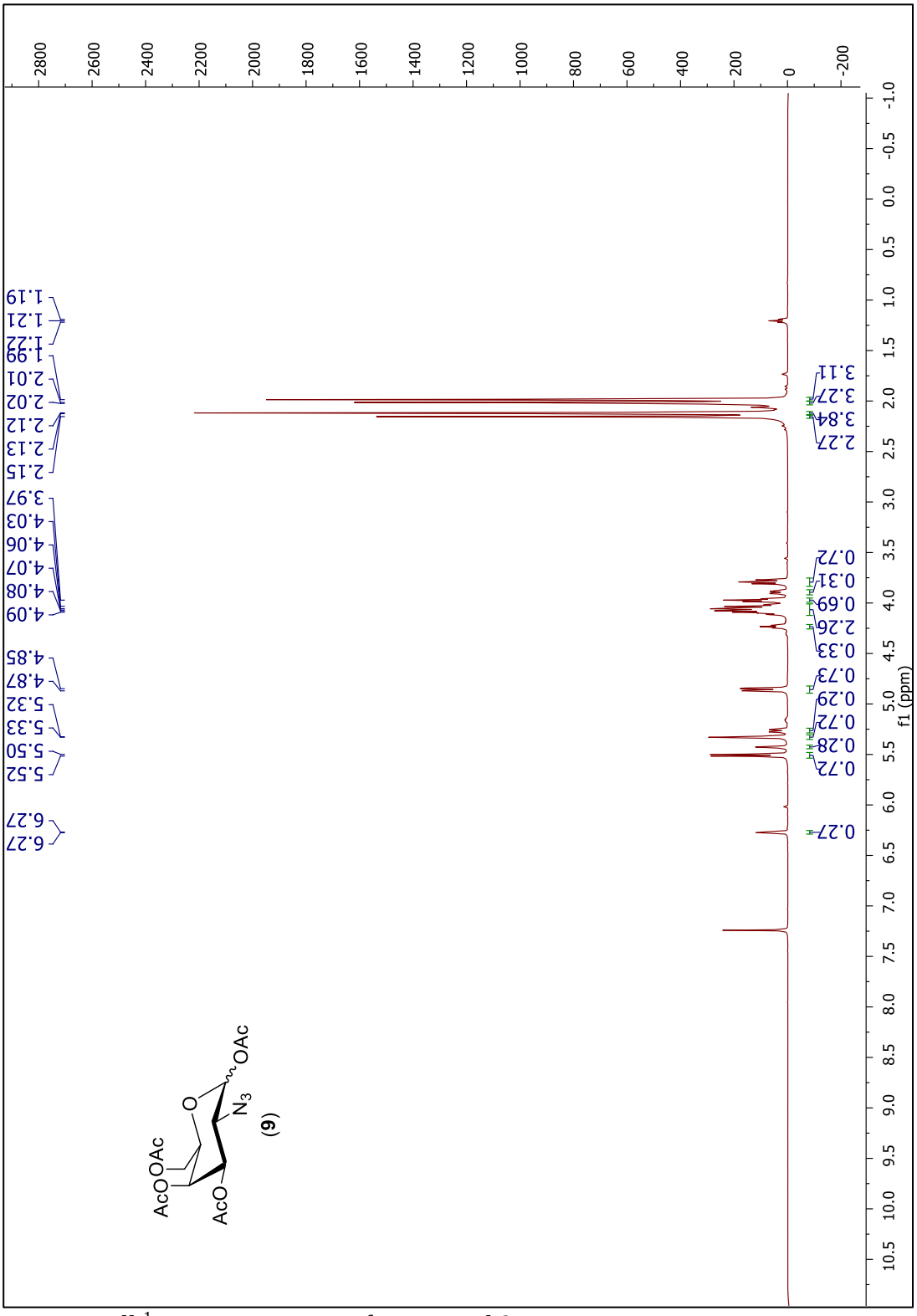


Figure 52. Full ^{1}H NMR spectrum of compound **9**.

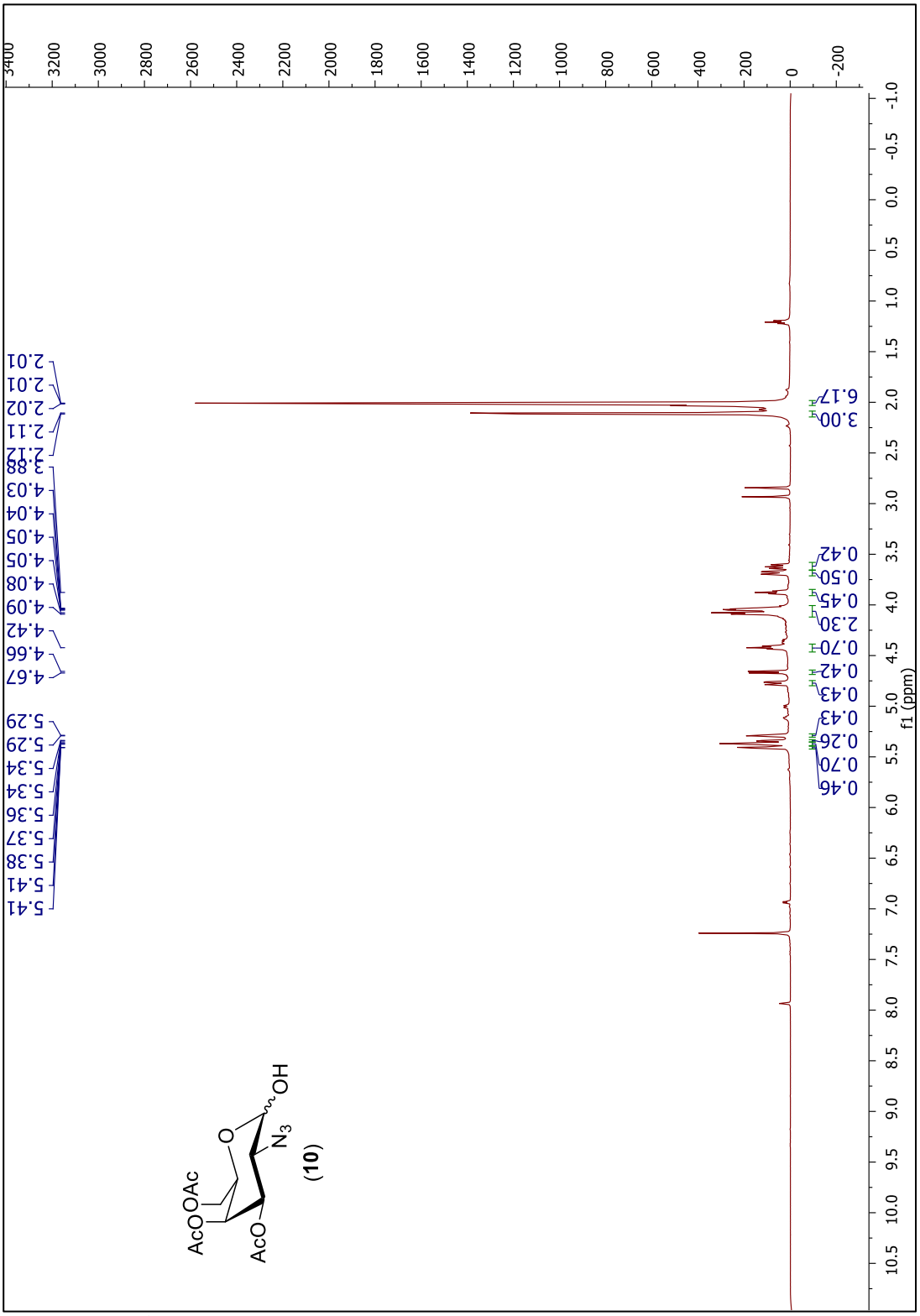


Figure 53. Full ^{1}H NMR spectrum of compound **10**.

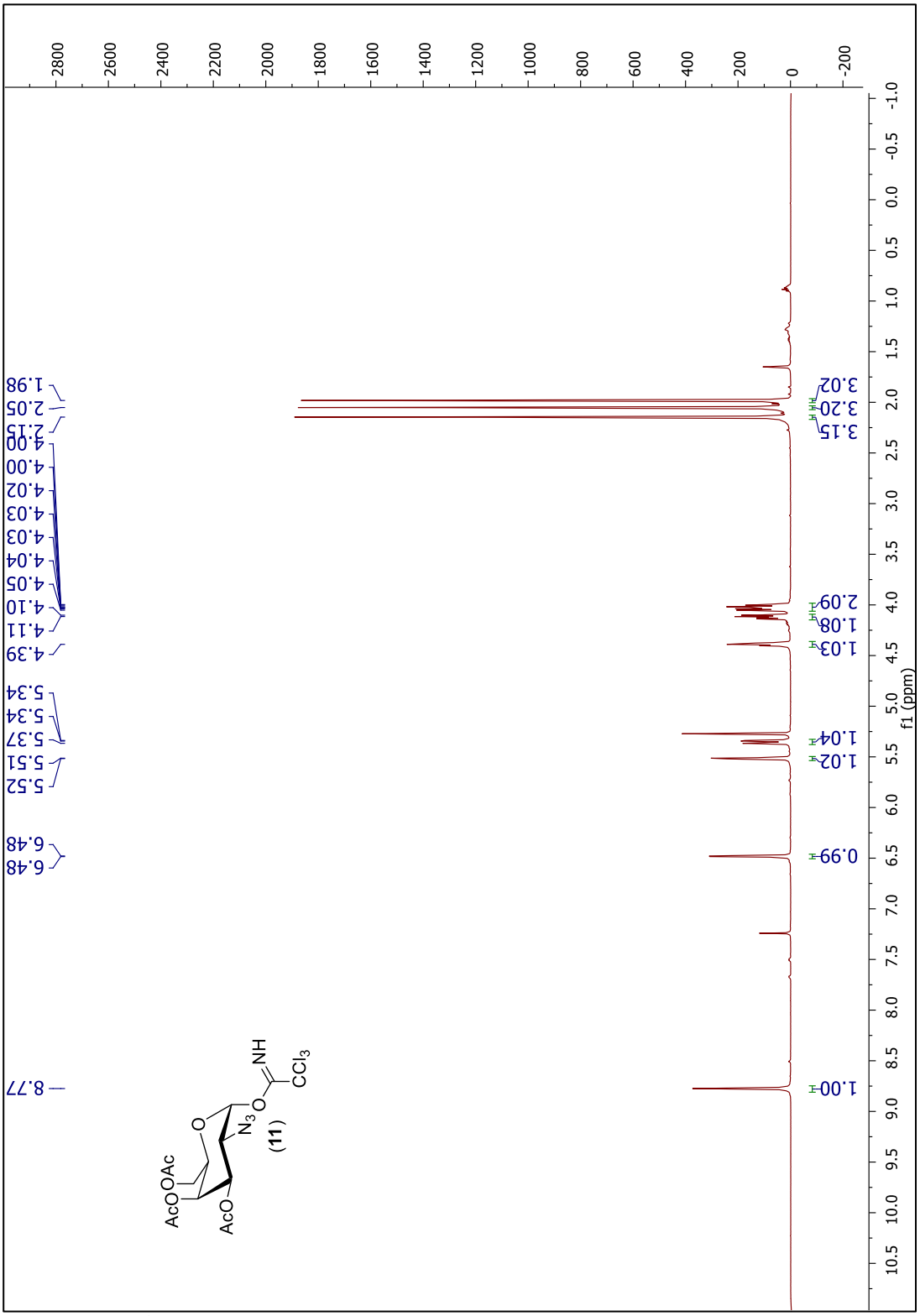


Figure 54. Full ^{1}H NMR spectrum of compound **11**.

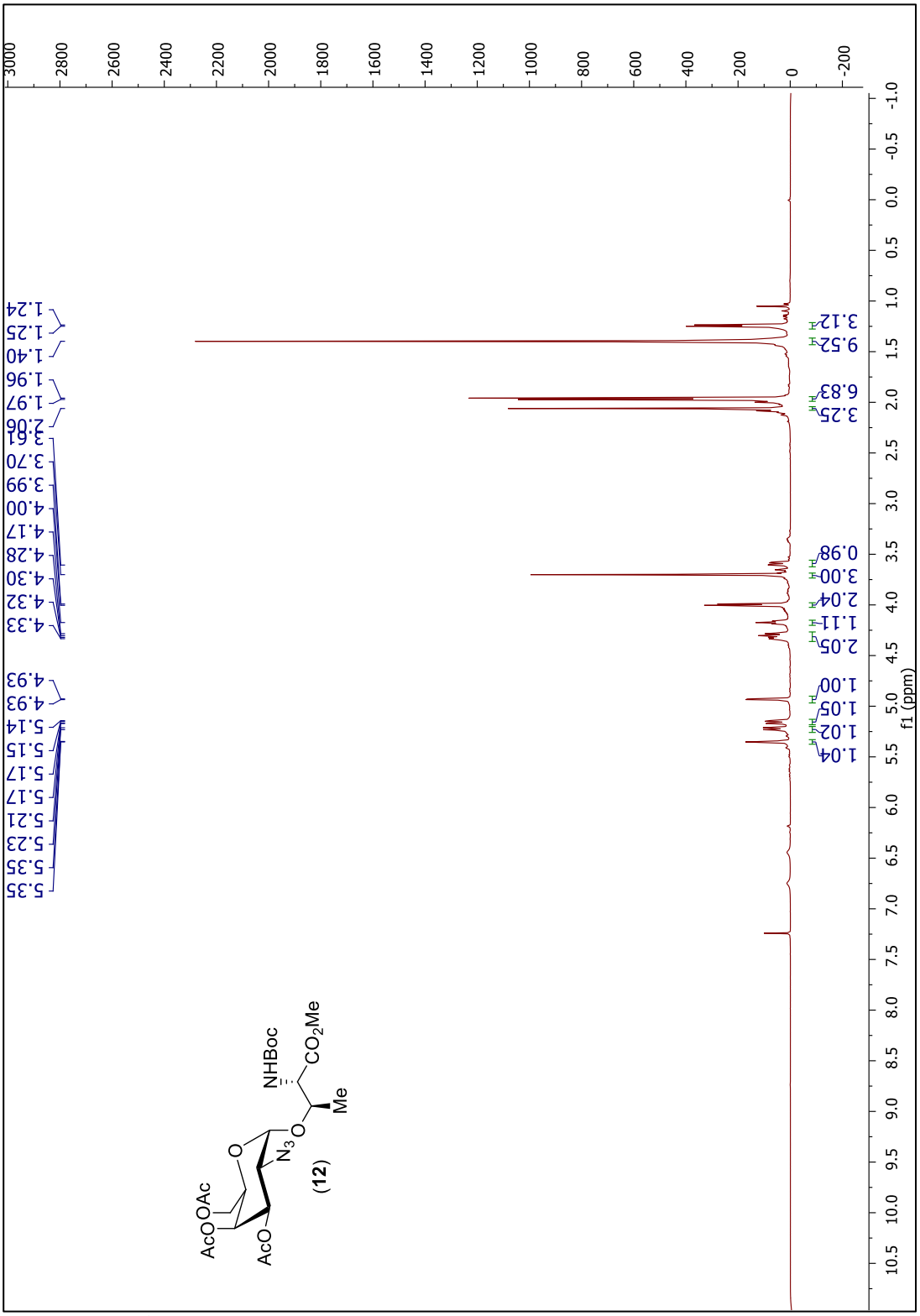


Figure 55. Full ^{1}H NMR spectrum of compound **12**.

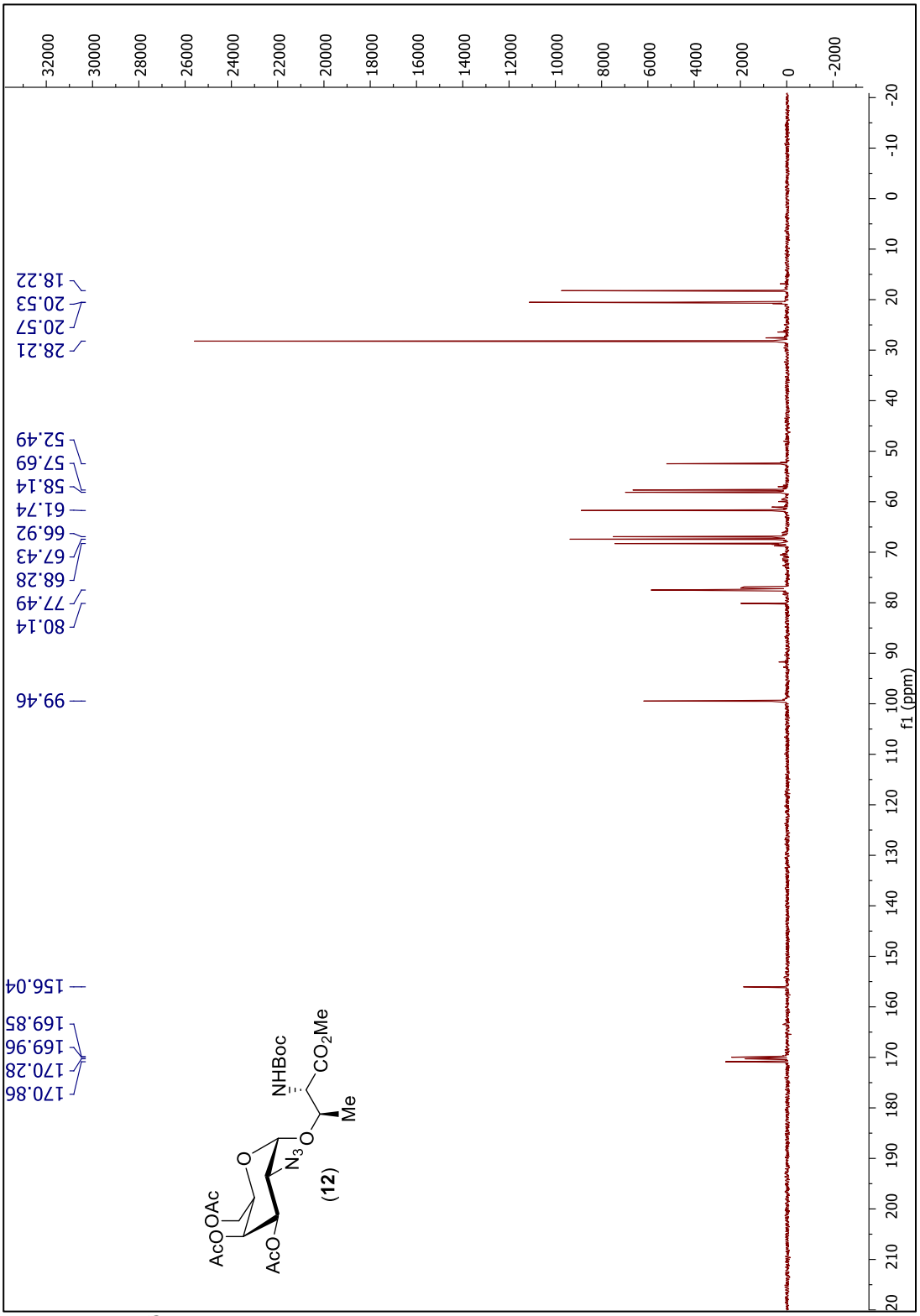


Figure 56. Full ^{13}C NMR spectrum of compound **12**.

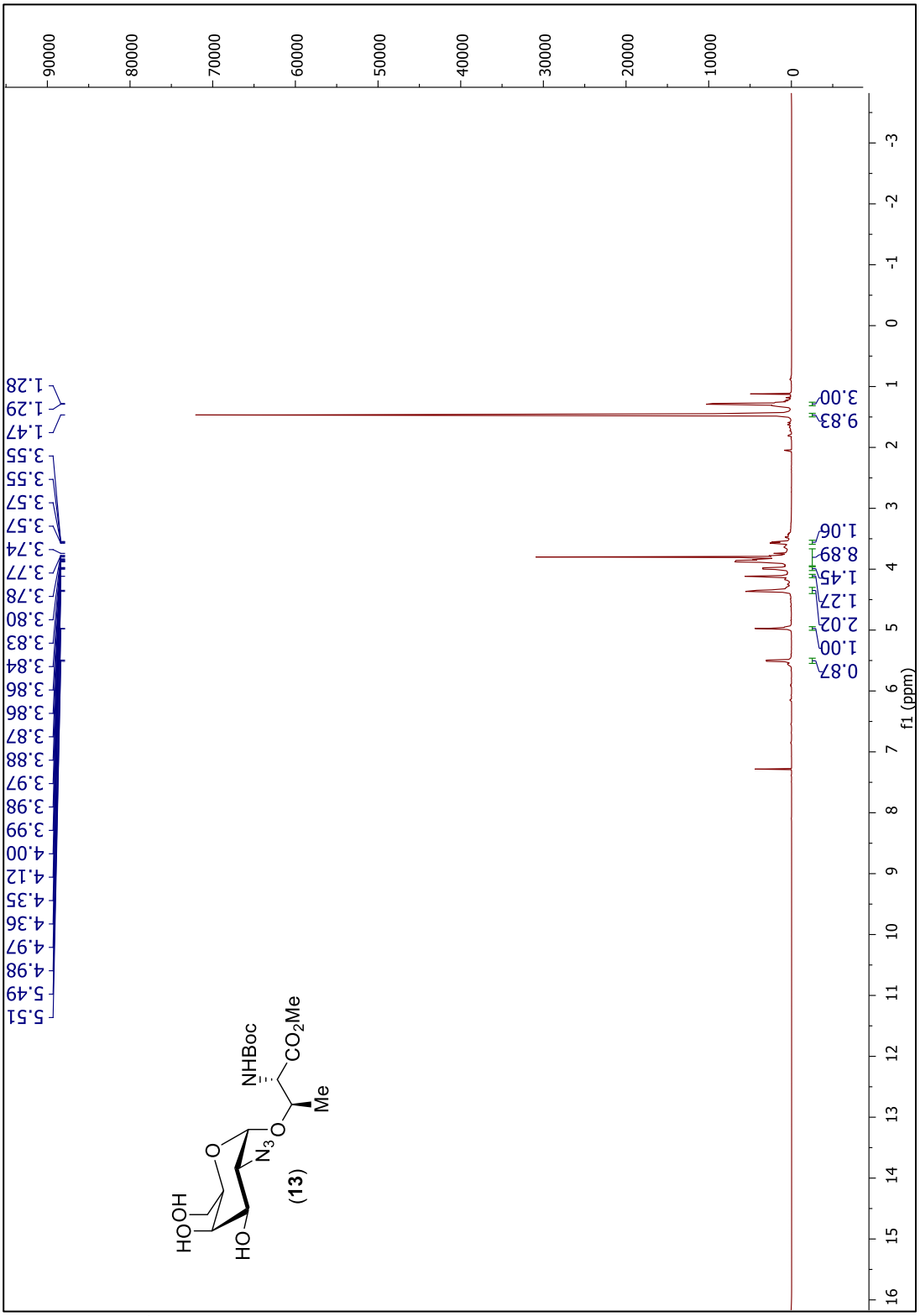


Figure 57. Full ^{1}H NMR spectrum of compound **13**.

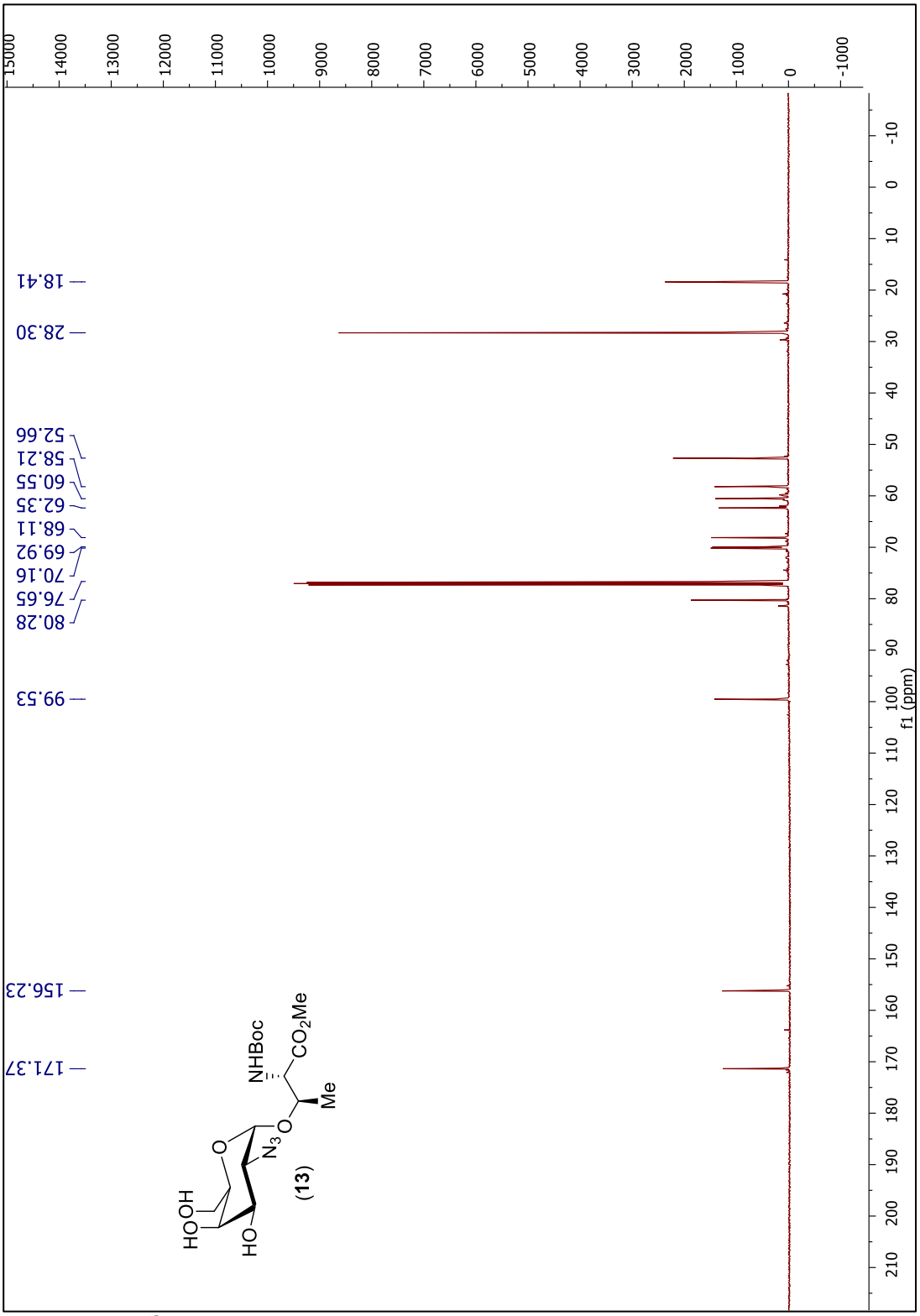


Figure 58. Full ^{13}C NMR spectrum of compound **13**.

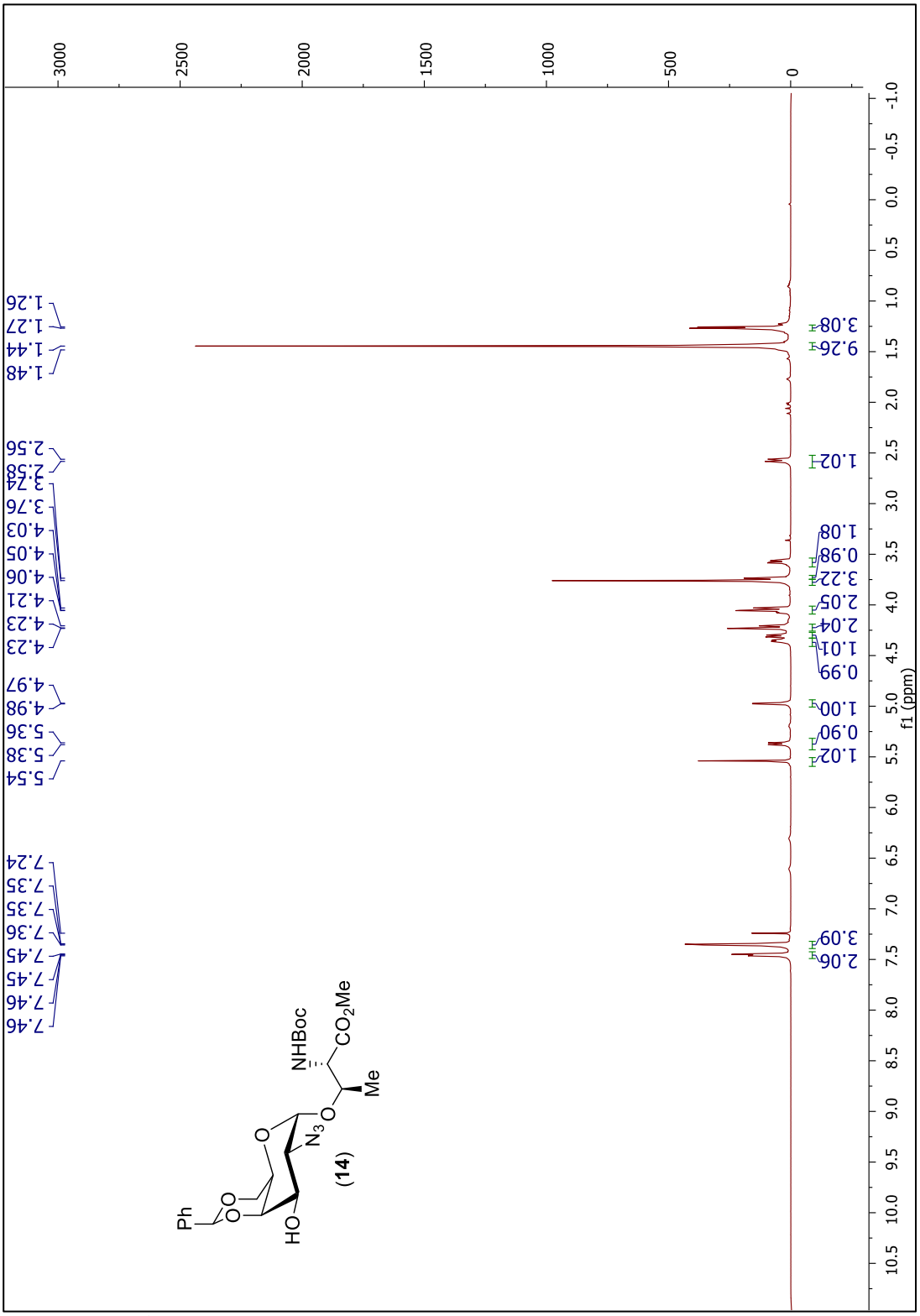


Figure 59. Full ^{1}H NMR spectrum of compound **14**.

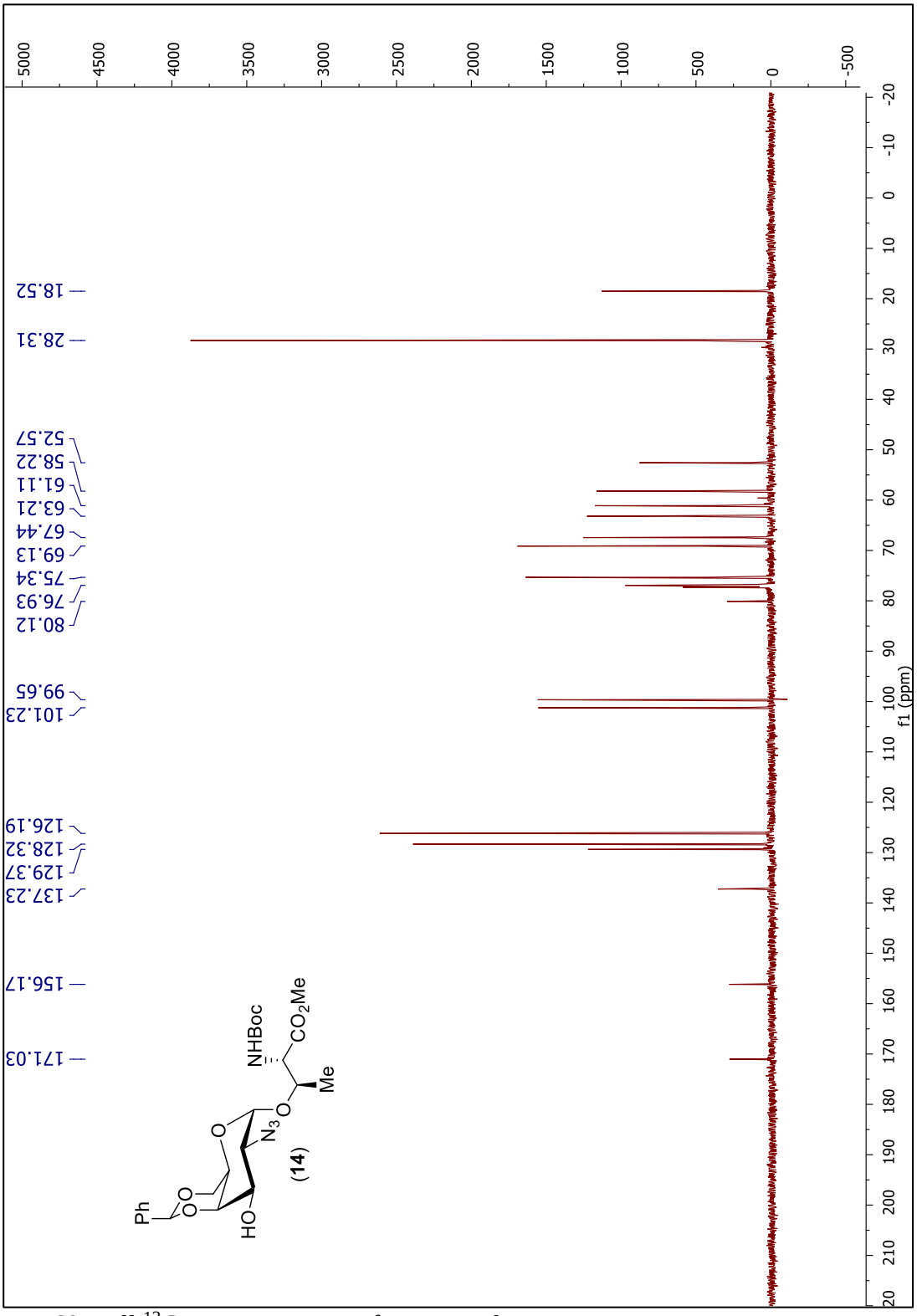


Figure 60. Full ^{13}C NMR spectrum of compound **14**.

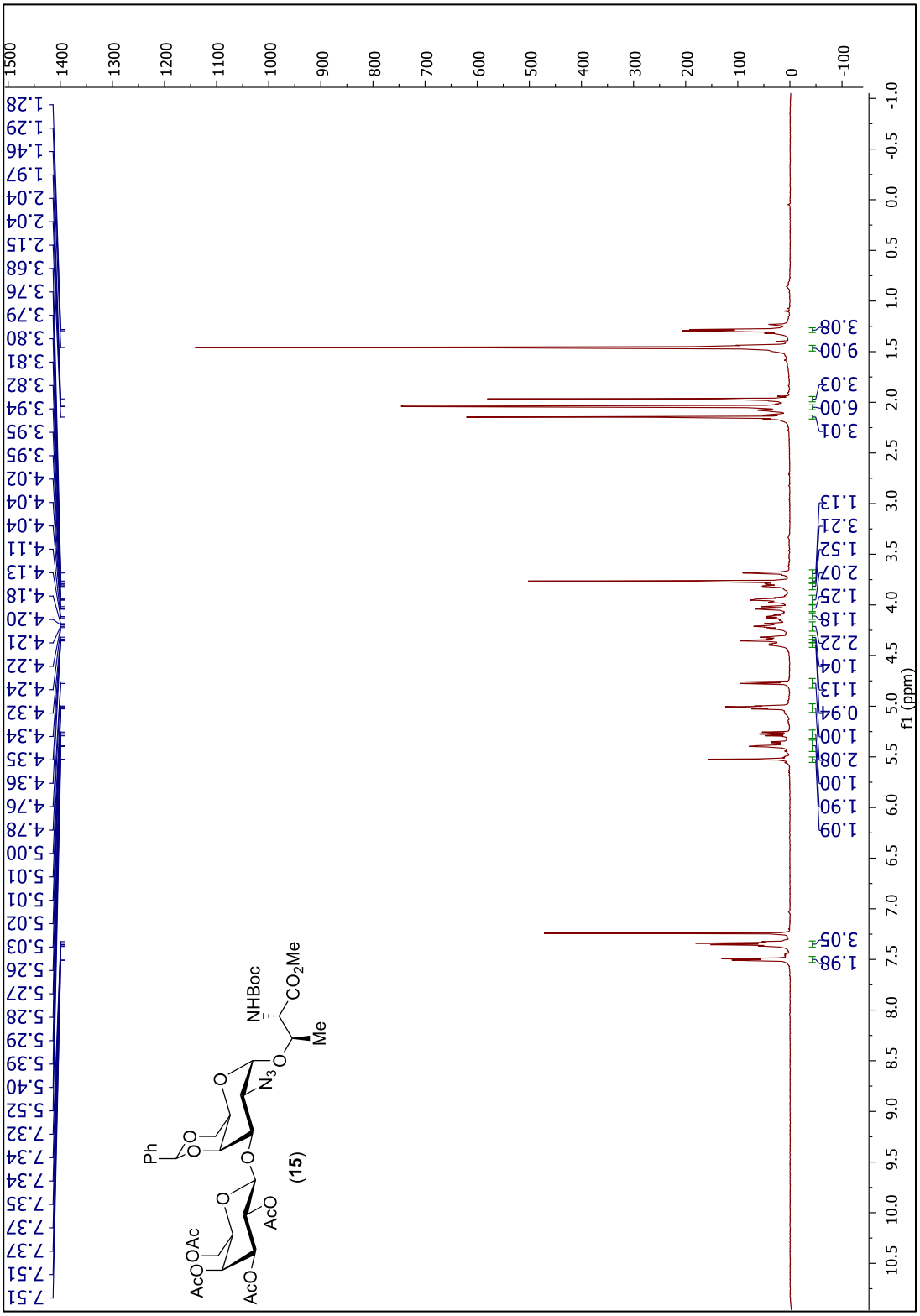


Figure 61. Full ^{1}H NMR spectrum of compound **15**.

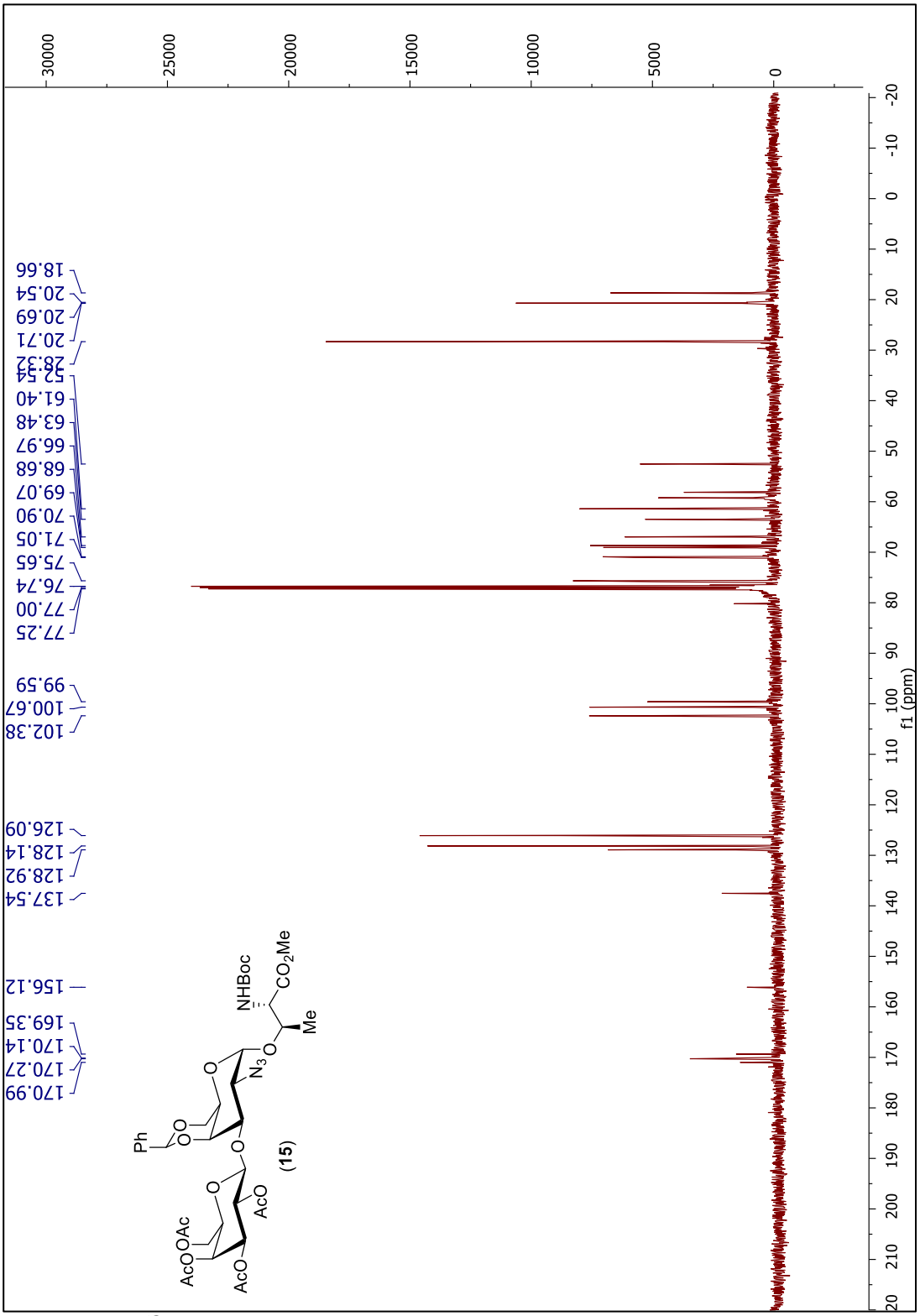


Figure 62. Full ^{13}C NMR spectrum of compound 1**5**.

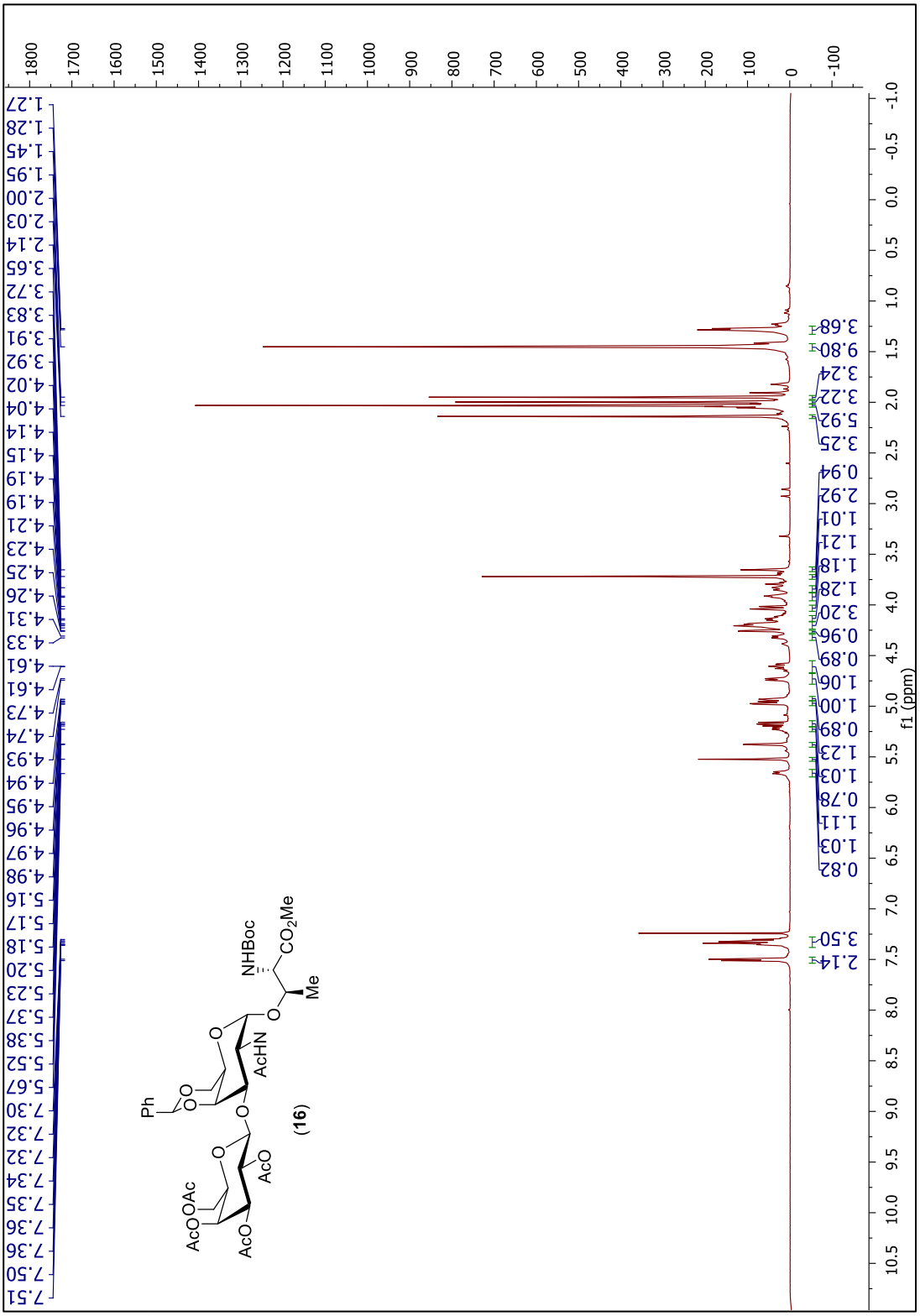


Figure 63. Full ^{1}H NMR spectrum of compound 1**6**.

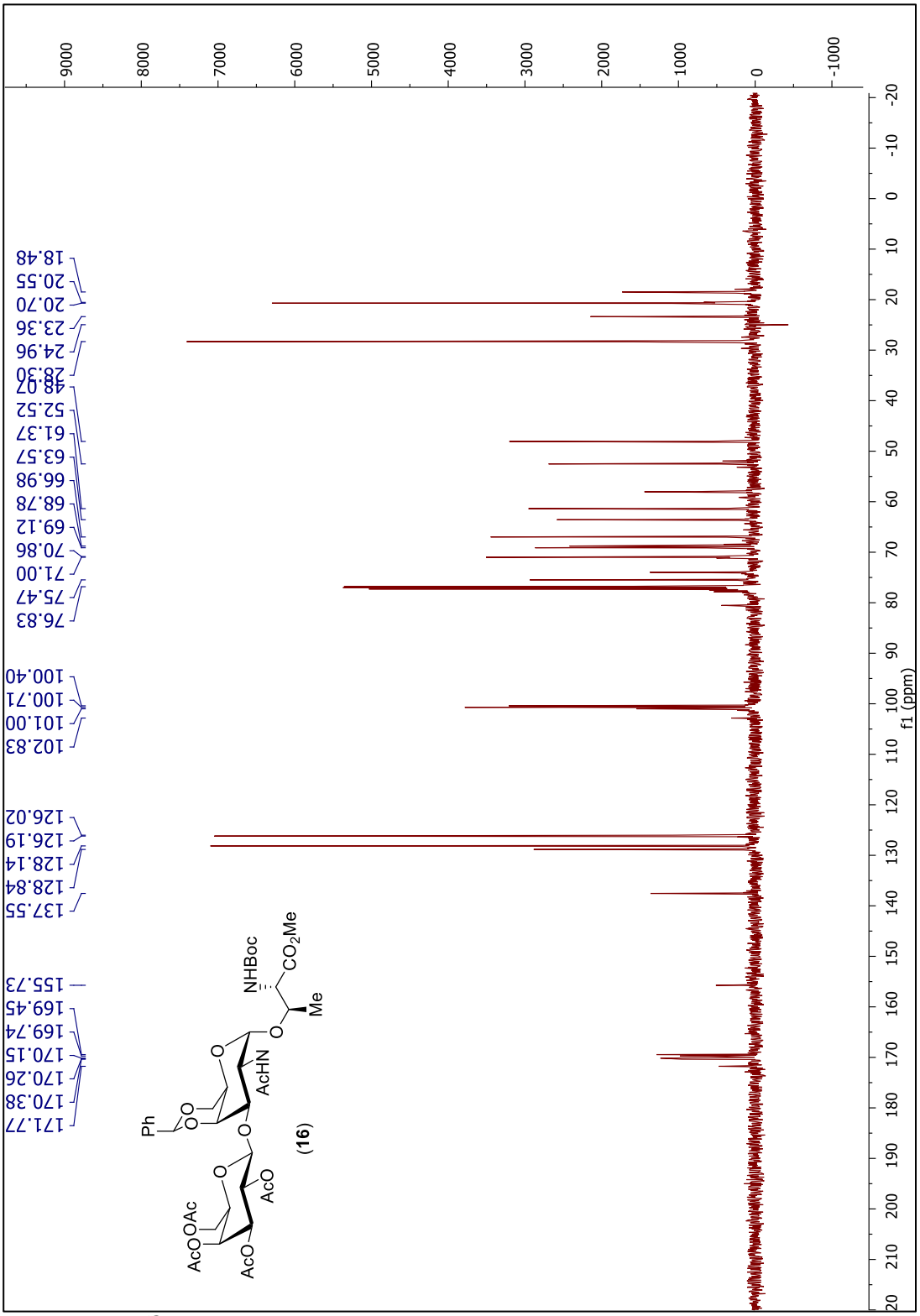


Figure 64. Full ^{13}C NMR spectrum of compound **16**.

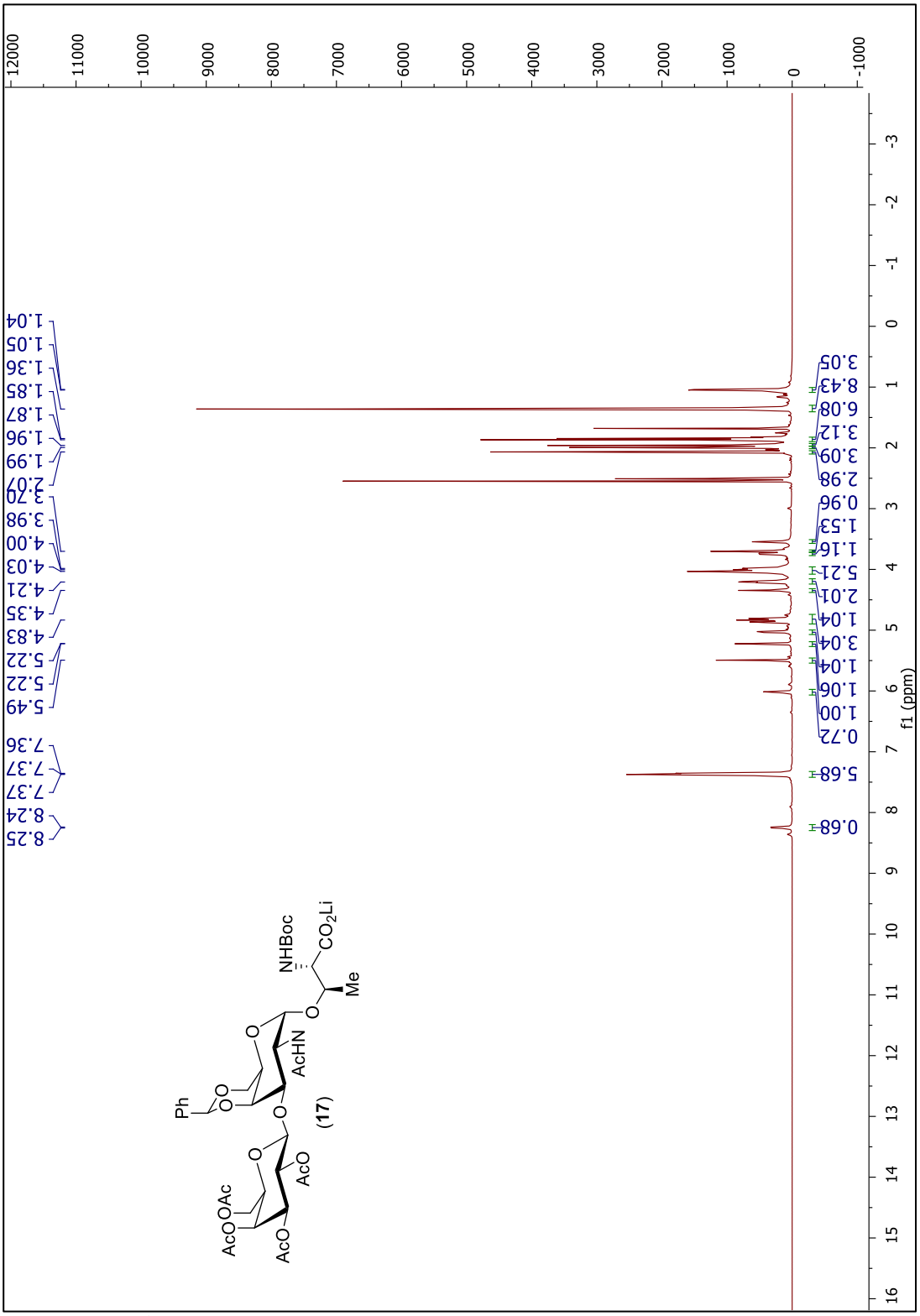


Figure 65. Full ^{1}H NMR spectrum of compound **17**.

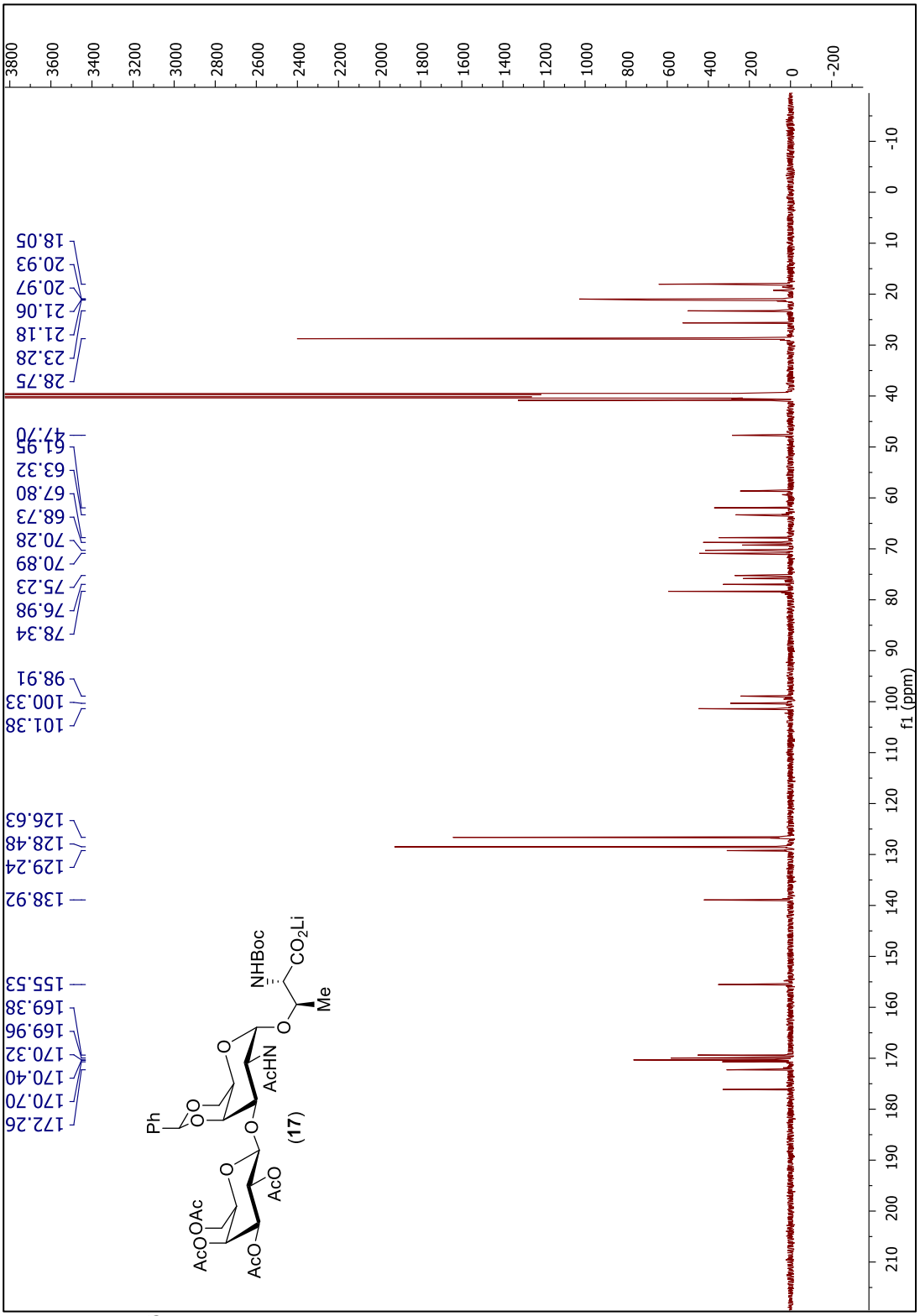


Figure 66. Full ^{13}C NMR spectrum of compound **17**.

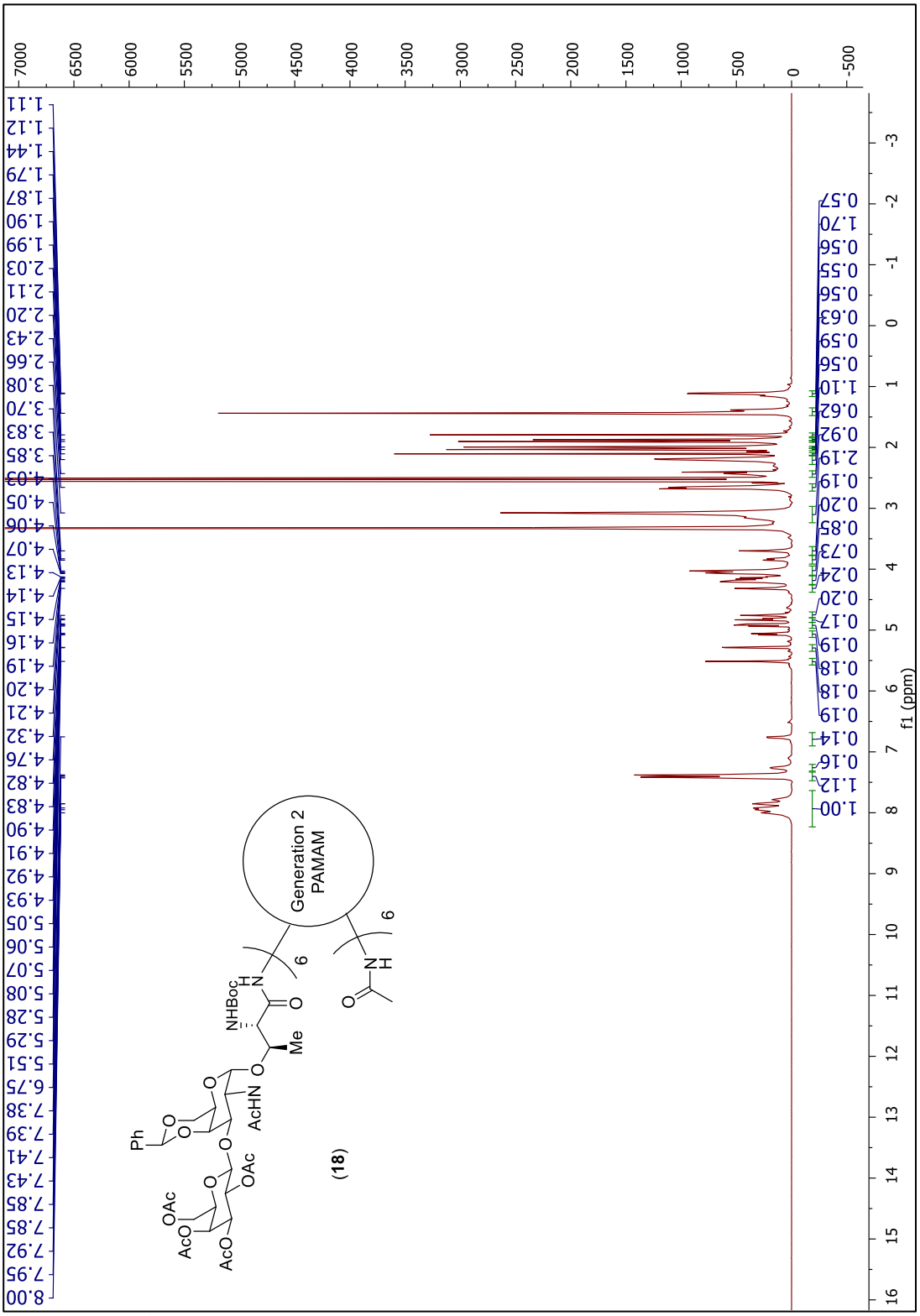


Figure 67. Full ^{1}H NMR spectrum of compound **18**.

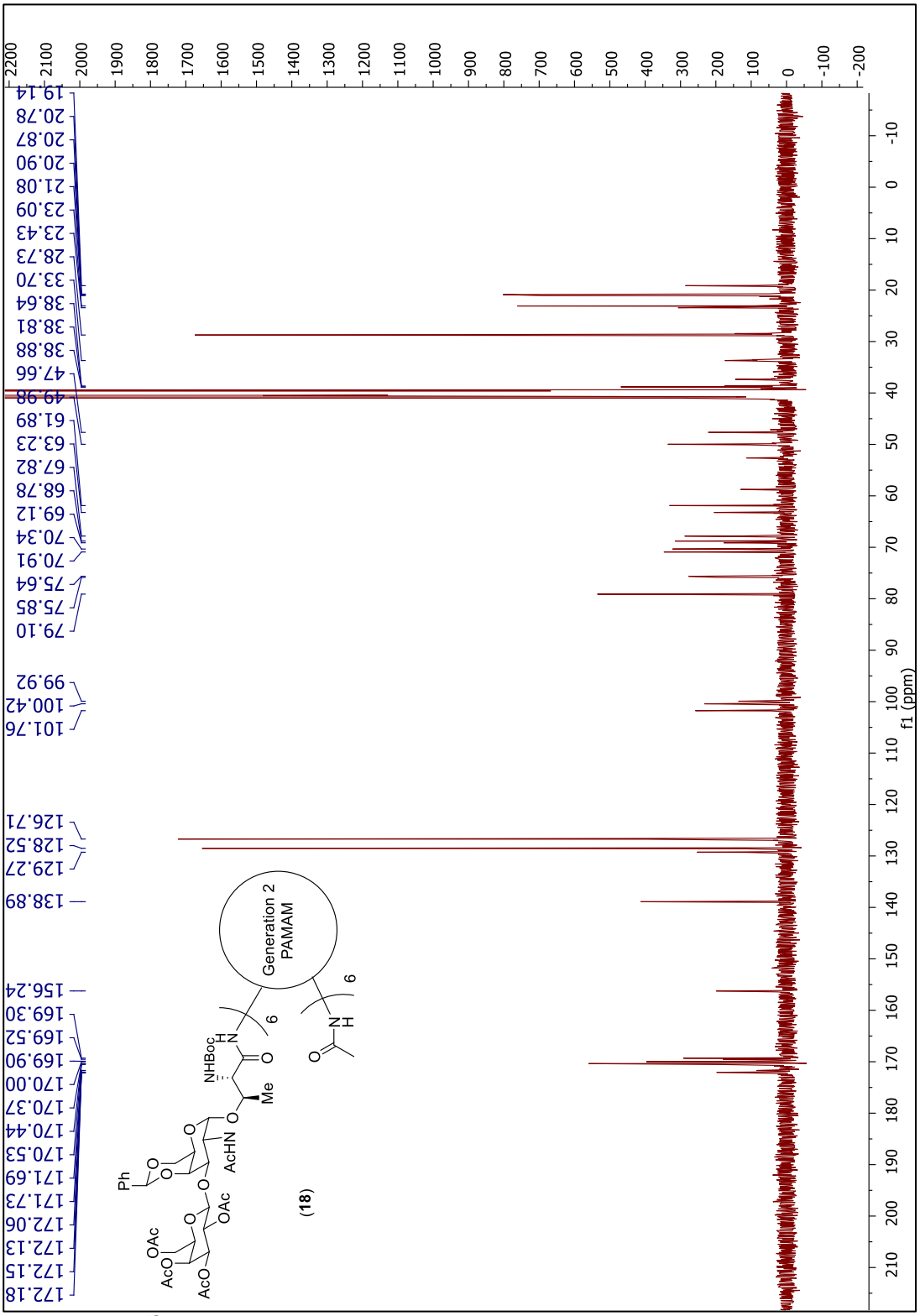


Figure 68. Full ^{13}C NMR spectrum of compound **18**.

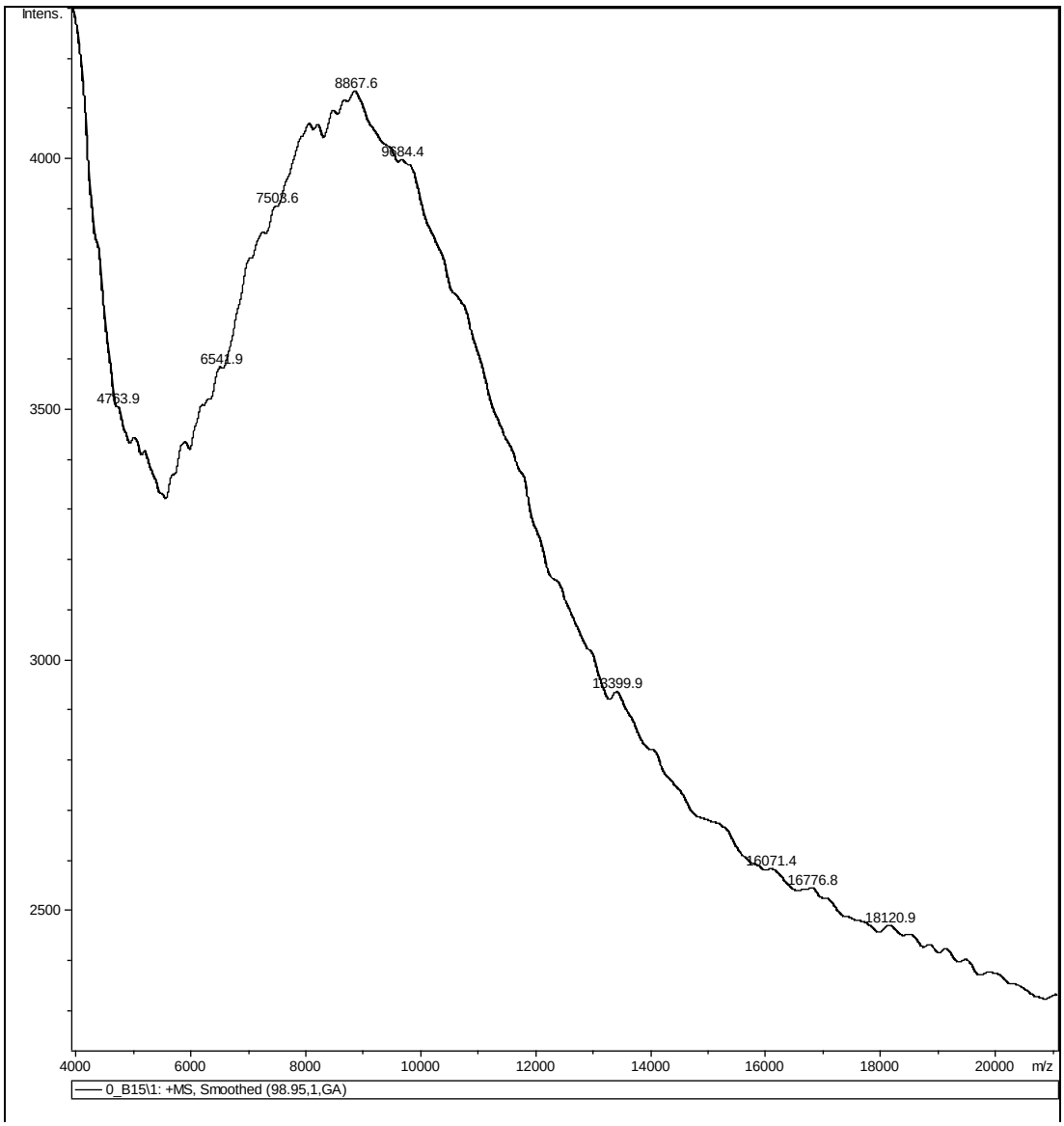


Figure 69. Smoothed MALDI TOF spectrum for compound **18**. M_w = 8895.

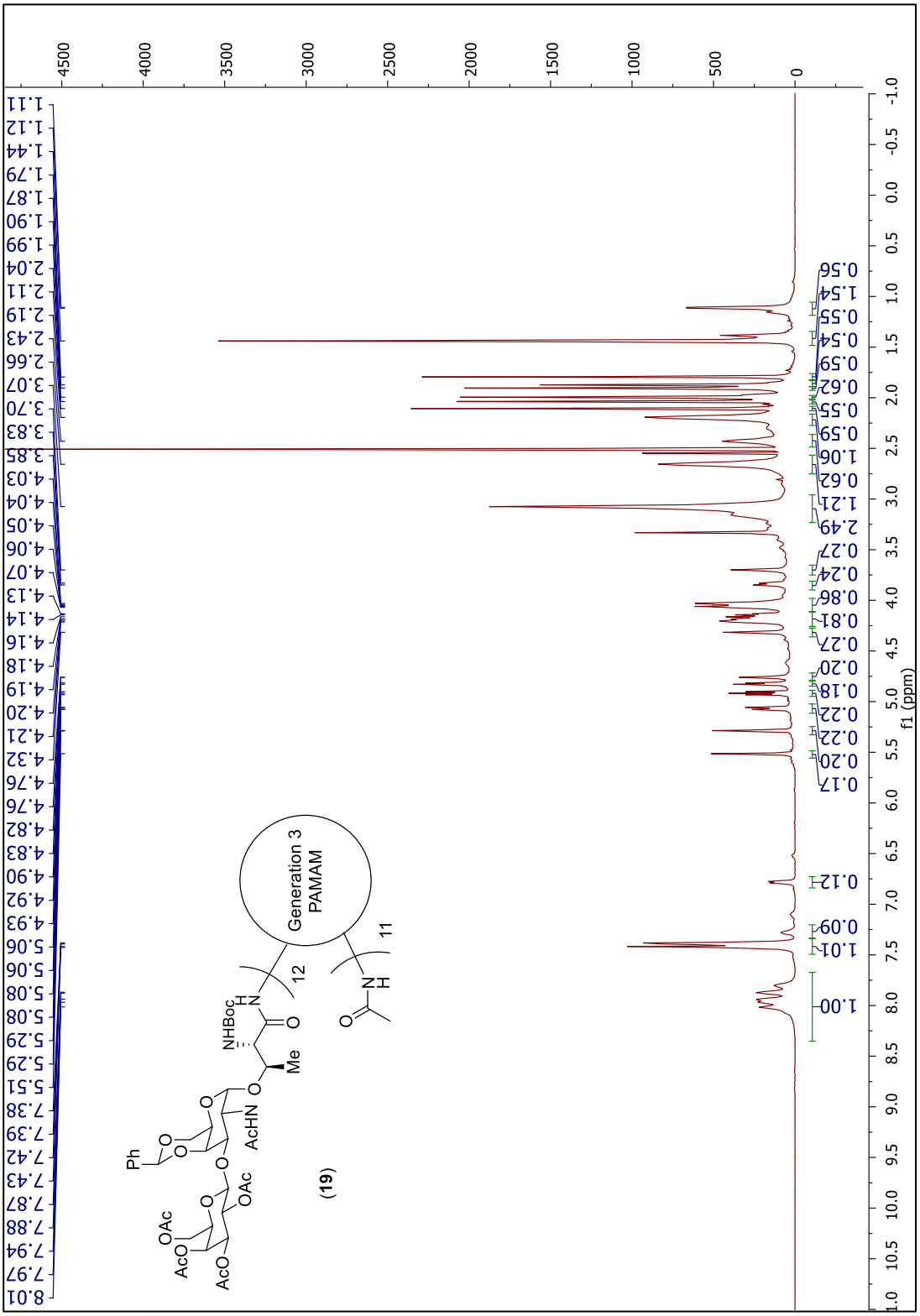


Figure 70. Full ^{1}H NMR spectrum of compound **19**.

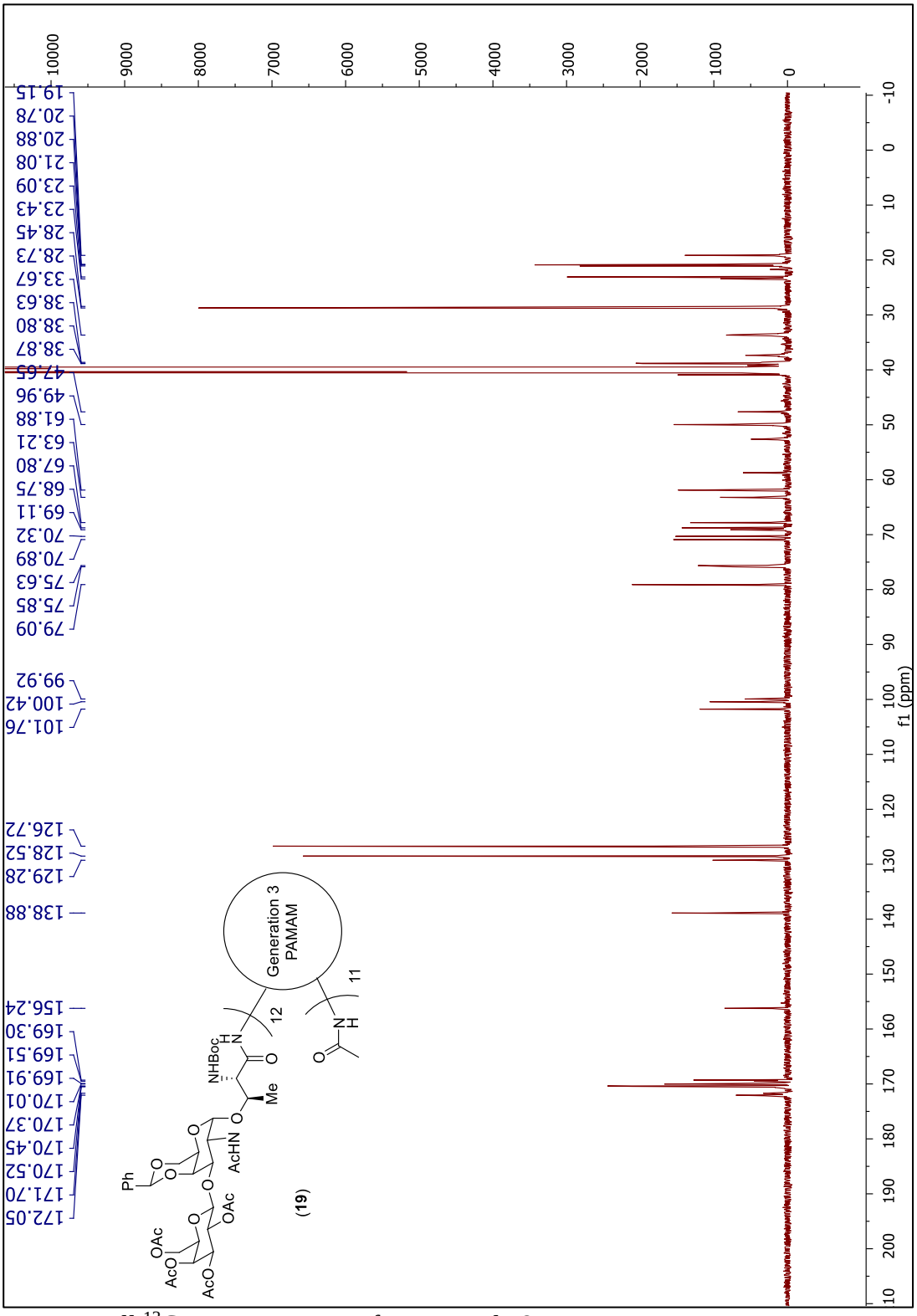


Figure 71. Full ^{13}C NMR spectrum of compound **19**.

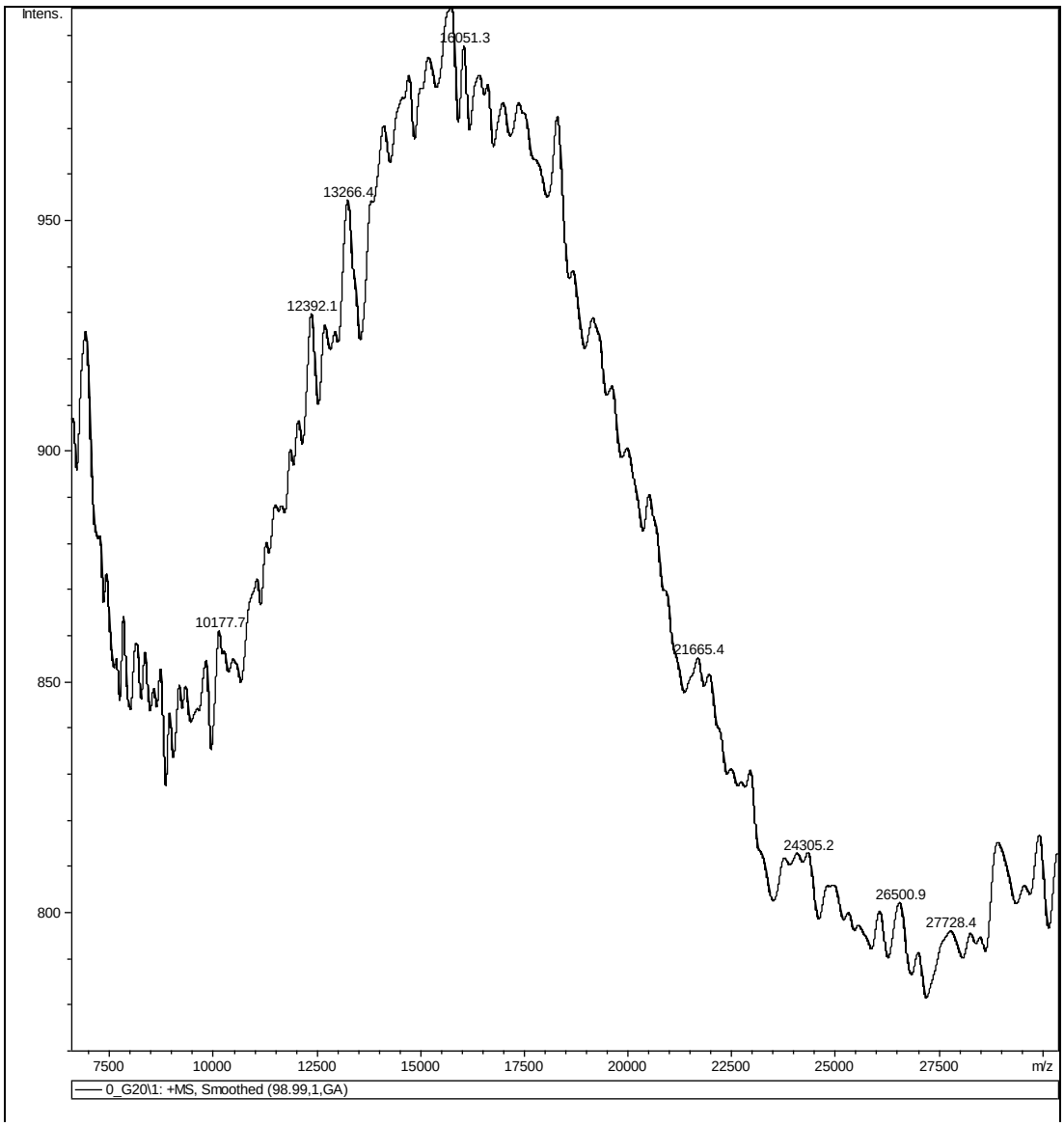


Figure 72. Smoothed MALDI TOF spectrum for compound **19**. M_w = 16220.

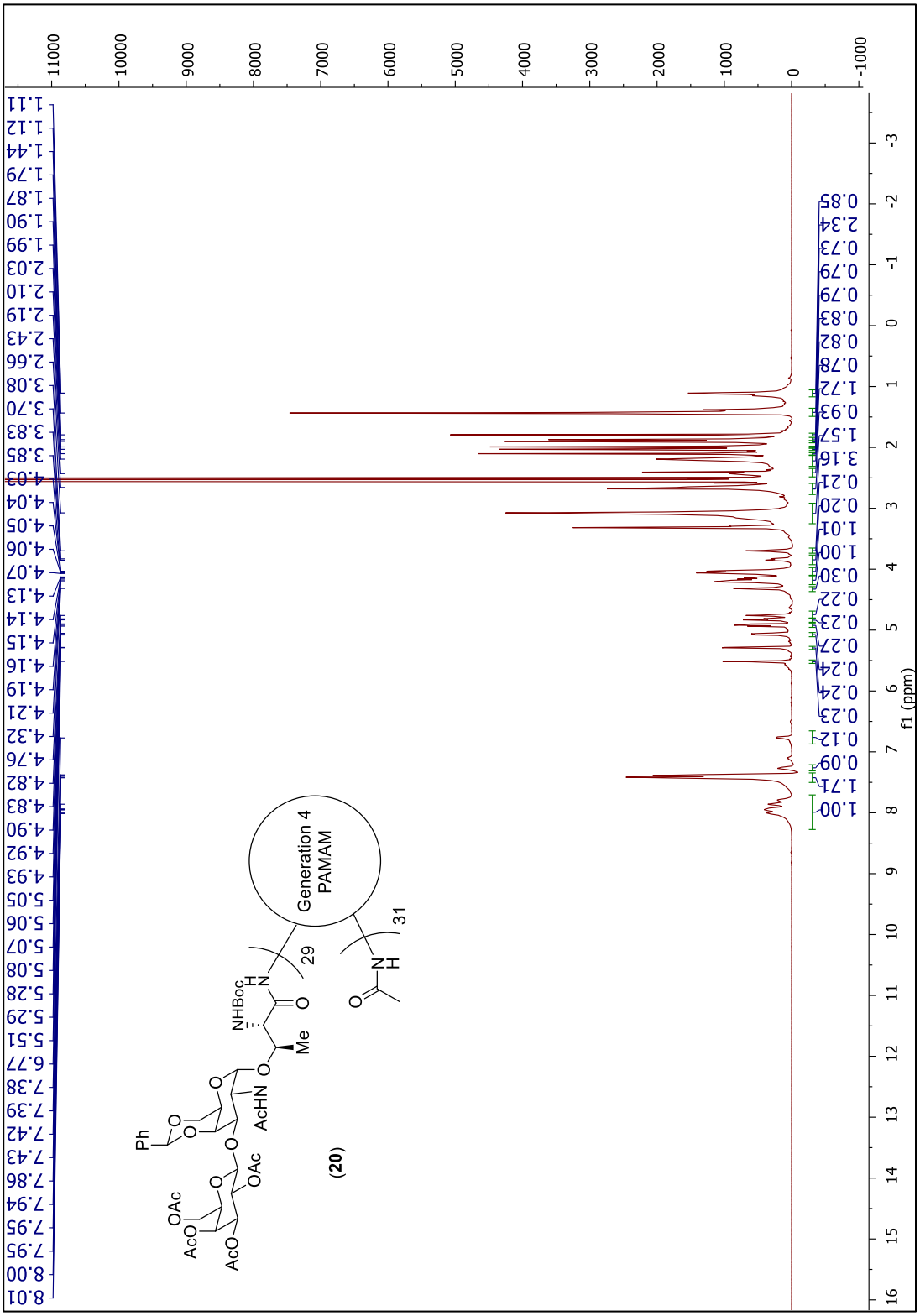


Figure 73. Full ^{1}H NMR spectrum of compound **20**.

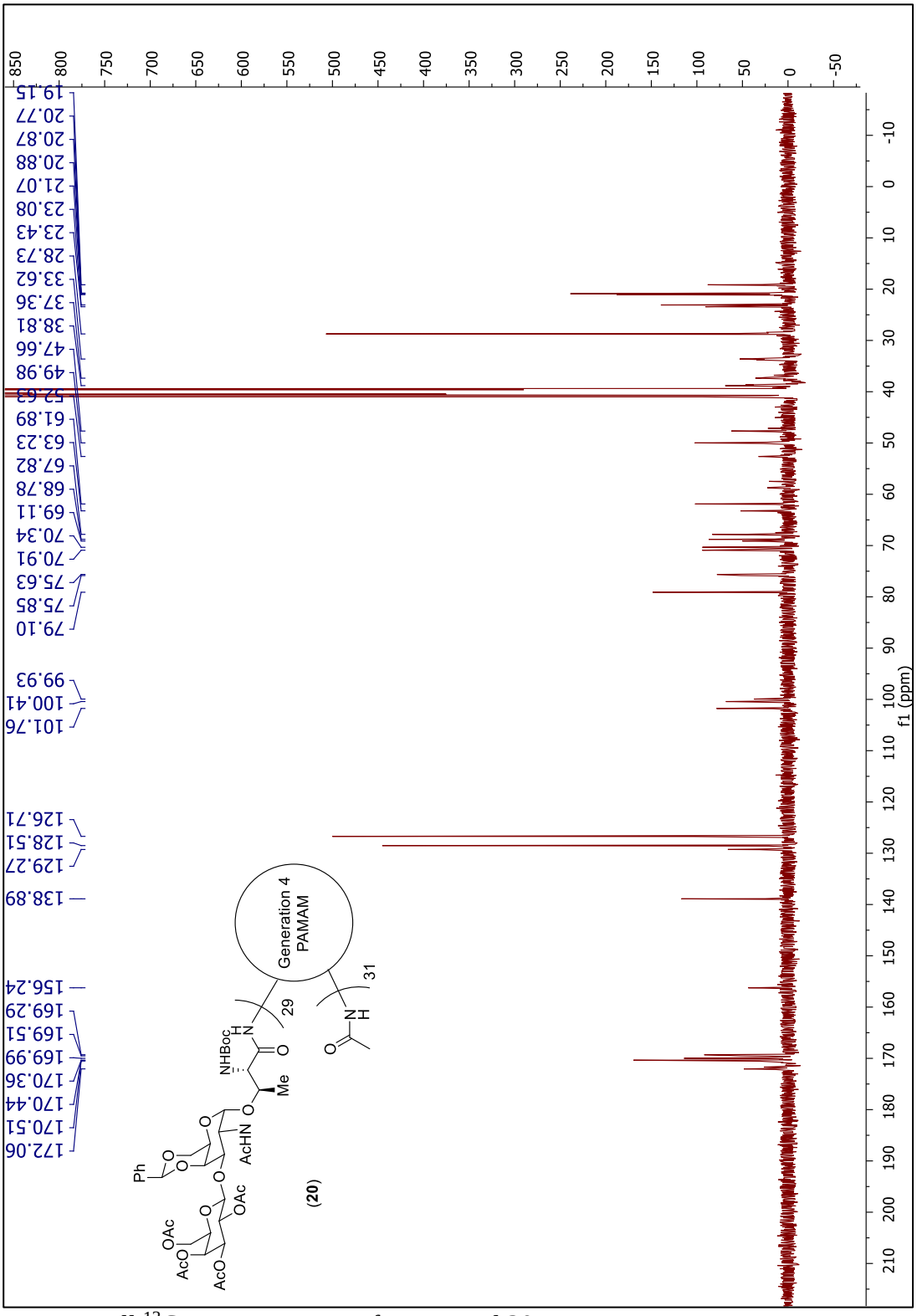


Figure 74. Full ^{13}C NMR spectrum of compound **20**.

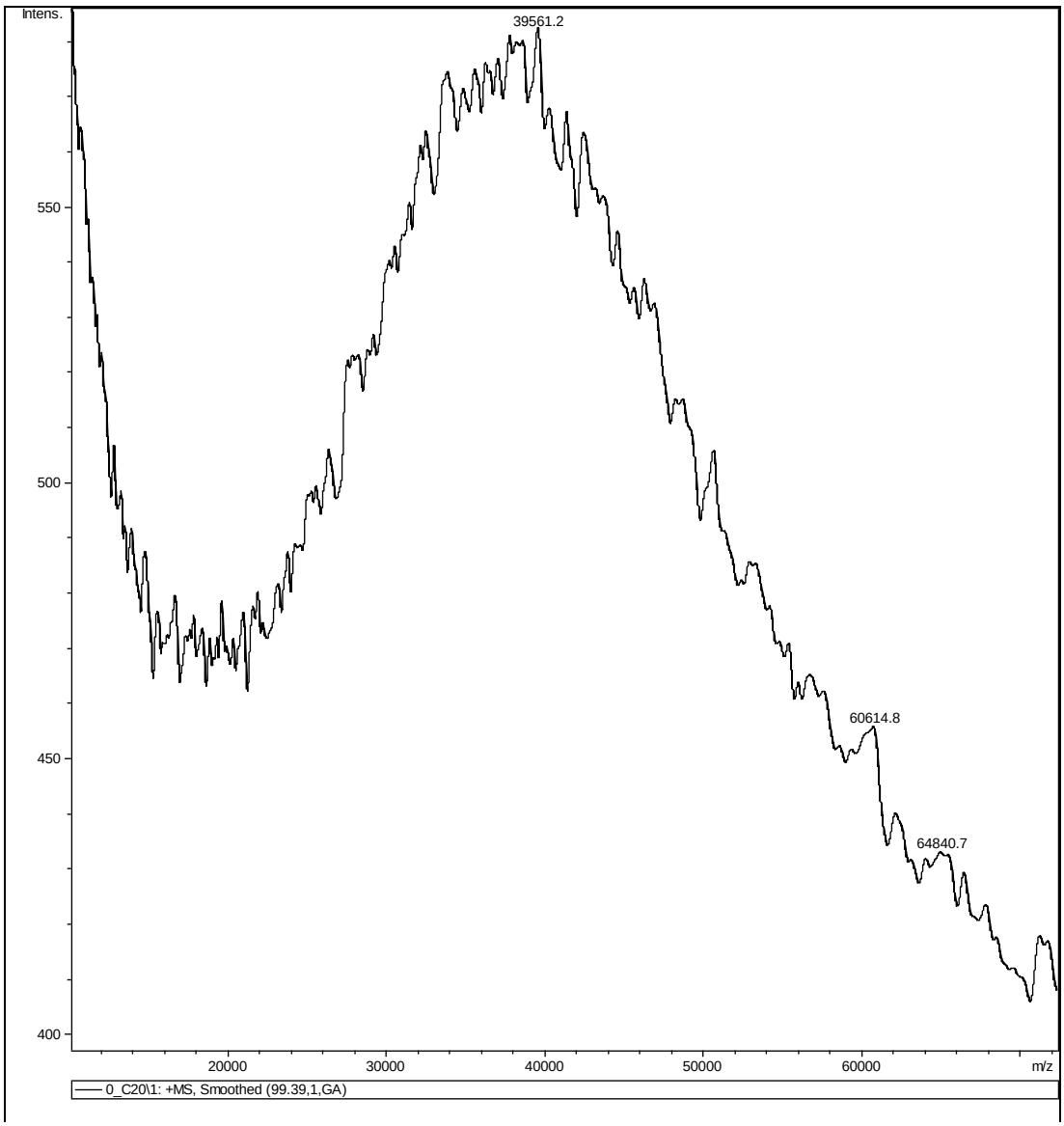


Figure 75. Smoothed MALDI TOF spectrum for compound **20**. M_w = 39225.

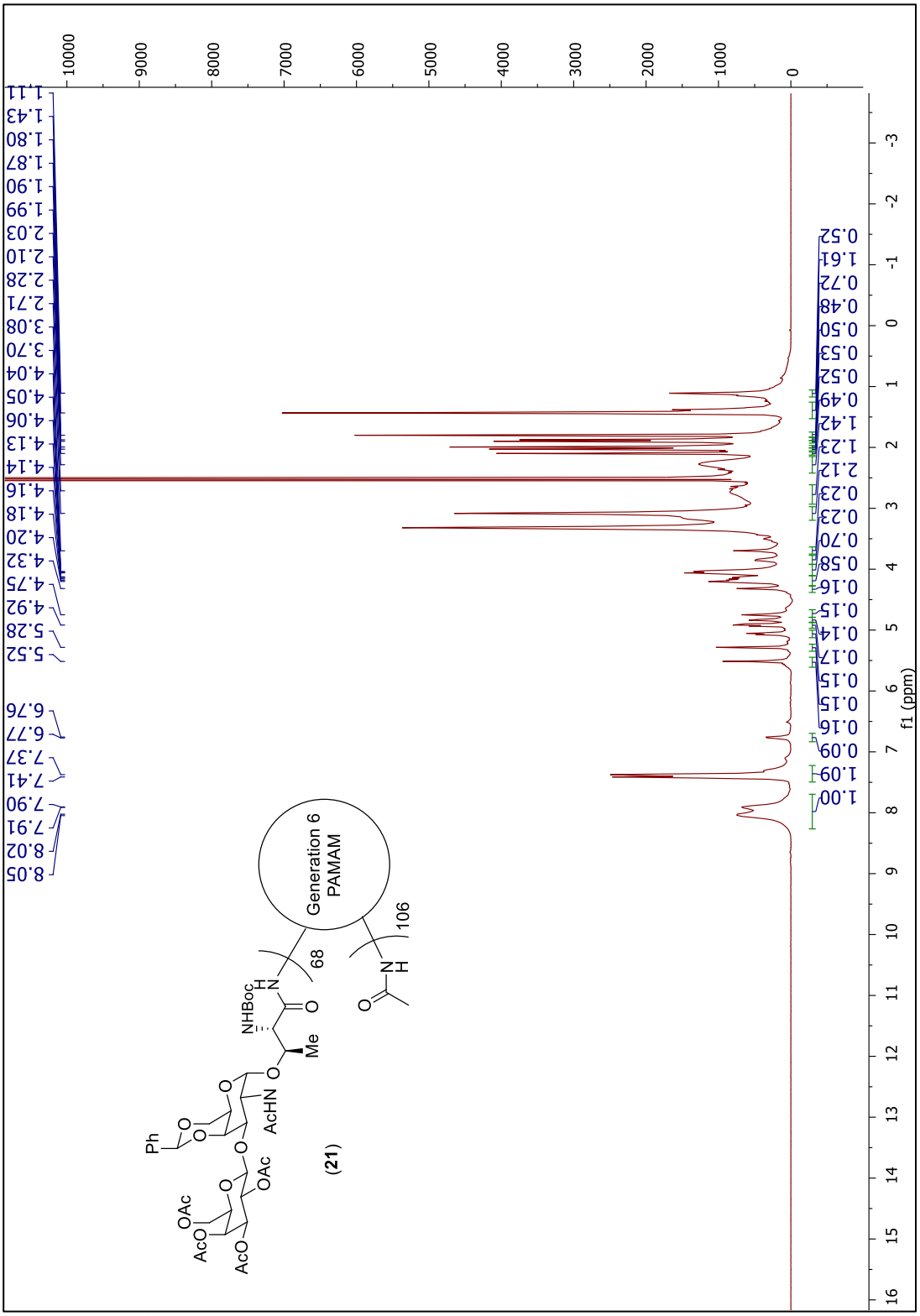


Figure 76. Full ^{1}H NMR spectrum of compound **21**.

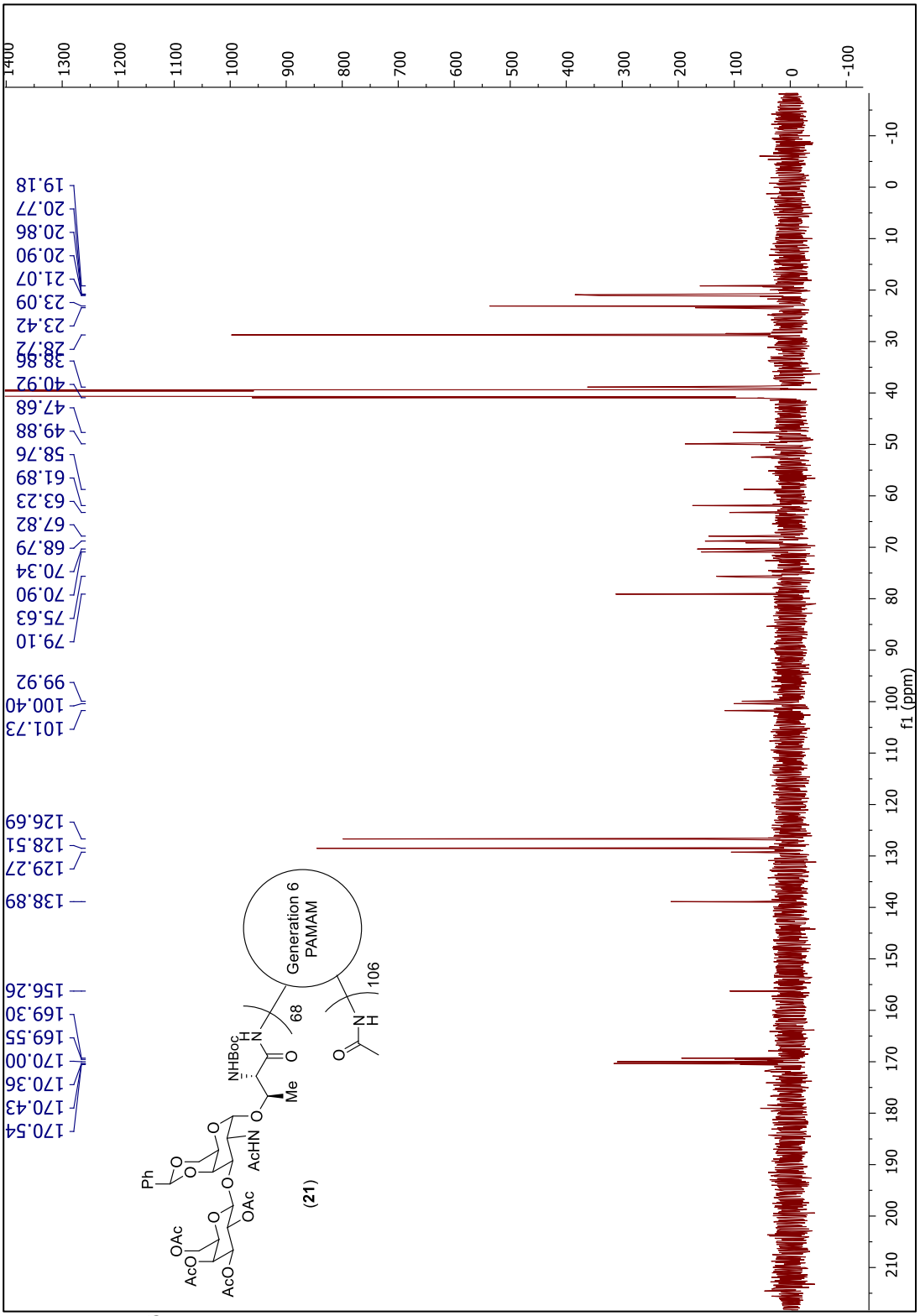


Figure 77. Full ^{13}C NMR spectrum of compound **21**.

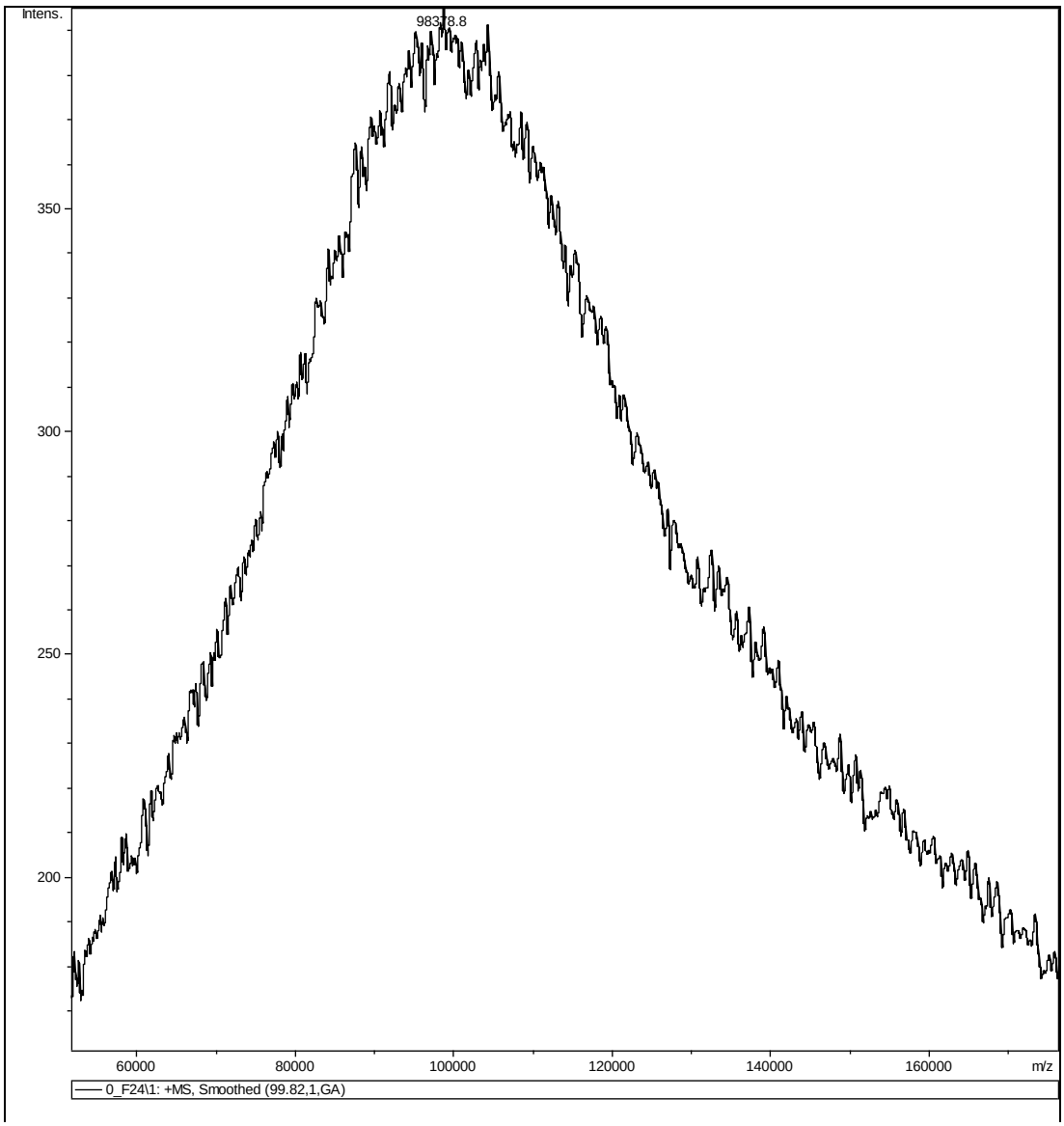


Figure 78. Smoothed MALDI TOF spectrum for compound **21**. M_w = 103355..

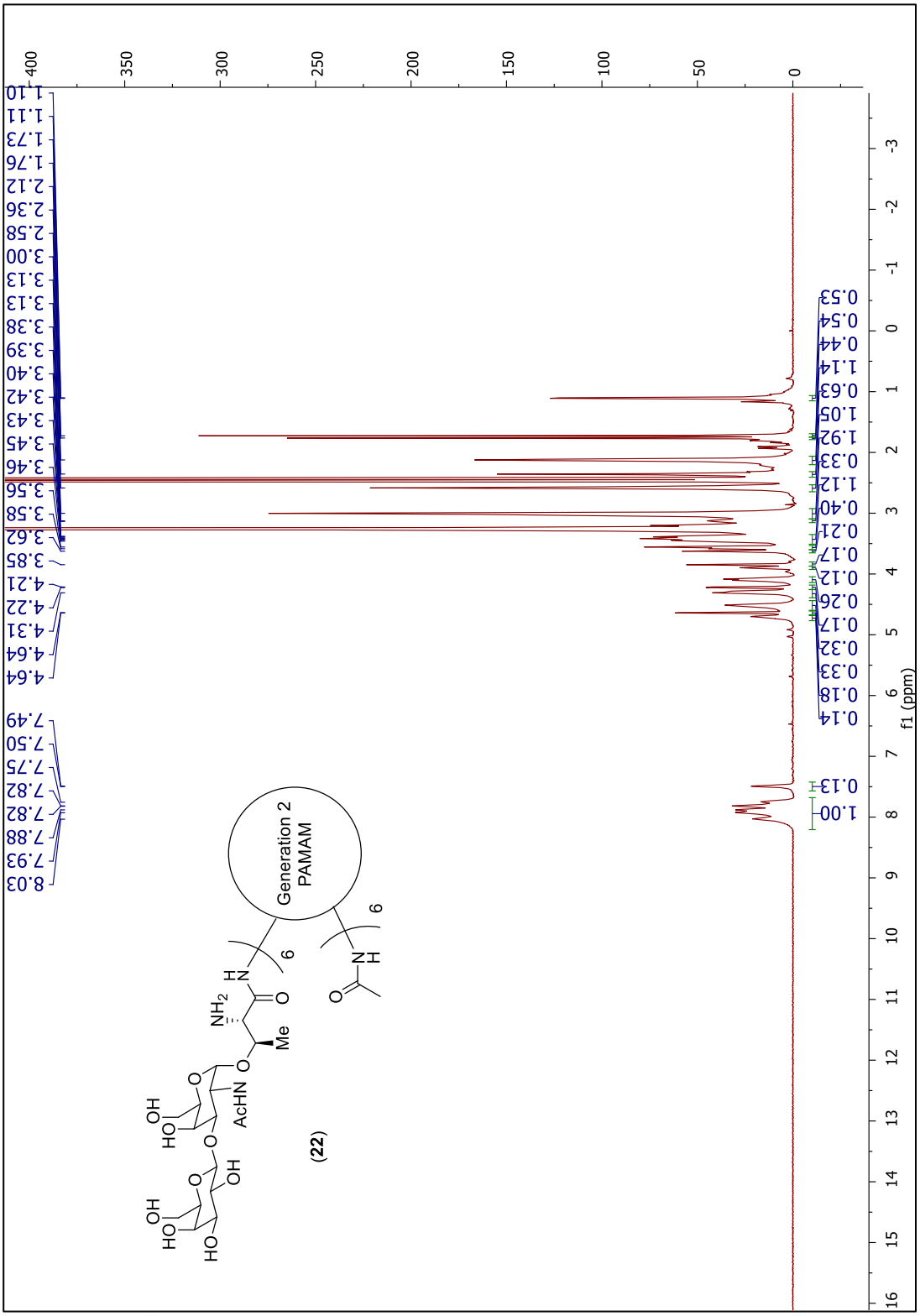


Figure 79. Full ^{1}H NMR spectrum of compound **22**.

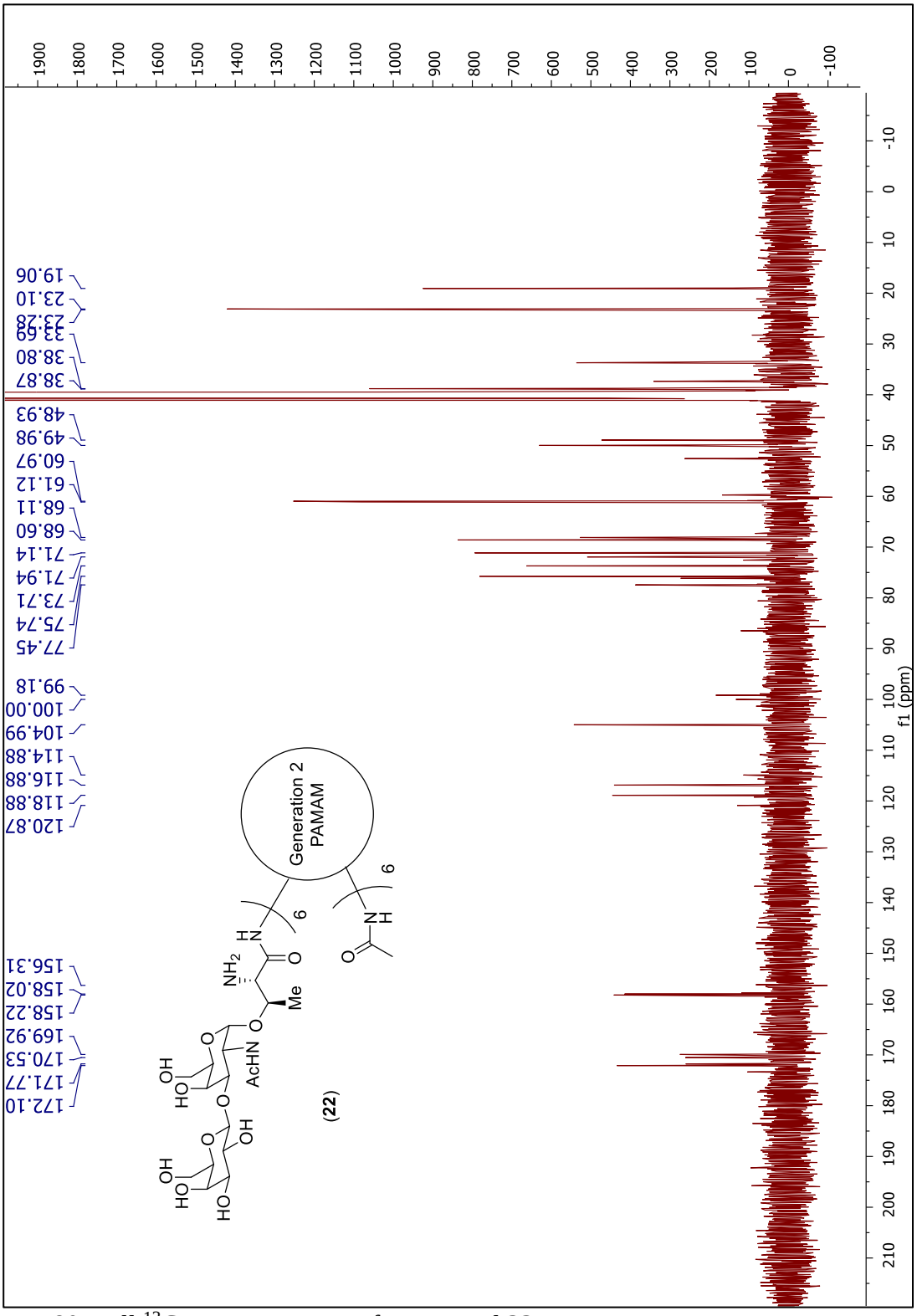


Figure 80. Full ^{13}C NMR spectrum of compound **22**.

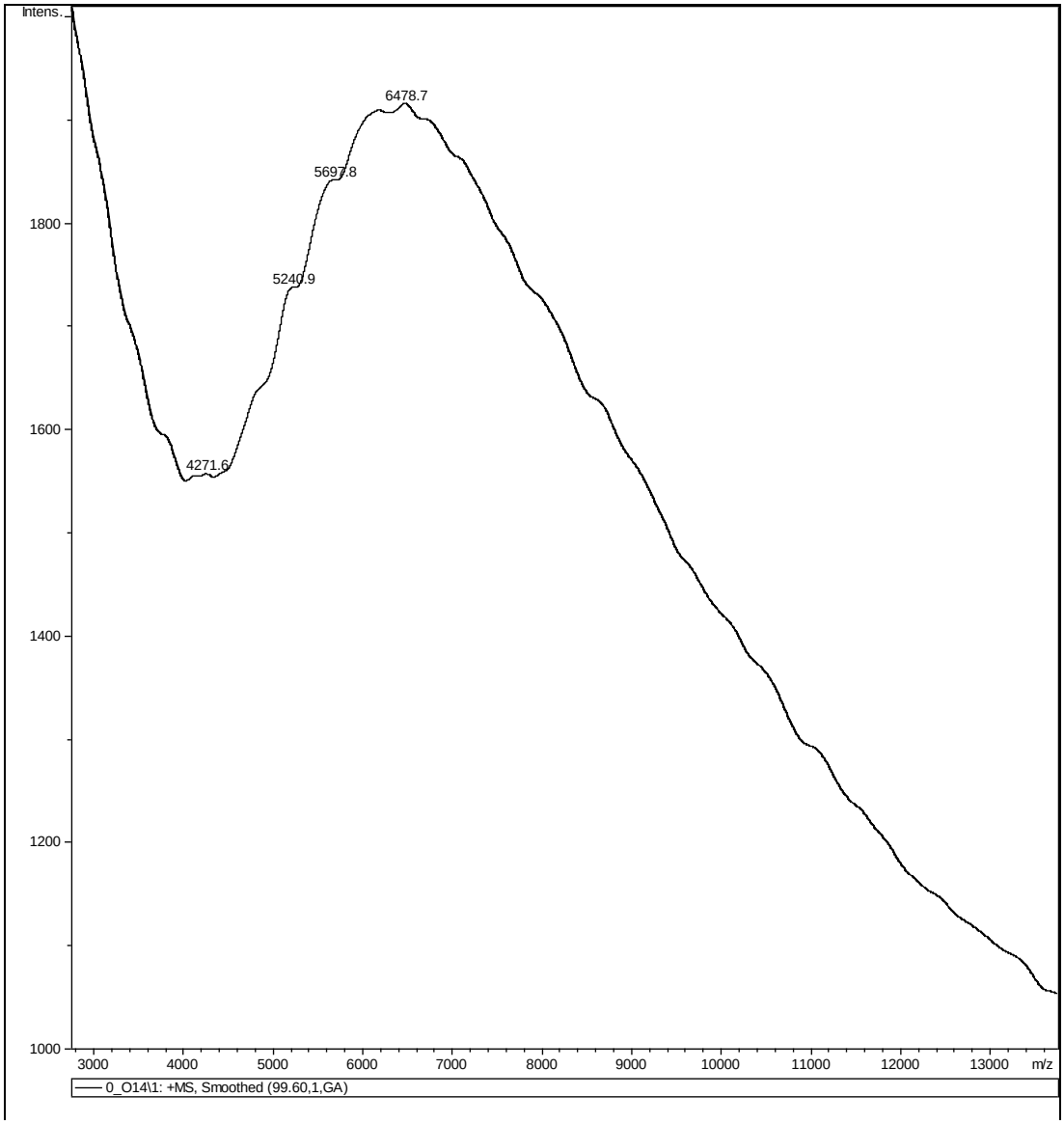


Figure 81. Smoothed MALDI TOF spectrum for compound **22**. M_w = 6540.

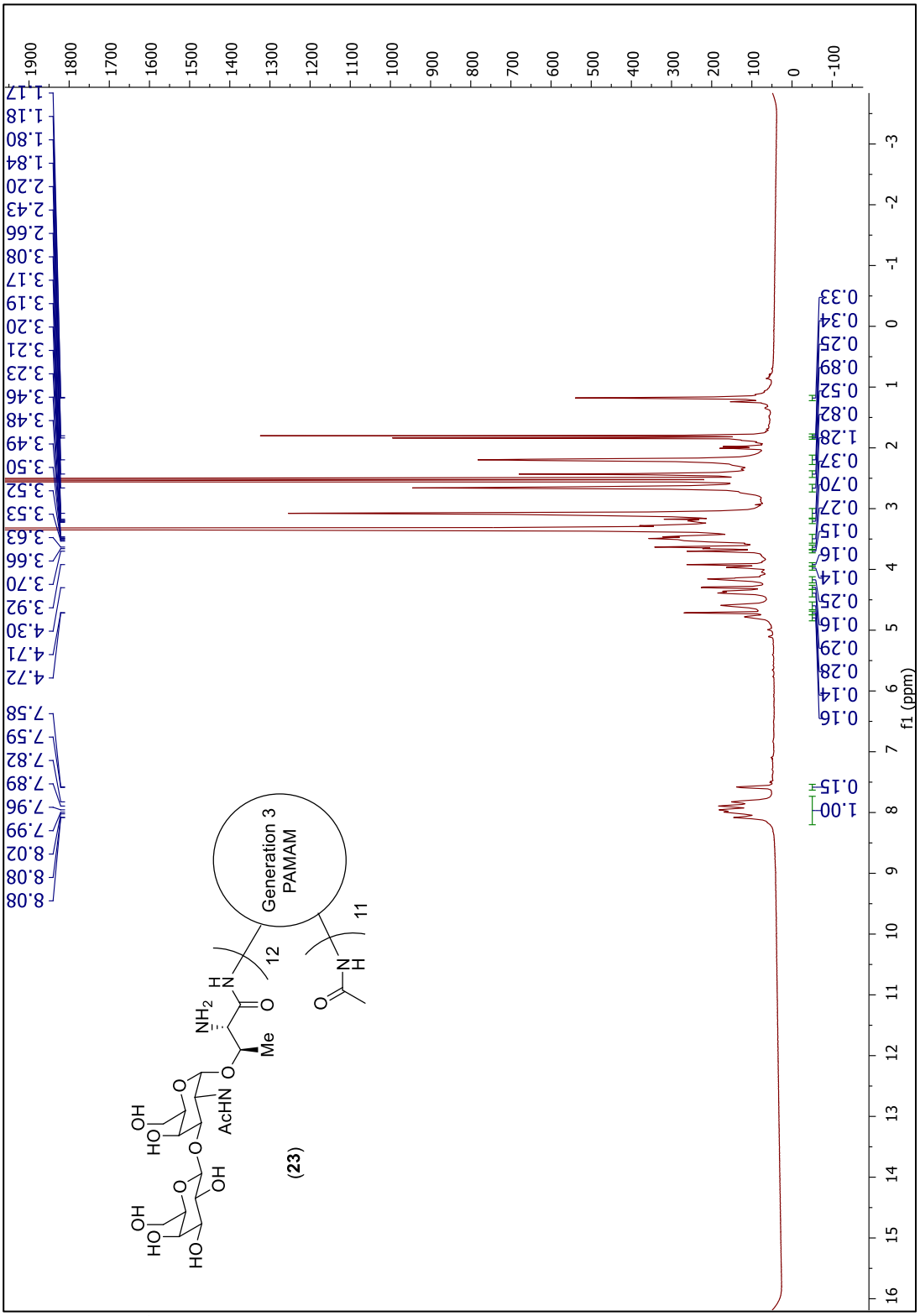


Figure 82. Full ^{1}H NMR spectrum of compound **23**.

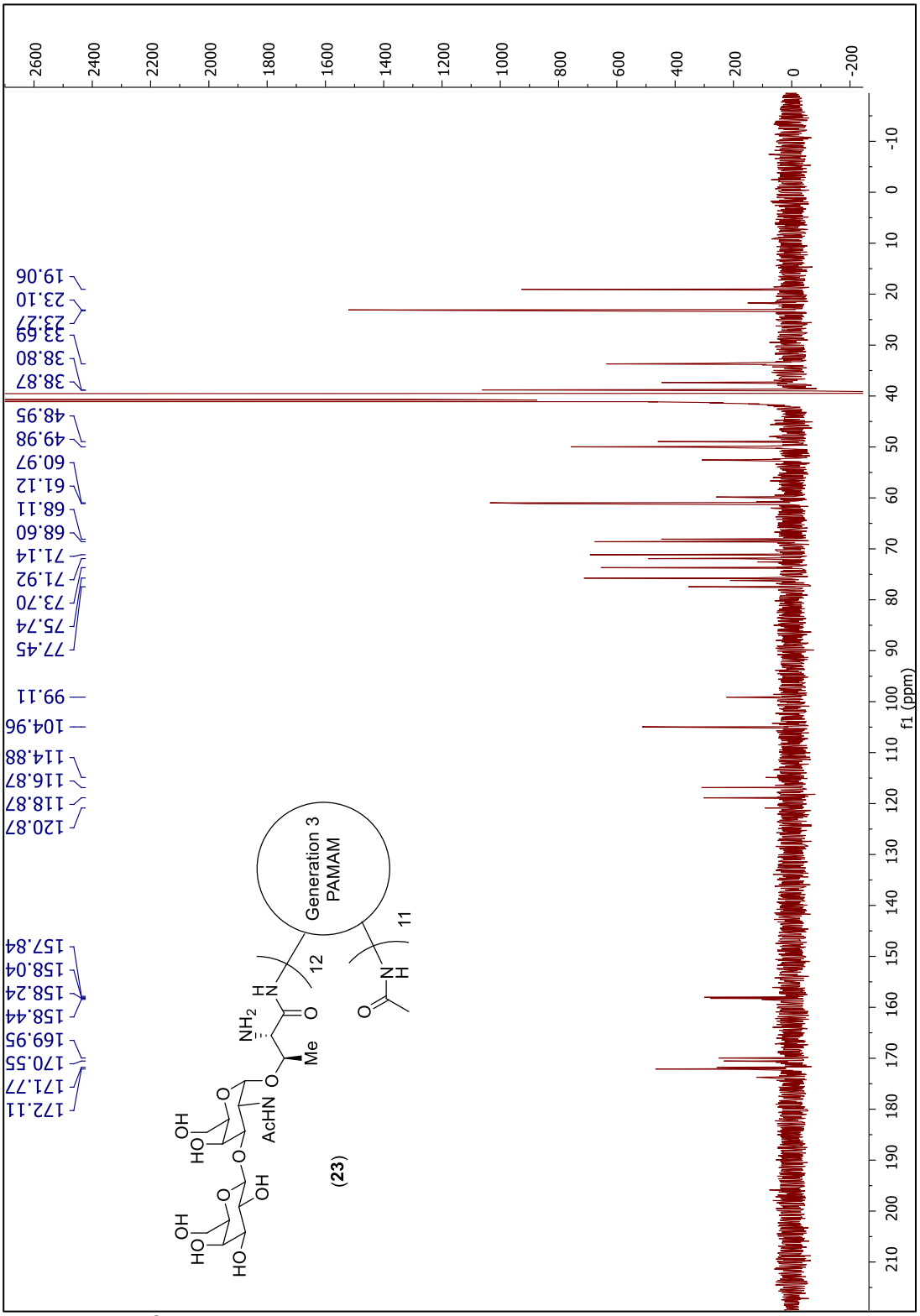


Figure 83. Full ^{13}C NMR spectrum of compound **23**.

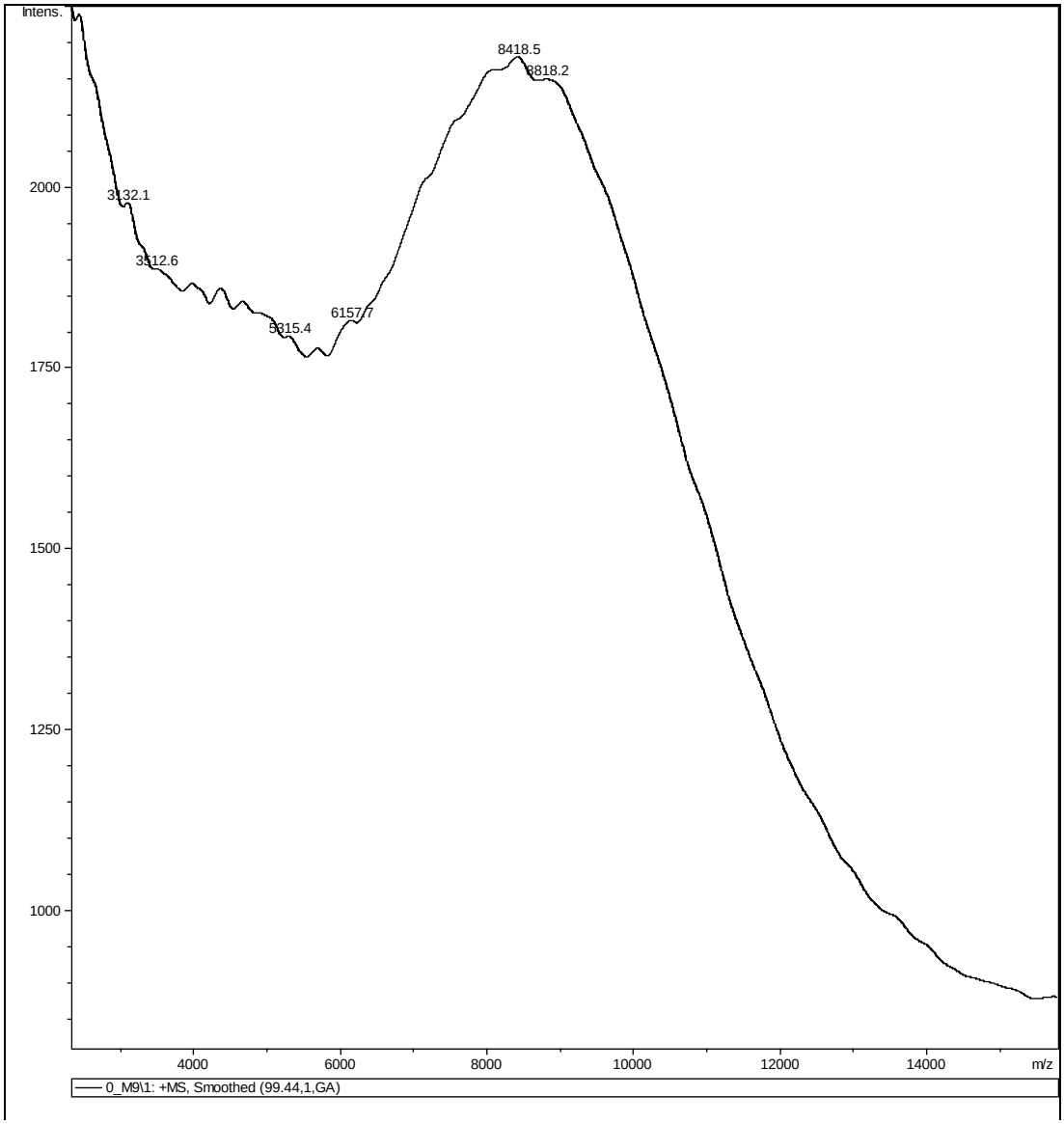


Figure 84. Smoothed MALDI TOF spectrum for compound **23**. M_w = 8550.

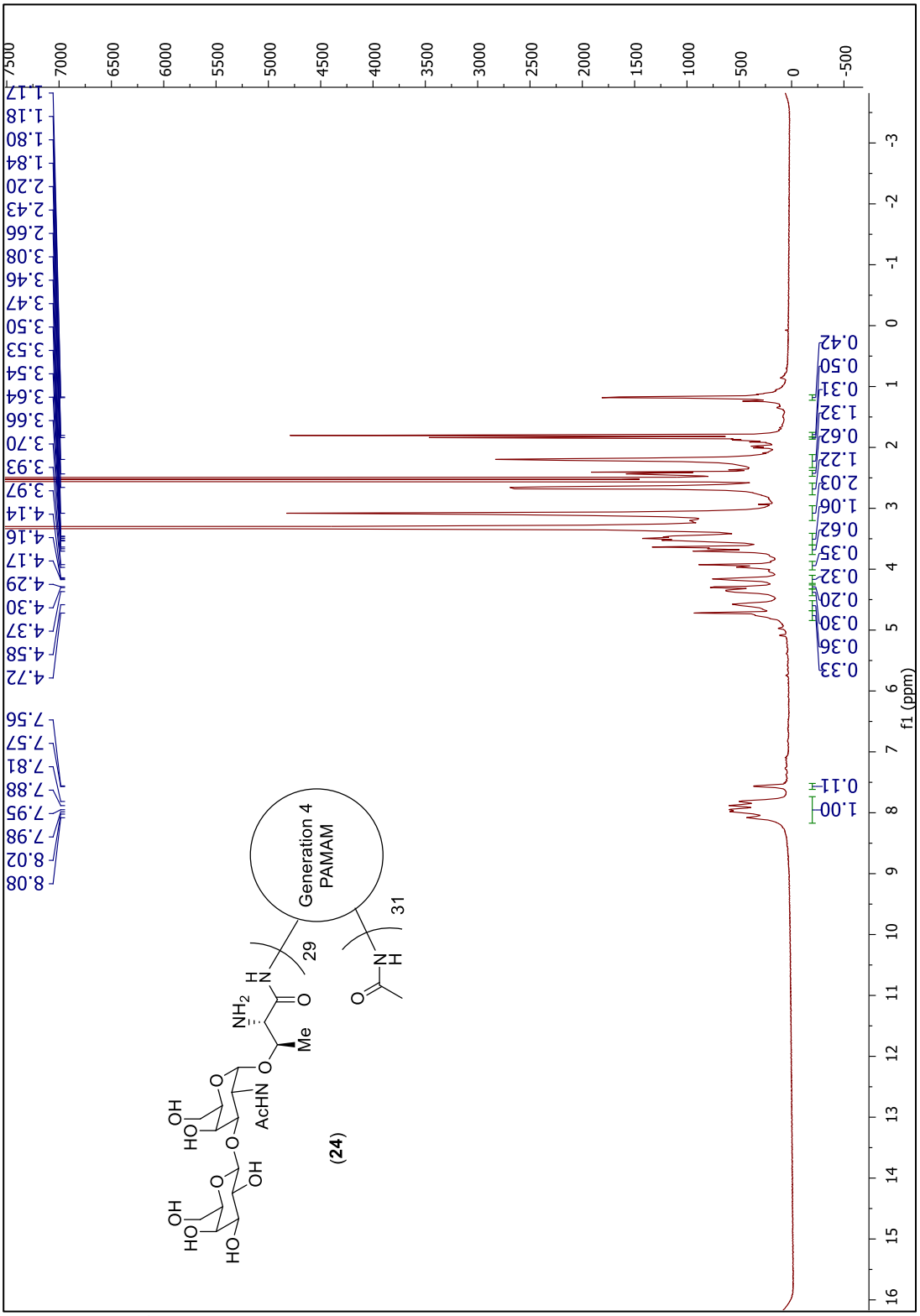


Figure 85. Full ^{1}H NMR spectrum of compound **24**.

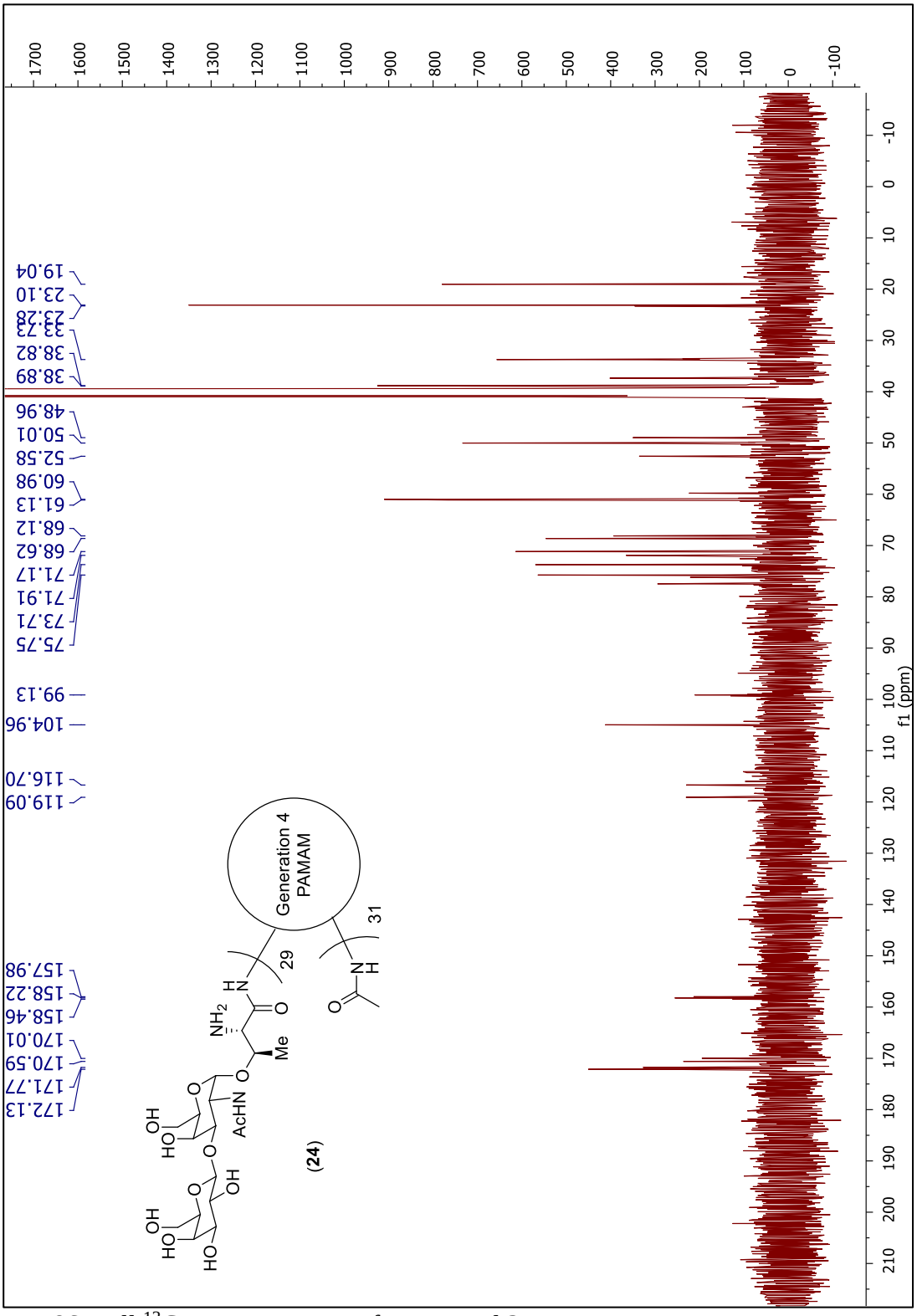


Figure 86. Full ^{13}C NMR spectrum of compound **24**.

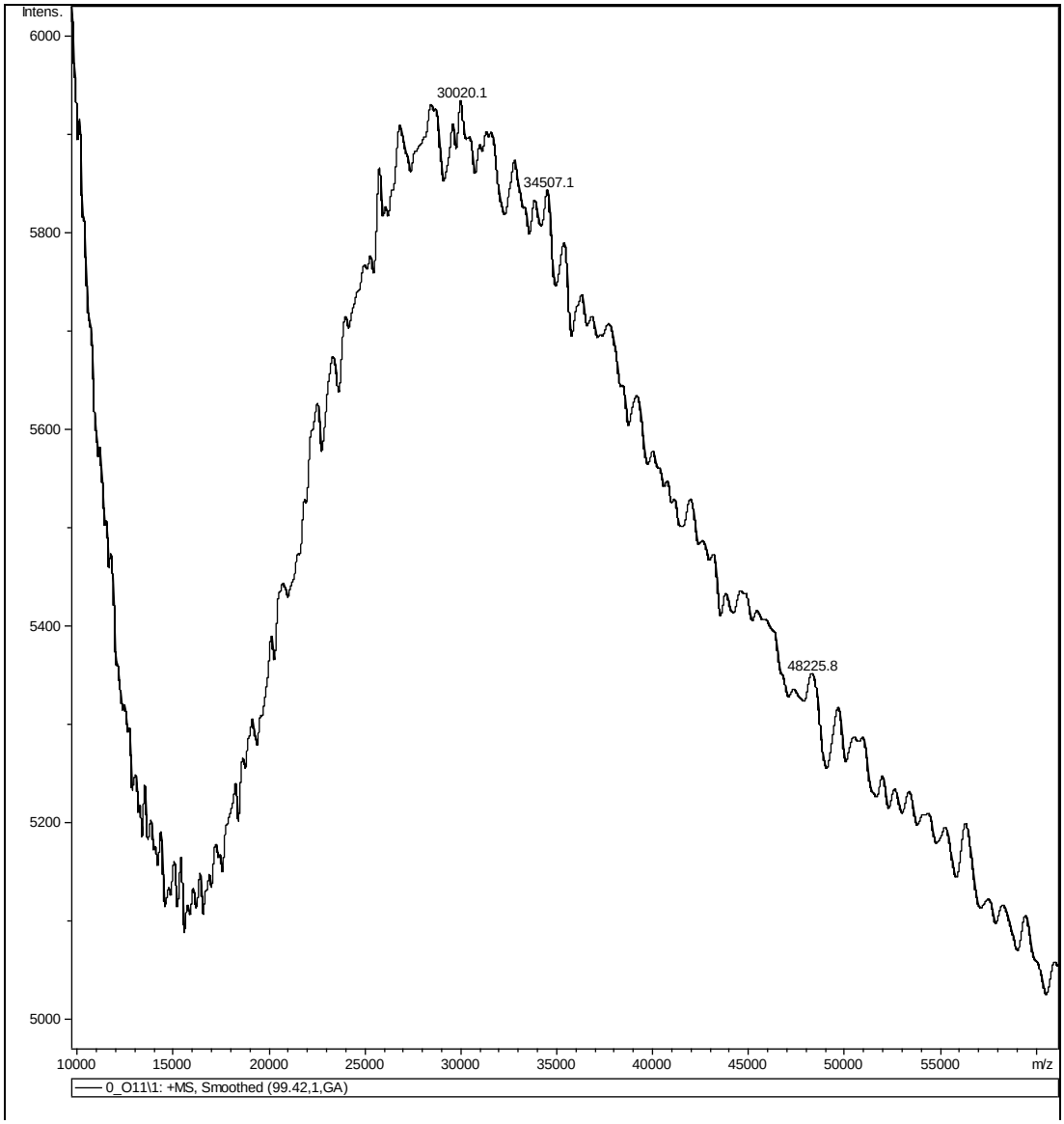


Figure 87. Smoothed MALDI TOF spectrum for compound **24**. M_w = 31510.

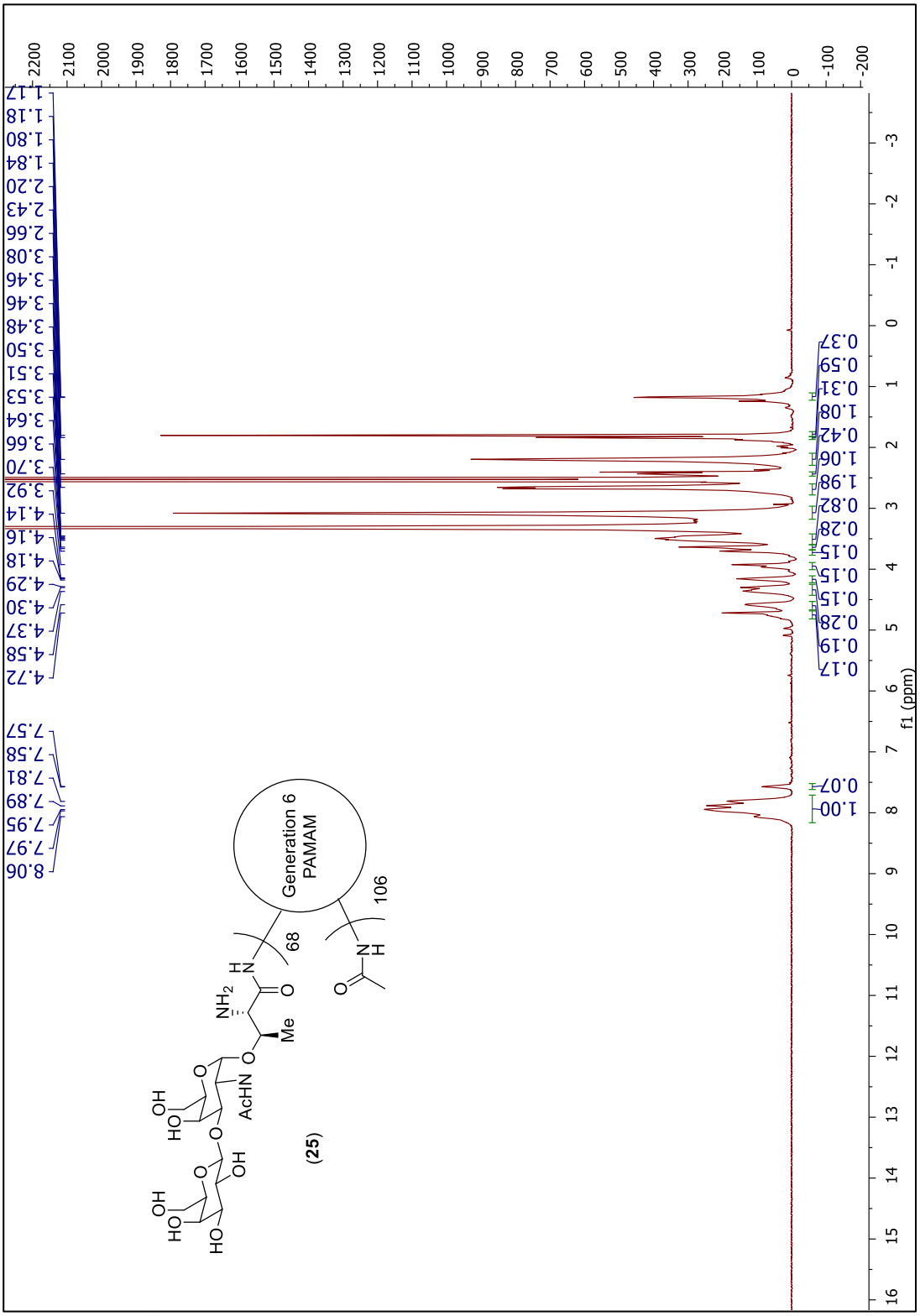


Figure 88. Full ^{1}H NMR spectrum of compound **25**.

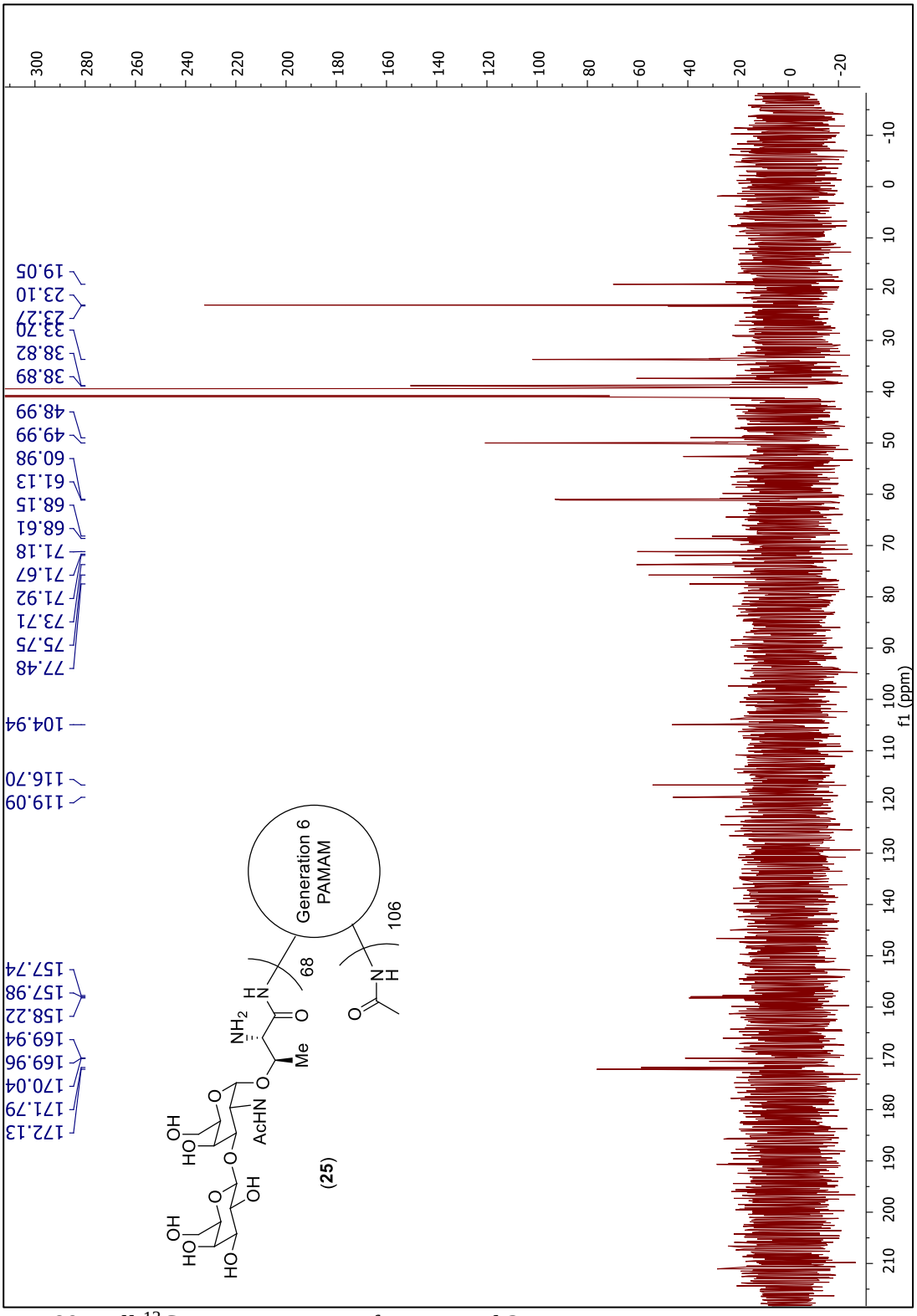


Figure 89. Full ^{13}C NMR spectrum of compound **25**.

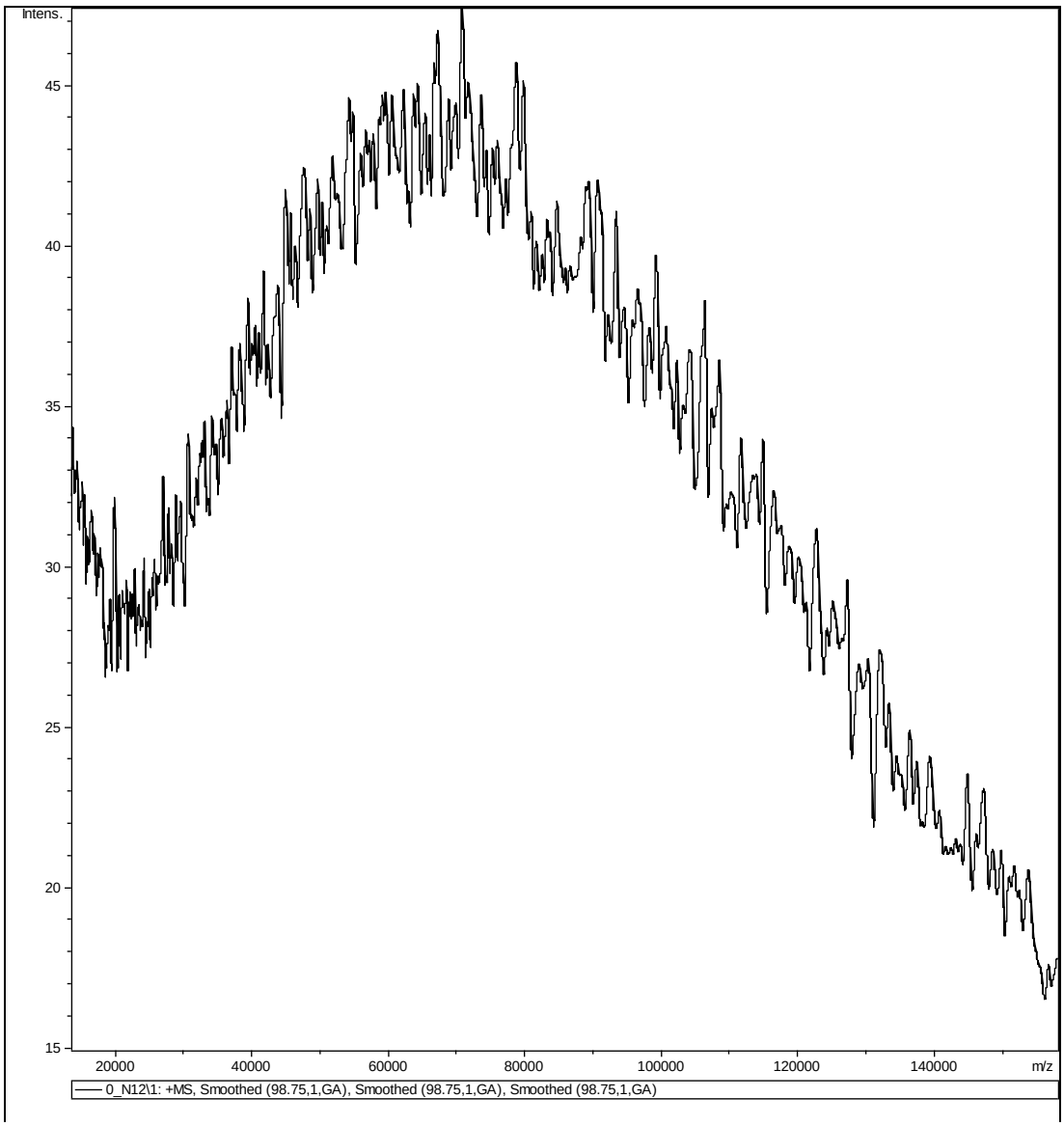


Figure 90. Smoothed MALDI TOF spectrum for compound **25**. M_w = 77880.

APPENDIX B

SUPPLEMENTAL DATA FROM CHAPTER THREE

Dendrimer	Amount Added, concentration	% Free Cells	Standard deviation	p-value
22	0 µL, 0 µM	80	±1.0	-
22	10 µL, 57 µM	79	±8.7	0.84
22	20 µL, 114 µM	73	±6.9	0.18
22	30 µL, 171 µM	59	±6.5	0.02
22	40 µL, 228 µM	60	±0.87	0.0009
23	0 µL, 0 µM	82	±3.6	-
23	10 µL, 33 µM	76	±9.1	0.40
23	20 µL, 66 µM	69	±11.4	0.16
23	30 µL, 99 µM	54	±15.4	0.08
23	40 µL, 132 µM	42	±12.7	0.03
24	0 µL, 0 µM	90	±4.2	-
24	10 µL, 12 µM	75	±2.0	0.03
24	20 µL, 24 µM	71	±4.6	0.01
24	30 µL, 36 µM	64	±15.5	0.15
24	40 µL, 48 µM	50	±11.5	0.05
25	0 µL, 0 µM	85	±7.5	-
25	10 µL, 4 µM	84	±5.9	0.91
25	20 µL, 8 µM	78	±7.1	0.002
25	30 µL, 12 µM	66	±5.9	0.006
25	40 µL, 16 µM	52	±14.2	0.04

Table 7: Summary of cellular aggregation assay data

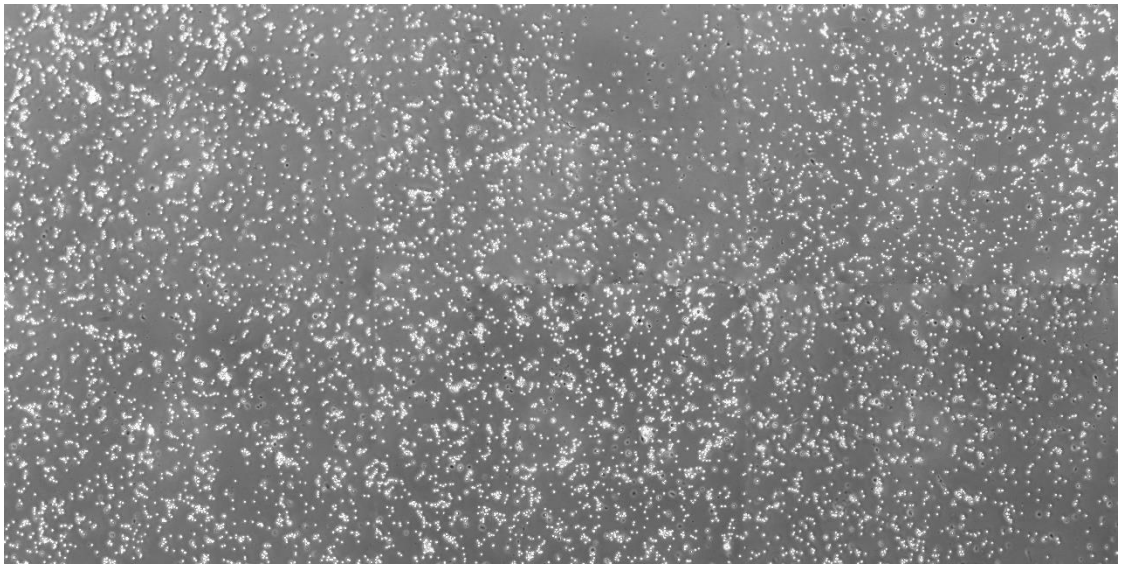


Figure 91: Untreated A549 cells

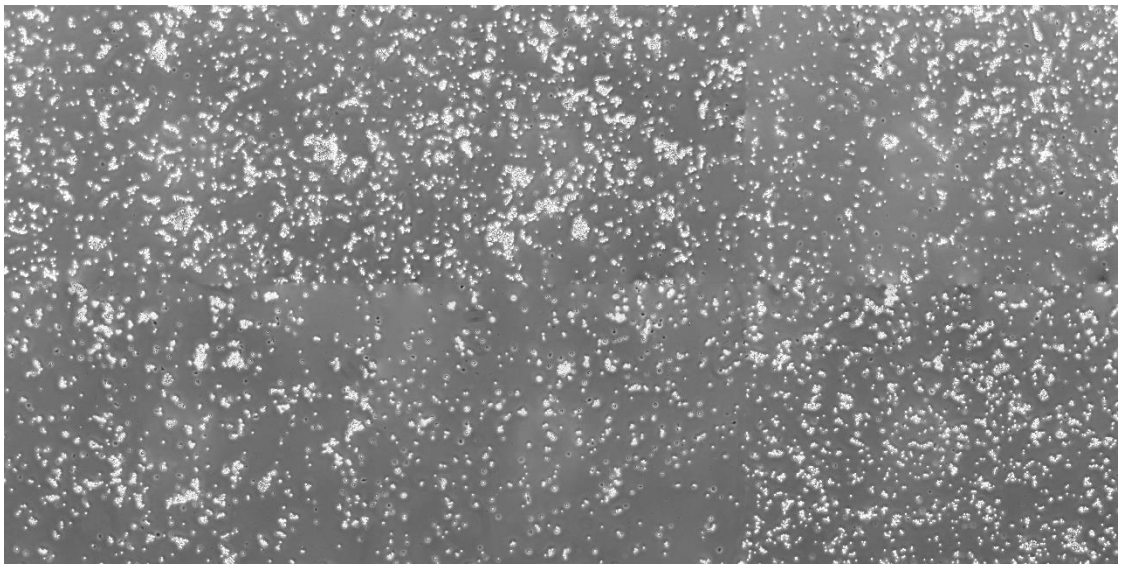


Figure 92: 57 µM G2-TF antigen functionalized dendrimer

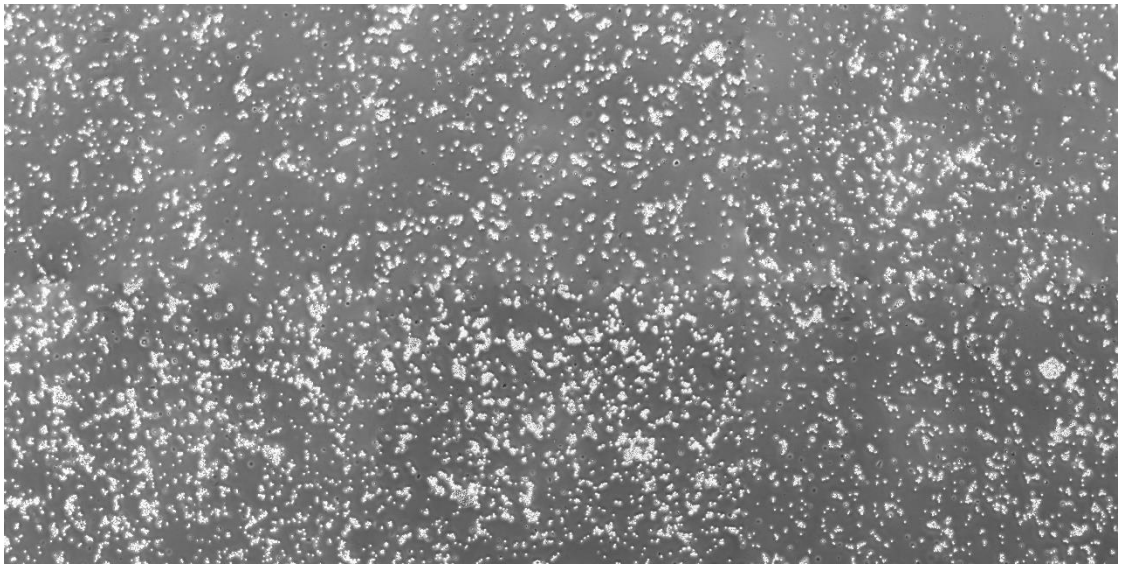


Figure 93: 114 µM G2-TF antigen functionalized dendrimer

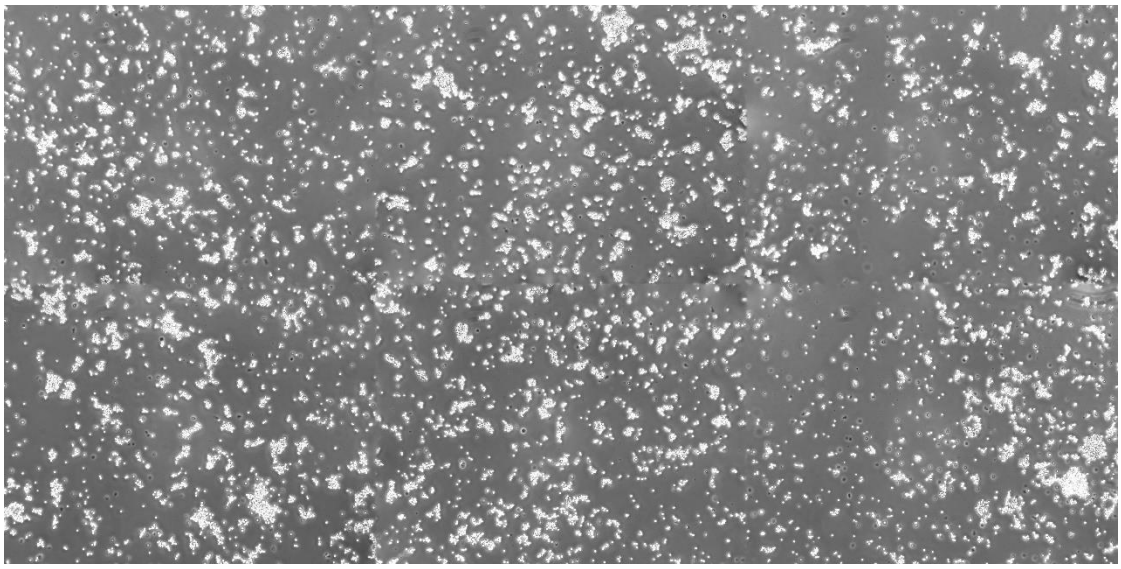


Figure 94: 171 µM G2-TF antigen functionalized dendrimer

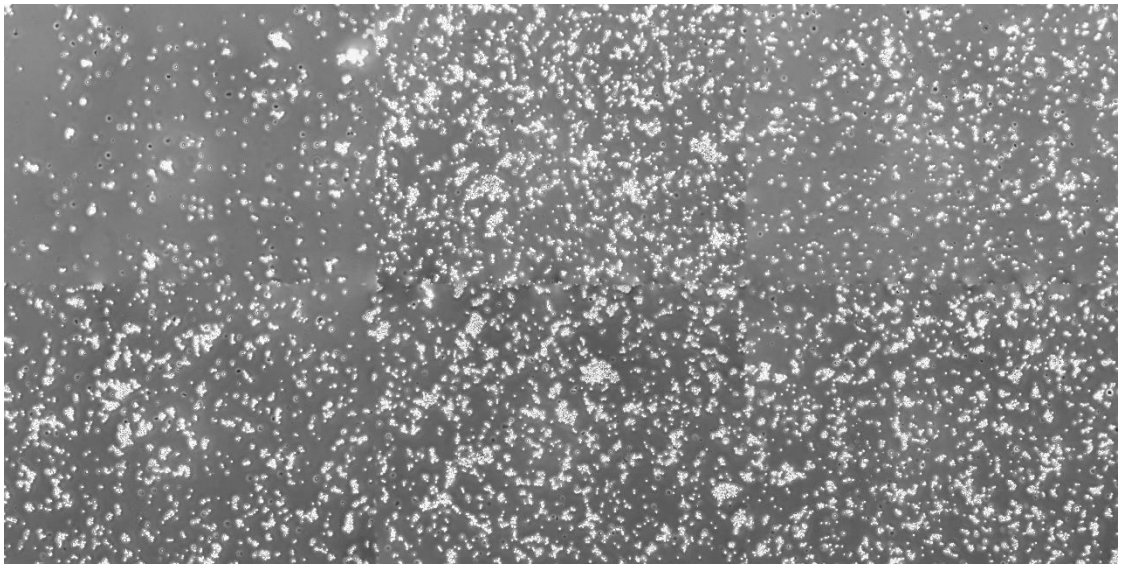


Figure 95: 228 µM G2-TF antigen functionalized dendrimer

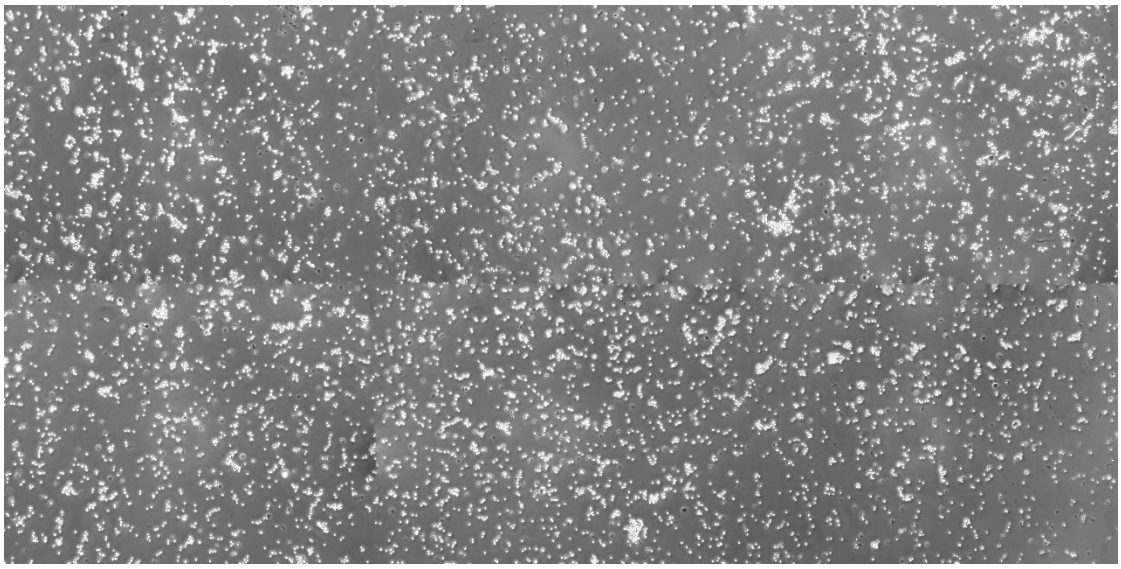


Figure 96: 33 µM G3-TF antigen functionalized dendrimer

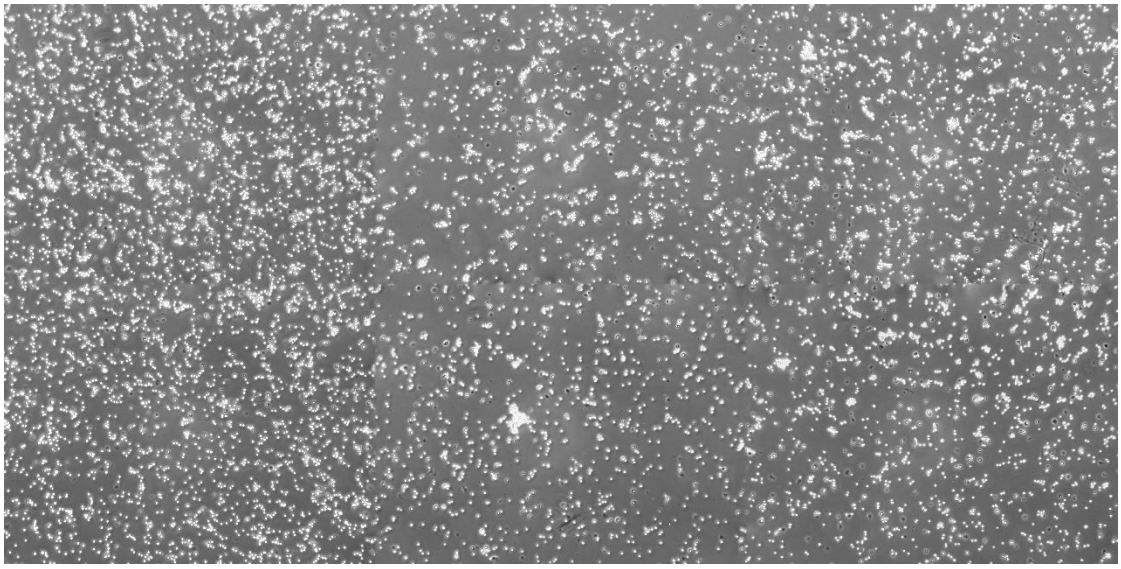


Figure 97: 66 µM G3-TF antigen functionalized dendrimer

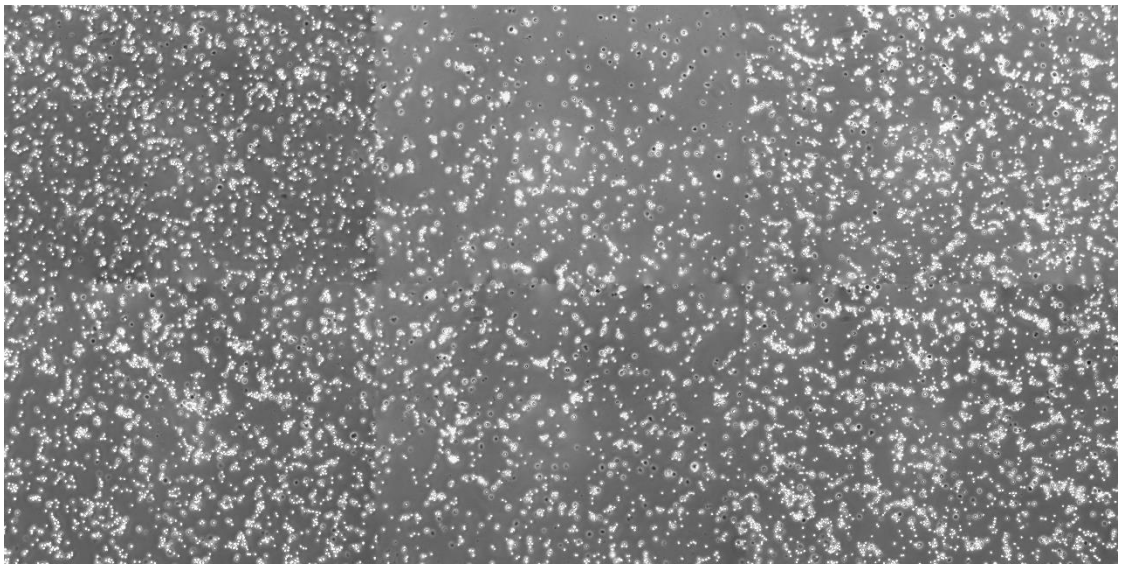


Figure 98: 99 µM G3-TF antigen functionalized dendrimer

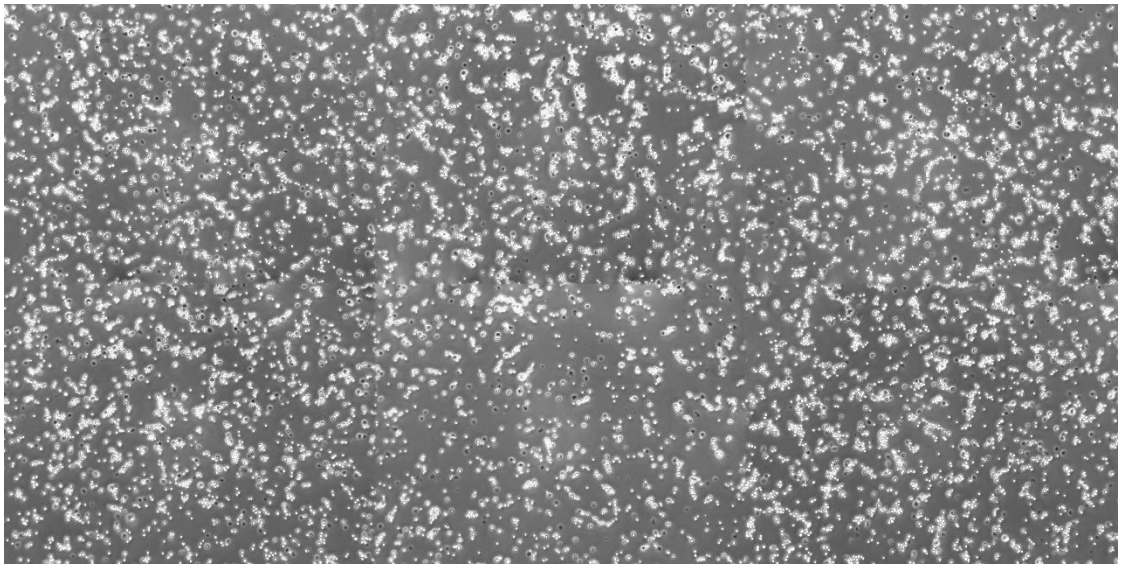


Figure 99: 132 µM G3-TF antigen functionalized dendrimer

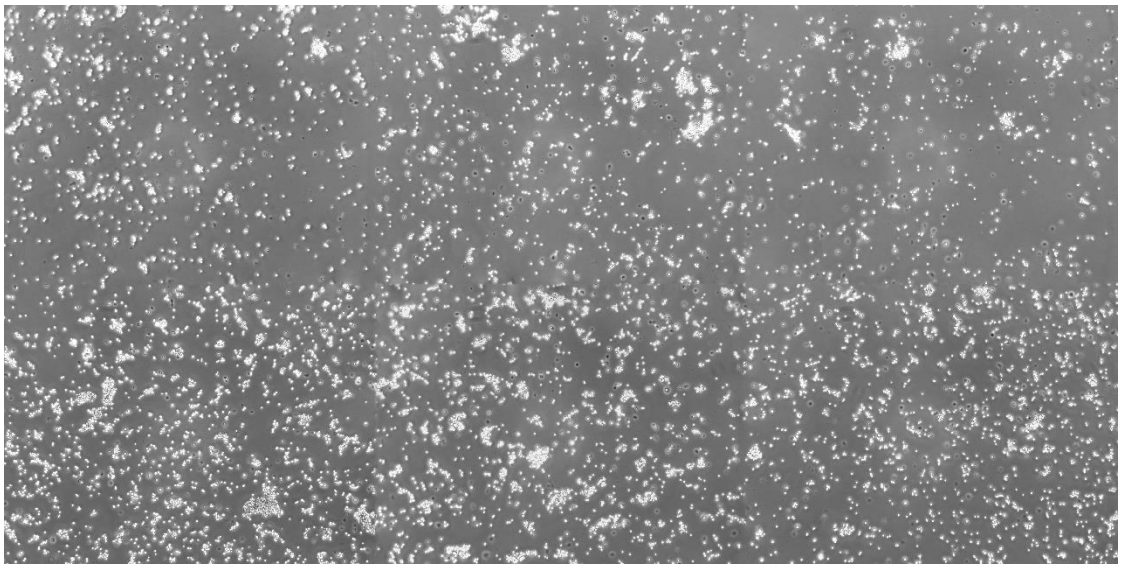


Figure 100: 12 µM G4-TF antigen functionalized dendrimer

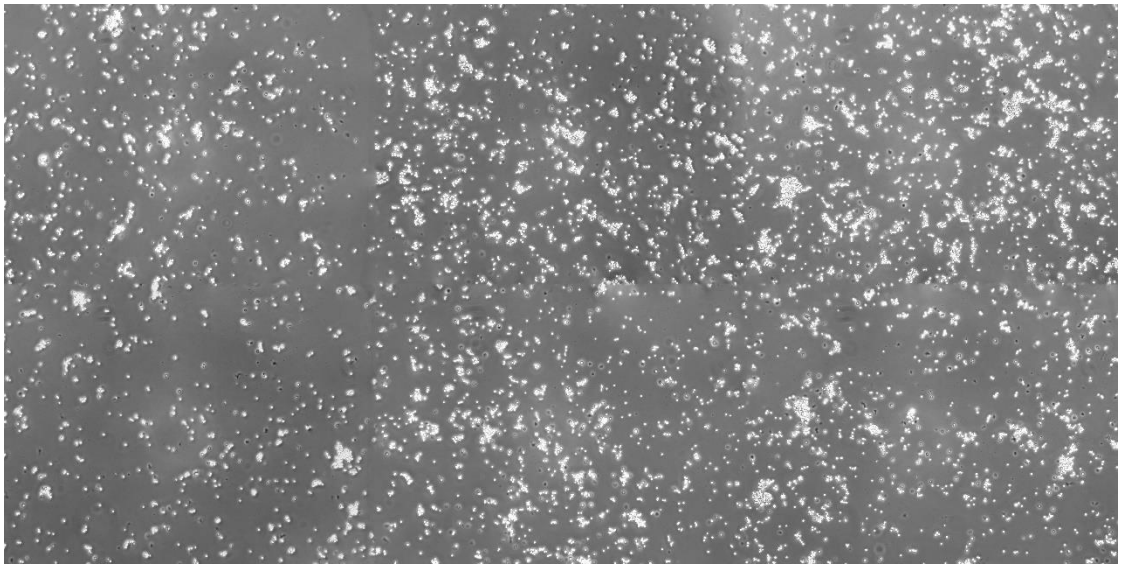


Figure 101: 24 µM G4-TF antigen functionalized dendrimer

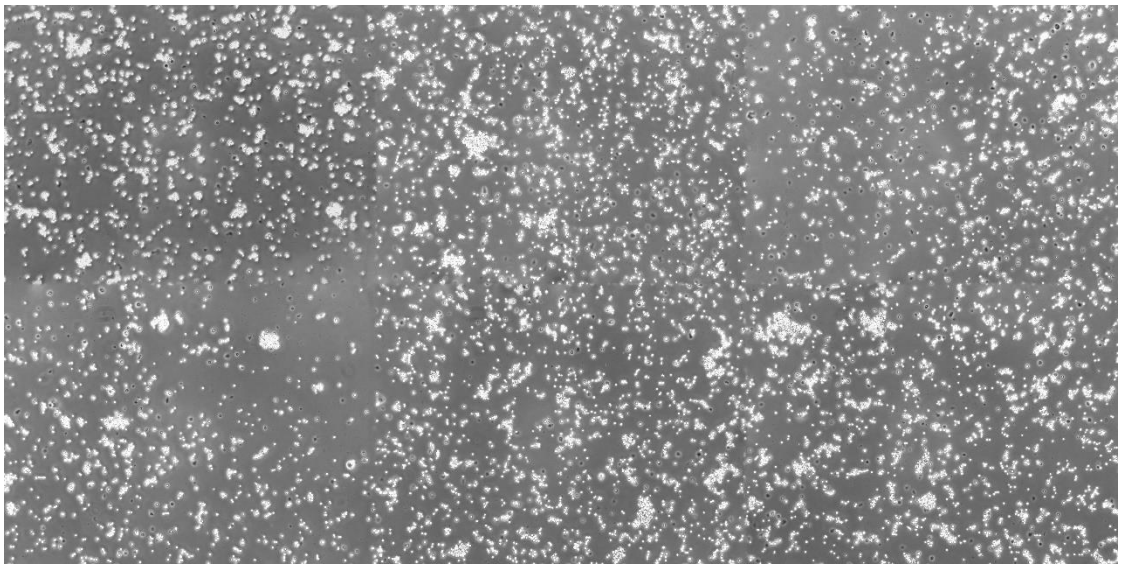


Figure 102: 36 µM G4-TF antigen functionalized dendrimer

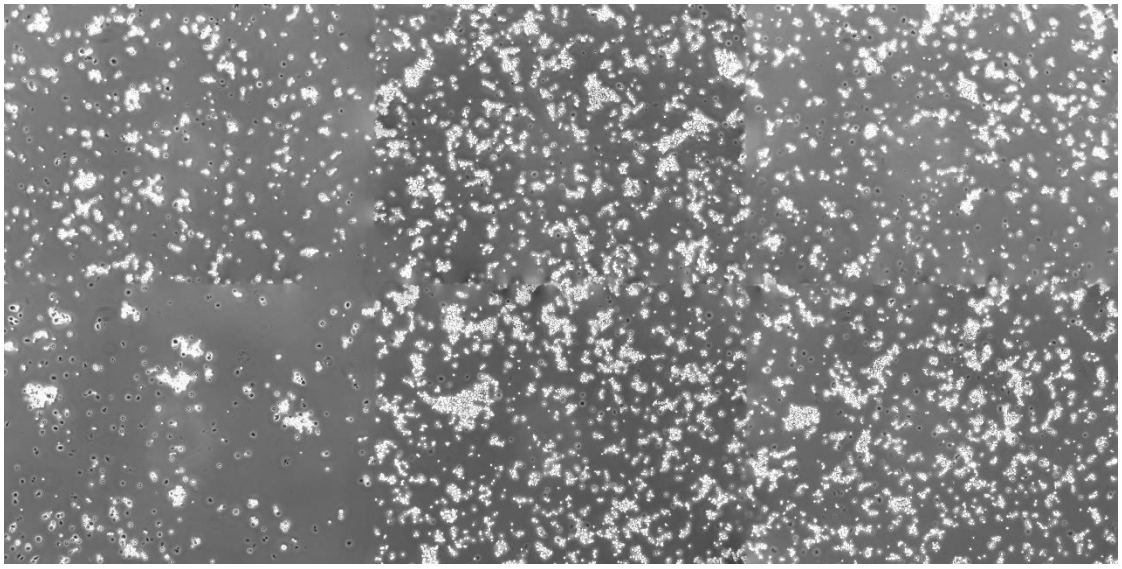


Figure 103: 48 µM G4-TF antigen functionalized dendrimer

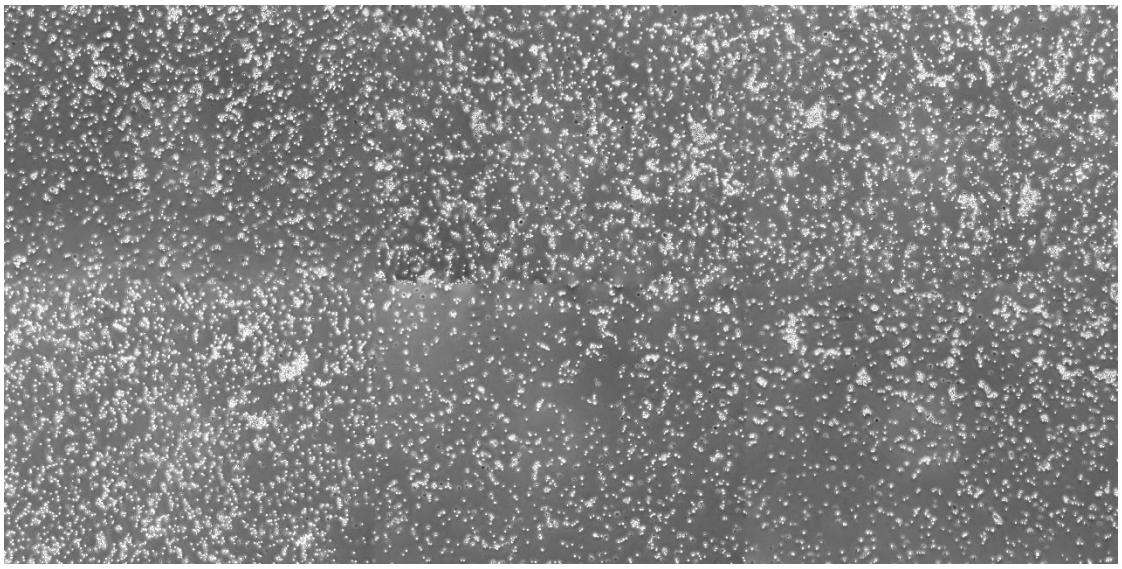


Figure 104: 4 µM G6-TF antigen functionalized dendrimer

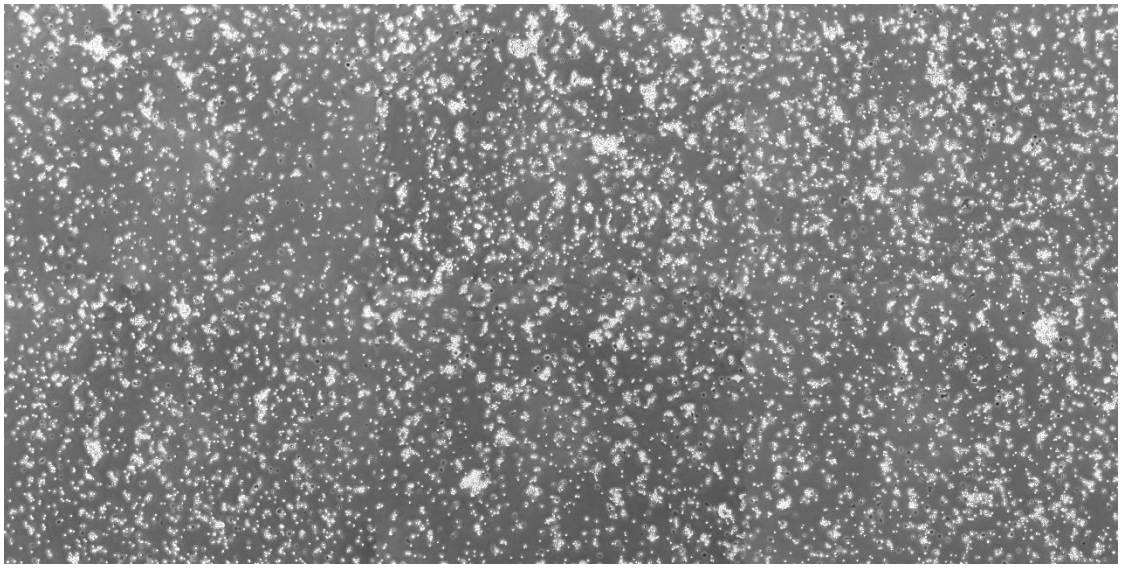


Figure 105: 8 µM G6-TF antigen functionalized dendrimer

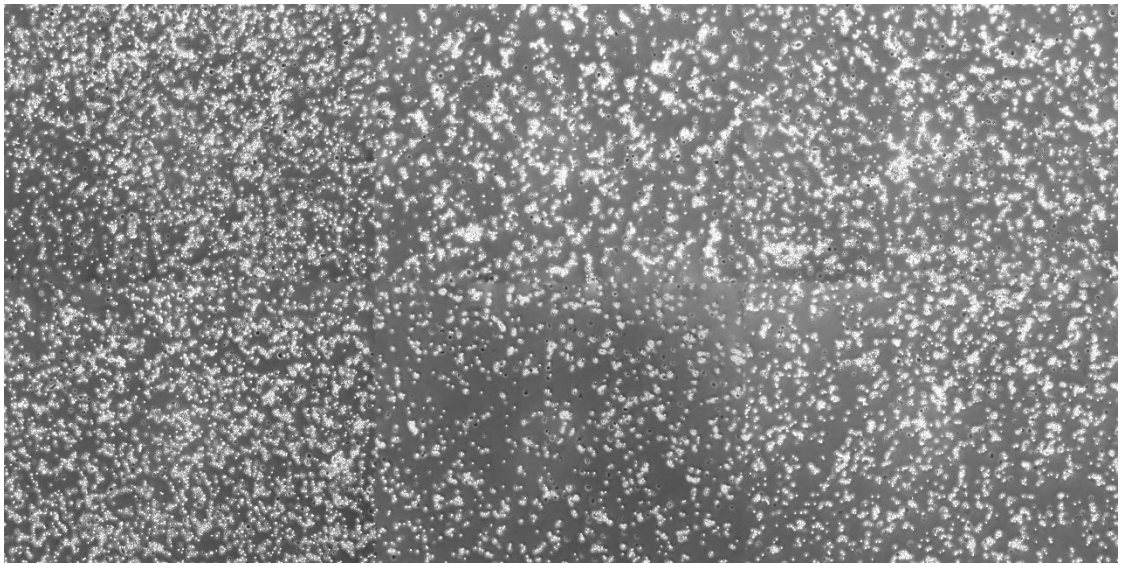


Figure 106: 12 µM G6-TF antigen functionalized dendrimer

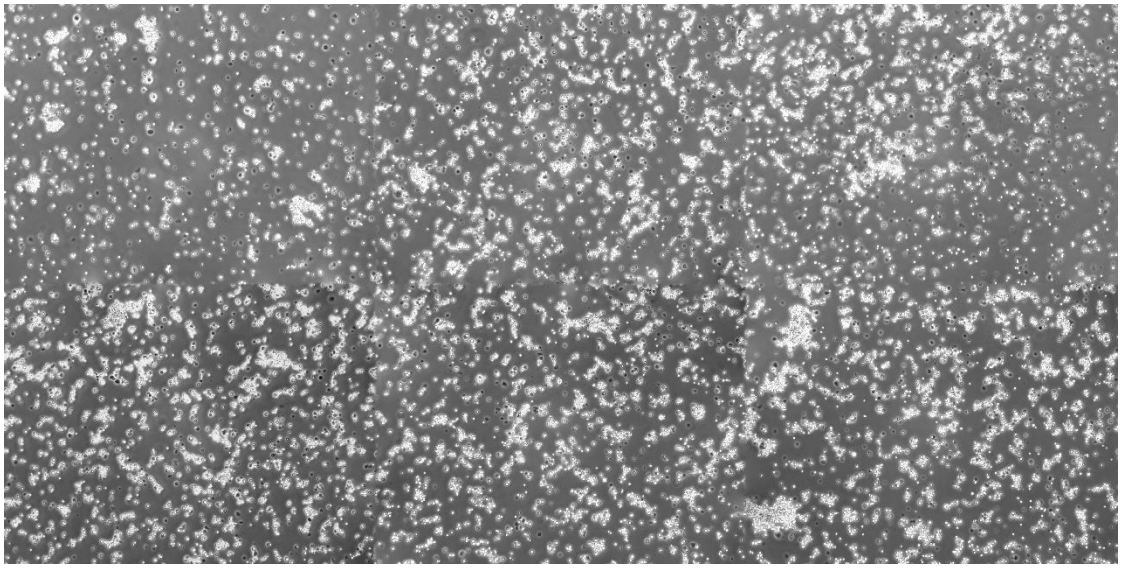


Figure 107: 16 µM G6-TF antigen functionalized dendrimer

APPENDIX C

RELEVANT SPECTRAL DATA FROM CHAPTER FOUR

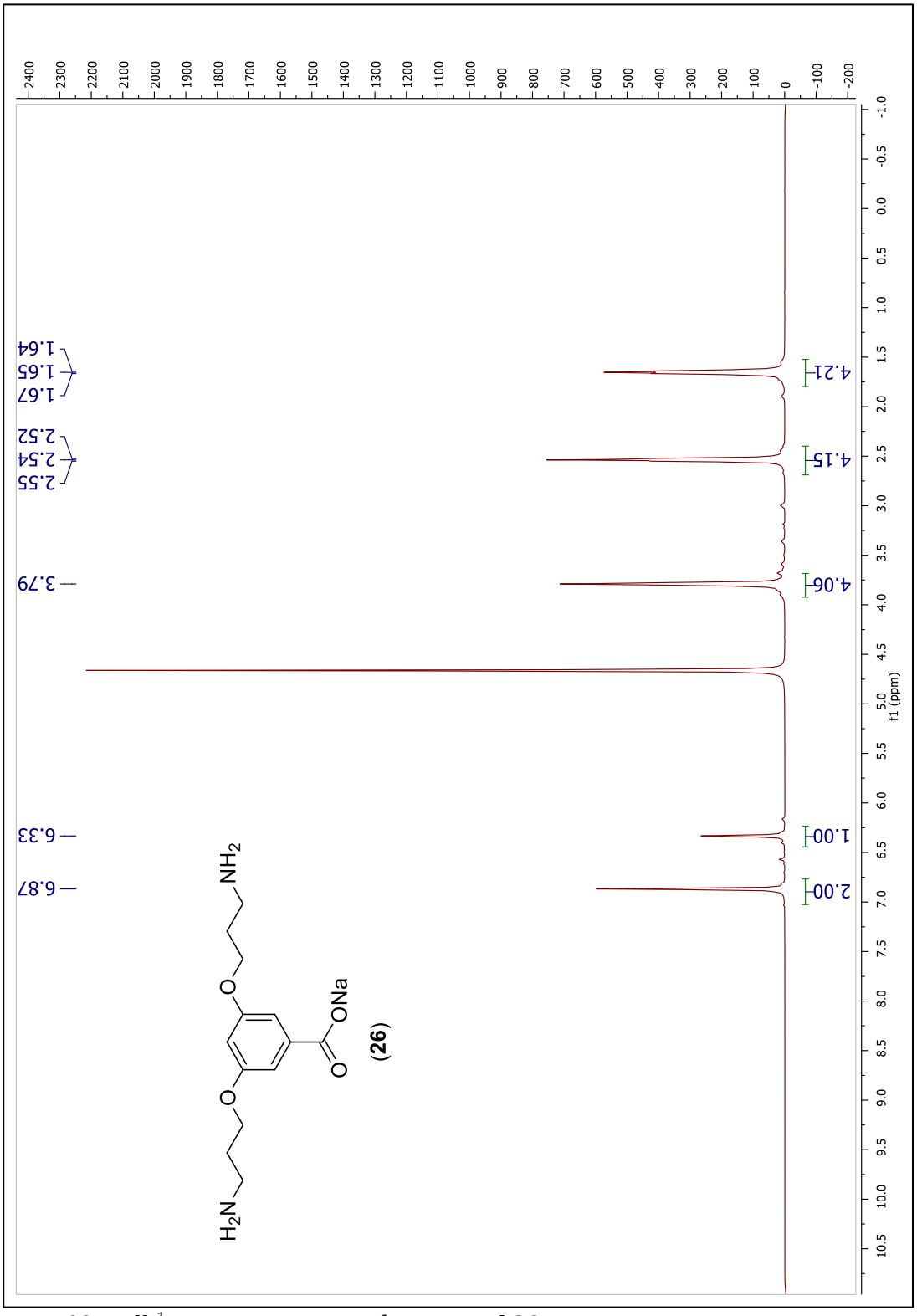


Figure 108. Full ^{1}H NMR spectrum of compound **26**.

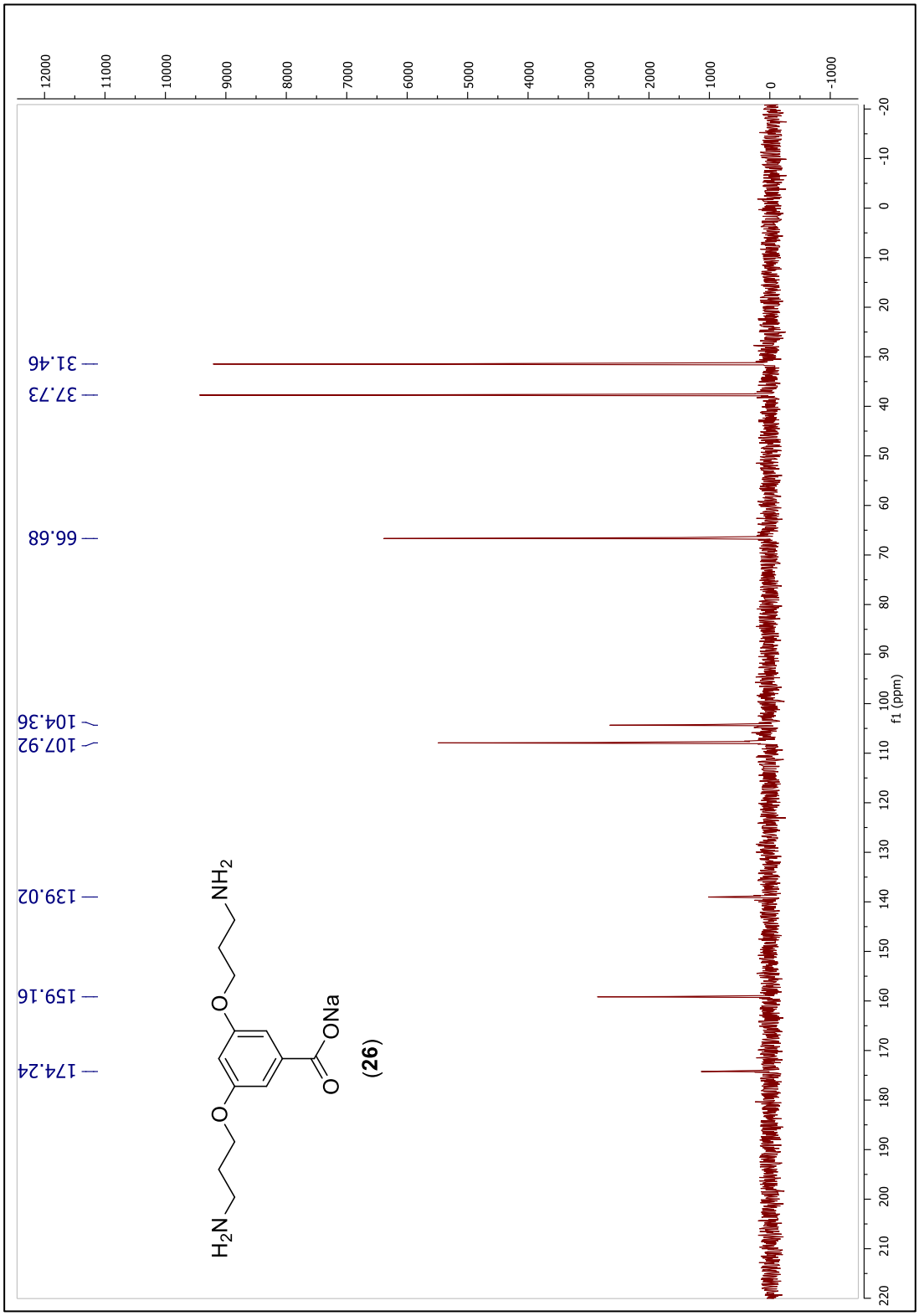


Figure 109. Full ^{13}C NMR spectrum of compound **26**.

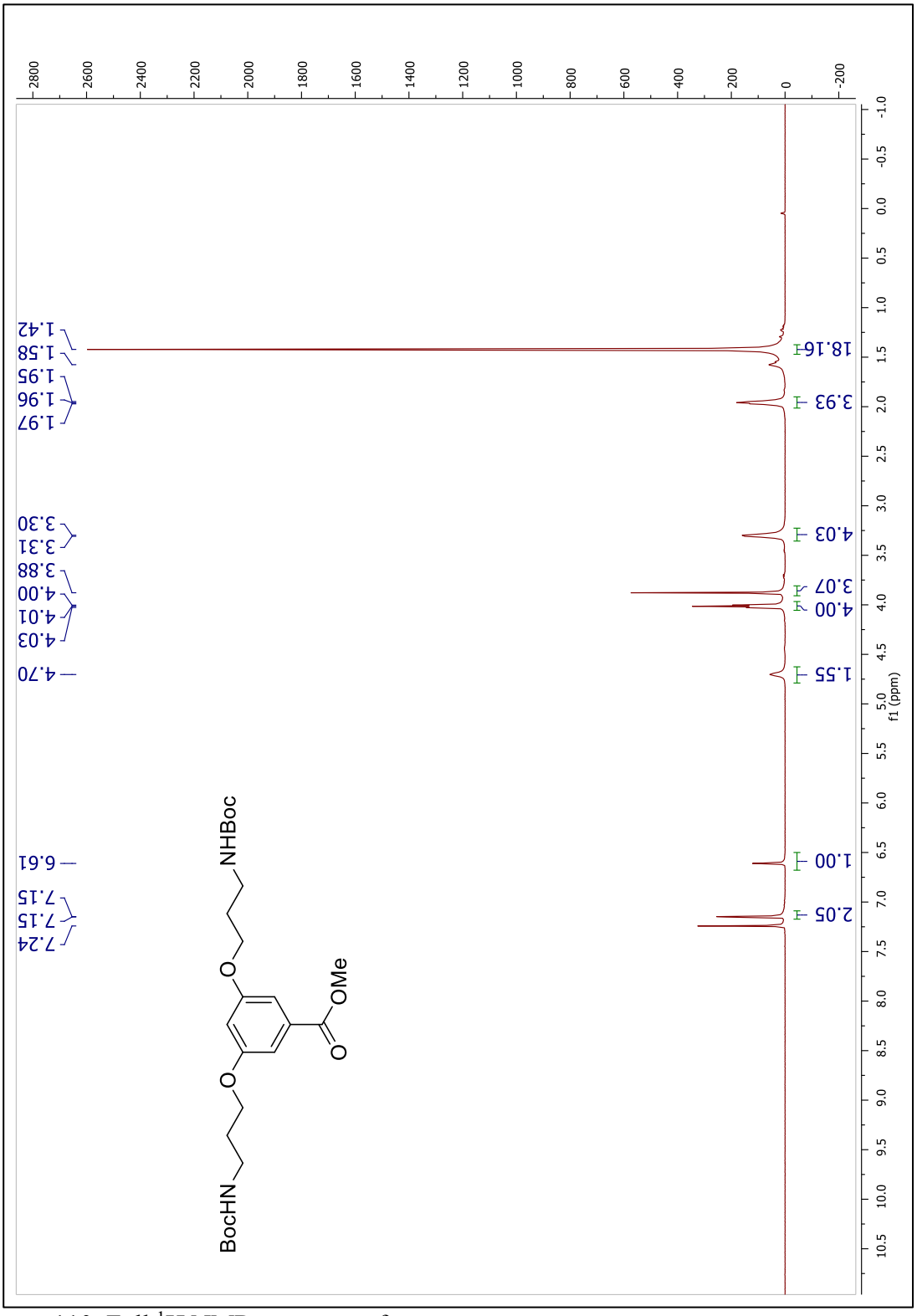


Figure 110. Full ^{1}H NMR spectrum of
Methyl 3,5-bis-(3-(tert-butyloxycarbonylamido)propoxy)benzoate.

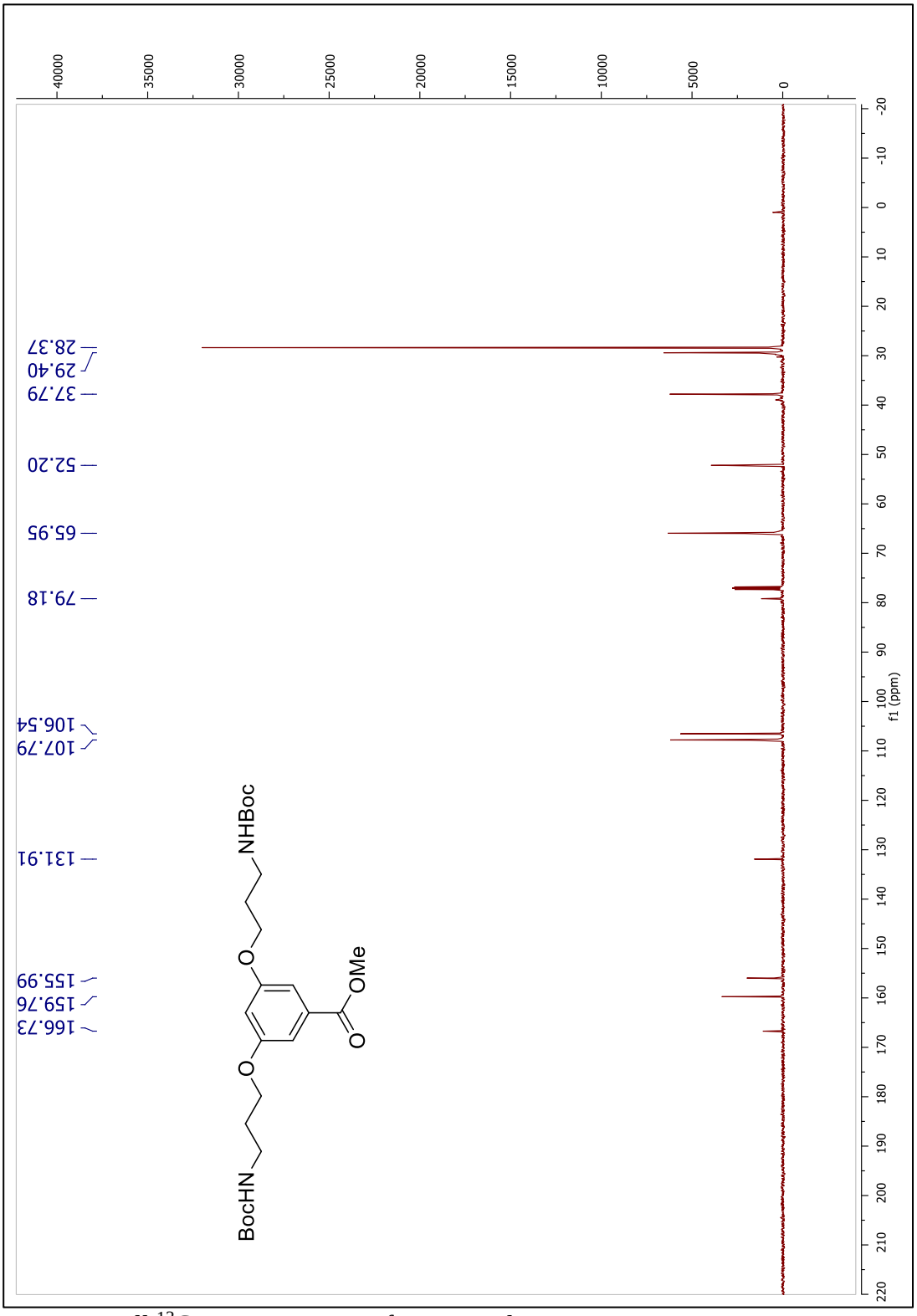


Figure 111. Full ^{13}C NMR spectrum of compound
Methyl 3,5-bis-(3-(tert-butyloxycarbonylamido)propoxy)benzoate.

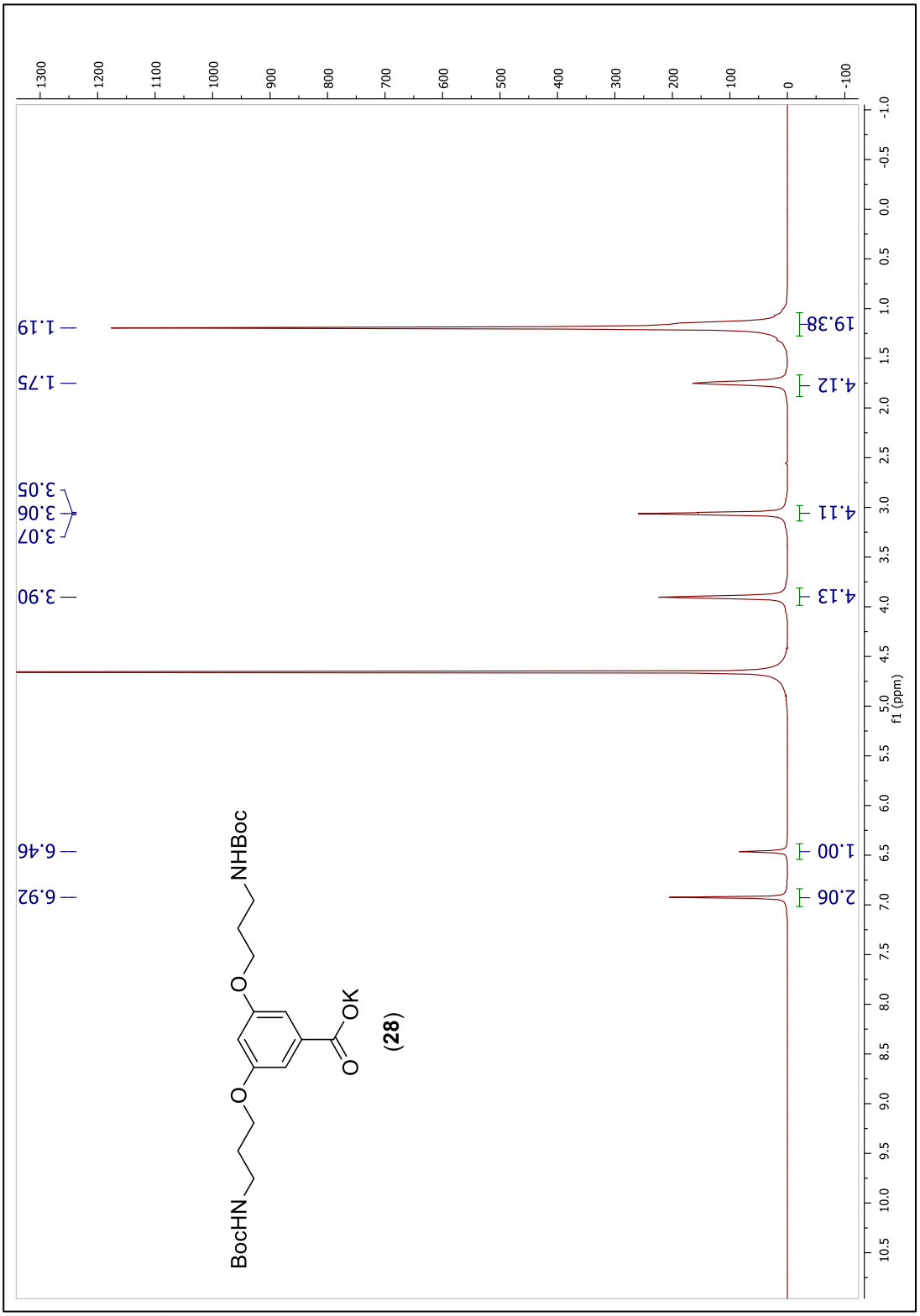


Figure 112. Full ^{1}H NMR spectrum of compound **28**.

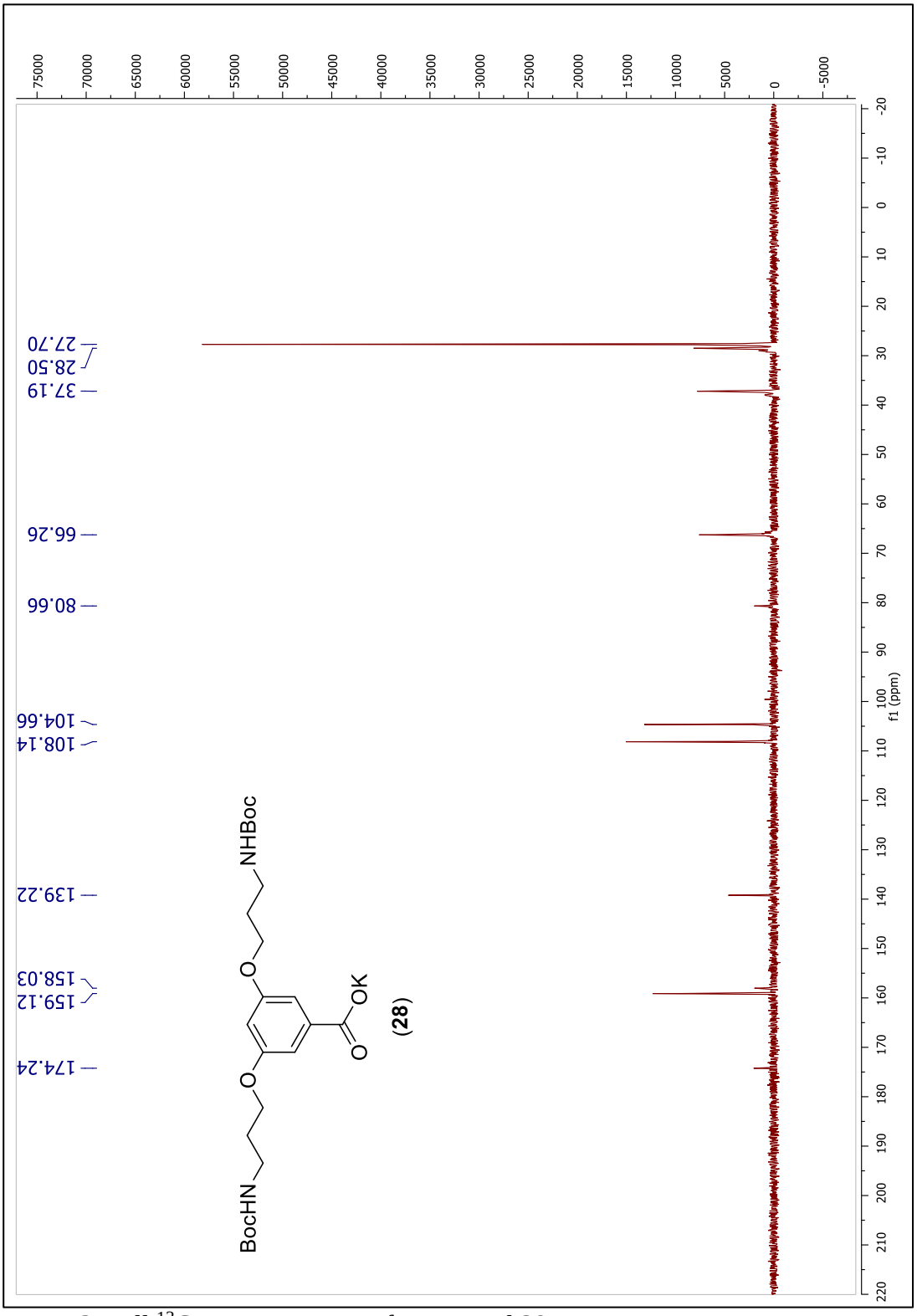


Figure 113. Full ^{13}C NMR spectrum of compound **28**.

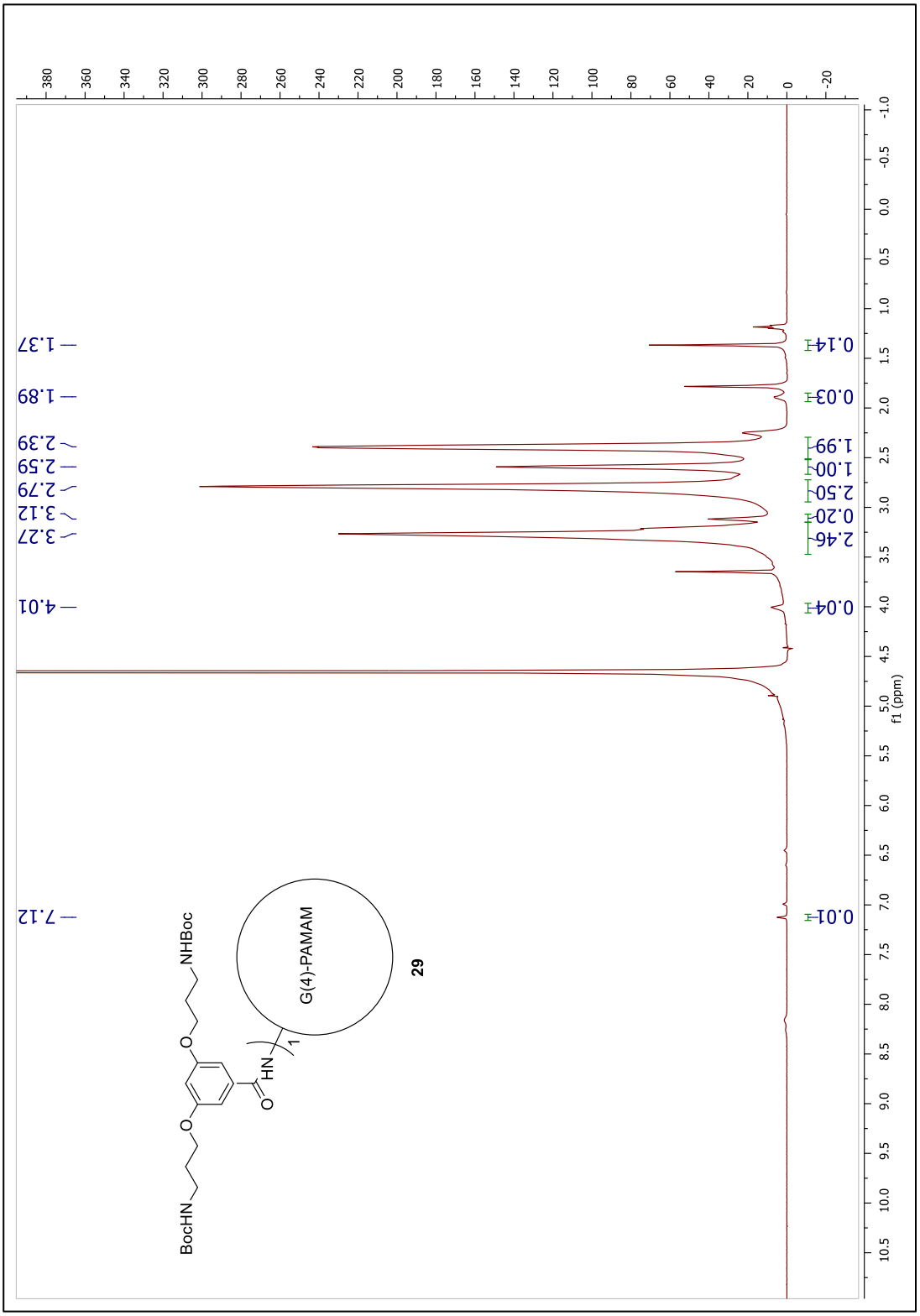


Figure 114. Full ^{1}H NMR spectrum of compound **29**.

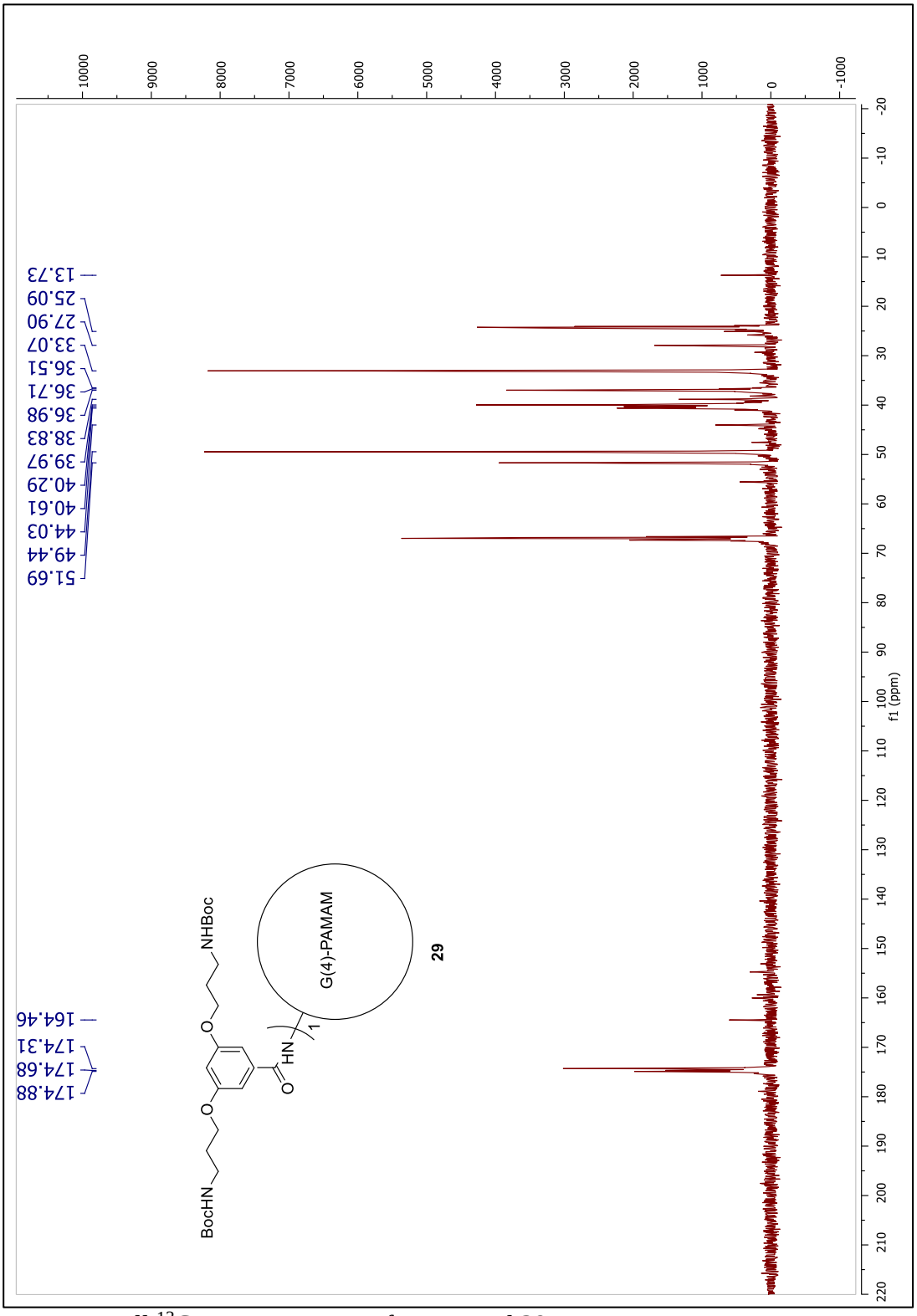


Figure 115. Full ^{13}C NMR spectrum of compound **29**.

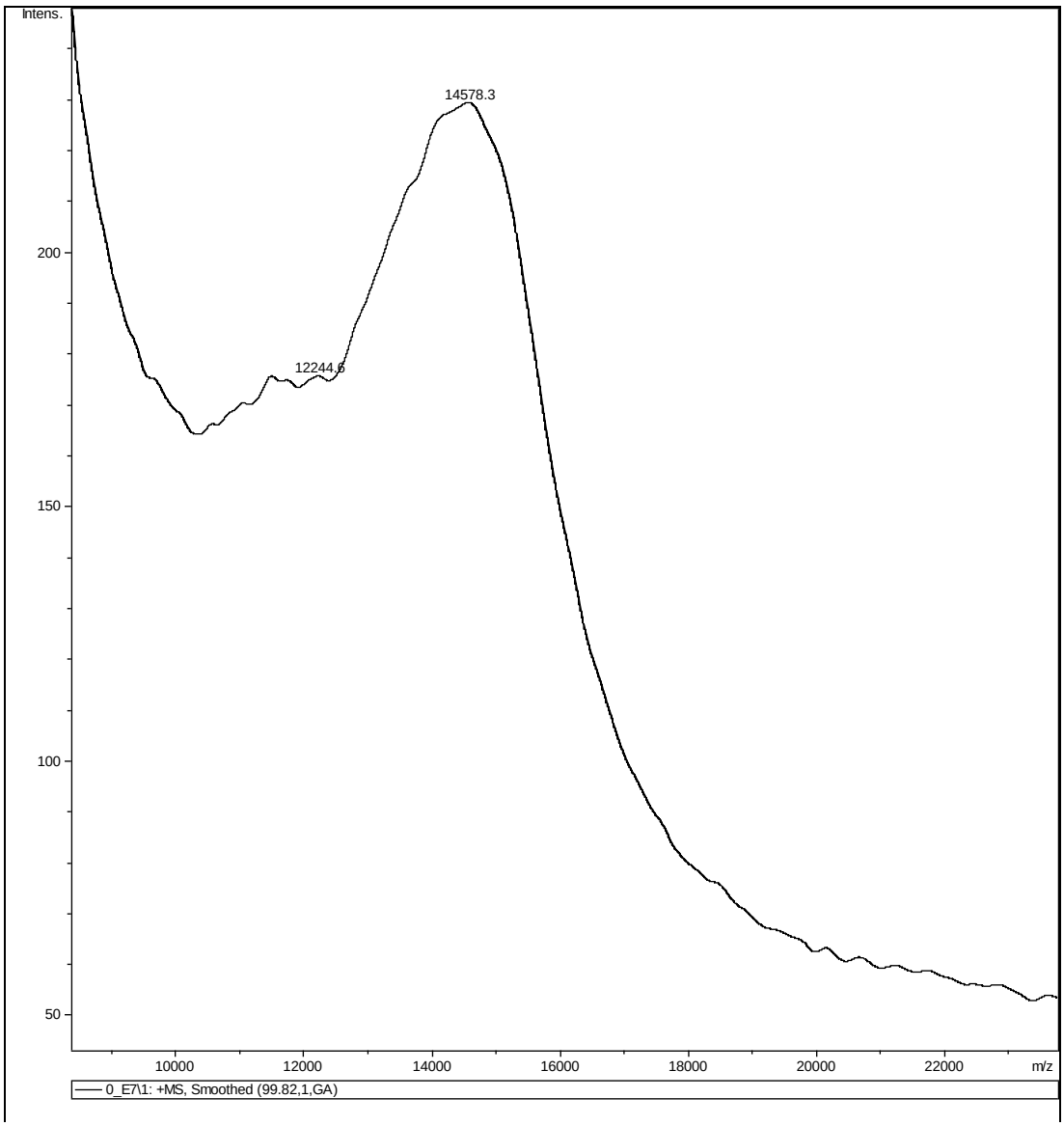


Figure 116. Smoothed MALDI TOF spectrum for compound **29**. M_w = 14100.

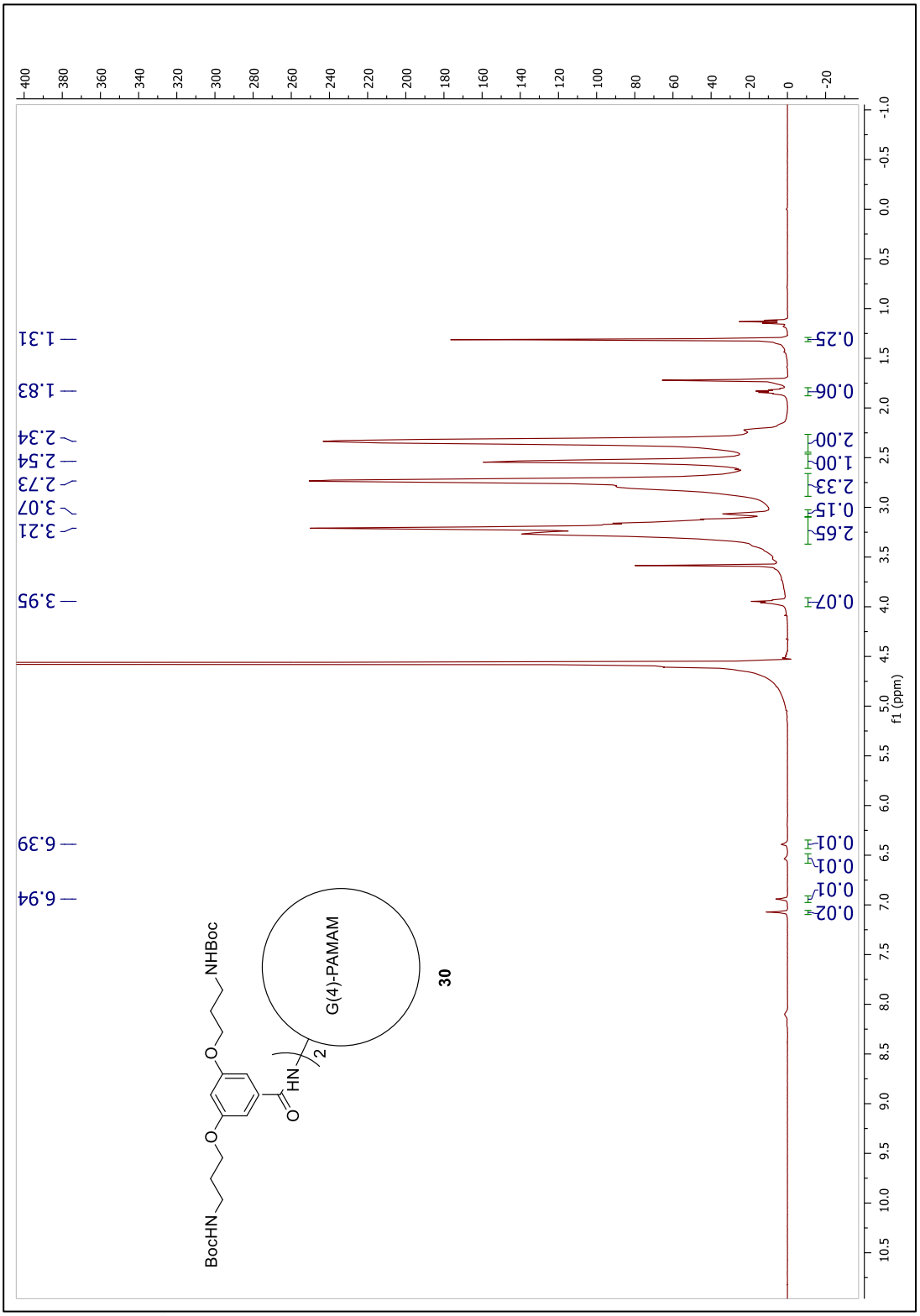


Figure 117. Full ^{1}H NMR spectrum of compound **30**.

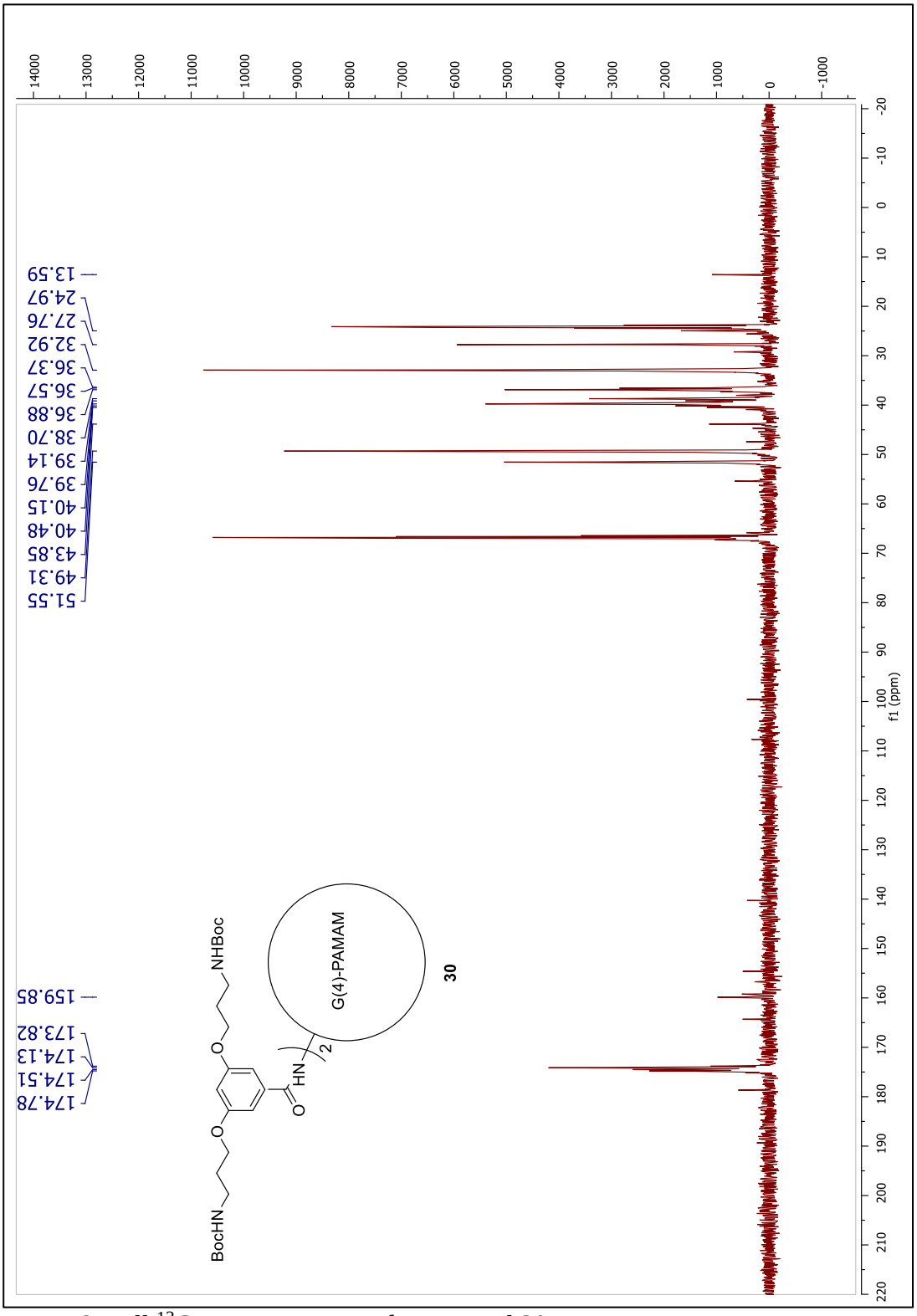


Figure 118. Full ^{13}C NMR spectrum of compound **30**.

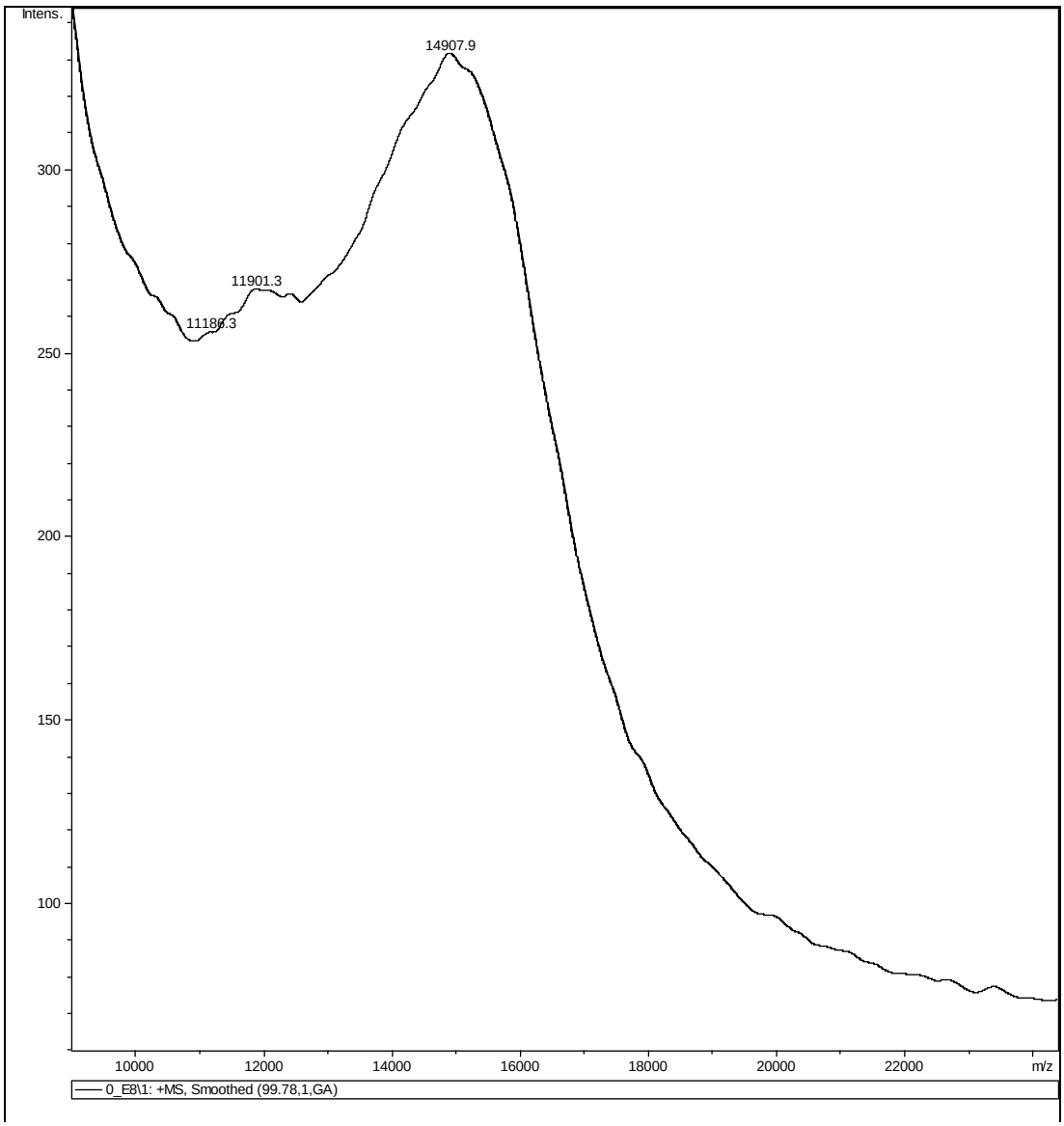


Figure 119. Smoothed MALDI TOF spectrum for compound **30**. M_w = 14400.

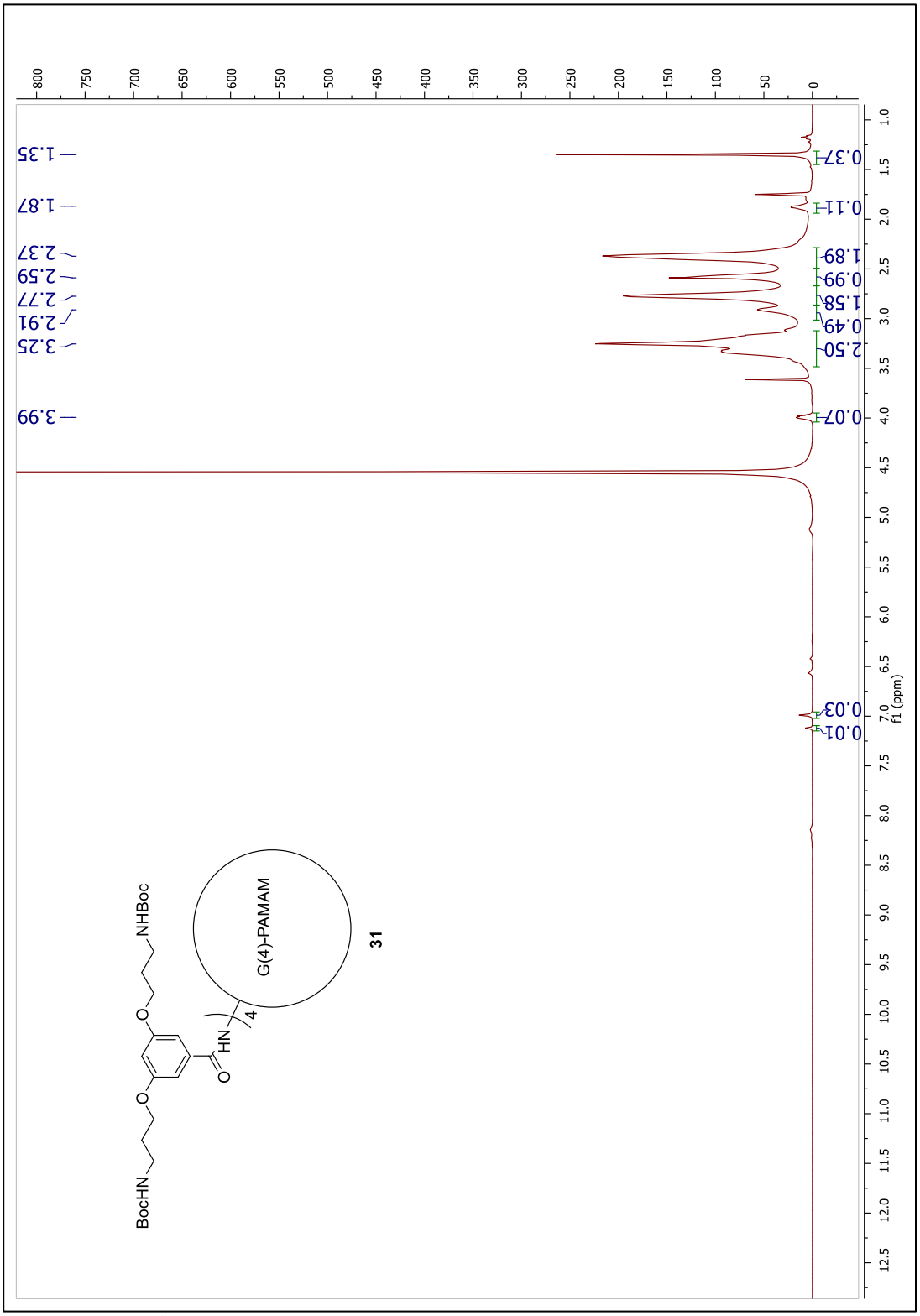


Figure 120. Full ^{1}H NMR spectrum of compound **31**.

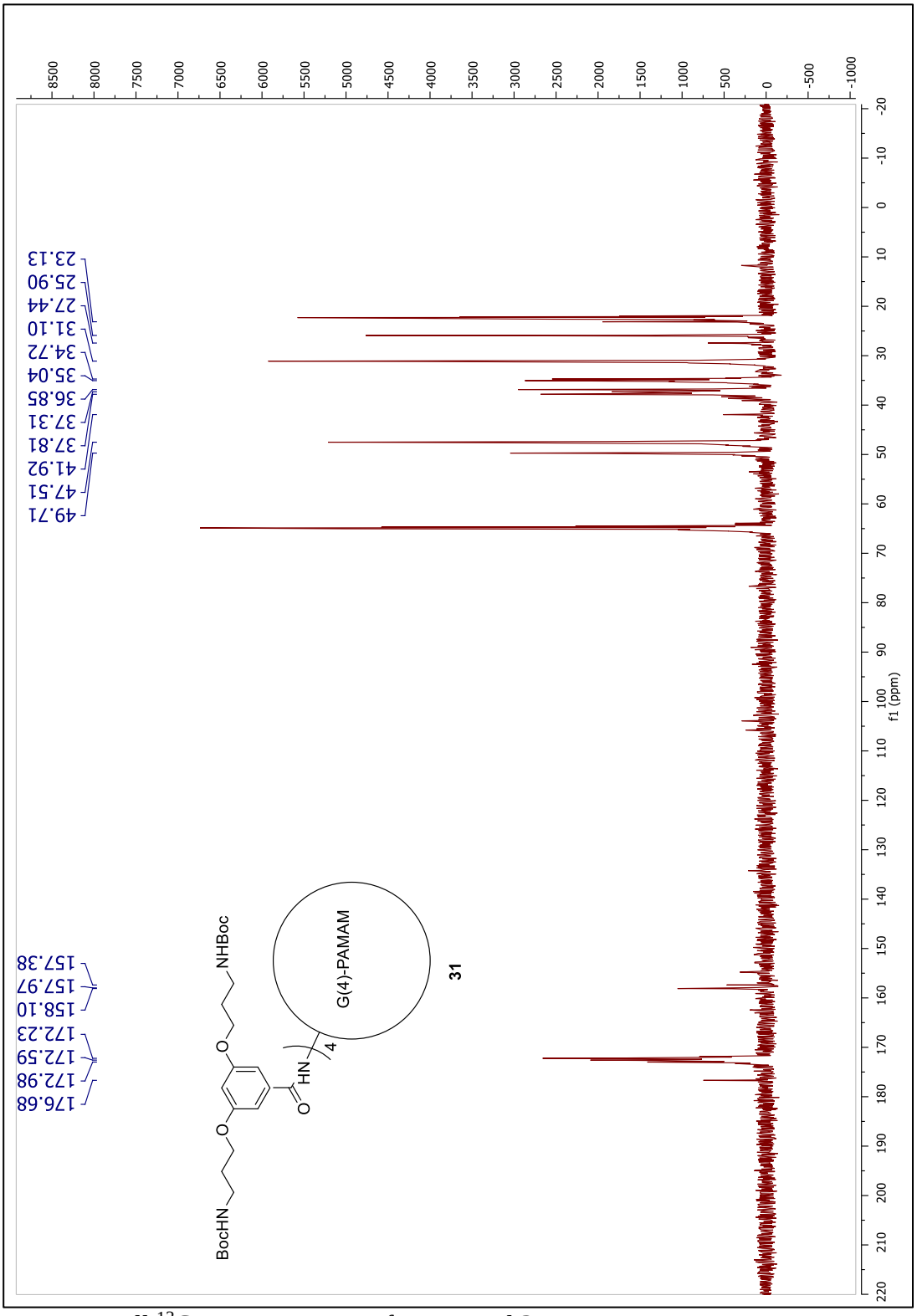


Figure 121. Full ^{13}C NMR spectrum of compound **31**.

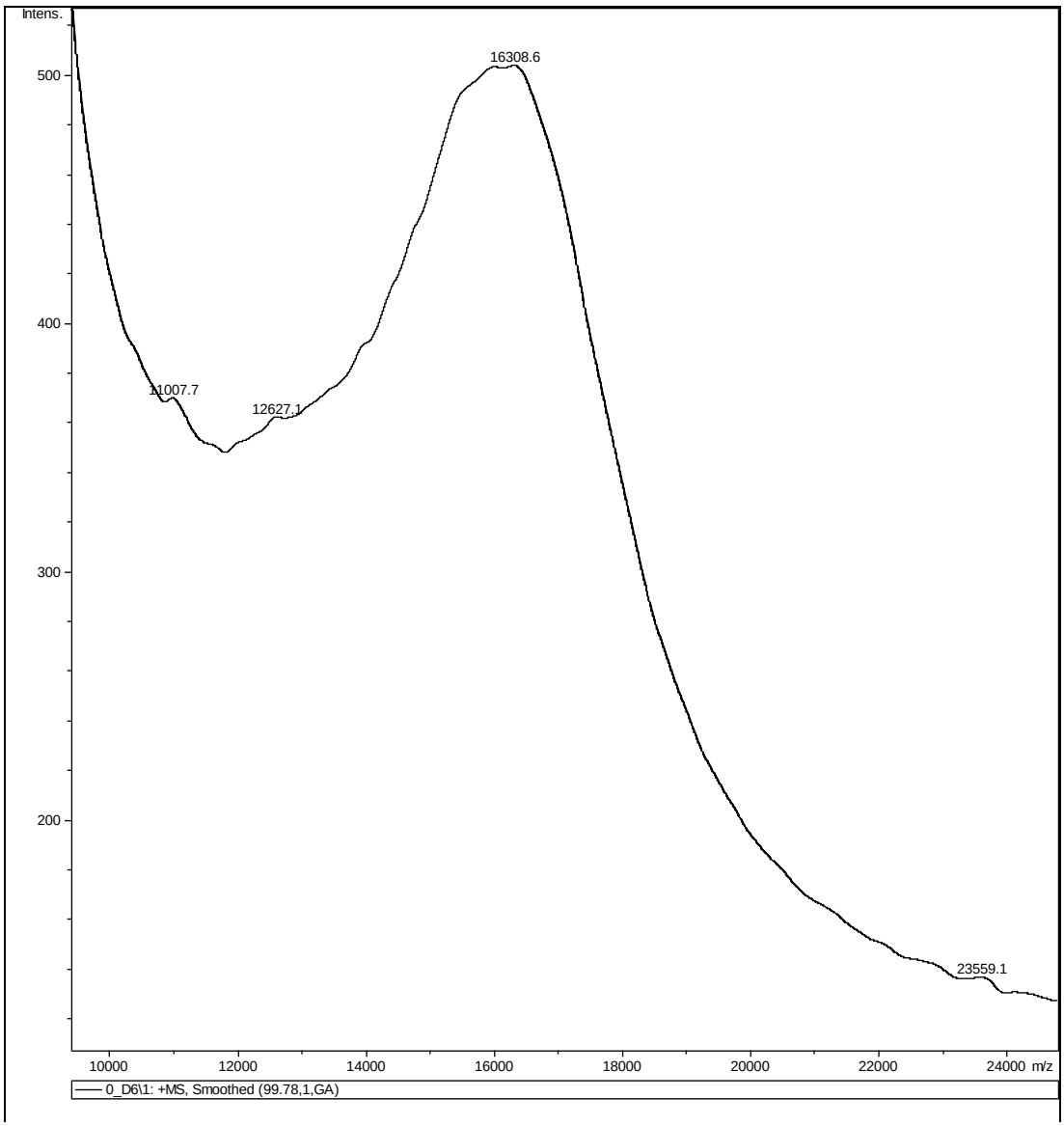


Figure 122. Smoothed MALDI TOF spectrum for compound **31**. M_w = 15400.

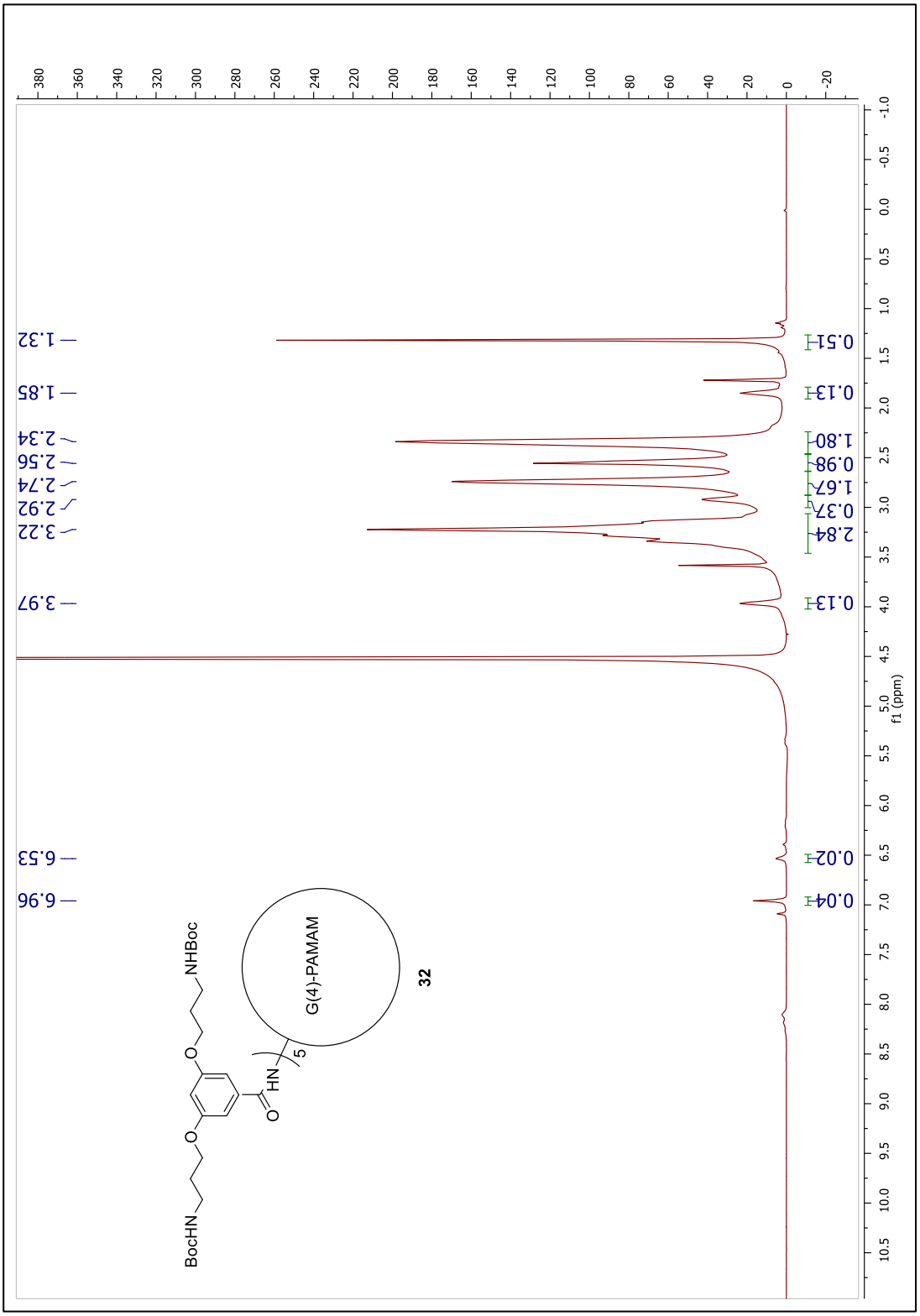


Figure 123. Full ^{1}H NMR spectrum of compound **32**.

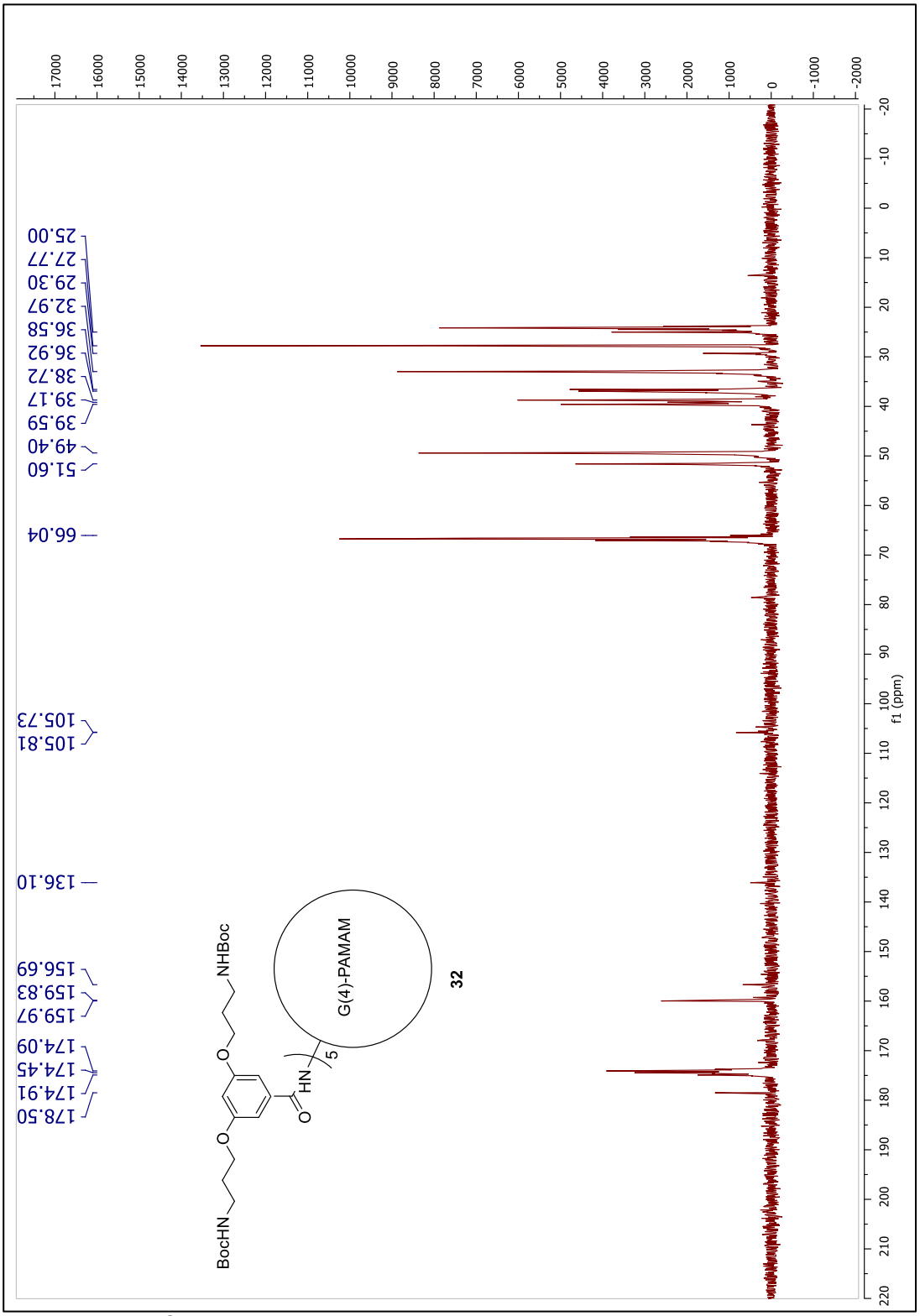


Figure 124. Full ^{13}C NMR spectrum of compound **32**.

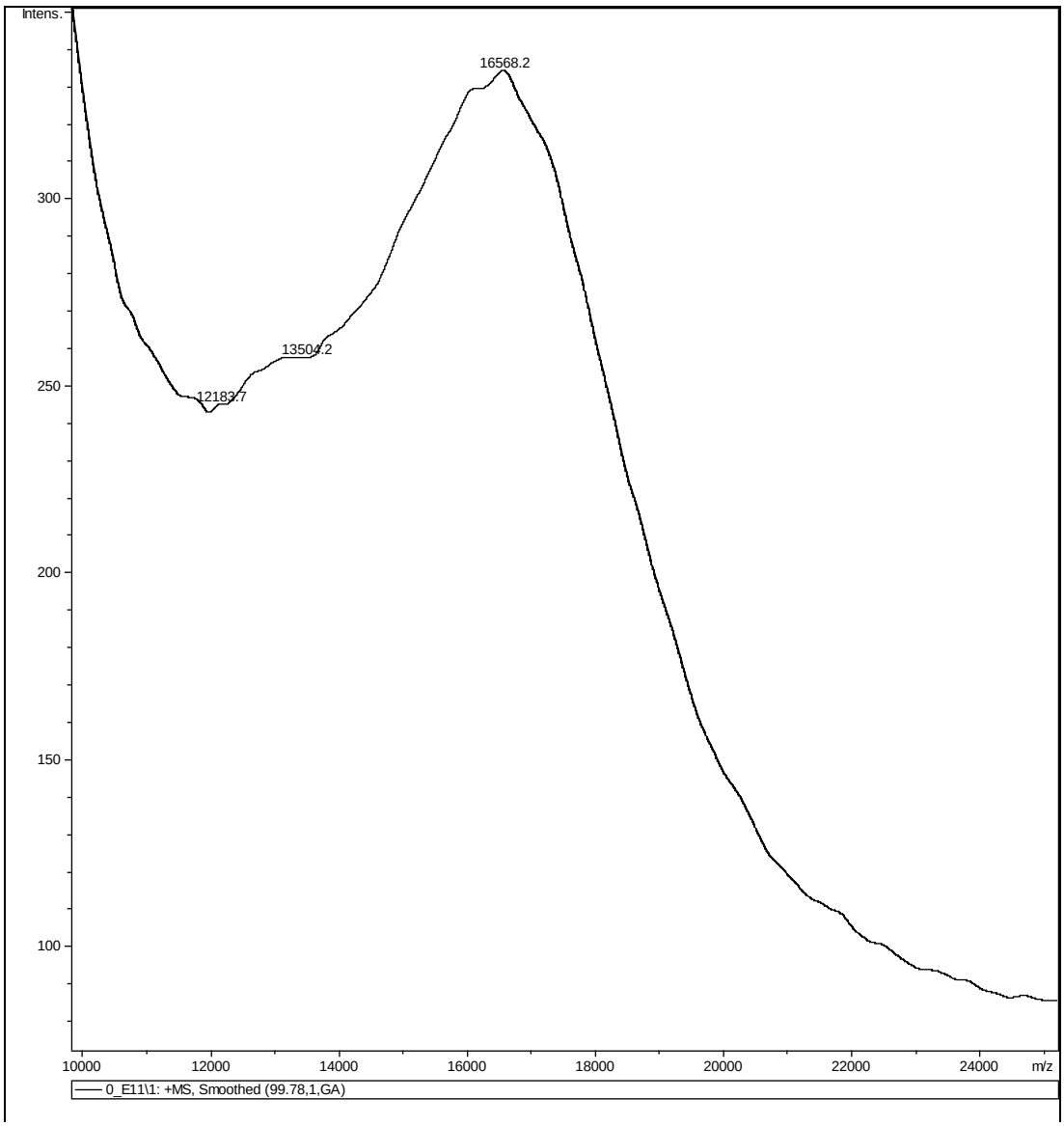


Figure 125. Smoothed MALDI TOF spectrum for compound **32**. M_w = 15900.

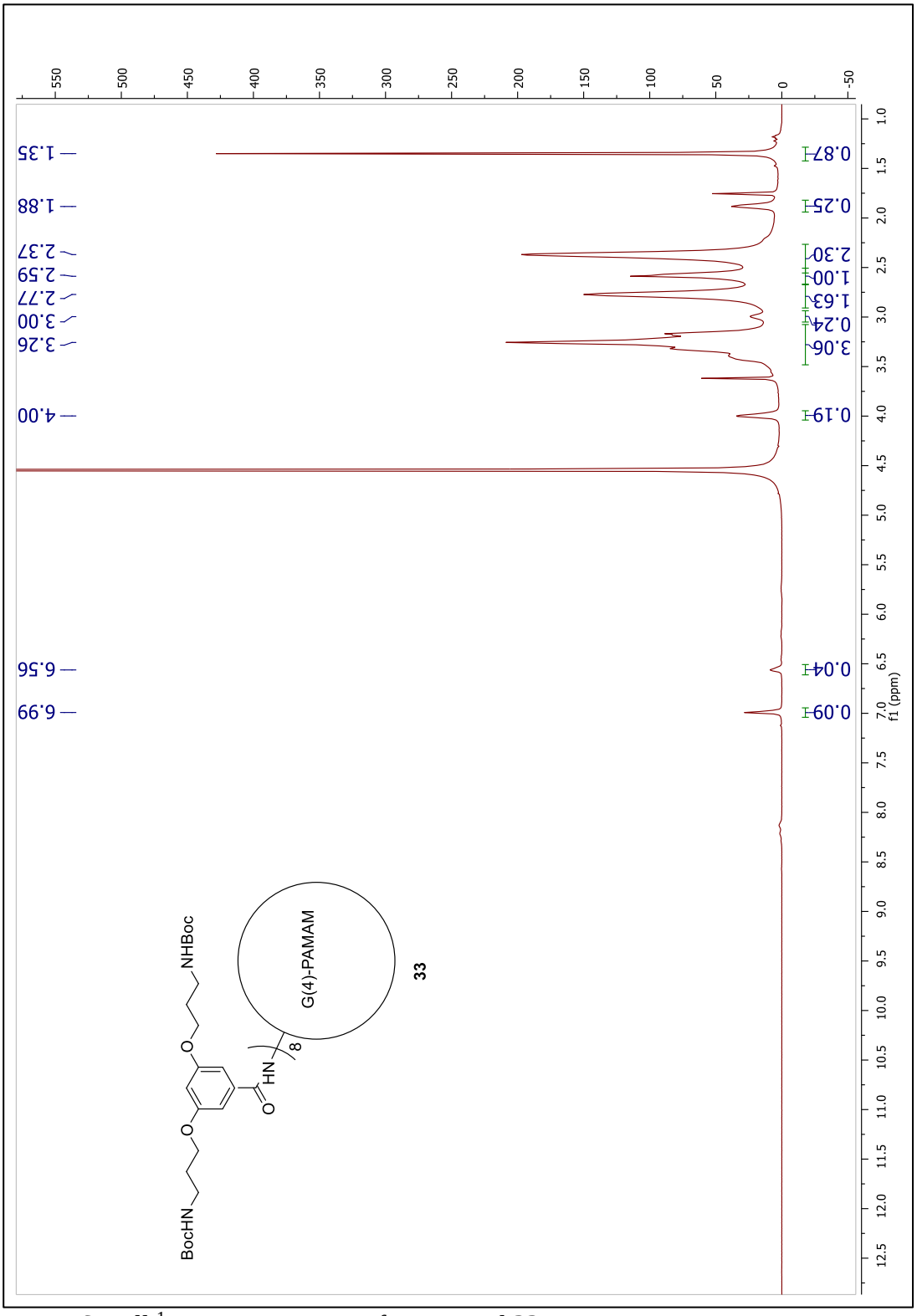


Figure 126. Full ^{1}H NMR spectrum of compound **33**.

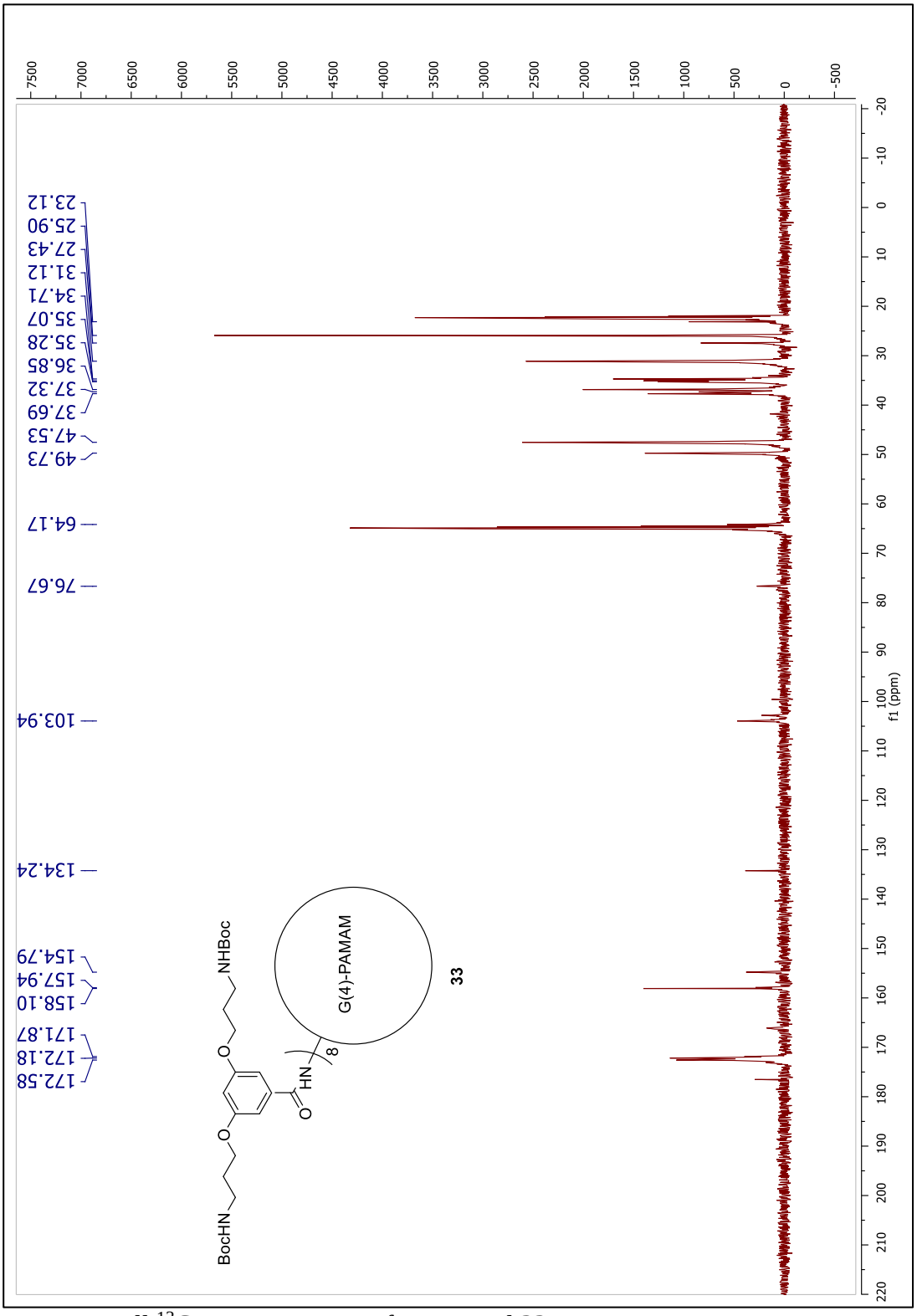


Figure 127. Full ^{13}C NMR spectrum of compound **33**.

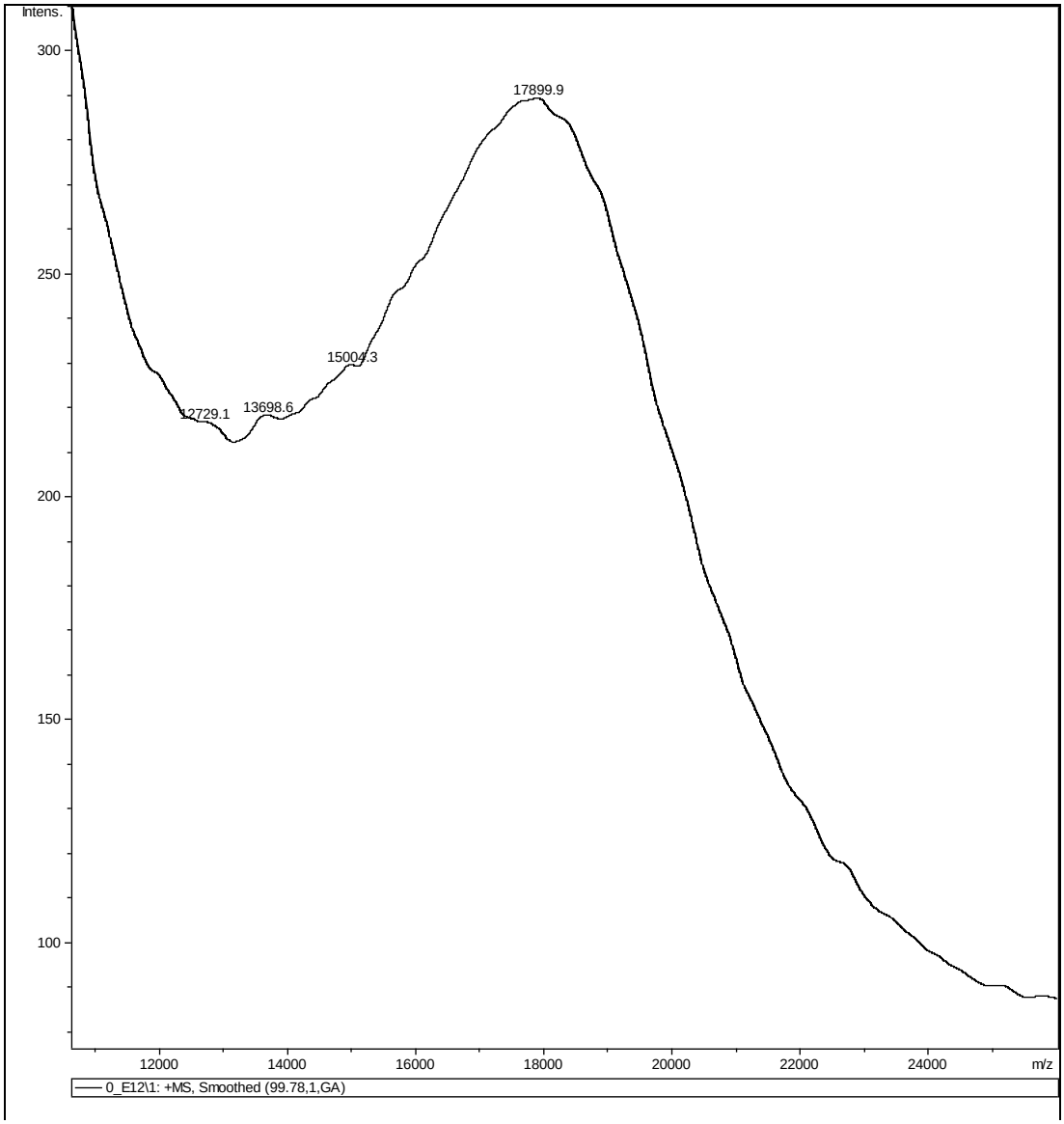


Figure 128. Smoothed MALDI TOF spectrum for compound **33**. M_w = 17000.

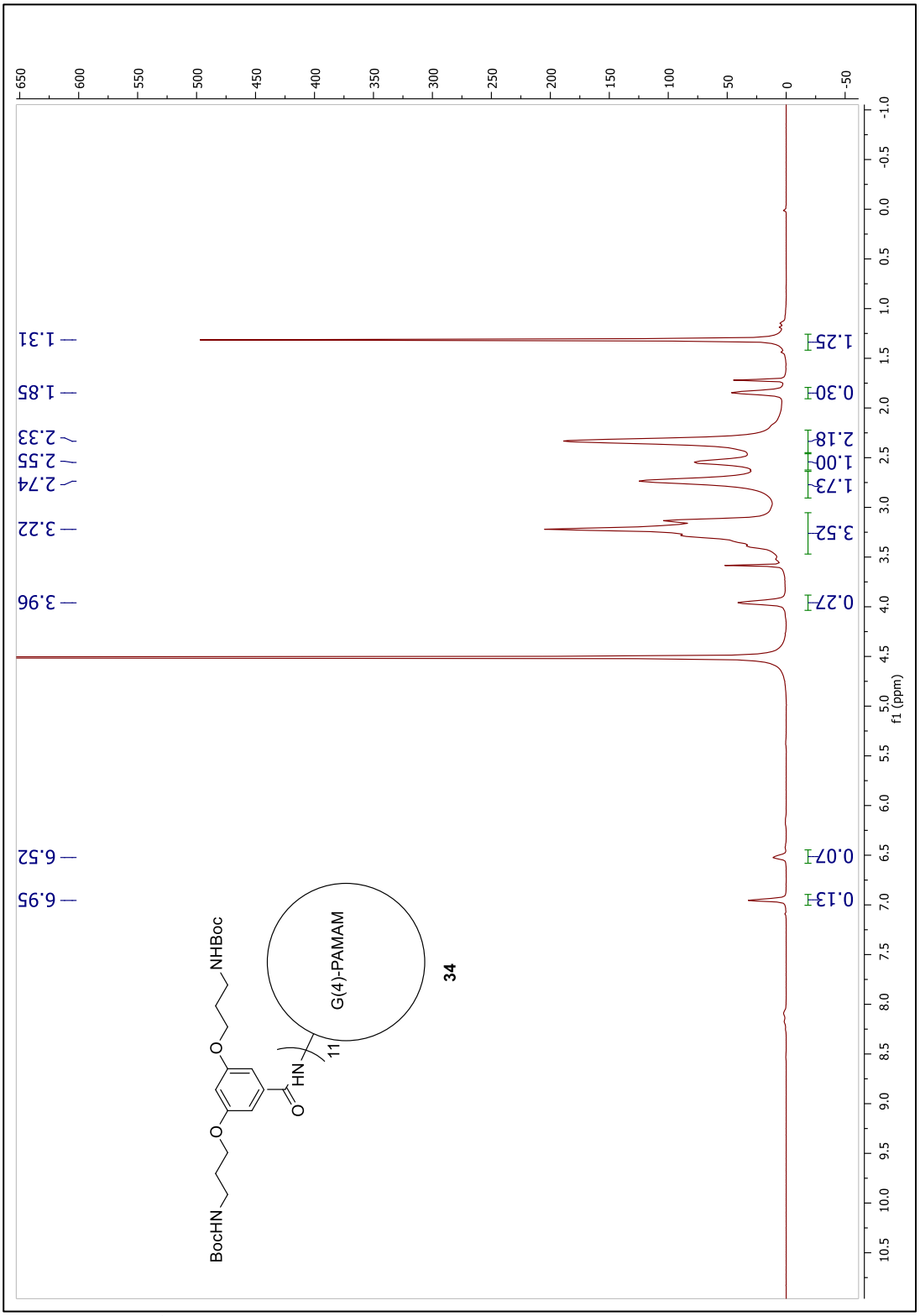


Figure 129. Full ^{1}H NMR spectrum of compound **34**.

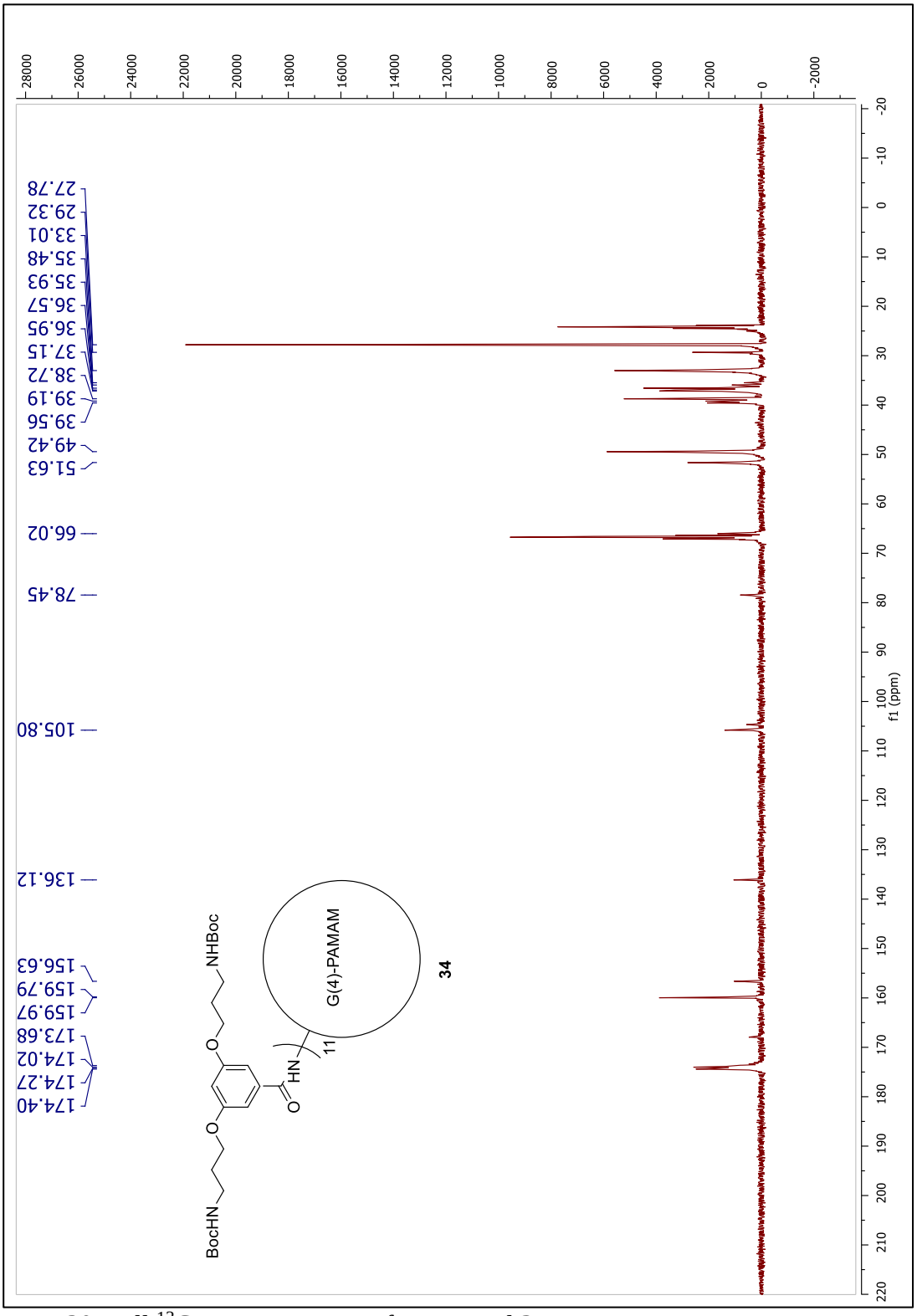


Figure 130. Full ^{13}C NMR spectrum of compound **34**.

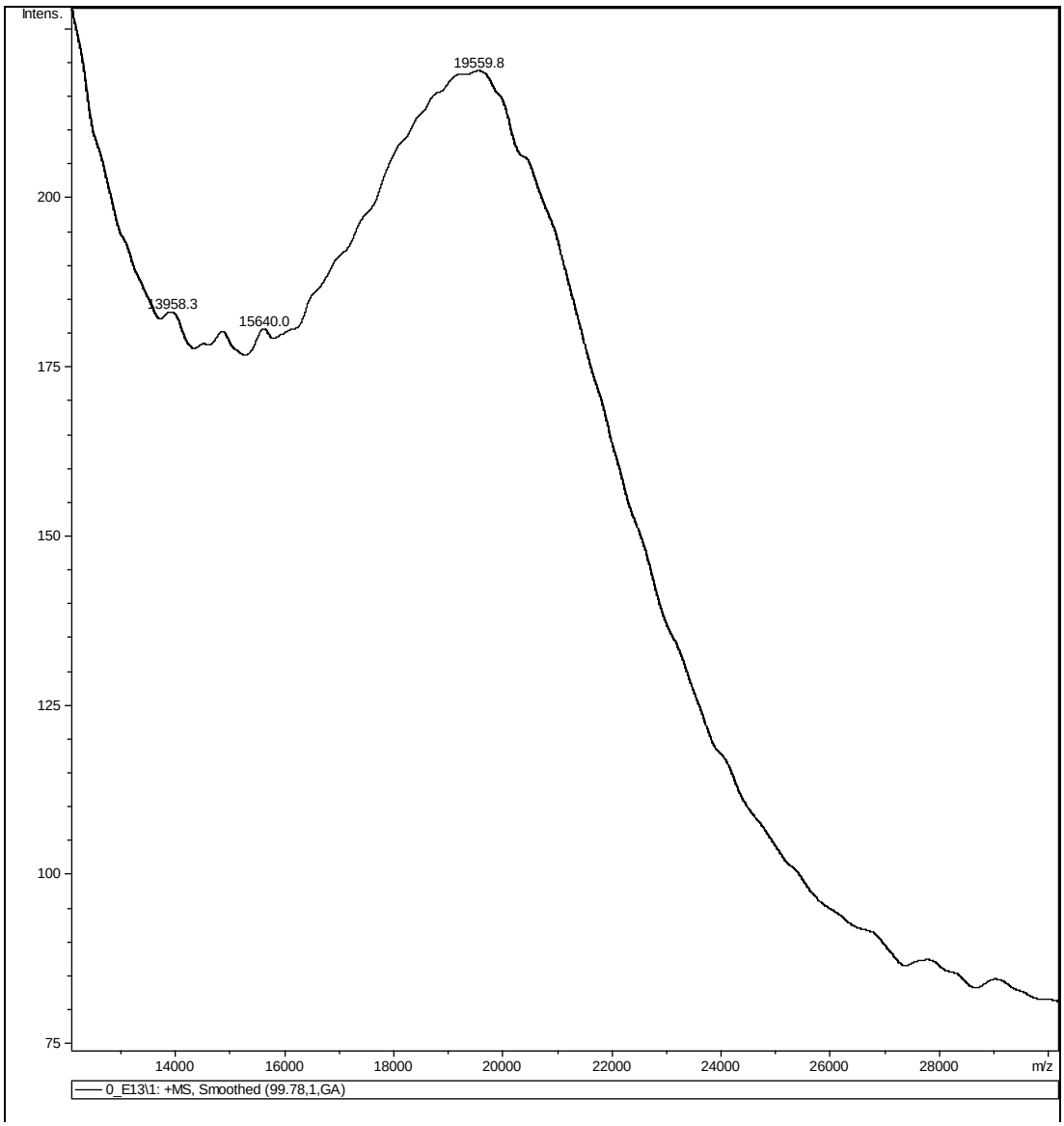


Figure 131. Smoothed MALDI TOF spectrum for compound **34**. M_w = 18500.

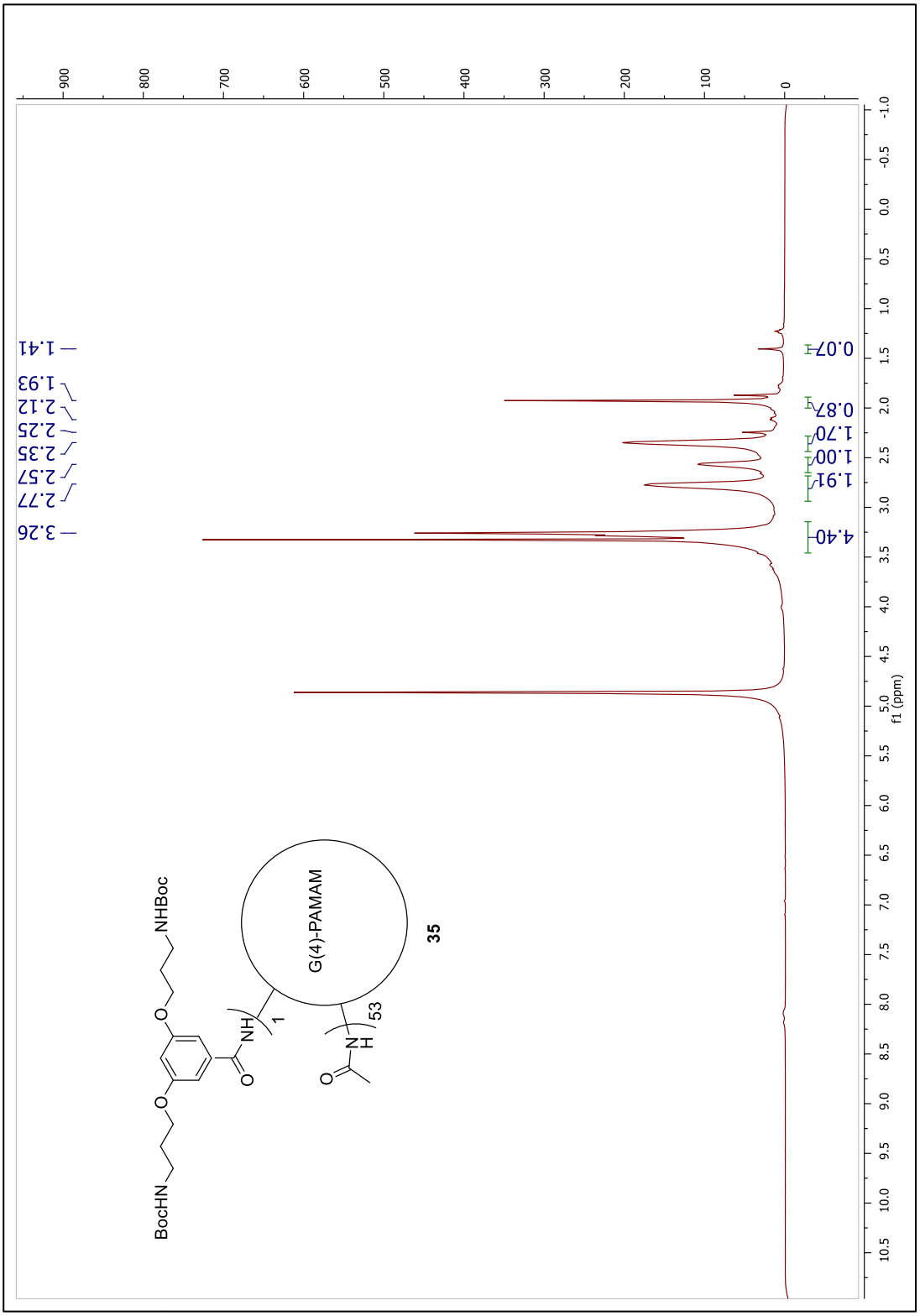


Figure 132. Full ^{1}H NMR spectrum of compound **35**.

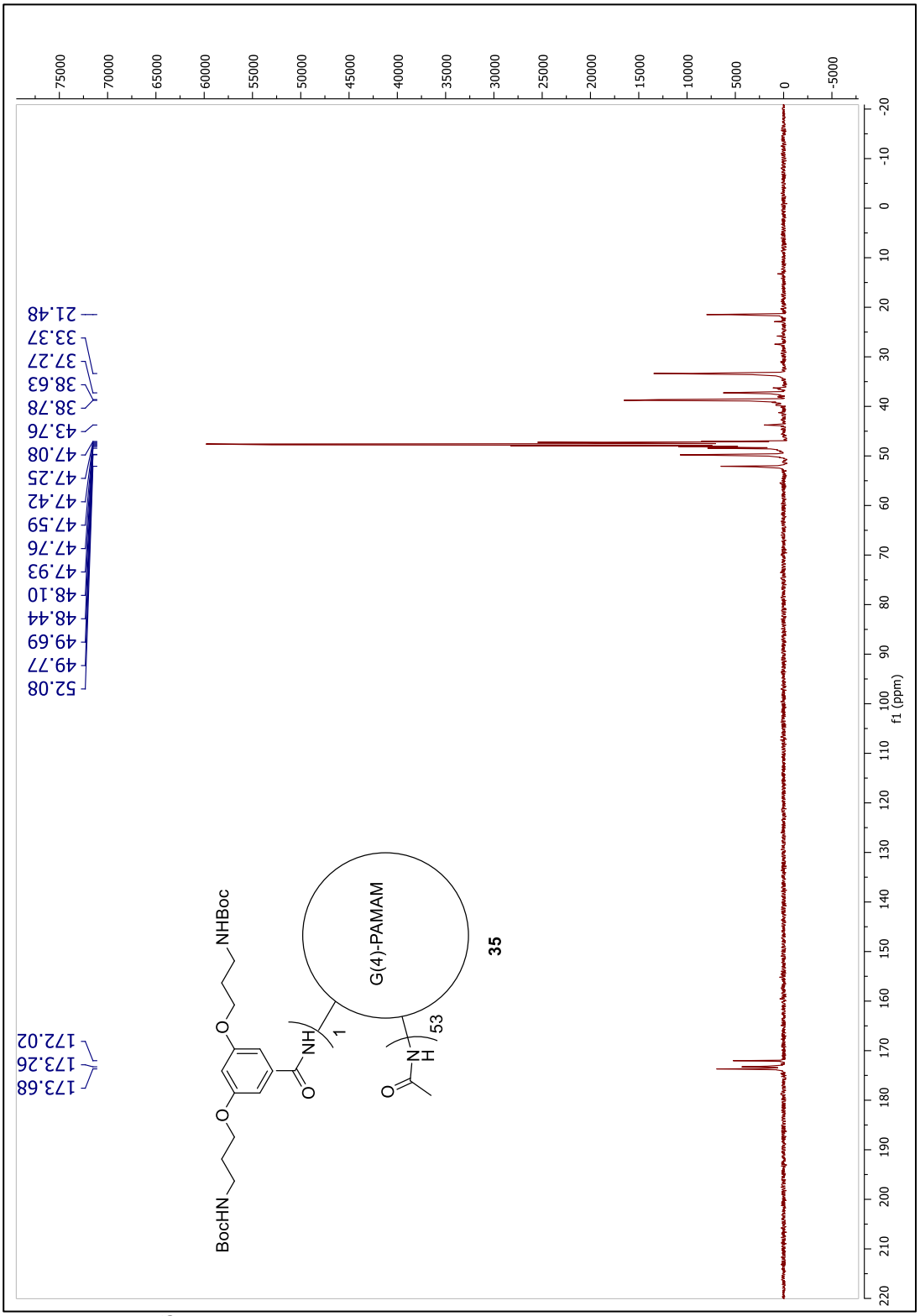


Figure 133. Full ^{13}C NMR spectrum of compound **35**.

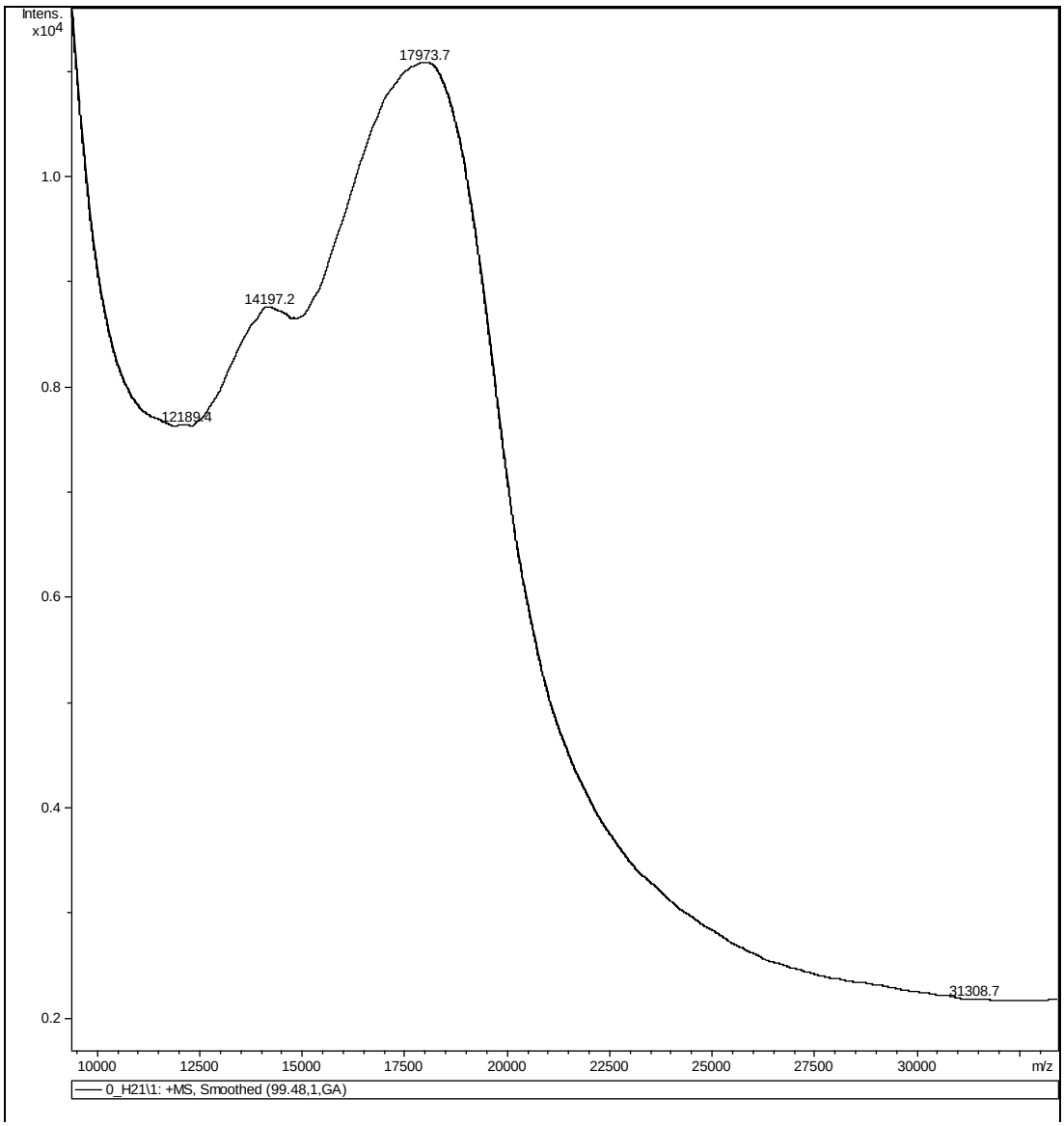


Figure 134. Smoothed MALDI TOF spectrum for compound **35**. M_w = 16800.

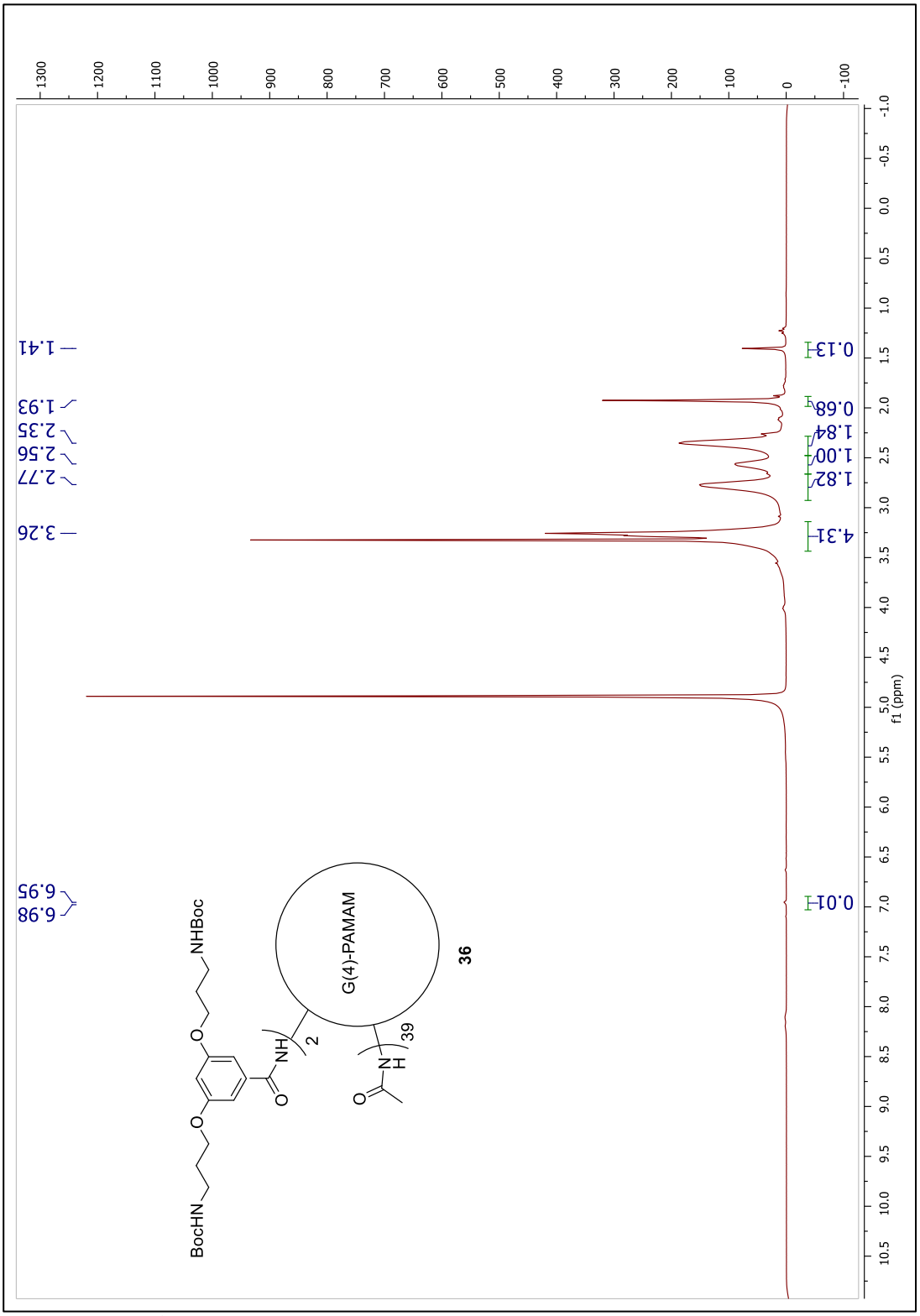


Figure 135. Full ^{1}H NMR spectrum of compound **36**.

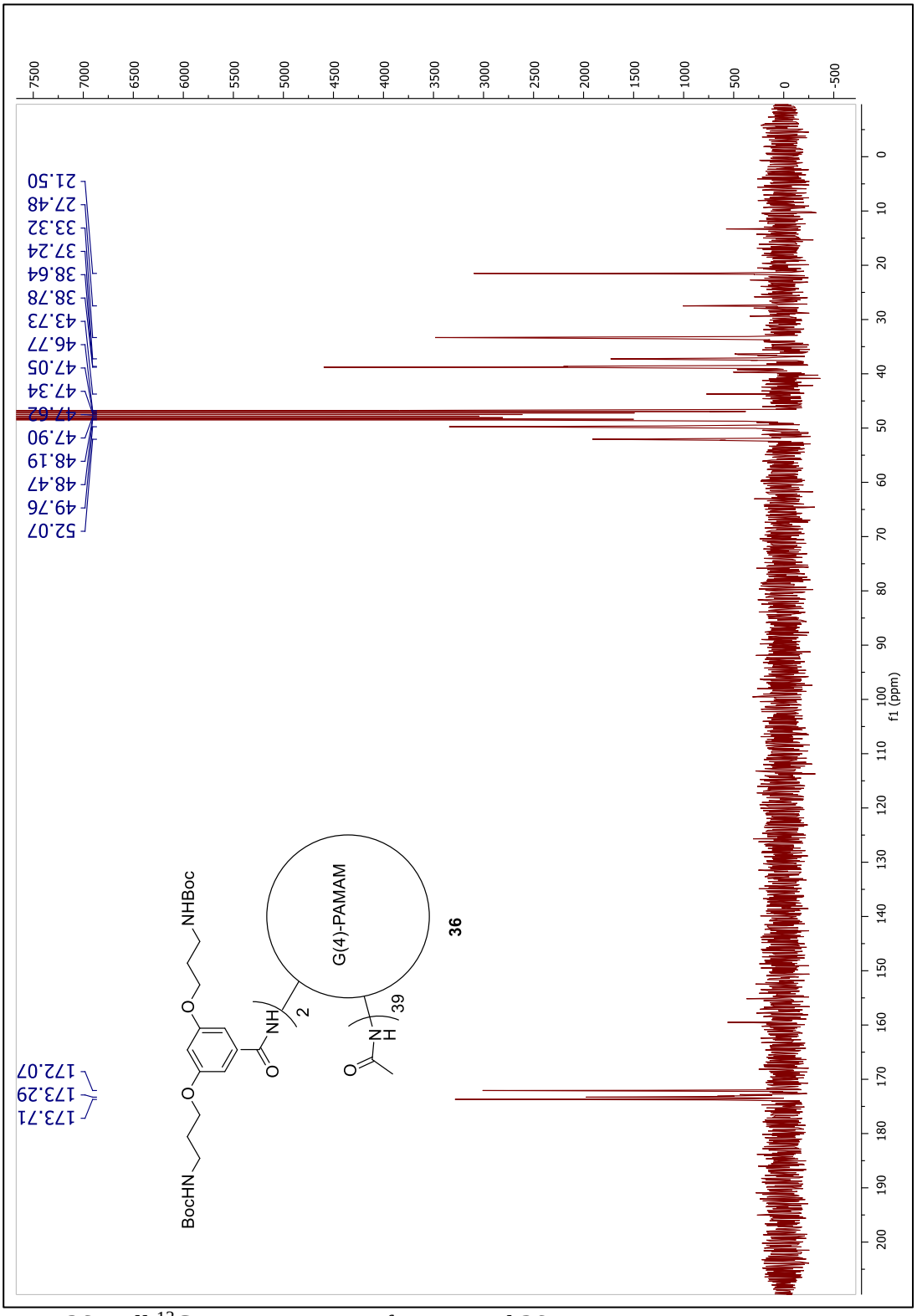


Figure 136. Full ^{13}C NMR spectrum of compound **36**.

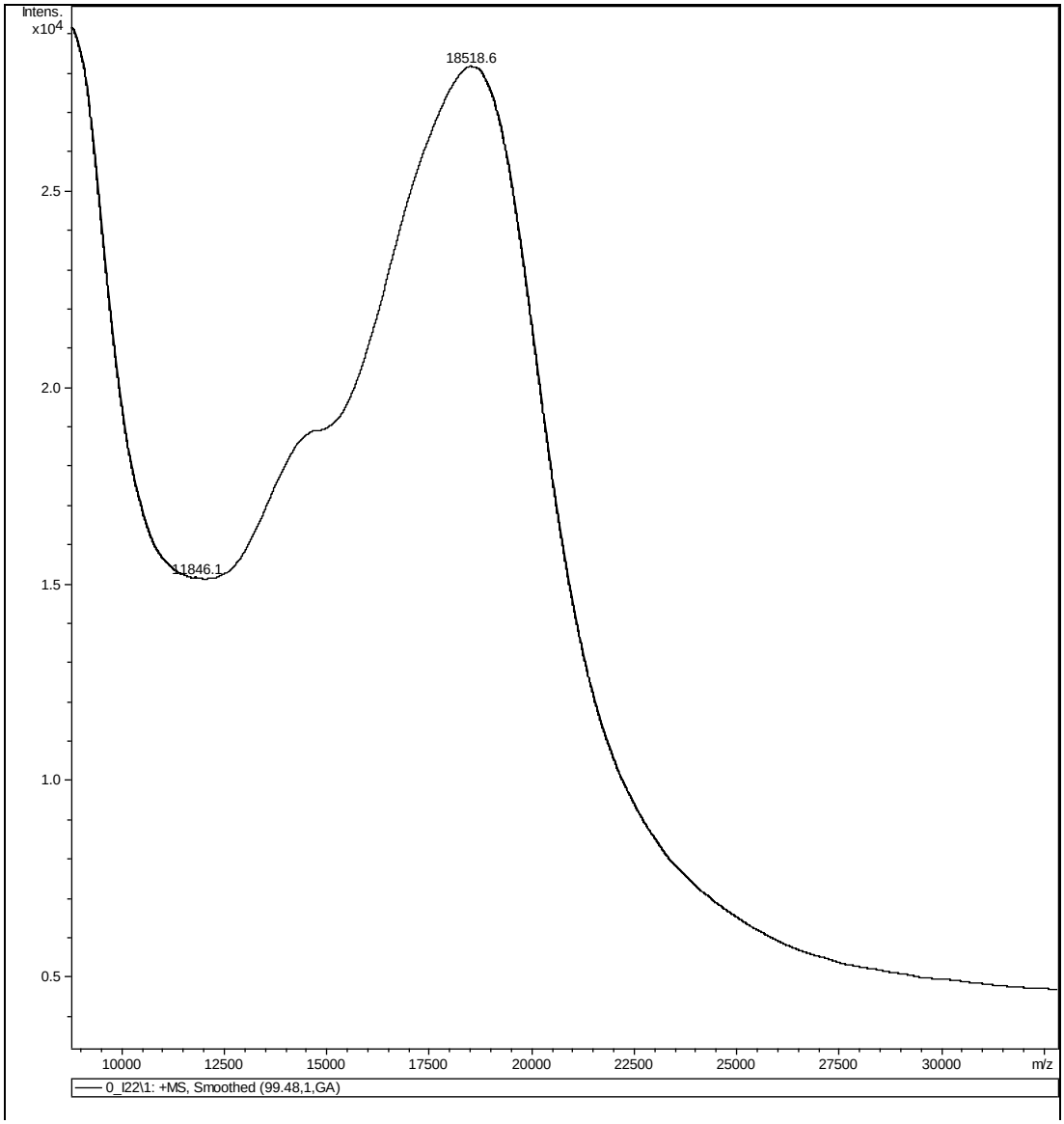


Figure 137. Smoothed MALDI TOF spectrum for compound **36**. M_w = 16800.

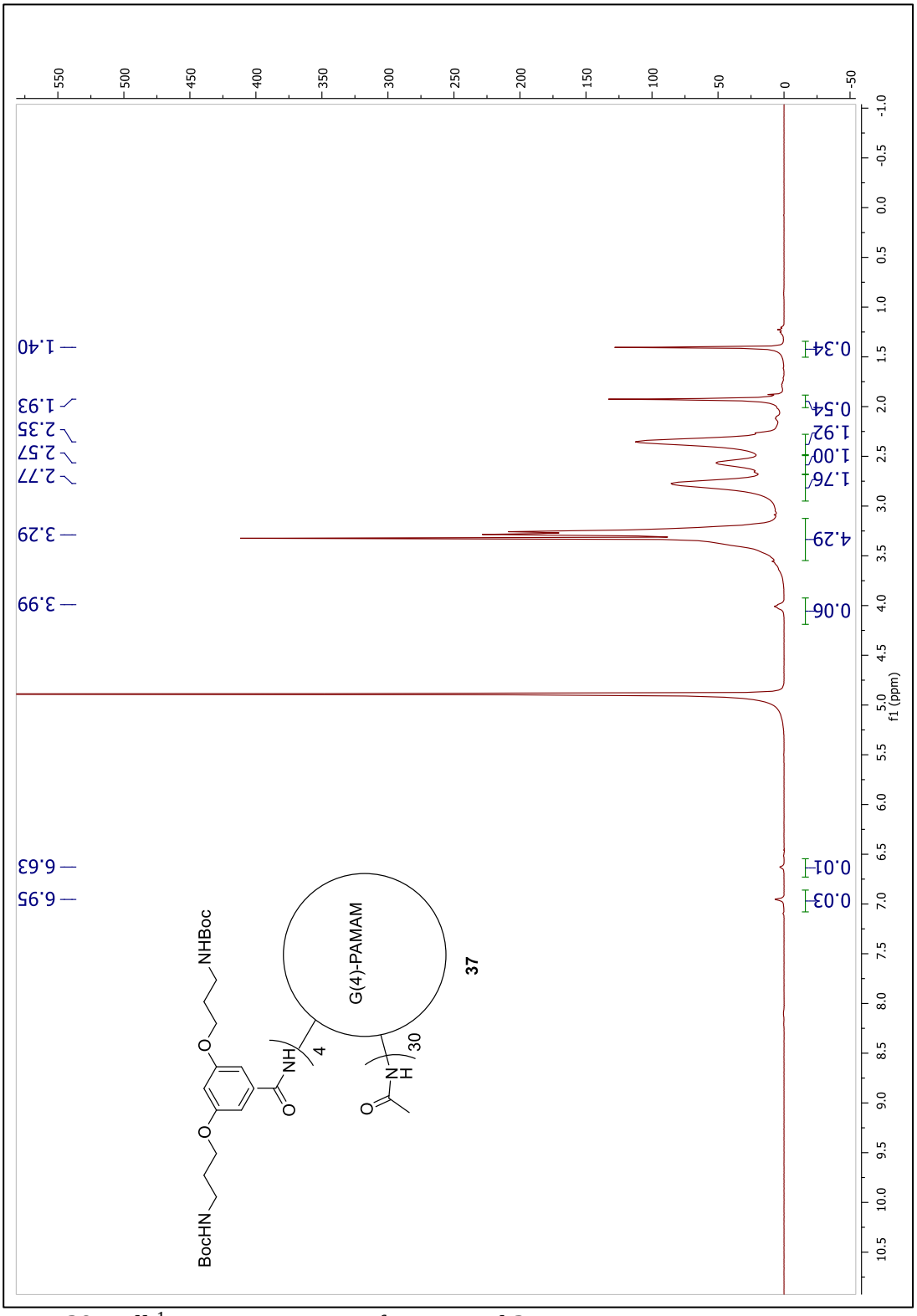


Figure 138. Full ^{1}H NMR spectrum of compound **37**.

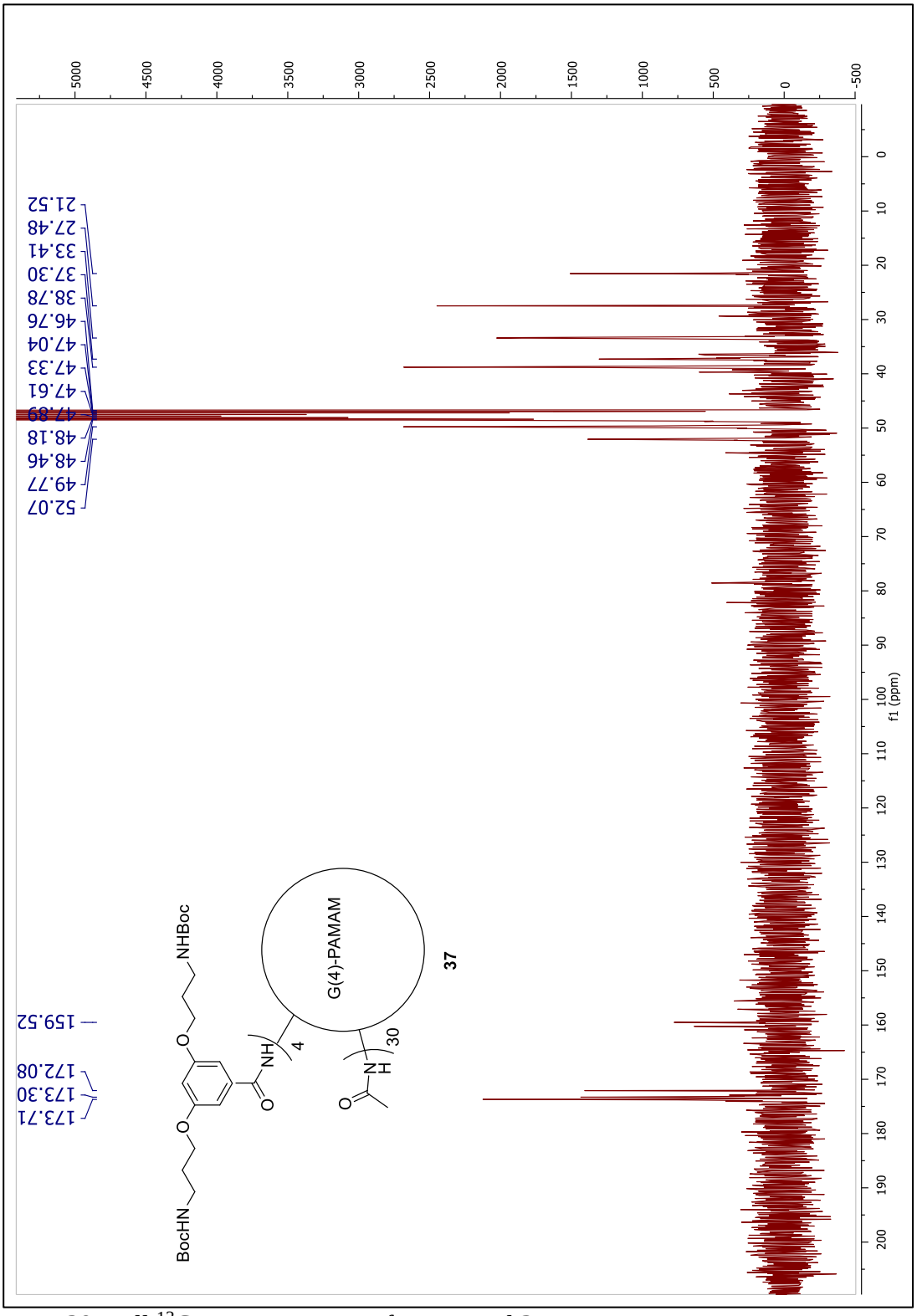


Figure 139. Full ^{13}C NMR spectrum of compound **37**.

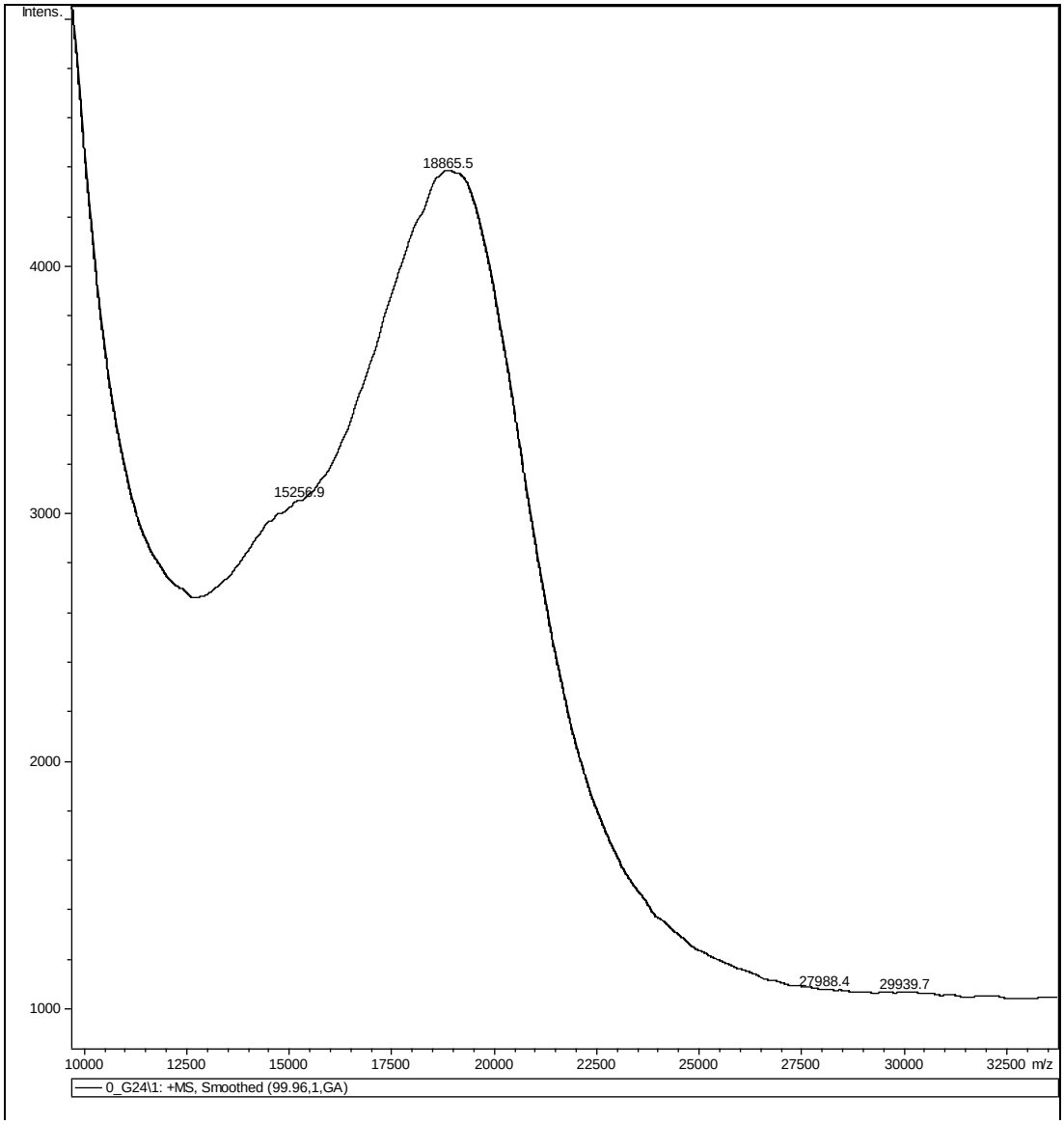


Figure 140. Smoothed MALDI TOF spectrum for compound **37**. M_w = 17200.

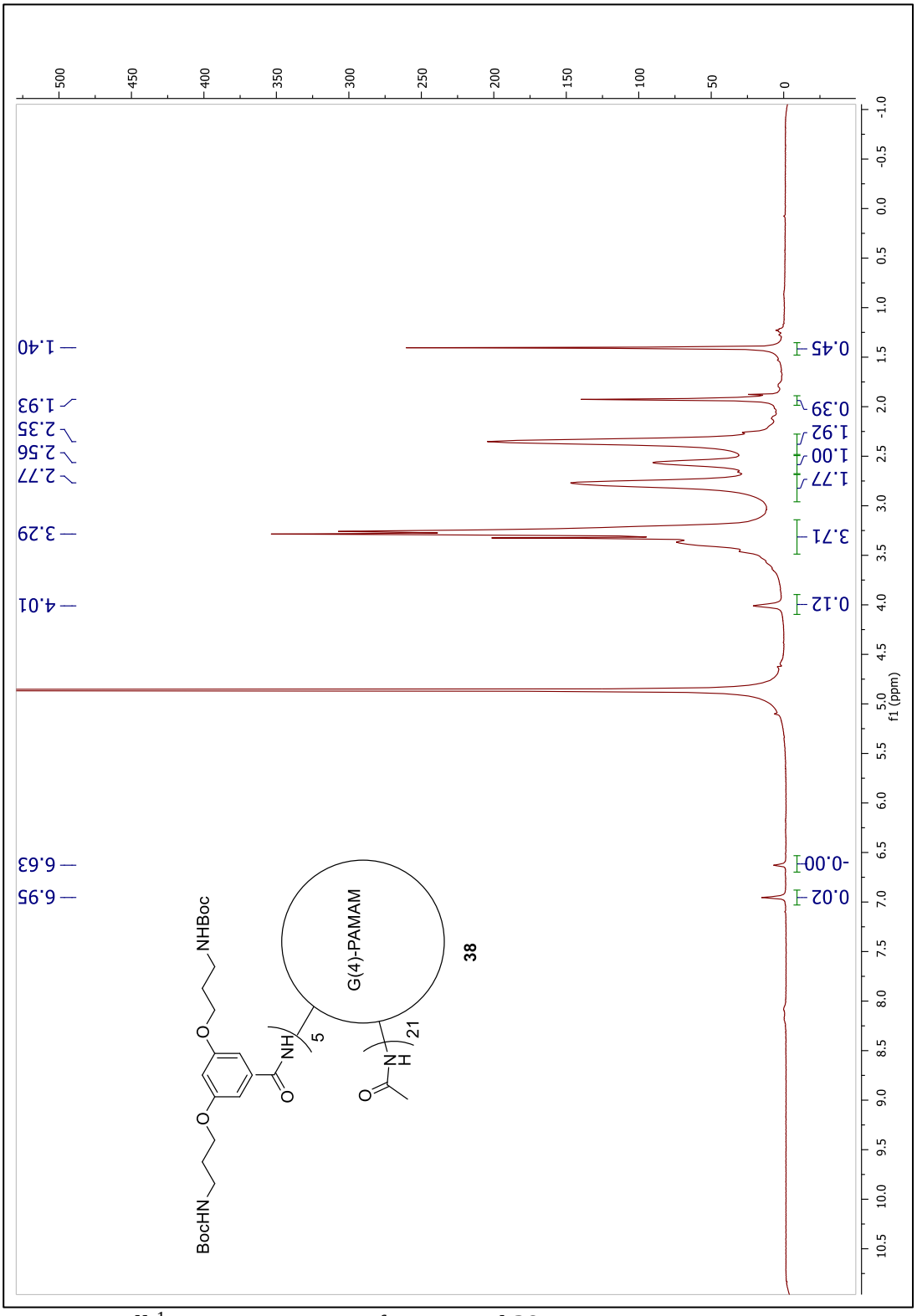


Figure 141. Full ^{1}H NMR spectrum of compound **38**.

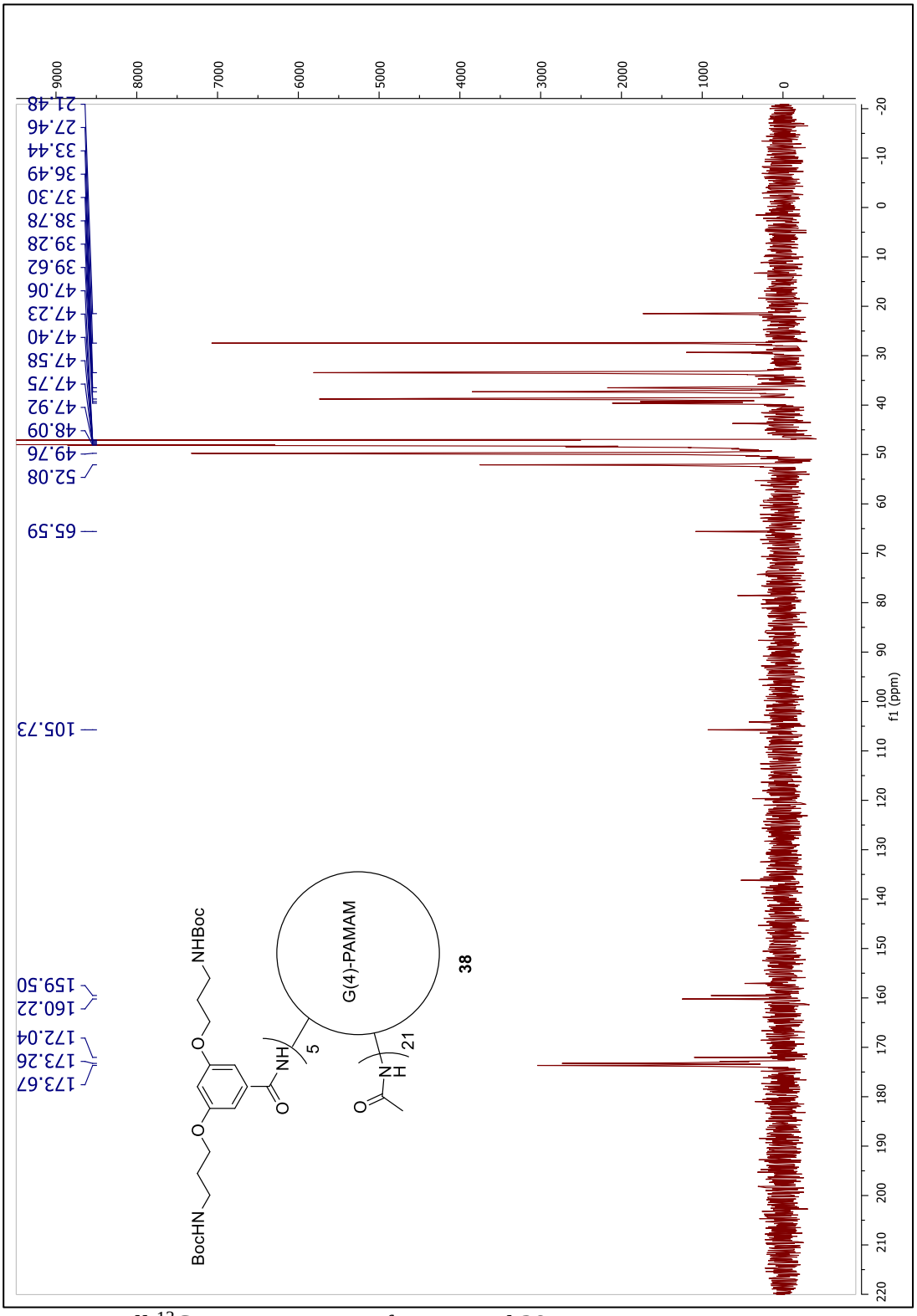


Figure 142. Full ^{13}C NMR spectrum of compound **38**.

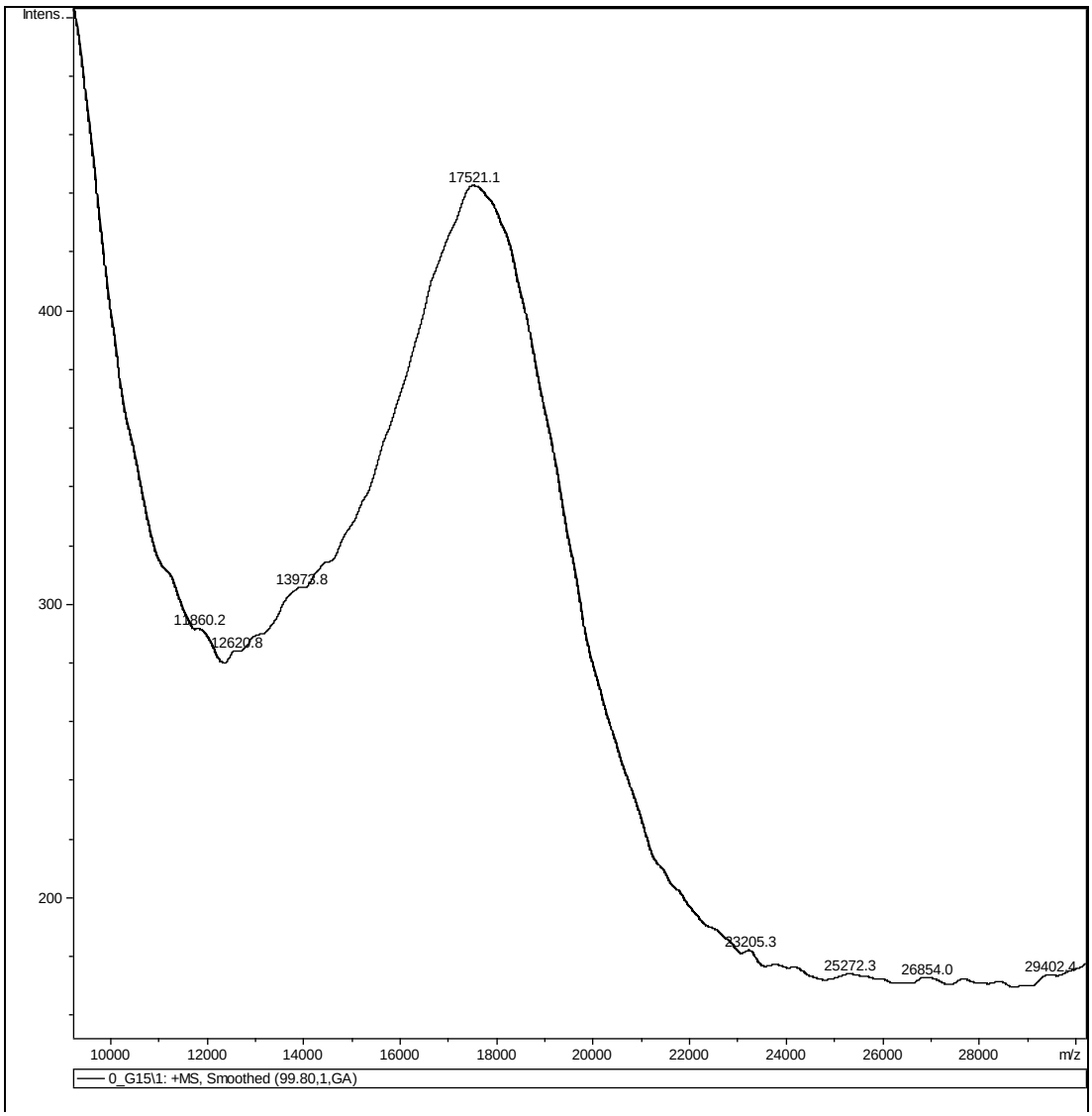


Figure 143. Smoothed MALDI TOF spectrum for compound **38**. M_w = 16600.

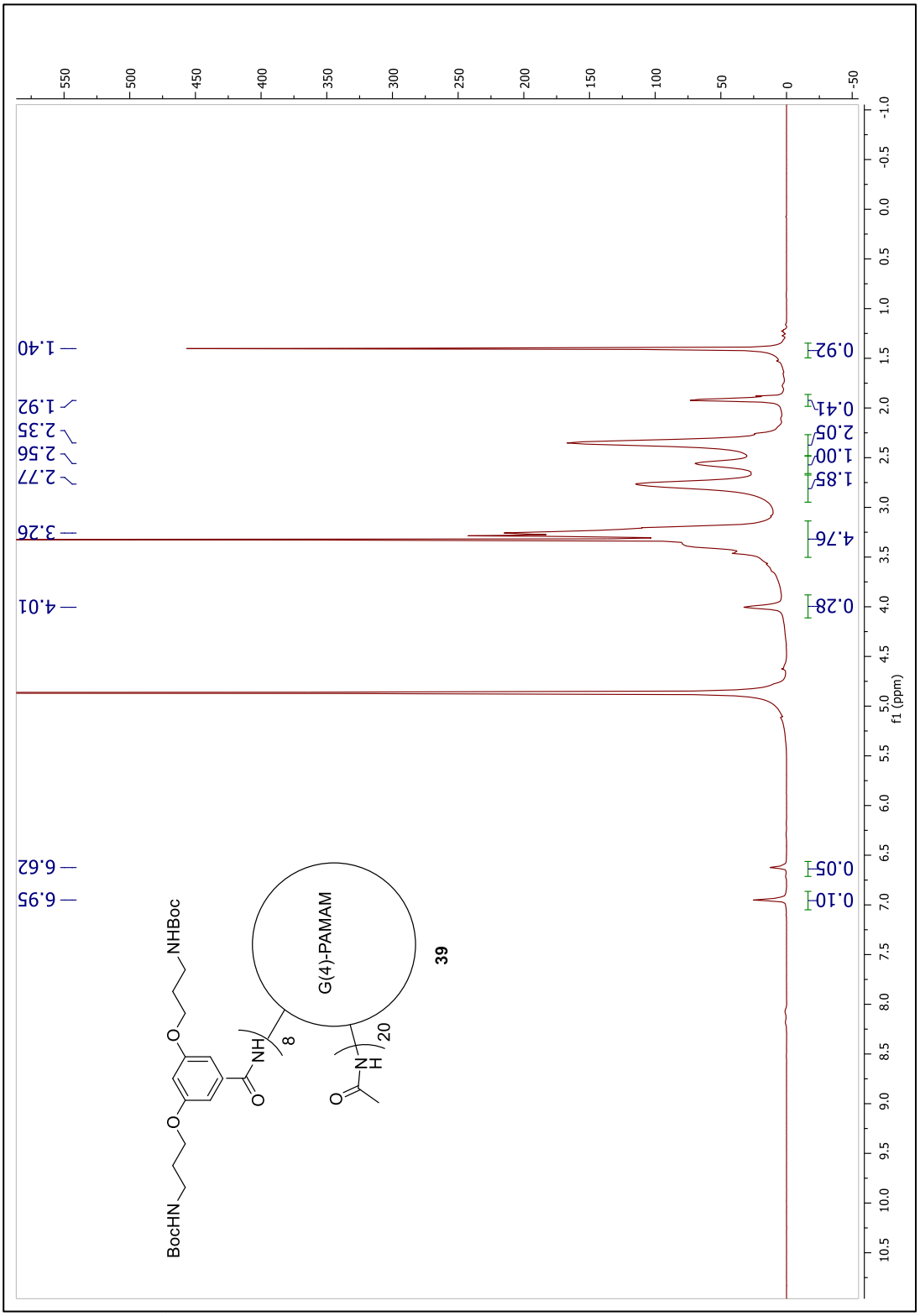


Figure 144. Full ^{1}H NMR spectrum of compound **39**.

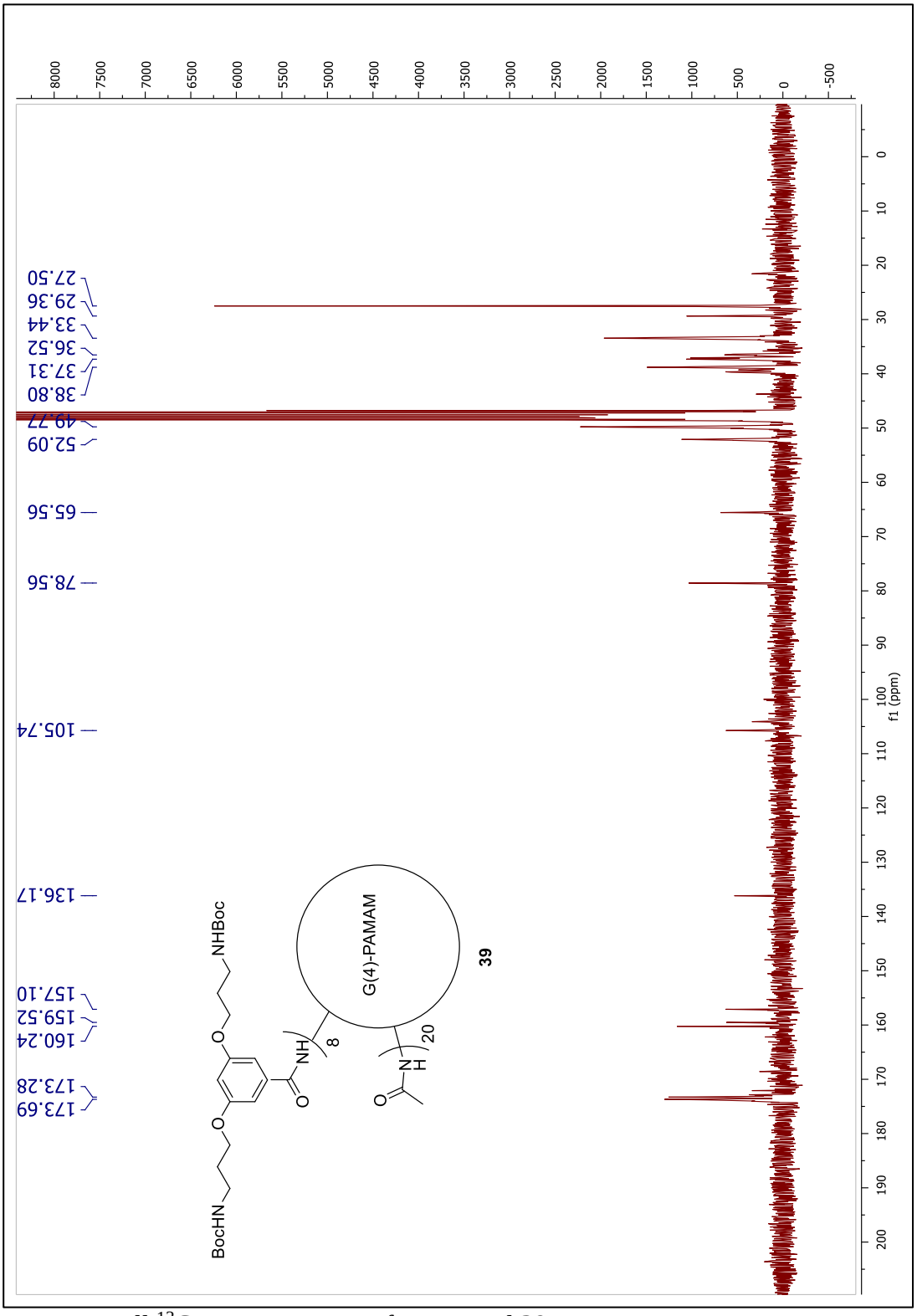


Figure 145. Full ^{13}C NMR spectrum of compound **39**.

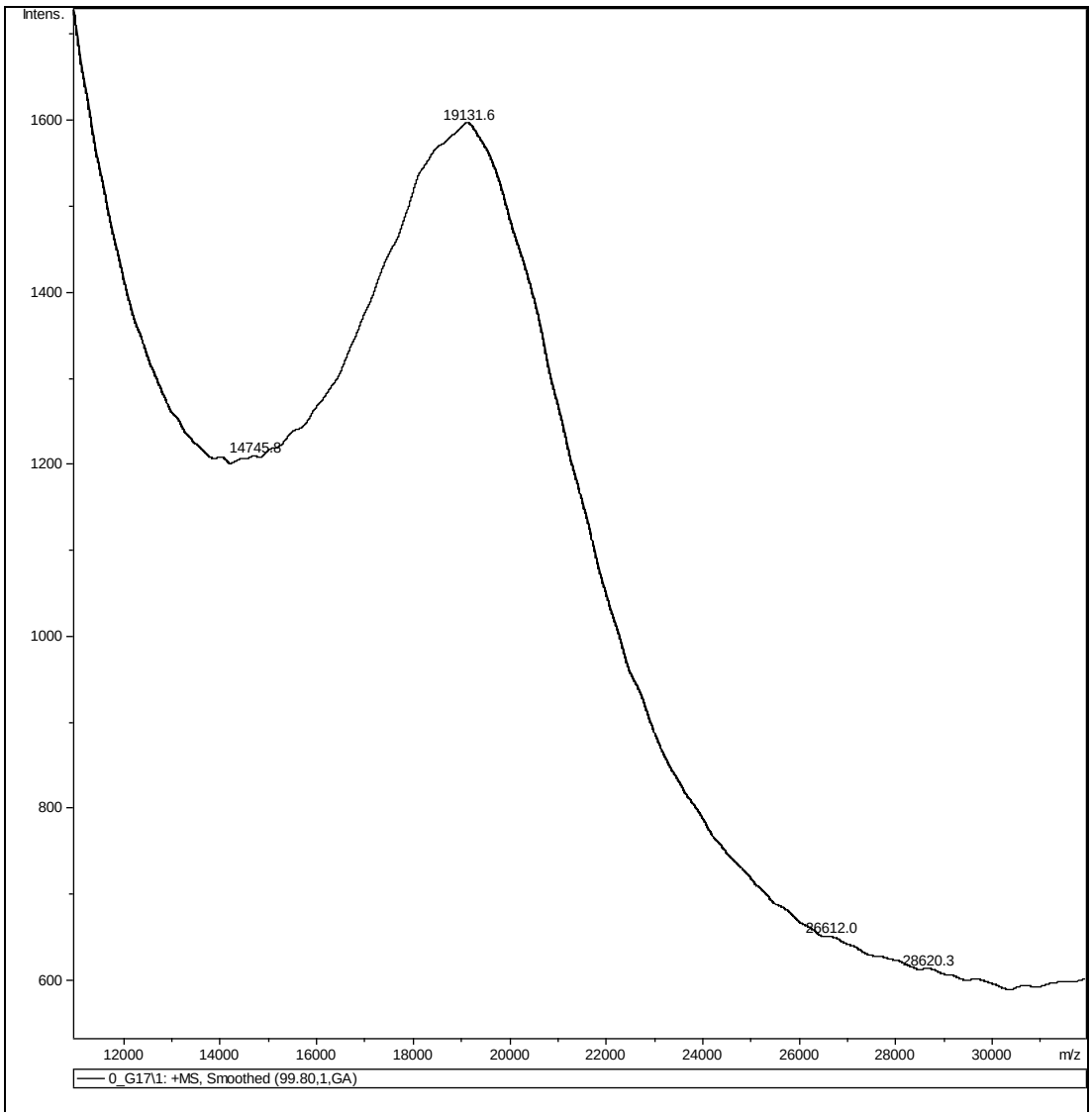


Figure 146. Smoothed MALDI TOF spectrum for compound **39**. M_w = 17800.

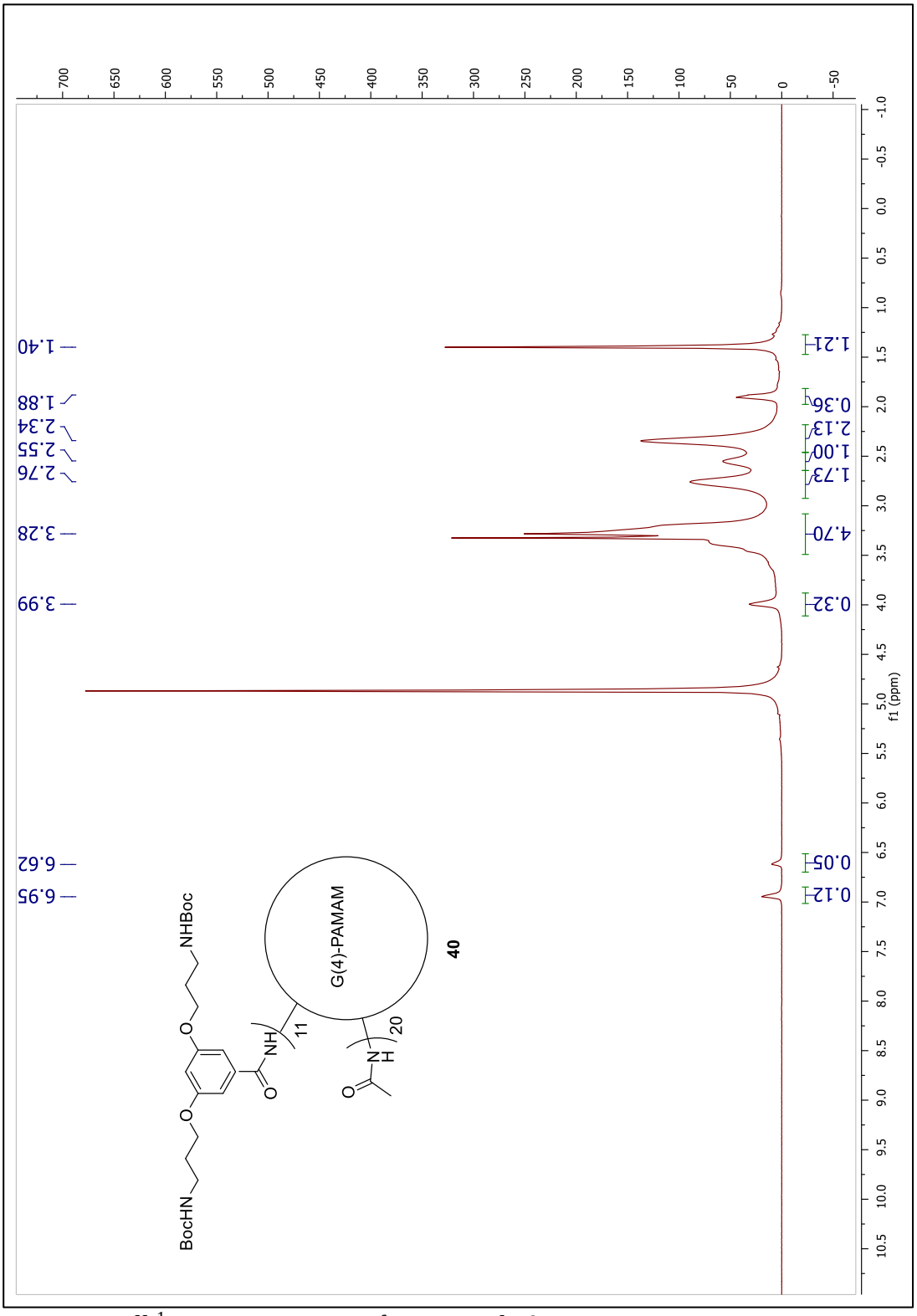


Figure 147. Full ^{1}H NMR spectrum of compound **40**.

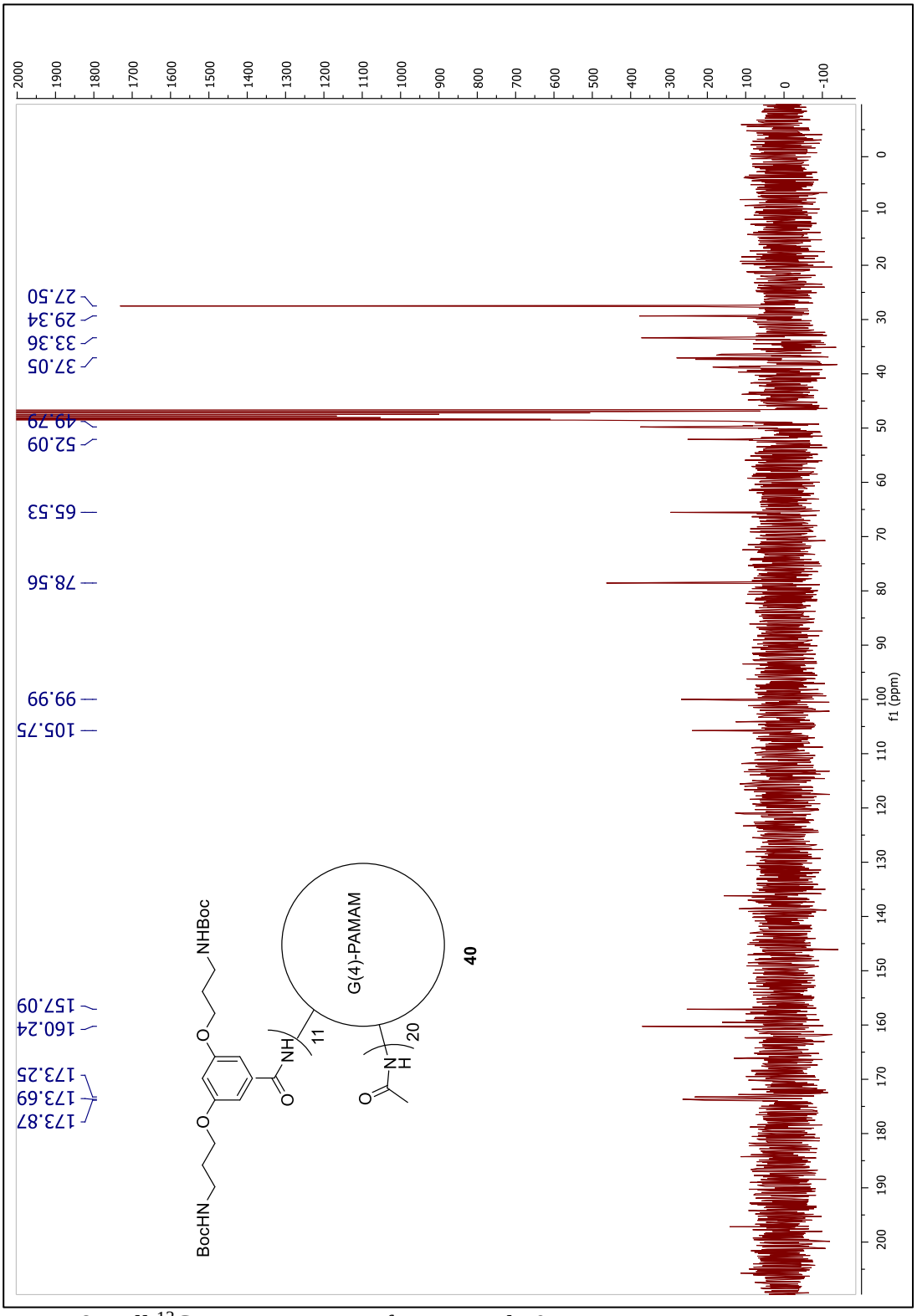


Figure 148. Full ^{13}C NMR spectrum of compound **40**.

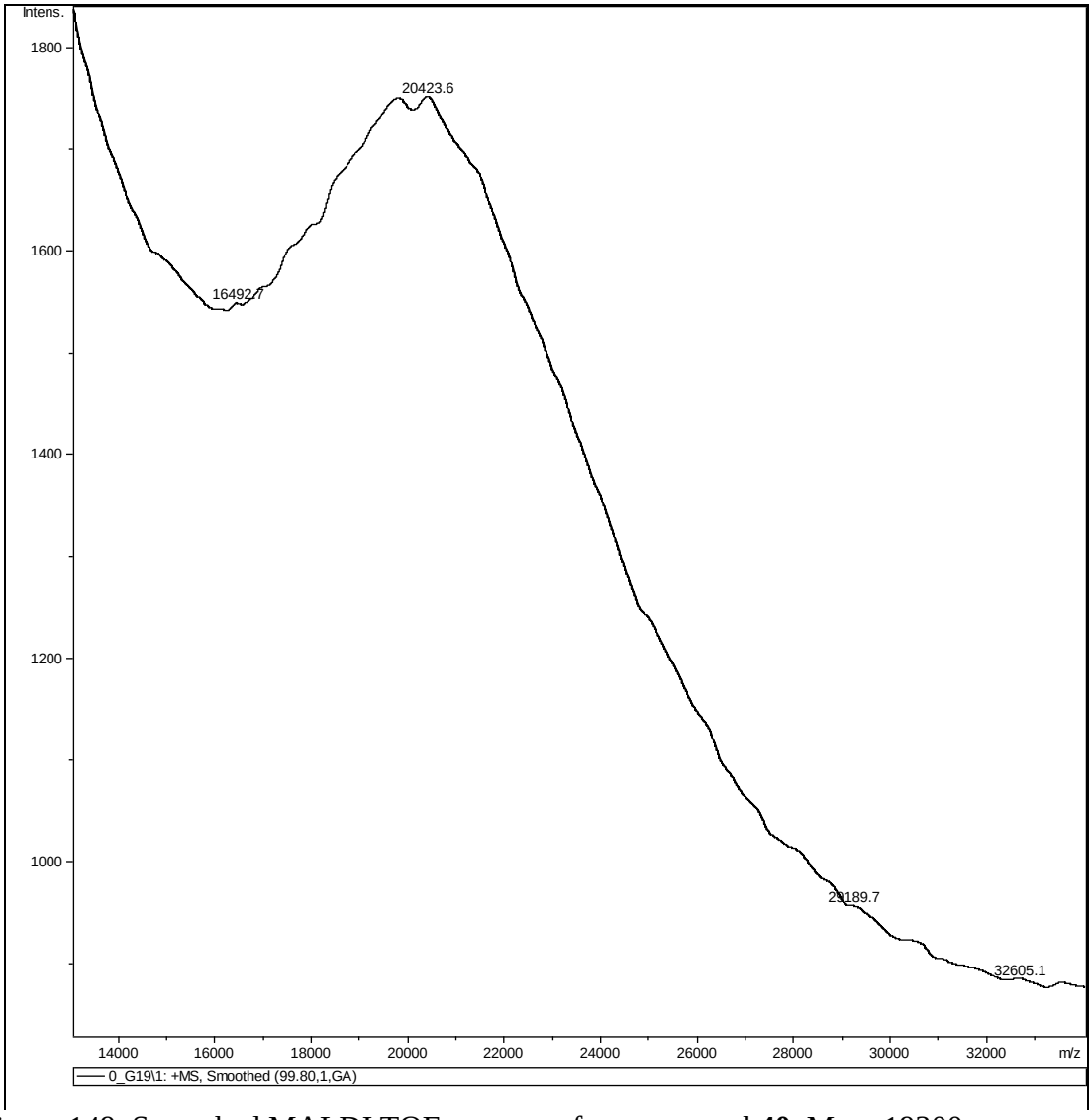


Figure 149. Smoothed MALDI TOF spectrum for compound **40**. M_w = 19300.

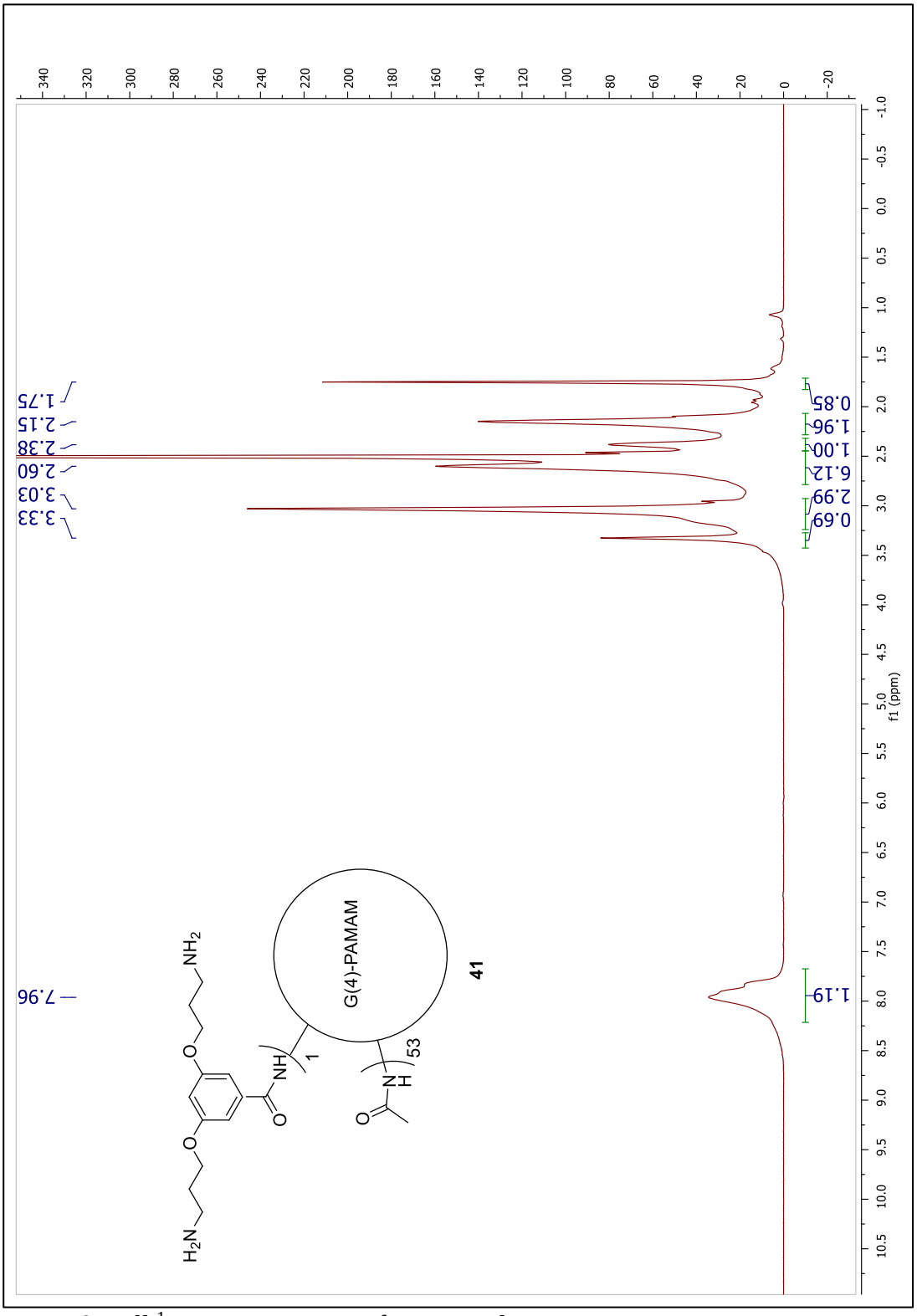


Figure 150. Full ^{1}H NMR spectrum of compound **41**.

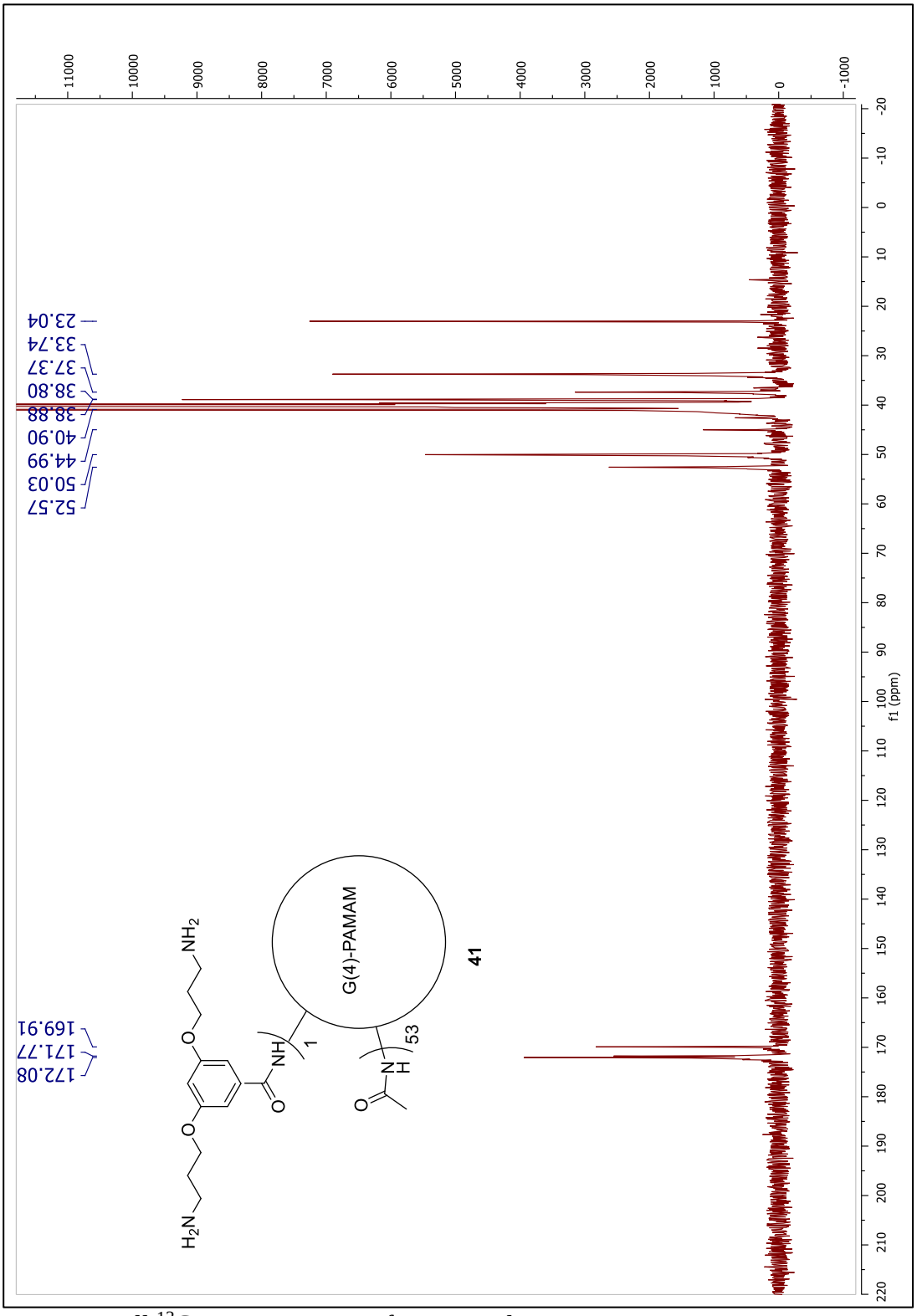


Figure 151. Full ^{13}C NMR spectrum of compound **41**.

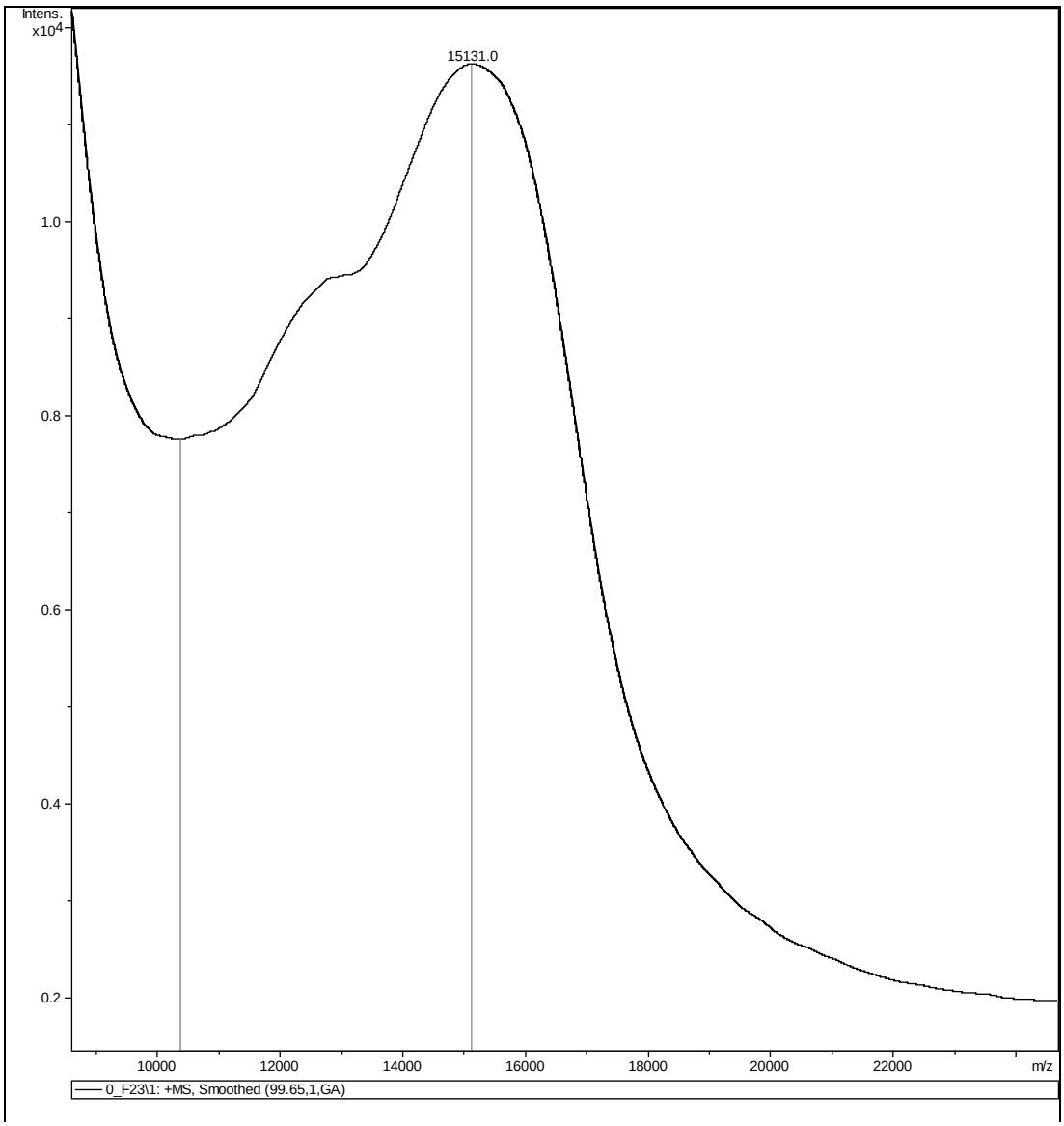


Figure 152. Smoothed MALDI TOF spectrum for compound **41**. M_w = 14900.

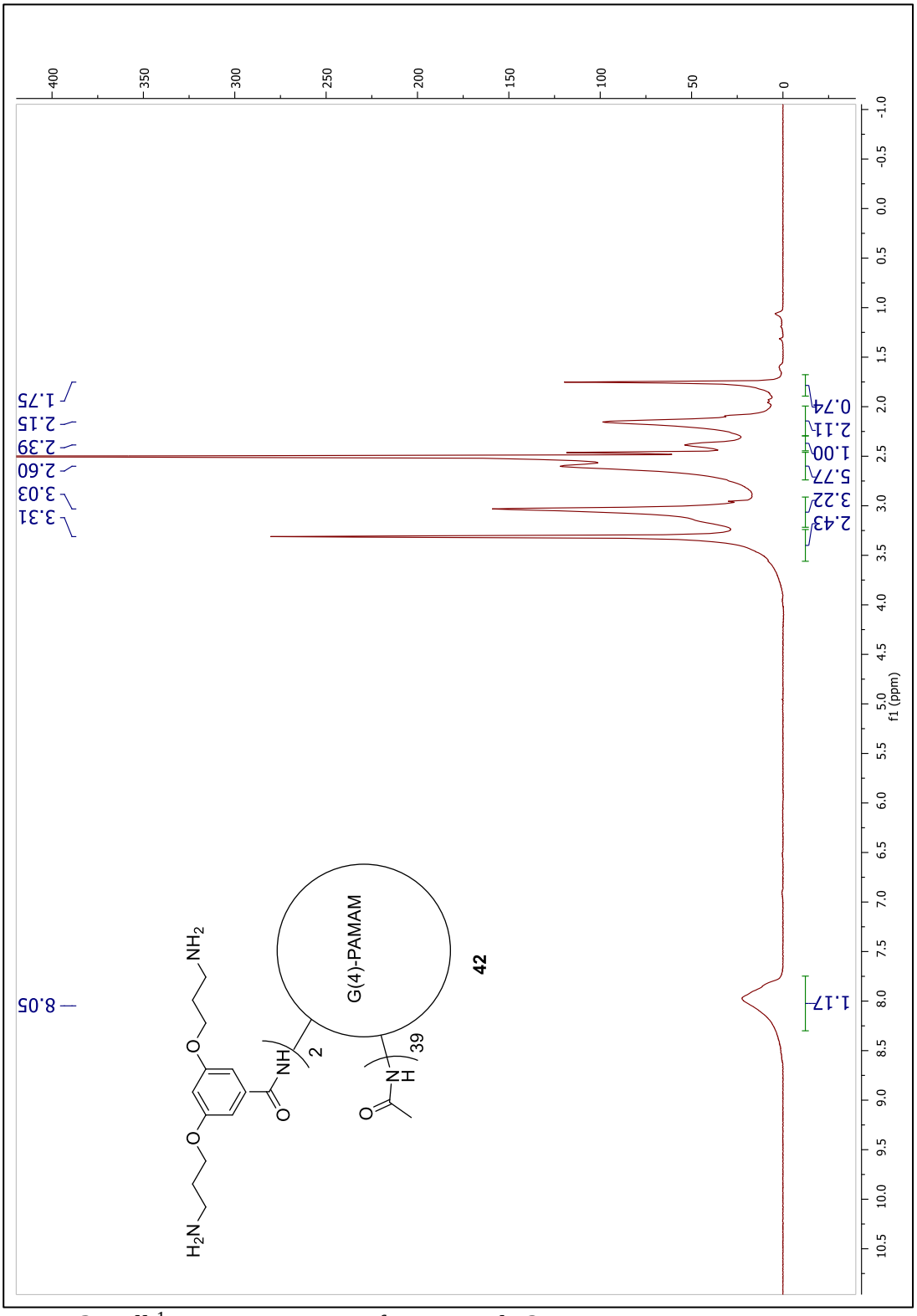


Figure 153. Full ^{1}H NMR spectrum of compound **42**.

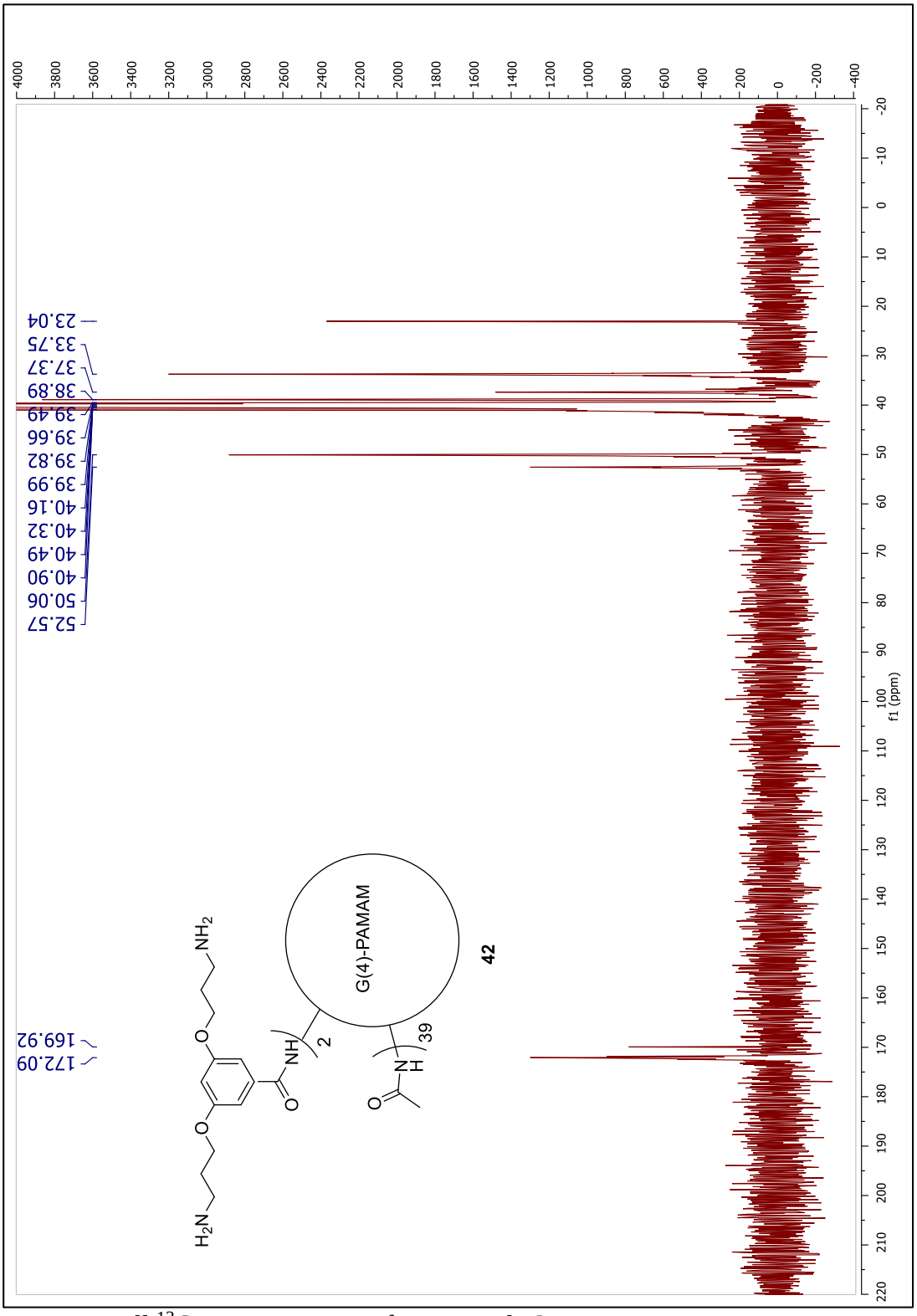


Figure 154. Full ^{13}C NMR spectrum of compound **42**.

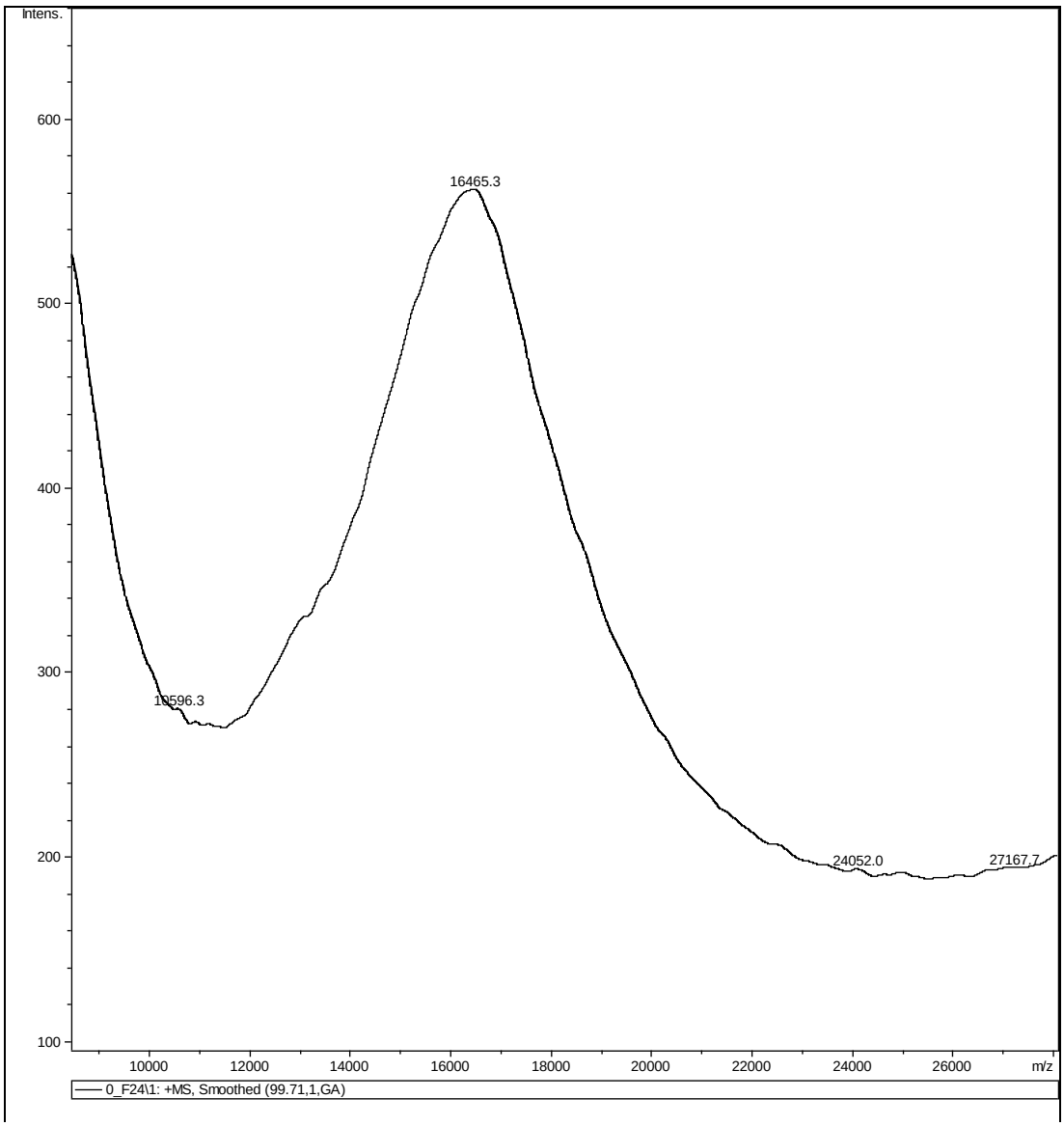


Figure 155. Smoothed MALDI TOF spectrum for compound **42**. M_w = 16100.

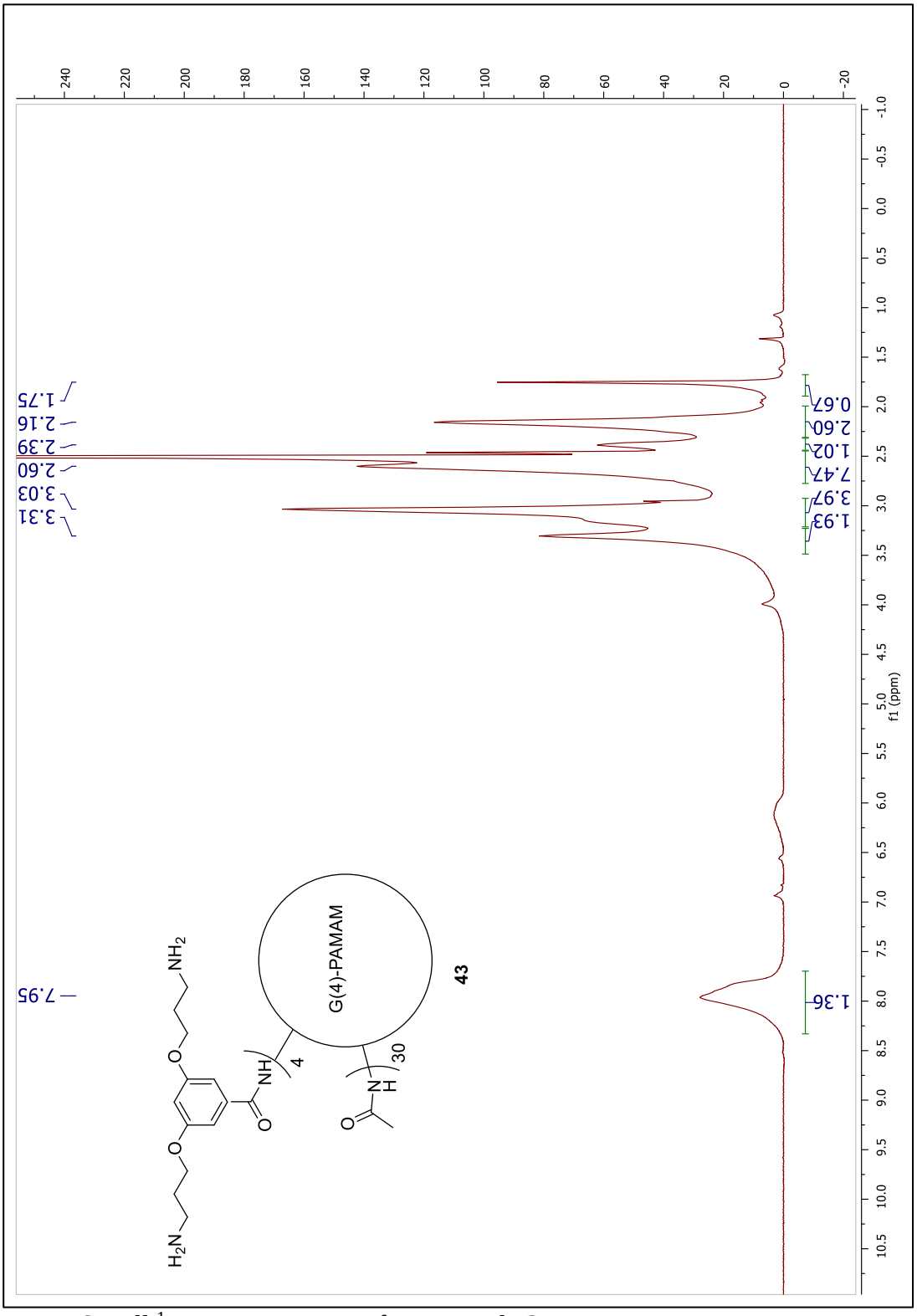


Figure 156. Full ^{1}H NMR spectrum of compound **43**.

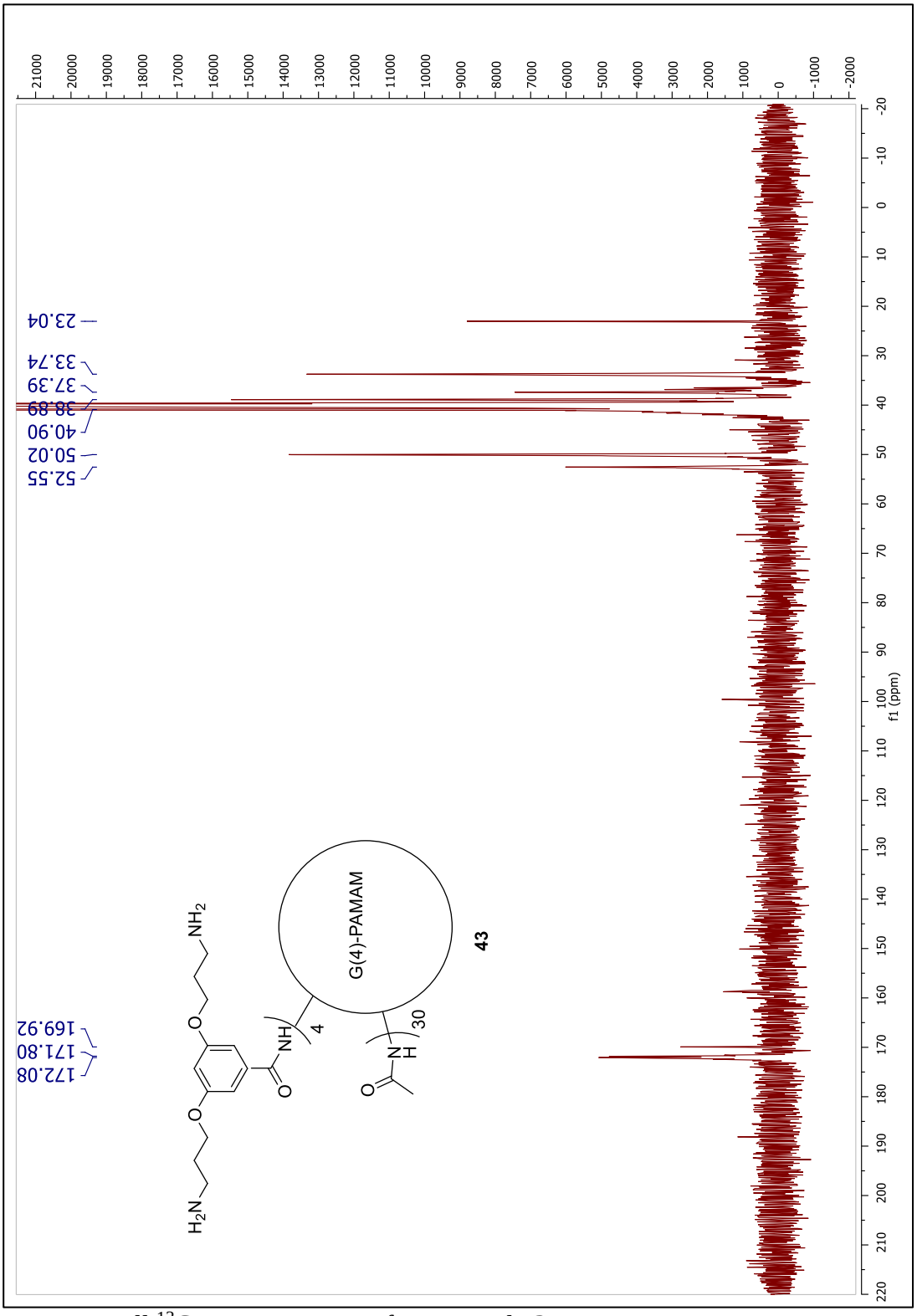


Figure 157. Full ^{13}C NMR spectrum of compound **43**.

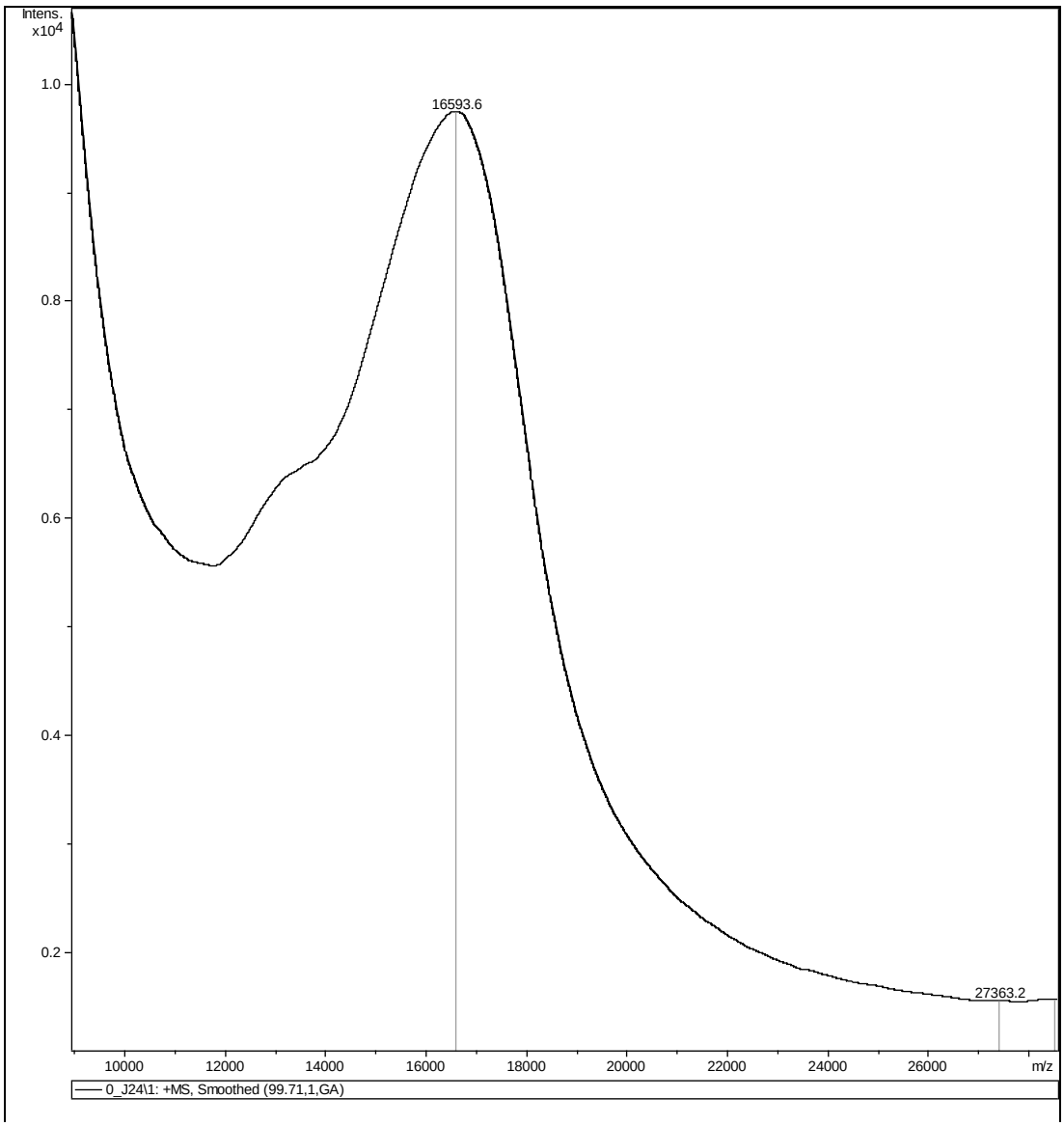


Figure 158. Smoothed MALDI TOF spectrum for compound **43**. M_w = 16000.

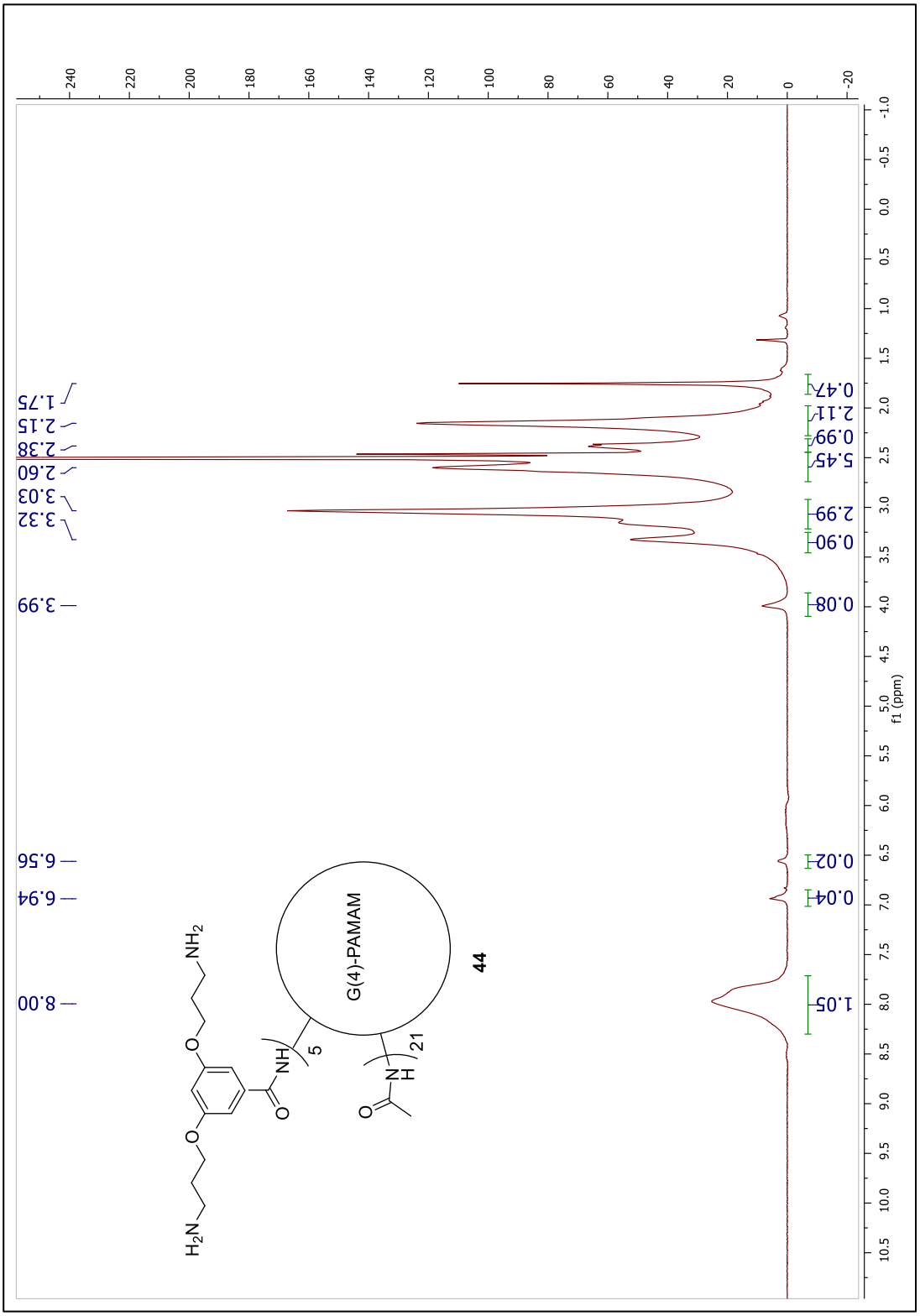


Figure 159. Full ^{1}H NMR spectrum of compound **44**.

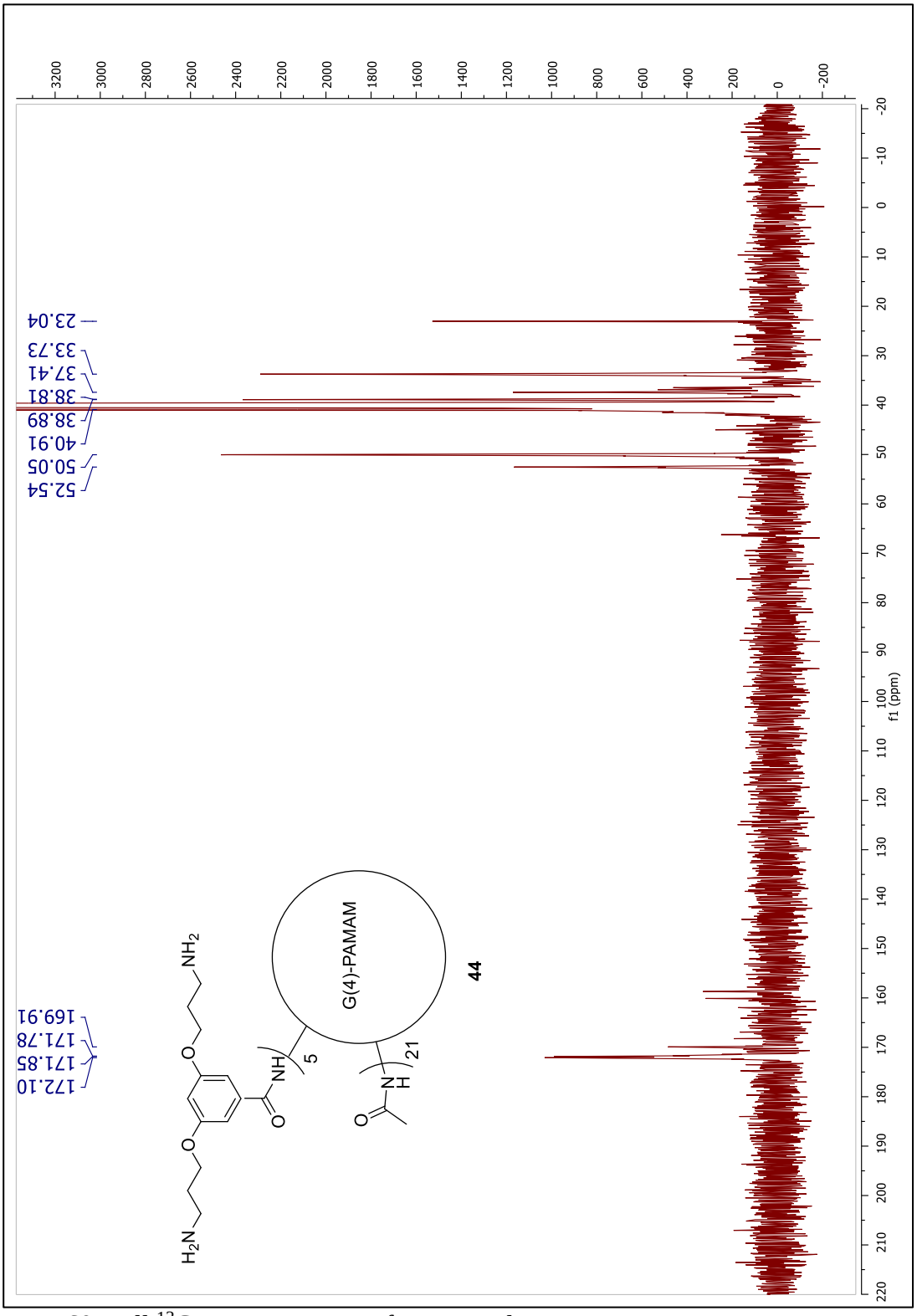


Figure 160. Full ^{13}C NMR spectrum of compound **44**.

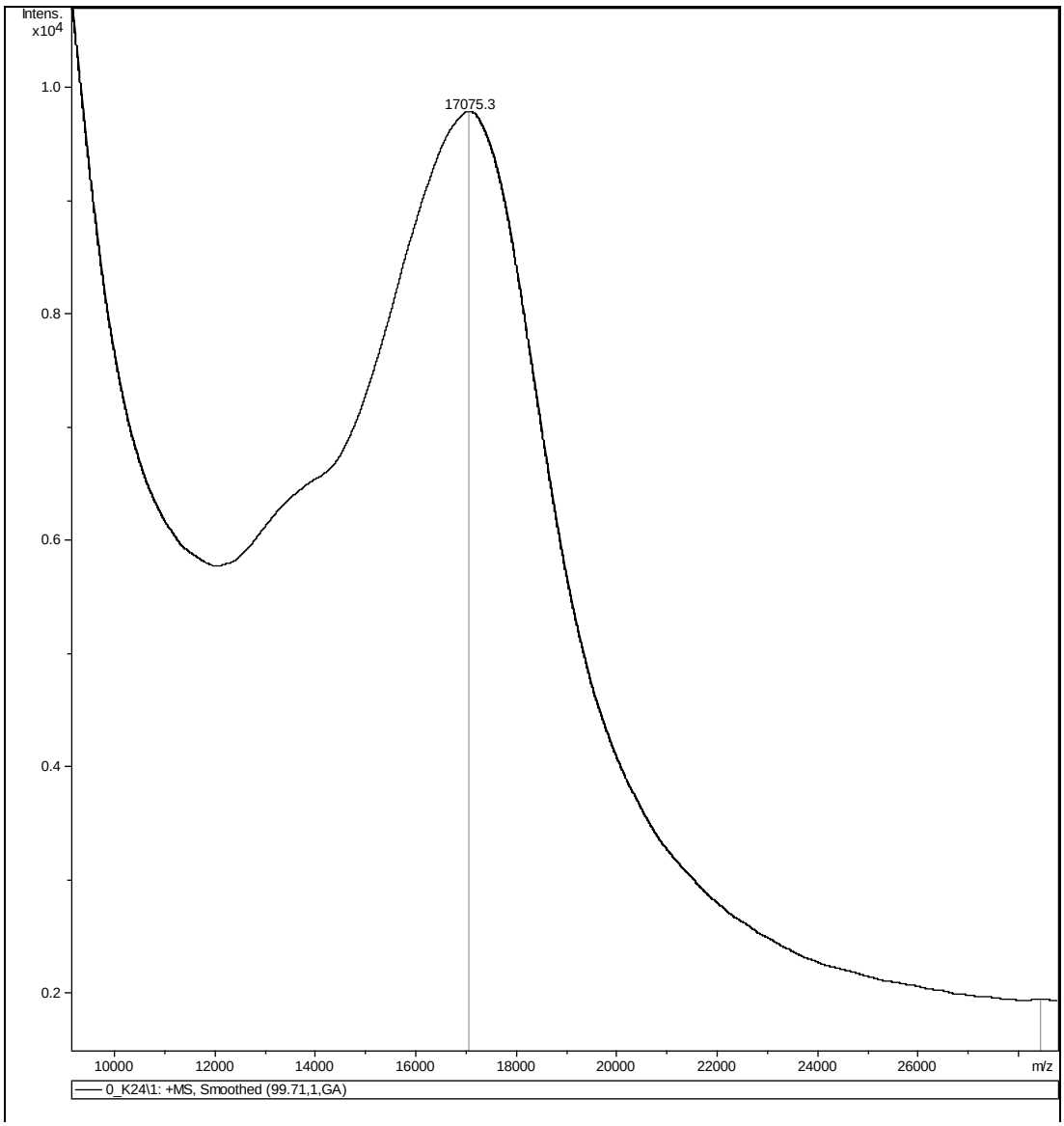


Figure 161. Smoothed MALDI TOF spectrum for compound **44**. M_w = 16500.

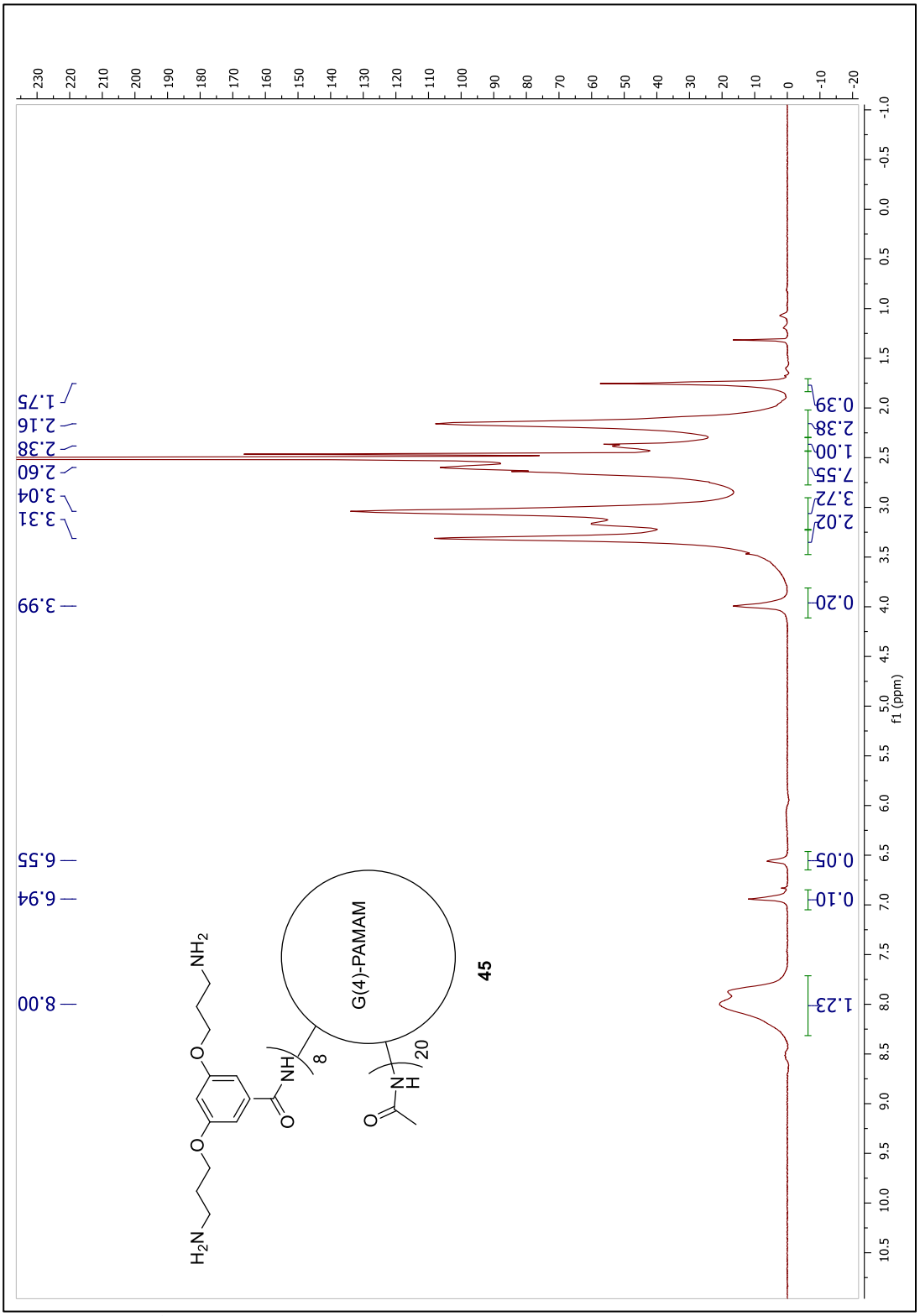


Figure 162. Full ^{1}H NMR spectrum of compound **45**.

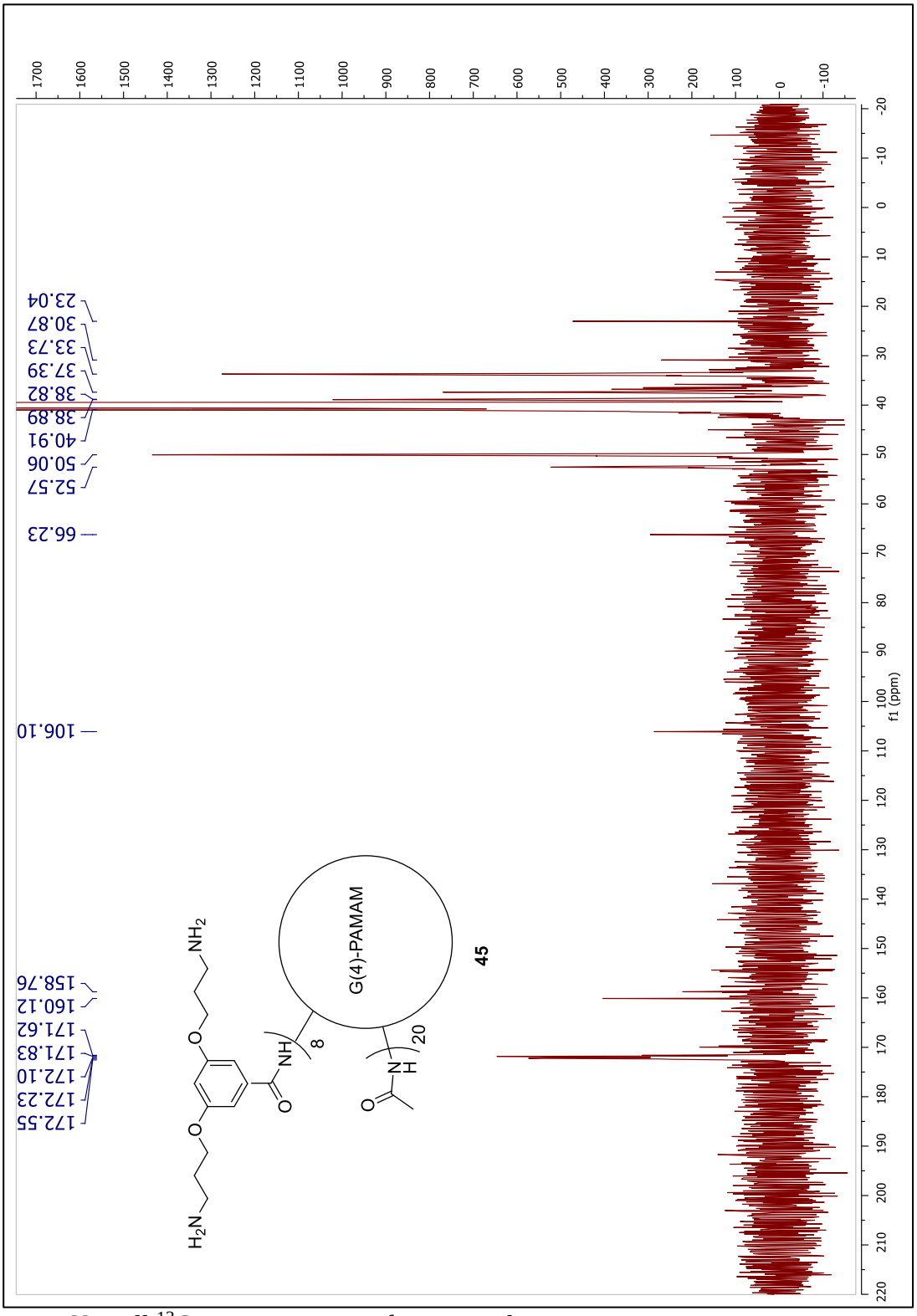


Figure 163. Full ^{13}C NMR spectrum of compound **45**.

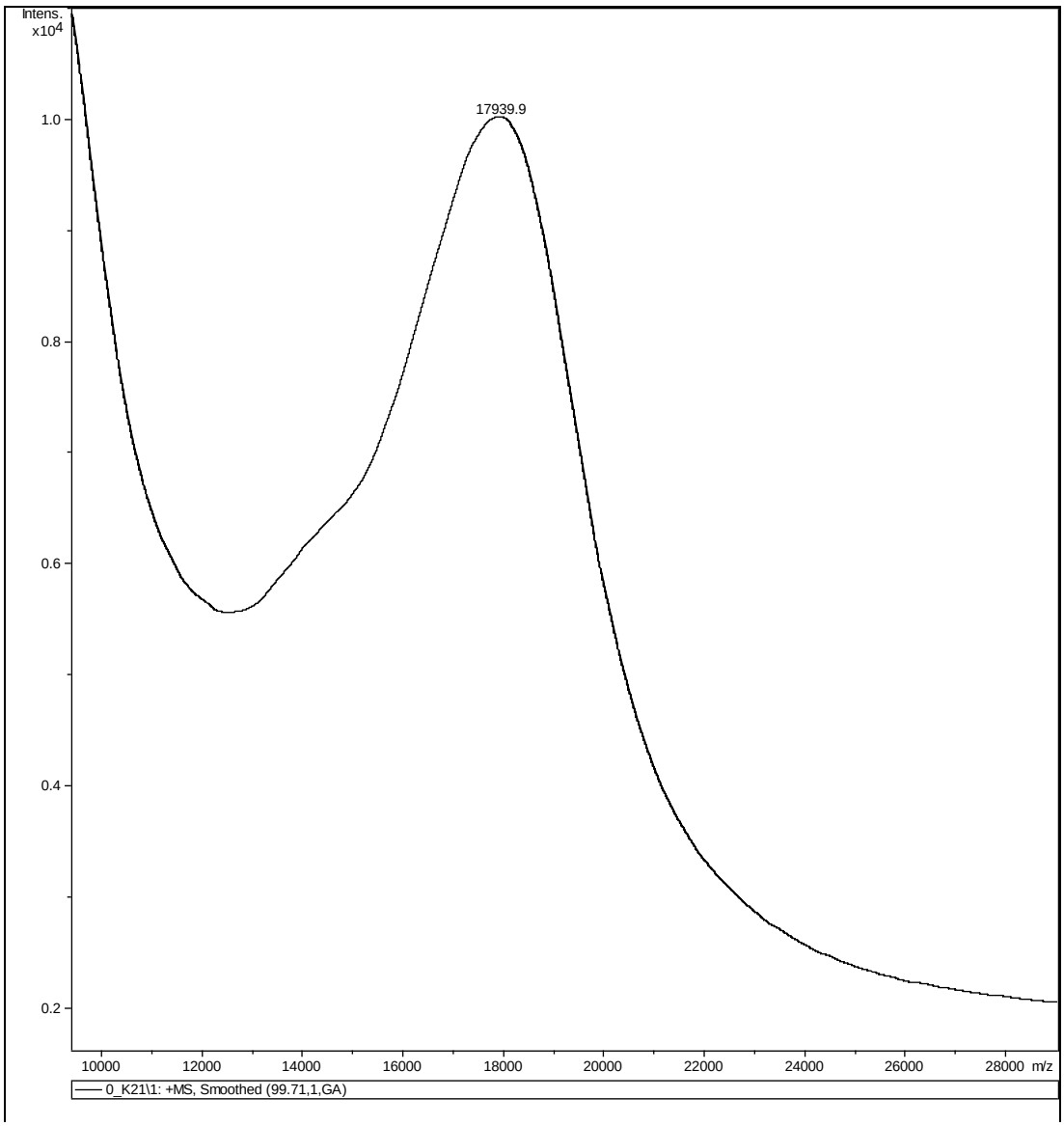


Figure 164. Smoothed MALDI TOF spectrum for compound **45**. M_w = 17300.

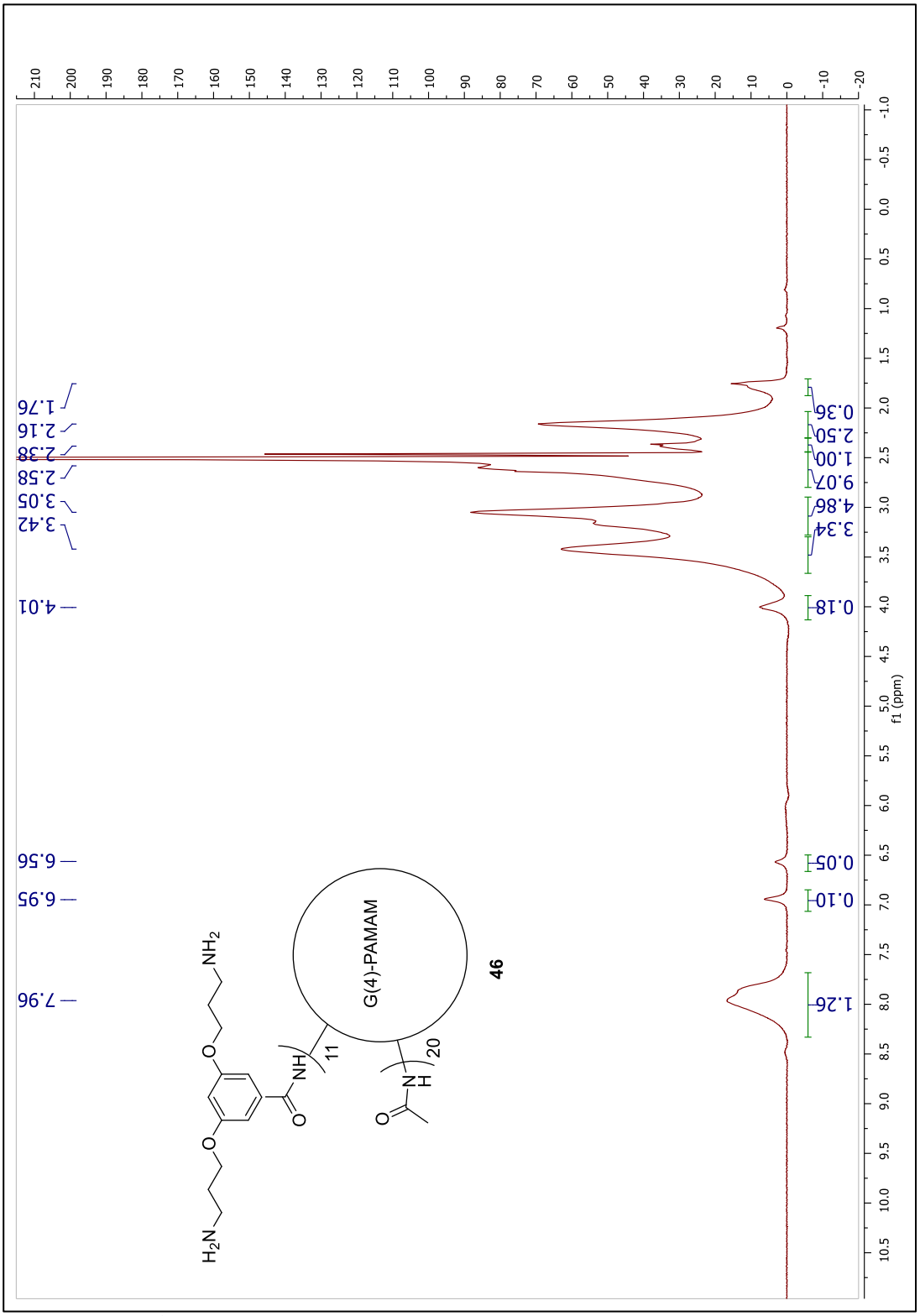


Figure 165. Full ^{1}H NMR spectrum of compound **46**.

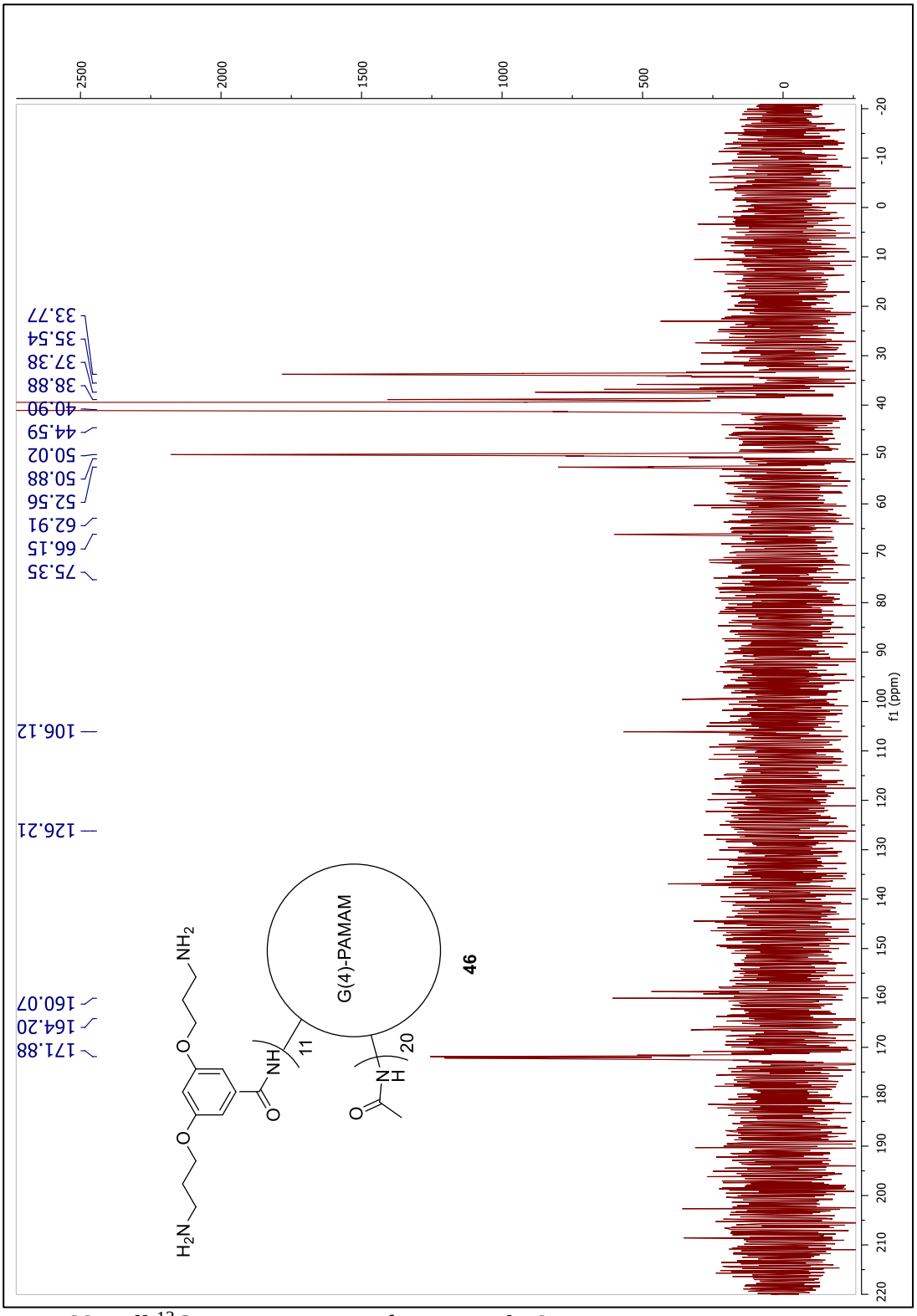


Figure 166. Full ^{13}C NMR spectrum of compound **46**.

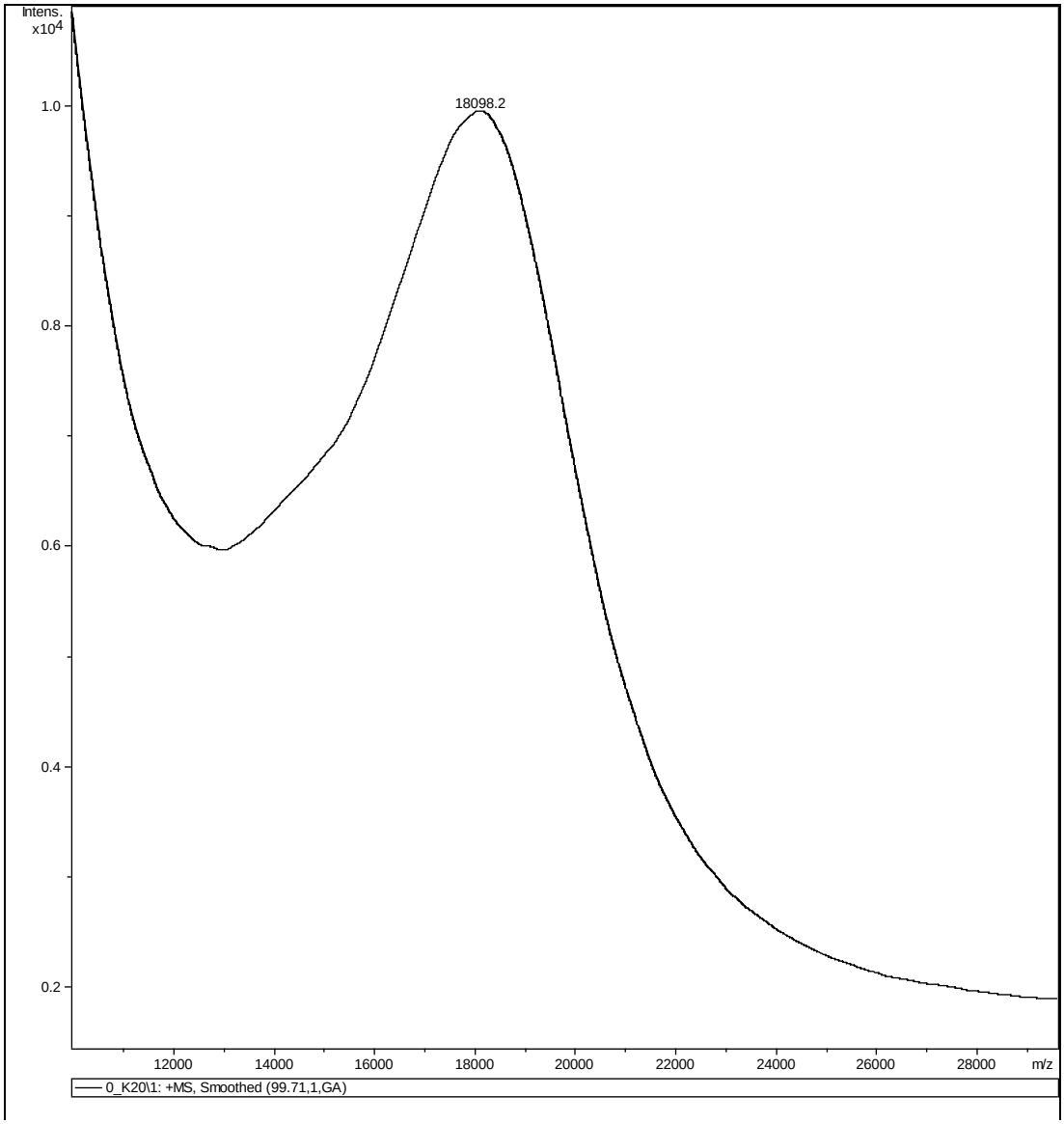


Figure 167. Smoothed MALDI TOF spectrum for compound **46**. M_w = 17600.

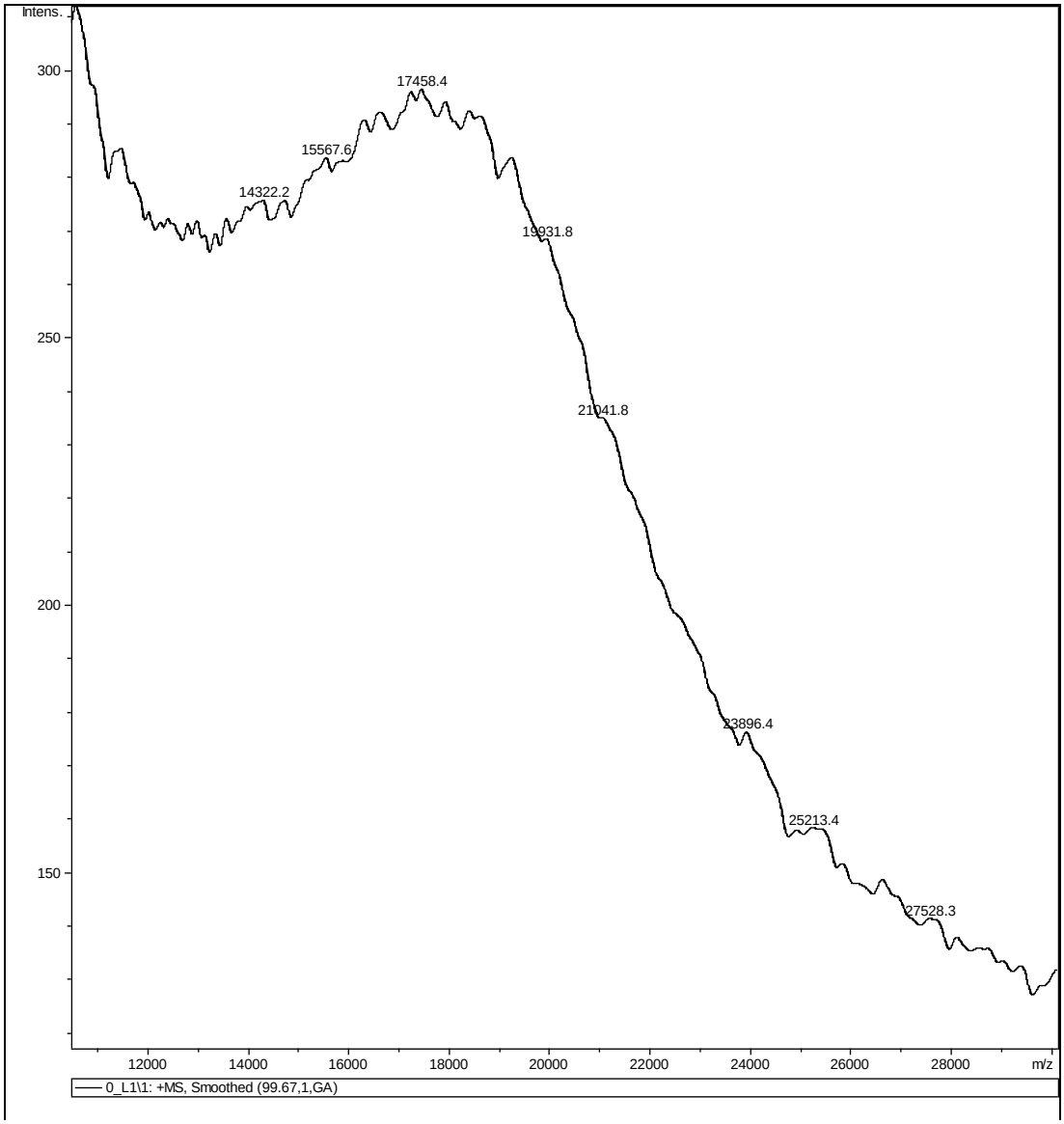


Figure 168. Smoothed MALDI TOF spectrum for compound **47**. M_w = 16600.

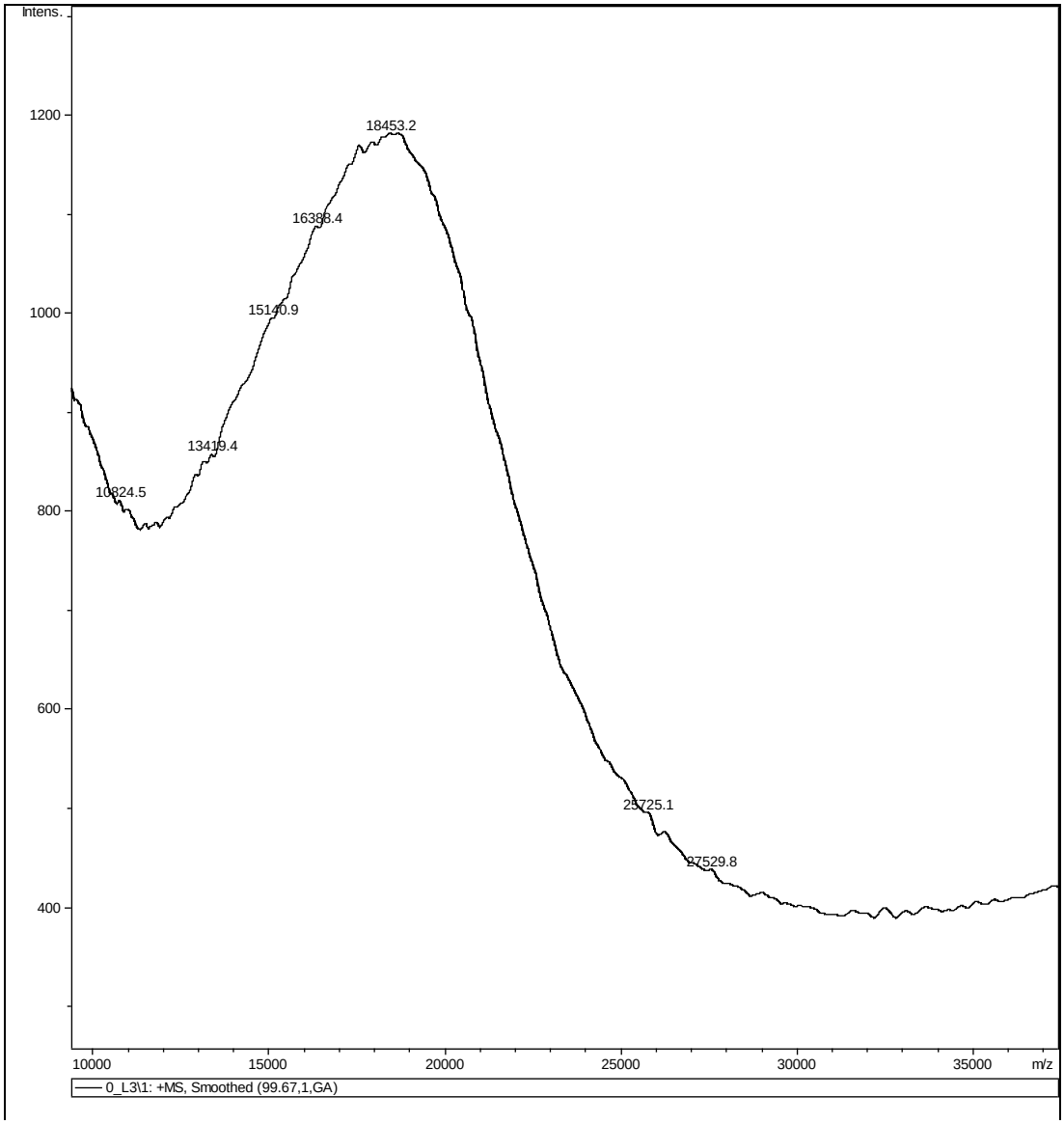


Figure 169. Smoothed MALDI TOF spectrum for compound **48**. M_w = 16900.

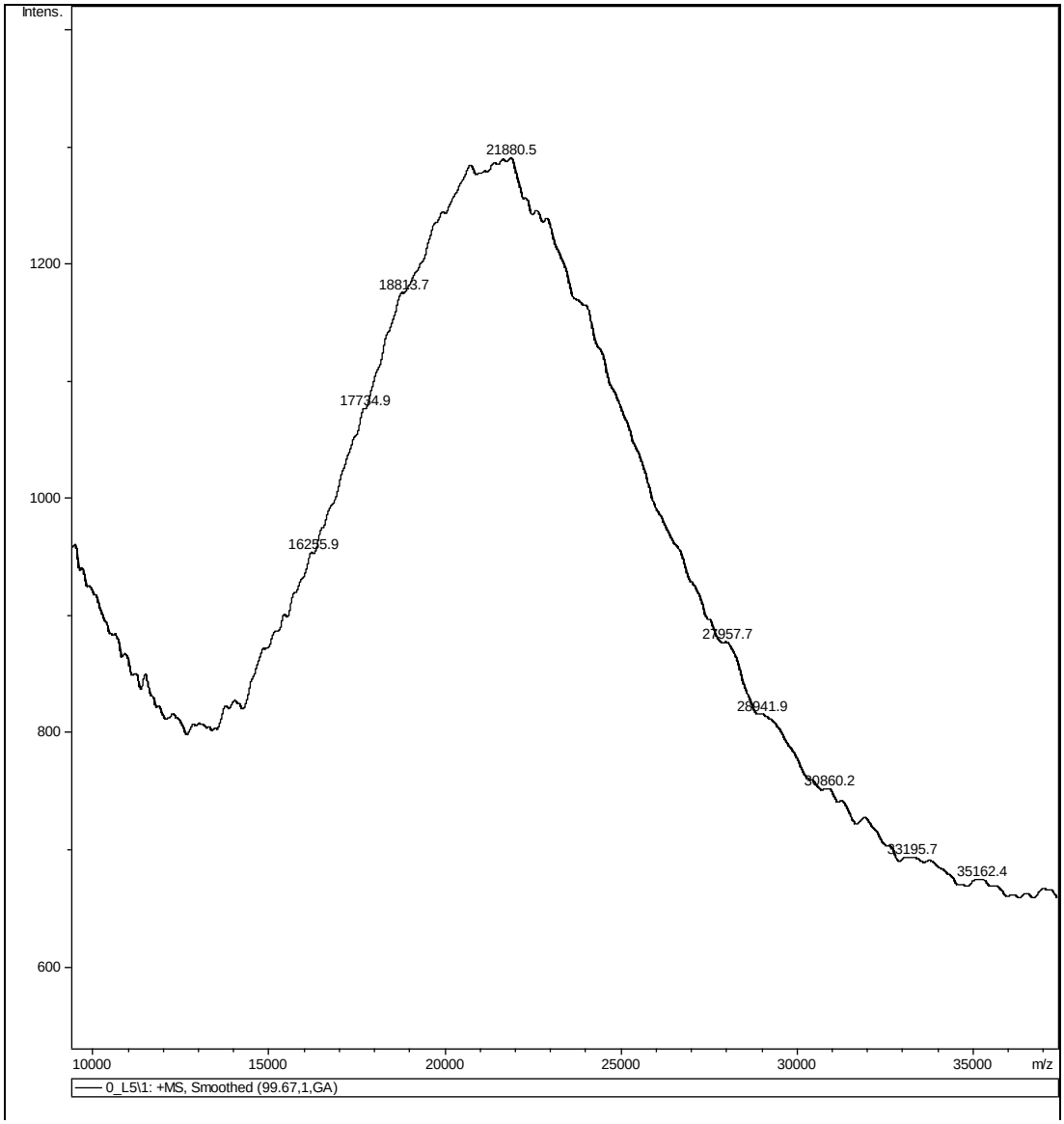


Figure 170. Smoothed MALDI TOF spectrum for compound **49**. M_w = 21300.

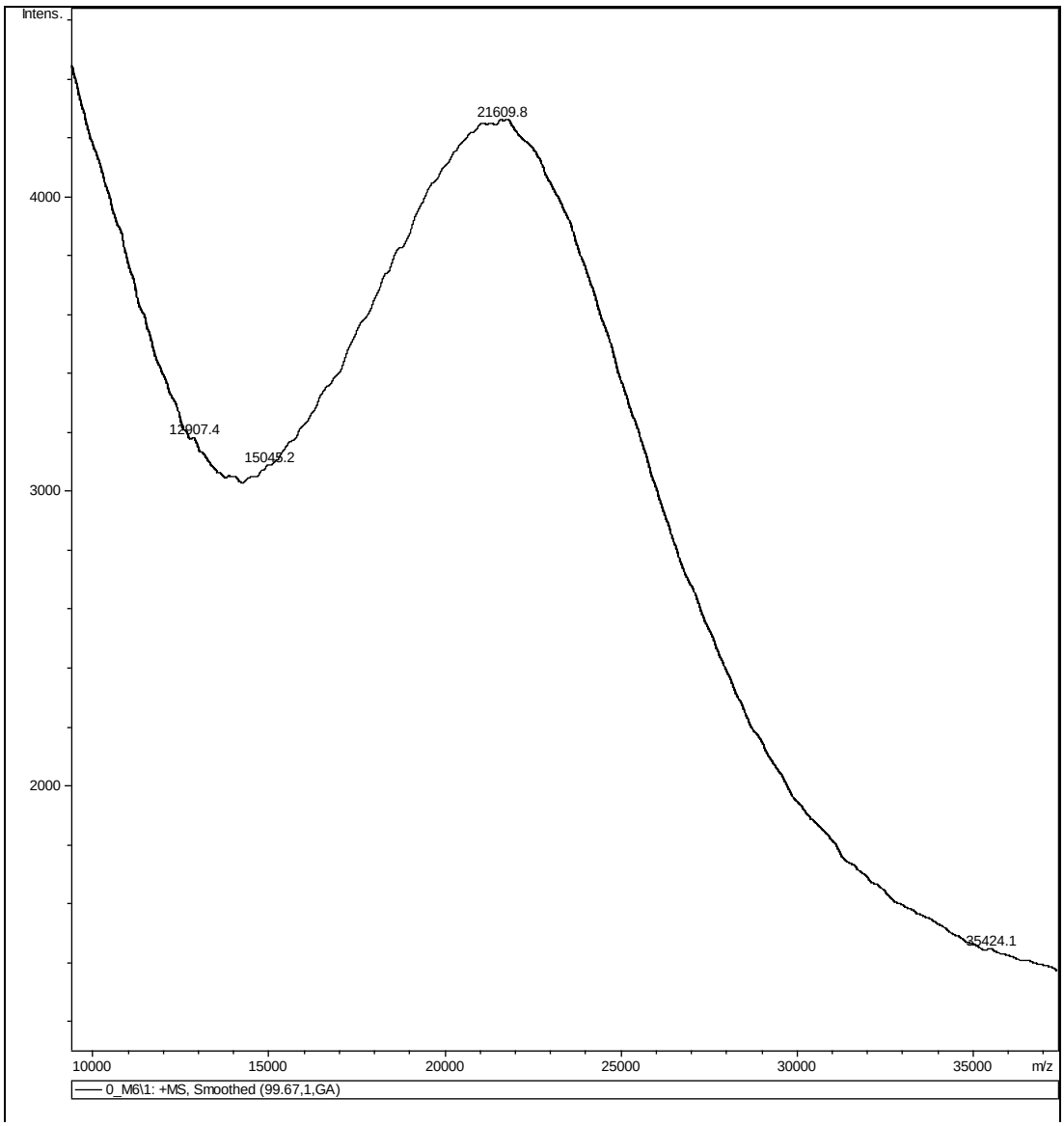


Figure 171. Smoothed MALDI TOF spectrum for compound **50**. M_w = 20800.

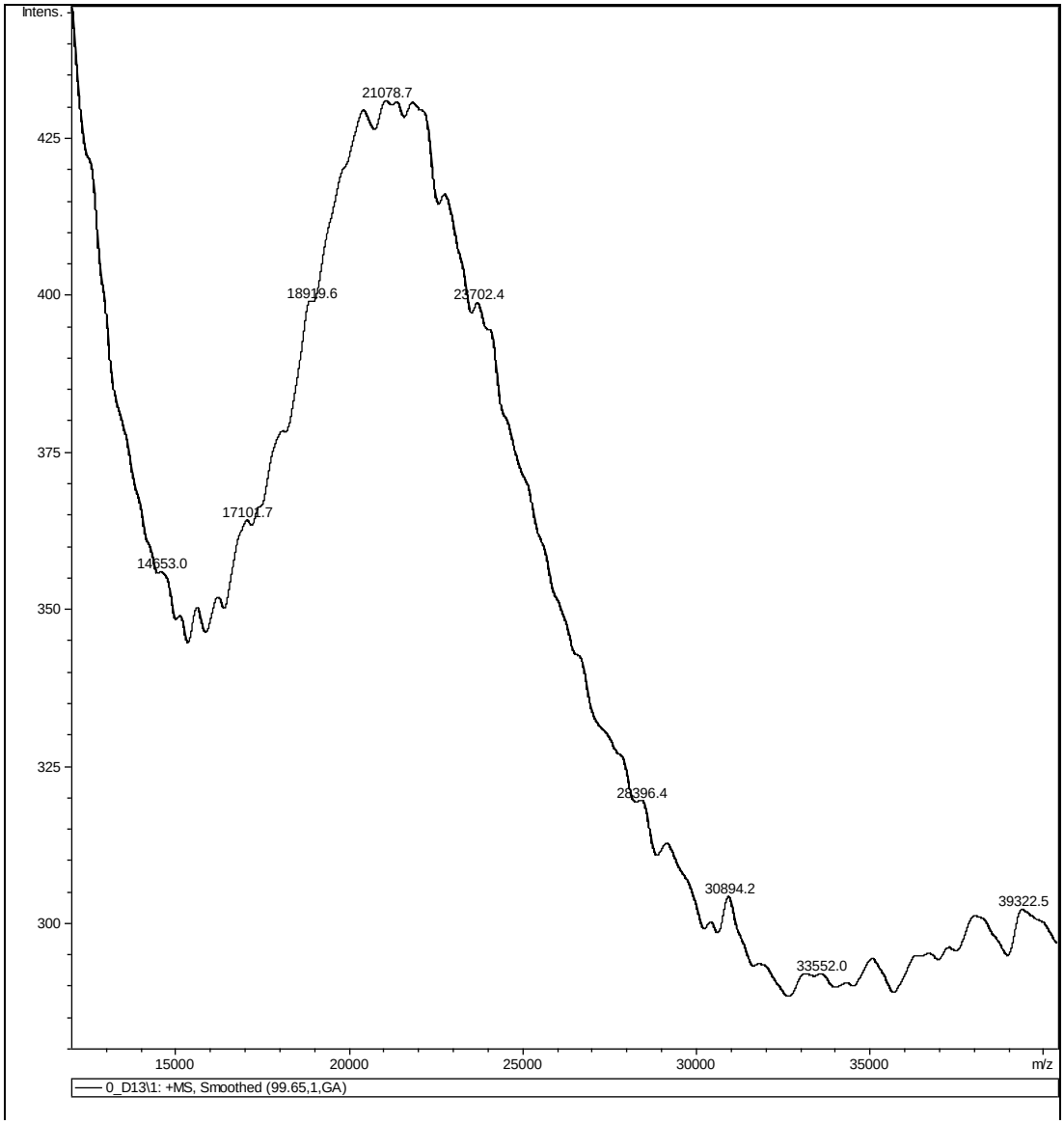


Figure 172. Smoothed MALDI TOF spectrum for compound **51**. M_w = 20800.

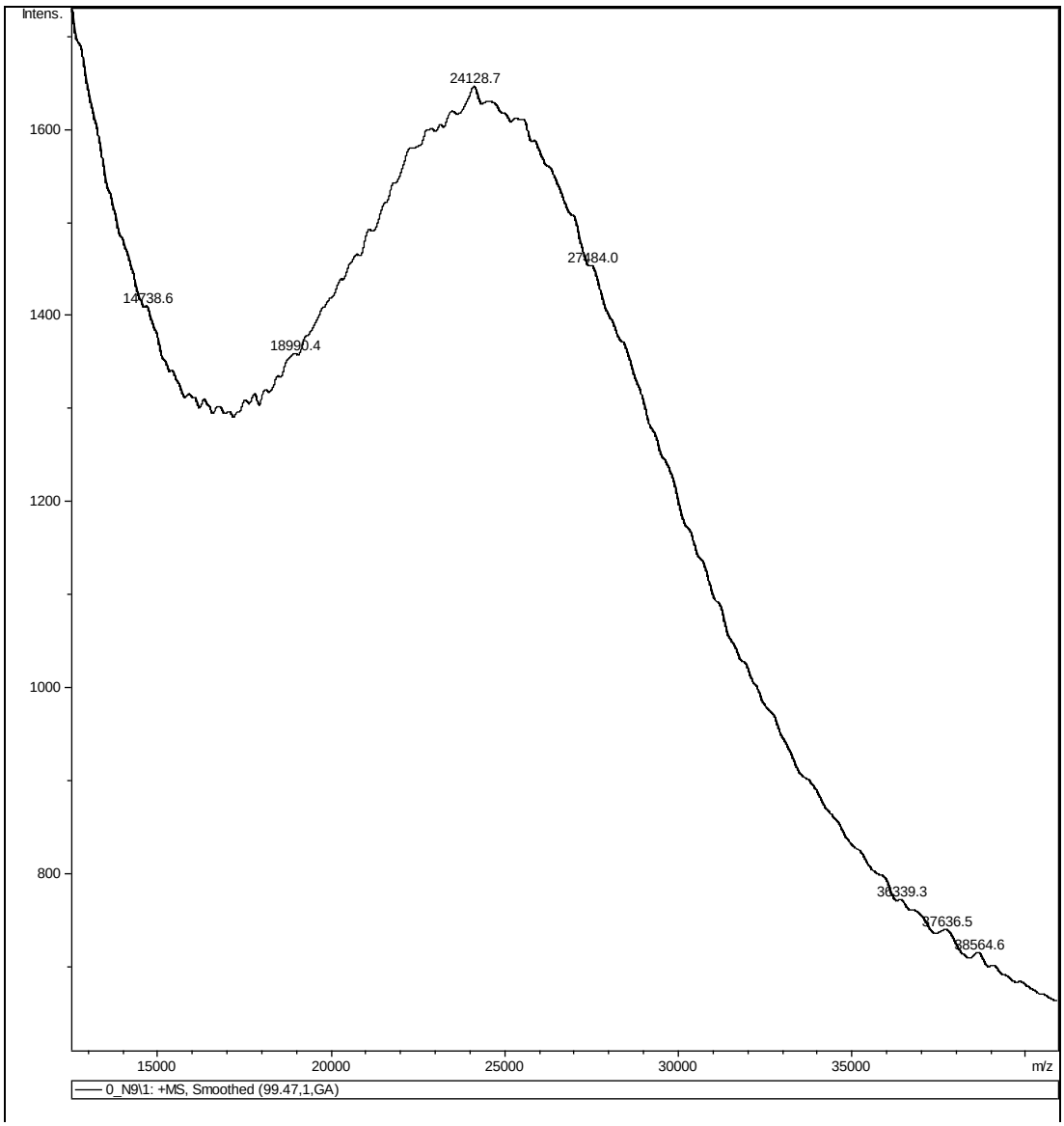


Figure 173. Smoothed MALDI TOF spectrum for compound **52**. M_w = 22500.

APPENDIX D

RELEVANT SPECTRAL DATA FROM CHAPTER FIVE

(Only compounds synthesized by Amanda L. Mattson)

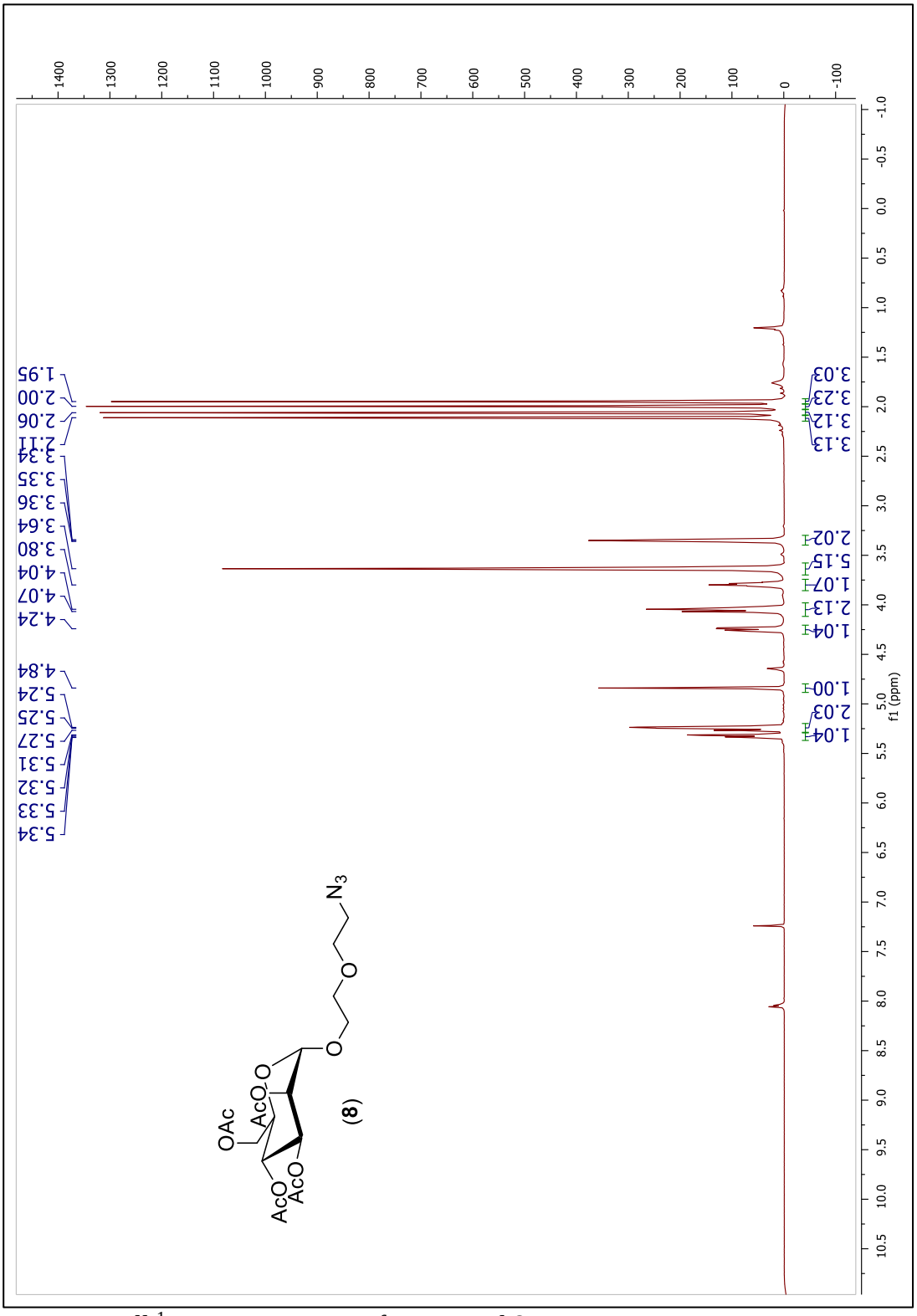


Figure 174. Full ^{1}H NMR spectrum of compound **8**.

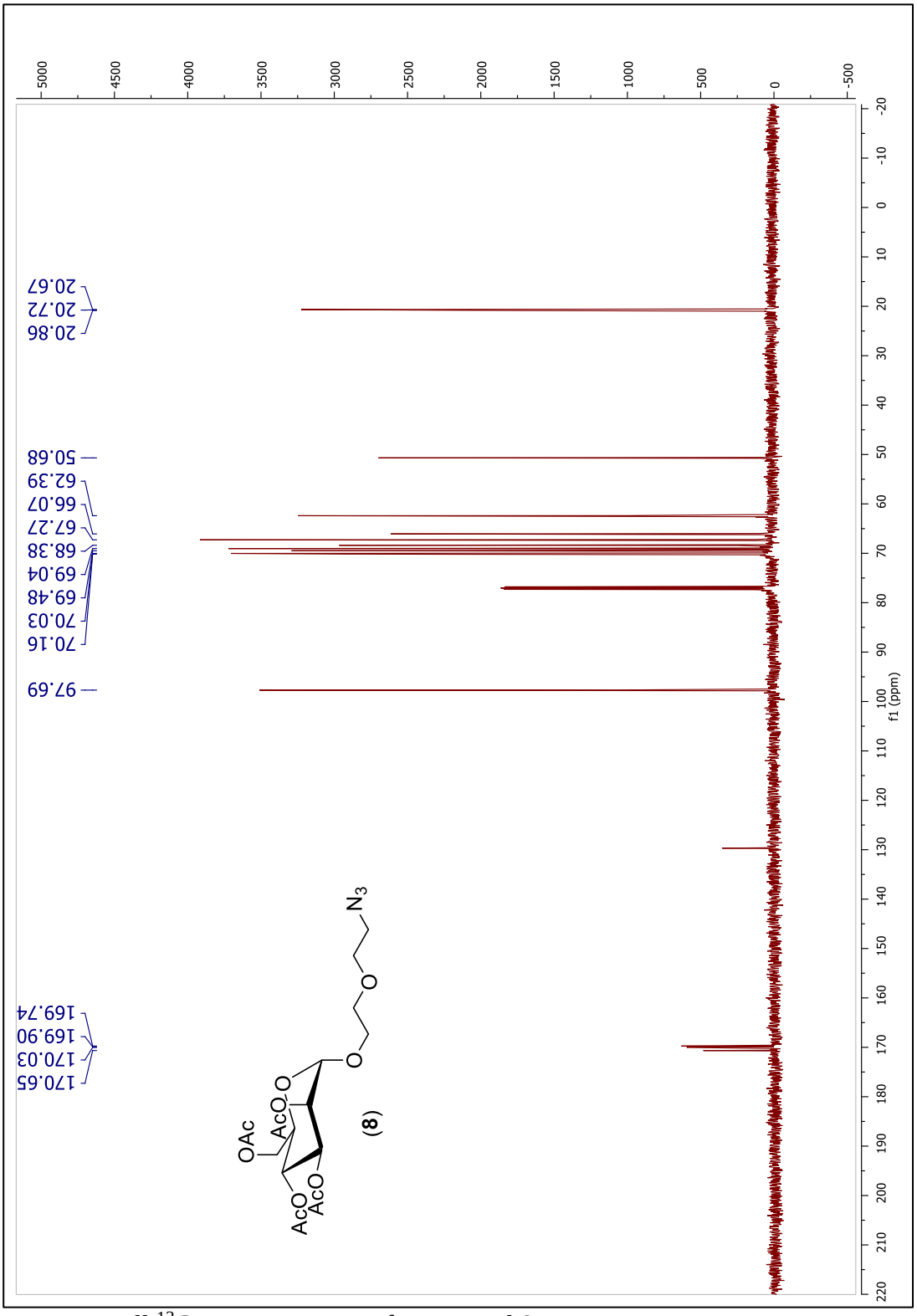


Figure 175. Full ^{13}C NMR spectrum of compound **8**.

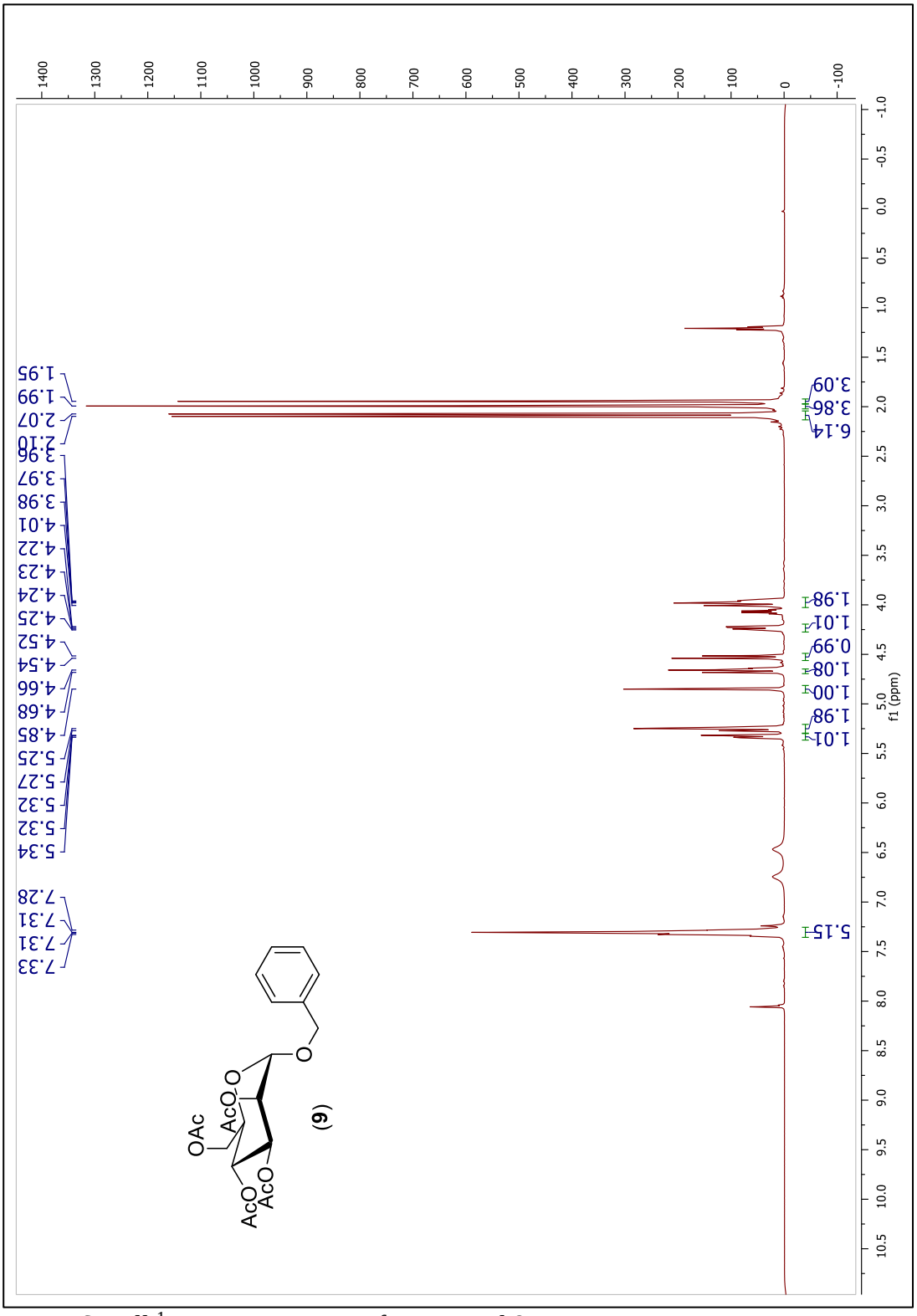


Figure 176. Full ^{1}H NMR spectrum of compound **9**.

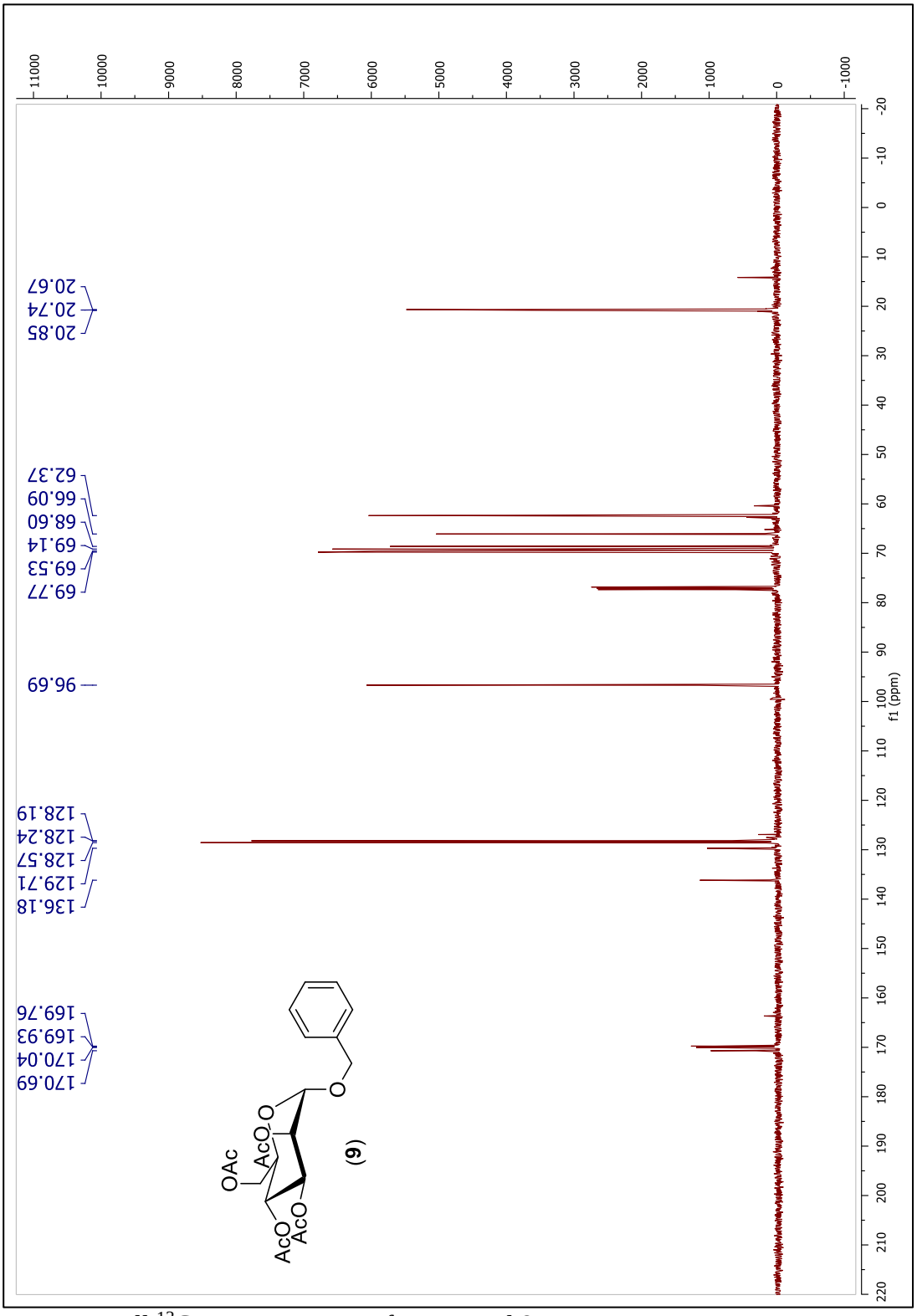


Figure 177. Full ^{13}C NMR spectrum of compound **9**.

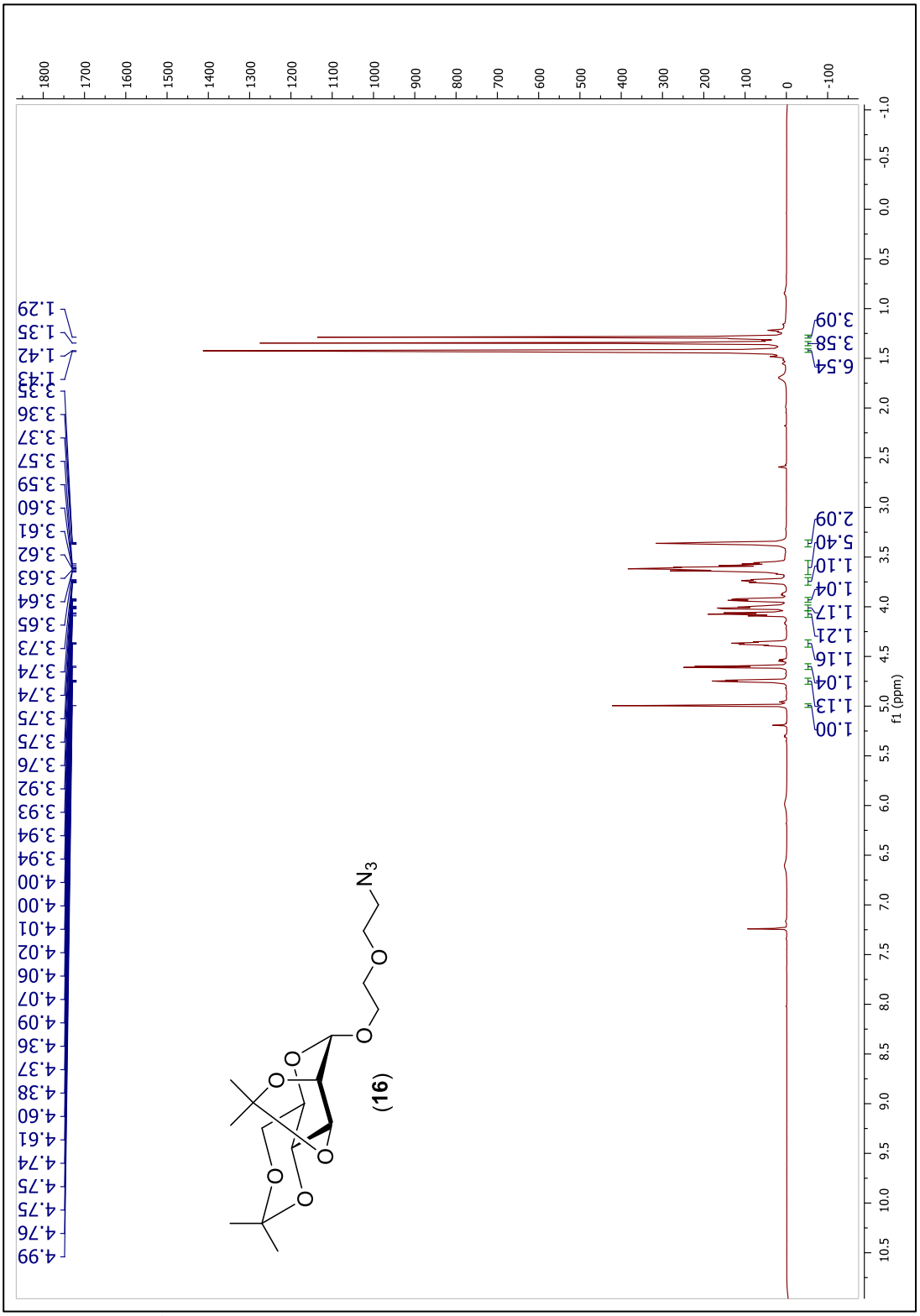


Figure 178. Full ^{1}H NMR spectrum of compound **16**.

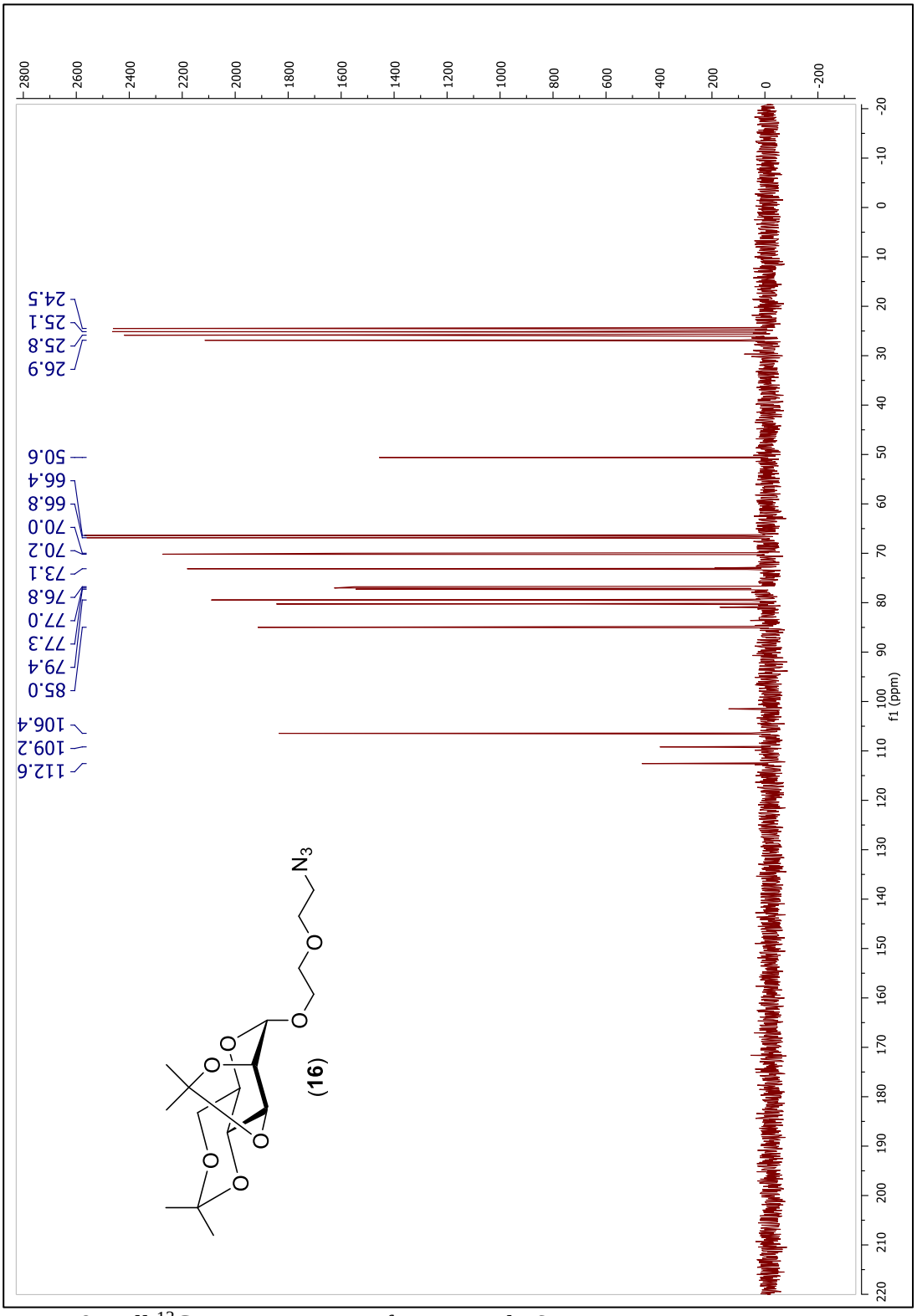


Figure 179. Full ^{13}C NMR spectrum of compound **16**.

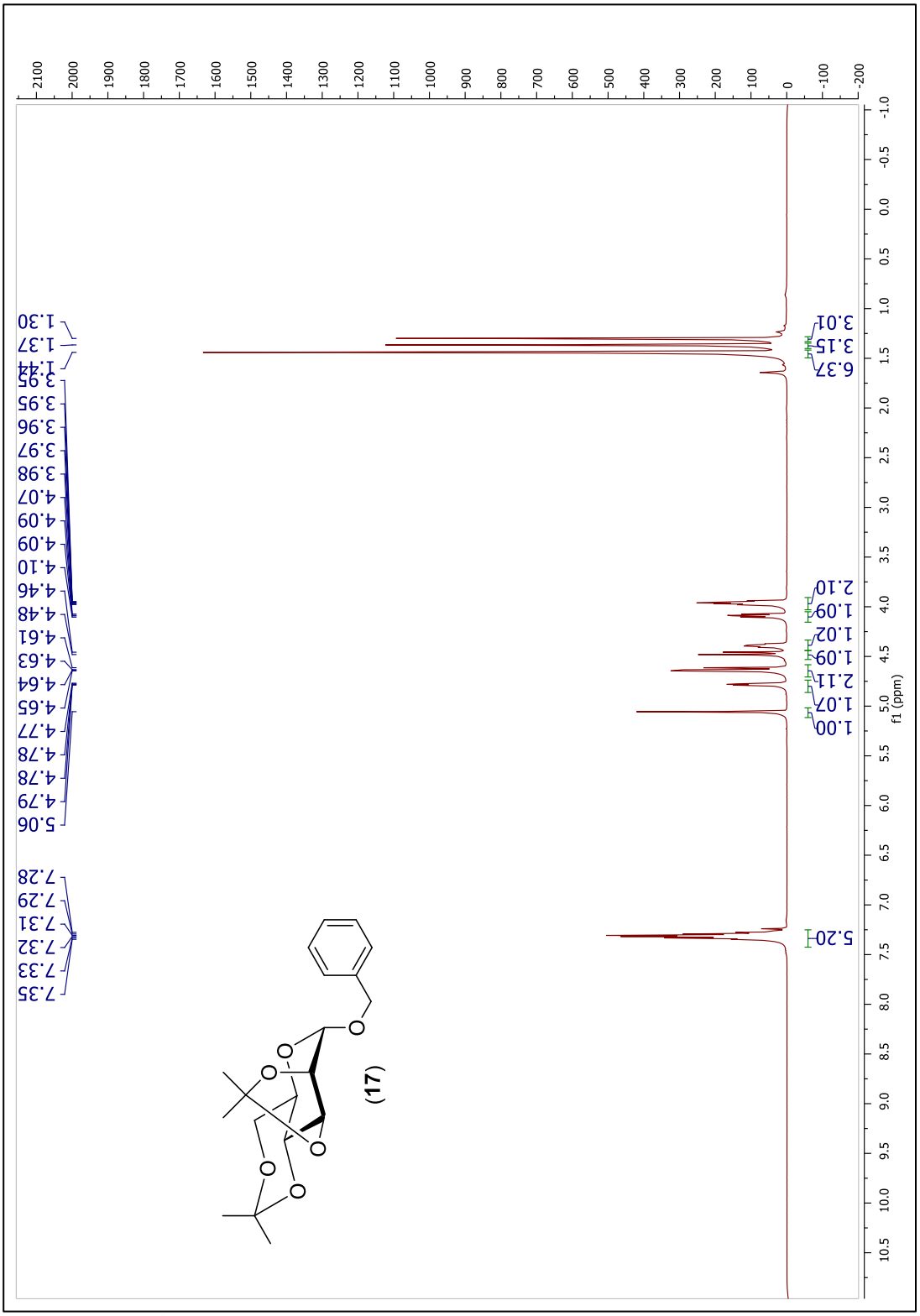


Figure 180. Full ^{1}H NMR spectrum of compound **17**.

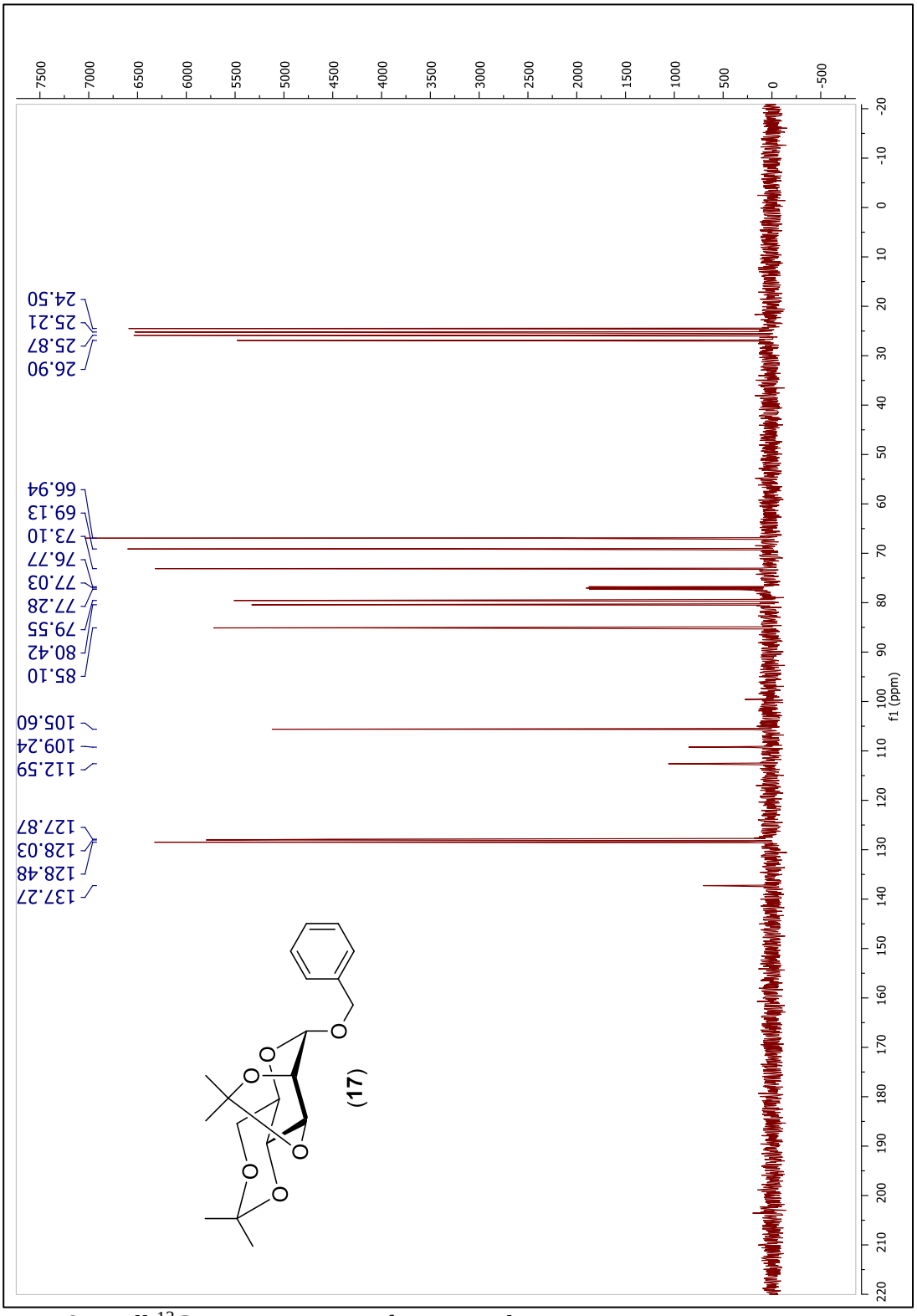


Figure 181. Full ^{13}C NMR spectrum of compound **17**.

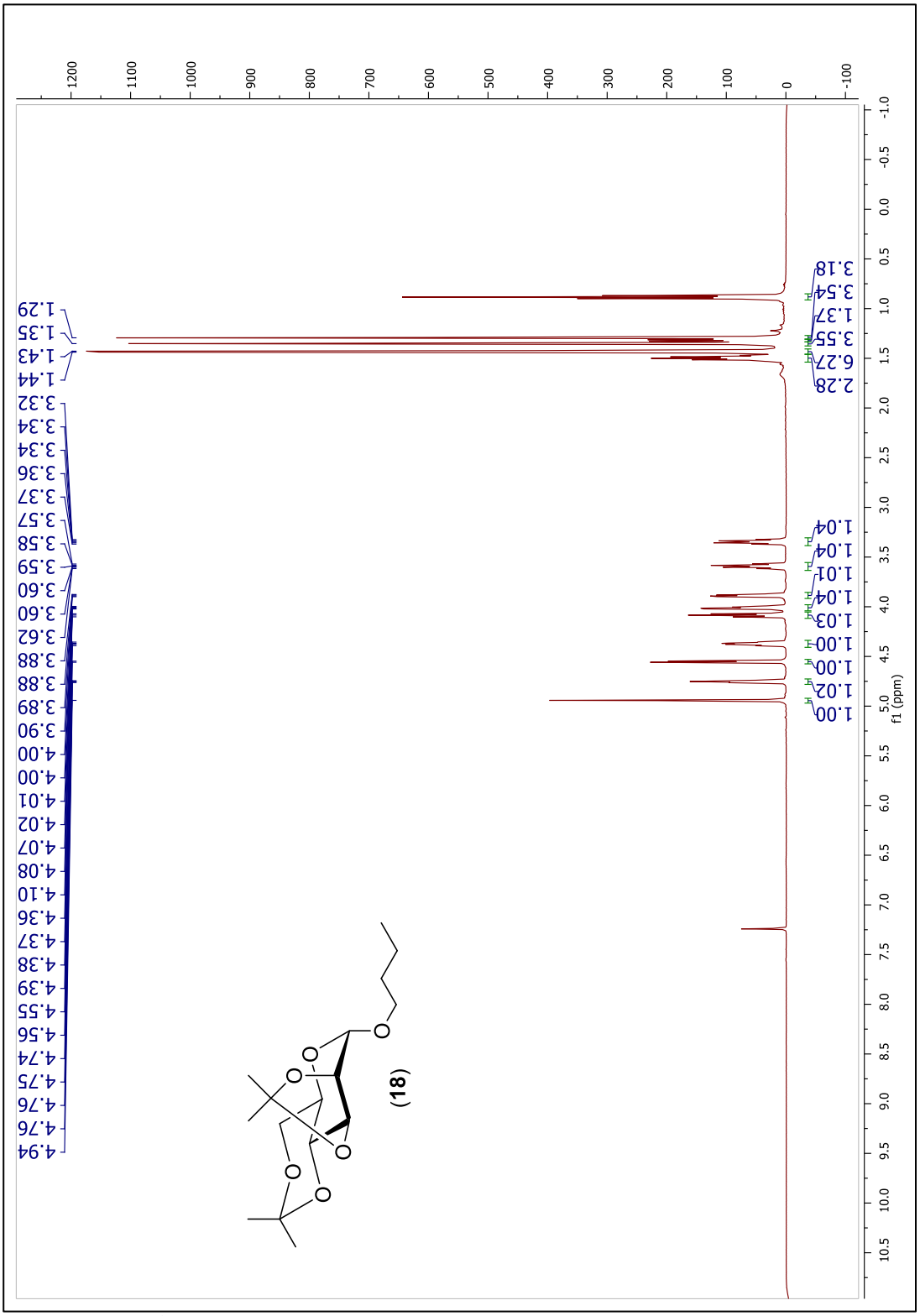


Figure 182. Full ^{1}H NMR spectrum of compound **18**.

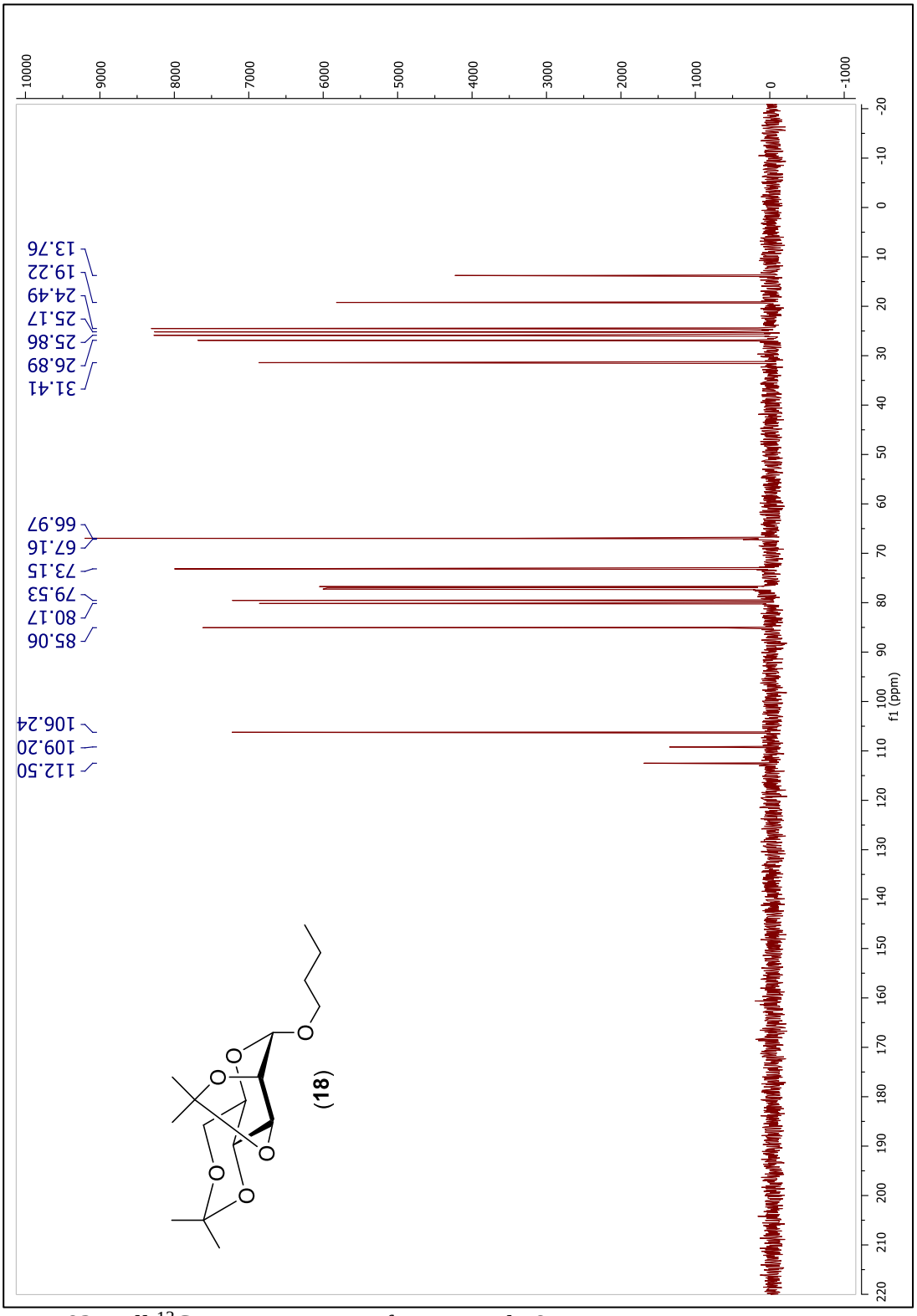


Figure 183. Full ^{13}C NMR spectrum of compound **18**.

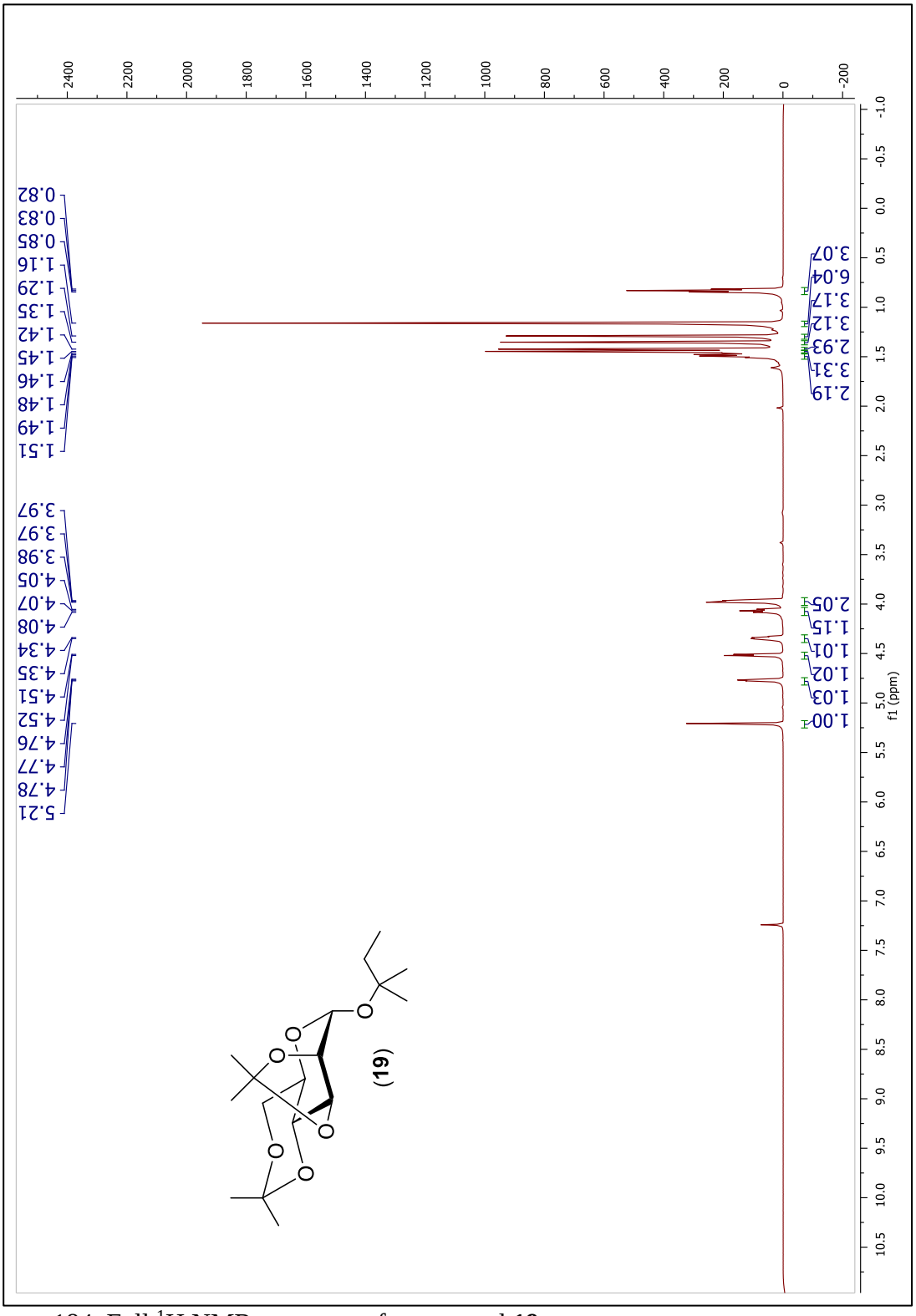


Figure 184. Full ^{1}H NMR spectrum of compound **19**.

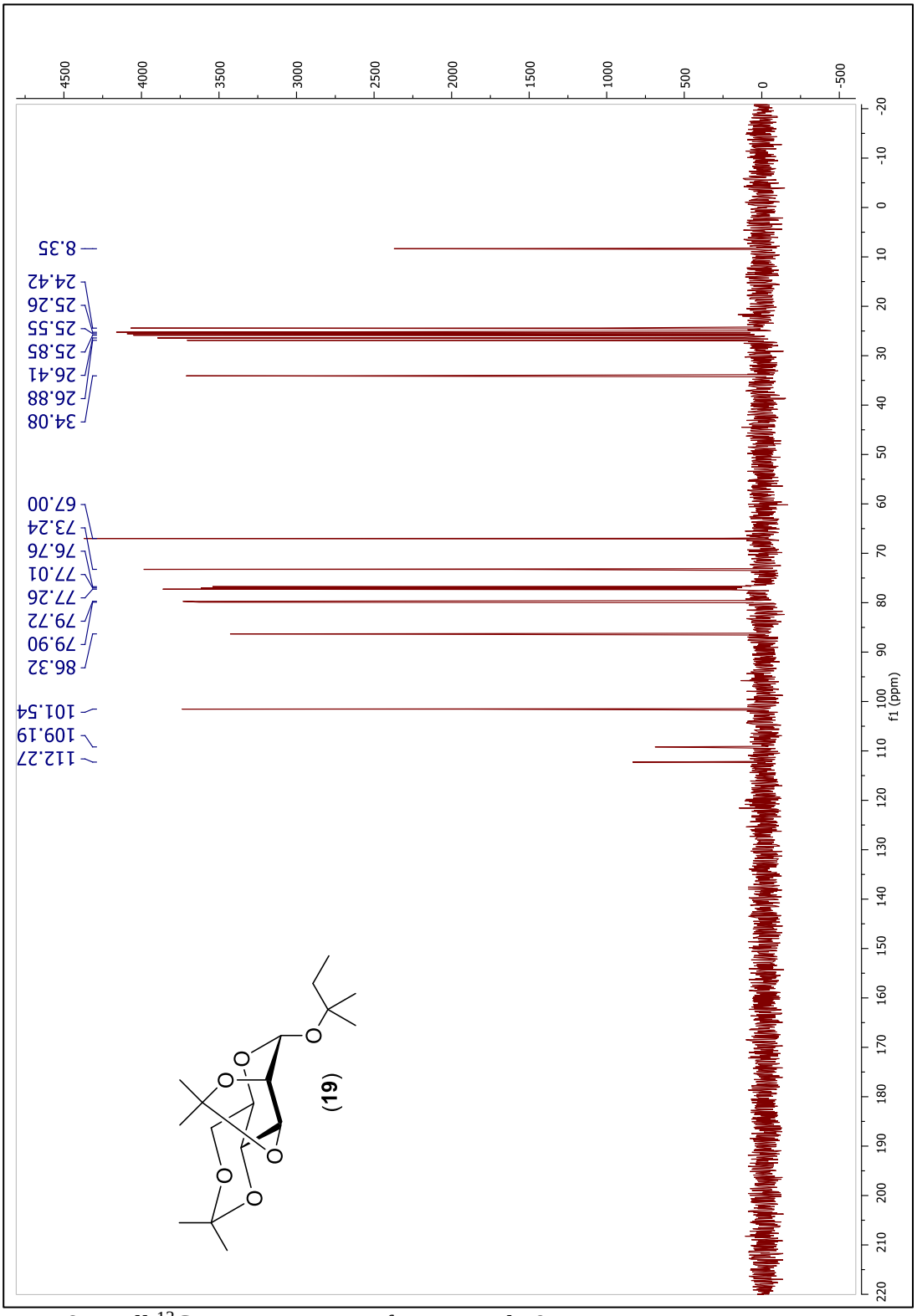


Figure 185. Full ^{13}C NMR spectrum of compound **19**.

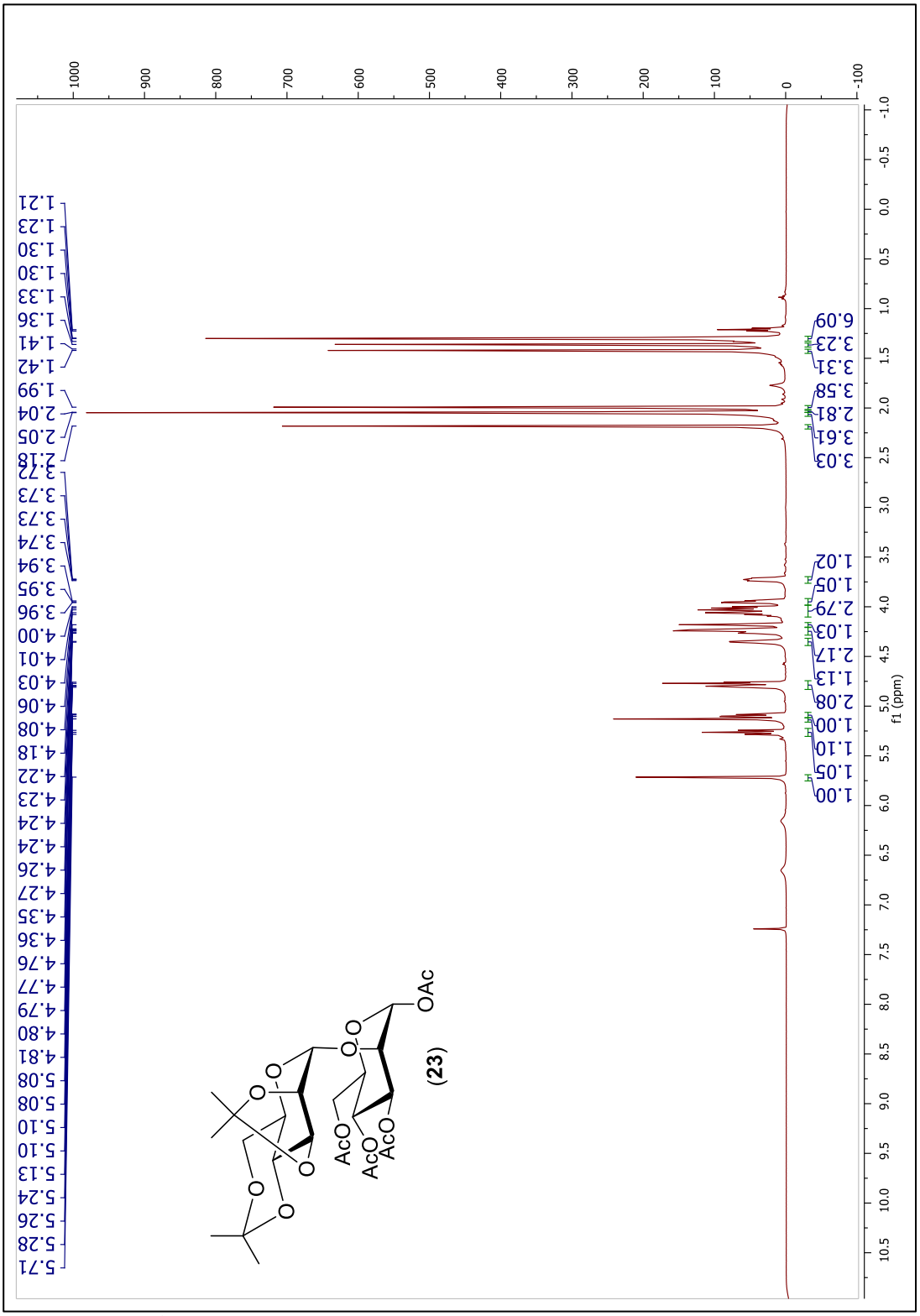


Figure 186. Full ^{1}H NMR spectrum of compound **23**.

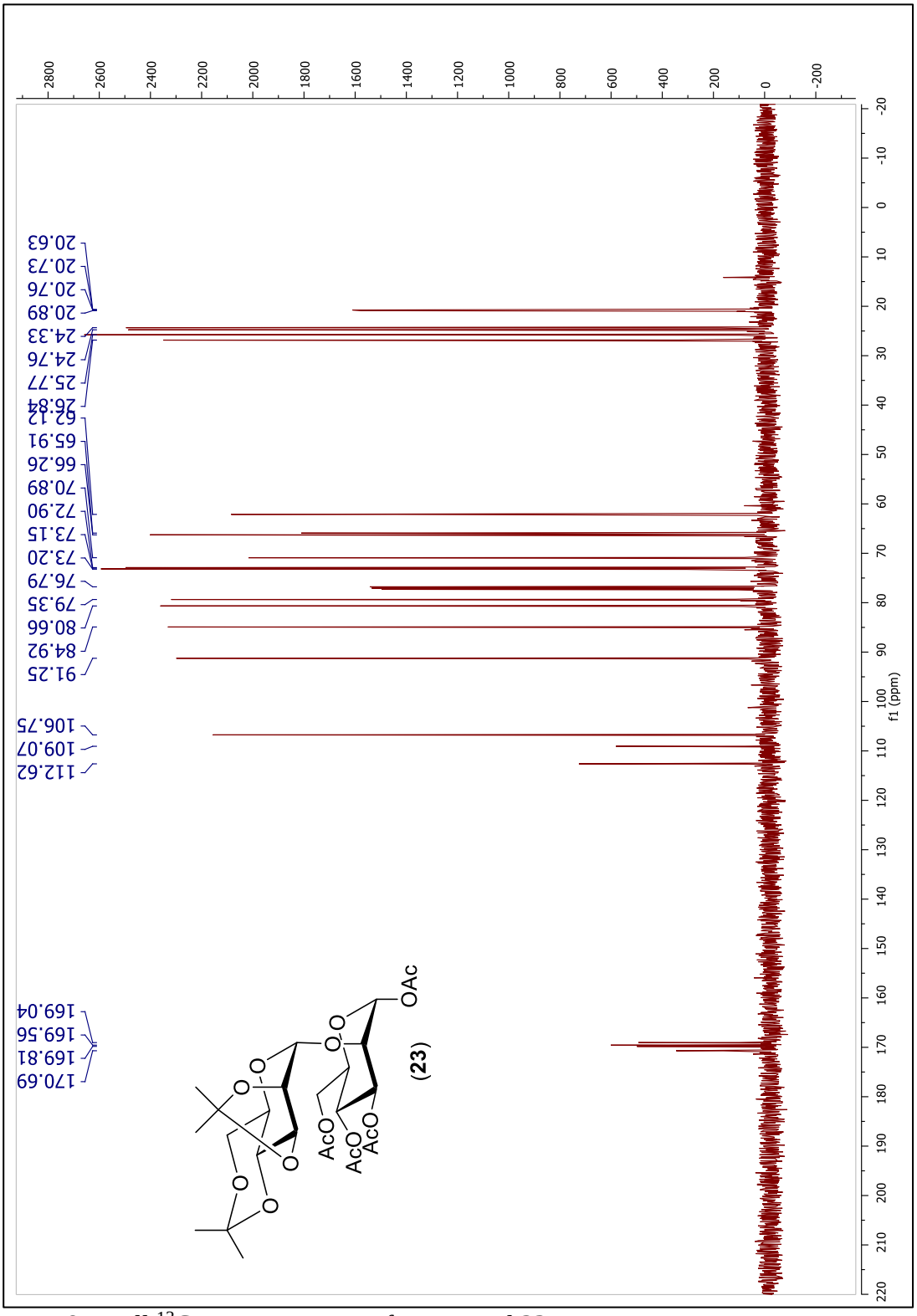


Figure 187. Full ^{13}C NMR spectrum of compound **23**.

APPENDIX E

COPYRIGHT INFORMATION FOR REPRINTED MATERIALS

Figure 2.

Brayman, M.; Thathiah, A.; Carson, D. D., MUC1: A multifunctional cell surface component of reproductive tissue epithelia. *Reproductive biology and endocrinology : RB&E* **2004,** *2*, 4-4. doi: 10.1186/1477-7827-2-4

This article is published under creative commons attribution license 4.0 (https://creativecommons.org/licenses/by/4.0/legalcode).
© Brayman et al; licensee BioMed Central Ltd. 2004
This article is published under license to BioMed Central Ltd. This is an Open Access article: verbatim copying and redistribution of this article are permitted in all media for any purpose, provided this notice is preserved along with the article's original URL.

Figures 5 and 6.

Bian, C.-F.; Zhang, Y.; Sun, H.; Li, D.-F.; Wang, D.-C., Structural Basis for Distinct Binding Properties of the Human Galectins to Thomsen-Friedenreich Antigen. *PLoS ONE* **2011,** *6* (9), e25007. doi: 10.1371/journal.pone.0025007

This article is published under creative commons attribution license 4.0 (https://creativecommons.org/licenses/by/4.0/legalcode).

Copyright: © 2011 Bian et al. This is an open-access article distributed under the terms of the Creative Commons Attribution License, which permits unrestricted use, distribution, and reproduction in any medium, provided the original author and source are credited.

Figures 7, 16, 17, 18.

JOHN WILEY AND SONS LICENSE TERMS AND CONDITIONS

Mar 28, 2017

This Agreement between Amanda L Mattson ("You") and John Wiley and Sons ("John Wiley and Sons") consists of your license details and the terms and conditions provided by John Wiley and Sons and Copyright Clearance Center.

License Number	4077880792785
License date	Mar 28, 2017
Licensed Content Publisher	John Wiley and Sons
Licensed Content Publication	ChemBioChem
Licensed Content Title	Lactose-Functionalized Dendrimers Arbitrate the Interaction of Galectin-3/MUC1 Mediated Cancer Cellular Aggregation
Licensed Content Author	Anna K. Michel,Pratima Nangia-Makker,Avraham Raz,Mary J. Cloninger
Licensed Content Date	Aug 19, 2014
Licensed Content Pages	7
Type of use	Dissertation/Thesis
Requestor type	University/Academic
Format	Print and electronic
Portion	Figure/table
Number of figures/tables	6
Original Wiley figure/table number(s)	Figure 1. Figure 2 (a-d) Figure 6
Will you be translating?	No
Title of your thesis / dissertation	The synthesis and study of TF antigen functionalized dendrimers
Expected completion date	Apr 2017
Expected size (number of pages)	350
Requestor Location	Amanda L Mattson 103 Chemistry and Biochemistry Building Montana State University BOZEMAN, MT 59717 United States Attn: Amanda L Mattson

Publisher Tax ID	EU826007151
Billing Type	Invoice
Billing Address	Amanda L Mattson 103 Chemistry and Biochemistry Building Montana State University BOZEMAN, MT 59717 United States Attn: Amanda L Mattson
Total	0.00 USD

Terms and Conditions

TERMS AND CONDITIONS

This copyrighted material is owned by or exclusively licensed to John Wiley & Sons, Inc. or one of its group companies (each a"Wiley Company") or handled on behalf of a society with which a Wiley Company has exclusive publishing rights in relation to a particular work (collectively "WILEY"). By clicking "accept" in connection with completing this licensing transaction, you agree that the following terms and conditions apply to this transaction (along with the billing and payment terms and conditions established by the Copyright Clearance Center Inc., ("CCC's Billing and Payment terms and conditions"), at the time that you opened your RightsLink account (these are available at any time at http://myaccount.copyright.com).

Terms and Conditions

- The materials you have requested permission to reproduce or reuse (the "Wiley Materials") are protected by copyright.
- You are hereby granted a personal, non-exclusive, non-sub licensable (on a stand-alone basis), non-transferable, worldwide, limited license to reproduce the Wiley Materials for the purpose specified in the licensing process. This license, **and any CONTENT (PDF or image file) purchased as part of your order,** is for a one-time use only and limited to any maximum distribution number specified in the license. The first instance of republication or reuse granted by this license must be completed within two years of the date of the grant of this license (although copies prepared before the end date may be distributed thereafter). The Wiley Materials shall not be used in any other manner or for any other purpose, beyond what is granted in the license. Permission is granted subject to an appropriate acknowledgement given to the author, title of the material/book/journal and the publisher. You shall also duplicate the copyright notice that appears in the Wiley publication in your use of the Wiley Material. Permission is also granted on the understanding that nowhere in the text is a previously published source acknowledged for all or part of this Wiley Material. Any third party content is expressly excluded from this permission.

- With respect to the Wiley Materials, all rights are reserved. Except as expressly granted by the terms of the license, no part of the Wiley Materials may be copied, modified, adapted (except for minor reformatting required by the new Publication), translated, reproduced, transferred or distributed, in any form or by any means, and no derivative works may be made based on the Wiley Materials without the prior permission of the respective copyright owner.**For STM Signatory Publishers clearing permission under the terms of the STM Permissions Guidelines only, the terms of the license are extended to include subsequent editions and for editions in other languages, provided such editions are for the work as a whole in situ and does not involve the separate exploitation of the permitted figures or extracts,** You may not alter, remove or suppress in any manner any copyright, trademark or other notices displayed by the Wiley Materials. You may not license, rent, sell, loan, lease, pledge, offer as security, transfer or assign the Wiley Materials on a stand-alone basis, or any of the rights granted to you hereunder to any other person.

- The Wiley Materials and all of the intellectual property rights therein shall at all times remain the exclusive property of John Wiley & Sons Inc, the Wiley Companies, or their respective licensors, and your interest therein is only that of having possession of and the right to reproduce the Wiley Materials pursuant to Section 2 herein during the continuance of this Agreement. You agree that you own no right, title or interest in or to the Wiley Materials or any of the intellectual property rights therein. You shall have no rights hereunder other than the license as provided for above in Section 2. No right, license or interest to any trademark, trade name, service mark or other branding ("Marks") of WILEY or its licensors is granted hereunder, and you agree that you shall not assert any such right, license or interest with respect thereto

- NEITHER WILEY NOR ITS LICENSORS MAKES ANY WARRANTY OR REPRESENTATION OF ANY KIND TO YOU OR ANY THIRD PARTY, EXPRESS, IMPLIED OR STATUTORY, WITH RESPECT TO THE MATERIALS OR THE ACCURACY OF ANY INFORMATION CONTAINED IN THE MATERIALS, INCLUDING, WITHOUT LIMITATION, ANY IMPLIED WARRANTY OF MERCHANTABILITY, ACCURACY, SATISFACTORY QUALITY, FITNESS FOR A PARTICULAR PURPOSE, USABILITY, INTEGRATION OR NON-INFRINGEMENT AND ALL SUCH WARRANTIES ARE HEREBY EXCLUDED BY WILEY AND ITS LICENSORS AND WAIVED BY YOU.

- WILEY shall have the right to terminate this Agreement immediately upon breach of this Agreement by you.

- You shall indemnify, defend and hold harmless WILEY, its Licensors and their respective directors, officers, agents and employees, from and against any actual or

threatened claims, demands, causes of action or proceedings arising from any breach of this Agreement by you.

- IN NO EVENT SHALL WILEY OR ITS LICENSORS BE LIABLE TO YOU OR ANY OTHER PARTY OR ANY OTHER PERSON OR ENTITY FOR ANY SPECIAL, CONSEQUENTIAL, INCIDENTAL, INDIRECT, EXEMPLARY OR PUNITIVE DAMAGES, HOWEVER CAUSED, ARISING OUT OF OR IN CONNECTION WITH THE DOWNLOADING, PROVISIONING, VIEWING OR USE OF THE MATERIALS REGARDLESS OF THE FORM OF ACTION, WHETHER FOR BREACH OF CONTRACT, BREACH OF WARRANTY, TORT, NEGLIGENCE, INFRINGEMENT OR OTHERWISE (INCLUDING, WITHOUT LIMITATION, DAMAGES BASED ON LOSS OF PROFITS, DATA, FILES, USE, BUSINESS OPPORTUNITY OR CLAIMS OF THIRD PARTIES), AND WHETHER OR NOT THE PARTY HAS BEEN ADVISED OF THE POSSIBILITY OF SUCH DAMAGES. THIS LIMITATION SHALL APPLY NOTWITHSTANDING ANY FAILURE OF ESSENTIAL PURPOSE OF ANY LIMITED REMEDY PROVIDED HEREIN.

- Should any provision of this Agreement be held by a court of competent jurisdiction to be illegal, invalid, or unenforceable, that provision shall be deemed amended to achieve as nearly as possible the same economic effect as the original provision, and the legality, validity and enforceability of the remaining provisions of this Agreement shall not be affected or impaired thereby.

- The failure of either party to enforce any term or condition of this Agreement shall not constitute a waiver of either party's right to enforce each and every term and condition of this Agreement. No breach under this agreement shall be deemed waived or excused by either party unless such waiver or consent is in writing signed by the party granting such waiver or consent. The waiver by or consent of a party to a breach of any provision of this Agreement shall not operate or be construed as a waiver of or consent to any other or subsequent breach by such other party.

- This Agreement may not be assigned (including by operation of law or otherwise) by you without WILEY's prior written consent.

- Any fee required for this permission shall be non-refundable after thirty (30) days from receipt by the CCC.

- These terms and conditions together with CCC's Billing and Payment terms and conditions (which are incorporated herein) form the entire agreement between you and WILEY concerning this licensing transaction and (in the absence of fraud) supersedes all prior agreements and representations of the parties, oral or written. This Agreement may not be amended except in writing signed by both parties. This

Agreement shall be binding upon and inure to the benefit of the parties' successors, legal representatives, and authorized assigns.

- In the event of any conflict between your obligations established by these terms and conditions and those established by CCC's Billing and Payment terms and conditions, these terms and conditions shall prevail.

- WILEY expressly reserves all rights not specifically granted in the combination of (i) the license details provided by you and accepted in the course of this licensing transaction, (ii) these terms and conditions and (iii) CCC's Billing and Payment terms and conditions.

- This Agreement will be void if the Type of Use, Format, Circulation, or Requestor Type was misrepresented during the licensing process.

- This Agreement shall be governed by and construed in accordance with the laws of the State of New York, USA, without regards to such state's conflict of law rules. Any legal action, suit or proceeding arising out of or relating to these Terms and Conditions or the breach thereof shall be instituted in a court of competent jurisdiction in New York County in the State of New York in the United States of America and each party hereby consents and submits to the personal jurisdiction of such court, waives any objection to venue in such court and consents to service of process by registered or certified mail, return receipt requested, at the last known address of such party.

WILEY OPEN ACCESS TERMS AND CONDITIONS

Wiley Publishes Open Access Articles in fully Open Access Journals and in Subscription journals offering Online Open. Although most of the fully Open Access journals publish open access articles under the terms of the Creative Commons Attribution (CC BY) License only, the subscription journals and a few of the Open Access Journals offer a choice of Creative Commons Licenses. The license type is clearly identified on the article.

The Creative Commons Attribution License

The Creative Commons Attribution License (CC-BY) allows users to copy, distribute and transmit an article, adapt the article and make commercial use of the article. The CC-BY license permits commercial and non-

Creative Commons Attribution Non-Commercial License

The Creative Commons Attribution Non-Commercial (CC-BY-NC)License permits use, distribution and reproduction in any medium, provided the original work is properly cited and is not used for commercial purposes.(see below)

Creative Commons Attribution-Non-Commercial-NoDerivs License

The Creative Commons Attribution Non-Commercial-NoDerivs License (CC-BY-NC-ND) permits use, distribution and reproduction in any medium, provided the original work is properly cited, is not used for commercial purposes and no modifications or adaptations are made. (see below)

Use by commercial "for-profit" organizations
Use of Wiley Open Access articles for commercial, promotional, or marketing purposes requires further explicit permission from Wiley and will be subject to a fee.
Further details can be found on Wiley Online
Library http://olabout.wiley.com/WileyCDA/Section/id-410895.html

Figure 9.

JOHN WILEY AND SONS LICENSE TERMS AND CONDITIONS

Mar 28, 2017

This Agreement between Amanda L Mattson ("You") and John Wiley and Sons ("John Wiley and Sons") consists of your license details and the terms and conditions provided by John Wiley and Sons and Copyright Clearance Center.

License Number	4077881287618
License date	Mar 28, 2017
Licensed Content Publisher	John Wiley and Sons
Licensed Content Publication	Angewandte Chemie International Edition
Licensed Content Title	Synthetic Antitumor Vaccines from Tetanus Toxoid Conjugates of MUC1 Glycopeptides with the Thomsen–Friedenreich Antigen and a Fluorine-Substituted Analogue
Licensed Content Author	Anja Hoffmann-Röder,Anton Kaiser,Sarah Wagner,Nikola Gaidzik,Danuta Kowalczyk,Ulrika Westerlind,Bastian Gerlitzki,Edgar Schmitt,Horst Kunz
Licensed Content Date	Sep 28, 2010
Licensed Content Pages	6
Type of use	Dissertation/Thesis
Requestor type	University/Academic
Format	Print and electronic
Portion	Figure/table
Number of figures/tables	1
Original Wiley figure/table number(s)	scheme 1
Will you be translating?	No
Title of your thesis / dissertation	The synthesis and study of TF antigen functionalized dendrimers
Expected completion date	Apr 2017
Expected size (number of pages)	350
Requestor Location	Amanda L Mattson 103 Chemistry and Biochemistry Building Montana State University BOZEMAN, MT 59717

	United States Attn: Amanda L Mattson
Publisher Tax ID	EU826007151
Billing Type	Invoice
Billing Address	Amanda L Mattson 103 Chemistry and Biochemistry Building Montana State University BOZEMAN, MT 59717 United States Attn: Amanda L Mattson
Total	0.00 USD
Terms and Conditions	

TERMS AND CONDITIONS

This copyrighted material is owned by or exclusively licensed to John Wiley & Sons, Inc. or one of its group companies (each a"Wiley Company") or handled on behalf of a society with which a Wiley Company has exclusive publishing rights in relation to a particular work (collectively "WILEY"). By clicking "accept" in connection with completing this licensing transaction, you agree that the following terms and conditions apply to this transaction (along with the billing and payment terms and conditions established by the Copyright Clearance Center Inc., ("CCC's Billing and Payment terms and conditions"), at the time that you opened your RightsLink account (these are available at any time at http://myaccount.copyright.com).

Terms and Conditions

- The materials you have requested permission to reproduce or reuse (the "Wiley Materials") are protected by copyright.

- You are hereby granted a personal, non-exclusive, non-sub licensable (on a stand-alone basis), non-transferable, worldwide, limited license to reproduce the Wiley Materials for the purpose specified in the licensing process. This license, **and any CONTENT (PDF or image file) purchased as part of your order,** is for a one-time use only and limited to any maximum distribution number specified in the license. The first instance of republication or reuse granted by this license must be completed within two years of the date of the grant of this license (although copies prepared before the end date may be distributed thereafter). The Wiley Materials shall not be used in any other manner or

for any other purpose, beyond what is granted in the license. Permission is granted subject to an appropriate acknowledgement given to the author, title of the material/book/journal and the publisher. You shall also duplicate the copyright notice that appears in the Wiley publication in your use of the Wiley Material. Permission is also granted on the understanding that nowhere in the text is a previously published source acknowledged for all or part of this Wiley Material. Any third party content is expressly excluded from this permission.

- With respect to the Wiley Materials, all rights are reserved. Except as expressly granted by the terms of the license, no part of the Wiley Materials may be copied, modified, adapted (except for minor reformatting required by the new Publication), translated, reproduced, transferred or distributed, in any form or by any means, and no derivative works may be made based on the Wiley Materials without the prior permission of the respective copyright owner.**For STM Signatory Publishers clearing permission under the terms of the STM Permissions Guidelines only, the terms of the license are extended to include subsequent editions and for editions in other languages, provided such editions are for the work as a whole in situ and does not involve the separate exploitation of the permitted figures or extracts,** You may not alter, remove or suppress in any manner any copyright, trademark or other notices displayed by the Wiley Materials. You may not license, rent, sell, loan, lease, pledge, offer as security, transfer or assign the Wiley Materials on a stand-alone basis, or any of the rights granted to you hereunder to any other person.

- The Wiley Materials and all of the intellectual property rights therein shall at all times remain the exclusive property of John Wiley & Sons Inc, the Wiley Companies, or their respective licensors, and your interest therein is only that of having possession of and the right to reproduce the Wiley Materials pursuant to Section 2 herein during the continuance of this Agreement. You agree that you own no right, title or interest in or to the Wiley Materials or any of the intellectual property rights therein. You shall have no rights hereunder other than the license as provided for above in Section 2. No right, license or interest to any trademark, trade name, service mark or other branding ("Marks") of WILEY or its licensors is

granted hereunder, and you agree that you shall not assert any such right, license or interest with respect thereto

- NEITHER WILEY NOR ITS LICENSORS MAKES ANY WARRANTY OR REPRESENTATION OF ANY KIND TO YOU OR ANY THIRD PARTY, EXPRESS, IMPLIED OR STATUTORY, WITH RESPECT TO THE MATERIALS OR THE ACCURACY OF ANY INFORMATION CONTAINED IN THE MATERIALS, INCLUDING, WITHOUT LIMITATION, ANY IMPLIED WARRANTY OF MERCHANTABILITY, ACCURACY, SATISFACTORY QUALITY, FITNESS FOR A PARTICULAR PURPOSE, USABILITY, INTEGRATION OR NON-INFRINGEMENT AND ALL SUCH WARRANTIES ARE HEREBY EXCLUDED BY WILEY AND ITS LICENSORS AND WAIVED BY YOU.

- WILEY shall have the right to terminate this Agreement immediately upon breach of this Agreement by you.

- You shall indemnify, defend and hold harmless WILEY, its Licensors and their respective directors, officers, agents and employees, from and against any actual or threatened claims, demands, causes of action or proceedings arising from any breach of this Agreement by you.

- IN NO EVENT SHALL WILEY OR ITS LICENSORS BE LIABLE TO YOU OR ANY OTHER PARTY OR ANY OTHER PERSON OR ENTITY FOR ANY SPECIAL, CONSEQUENTIAL, INCIDENTAL, INDIRECT, EXEMPLARY OR PUNITIVE DAMAGES, HOWEVER CAUSED, ARISING OUT OF OR IN CONNECTION WITH THE DOWNLOADING, PROVISIONING, VIEWING OR USE OF THE MATERIALS REGARDLESS OF THE FORM OF ACTION, WHETHER FOR BREACH OF CONTRACT, BREACH OF WARRANTY, TORT, NEGLIGENCE, INFRINGEMENT OR OTHERWISE (INCLUDING, WITHOUT LIMITATION, DAMAGES BASED ON LOSS OF PROFITS, DATA, FILES, USE, BUSINESS OPPORTUNITY OR CLAIMS OF THIRD PARTIES), AND WHETHER OR NOT THE PARTY HAS BEEN ADVISED OF THE POSSIBILITY OF SUCH DAMAGES. THIS LIMITATION SHALL APPLY NOTWITHSTANDING ANY FAILURE OF ESSENTIAL PURPOSE OF ANY LIMITED REMEDY PROVIDED HEREIN.

- Should any provision of this Agreement be held by a court of competent jurisdiction to be illegal, invalid, or unenforceable, that provision shall be deemed amended to achieve as nearly as possible the same economic effect as the original provision, and the legality, validity and enforceability of the remaining provisions of this Agreement shall not be affected or impaired thereby.

- The failure of either party to enforce any term or condition of this Agreement shall not constitute a waiver of either party's right to enforce each and every term and condition of this Agreement. No breach under this agreement shall be deemed waived or excused by either party unless such waiver or consent is in writing signed by the party granting such waiver or consent. The waiver by or consent of a party to a breach of any provision of this Agreement shall not operate or be construed as a waiver of or consent to any other or subsequent breach by such other party.

- This Agreement may not be assigned (including by operation of law or otherwise) by you without WILEY's prior written consent.

- Any fee required for this permission shall be non-refundable after thirty (30) days from receipt by the CCC.

- These terms and conditions together with CCC's Billing and Payment terms and conditions (which are incorporated herein) form the entire agreement between you and WILEY concerning this licensing transaction and (in the absence of fraud) supersedes all prior agreements and representations of the parties, oral or written. This Agreement may not be amended except in writing signed by both parties. This Agreement shall be binding upon and inure to the benefit of the parties' successors, legal representatives, and authorized assigns.

- In the event of any conflict between your obligations established by these terms and conditions and those established by CCC's Billing and Payment terms and conditions, these terms and conditions shall prevail.

- WILEY expressly reserves all rights not specifically granted in the combination of (i) the license details provided by you and accepted in the course of this licensing transaction, (ii) these terms and conditions and (iii) CCC's Billing and Payment terms and conditions.

- This Agreement will be void if the Type of Use, Format, Circulation, or Requestor Type was misrepresented during the licensing process.

- This Agreement shall be governed by and construed in accordance with the laws of the State of New York, USA, without regards to such state's conflict of law rules. Any legal action, suit or proceeding arising out of or relating to these Terms and Conditions or the breach thereof shall be instituted in a court of competent jurisdiction in New York County in the State of New York in the United States of America and each party hereby consents and submits to the personal jurisdiction of such court, waives any objection to venue in such court and consents to service of process by registered or certified mail, return receipt requested, at the last known address of such party.

WILEY OPEN ACCESS TERMS AND CONDITIONS

Wiley Publishes Open Access Articles in fully Open Access Journals and in Subscription journals offering Online Open. Although most of the fully Open Access journals publish open access articles under the terms of the Creative Commons Attribution (CC BY) License only, the subscription journals and a few of the Open Access Journals offer a choice of Creative Commons Licenses. The license type is clearly identified on the article.

The Creative Commons Attribution License

The Creative Commons Attribution License (CC-BY) allows users to copy, distribute and transmit an article, adapt the article and make commercial use of the article. The CC-BY license permits commercial and non-

Creative Commons Attribution Non-Commercial License

The Creative Commons Attribution Non-Commercial (CC-BY-NC)License permits use, distribution and reproduction in any medium, provided the original work is properly cited and is not used for commercial purposes.(see below)

Creative Commons Attribution-Non-Commercial-NoDerivs License

The Creative Commons Attribution Non-Commercial-NoDerivs License (CC-BY-NC-ND) permits use, distribution and reproduction in any medium, provided the original work is properly cited, is not used for commercial purposes and no modifications or adaptations are made. (see below)

Use by commercial "for-profit" organizations

Use of Wiley Open Access articles for commercial, promotional, or marketing purposes requires further explicit permission from Wiley and will be subject to a fee.
Further details can be found on Wiley Online Library http://olabout.wiley.com/WileyCDA/Section/id-410895.html

Other Terms and Conditions:

v1.10 Last updated September 2015

Questions? customercare@copyright.com or +1-855-239-3415 (toll free in the US) or +1-978-646-2777.

Figure 10.

Copyright Clearance Center RightsLink®

ACS Publications Most Trusted. Most Cited. Most Read.

Title: From Synthesis to Biologics: Preclinical Data on a Chemistry Derived Anticancer Vaccine

Author: Jianglong Zhu, Qian Wan, Dongjoo Lee, et al

Publication: Journal of the American Chemical Society

Publisher: American Chemical Society

Date: Jul 1, 2009

Copyright © 2009, American Chemical Society

PERMISSION/LICENSE IS GRANTED FOR YOUR ORDER AT NO CHARGE

This type of permission/license, instead of the standard Terms & Conditions, is sent to you because no fee is being charged for your order. Please note the following:

- Permission is granted for your request in both print and electronic formats, and translations.
- If figures and/or tables were requested, they may be adapted or used in part.
- Please print this page for your records and send a copy of it to your publisher/graduate school.
- Appropriate credit for the requested material should be given as follows: "Reprinted (adapted) with permission from (COMPLETE REFERENCE CITATION). Copyright (YEAR) American Chemical Society." Insert appropriate information in place of the capitalized words.
- One-time permission is granted only for the use specified in your request. No additional uses are granted (such as derivative works or other editions). For any other uses, please submit a new request.

If credit is given to another source for the material you requested, permission must be obtained from that source.

Copyright © 2017 Copyright Clearance Center, Inc. All Rights Reserved. Privacy statement. Terms and Conditions.
Comments? We would like to hear from you. E-mail us at customercare@copyright.com

Figure 11.

ELSEVIER LICENSE
TERMS AND CONDITIONS

Mar 28, 2017

This Agreement between Amanda L Mattson ("You") and Elsevier ("Elsevier") consists of your license details and the terms and conditions provided by Elsevier and Copyright Clearance Center.

License Number	4077911156046
License date	Mar 28, 2017
Licensed Content Publisher	Elsevier
Licensed Content Publication	Carbohydrate Research
Licensed Content Title	Synthesis and cell-selective antitumor properties of amino acid conjugated tumor-associated carbohydrate antigen-coated gold nanoparticles
Licensed Content Author	Souvik Biswas,Scott H. Medina,Joseph J. Barchi
Licensed Content Date	20 March 2015
Licensed Content Volume	405
Licensed Content Issue	n/a
Licensed Content Pages	9
Start Page	93
End Page	101
Type of Use	reuse in a thesis/dissertation
Intended publisher of new work	other
Portion	figures/tables/illustrations
Number of figures/tables/illustrations	1
Format	both print and electronic
Are you the author of this Elsevier article?	No
Will you be translating?	No
Order reference number	
Original figure numbers	Figure 1A
Title of your thesis/dissertation	The synthesis and study of TF antigen functionalized dendrimers
Expected completion date	Apr 2017

Estimated size (number of pages)	350
Elsevier VAT number	GB 494 6272 12
Requestor Location	Amanda L Mattson 103 Chemistry and Biochemistry Building Montana State University BOZEMAN, MT 59717 United States Attn: Amanda L Mattson
Publisher Tax ID	98-0397604
Total	0.00 USD
Terms and Conditions	

INTRODUCTION

1. The publisher for this copyrighted material is Elsevier. By clicking "accept" in connection with completing this licensing transaction, you agree that the following terms and conditions apply to this transaction (along with the Billing and Payment terms and conditions established by Copyright Clearance Center, Inc. ("CCC"), at the time that you opened your Rightslink account and that are available at any time at http://myaccount.copyright.com).

GENERAL TERMS

2. Elsevier hereby grants you permission to reproduce the aforementioned material subject to the terms and conditions indicated.
3. Acknowledgement: If any part of the material to be used (for example, figures) has appeared in our publication with credit or acknowledgement to another source, permission must also be sought from that source. If such permission is not obtained then that material may not be included in your publication/copies. Suitable acknowledgement to the source must be made, either as a footnote or in a reference list at the end of your publication, as follows:
"Reprinted from Publication title, Vol /edition number, Author(s), Title of article / title of chapter, Pages No., Copyright (Year), with permission from Elsevier [OR APPLICABLE SOCIETY COPYRIGHT OWNER]." Also Lancet special credit - "Reprinted from The Lancet, Vol. number, Author(s), Title of article, Pages No., Copyright (Year), with permission from Elsevier."
4. Reproduction of this material is confined to the purpose and/or media for which permission is hereby given.
5. Altering/Modifying Material: Not Permitted. However figures and illustrations may be altered/adapted minimally to serve your work. Any other abbreviations, additions, deletions and/or any other alterations shall be made only with prior written authorization of Elsevier Ltd. (Please contact Elsevier at permissions@elsevier.com). No modifications can be made to any Lancet figures/tables and they must be reproduced in full.
6. If the permission fee for the requested use of our material is waived in this instance, please be advised that your future requests for Elsevier materials may attract a fee.
7. Reservation of Rights: Publisher reserves all rights not specifically granted in the combination of (i) the license details provided by you and accepted in the course of this

licensing transaction, (ii) these terms and conditions and (iii) CCC's Billing and Payment terms and conditions.

8. License Contingent Upon Payment: While you may exercise the rights licensed immediately upon issuance of the license at the end of the licensing process for the transaction, provided that you have disclosed complete and accurate details of your proposed use, no license is finally effective unless and until full payment is received from you (either by publisher or by CCC) as provided in CCC's Billing and Payment terms and conditions. If full payment is not received on a timely basis, then any license preliminarily granted shall be deemed automatically revoked and shall be void as if never granted. Further, in the event that you breach any of these terms and conditions or any of CCC's Billing and Payment terms and conditions, the license is automatically revoked and shall be void as if never granted. Use of materials as described in a revoked license, as well as any use of the materials beyond the scope of an unrevoked license, may constitute copyright infringement and publisher reserves the right to take any and all action to protect its copyright in the materials.

9. Warranties: Publisher makes no representations or warranties with respect to the licensed material.

10. Indemnity: You hereby indemnify and agree to hold harmless publisher and CCC, and their respective officers, directors, employees and agents, from and against any and all claims arising out of your use of the licensed material other than as specifically authorized pursuant to this license.

11. No Transfer of License: This license is personal to you and may not be sublicensed, assigned, or transferred by you to any other person without publisher's written permission.

12. No Amendment Except in Writing: This license may not be amended except in a writing signed by both parties (or, in the case of publisher, by CCC on publisher's behalf).

13. Objection to Contrary Terms: Publisher hereby objects to any terms contained in any purchase order, acknowledgment, check endorsement or other writing prepared by you, which terms are inconsistent with these terms and conditions or CCC's Billing and Payment terms and conditions. These terms and conditions, together with CCC's Billing and Payment terms and conditions (which are incorporated herein), comprise the entire agreement between you and publisher (and CCC) concerning this licensing transaction. In the event of any conflict between your obligations established by these terms and conditions and those established by CCC's Billing and Payment terms and conditions, these terms and conditions shall control.

14. Revocation: Elsevier or Copyright Clearance Center may deny the permissions described in this License at their sole discretion, for any reason or no reason, with a full refund payable to you. Notice of such denial will be made using the contact information provided by you. Failure to receive such notice will not alter or invalidate the denial. In no event will Elsevier or Copyright Clearance Center be responsible or liable for any costs, expenses or damage incurred by you as a result of a denial of your permission request, other than a refund of the amount(s) paid by you to Elsevier and/or Copyright Clearance Center for denied permissions.

LIMITED LICENSE

The following terms and conditions apply only to specific license types:

15. **Translation**: This permission is granted for non-exclusive world **English** rights only unless your license was granted for translation rights. If you licensed translation rights you may only translate this content into the languages you requested. A professional translator must perform all translations and reproduce the content word for word preserving the integrity of the article.
16. **Posting licensed content on any Website**: The following terms and conditions apply as follows: Licensing material from an Elsevier journal: All content posted to the web site must maintain the copyright information line on the bottom of each image; A hyper-text must be included to the Homepage of the journal from which you are licensing at http://www.sciencedirect.com/science/journal/xxxxx or the Elsevier homepage for books at http://www.elsevier.com; Central Storage: This license does not include permission for a scanned version of the material to be stored in a central repository such as that provided by Heron/XanEdu.
Licensing material from an Elsevier book: A hyper-text link must be included to the Elsevier homepage at http://www.elsevier.com . All content posted to the web site must maintain the copyright information line on the bottom of each image.

Posting licensed content on Electronic reserve: In addition to the above the following clauses are applicable: The web site must be password-protected and made available only to bona fide students registered on a relevant course. This permission is granted for 1 year only. You may obtain a new license for future website posting.
17. **For journal authors:** the following clauses are applicable in addition to the above:
Preprints:
A preprint is an author's own write-up of research results and analysis, it has not been peer-reviewed, nor has it had any other value added to it by a publisher (such as formatting, copyright, technical enhancement etc.).
Authors can share their preprints anywhere at any time. Preprints should not be added to or enhanced in any way in order to appear more like, or to substitute for, the final versions of articles however authors can update their preprints on arXiv or RePEc with their Accepted Author Manuscript (see below).
If accepted for publication, we encourage authors to link from the preprint to their formal publication via its DOI. Millions of researchers have access to the formal publications on ScienceDirect, and so links will help users to find, access, cite and use the best available version. Please note that Cell Press, The Lancet and some society-owned have different preprint policies. Information on these policies is available on the journal homepage.
Accepted Author Manuscripts: An accepted author manuscript is the manuscript of an article that has been accepted for publication and which typically includes author-incorporated changes suggested during submission, peer review and editor-author communications.
Authors can share their accepted author manuscript:

- immediately
    - via their non-commercial person homepage or blog
    - by updating a preprint in arXiv or RePEc with the accepted manuscript

  - via their research institute or institutional repository for internal institutional uses or as part of an invitation-only research collaboration work-group
  - directly by providing copies to their students or to research collaborators for their personal use
  - for private scholarly sharing as part of an invitation-only work group on commercial sites with which Elsevier has an agreement
- After the embargo period
  - via non-commercial hosting platforms such as their institutional repository
  - via commercial sites with which Elsevier has an agreement

In all cases accepted manuscripts should:

- link to the formal publication via its DOI
- bear a CC-BY-NC-ND license - this is easy to do
- if aggregated with other manuscripts, for example in a repository or other site, be shared in alignment with our hosting policy not be added to or enhanced in any way to appear more like, or to substitute for, the published journal article.

Published journal article (JPA): A published journal article (PJA) is the definitive final record of published research that appears or will appear in the journal and embodies all value-adding publishing activities including peer review co-ordination, copy-editing, formatting, (if relevant) pagination and online enrichment.
Policies for sharing publishing journal articles differ for subscription and gold open access articles:
Subscription Articles: If you are an author, please share a link to your article rather than the full-text. Millions of researchers have access to the formal publications on ScienceDirect, and so links will help your users to find, access, cite, and use the best available version.
Theses and dissertations which contain embedded PJAs as part of the formal submission can be posted publicly by the awarding institution with DOI links back to the formal publications on ScienceDirect.
If you are affiliated with a library that subscribes to ScienceDirect you have additional private sharing rights for others' research accessed under that agreement. This includes use for classroom teaching and internal training at the institution (including use in course packs and courseware programs), and inclusion of the article for grant funding purposes.
Gold Open Access Articles: May be shared according to the author-selected end-user license and should contain a CrossMark logo, the end user license, and a DOI link to the formal publication on ScienceDirect.
Please refer to Elsevier's posting policy for further information.
18. **For book authors** the following clauses are applicable in addition to the above: Authors are permitted to place a brief summary of their work online only. You are not allowed to download and post the published electronic version of your chapter, nor may you scan the printed edition to create an electronic version. **Posting to a**

repository: Authors are permitted to post a summary of their chapter only in their institution's repository.

19. **Thesis/Dissertation**: If your license is for use in a thesis/dissertation your thesis may be submitted to your institution in either print or electronic form. Should your thesis be published commercially, please reapply for permission. These requirements include permission for the Library and Archives of Canada to supply single copies, on demand, of the complete thesis and include permission for Proquest/UMI to supply single copies, on demand, of the complete thesis. Should your thesis be published commercially, please reapply for permission. Theses and dissertations which contain embedded PJAs as part of the formal submission can be posted publicly by the awarding institution with DOI links back to the formal publications on ScienceDirect.

Elsevier Open Access Terms and Conditions

You can publish open access with Elsevier in hundreds of open access journals or in nearly 2000 established subscription journals that support open access publishing. Permitted third party re-use of these open access articles is defined by the author's choice of Creative Commons user license. See our open access license policy for more information.

Terms & Conditions applicable to all Open Access articles published with Elsevier:

Any reuse of the article must not represent the author as endorsing the adaptation of the article nor should the article be modified in such a way as to damage the author's honour or reputation. If any changes have been made, such changes must be clearly indicated. The author(s) must be appropriately credited and we ask that you include the end user license and a DOI link to the formal publication on ScienceDirect.

If any part of the material to be used (for example, figures) has appeared in our publication with credit or acknowledgement to another source it is the responsibility of the user to ensure their reuse complies with the terms and conditions determined by the rights holder.

Additional Terms & Conditions applicable to each Creative Commons user license:

CC BY: The CC-BY license allows users to copy, to create extracts, abstracts and new works from the Article, to alter and revise the Article and to make commercial use of the Article (including reuse and/or resale of the Article by commercial entities), provided the user gives appropriate credit (with a link to the formal publication through the relevant DOI), provides a link to the license, indicates if changes were made and the licensor is not represented as endorsing the use made of the work. The full details of the license are available at http://creativecommons.org/licenses/by/4.0.

CC BY NC SA: The CC BY-NC-SA license allows users to copy, to create extracts, abstracts and new works from the Article, to alter and revise the Article, provided this is not done for commercial purposes, and that the user gives appropriate credit (with a link to the formal publication through the relevant DOI), provides a link to the license, indicates if changes were made and the licensor is not represented as endorsing the use made of the work. Further, any new works must be made available on the same conditions. The full details of the license are available at http://creativecommons.org/licenses/by-nc-sa/4.0.

CC BY NC ND: The CC BY-NC-ND license allows users to copy and distribute the Article, provided this is not done for commercial purposes and further does not permit distribution of the Article if it is changed or edited in any way, and provided the user gives appropriate credit (with a link to the formal publication through the relevant DOI), provides a link to the license, and that the licensor is not represented as endorsing the use made of the work. The full details of the license are available at http://creativecommons.org/licenses/by-nc-nd/4.0. Any commercial reuse of Open Access articles published with a CC BY NC SA or CC BY NC ND license requires permission from Elsevier and will be subject to a fee.
Commercial reuse includes:

- Associating advertising with the full text of the Article
- Charging fees for document delivery or access
- Article aggregation
- Systematic distribution via e-mail lists or share buttons

Posting or linking by commercial companies for use by customers of those companies.

20. **Other Conditions**:

v1.9

Questions? customercare@copyright.com or +1-855-239-3415 (toll free in the US) or +1-978-646-2777.

Figure 25.





Title:	Characterization of Heterogeneously Functionalized Dendrimers by Mass Spectrometry and EPR Spectroscopy
Author:	Eric D. Walter, Karl B. Sebby, Robert J. Usselman, et al
Publication:	The Journal of Physical Chemistry B
Publisher:	American Chemical Society
Date:	Nov 1, 2005

Copyright © 2005, American Chemical Society

This type of permission/license, instead of the standard Terms & Conditions, is sent to you because no fee is being charged for your order. Please note the following:

- Permission is granted for your request in both print and electronic formats, and translations.
- If figures and/or tables were requested, they may be adapted or used in part.
- Please print this page for your records and send a copy of it to your publisher/graduate school.
- Appropriate credit for the requested material should be given as follows: "Reprinted (adapted) with permission from (COMPLETE REFERENCE CITATION). Copyright (YEAR) American Chemical Society." Insert appropriate information in place of the capitalized words.
- One-time permission is granted only for the use specified in your request. No additional uses are granted (such as derivative works or other editions). For any other uses, please submit a new request.

If credit is given to another source for the material you requested, permission must be obtained from that source.

Copyright © 2017 Copyright Clearance Center, Inc. All Rights Reserved. Privacy statement. Terms and Conditions.
Comments? We would like to hear from you. E-mail us at customercare@copyright.com

Chapter 5.

ELSEVIER LICENSE
TERMS AND CONDITIONS

Mar 28, 2017

This Agreement between Amanda L Mattson ("You") and Elsevier ("Elsevier") consists of your license details and the terms and conditions provided by Elsevier and Copyright Clearance Center.

License Number	4077911441717
License date	Mar 28, 2017
Licensed Content Publisher	Elsevier
Licensed Content Publication	Carbohydrate Research
Licensed Content Title	Using In(III) as a promoter for glycosylation
Licensed Content Author	Amanda L. Mattson,Anna K. Michel,Mary J. Cloninger
Licensed Content Date	10 January 2012
Licensed Content Volume	347
Licensed Content Issue	1
Licensed Content Pages	5
Start Page	142
End Page	146
Type of Use	reuse in a thesis/dissertation
Intended publisher of new work	other
Portion	full article
Format	both print and electronic
Are you the author of this Elsevier article?	Yes
Will you be translating?	No
Order reference number	
Title of your thesis/dissertation	The synthesis and study of TF antigen functionalized dendrimers
Expected completion date	Apr 2017
Estimated size (number of pages)	350
Elsevier VAT number	GB 494 6272 12
Requestor Location	Amanda L Mattson 103 Chemistry and Biochemistry Building Montana State University BOZEMAN, MT 59717

	United States Attn: Amanda L Mattson
Publisher Tax ID	98-0397604
Total	0.00 USD
Terms and Conditions	

INTRODUCTION

1. The publisher for this copyrighted material is Elsevier. By clicking "accept" in connection with completing this licensing transaction, you agree that the following terms and conditions apply to this transaction (along with the Billing and Payment terms and conditions established by Copyright Clearance Center, Inc. ("CCC"), at the time that you opened your Rightslink account and that are available at any time at http://myaccount.copyright.com).

GENERAL TERMS

2. Elsevier hereby grants you permission to reproduce the aforementioned material subject to the terms and conditions indicated.
3. Acknowledgement: If any part of the material to be used (for example, figures) has appeared in our publication with credit or acknowledgement to another source, permission must also be sought from that source. If such permission is not obtained then that material may not be included in your publication/copies. Suitable acknowledgement to the source must be made, either as a footnote or in a reference list at the end of your publication, as follows:
"Reprinted from Publication title, Vol /edition number, Author(s), Title of article / title of chapter, Pages No., Copyright (Year), with permission from Elsevier [OR APPLICABLE SOCIETY COPYRIGHT OWNER]." Also Lancet special credit - "Reprinted from The Lancet, Vol. number, Author(s), Title of article, Pages No., Copyright (Year), with permission from Elsevier."
4. Reproduction of this material is confined to the purpose and/or media for which permission is hereby given.
5. Altering/Modifying Material: Not Permitted. However figures and illustrations may be altered/adapted minimally to serve your work. Any other abbreviations, additions, deletions and/or any other alterations shall be made only with prior written authorization of Elsevier Ltd. (Please contact Elsevier at permissions@elsevier.com). No modifications can be made to any Lancet figures/tables and they must be reproduced in full.
6. If the permission fee for the requested use of our material is waived in this instance, please be advised that your future requests for Elsevier materials may attract a fee.
7. Reservation of Rights: Publisher reserves all rights not specifically granted in the combination of (i) the license details provided by you and accepted in the course of this licensing transaction, (ii) these terms and conditions and (iii) CCC's Billing and Payment terms and conditions.
8. License Contingent Upon Payment: While you may exercise the rights licensed immediately upon issuance of the license at the end of the licensing process for the transaction, provided that you have disclosed complete and accurate details of your proposed use, no license is finally effective unless and until full payment is received from

you (either by publisher or by CCC) as provided in CCC's Billing and Payment terms and conditions. If full payment is not received on a timely basis, then any license preliminarily granted shall be deemed automatically revoked and shall be void as if never granted. Further, in the event that you breach any of these terms and conditions or any of CCC's Billing and Payment terms and conditions, the license is automatically revoked and shall be void as if never granted. Use of materials as described in a revoked license, as well as any use of the materials beyond the scope of an unrevoked license, may constitute copyright infringement and publisher reserves the right to take any and all action to protect its copyright in the materials.

9. Warranties: Publisher makes no representations or warranties with respect to the licensed material.

10. Indemnity: You hereby indemnify and agree to hold harmless publisher and CCC, and their respective officers, directors, employees and agents, from and against any and all claims arising out of your use of the licensed material other than as specifically authorized pursuant to this license.

11. No Transfer of License: This license is personal to you and may not be sublicensed, assigned, or transferred by you to any other person without publisher's written permission.

12. No Amendment Except in Writing: This license may not be amended except in a writing signed by both parties (or, in the case of publisher, by CCC on publisher's behalf).

13. Objection to Contrary Terms: Publisher hereby objects to any terms contained in any purchase order, acknowledgment, check endorsement or other writing prepared by you, which terms are inconsistent with these terms and conditions or CCC's Billing and Payment terms and conditions. These terms and conditions, together with CCC's Billing and Payment terms and conditions (which are incorporated herein), comprise the entire agreement between you and publisher (and CCC) concerning this licensing transaction. In the event of any conflict between your obligations established by these terms and conditions and those established by CCC's Billing and Payment terms and conditions, these terms and conditions shall control.

14. Revocation: Elsevier or Copyright Clearance Center may deny the permissions described in this License at their sole discretion, for any reason or no reason, with a full refund payable to you. Notice of such denial will be made using the contact information provided by you. Failure to receive such notice will not alter or invalidate the denial. In no event will Elsevier or Copyright Clearance Center be responsible or liable for any costs, expenses or damage incurred by you as a result of a denial of your permission request, other than a refund of the amount(s) paid by you to Elsevier and/or Copyright Clearance Center for denied permissions.

LIMITED LICENSE

The following terms and conditions apply only to specific license types:

15. **Translation**: This permission is granted for non-exclusive world **English** rights only unless your license was granted for translation rights. If you licensed translation rights you may only translate this content into the languages you requested. A professional translator must perform all translations and reproduce the content word for word preserving the integrity of the article.

16. **Posting licensed content on any Website**: The following terms and conditions apply as follows: Licensing material from an Elsevier journal: All content posted to the web site must maintain the copyright information line on the bottom of each image; A hyper-text must be included to the Homepage of the journal from which you are licensing at http://www.sciencedirect.com/science/journal/xxxxx or the Elsevier homepage for books at http://www.elsevier.com; Central Storage: This license does not include permission for a scanned version of the material to be stored in a central repository such as that provided by Heron/XanEdu.
Licensing material from an Elsevier book: A hyper-text link must be included to the Elsevier homepage at http://www.elsevier.com . All content posted to the web site must maintain the copyright information line on the bottom of each image.

Posting licensed content on Electronic reserve: In addition to the above the following clauses are applicable: The web site must be password-protected and made available only to bona fide students registered on a relevant course. This permission is granted for 1 year only. You may obtain a new license for future website posting.
17. **For journal authors:** the following clauses are applicable in addition to the above:
Preprints:
A preprint is an author's own write-up of research results and analysis, it has not been peer-reviewed, nor has it had any other value added to it by a publisher (such as formatting, copyright, technical enhancement etc.).
Authors can share their preprints anywhere at any time. Preprints should not be added to or enhanced in any way in order to appear more like, or to substitute for, the final versions of articles however authors can update their preprints on arXiv or RePEc with their Accepted Author Manuscript (see below).
If accepted for publication, we encourage authors to link from the preprint to their formal publication via its DOI. Millions of researchers have access to the formal publications on ScienceDirect, and so links will help users to find, access, cite and use the best available version. Please note that Cell Press, The Lancet and some society-owned have different preprint policies. Information on these policies is available on the journal homepage.
Accepted Author Manuscripts: An accepted author manuscript is the manuscript of an article that has been accepted for publication and which typically includes author-incorporated changes suggested during submission, peer review and editor-author communications.
Authors can share their accepted author manuscript:

- immediately
    - via their non-commercial person homepage or blog
    - by updating a preprint in arXiv or RePEc with the accepted manuscript
    - via their research institute or institutional repository for internal institutional uses or as part of an invitation-only research collaboration work-group
    - directly by providing copies to their students or to research collaborators for their personal use

    - for private scholarly sharing as part of an invitation-only work group on commercial sites with which Elsevier has an agreement
- After the embargo period
    - via non-commercial hosting platforms such as their institutional repository
    - via commercial sites with which Elsevier has an agreement

In all cases accepted manuscripts should:

- link to the formal publication via its DOI
- bear a CC-BY-NC-ND license - this is easy to do
- if aggregated with other manuscripts, for example in a repository or other site, be shared in alignment with our hosting policy not be added to or enhanced in any way to appear more like, or to substitute for, the published journal article.

Published journal article (JPA): A published journal article (PJA) is the definitive final record of published research that appears or will appear in the journal and embodies all value-adding publishing activities including peer review co-ordination, copy-editing, formatting, (if relevant) pagination and online enrichment.
Policies for sharing publishing journal articles differ for subscription and gold open access articles:
Subscription Articles: If you are an author, please share a link to your article rather than the full-text. Millions of researchers have access to the formal publications on ScienceDirect, and so links will help your users to find, access, cite, and use the best available version.
Theses and dissertations which contain embedded PJAs as part of the formal submission can be posted publicly by the awarding institution with DOI links back to the formal publications on ScienceDirect.
If you are affiliated with a library that subscribes to ScienceDirect you have additional private sharing rights for others' research accessed under that agreement. This includes use for classroom teaching and internal training at the institution (including use in course packs and courseware programs), and inclusion of the article for grant funding purposes.
Gold Open Access Articles: May be shared according to the author-selected end-user license and should contain a CrossMark logo, the end user license, and a DOI link to the formal publication on ScienceDirect.
Please refer to Elsevier's posting policy for further information.
18. **For book authors** the following clauses are applicable in addition to the above: Authors are permitted to place a brief summary of their work online only. You are not allowed to download and post the published electronic version of your chapter, nor may you scan the printed edition to create an electronic version. **Posting to a repository:** Authors are permitted to post a summary of their chapter only in their institution's repository.
19. **Thesis/Dissertation**: If your license is for use in a thesis/dissertation your thesis may be submitted to your institution in either print or electronic form. Should your thesis be published commercially, please reapply for permission. These requirements include

permission for the Library and Archives of Canada to supply single copies, on demand, of the complete thesis and include permission for Proquest/UMI to supply single copies, on demand, of the complete thesis. Should your thesis be published commercially, please reapply for permission. Theses and dissertations which contain embedded PJAs as part of the formal submission can be posted publicly by the awarding institution with DOI links back to the formal publications on ScienceDirect.

Elsevier Open Access Terms and Conditions
You can publish open access with Elsevier in hundreds of open access journals or in nearly 2000 established subscription journals that support open access publishing. Permitted third party re-use of these open access articles is defined by the author's choice of Creative Commons user license. See our open access license policy for more information.
Terms & Conditions applicable to all Open Access articles published with Elsevier:
Any reuse of the article must not represent the author as endorsing the adaptation of the article nor should the article be modified in such a way as to damage the author's honour or reputation. If any changes have been made, such changes must be clearly indicated. The author(s) must be appropriately credited and we ask that you include the end user license and a DOI link to the formal publication on ScienceDirect.
If any part of the material to be used (for example, figures) has appeared in our publication with credit or acknowledgement to another source it is the responsibility of the user to ensure their reuse complies with the terms and conditions determined by the rights holder.
Additional Terms & Conditions applicable to each Creative Commons user license:
CC BY: The CC-BY license allows users to copy, to create extracts, abstracts and new works from the Article, to alter and revise the Article and to make commercial use of the Article (including reuse and/or resale of the Article by commercial entities), provided the user gives appropriate credit (with a link to the formal publication through the relevant DOI), provides a link to the license, indicates if changes were made and the licensor is not represented as endorsing the use made of the work. The full details of the license are available at http://creativecommons.org/licenses/by/4.0.
CC BY NC SA: The CC BY-NC-SA license allows users to copy, to create extracts, abstracts and new works from the Article, to alter and revise the Article, provided this is not done for commercial purposes, and that the user gives appropriate credit (with a link to the formal publication through the relevant DOI), provides a link to the license, indicates if changes were made and the licensor is not represented as endorsing the use made of the work. Further, any new works must be made available on the same conditions. The full details of the license are available at http://creativecommons.org/licenses/by-nc-sa/4.0.
CC BY NC ND: The CC BY-NC-ND license allows users to copy and distribute the Article, provided this is not done for commercial purposes and further does not permit distribution of the Article if it is changed or edited in any way, and provided the user gives appropriate credit (with a link to the formal publication through the relevant DOI), provides a link to the license, and that the licensor is not represented as endorsing the use

made of the work. The full details of the license are available at http://creativecommons.org/licenses/by-nc-nd/4.0. Any commercial reuse of Open Access articles published with a CC BY NC SA or CC BY NC ND license requires permission from Elsevier and will be subject to a fee.
Commercial reuse includes:

- Associating advertising with the full text of the Article
- Charging fees for document delivery or access
- Article aggregation
- Systematic distribution via e-mail lists or share buttons

Posting or linking by commercial companies for use by customers of those companies.

20. **Other Conditions**:

v1.9

Questions? customercare@copyright.com or +1-855-239-3415 (toll free in the US) or +1-978-646-2777.